DYNAMICS OF BIOCHEMICAL SYSTEMS

Symposia Biologica Hungarica 30

DYNAMICS OF BIOCHEMICAL SYSTEMS

30

Akadémiai Kiadó, Budapest

DYNAMICS OF BIOCHEMICAL SYSTEMS

Edited by
S. DAMJANOVICH, T. KELETI,
L. TRÓN

Symposia Biologica Hungarica
30

This volume brings together studies from a number of different laboratories working on the dynamics of micromolecular and cellular systems. It contains the lectures presented at a FEBS advanced course held in Debrecen, Hungary, August 1985 along with the entire discussion material. Leading experts have contributed new unpublished experimental and theoretical results as up-to-date short accounts of the achievements in their special lines.

The book includes four major sections:

- Dynamics of protein and nucleic structure
- Dynamics of multienzyme complexes and metabolic pathways
- Receptor dynamics
- Membrane dynamics and
- transport

Selected topics, among others: interactions between metabolic pathways—interaction of sequential metabolic enzymes—dynamics of enzyme quaternary structure—relationship of conformational dynamics of enzymes and substrate binding—protein dynamics and free energy transduction—model discrimination and parameter esti-

Symposia
Biologica
Hungarica
30

Symposia Biologica Hungarica

Vol. 30

Redigunt

S. Damjanovich
T. Keleti
L. Trón

AKADÉMIAI KIADÓ, BUDAPEST 1986

DYNAMICS OF BIOCHEMICAL SYSTEMS

Lectures Presented at the
FEBS ADVANCED COURSE
and
ROUND TABLE DISCUSSION of the
IUB INTEREST GROUP on KINETICS and MECHANISMS of
ENZYMES and METABOLIC NETWORKS

Debrecen, Hungary
18–24 August 1985

Edited by

S. DAMJANOVICH
Department of Biophysics
University Medical School of Debrecen
Debrecen, Hungary

T. KELETI
Institute of Enzymology
Biological Research Center, Hungarian Academy of Sciences
Budapest, Hungary

L. TRÓN
Department of Biophysics
University Medical School of Debrecen
Debrecen, Hungary

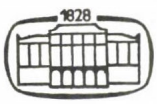

AKADÉMIAI KIADÓ, BUDAPEST 1986

Joint edition published by Elsevier Science Publishers, Amsterdam, The Netherlands
and
Akadémiai Kiadó, The Publishing House of the Hungarian Academy of Sciences,
Budapest, Hungary

ISBN 963 05 4356 7

Printed in Hungary

PREFACE

Contemporary science (as scientists know only too well) is flooded with an ocean of unselected information. Despite international efforts to bring order among the immense number of scientific meetings held each year and to rank the wild forest of journals according to their immediacy, impact factor and many other indices characterizing their values, the jungle of information is becoming larger and more disorganized day by day. Creative scientific communities are trying to safeguard their integrity - of course without losing the unquestionable benefit of quick information exchange - by organizing small symposia, attended mostly by invited persons, where narrower scientific fields can be thoroughly treated and dicussed by the well-known celebrities of that field.

Everyone has to start his scientific career as a beginner with the possible exception of a genius. To avoid the exclusion of very promising young scientists from a mini-symposium and to take full advantage of the opportunity for these young people to meet an excellent selection of internationally known scientists, a new organizational form was tested. At the Debrecen Medical University School of Hungary all the necessary facilities are provided for the organization of successful small meetings on selected scientific topics. The experimental institutes of this university campus in Eastern Hungary have long traditions and the necessary organizational skill. This year, for the first time in the long line of earlier, really successful symposia, such a mini-symposium was combined with an advanced course for young scientists. Thus, the original aim,

i.e., the possibility of high level discussions among selected renowned scientists, was maintained without losing the opportunity to include promising members of the younger generation.

The Department of Biophysics was host to the experimental lessons, and the themes were coorganized with the Institute of Enzymology of the Hungarian Academy of Sciences.

The topics of the theoretical lessons could clearly be divided into five main parts:

1) Kinetics and mechanism of enzymes and metabolic networks
2) Dynamics of protein and nucleic acid structure
3) Dynamics of multienzyme complexes and metabolic pathways
4) Enzyme kinetics and regulation
5) Membrane dynamics

For those who are familiar with these fields it is immediately obvious that the first four subjects represent a broader field and the last subject is strongly interdependent with the four others. The content of this book reflects the high scientific quality of the presentations, and the discussions following the presentations give the reader an insight into the sometimes heated, but always relevant and objective, arguing of eminent scientists about their very up-to-date results and concepts. Although the experimental parts could not be included here, all participants of the summer school received them before the actual experimental hours.

Thanks are due to those organizations who supported this fruitful meeting: among them the Federation of European Biochemical Societies, the International Union of Biochemistry, the Hungarian Academy of Sciences, the Hungarian Societies of Biochemistry and Biophysics, the Regional Committee of the Hungarian Academy of Sciences and last, but not at all least, the two organizing institutes: the Institute of Enzymology of the Hungarian Academy of Sciences and the Department of Biophysics of the Debrecen Medical University School.

The skilled contribution of many coworkers is gratefully acknowledged. We hope that all guests and participants were

satisfied with the pleasant atmosphere of the surroundings and enjoyed their stay with us.

The rapid publication of the proceedings with the generous help of the Publishing House of the Hungarian Academy of Sciences is part of our cherished traditions.

The Editors

CONTENTS

PREFACE V

KINETICS AND MECHANISM OF ENZYMES AND METABOLIC NETWORKS

T. KELETI and B. VÉRTESSY
Kinetic power and theory of control 3

M. MARKUS and B. HESS
Hysteresis and crises in the dynamics of glycolysis 11
Discussion 24

L. ERNSTER, V. KONJI, A. MONTAG, K. NORDENBRAND and G. SANDRI
Mitochondrial transport of divalent cations: pathways, mechanisms, regulation 27
Discussion 40

J.J. ARAGÓN
Simulation of intracellular concentrations of enzyme for kinetic studies: application to phosphofructokinase 41
Discussion 53

DYNAMICS OF PROTEIN AND NUCLEIC ACID STRUCTURE

B.N. GOLDSTEIN
Graph theoretic approach to dynamics of enzyme quaternary structure 59
Discussion 71

J. RICARD and G. NOAT
Dynamics of conformational changes of enzymes and the modulation of substrate binding and catalysis. Evolutionary considerations 73
Discussion 87

M.D. FRANK-KAMENETSKII
Dynamics of DNA structure 91

A. ROSENBERG and B. SOMOGYI
Conformational fluctuations, thermal stability and hydration of proteins. Studies by hydrogen exchange kinetics 101

B. SOMOGYI and A. ROSENBERG
Protein dynamics as revealed by fluorescence quenching 113
Discussion 125

DYNAMICS OF MULTIENZYME COMPLEXES AND METABOLIC PATHWAYS

D.E. ATKINSON
Dynamic interactions between metabolic sequences 129
Discussion 142

J.S. EASTERBY
Application of the transient kinetic behaviour of coupled enzyme reactions to the analysis of metabolic pathway dynamics 145
Discussion 157

J.B. ROBINSON, Jr. and P.A. SRERE
Interactions of sequential metabolic enzymes of the mitochondria: a role in metabolic regulation 159
Discussion 170

P. FRIEDRICH
Characterization of metabolite pools by "enzyme probes" 173
Discussion 183

V.V. DYNNIK, R.H. DJAFAROV and I.M. DJAFAROVA
Dynamics of aerobic energy metabolism. Coenzyme cycles, feedback and feedforward control and homeostasis 185
Discussion 201

J. OVÁDI
Dynamic assembly of enzymes related to triosephosphates 203
Discussion 216

G.R. WELCH
Viscosity and biochemical dynamics in vivo 217
Discussion 227

B.I. KURGANOV
The general principles of the control of functioning enzymes and multienzyme complexes 231
Discussion 243

J. BATKE and P. TOMPA
The dynamic character of the enzyme-enzyme interactions in the cytoplasm of evolutionary distant species 247
Discussion 262

ENZYME KINETICS AND REGULATION

W.G. BARDSLEY
Model discrimination. Conditions when the current model can be identified for transient, steady-state and binding data 267
Discussion 282

M. BEZEAU, M.J. CLEMENTS, A. CORNISH-BOWDEN, L. ENDRENYI and J. WANG
Design and analysis of enzyme kinetic experiments. Efficiency and robustness of the parameters 289
Discussion 305

A. CORNISH-BOWDEN and L. ENDRENYI
Estimation of enzyme kinetic parameters without prior information about weights or error distribution 309
Discussion 320

B. MANNERVIK and U.H. DANIELSON
Empirical error functions for model discrimination and parameter estimation in enzyme kinetics 323
Discussion 335

MEMBRANE DYNAMICS

D.M. SEGAL, B. KARPOVSKY, D.A. STEPHANY, P. PEREZ, J.A. TITUS and D.V. COVELL
The role of Fcγ receptors in mediating conjugate formation and target cell lysis 341
Discussion 357

E.L. ELSON
Biophysical applications of fluorescence correlation spectroscopy and photobleaching recovery 359
Discussion 377

Ch. DELISI and M. GEX-FABRY
The dynamics of endocytic processing 381

M. EDIDIN
Interactions between major histocompatibility complex glycoproteins and peptide hormone receptors 393
Discussion 404

J. GERGELY and G. SÁRMAY
Two-binding-site model of Fc receptors on human K cells 409
Discussion 415

L. TRÓN, S. DAMJANOVICH, A. ASZALOS, J. SZÖLLŐSI, S.A. MULHERN and M.J. FULWYLER
On the role of cell surface dynamics and transmembrane information transfer: cyclosporin A changes physical properties of cell membranes 417
Discussion 441

A. ASZALOS, M.M. GOTTESMAN and S. DAMJANOVICH
Depolymerization of microtubules increases motional freedom of lipid and protein probes in the cellular membrane and alters plasma membrane potential 443
Discussion 459

A. IKEGAMI and K. KINOSITA, Jr.
Dynamic structure of biological membranes 461

I. PECHT, B. RIVNAY and A. CORCIA
Calcium channels linking antigen stimulation with secretion from mast cells and basophils 473
Discussion 483

R.J. CHERRY
Effects of melittin and membrane potential on the mobility of band 3 proteins in human erythrocyte membranes 487
Discussion 497

R. ZIDOVETZKI, U. BANERJEE, R.R. BIRGE and S.I. CHAN
Nuclear magnetic resonance study of the interaction of phospholipid bilayers with polypeptide antibiotics 501
Discussion 518

C.M. SLUSE-GOFFART and F.E. SLUSE
Kinetics as a tool for the study of transmembrane exchange exemplified by the study of the oxoglutarate translocator 521
Discussion 534

R.M. KRUPKA and R. DEVES
Access channels in carrier systems: evidence derived from inhibition studies of the choline and glucose transport systems of erythrocytes 537
Discussion 549

LIST OF PARTICIPANTS 553

INDEX 557

KINETICS AND MECHANISM OF ENZYMES AND METABOLIC NETWORKS

Dynamics of Biochemical Systems
S. Damjanovich, T. Keleti, L. Trón (Eds)

KINETIC POWER AND THEORY OF CONTROL

KELETI, T. and VÉRTESSY, B.

Institute of Enzymology, Biological Research Center,
Hungarian Academy of Sciences, Budapest, Hungary
H-1502 Pf. 7

The evolution of living beings is based on the evolution of the 1./ individual macromolecules, 2./ metabolic pathways, 3./ regulation of the organism.

The evolution of the individual enzymes is considered to be linked to the free-energy change associated with the transient state barrier (Welch and Keleti 1981). The measure of the evolutionary "perfection" is the kinetic power, i.e. $V_{max}/K_M = k_f$ (Keleti and Welch 1984). The resultant of individual transition-state barriers (of the optimally evolved kinetic powers) influences the efficacy of the overall metabolic pathway in which the considered enzymes take place. Consequently the metabolic pathways which, at one hand, are the result of biological evolution, on the other hand, are also subject of the evolution. As a result of selection processes the metabolic pathways are characterized by more and more effective coherent functioning of the various elements and subsystems. Such a selection pressure leads to the formation of the cytosociological behaviour of the enzymes which renders them able to respond to the complete spectrum of extrinsic factors (Welch and Keleti 1981). Therefore, the whole multienzyme sequence of a given biochemical pathway is the most likely focus in the evolutionary optimization of the metabolism. Since the regulation of an organism depends on the coherent functioning of the different metabolic pathways the cytosociological behaviour of the enzymes should be reflected in the cytosociological adaptation of biochemical pathways to

each other.

The stabilization of the formed biochemical pathways and the evolving of their cytosociological adaptation lead to the formation of dynamically or statically interacting enzyme aggregates, i.e. organized multienzyme complexes. Their major benefit is the compartmentation of metabolites and the concomitant decrease in (or elimination of) the steady-state transient time (Friedrich 1974, 1984, 1985, Welch 1977, Welch and Keleti 1981, Keleti 1984, Keleti et al. 1985).

In a consecutive reaction of two enzymes the transient time, τ , generally equals (Bartha and Keleti 1979):

$$\tau = ([E_2]_o + K_M)/k_2 [E_2]_o \qquad (1)$$

If $[E_2]_o \ll K_M$

$$\tau = K_M/k_2 [E_2]_o \qquad (2)$$

(cf. Hess and Wurster 1970) where $[E_2]_o$ is the total concentration of the second enzyme in the consecutive reaction of two enzymes, K_M is the Michaelis constant of the substrate for the second enzyme and k_2 is the first order rate constant of the rate limiting step of the reaction catalyzed by the second enzyme. From (1)

$$\tau = 1/k_2 + K_M/V_{max} = 1/k_2 + 1/k_r \qquad (3)$$

or if $[E_2]_o \ll K_M$, from (2)

$$\tau = 1/k_r \qquad (4)$$

(cf. Easterby 1973, Welch 1977a).

The "measure of perfection" is the magnitude of k_r (Keleti and Welch 1984).

If $1/k_r \ll 1/k_2$, from (3)

$$\tau \approx 1/k_2 \qquad (5)$$

If k_r is very high and $[E_2]_0 \ll K_M$, from (4)

$$\tau \approx 0 \qquad (6)$$

In the case of a consecutive reaction of n enzymes $\tau = \sum_2^n \tau_i$ (i=1,2...n). Consequently in a best evolved multienzyme complex $\tau = \sum_2^n 1/k_i$ (in the general case) or $\tau = 0$ (if $[E_i]_0 \ll K_{M,i}$, for i=2,...n).

This means that the "extremal principle" of the evolution of multienzyme systems is the same as that of the individual enzymes (Welch and Keleti 1981, Keleti and Welch 1984).

For the description of regulatory properties of metabolic pathways a "theory of control" was developed (Kacser and Burns 1973, 1979, Kacser 1983, Heinrich and Rapoport 1973, 1974, 1983, Heinrich et al. 1977) and improved (Westerhoff et al. 1984, Fell and Sauro 1985).

Obviously, the more effective the control is, the more elastic the metabolic pathway will be, consequently it will be more able to respond to the changes in external conditions. The best controllable, the most elastic metabolic pathway can be considered to be the most "perfectly" evolved.

Every enzyme reaction of a metabolic pathway is coupled to the neighbouring enzymes through its substrate(s) and product(s). The change in substrate concentration (since enzymes in vivo work distant from saturation values) causes change in enzyme activity and the value of this change depends on the nature of the enzyme and the substrate participating in the reaction. The factor describing the response of the rate to an infinitesimal change in substrate concentration is

the "elasticity coefficient": $(\delta v/v)/(\delta S/S) = \epsilon^v_S$. The magnitude of the elasticity coefficient depends on the concentration of all participants and on the associated kinetic constants. In the case of Michaelis-Menten kinetics (single enzyme-substrate complex and rate determining irreversible step of product formation):

$$(\delta v/v)/(\delta S/S) \approx (dv/dS)(S/v) = S(V_{max}-v)^2/vV_{max}K_M =$$

$$= V_{max}S/K_Mv - (S/K_M)(2-v/V_{max}) =$$

$$= (K_M+S)/K_M - (S/K_M)\left[(2K_M+S)/(K_M+S)\right] =$$

$$= K_M/(K_M+S) \qquad (7)$$

Elasticity coefficient =

$$= \epsilon^v_S = K_M/(K_M+S) = V_{max}/(V_{max}+k_f S) \qquad (8)$$

$$\epsilon^v_S = \begin{cases} 1 & \text{if } (S \ll K_M) \equiv (k_f S \ll V_{max}) \\ K_M/S = V_{max}/k_f S & \text{if } (S \gg K_M) \equiv (k_f S \gg V_{max}) \\ 0 & \text{if } S \longrightarrow \infty \end{cases}$$

This means that at substrate saturation no elasticity, at high substrate concentration small elasticity can be observed. The elasticity is optimal at low substrate concentration and this is the normal circumstance in the living cells.

The factor describing the response of the overall rate to an infinitesimal change in enzyme concentration is the "control coefficient":

$C^V_P = (\delta V/V)/(\delta P/P) = (\delta \ln V/\delta \ln P)$, where V = flux = F and P = enzyme concentration = E, i.e. $C^V_P = C^F_E$.

Since in a coupled reaction of two enzymes catalyzing reversible reactions (cf. Kacser and Burns 1983):

$$S_1 \overset{E_1}{\rightleftharpoons} S_2 \overset{E_2}{\rightleftharpoons} S_3$$

$$C^{F}_{E_1 1} \in^{v}_{S_1 1} + C^{F}_{E_2 1} \in^{v}_{S_2 2} = 0 \qquad (9)$$

$$C^{F}_{E_1 1}/C^{F}_{E_2 1} = -\in^{v}_{S_2 2}/\in^{v}_{S_1 1}$$

If $S_1/K^{E_1}_{M,S_1} + S_2/K^{E_1}_{M,S_2} \ll 1$

$$v_1 = k_{\Gamma,1}/(S_1 - S_2/K_{eq,1}) \qquad (10)$$

$$v_2 = k_{\Gamma,2}/(S_2 - S_3/K_{eq,2}) \qquad (11)$$

where $K_{eq,1}$ is the equilibrium constant between the pools of S_1 and S_2, $K_{eq,2}$ that between the pools of S_2 and S_3.

Applying further equations derived by Kacser and Burns (1973) for more consecutive reactions :

$$C^{F_1}_{E_1} : C^{F_1}_{E_2} : C^{F_1}_{E_3} : \ldots = 1/k_{\Gamma,1} : 1/k_{\Gamma,2}K_{eq,1} : 1/k_{\Gamma,3}K_{eq,1}K_{eq,2} : \cdots \qquad (12)$$

and

$$C^{F_1}_{E_1} = (1/k_{\Gamma,1})/(1/k_{\Gamma,1} + 1/k_{\Gamma,2}K_{eq,1} + \ldots) \qquad (13)$$

$$C^{F_1}_{E_2} = (1/k_{\Gamma,2}K_{eq,1})/(1/k_{\Gamma,1} + 1/k_{\Gamma,2}K_{eq,1} + \ldots) \qquad (14)$$

$$C^{F_1}_{E_3} = (1/k_{\Gamma,3}K_{eq,1}K_{eq,2})/(1/k_{\Gamma,1} + 1/k_{\Gamma,2}K_{eq,1} + \ldots) \qquad (15)$$

i.e. $$C_{E_1}^{F_1} + C_{E_2}^{F_1} + C_{E_3}^{F_1} + \ldots = 1 \qquad (16)$$

Consequently k_Γ is the measure not only of the evolution of the individual enzymes (Keleti and Welch 1984) or of the coupled reactions (cf. equ.s (3), (4)) but also of the control parameters of the metabolic pathways, namely the elasticity coefficient and the control coefficient. The greater k_Γ is, the more "evolved", more "perfect" the enzyme is. The greater k_Γ is, the smaller the transient time of the coupled reaction is. At low $[S]$, which is the case under physiological conditions, the greater k_Γ is the more effective the elasticity is (cf. equ. (8)), and the velocity of the enzyme reactions in the metabolic pathway is greater (cf. equ.s (10), (11)).

In the course of evolution, first the enzymes developed individually - here the purpose is to increase the power (rate) and the specificity of enzyme catalysis. We can estimate how far in evolution the individual enzyme molecule can go, in optimizing (increasing) its kinetic power under the conditions of cell metabolism. According to an "evolutionary compromise" condition we get an approximate upper limit of $k_\Gamma = k_D[E]_T/2$ (cf. Keleti and Welch 1984), where k_D is the rate constant of diffusion. However, evolution can go much further in tailoring the regulatory character of cell metabolism, where the enzyme molecule is imbedded in its natural setting, and is connected with other enzymes through substrates and products. In this part of evolution the main purpose is to achieve the most perfect regulation, control mechanism, elasticity - even if it calls forth accidental decrease in some k_Γ values of individual reactions (- and perhaps increase in others).

Therefore, the fact that changes in more than one k_Γ value (increases in some and decreases in others) can equally increase or decrease C_E^F values (cf. equ.s (12)-(16)) does not contradict our previous observations. For instance, we can easily see that $\delta C_{E_i}^{F_1} / \delta k_{\Gamma,i}$ is always negative, while

$\partial C^{F}_{E_i 1}/\partial k_{\Gamma,j}$ $(j \neq i)$ is always positive which means that increase in $k_{\Gamma,i}$ decreases while increase in $k_{\Gamma,j}$ $(j \neq i)$ increases the respective $C^{F}_{E_i 1}$, i.e. the measure of the control importance of the step per se. Since the sum of all control coefficients of a given metabolic pathway equals unity, only one could approach full control importance, but it is equally possible that none of the enzymes is a "pace-maker", "bottleneck" or "key" enzyme. Consequently, changes in k_{Γ} values and the concomitant increase or decrease in C^{V}_{P} values may be equally useful for evolution, depending on whether a single-enzyme controlled or all enzymes controlled metabolic pathway is more powerful for the regulation in a given organism. Moreover, one should be aware that by changing the circumstances a single-enzyme controlled pathway may change into an all enzymes controlled one, and vice versa.

We have shown some considerations which say that the "extremal principle" of the evolution of enzymes, enzyme systems, metabolic pathways and their regulation is identical, namely the kinetic power, i.e. $V_{max}/K_M = k_{\Gamma}$.

One should be aware of the fact that all these considerations refer to a homogeneous "bulk" medium. The application of the theory to structuralized, organized states (which is the living cell) is under way (Welch et al. 1986).

References

Bartha,F., Keleti,T. (1979) Oxid.Commun. 1,75-84

Easterby,J.S. (1973) Biochim.Biophys.Acta 293,552-558

Fell,D.A., Sauro,H.M. (1985) Eur.J.Biochem. 148,555-561

Friedrich,P. (1974) Acta Biochim.Biophys.Acad.Sci.Hung. 9, 159-175

Friedrich,P. (1984) Supramolecular Enzyme Organization. Quaternary Structure and Beyond. Pergamon Press, Oxford and Akadémiai Kiadó, Budapest

Friedrich,P. (1985) Dynamic Compartmentation in Soluble Multienzyme System. In Welch,G.R. ed.: Catalytic Facilitation in Organized Multienzyme Systems. Acad.Press, New York

Heinrich,R., Rapoport,T.A. (1973) Acta Biol.Med.Germ. 31, 479-494

Heinrich,R., Rapoport,T.A. (1974) Eur.J.Biochem. 42,89-95

Heinrich,R., Rapoport,T.A. (1983) Biochem.Soc.Trans. 11,31-35

Heinrich,R., Rapoport,T.A., Rapoport,S.M. (1977) Progr.Biophys. Mol.Biol. 32,1-82

Hess,B., Wurster,B. (1970) FEBS Lett. 9,73-77

Kacser,H. (1983) Biochem.Soc.Trans. 11,35-40

Kacser,H., Burns,J.A. (1973) The Control of Flux. In Symp.Soc. Exp.Biol.XXVII. Rate Control of Biological Processes.Univ. Press, Cambridge

Kacser,H., Burns,J.A. (1979) Biochem.Soc.Trans. 7,1149-1160

Keleti,T. (1984) Channelling in Enzyme Complexes. In Ricard,J., Cornish-Bowden,A. eds.: Dynamics of Biochemical Systems. Plenum Press, New York, London, Washington, Boston. pp. 103-114

Keleti,T., Welch,G.R. (1984) Biochem.J. 223,299-303

Keleti,T., Ovádi,J., Batke,J., (1985) Kinetic and Physiochemical Analysis of Enzyme Complexes. In Klyosov,A.A., Varfolomeev,S.D., Welch,G.R. eds.: Towards a Cellular Enzymology. Plenum Press, New York

Welch,G.R. (1977) Progr.Biophys.Mol.Biol. 32,103-191

Welch,G.R. (1977a) J.Theor.Biol. 68,267-291

Welch,G.R., Keleti,T. (1981) J.Theor.Biol. 93,701-735

Welch,G.R., Keleti,T., Vértessy,B. (1986) in preparation

Westerhoff,H.V., Groen,A.K., Wanders,J.A. (1984) Biosci.Rep. 4,1-22

Dynamics of Biochemical Systems
S. Damjanovich, T. Keleti, L. Trón (Eds)

HYSTERESIS AND CRISES IN THE DYNAMICS OF GLYCOLYSIS

MARIO MARKUS and BENNO HESS

Max-Planck-Institut für Ernährungsphysiologie
Rheinlanddamm 201, 4600 Dortmund 1, FRG

INTRODUCTION

Until a few decades ago, the analysis of metabolic pathways has relied on the classical assumption of self-regulation leading to steady states. The biochemical community then became aware of periodic reactions being a widespread feature of metabolic processes (for reviews, see [1,2]). Recently, more complicated dynamic states, namely aperiodic (chaotic) oscillations have been discovered in biochemistry: first in a single-enzyme system (the peroxidase-oxidase reaction [3]) and then in glycolyzing cell extracts. In the latter system, chaos was first predicted theoretically [4,5] and then found experimentally [6-8] under the conditions of coupling of periodic glycolytic oscillations and periodic substrate flux. Coupled periodic processes play an important role at all levels of biological organization (see [9]). In particular, coupling between oscillatory metabolic processes was demonstrated in yeast cells [10,11] and the slime mould [12].

Our investigations showed that glycolysis is able to convert a sinusoidal input flux into a variety of periodic, quasiperiodic, intermittent and chaotic oscillations [4-9]. Thus, instead of just speaking of a frequency converter mechanism, as in [13], one may more generally speak of a time pattern converter. But this is not all: glycolysis may display more than one (two, three or four) types of oscillations under exactly the same conditions, depending on the previous history. The system then shows hysteretic behaviour [5,9,11]. In such cases, different

attractors coexist in phase space (i.e. in a space of variables describing the dynamics of the system), each one having its own basin of attraction, and there are in general two ways of changing the system time pattern: 1. By perturbing the system so that it may jump in phase space from one attractor to another at constant external conditions ("switching" process). 2. By changing the external conditions. However, if this change is performed gradually one may not always expect a gradual change in the dynamic properties of the system, since abrupt transitions (bifurcations) may occur. There are many types of bifurcations, such as the well-known saddle-node bifurcations, the period-doubling cascades [14,15] and the so-called crises, which have recently been found in simple mathematical mappings [16,17].

In what follows, we will discuss some new examples of glycolytic processes illustrating hysteresis, switching and crises.

THE MODEL AND METHODS OF DISPLAY

In spite of the complexity of the glycolytic pathway, we have shown that the dynamics of glycolysis can be sufficiently well described by a simplified model containing three rates: that of the input flux and those of the key enzymes phosphofructokinase (PFK) and pyruvate kinase (PK). The model is described in detail in references [4,5]. It contains rate laws for PFK and PK that had accurately been determined from extensive kinetic measurements. These rate laws depend on the concentrations of ADP, ATP, fructose-6-phosphate, fructose 1,6-bisphosphate, phosphoenolpyruvate (PEP), magnesium and potassium. The input flux rate V_{in} is written as the sum of a constant flux $\overline{V}_{in}$ and a sinusoidal flux $A \sin \omega_e t$. Unless otherwise stated, the control conditions are set as given in reference [5].

HYSTERESIS

In Fig. 1 we show a number of hysteresis loops obtained from the glycolytic model. The ordinates (resp. abscissas) show different dependent (resp. independent) variables of the dynamics of glycolysis.

As dependent variables in the examples shown in Fig. 1 we

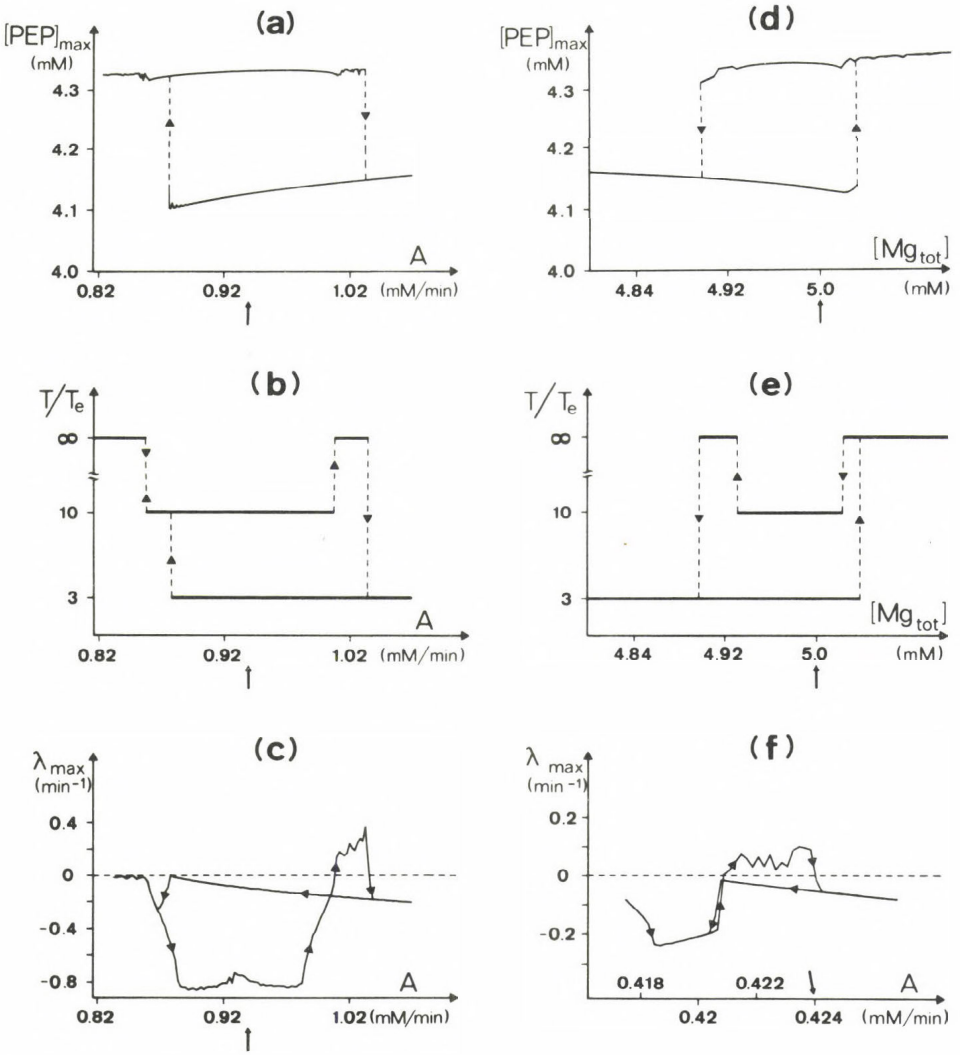

Fig. 1. Hysteresis of the dynamics of glycolysis. A and T_e are the input flux amplitude and period, respectively. T is the response period. λ_{max} is the maximum Liapunov exponent per unit time. The conditions are: (a), (b) and (c): ω_e=14 min^{-1}, $[Mg_{tot}]$ =5 mM; (d) and (e): ω_e=14 min^{-1}, A=0.94 mM/min; (f): ω_e=6.4 min^{-1}, $[Mg_{tot}]$= 5 mM. $[Mg_{tot}]$ is the total magnesium concentration (bound plus unbound). The arrows pointing to the abscissas of (a) to (e) correspond to Fig. 2. The arrow pointing to the abscissa in (f) corresponds to Figs. 3 and 4b

have chosen: 1. The maximum value of [PEP] ($[PEP]_{max}$) attained during the oscillations. 2. The period T of the response oscillation relative to the external (input) period T_e. 3. The maximum Liapunov exponent per unit time λ_{max} (see [18]), which is a measure of the average stability of the orbit. For chaotic orbits, λ_{max} is larger than 0 and is equal to the reciprocal of the shortest average time in which a perturbation doubles its size. For periodic orbits, λ_{max} is smaller than 0 and is equal to the reciprocal of the longest average time in which a perturbation decays to one half. Quasiperiodic oscillations (mixing of periodic oscillations having inconmensurate frequencies) are characterized by $\lambda_{max}=0$.

As independent variables in Fig. 1 we have chosen the input flux amplitude A and the total magnesium concentration $[Mg_{tot}]$. Note that only a fraction (about 25% in the present range of concentrations) is free as a divalent cation, the rest being bound to other solutes, as investigated in [19]. The abscissas in Fig. 1 were varied slowly enough so that the system remained in the neighbourhood of an attractor and leaving enough time for an accurate estimation of the ordinate ("slow time" method). We have described this procedure in detail in reference [5] for the special case of T/T_e versus A.

For each abscissa value of Fig. 1 one or two ordinate values are given. The latter case corresponds to two coexisting attractors ("birhythmicity"). For other control conditions, we have obtained loops of higher complexity involving three or four coexisting attractors ("tri"- and "tetrarhythmicity",[5,9,11]).

Fig. 1 illustrates how manifold the differences between coexisting attractors can be. Besides the differences in response period (given by Figs. 1b and 1e), there are differences in response amplitude (Figs. 1a and 1d) and differences in response stability (Figs. 1c and 1f). Fig. 1c (recorded under the same conditions as Figs. 1a and 1b) shows two coexisting periodic responses, one with very low stability (period $3T_e$) and one with very high stability (period $10T_e$). In fact, while λ_{max} for $3T_e$ is close to 0, λ_{max} for $10T_e$ shows a deep minimum. We

have called systems displaying such a minimum "hyperstable" [4]. The functional relevance of such systems relies in their extreme insensitivity to perturbations. Figs. 1c and 1f show chaotic regions ($\lambda_{max} > 0$).

We now pose the question: Which is the "watershed" in phase space separating the basins of attraction between two coexisting attractors ? The answer would tell us which starting points in phase space lead to which attractors, and how we have to perturbate the system in order to drive it from one attractor to the other (and thus from one time pattern to the other) and conversely. The method to obtain the "watershed" in phase space (see [16,20]) is illustrated for the glycolytic case in Fig. 2. In this figure, we show two phase variables ([ADP] and

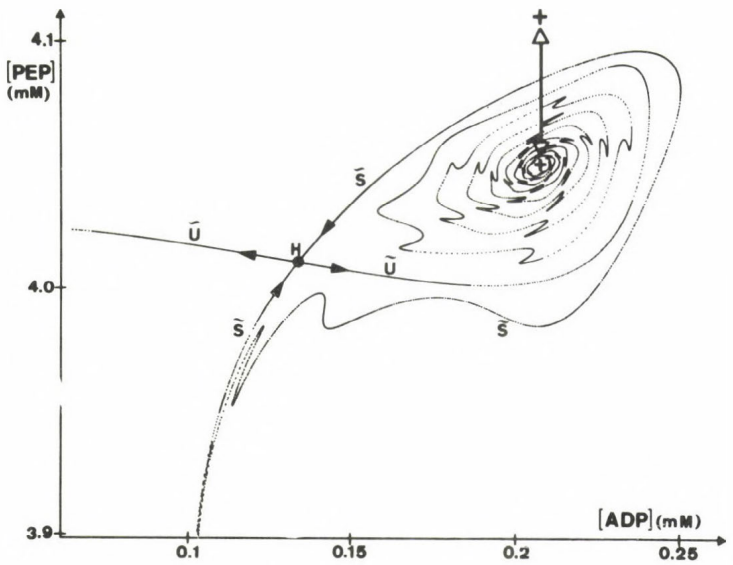

Fig. 2. Watershed ($\widetilde{S}$) between different periodicities (periods $3T_e$ and $10T_e$, T_e: input period), as obtained from the glycolytic model in a stroboscopic representation. H is a saddle point, $\widetilde{U}$ and $\widetilde{S}$ its unstable and stable manifolds, respectively. The double-arrow in the upper right side indicates switching from $3T_e$ (inside $\widetilde{S}$) to $10T_e$ (outside $\widetilde{S}$), and vice-versa. The conditions are the same as those at the arrows pointing to the abscissas of Figs. 1a, b, c, d and e

[PEP]) in a stroboscopic representation, in which the phase variables are plotted at times nT_e , n=1,2,3,.... A periodic solution with period mT_e leads to m points in this representation. The cross at the lower end of the double-arrow in Fig. 2 is one of the stroboscopic points corresponding to period $3T_e$. The upper cross is one of the stroboscopic points corresponding to $10T_e$. The other stroboscopic points are out of the scope of the figure. Point H is an unstable fixed point (saddle type, period $3T_e$), which was obtained using an extension of Newton's method (subroutine NS01AD from [21]).

The boundary between the basins of attraction of $3T_e$ and $10T_e$ is given by the stable manifold $\tilde{S}$ of H [16,20]. Thus, any initial condition lying inside the area delimited by $\tilde{S}$ leads to $3T_e$ and any initial condition lying outside this area leads to $10T_e$. The double-arrow indicates a direct switching process from $3T_e$ to $10T_e$ by addition of PEP (arrow pointing upwards) and from $10T_e$ to $3T_e$ by consumption of PEP (arrow pointing downwards). At an appropriate phase, the reverse is possible, namely direct switching from $3T_e$ to $10T_e$ by consumption of PEP and from $10T_e$ to $3T_e$ by addition of PEP. At an arbitrary phase, any transition from one basin to the other is of course possible, but transients have to be taken into account before the system settles on the final attractor (see [9]).

$\tilde{S}$ in Fig. 2 was obtained by integrating the differential equations backwards in time starting from H . The unstable manifold $\tilde{U}$ (obtained by integrating forwards starting from H) displays a long-winded transient spiral leading to period $3T_e$.

CRISES

Recently, new types of bifurcations, namely so-called crises, have been described [16,17]. In case of a "boundary-crisis", the disappearance of a chaotic attractor by colliding with its basin boundary is observed. In our model, such a collision takes place at the arrow pointing to the abscissa in Fig. 1f, causing the sudden disappearance of a chaotic time pattern in favour of a periodic time pattern (period $5T_e$). The collision is illustrated in Figs. 3 and 4. Fig. 3 shows in a stroboscopic representation

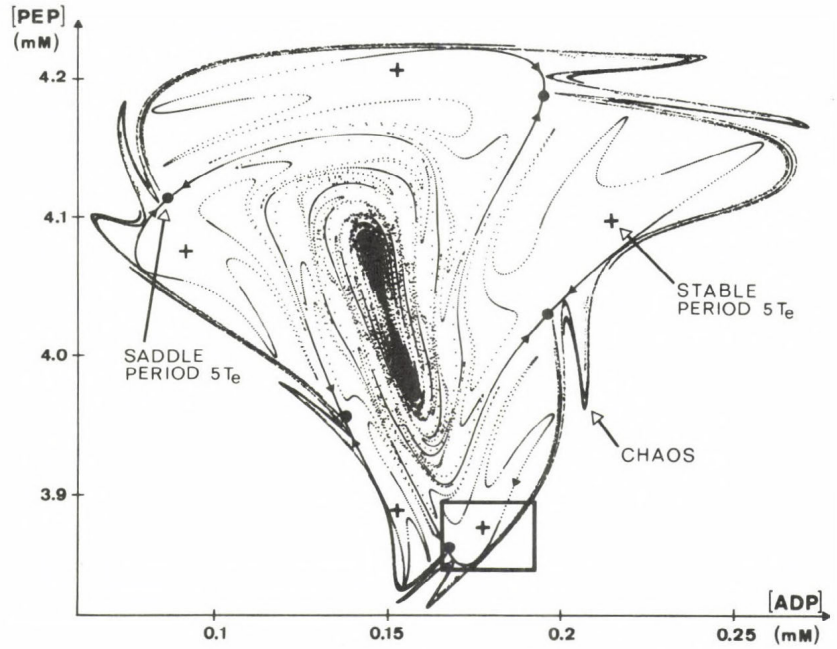

Fig. 3. Stroboscopic plot illustrating a crisis. The chaotic attractor can collapse as it touches its basin boundary. This boundary is given by the stable manifold of the saddle of period $5T_e$ (T_e: input period). The conditions correspond to the arrow pointing to the abscissa of Fig. 1f. The rectangle down below in the right indicates the region that is shown enlarged in Fig. 4

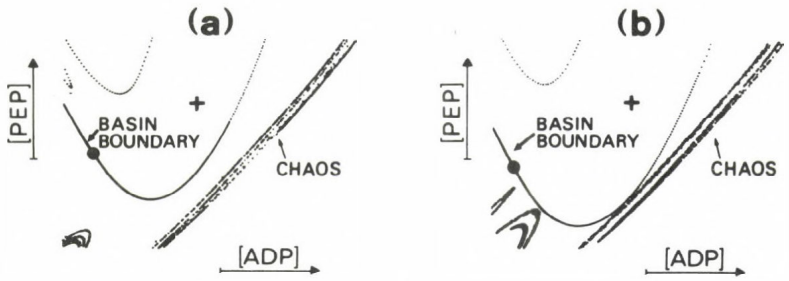

Fig. 4. Enlarged section of the plane from Fig. 3. (a): Non-vanishing chaos at A=0.423 mM/min (the chaotic attractor does not touch its basin boundary) (b): Crisis at A=0.424 mM/min (the chaotic attractor collides with its basin boundary)

a chaotic attractor under the conditions where it collides with the stable manifold of a saddle with period $5T_e$, which is the boundary that separates its basin from that of a stable orbit with period $5T_e$. In the centre of the picture, we see stable manifold winds in an eight-shaped manner around an unstable orbit with period $2T_e$.

Fig. 4b shows an enlarged section of Fig. 3. Fig. 4a shows the same section but at a slightly smaller value of A. Under the conditions of Fig. 4a (A=0.423 mM/min) the two attractors can coexist, but a small increase of A causes the crisis (A= 0.424 mM/min).

We would now like to point to the phenomenon of "long-lived chaotic transients", which has been gaining some attention for the last two years in the analysis of simple theoretical mappings [16,17]. We explain this phenomenon with the help of the plots in Figs. 3 and 4b. A start on the chaotic points in these plots may imply that the system stays on it for hundreds of T_e. Only when a point in contact with the boundary is reached in the course of the oscillations, a transition to a periodic oscillation can actually take place. This is illustrated in Fig. 5, where we show the chaotic time pattern (period $5T_e$) after about 4.5 hours. For somewhat larger values of A than in

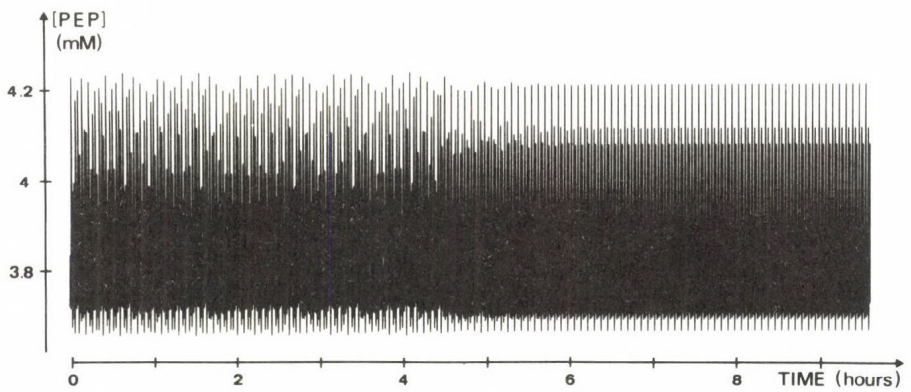

Fig. 5. Autonomous transition from chaos to order due to a crisis. The conditions are those of Figs. 3 and 4b.

Fig. 5, the transients have a shorter life. Conversely, if A is decreased, the chaotic transients become longer and longer until they reach infinity, and then a new chaotic attractor is born. In other words, the reverse effect of a crisis is a route to chaos. In the presence of noise, long-lived transients tend to become shorter, since noise facilitates the crossing over the basin boundary.

DISCUSSION

We have investigated here some new forms of possible metabolic control. The quantitative knowledge of the enzymic rate laws has allowed us to determine actual metabolite concentrations, such as [ADP] and [PEP], as functions of time, and to analyze the system's response as a function of control parameters such as the magnesium concentration.

It is important to note that the phenomena investigated here pose restrictions on the applicability of control coefficients [22], even if these may be generalized from steady states to oscillatory systems by considering response quantities such as λ_{max} or $[PEP]_{max}$ as functions of independent variables. In fact, control coefficients are well defined derivatives, the determination of which relies on the assumption that the behaviour of the system is unique and continuous. These conditions are not always fulfilled in the cases treated here, where multivaluedness arises as a cause of the system's dependence on its previous history, and discontinuities, such as crises, occur. General considerations show that in principle any number of coexisting attractors is possible in an enzymic system [23], while the actually measured enzymic rate laws in our concrete case reveal up to four such coexisting attractors [5]. Although this multivaluedness may seem disadvantageous at first sight it could, however, provide a memory capacity to the system. Furthermore, noise may become amplified since fluctuations cause jumps between the basins of attraction without ever allowing the system to settle on a well defined attractor [9]. Multivaluedness, just as deterministic chaos, may thus provide a random generator to the system. When the biological meaning of a random generator is considered

in the literature, one occasionally speaks about aperiodic oscillations as "dynamic diseases" (e.g. in neural disturbances; for a review see [24]). But, on the other hand, it has been shown that searching processes in all sorts of complex systems may be greatly improved by introducing randomness [25]. In biology, a search may be useful in chemotaxis and evolution, as well as in complex neural phenomena, such as searching memory and decision making. In predator-prey systems, randomness decreases the predictability of behaviour, and may thus serve as a disguising mechanism for prey behaviour [26]. Furthermore, cell cycle variability in cell populations can be simulated by a chaotic model [27].

We have shown here the existence of crises in a glycolytic model, as one of the sources of dynamic discontinuities. A remarkable feature in the neighbourhood of a crisis is the appearance of long-lived transients. The knowledge of such transients should be a warning to experimentalists: not everything that looks like a stable time pattern may stay forever, even if all conditions remain unchanged. Long-lived transients are part of the dynamic diversity of such a system, and they should be expected in biological experimentation, being possible phases in "time pattern morphogenesis".

The glycolytic system is indeed extraordinarily rich and one should consider this richness as being a reflexion of the functional properties of a system composed of two allosteric enzymes, widespread in living nature. Our considerations should be understood in terms of the most delicate regulatory properties of such systems. It should be kept in mind that similar processes may occur in any system including allosteric proteins or membrane transport.

ACKNOWLEDGEMENTS

We thank Miss Heike Kessel for programming assistance and Mrs. Marion Wilson for efficient typing of the manuscript. One of us (M.M.) participated in the meeting in Debrecen and would like to thank the organizers for excellent organization and hospitality.

REFERENCES

[1] Hess, B. and Boiteux, A., Oscillatory Phenomena in Biochemistry, Annual Rev. Biochem. 40, 237-258 (1971)

[2] Biological and Biochemical Oscillations, ed. by Chance, B., Pye, E.K., Ghosh, A.K. and Hess, B. (Academic Press, N.Y., London, 1973)

[3] Olsen, L.F. and Degn, H., Chaos in an Enzyme Reaction, Nature 267, 177-178 (1977)

[4] Hess, B. and Markus, M., Time Pattern Transitions in Biochemical Processes, in: Synergetics - from Microscopic to Macroscopic Order, ed. by Frehland, F. (Springer-Verlag, Berlin, 1984) pp. 6-16

[5] Markus, M. and Hess, B., Transitions Between Oscillatory Modes in a Glycolytic Model System, Proc. Natl. Acad. Sci. USA 81, 4394-4398 (1984)

[6] Markus, M., Kuschmitz, D. and Hess, B., Chaotic Dynamics in Yeast Glycolysis Under Periodic Substrate Input Flux, FEBS Lett. 172, 235-238 (1984)

[7] Markus, M., Müller, S.C. and Hess, B., Observation of Entrainment, Quasiperiodicity and Chaos in Glycolyzing Yeast Extract Under Periodic Glucose Input, Ber. Bunsenges. Phys. Chem. 89, 651-654 (1985)

[8] Markus, M., Kuschmitz, D. and Hess, B., Properties of Strange Attractors in Yeast Glycolysis, Biophysical Chemistry, 22, 95-105 (1985)

[9] Hess, B. and Markus, M., The Diversity of Biochemical Time Patterns, Ber. Bunsenges. Phys. Chem. 89, 642-651 (1985)

[10] Hess, B., Boiteux, A. and Kuschmitz, D., Regulation of Glycolysis, in: Biological Oxidations, ed. by Sund, H. and Ullrich, V. (Springer-Verlag, Berlin, 1983) pp. 249-266

[11] Hess, B., Kuschmitz, D. and Markus, M., Dynamic Coupling and Time Patterns in Glycolysis, in: Dynamics of Biochemical Systems, ed. by Ricard, J. and Cornish-Bowden, A. (Plenum Press, N.Y., 1984) pp. 213-226

[12] Gerisch, G. and Hess, B., Cyclic-AMP-Controlled Oscillations in Suspended Dictyostelium Cells: Their Relation to Morphogenetic Cell Interactions, Proc. Natl. Acad. Sci.

USA 71, 2118-2122 (1974)

[13] Okamoto, M. and Hayashi, K., Frequency Conversion Mechanism in Enzymatic Feedback Systems, J. Theor. Biol. 108, 529-537 (1984)

[14] Feigenbaum, M., Quantitative Universality for a Class of Nonlinear Transformations, J. Stat. Phys. 19, 25-52 (1978)

[15] Feigenbaum, M., The Universal Metric Properties of Nonlinear Transformations, J. Stat. Phys. 21, 669-706 (1979)

[16] Grebogi, C., Ott, E. and Yorke, J.A., Crises, Sudden Changes in Chaotic Attractors, and Tansient Chaos, Physica 7D, 181-200 (1983)

[17] Grebogi, C., Ott, E. and Yorke, J.A., Fractial Basin Boundaries, Long-Lived Chaotic Transients, and Unstable-Unstable Pair Bifurcation, Phys. Rev. Lett. 50, 935-938 (1983)

[18] Shimada, I. and Nagashima, T., A Numerical Approach to Ergodic Problem of Dissipative Dynamical Systems, Progr. Theor. Phys. 61, 1605-1616 (1979)

[19] Markus, M., Plesser, Th., Boiteux, A., Hess, B. and Malcovati, M., Analysis of Progress Curves: Rate Law of Pyruvate Kinase Type I from Escherichia coli, Biochem. J. 189, 421-433 (1980)

[20] Hayashi, C., Nonlinear Oscillations in Physical Systems, (McGraw Hill, N.Y., 1964)

[21] Harwell Subroutine Library, A Catalogue of Subroutines, compiled by Hopper, M.J. (Computer Science and Systems Division, A.E.R.E., Harwell, Oxfordshire, England, 1978)p.33

[22] Burns, J.A., Cornish-Bowden, A., Groen, A.K., Heinrich, R., Kacser, H., Porteus, J.W., Rapoport, S.M., Rapoport, T.A., Stucki, J.W., Tager, J.M., Wanders, R.J.A., Westerhoff, H.V., Control Analysis and Metabolic Systems, Trends in Biochem. Sci., Jan. (1985), p. 16

[23] Erle, D., Nonuniqueness of Stable Limit Cycles in a Class of Enzyme Catalyzed Reactions, J. Math. Analysis and Appl. 82, 386-391 (1981)

[24] Rapp, P.E., Zimmermann, I.D., Albano, A.M., deGuzman, G.C., Greenbaum, N.N. and Bashore, T.R., Experimental Studies of Chaotic Neural Behaviour: Cellular Activity and Electroencephalographic Signals, in: Nonlinear Oscillations in Che-

mistry and Biology, ed. by Othmer, H.G. (Springer-Verlag, N.Y.), in press

[25] Kolata, G., Order Out of Chaos in Computers, Science 223, 917-919 (1984)

[26] Schulmeister, Th., Some Comments on Chaos in Models of Biochemical Reactions, Studia Biophysica 105, 5-10 (1985)

[27] Mackey, M.C., A Deterministic Cell Cycle Model with Transition Probability-Like Behaviour, in: Temporal Order, ed. by Rensing, L. and Jaeger, N.I. (Springer-Verlag, Berlin, 1985) pp. 315-320

DISCUSSION

DYNNIK:

If I am not mistaken, quasiperiodic or even stochastic oscillations were obtained experimentally about 15 years ago by Hess and Boiteux in yeast extracts at a fixed velocity of substrate injection. Is it possible to realize such regimes in your model, say by including an additional regulation of PFK by fructose 1,6-bisphosphate?

MARKUS:

The aperiodic measurements of A. Boiteux and B. Hess at constant input flux were too short in time to be identified as chaos or quasiperiodicity. They could have been transient oscillations. However, it is possible that chaos or quasiperiodicity may occur under such conditions, as has been predicted in a qualitative model (O. Decroly and A. Goldbeter, Proc. Natl. Acad. Sci. USA, 79, 6817-6921, 1982). We are at present working on a quantitative extension of our model, based on experimentally determined kinetic parameters, in order to investigate such effects.

DAMJANOVICH:

Of course, the quasiperiodic and chaotic states of the system are not to be considered as steady states. However, if you take the mean of the periods or a weighted average of the chaos you may make use of the catastrophe theory for the description of the sudden changes. On the other hand, the individual components of the quasiperiodic or periodic states can also be described as Markovian chains, since the component n determines the whereabouts of component n+1. Of course, this is the opposite for the chaos. Could you please comment on these remarks?

MARKUS:

Sudden changes, such as crises, may certainly be considered as "catastrophes" in a general sense. However, the mathematical theory as formulated by René Thom is too special to be applicable here: it describes these phenomena as combinations of seven elementary catastrophes, relying on the assumption that a potential can be defined and that the system comes to a rest at a potential minimum. I do not know of any mathematical generalization of this special approach that makes it possible to include multiple oscillatory states as described here. As to Markovian chains, it has been shown in calculations of the Kolmogorov-Sinai-entropy that in some special cases (not in general) chaotic processes can be described by Markovian chains. For details on this topic you may consult the paper by G. Györgyi and P. Szépfalusy (from Eötvös University) in Phys. Rev. A, 31, 3477-3479 (1985).

Dynamics of Biochemical Systems
S. Damjanovich, T. Keleti, L. Trón (Eds)

MITOCHONDRIAL TRANSPORT OF DIVALENT CATIONS: PATHWAYS, MECHANISMS, REGULATION

LARS ERNSTER, VICTOR KONJI*, ANNIKA MONTAG†, KERSTIN NORDENBRAND and GABRIELLA SANDRI**

Department of Biochemistry, Arrhenius Laboratory, University of Stockholm, S-106 91 Stockholm, Sweden

†Department of Experimental Medicine, Pharmacia AB, S-751 05 Uppsala, Sweden

INTRODUCTION

It is now generally recognized that there exist multiple pathways for the transport of divalent cations across the mitochondrial inner membrane (1). The longest-known of these is an electrogenic uniporter, present in most animal tissues, that can accumulate Ca^{2+} and other divalent cations (Mn^{2+}, Ba^{2+} and Sr^{2+} but not Mg^{2+}) at the expense of an electrochemical proton gradient generated by electron transport or ATP hydrolysis (2-5). It is inhibited by ruthenium red (6), and probably involves the Ca^{2+}-binding protein known as calvectin (1, 7). This pathway is reversible, in the sense that in the absence of an electrochemical proton gradient it can serve as a pathway for the release of accumulated Ca^{2+} from the mitochondria.

There are at present two pathways known which seem to be involved specifically in the release of Ca^{2+} from mitochondria. A Na^{+}-dependent pathway (8, 9), which occurs in excitable tissues such as heart (8), brain (9) and brown fat (10), consists of an electroneutral exchange of intramitochondrial Ca^{2+} against extramitochondrial Na^{+}. A second release pathway (11, 12), occurring in heart and liver, as well as in certain tumors, is activated by the oxidation of intramitochondrial nicotinamide nucleotides and involves an exchange of intramitochondrial Ca^{2+} against extramitochondrial H^{+}. These two pathways are insensitive to ruthenium red (8, 11) and their specificity for divalent cations has not yet been investigated in detail.

This paper summarizes some recent results from our laboratory relating to the above pathways of divalent-cation transport by mitochondria. Our studies of the electrogenic uniporter and the Na^{+}-dependent efflux systems have primarily concerned the cation specificity of these proces-

Abbreviation: CCCP, carbonyl-cyanide m-chlorophenylhydrazone

*Fellow of International Seminar of Chemistry, University of Uppsala. Permanent address: Department of Biochemistry, University of Nairobi, Nairobi, Kenya

**Permanent address: Dipartimento di Biochimica, Biofisica e Chimica delle Macromolecole, Università di Trieste, Trieste, Italy

ses, especially regarding the cooperativity of Ca^{2+} and Mn^{2+} uptake and its modulation by extramitochondrial Mg^{2+}. The nicotinamide nucleotide-induced release of Ca^{2+} was investigated mainly from the point of view of nicotinamide nucleotide specificity and the possible regulatory roles of adenine nucleotides in this process.

ENERGY-LINKED UPTAKE AND Na^{+}-DEPENDENT RELEASE OF Ca^{2+} AND Mn^{2+} BY MITOCHONDRIA FROM RAT LIVER, HEART AND BRAIN

Our interest in the effects of Ca^{2+} and Mn^{2+} on mitochondria originates from observations reported over 30 years ago. In 1953 Slater and Cleland (13) demonstrated that Ca^{2+} causes a swelling of mitochondria and an uncoupling of oxidative phosphorylation. The following year Lindberg and Ernster (14) reported that Mn^{2+} prevents the uncoupling effect of Ca^{2+} and can even reverse it in the presence of ATP. Mn^{2+} and ATP were also shown to induce a contraction of swollen mitochondria (15). Mg^{2+} had an effect similar to that of Mn^{2+} although at higher concentrations (16).

Following the demonstration in the early 1960s that mitochondria can accumulate Ca^{2+} (17, 18) and Mn^{2+} (19) in an energy-dependent manner, we investigated the uptake of the two cations when added simultaneously to rat liver mitochondria. We found that Ca^{2+} accelerates the uptake of Mn^{2+} and Mn^{2+} retards the uptake of Ca^{2+} (20, 21). Similar findings were independently reported by Chance and Mela (22, 23). We further found that extramitochondrial Mg^{2+}, which was not taken up by the mitochondria, was capable of maintaining the enhancement of Mn^{2+} uptake by Ca^{2+} even after terminated Ca^{2+} uptake (24).

The cooperative uptake of Ca^{2+} and Mn^{2+} and its modulation by Mg^{2+} were subseqeuntly investigated in some detail by several laboratories (25-28), with essentially similar results. Our studies were performed with rat liver mitochondria respiring in the presence of succinate and glutamate as substrates and in the absence and presence of P_i i.e., under limited and massive loading conditions. The following parameters were investigated: uptake of the radioactive cations ($^{45}Ca^{2+}$ or $^{54}Mn^{2+}$) using a rapid filtration technique; H^{+} ejection accompanying cations uptake, using a glass electrode; stimulation of state 4 respiration, using an O_2 electrode; intramitochondrial nicotinamide nucleotide oxidoreduction, monitored fluorometrically. Illustrative data are shown in Figs. 1 and 2. Fig. 1 shows the time course of the respiration-dependent uptake of Ca^{2+} and Mn^{2+} in the absence and presence of P_i using radioisotopes. Ca^{2+} uptake is more rapid in the presence than in the absence of P_i, and its rate in both cases is diminished by Mn^{2+}. Conversely, Mn^{2+} uptake is relatively slow in both cases and its rate is markedly enhanced by Ca^{2+}, especially in the presence of P_i. The stimulation of Mn^{2+} uptake by Ca^{2+} in the presence of P_i is further illustrated by measurements of O_2 uptake, nicotinamide nucleotide oxidoreduction and H^{+} ejection, shown in Fig. 2.

Using the above parameters and a variety of experimental conditions, the following results were obtained (24):

1. The cooperative uptake of Ca^{2+} and Mn^{2+} required the simultaneous presence of the two cations; when Mn^{2+} was added after terminated Ca^{2+} uptake, its rate of uptake was no longer enhanced. However, the two

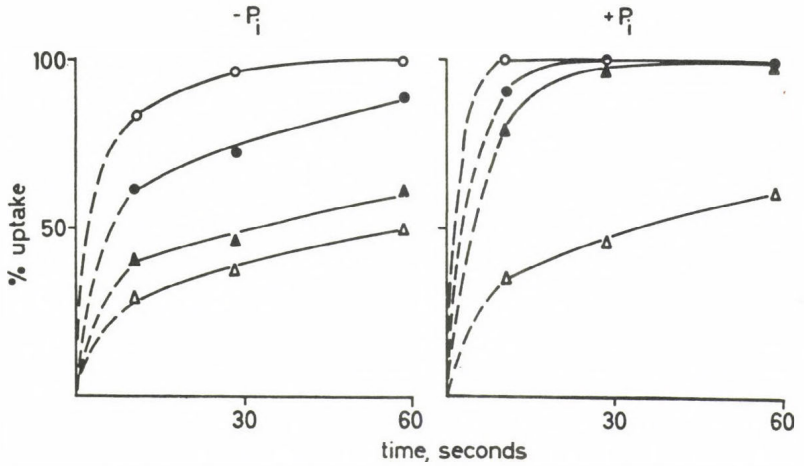

Fig. 1. Uptake of Ca^{2+} and Mn^{2+} by rat liver mitochondria in the absence and presence of P_i. From ref. 24. Rat liver mitochondria (1.9 mg protein/ml) were incubated in a medium containing 20 mM Tris-Cl, pH 7.2, 100 mM KCl, 5 mM succinate, 5 mM glutamate. 3.3 mM P_i and 133 µM Ca^{2+} and/or 133 µM Mn^{2+} were added when indicated. At the time intervals indicated an aliquot was rapidly filtered and the radioactivity determined. o-o $^{45}Ca^{2+}$; ●-● $^{45}Ca^{2+}$ + Mn^{2+}; △-△ $^{54}Mn^{2+}$; ▲-▲ $^{54}Mn^{2+}$ + Ca^{2+}.

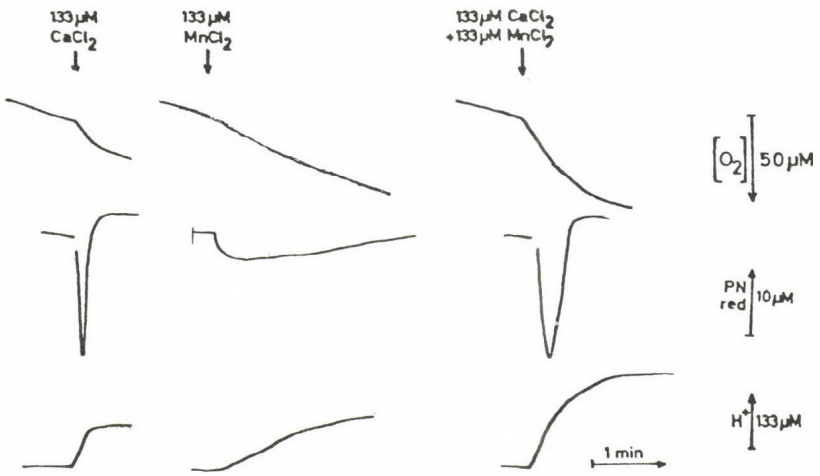

Fig. 2. Respiratory stimulation, nicotinamide nucleotide (PN) redox cycle, and H^+ ejection accompanying the uptake of Ca^{2+} and/or Mn^{2+} by rat liver mitochondria in the presence of P_i. From ref. 24. The incubation mixture contained 20 mM Tris-Cl, pH 7.2, 100 mM KCl, 2.5 mM succinate, 2.5 mM glutamate, 1.7 mM P_i and 1.4 mg prot/ml.

cations were not taken up at the same rate, and, once initiated, Mn^{2+} uptake was maintained at an accelerated rate even after virtually all Ca^{2+} had been incorporated.

2. The cooperativity between the Ca^{2+} and Mn^{2+} uptakes was independent of the presence of P_i, indicating that the same carrier was involved in the massive and limited uptake processes.

3. The cooperativity and kinetics of Ca^{2+} and Mn^{2+} uptake were not noticeably influenced by univalent cations (K^+, Na^+, NH_4^+).

4. Mn^{2+} inhibited and Ca^{2+} stimulated the uptake of Sr^{2+} and Ba^{2+}.

5. Mg^{2+} was not taken up by the mitochondria, but its presence in the incubation medium resulted in a maintenance of the accelerating effect of Ca^{2+} on Mn^{2+} uptake even when Mn^{2+} was added after completed Ca^{2+} uptake; this effect also occurred both in the presence and absence of P_i.

6. Ca^{2+} and Mn^{2+} mutually eliminated the oscillatory kinetics of uptake found with either cation when present alone. Again, Mg^{2+} had an effect similar to that of Mn^{2+}. The relative concentrations of the three cations exhibiting these effects were similar to those needed for the prevention of Ca^{2+}-induced mitochondrial swelling and uncoupling of oxidative phosphorylation by means of Mn^{2+} and Mg^{2+}.

These data were interpreted to indicate that the energy-linked electrogenic divalent-cation carrier of liver mitochondria is controlled with regard to its cation specificity by a regulatory site that is situated on the outer surface of the inner membrane. Mg^{2+} (and possibly Mn^{2+}) in the intermembrane space act as effectors of the carrier. In their absence, the carrier is highly active with Ca^{2+} and has a relatively low activity with Mn^{2+}. In the presence of Mg^{2+} (or Mn^{2+}) at the regulatory site, the activity of the carrier with Ca^{2+} decreases, and that with Mn^{2+} increases; Sr^{2+} and Ba^{2+} behave similarly to Mn^{2+}. Binding of Mg^{2+} (or Mn^{2+}) to the regulatory site occurs only in the presence of Ca^{2+}, which thus acts as a "feedback" regulator of the carrier. Although the relationship of this mechanism to the regulation of the structural and functional state of liver mitochondria remains unclear, it was pointed out that the striking antagonistic effects of Ca^{2+} on one hand, and of Mn^{2+} and Mg^{2+} on the other, on mitochondrial energy coupling and membrane structure may be reflections of this mechanism.

More recently these studies were extended to include mitochondria from rat heart and brain. The results, a detailed account which is being published elsewhere (29), were essentially similar to those earlier obtained with liver mitochondria regarding both the cooperativity between Ca^{2+} and Mn^{2+} uptake and its modulation by Mg^{2+}. The enhancement of Mn^{2+} uptake by Ca^{2+} is most pronounced in liver, and the inhibition of Ca^{2+} uptake by Mn^{2+} or Mg^{2+} is strongest in heart. Brain mitochondria take up Mn^{2+} relatively rapidly even in the absence of Ca^{2+}.

In these recent studies we have also investigated the efflux of Ca^{2+} and Mn^{2+} from rat liver, heart and brain mitochondria as induced either by the uncoupler CCCP or by Na^+ according to the mechanism first

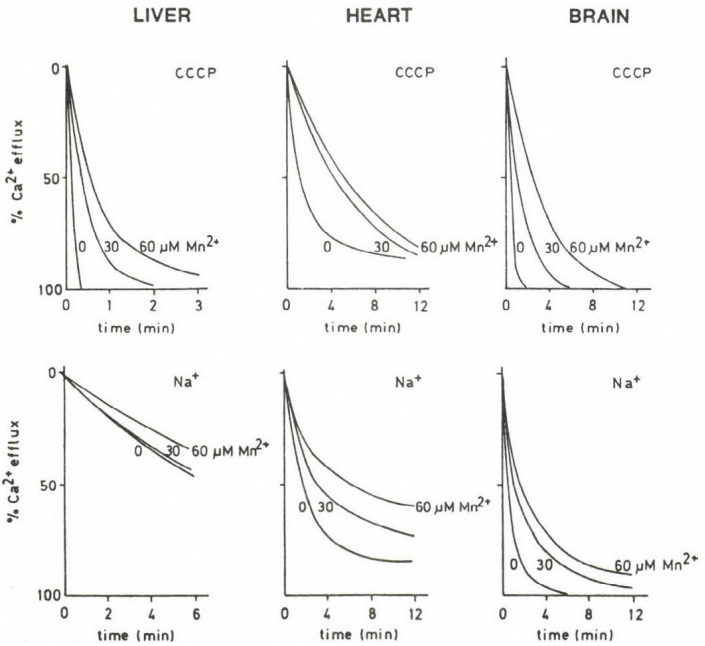

Fig. 3. Effect of CCCP and Na^+ on the efflux of Ca^{2+} from mitochondria from rat liver, heart and brain. From ref. 29. The incubation mixture contained 20 mM Tris-Cl, pH 7.5, 100 mM KCl, 5 mM glutamate, 5 mM malate, 3 mM P_i, 100 μM Arsenazo III, 0.5 mg mitochondrial protein/ml, 30 μM Ca^{2+} and Mn^{2+} as indicated. After Ca^{2+} was taken up, 1 μM ruthenium red was added followed by either 3 μM CCCP or 10 mM Na^+.

described by Crompton et al. (8, 9) for mitochondria from excitable tissues.

Ca^{2+} efflux was monitored spectrophotometrically using the non-penetrant metallochromic dye Arsenazo III after loading the mitochondria with Ca^{2+} in the presence of substrate and P_i and the addition of ruthenium red to inhibit the reuptake of Ca^{2+}. As shown in Fig. 3, CCCP caused a release of Ca^{2+} from all three sources of mitochondria and the rate of the release was diminished by Mn^{2+}. Na^+ induced as expected a release of Ca^{2+} from heart and brain but not from liver mitochondria and the rate of the Na^+-induced Ca^{2+} release was likewise diminished by Mn^{2+}.

Mn^{2+} efflux was measured by determining the $^{54}Mn^{2+}$ released from the mitochondria using a rapid filtration technique. Mn^{2+} loading was carried out in the presence of substrate but in the absence of P_i since it was found that P_i prevents Mn^{2+} release by either CCCP or Na^+, probably because of the precipitation of insoluble manganese phosphate. Ruthenium red was again added to prevent reuptake. As shown in Fig. 4, Mn^{2+} efflux was induced by CCCP in all three sources of mitochondria and its rate was accelerated by Ca^{2+}. Na^+ enhanced Mn^{2+} efflux in the case of brain and heart but not in the case of liver mitochondria. The Na^+-indu-

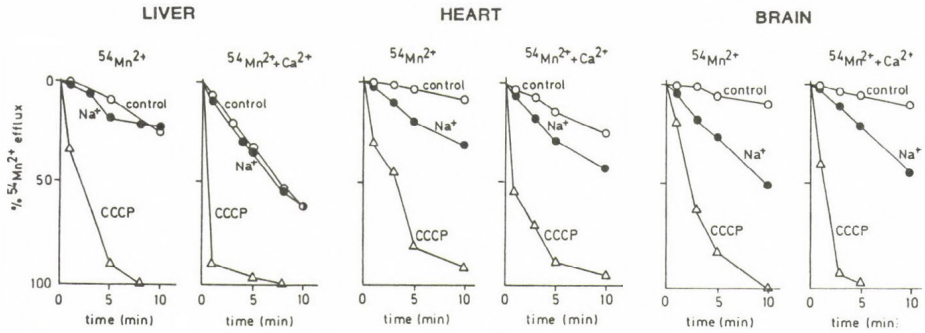

Fig. 4. Effect of CCCP and Na^+ on the efflux of Mn^{2+} from mitochondria from rat liver, heart and brain. From ref. 29. The incubation mixture contained 20 mM Tris-Cl, pH 7.5, 100 mM KCl, 5 mM glutamate, 5 mM malate 0.5 mg mitochondrial protein/ml and 30 μM $^{54}Mn^{2+}$ + 30 μM unlabelled Ca^{2+}. After Mn^{2+} was taken up, 1 μM ruthenium red was added followed by either 3 μM CCCP or 10 mM Na^+. At the time intervals indicated an aliquot was rapidly filtered and the radioactivity determined.

ced release in contrast to that induced by CCCP was not significantly affected by Ca^{2+}.

From these results it appears that the uncoupler-induced release of Ca^{2+} and Mn^{2+} display a cooperativity similar to the energy-linked uptake, consistent with the notion that it proceeds by way of the electrogenic uniporter operating in the reverse direction. That this efflux is insensitive to ruthenium red can be explained as proposed by Bernardi et al. (30) on kinetic grounds, by assuming that it is the uncoupler-induced H^+-uptake rather than the cation release itself which is rate-limiting. The Na^+-Ca^{2+} exchange carrier present in heart and brain mitochondria can evidently also catalyze Na^+-Mn^{2+} exchange. However there is no evidence for a cooperativity between Ca^{2+} and Mn^{2+} transport through this carrier similar to that found with the electrogenic uniporter.

Ca^{2+} EFFLUX FROM MITOCHONDRIA AS INDUCED BY OXIDATION OF INTRAMITOCHONDRIAL NICOTINAMIDE NUCLEOTIDES

Much interest has recently been directed to the oxidation-reduction state of intramitochondrial nicotinamide nucleotides as a potential regulator of Ca^{2+} release. It has been shown that a net Ca^+ release from liver and heart mitochondria can be induced by shifting the redox state of mitochondrial nicotinamide nucleotides to the oxidized state using either oxaloacetate or acetoacetate (11), t-butylhydroperoxide (t-BuOOH) (31), or menadione (32). Acetoacetate and oxaloacetate oxidize NADH selectively, through β-hydroxybutyrate dehydrogenase and malate dehydrogenase respectively. Menadione and t-BuOOH cause an oxidation of both NADH and NADPH, the former via DT diaphorase and the latter via glutathione peroxidase, glutathione reductase and the energy-linked nicotinamide nucleotide transhydrogenase. From these findings alone it would seem that

it is the oxidation of NADH rather than NADPH which is responsible for the Ca^{2+} release. Indeed Panfili et al. (33) arrived at this conclusion from experiments demonstrating a specific binding of NAD^+ to the Ca^{2+}-binding protein calvectin. Moreover Lötscher et al. (31, 34) found that the oxidized forms of both NAD^+ and $NADP^+$ are split by mitochondrial glycohydrolase and that ADP-ribose derived from NAD^+ binds to a protein which may thereby be activated to promote Ca^{+2} release. This glycohydrolase is inhibited by ATP (35) which has been shown to inhibit Ca^{2+} release (36). Other laboratories on the other hand have arrived at the conclusion that oxidation of NADPH may be primarily responsible for the Ca^{2+} release (37-41).

In an attempt to clarify the nicotinamide nucleotide specificity of the Ca^{2+} release we carried out a series of experiments in which we compared the effects of oxaloacetate, t-BuOOH, menadione and α-ketoglutarate + NH_4^+ on this process. Under the conditions employed α-ketoglutarate + NH_4^+ cause an oxidation of NADPH but not of NADH (42). This is shown in Fig. 5 which compares the redox states of NAD(H) and NADP(H) as a function of time after treatment with oxaloacetate, menadione, t-BuOOH and α-ketoglutarate + NH_4^+. It may be seen that, as expected, oxaloacetate induced a selective oxidation of NADH, menadione and t-BuOOH oxidized both NADH and NADPH, and α-ketoglutarate + NH_4^+ caused a selective oxidation of NADPH. It may also be seen that in all cases there was a disappearance of oxidized nicotinamide nucleotides, provided that Ca^{2+} was present in the incubation medium, and that this effect was inhibited by ATP.

In Fig. 6 it is shown that oxaloacetate, menadione and t-BuOOH induced a release of Ca^{2+} from the mitochondria, which was virtually complete after 5 minutes following the addition of these agents. This effect was correlated in time with the disappearance of NAD^+ and was completely abolished by 0.1 mM ATP (not shown). No release of Ca^{2+} occurred within 10 minutes after the addition of α-ketoglutarate and NH_4^+. These data strongly support the conclusion that the Ca^{2+} efflux occurring upon the oxidation of intramitochondrial nicotinamide nucleotides is: 1) dependent specifically on NADH oxidation; 2) requires a cleavage of NAD^+; 3) is inhibited by ATP which also inhibits NAD^+ cleavage; and 4) requires the presence of intramitochondrial Ca^{2+}, without which NAD^+ is not cleaved. These conclusions are in accordance with those reached by Richter and associates (31, 34-36, 43, 44).

Fig. 7 shows in a schematic form our tentative interpretation of the present findings. In accordance with earlier proposals by Lötscher et al. (31, 34), our data support the conclusion that Ca^{2+} efflux requires activation by ADP-ribose which is formed from NAD^+ through an ATP-sensitive NAD-glycohydrolase. Moser et al. (35), have indeed isolated such an enzyme from mitochondria and have also demonstrated the occurrence in mitochondria of a cleavage of NAD^+ into ADP-ribose and nicotinamide as well as the ADP-ribosylation of a protein (42). We further propose that intramitochondrial Ca^{2+}, which is not required for the activity of the NAD^+ glycohydrolase per se (35) may inhibit the resynthesis of NAD^+ from ADP-ribose and nicotinamide; the latter reaction has been demonstrated by Frei et al. (44) using radioactive nicotinamide. By this inhibition intramitochondrial Ca^{2+} may enhance the steady-state level of ADP-ribose and thereby the activation of the ADP-ribose dependent Ca^{2+}-release protein.

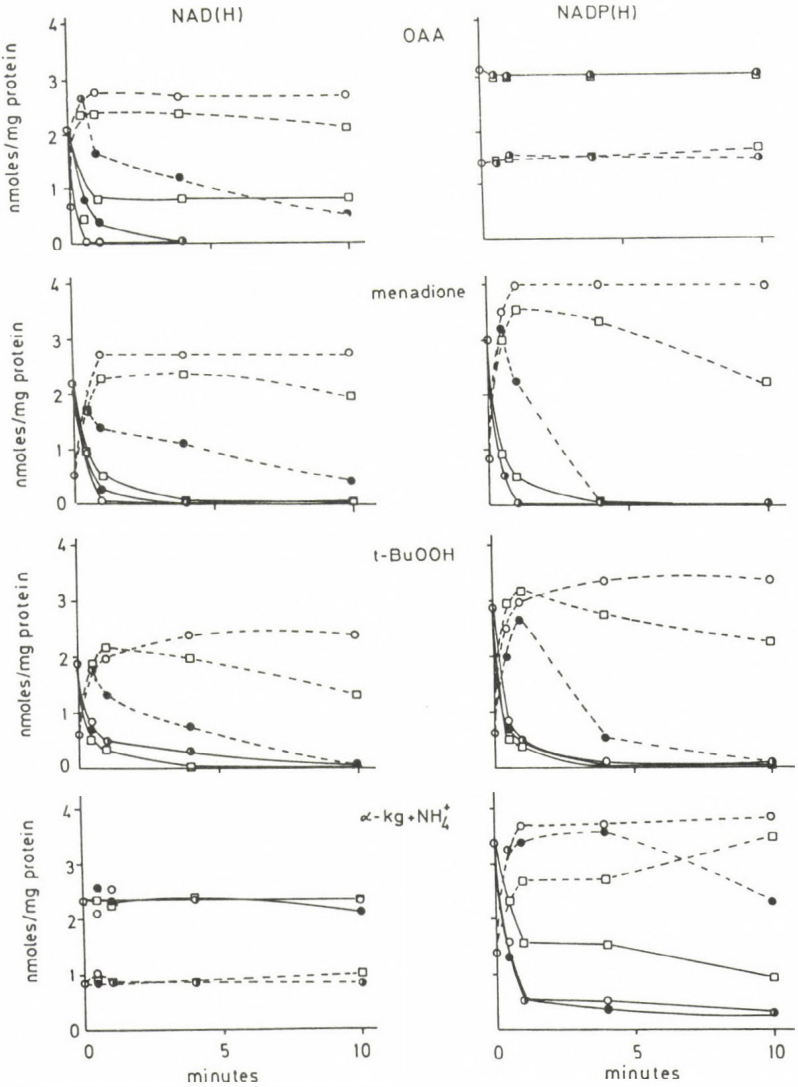

Fig. 5. Changes of reduced and oxidized nicotinamide nucleotides induced by oxaloacetate (OAA), menadione, t-BuOOH or α-ketoglutarate (α-kg) and NH_4^+. Mitochondria (2 mg protein/ml) were incubated in a medium containing 210 mM mannitol, 10 mM sucrose, 10 mM Tris-Cl, pH 7,4, 0.5 mg/ml bovine serum albumin, 15 mM succinate, 9 µM rotenone 30 µM Ca^{2+} and 0.1 mM ATP were present when indicated. After 2 minutes incubation, the oxidizing agents were added; 2 mM OAA, 0.3 mM menadione, 2 mM t-BuOOH or 2 mM α-kg and 2 mM NH_4^+. At times indicated the reaction was stopped by the addition of acid or alkali. $NAD(P)^+$ and NAD(P)H were determined enzymically in the acid and alkali extracts respectively (see ref. 45). o——o NAD(P)H; ●——● NAD(P)H + Ca^{2+}; □——□ NAD(P)H + Ca^{2+} + ATP; o---o $NAD(P)^+$; ●---● $NAD(P)^+$ + Ca^{2+}; □ ---□ $NAD(P)^+$ + Ca^{2+} + ATP. (From ref. 46)

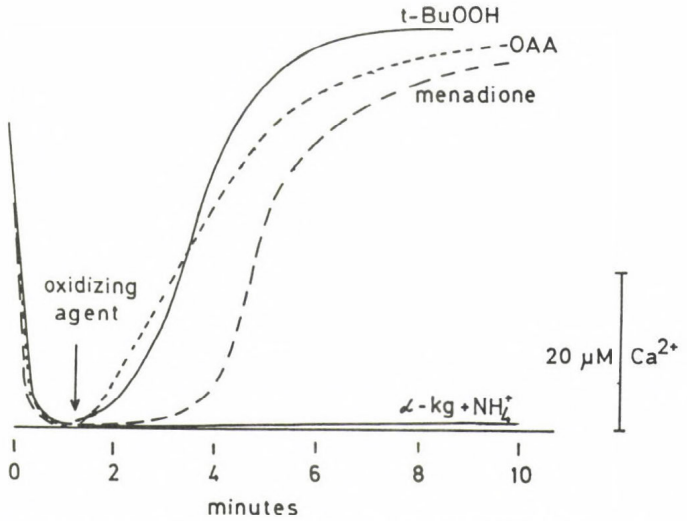

Fig. 6. Ca^{2+} release induced by oxaloacetate (OAA), menadione, t-BuOOH or α-ketoglutarate (α-kg) + NH_4^+. Mitochondria (2 mg protein/ml) were incubated in a medium containing 210 mM mannitol, 70 mM sucrose, 10 mM Tris-Cl, pH 7.4, BSA (0.5 mg/ml), 5 mM succinate, 3 µM rotenone, 100 µM Arsenazo III. At time zero, 50 µM Ca^{2+} was added. When indicated 2 mM OAA, 0.3 mM menadione, 2 mM t-BuOOH or 2 mM α-kg + 2 mM NH_4^+ was added. Ca^{2+} uptake and release were followed spectrophotometrically at 665-685 nm. (From ref. 46)

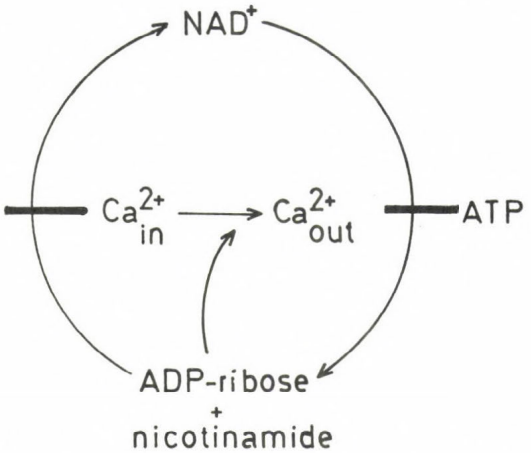

Fig. 7. Hypothetic scheme of the regulation of Ca^{2+} efflux by NAD^+ cleavage and ATP. In accordance with Richter and associates (31, 34-36, 43, 44) it is proposed that Ca^{2+} uptake through the electrogenic uniporter results in a lowering of the intramiatochondrial ATP concentration and thereby a relief of the inhibition of NAD^+-glycohydrolase. At the same time, intramitochondrial Ca^{2+} inhibits the resynthesis of NAD^+. As a result, the level of ADP-ribose increases and this activates Ca^{2+} release. For further explanation, see text.

The proposed mechanism explains a) how a decrease in mitochondrial ATP level, due to active Ca^{2+}-uptake, may promote NAD^+-cleavage; and b) why intramitochondrial Ca^{2+} is needed for this cleavage. The resulting increase in ADP-ribose activates Ca^{2+} efflux. Thus, the cycle as a whole regulates Ca^{2+} efflux in relation to Ca^{2+} uptake. A detailed account of these results and conclusions will be published elsewhere (46).

CONCLUDING REMARKS

The possible role of the three mitochondrial Ca^{2+}-transport systems in the regulation of cellular Ca^{2+} homeostasis is widely recognized (see e.g. refs. 1 and 47-49 for review). The electrogenic uniporter is generally regarded as an efficient mechanism for sequestering Ca^{2+}, especially in emergency situations where there is an increased influx of Ca^{2+} from the extracellular space due to a decreased cellular energy level, e.g. in ischemia (50). The protective effect of Mn^{2+} against mitochondrial injury caused by high Ca^{2+} concentrations may constitute an important defence mechanism (29, 51). In addition there is growing evidence that the mitochondrial transport of Mn^{2+} may have a function in regulating intra- and extramitochondrial Mn^{2+}-dependent enzymes (52).

The Na^+-dependent Ca^{2+}-efflux system in mitochondria of excitable tissues may play an important role in the regulation of cytosolic Ca^{2+} concentration, and thereby of Ca^{2+}-dependent enzymes in the cytosol, in relation to the prevailing action potential.

The Ca^{2+}-efflux mechanism induced by mitochondrial nicotinamide nucleotide oxidation and cleavage is another conceivable regulator of cytosolic Ca^{2+} concentration. The physiological role of this system is not yet fully understood. However, this mechanism has been implicated in cell injury caused by oxidative stress, such as exposure of cells to organic hydroperoxides or to agents that give rise to the formation of the superoxide radical and hydrogen peroxide, e.g. quinones (32, 53, 54). These treatments lead to an extensive oxidation of mitochondrial NAD(P)H via glutathione peroxidase, glutathione reductase and the energy-linked transhydrogenase. The ensuing increase in cytosolic Ca^{2+} concentration causes a collapse of the cytoskeleton, with a damage of the cell membrane as a consequence.

ACKNOWLEDGEMENT

This work has been supported by the Swedish Natural-Science Research Council and Pharmacia AB, Uppsala.

REFERENCES

1. Carafoli, E. and Sottocasa, G.L. (1984) In Bioenergetics, New Comprehensive Biochemistry (Ernster, L., ed.) vol. 9, Elsevier, Amsterdam, pp. 268-289.

2. Lehninger, A.L., Carafoli, E. and Rossi, C.S. (1967) Adv. Enzymol. 29, 259-320.

3. Carafoli, E. and Crompton, M. (1976) In Calcium in Biological Systems (Duncan, C.J., ed.), Cambridge Univ. Press, Cambridge, pp. 89-115.

4. Bygrave, F.L. (1977) Curr. Top. Bioenerg. 6, 259-318.

5. Saris, N.-E.L. and Åkerman, K. (1980) Curr. Top. Membranes Transp. 10, 151-216.

6. Moore, C.L. (1971) Biochem. Biophys. Res. Commun. 42, 298-305.

7. Sottocasa, G.L., Sandri, G., Panfili, E. and de Bernard, B. (1971) FEBS Lett. 17, 100-105.

8. Crompton, M., Capano, M. and Carafoli, E. (1976) Eur. J. Biochem. 69, 453-462.

9. Crompton, M., Moser, R., Lüdi, H. and Carafoli, E. (1978) Eur. J. Biochem. 82, 25-31.

10. Al-Shaikhaly, M.H.M., Nedergaard, J. and Cannon, B. (1979) Proc. Natl. Acad. Sci. USA 76, 2350-2353.

11. Lehninger, A.L., Vercesi, A. and Bababunmi, E.A. (1978) Proc. Natl. Acad. Sci. USA 75, 1690-1694.

12. Fiskum, G. and Lehninger, A.L. (1979) J. Biol. Chem. 254, 6236-6239.

13. Slater, E.C. and Cleland, K.W. (1953) Biochem. J. 55, 565-580.

14. Lindberg, O. and Ernster, L. (1954) Nature 173, 1038-1040.

15. Beyer, R.E., Ernster, L., Löw, H. and Beyer, T. (1955) Exptl. Cell Res. 8, 586-588.

16. Ernster, L. and Löw, H. (1955) Exptl. Cell Res. Suppl. 3, 133-153.

17. Vasington, F.D. and Murphy, J.V. (1962) J. Biol. Chem. 237, 2670-2677.

18. DeLuca, H.F. and Engström, G. (1961) Proc. Natl. Acad. Sci. USA 47, 1744-1750.

19. Chappell, J.B., Cohn, M. and Greville, G.D. (1963) In Energy-linked Functions of Mitochondria (Chance, B., ed.) Academic Press, New York, pp. 219-231.

20. Ernster, L. and Nordenbrand, K. (1967) Abstr. 4th FEBS Meeting, Oslo, p. 108.

21. Ernster, L., Hollander, P., Nakazawa, T. and Nordenbrand, K. (1969) In Energy Level and Metabolic Control in Mitochondria (Papa, S., Tager, J.M., Quagliariello, E., Slater, E.C., eds.) Adriatica Editrice, Bari, pp. 97-113.

22. Chance, B. and Mela, L. (1966) Biochemistry 5, 3220-3223.

23. Mela, L. and Chance, B. (1968) Biochemistry 7, 4059-4063.

24. Ernster, L., Nakazawa, T. and Nordenbrand, K. (1978) In The Proton and Calcium Pump (Azzone, G.F., Avron, M., Metcalfe, J.C., Quagliariello, E., Siliprandi, N., eds.) Elsevier/North Holland Biomedical Press, Amsterdam, pp. 163-176.

25. Vainio, H., Mela, L. and Chance, B. (1970) Eur. J. Biochem. 12, 387-391.

26. Vinogradov, A. and Scarpa, A. (1973) J. Biol. Chem. 248, 5527-5531.

27. Hughes, B.P. and Exton, J.H. (1983) Biochem. J. 212, 773-782.

28. Allshire, A., Bernardi, P. and Saris, N.-E.L. (1985) Biochim. Biophys. Acta 807, 202-209.

29. Konji, V., Montag, A., Sandri, G., Nordenbrand, K. and Ernster, L. Biochimie, in press.

30. Bernardi, P., Paradisi, V., Pozzan, T. and Azzone, G.F. (1984) Biochemistry 23, 1645-1651.

31. Lötscher, H.R., Winterhalter, K.H., Carafoli, E. and Richter, C. (1979) Proc. Natl. Acad. Sci. USA 76, 4340-4344.

32. Bellomo, G., Jewell, S.A. and Orrenius, S. (1982) J. Biol. Chem. 257, 11558-11562.

33. Panfili, E., Sottocasa, G.L., Sandri, G. and Liut, G. (1980) Eur. J. Biochem. 105, 205-210.

34. Lötscher, H.R., Winterhalter, K.H., Carafoli, E. and Richter, C. (1980) J. Biol. Chem. 255, 9325-9330.

35. Moser, B., Winterhalter, K.H. and Richter, C. (1983) Arch. Biochem. Biophys. 224, 358-364.

36. Hofstetter, W., Mühlebach, T., Lötscher, H.R., Winterhalter, K.M. and Richter, C. (1981) Eur. J. Biochem. 117, 361-367.

37. Bellomo, G., Martino, A., Richelmi, P., Moore, G.A., Jewell, S.A. and Orrenius, S. (1984) Eur. J. Biochem. 140, 1-6.

38. Prpić, V. and Bygrave, F.L. (1980) J. Biol. Chem. 255, 6193-6199.

39. Roth, Z. and Dikstein, S. (1982) Biochem. Biophys. Res. Commun. 105, 991-996.

40. Vercesi, A.E. and Lehninger, A.L. (1982) Fed. Proc. 41, 1434.

41. Vercesi, A.E. (1984) Biochem. Biophys. Res. Commun. 119, 305-310.

42. Hoek, J.B., Ernster, L., De Haan, E.J. and Tager, J.M. (1974) Biochim. Biophys. Acta 333, 546-559.

43. Richter, C., Winterhalter, K.H., Baumhüfer, S., Lötscher, M.R. and Moser, B. (1983) Proc. Natl. Acad. Sci. USA 80, 3188-3192.

44. Frei, B., Winterhalter, K.H. and Richter, C. (1985) Eur. J. Biochem. 149, 633-639.

45. Klingenberg, M. (1963) In Methods of Enzymatic Analysis (Bergmeyer, H.U., ed.) Academic Press, New York, pp. 528-538.

46. Konji, V., Montag, A., Nordenbrand, K., Sandri, G. and Ernster, L., in preparation.

47. Bygrave, F.L. (1978) Biol. Rev. 53, 43-79.

48. Nicholls, D. and Åkerman, K. (1982) Biochim. Biophys. Acta 638, 57-88.

49. Carafoli, E., Caroni, P., Chiesi, M. and Famulski, K. (1982) In Metabolic Compartmentation (Sies, H., ed.) Academic Press, London, pp. 521-547.

50. Hossmann, K.-A., Paschen, W., Csiba, L. (1983) J. Cereb. Blood Flow Metabol. 3, 346-353.

51. Hillered, L., Muchiri, P.M., Nordenbrand, K. and Ernster, L. (1983) FEBS Lett. 154, 247-250.

52. Schramm, V.L. (1982) TIBS 2, 369-371.

53. Jewell, S.A., Bellomo, G., Thor, H., Orrenius, S. and Smith, M.T. (1982) Science 217, 1257-1259.

54. Bellomo, G., Jewell, S.A., Thor, H. and Orrenius, S. (1982) Proc. Natl. Acad. Sci. USA 79, 6842-6846.

RICARD:

I wonder whether you have any working hypothesis about the molecular nature of this memory effect? Is this memory effect related to a "slow" conformation change of the protein?

ERNSTER:

That sounds like a reasonable explanation. But we need more data in order to answer this question.

KACSER:

Is not the time constant involved in the hysteresis rather large? It seems to be of the order of minutes.

ERNSTER:

A hysteresis may indeed involve a slow conformational change of protein.

Dynamics of Biochemical Systems
S. Damjanovich, T. Keleti, L. Trón (Eds)

SIMULATION OF INTRACELLULAR CONCENTRATIONS OF ENZYME FOR KINETIC STUDIES: APPLICATION TO PHOSPHOFRUCTOKINASES

JUAN J. ARAGÓN

Departamento de Enzimologia del Instituto de Investigaciones Biomédicas del CSIC y Departamento de Bioquímica de la Facultad de Medicina de la Universidad Autónoma, 28029 Madrid, Spain

1. INTRODUCTION

It is well known that many intracellular enzymes are present in high concentrations (Srere, 1967; Sols and Marco, 1970). Then, protein-protein interactions, both homologous (Hulme and Tipton, 1971) and heterologous (Hess and Boiteux, 1972), could induce intracellular changes in some properties of the enzymes important for metabolic regulation. This may be significant for phosphofructokinase, a highly modulated enzyme whose activity was reported to show a concentration dependent behavior (Hulme and Tipton, 1971; Hofer, 1971). Several procedures suitable for kinetic studies have been reported as approximations to intracellular conditions concerning protein concentration, one of the factors in which assays in vitro used to be markedly different from in vivo, mainly due to technical reasons. The measurement of enzyme activity in permeabilized cells, designated as the in situ approach, has been used to study a number of enzymes (Sols, 1975; Aragón et al. 1980). In the case of phosphofructokinase we have also used the purified enzyme at a concentration in the physiological level in an attempt to reproduce in vitro the behavior observed in situ, as well as the addition of polyethylene glycol (PEG) to increase the local protein concentration (Boscá, et al, 1985; Aragón and Sánchez, 1985). The later approach has additionally been employed to study the activity of other enzymes (Medina et al, 1985).

This article presents the kinetic studies that we have carried out to simulate in vivo conditions related to enzyme concentration. Most of these studies are focused on the regulation of several eukaryotic phosphofructokinases.

2. THE IN SITU APPROACH

Reeves and Sols (1973) developed the in situ approach for the study of the activity of intracellular enzymes in permeabilized E. coli by toluene treatment to disintegrate the cell membrane. By now, several dozens of enzymes have been studied in situ in microorganisms (Sols et al. 1976; Bañuelos and Gancedo, 1978); with most of them the parameters measured were similar in situ and in vitro although some differences were pointed out in a significant proportion of cases.

A general method for the kinetic study of enzymes in animal cells was developed by Aragón et al (1980) by treatment with bifunctional reagents to crosslink proteins and subsequent permeabilization by delipidation with digitonin without scape of intracellular proteins. The procedure, originally described for erythrocytes, could be applied to ascites tumor cells (Lazo and Sols, 1980) and other types of cells, but not to hepatocytes. With this approach a systematic exploration of the kinetic behavior of the glycolytic enzymes in erythrocytes was carried out. As shown in Table 1 the Km and Vmax values for the majority of the enzymes were essentially the same in situ as in vitro (a diluted hemolysate). The most significant difference was exhibited by phosphofructokinase, which will be described in the next section.

In addition to the study of individual enzymes, the in situ approach provides the possibility of evaluating the flux of a metabolic pathway starting from any of its intermediates under near physiological conditions. Fig. 1 shows the production of lactate in situ in erythrocytes from several glycolytic intermediates. As indicated, the generation of lactate was higher from glucose-6-P than from glucose supporting the idea that hexokinase may limitate the glycolytic flux in vivo in these cells. The rate of the pathway from glucose-6-P and glyceraldehyde-3-P was in the order of the activity of the limiting enzymes below these intermediates, presumably aldolase and phosphoglyceromutase.

Several other methods for partial permeabilization of animal cells have been published by other investigators (for a review see Aragón et al, 1980). Some of them imply insufficient permeabilization to metabolites while incomplete retention of proteins is brought about by others. Faced with this dilemma, the approach described above may be the most practical one for kinetic studies of enzymes, even at the expense of potential arti-

Table 1.

Glycolytic enzymes of rat erythrocytes *in situ* and *in vitro*.

(From Aragón et al, 1980)

Enzyme[a]	Vmax: In vitro units/g	Vmax: In situ[b] %	Substrate	$S_{0.5}$ mM: in situ	$S_{0.5}$ mM: in vitro
HK	0.08	33 (TDI)	Glc	0.2	0.2
			ATP	0.15;1.5	0.3
PGI	15[c]	47 (TDI)	Fru-6-P	0.1	0.1
PFK	8	48 (DMS)	Fru-6-P	0.2 (0.04)[d]	2 (0.025)[d]
			ITP	0.3	0.3
ALD	0.5	40 (TDI)	Fru-1,6-P_2	0.02	0.02
TIM	200	40 (TDI)	Gra-3-P[e]	0.4	0.4
GAPDH	9	57 (DMS)	Gra-3-P	0.3	0.3
			NAD^+	0.18	0.05
			Pi	10	10
PGK	16	44 (DMS)	3-P-Gri[e]	0.7	0.7
PGM	0.7	62 (DMS)	3-P-Gri	0.1	0.1
ENO	8	57 (TDI)	2-P-Gri	0.02	0.02
PK	6	58 (DMS)	P-enol-pyruvate	1.5	0.8
LDH	44	51 (DMS)	Pyruvate	0.2	0.2
			NADH	0.03	0.03

a) The abbreviations correspond to the 11 enzymes of the pathway ordered as they operate in the glycolytic direction.

b) Shown as % of value *in vitro*. The reagent used for crosslinking is shown in parentheses: TDI, toluene diisocyanate; DMS, dimethyl suberimidate.

c) In the reverse reaction with respect to glycolysis.

d) Numbers in parentheses are the values in the presence of positive effectors.

e) Gra, glyceraldehyde; Gri, glycerate.

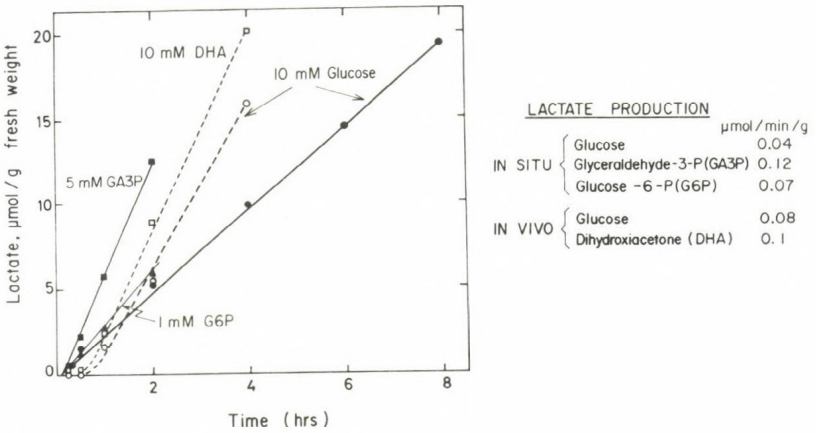

Fig. 1 Glycolysis in situ (●, ▲, ■) and in vivo (○, □) in rat erythrocytes. The reaction mixture contained 6 mM MgITP, 5 mM MgADP, 0.5 mM NAD^+, 20 mM Pi, 0.1 mM AMP, 1 mM NH_4^+, 0.1 mM p^1,p^5-di(adenosine-5'-)pentaphosphate, 1 mM DTE.

facts mediated by the crosslinking of some intracellular proteins.

3. REGULATION OF EUKARYOTIC PHOSPHOFRUCTOKINASES AT PHYSIOLOGICAL CONCENTRATION OF ENZYME.

Phosphofructokinase is a key regulatory enzyme of the glycolytic pathway whose activity responds to a variety of metabolic signals (Sols et al, 1981). Several eukaryotic phosphofructokinases have been studied to examine the influence of enzyme concentration on their allosteric regulation as described below.

Animal phosphofructokinases

Among the enzymes studied in situ in erythrocytes, phosphofructokinase exhibited the most striking difference with respect to the in vivo assay. As indicated in Fig. 2, the enzyme in situ showed an affinity for fructose-6-P in the absence of positive effectors, such as Pi, AMP and NH_4^+, markedly higher than in vitro . A concomitant reduction in the ATP inhibition was also observed (Sols et al, 1981).

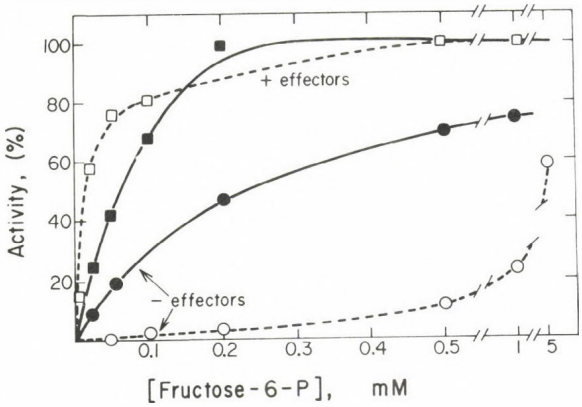

Fig. 2. Phosphofructokinase activity of rat erythrocytes in situ and in vitro. $MgATP^{2-}$ was 1 mM. Effectors were 5 mM Pi, 0.1 mM AMP and 1 mM NH_4^+. ●, ■, In situ; ○, □, in vitro. The pH was 7.4 (From Aragón et al, 1980).

Although these results suggested that the intracellular concentration of enzyme may contribute to the change observed in its kinetic behavior, they could also be related to some chemical modification of the enzyme produced by the permeabilization procedure. To test this possibility we studied the allosteric regulation of phosphofructokinase in vitro but employing concentrations of enzyme in the physiological range. Fig. 3A shows that the affinity for fructose-6-P was decreased when the purified muscle enzyme was assayed at a concentration of 0.6 mg/ml, which is in the order of its physiological level in muscle (Ling et al, 1965; Tornheim and Lowenstein, 1976) as compared to 100-fold more diluted concentration of enzyme. To measure the activity of the concentrated enzyme we used a very low Mg^{2+}/ATP ratio to decrease the reaction velocity. The increase on the apparent affinity for fructose-6-P reflected a drastic reduction in the ATP inhibition, as indicated in Fig. 3B.

As another way to simulate a high concentration of enzyme we included PEG (Mr = 6000) in the kinetic assay as a "crowding" agent to increase the local protein concentration, and thus favoring the aggregation of the diluted enzyme (Reinhart, 1980). Fig. 3 shows that phosphofructokinase exhibited a roughly similar behavior in the presence of PEG as when the enzyme was used at physiological concentration, and also similar to what we previously observed with the in situ approach. Then, essentially the same

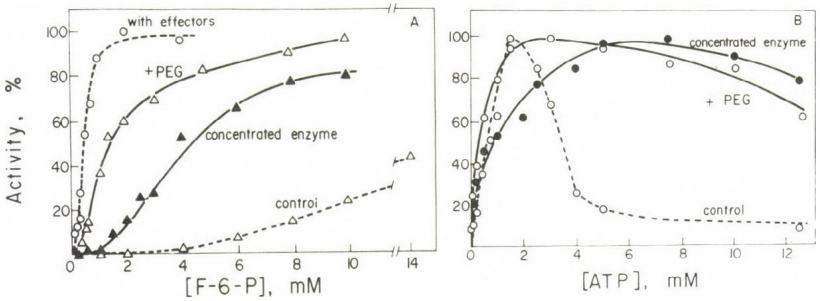

Fig. 3. Effect of physiological concentration of enzyme and polyethylene glycol on muscle phosphofructokinase. Purified rabbit muscle phosphofructokinase was used at 0.6 µg/ml (open symbols) and 0.6 mg/ml (solid symbols). Addition of 10% PEG as indicated. $MgCl_2$ was in excess over ATP with the diluted enzyme and was only 1% of that of ATP and with 4 mM EDTA in the case of the concentrated enzyme. Effectors were 5 mM Pi, 0.1 mM AMP, and 1 mM NH_4^+; △,▲, without effectors; ○,●, with effectors. A, ATP was 5 mM and the pH was 7.0. B, fructose-6-P was 0.5 mM and the pH was 6.8 (From Boscá et al, 1985).

result has been obtained by employing three different procedures, which have in common the use of concentrations of enzyme in the physiological range. The reduction in the ATP inhibition was also observed in the presence of a mixture of relevant phosphofructokinase effectors used at concentrations that prevail in working muscle (Boscá et al, 1985). A similar influence of the enzyme concentration on phosphofructokinases from other animal sources as liver and ascites tumor cells has been shown (Boscá et al, 1985; Lazo and Sols, 1980). Accordingly, these results suggest that the regulation of phosphofructokinase is among other factors dependent on its high concentration in vivo, leading to a sensitivity to inhibition by ATP compatible with high levels of activity, as it is the case in working muscle, without the need for a lowering of the endogenous concentration of ATP. Our results agree with prior observations by several investigators which were suggestive of a possible concentration dependent activity for animal phosphofructokinase, although the extrapolation to physiological

concentration was uncertain (Hulme and Tipton, 1971; Hofer, 1971; Wenzel et al, 1976; Reinhart, 1980).

The utilization of phosphofructokinase at physiological concentrations affords the possibility of measuring the ATPase and fructose-1,6-bisphosphatase minor activities of the enzyme. Fructose-2,6-P_2 and citrate affected the ATPase activity but not the fructose-1,6-bisphosphatase activity, in which assay ATP is not present. These results suggest that both citrate and fructose-2,6-P_2 are mechanistically "secondary" allosteric effectors that require the presence of ATP to modify the activity of phosphofructokinase (Boscá et al, 1985).

Yeast phosphofructokinase

Yeast phosphofructokinase, in contrast to those in animal tissues, has been claimed not to exhibit a concentration dependent kinetic behavior on the basis of both *in situ* studies (Bañuelos and Gancedo, 1978) and *in vitro* assays at a wide range of enzyme concentration (Laurent et al, 1979). The use of the three approaches described above to examine the influence of enzyme concentration gave us the opportunity to reinvestigate this possibility. As illustrated in Fig. 4, the enzyme studied *in situ* was markedly less sensitive to ATP in comparison to the assay in a cell free extract or *in situ*. Repetition of the same kinetic study by using purified yeast enzyme at physiological concentration led to a similar result (Fig. 5). PEG was able to reproduce the behavior observed in both cases, although it had to be added to the assay mixture at concentrations higher than the 10% concentration used with several mammalian phosphofructokinases and other enzymes.

These results strongly suggest that the ATP allosteric regulation of yeast phosphofructokinase can be affected by its intracellular concentration, as in the case of animal phosphofructokinase. Nevertheless, these observations do not contradict those previously described by Bañuelos and Gancedo (1978) and by Laurent et al (1979) because the lack of difference related to enzyme concentration was reported solely on the basis of fructose-6-P kinetics. We have confirmed this observation, not finding a significant change in the fructose-6-P saturation curve either with concentrated enzyme or in the presence of PEG (Aragón and Sánchez, 1985).

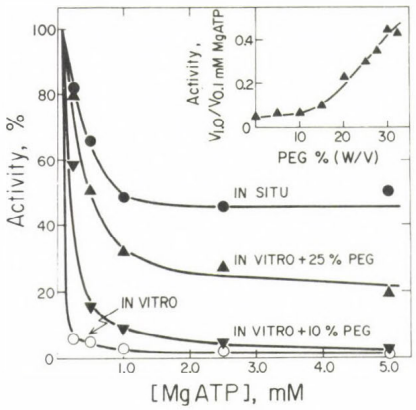

Fig. 4

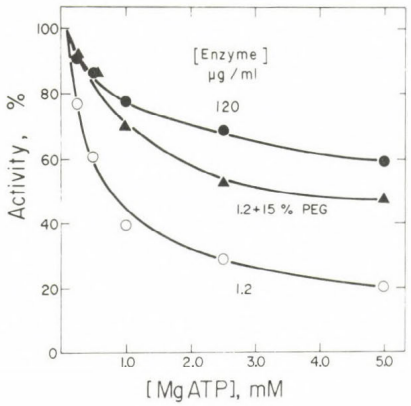

Fig. 5

Fig. 4. ATP inhibition of yeast phosphofructokinase in situ and in vitro. Fructose-6-P was 0.3 mM an the pH was 6.4. Activity at 0.1 mM MgATP was taken as 100%. Inset: effect of various concentrations of PEG on ATP inhibition in vitro. (From Aragón and Sánchez, 1985)

Fig. 5. ATP inhibition of purified yeast phosphofructokinase at high and low concentration of enzyme. Conditions as in Fig. 4. (From Aragón and Sánchez, 1985)

Dictyostelium discoideum phosphofructokinase.

In contrast to most phosphofructokinases, the enzyme from the slime mold D. discoideum has simple kinetic properties, it exhibits no sigmoidicity for fructose-6-P and no sensitivity to any of the typical allosteric effectors (Baumann and Wright, 1968), including fructose-2,6-P_2 as we have recently observed (unpublished results). This enzyme was chosen to test the effect of enzyme concentration on an apparently non-allosteric phosphofructokinase. Fig. 6 shows that this enzyme was very little sensitive to ATP inhibition, as compared to other phosphofructokinases and not affected by PEG. Concentrations of PEG higher than 10% had also no effect. This result suggest that some properties of the allosteric regulation of phosphofructokinase may be required to exhibit a concentration dependent activity, presumably the enzyme capability to aggregate.

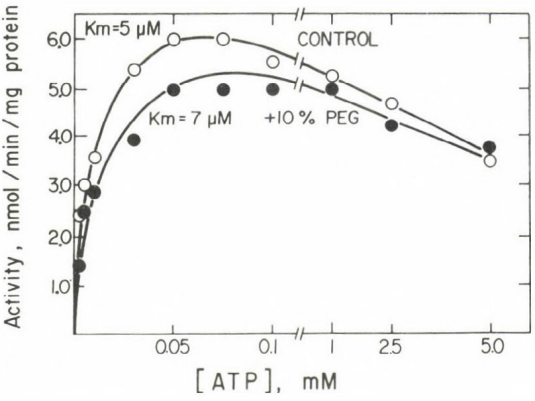

Fig. 6. Effect of polyethylene glycol on D. discoideum phosphofructokinase. Fructose-6-P was 15 μM and the pH 6.8. (Ospina, Sánchez and Aragón, unpublished results.)

4. OTHER ENZYMES AT PHYSIOLOGICAL CONCENTRATION.

Liver cells could not have been well permeabilized for kinetic studies. Then, we have used the PEG approach to study the influence of enzyme concentration on the kinetic parameters of other potentially regulatory liver enzymes. Among the enzymes examined, pyruvate kinase L was the most significantly affected, which affinity for P-enolpyruvate was markedly increased in the presence of PEG. In contrast with the liver enzyme, the behavior of muscle pyruvate kinase M, a non-regulatory isozyme, was not affected by PEG (Fig. 7). A similar decrease in the cooperativity for P-enolpyruvaste was observed when pyruvate kinase L was studied in situ in permeabilized erythrocytes (Aragón et al, 1980).

Out of the other enzymes tested only two were significantly affected by PEG: L-serine dehydratase, which showed an increase in the affinity for L-serine and a sigmoidal saturation curve in the presence of PEG, and glycogen phosphorylase a from muscle that exhibited a higher $S_{0.5}$ for Pi (Medina et al, 1985). The later result agrees with that reported by Eagle and Scopes (1981) for the enzyme assayed at high concentration.

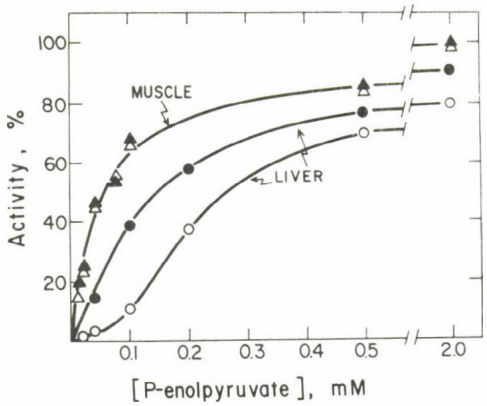

Fig. 7. Effect of polyethylene glycol on liver and muscle pyruvate kinase. ADP was 1 mM. ○,△, Control; ●,▲, plus 10% PEG. (From Medina et al, 1985)

5. CONCLUDING REMARKS

Three different approaches have been used for enzymatic kinetic studies at concentrations of enzyme in the physiological range. Phosphofructokinase was the enzyme most significantly affected by its concentration. The three procedures used in this study gave essentially similar results on the regulatory behavior of this enzyme. Each of these approaches involves a potentially damaging artifact. Nevertheless, the fact that the artifacts are different in each case cancel them as responsible of the marked differences in quantitative behavior relative to the usual in vitro assay. The common denominator is to favor the enzyme aggregation to its normal in vivo state. Hence, in relation with studies of physiological regulation of phosphofructokinase, the mere dilution of the enzyme typical of in vitro assays can markedly alter its allosteric behavior. This study also shows that the behavior of phosphofructokinase observed in situ can be explained on the basis of homologous protein-protein interactions, although other possibilities are not excluded.

Most other enzymes studied either in permeabilized cells or in the presence of PEG, did not show a significant change in their kinetic behavior, indicating that the majority of enzymes may not be affected by their concentrations in vivo. The exception seems to be the case of some regula-

tory enzymes such as phosphofructokinase and pyruvate kinase L. D. discoideum phosphofructokinase, as well as muscle pyruvate kinase, both apparently non-allosteric isozymes, were not affected by PEG, suggesting that the effect of enzyme concentration, when it occurs, may work mainly by adjusting some of the properties of regulatory enzymes.

Acknowledgements: I am indebted to Prof. A. Sols for valuable suggestions and critical reading of the manuscript, and to Ms. R. Clarys for typing the manuscript.

REFERENCES

Aragón, J.J., Felíu, J.E., Frenkel, R.A. and Sols, A. (1980) Permeabilization of animal cells for kinetic studies of intracellular enzymes: In situ behavior of the glycolytic enzymes of erythrocytes. Proc. Natl. Acad. Sci. USA 77, 6324-6328.

Aragón, J.J. and Sánchez, V. (1985) Enzyme concentration affects the allosteric behavior of yeast phosphofructokinase. Biochem. Biophys. Res. Commun. (In press)

Bañuelos, M. and Gancedo, C. (1978) In situ studies of the glycolytic pathway in Saccharomyces cerevisiae. Arch. Microbiol. 117, 197-201.

Baumann, P. and Wright, B.E. (1968) The phosphofructokinase of Dictyostelium discoideum. Biochemistry, 7, 3653-3661.

Boscá, L., Aragón, J.J. and Sols, A. (1985) Modulation of muscle phosphofructokinase at physiological concentration of enzyme. J. Biol. Chem. 260, 2100-2107.

Eagle, G. R. and Scopes, R.K. (1981) Inhibition of phosphorylase a by natural components of the sarcoplasm. Arch. Biochem. Biophys. 210, 540-548.

Hess, B. and Boiteux, A. (1972) Heterologous enzyme-enzyme interactions. In: Protein-Protein Interactions (Jaenicke, R., and Helmreich, E. eds.) pp. 271-296, Springer-Verlag, Berlin.

Hofer, H.W. (1971) Influence of enzyme concentration on the kinetic behavior of rabbit muscle phosphofructokinase. Hoppe-Seyler's Z. Physiol. Chem. 352, 997-1004.

Hulme, E.C. and Tipton, K.F. (1971) The dependence of phosphofructokinase kinetics upon protein concentration. FEBS Lett. 12, 197-200.

Laurent, M., Seydoux, F.J., and Dessen, P. (1979) Allosteric regulation of yeast phosphofructokinase. Correlation between equilibrium binding, spectroscopic and kinetic data. J. Biol. Chem. 254, 7515-7520.

Lazo, P.A., and Sols, A. (1980) Energetics of tumor cells: enzymatic basis of aerobic glycolysis. Biochem. Soc. Trans. 8, 579.

Ling, K.H., Marcus, F., and Lardy, H.A. (1965) Purification and some properties of rabbit skeletal muscle phosphofructokinase. J. Biol. Chem. 240, 1893-1899.

Medina, R., Aragón, J.J., and Sols, A. (1985) Effect of polyethylene glycol on the kinetic behavior of pyruvate kinase and other potentially regulatory liver enzymes. FEBS Lett. 180, 77-80.

Reeves, R.E., and Sols, A. (1973) Regulation of Escherichia coli phosphofructokinase in situ. Biochem. Biophys. Res. Commun. 50, 459-466.

Reinhart, G.D. (1980) Influence of polyethylene glycols on the kinetics of rat liver phosphofructokinase. J. Biol. Chem. 255, 10576-10578.

Sols, A. (1975) Regulation of enzymes in situ. In: Mechanism of Action and Regulation of Enzymes (Keleti, T. ed.) FEBS Symposia vol 32, pp. 211-221. North-Holland Publishing Co., Amsterdam.

Sols, A., and Marco, R. (1970) Concentrations of metabolites and binding sites. Implications in metabolic regulation. Curr. Top. Cell. Regul. 2, 227-273.

Sols, A., Felíu, J.E., and Aragón, J.J. (1976) Study of enzyme activity in animal cells in situ. In: Metabolic Interconversion of Enzymes 1975 (Shaltiel, S. ed.), pp. 191-197. Springer-Verlag, Berlin.

Sols, A., Castaño, J.G., Aragón, J.J., Domenech, C., Lazo, P.A., and Nieto, A. (1981) Multimodulation of phosphofructokinases in metabolic regulation. In Metabolic Interconversion of Enzymes 1980 (Holzer, H. ed) pp. 111-123, Springer-Verlag, Berlin.

Srere, P.A. (1967) Enzyme concentrations in tissues. Science, 158, 936-937.

Tornheim, K., and Lowenstein, J.M. (1976) Control of phosphofructokinase from rat skeletal muscle. Effects of fructose diphosphate, AMP, ATP, and citrate. J. Biol. Chem. 251, 7322-7328.

Wenzel, K.W., Kurganov, B.J., Zimmermann, G., Yakovlev, V.A., Schellenberger, W., and Hofmann, E. (1976) Self- association of human erythrocytes phosphofructokinase. Kinetic behavior in dependence of enzyme concentration and mode of association. Eur. J. Biochem. 61, 181-190.

DISCUSSION

KELETI:

About 10 years ago Jancsik et al. published (J. Mol. Catal. 1, 137, 1975) that polyvinylalcohol and polyvinylpyrrolidone depending on the molecular weight and concentration may activate or inhibit aldolase V_{max}. Aldolase is a pure Michaelis-Menten type enzyme in buffer but shows inhibition by excess substrate in the presence of the above mentioned polymers.

ARAGON:

In our hands, aldolase did not exhibit a concentration dependent behavior when it was studied either in permeabilized erythrocytes or by using the liver enzyme in the presence of polyethylene glycol. Nevertheless, this does not exclude that the enzyme from other sources, as muscle for instance, may show such a behavior. In any case, more than one approach should be used to extrapolate this type of results to physiological conditions to rule out possible artifacts.

WELCH:

Im am very interested in the results you have shown for phosphofructokinase (PFK), especially the polyethyleneglycol (PEG) effects. Indeed, PEG has been shown to affect the properties of many enzymes, in some cases by mimicking the heterogeneous environment in vivo. PFK from erythrocytes has been found to bind reversibly to cell "ghosts", the degree of association being influenced by regulatory effectors. (For example, see the review article by C. Masters in CRC Cricital Reviews of Biochemistry, 1981.) The bound form of PFK displays kinetic properties resembling those which you see with PEG. It seems, therefore, that some of your results with PEG might be due to the circumstance, that PEG is mimicking the in situ milieu of the membrane surface. (Incidentally,

one should note that toluenization of cells would disrupt this state of organization.)

ARAGON:

Yes, it can certainly be the case. Although concerning the binding of phosphofructokinase to the cell membrane we need to consider how significant the proportion of the bound enzyme is, and also the ionic strength used to study those interactions.

RICARD:

In order to compare kinetic properties of enzymes at very different enzyme concentrations, one has to be certain that the substrate concentration is in large excess with respect to the enzyme concentration. Is that the case even for very high substrate concentrations?

ARAGON:

Yes it is. The concentration of the enzyme we used in those studies was estimated to be around 1 μM considering the enzyme as a tetramer and that the subunit molecular weight of the muscle isozyme is about 90 000 daltons.

EASTERBY:

Muscle phosphofructokinase has been shown to be phosphorylatable in vivo and phosphorylation is proposed to stabilize the tetramer. Have you looked at the extent if any, of phosphorylation of your enzyme?

ARAGON:

This is a very interesting question. I did not mention the phosphorylation mechanism as another possibility for the regulation of phosphofructokinase because although this enzyme has been reported to undergo such a covalent modification, the physiological meaning of this phenomenon is unknown so far. Nevertheless, we though that perhaps the possible kinetic changes induced by the phosphorylation-

-dephosphorylation mechanism could be visualized by assaying the enzyme at a high concentration. Then we extracted the enzyme from resting and exercising skeletal muscle, when phosphofructokinase is subjected to a very high change in its activity. But unfortunately we did not observe any change in the kinetic behavior of the enzyme, even in the presence of polyethylene glycol (Miranda, M.E. and Aragon, J.J., unpublished results).

DYNAMICS OF PROTEIN AND NUCLEIC ACID STRUCTURE

Dynamics of Biochemical Systems
S. Damjanovich, T. Keleti, L. Trón (Eds)

GRAPH THEORETIC APPROACH TO DYNAMICS OF ENZYME QUATERNARY STRUCTURE

B.N. GOLDSTEIN

Institute of Biological Physics, USSR Academy of Sciences, Pushchino, Moscow Region, 142292, USSR

A number of models for allosteric enzymes proposed in the early 60's do not consider many multi-stage enzymic mechanisms with their complex conformational dynamics often induced through cascade systems.

New discoveries stimulate new approaches to the modelling of conformationally regulated enzyme systems. Using methods of the theory of graphs and taking the hierarchy of enzymic systems into account, we can study these systems in more details. At first the theory of graphs was used for some simpler enzyme reactions (Volkenstein and Goldstein, 1966). Ever since we have formulated the kinetic models in terms of schematic language commonly employed by biochemists. Our schemes (graphs) however not only illustrate the process but can also be quantitatively analyzed. Very complex graphs may be simplified in such a way as to obtain rate equations for multi-subunit enzymes. In the present paper we consider not only the interactions of enzymes with various ligands, but also their various equilibrium or non-equilibrium distributions among conformational states. We also investigate both linear (one-enzymic) and non-linear (multi-enzymic) processes, formulating in the last instance the conditions of their instability or self-oscillations.

Linear graphs for rapid equilibrium, steady-states and pre-steady states

Various states of an enzyme are pictured as graph "nodes"

and their interconversions - as directed "branches", if we use so-called "linear" graphs:

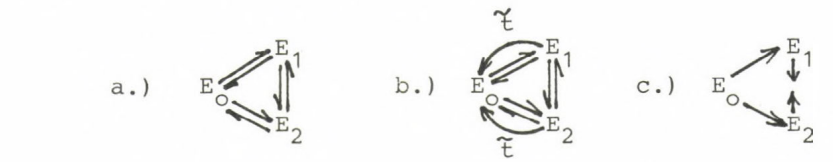

(1)

Complex graphs can be simplified according to our rules summarized elsewhere (Cornish-Bowden, 1976). Graph for pre-steady-state kinetics (1b) contains additional branches with $\tilde{t}$-values and directed from all nodes to initial nodes (Goldstein, 1983). $\tilde{t}$-value is a time variable transformed according to Laplace-Carson. In accordance with the laws of thermodynamics there are no cycles in the equilibrium graph (1c), this graph thus being a directed tree (Volkenstein and Goldstein, 1966,b). This equilibrium simplification of ours has been used by Cha (1968) for analysis of graphs with a number of equilibrium sub-graphs connected by slow stages.

For each of the graphs (1) the rate equation is obtained according to the rule:

$$v = \frac{\Sigma D_i k_+ - \Sigma D_j k_-}{\Sigma_i D_i} \qquad (2)$$

where D_i is a sum of tree values for trees directed to i-th node. For steady-states (graph 1a) without simplifications the rule (2) coincides with the rule of King-Altman (1956). Using graph (1b) we obtain reaction rate $v(\tilde{t})$ transformed according to Laplace-Carson. $v(\tilde{t})$ is informative by itself but may be re-transformed into time-dependent function v(t) which is a sum of exponential terms, their number being equal to the number of graph nodes minus one. On the experimental curves and for a time scale chosen only a few exponential terms (as a rule not more than two) are reliable. It means that a complete graph should be simplified by abolishing very slow as well as very rapid stages to obtain a graph with three nodes only. If

exponential terms are all of equal signs, their reliable separation may be difficult to obtain. For this reason it is desirable to choose such conditions which would give opposite signs for two exponential terms. In our laboratory such conditions were experimentally realized for lactate dehydrogenase pre-equilibrated with some ligands (Yagodina et al., in press). Two experimental curves shown in Fig. 1 exactly fitted the same rate equation with the only difference in parameter values:

$$P(t) = vt + \beta_1(1-e^{-\lambda_1 t}) + \beta_2(1-e^{-\lambda_2 t}) \qquad (3)$$

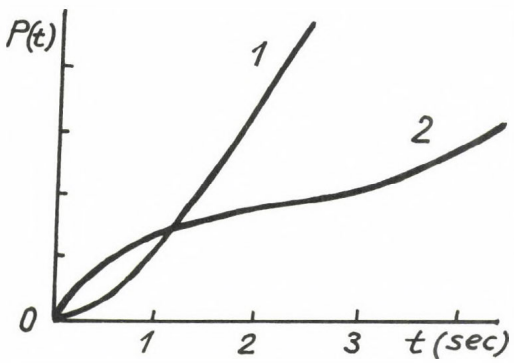

Fig. 1

Time-dependent rate of lactate dehydrogenase-catalyzed reaction (pH 8): 1 - without pre-equilibration, 2 - pre-equilibrated with 0.25 mM NAD^+ and 0.5 mM pyruvate (Yagodina et al., in press).

If we use graph (1b), we must change the number of $\tilde{t}$-branches to obtain different initial conditions and, as a consequence, different parameters of Eq. (3) (Goldstein, 1983). In this way the unusual inflection point ($\beta_1>0$, $\beta_2<0$, $\lambda_1>\lambda_2$) in curve 2 has been obtained. We interprete the two slow stages clearly revealed in curve 2 under conditions of pre-equilibration as slow pH-dependent enzyme conformational transitions.

Modifications of Monod-Wyman-Changeux model

The model proposed by Monod et al. (1965) is apt to undergo various modifications. According to this model, we can divide the whole complicated graph into a number of conformational blocks, each for identical independent enzyme subunits. For

two conformational states R and T we have two conformational sub-graphs connected by transition stages (see Fig. 2). Indices i, j refer here to different enzyme complexes with ligands, $L_{\pm i}$ are constants of conformational transitions (i=0, ..., n, ..., N), n is the number of subunits, N is the total number of enzymic complexes with ligands.

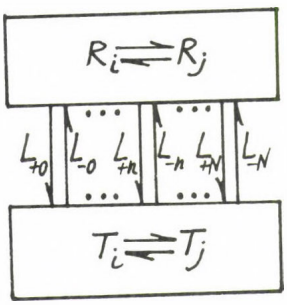

Fig. 2

Block-graph for two enzymic conformations and arbitrarily complicated reaction mechanisms

For all of different enzymic mechanisms consistent with block-graph of Fig. 2 we obtain the following rate equation:

$$v = nv_r \frac{1 + Qv_t/v_r}{1 + Q} \qquad (4)$$

where $Q = \Sigma_i T_i / \Sigma_i R_i$, v_r and v_t are reaction rates for a single active site in R and T conformations, respectively. The separation of conformational transitions (function Q) from reaction rates (v_t, v_r) is reflected in Eq. (4). Functions v_t and v_r in this context are supposed to be known. Function Q is easily obtained in two cases: 1.) rapid equilibration of different conformations, 2.) slow (as compared to other stages) conformational transitions.

The graph in the first case is the tree, thus, only single ($R_o \rightleftharpoons T_o$) transition between two sub-graphs R and T is to be considered. The function Q in this case is the following

(Popova et al., 1983):

$$Q = L_o \left(\frac{r_o}{r_o + \Sigma r_s} \Big/ \frac{t_o}{t_o + \Sigma t_s} \right)^n \qquad (5)$$

where r_s, t_s are concentrations of a single enzymic subunit in complexes with various ligands s = 1, 2, ... Function Q from Eq. (5) is easily applied to various mechanisms.

For example, for a two-substrate mechanism $r_o \rightleftharpoons rS_1 \rightleftharpoons rS_1S_2 \rightarrow r_o$ we have:

$$Q = L_o \left(\frac{1 + c_1 S_1 (1 + c_2 S_2)}{1 + S_1 (1 + S_2)} \right)^n \qquad (6)$$

where S_1, S_2 are dimensionless substrate concentrations and c_1 and c_2 are parameters. In the case of slow conformational transitions instead of Eq. (5) we have:

$$Q = L_o \left(\frac{r_o + \Sigma r_s 1_{+s}/1_{+o}}{r_o + \Sigma r_s} \Big/ \frac{t_o + \Sigma t_s 1_{-s}/1_{-o}}{t_o + \Sigma t_s} \right)^n \qquad (7)$$

where $1_{\pm s}$ are constants for single-subunit conformational transitions. It is Eq. (8) that may be deduced from Eq. (7) for the two-substrate mechanism:

$$Q = L_o \left(\frac{1 + c_1 S_1 (1 + c_2 S_2) + c_3 S_2}{1 + S_1 (1 + S_2) + c_4 S_2} \right)^n \cdot \left(\frac{1 + c_4 S_2 + S_1 (c_5 + c_6 S_2)}{1 + c_3 S_2 + S_1 (c_5 + c_7 S_2)} \right)^n \qquad (8)$$

The concentrational maximum exponent 2n in Eq. (8) is twice as greater as it is in Eq. (6). It means that in the case of non-equilibrated conformations an enzyme has "memory" of both its conformational states.

This effect results in complicated curves $v(S_1, S_2)$ with intermediate plateau or intermediate minimum (Popova et al.,

1983) similar to those shown in Fig. 3.

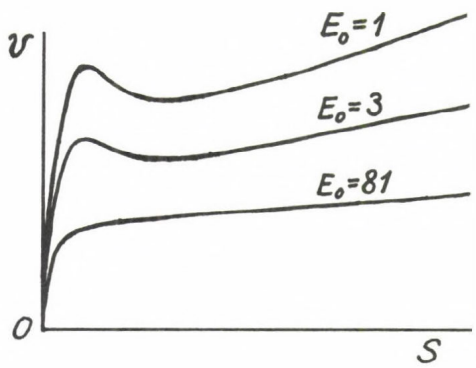

Fig. 3

Reaction rate versus substrate concentration for a slowly and reversibly dissociated oligomeric enzyme S (n=8; c_1=20; c_2=0.2; c_3=0.8; V_t/V_r=0.005).

Models of slow dissociating multi-subunit systems

The steady-state rate equation for slowly reversibly dissociating enzyme systems is similar to the one shown in Eq. (4) with the exception of another Q function. For dissociation into two halves and, in particular, for a single-substrate reaction we obtain:

$$Q = \frac{1}{2}\left(\sqrt{1+8E_oL_o\left(\frac{1+c_1S}{1+S}\cdot\frac{1+c_2S}{1+c_3S}\right)^n} - 1\right) \qquad (9)$$

Here E_o denotes the variable total enzyme concentration. Let's use now Eq. (4) with Q from Eq. (9) to interprete kinetic curves obtained for α-ketoglutarate dehydrogenase (Severin et al., 1976). Kinetic curves v(S) presented in Fig. 3 are fitted to experimental data according to Eqs. (4), (9). We see that the enzyme activity decreases and the intermediate minimum vanishes with the increase of enzyme concentration. Curves with an intermediate minimum may prove important, if such an enzymic system becomes an open one. The substrate inflow into such a system may cause unstabilities and, as a consequence, discrete regulation of enzyme activity.

Models for symmetry-changing conformational transitions

Many oligomeric enzymes are known to change their symmetry as a result of ligand binding. The half-asymmetry of oligomeric enzymes is well known and is used in so called "flip-flop" models (Lazdunski, 1974). Multi-enzyme complexes consisting of a large number of subunits are in their turn also organized into symmetrical structures. Dynamics of their quaternary structures may lead to lower symmetries, namely, to the subgroups of their point group of symmetry. We suppose, that in this way the identical subunits will fall into two or three or more conformational classes. During conformational transitions concerving a lower sub-symmetry subunits ma pass from one conformational class to another one like subunits in the "flip-flop" models do. Each of the conformational classes may correspond to a definite stage of a cyclic multi-stage enzymic process. As an example, three conformational states for each of 24 identical subunits, forming a cubic structure, may be quoted. The multi-enzymic complexes for dehydrogenases of α-keto acids do form such structures (Goldstein, Kornilov and Smetanitz, in press).

Now we would like to discuss a model for aspartate transcarbamylase using numerous data consistent with its symmetry-changing dynamics.

We consider three conformational states (Saifullin and Goldstein, in press):

1.) a fully symmetrical state in which two ligands (succinate S_1 and carbamoylphosphate S_2) are bound;

2.) a half-asymmetrical state arranged to bind succinate only at half of catalytic subunits;

3.) fully inactive state.

Using graph-theoretical approach we obtain for this model:

$$Y(S_1) = S_1 \frac{(1+S_2)\left[1+S_1(1+S_2)\right]^{n-1} + \frac{1}{2}Lc(1+cS_1)^{\frac{n}{2}-1}}{\left[1+S_1(1+S_2)\right]^{n} + L(1+cS_1)^{n/2} + L'} \qquad (10)$$

The Hill's coefficient n_H is computed from Eq. (10) in accordance with Eq. (11):

$$n_H = \frac{S_1}{Y(1-Y)} \cdot \frac{\delta Y}{\delta S_1} \qquad (11)$$

The value (n_H-1) is plotted then in Fig. 4 for various S_2 values. It is clearly seen from Fig. 4 that "cooperativity" - that is the value (n_H-1) - changes from initial positive values to negative ones and then to positive again with the increase of S_1. This kind of dependence, obtained in the model, agrees with the available experimental data.

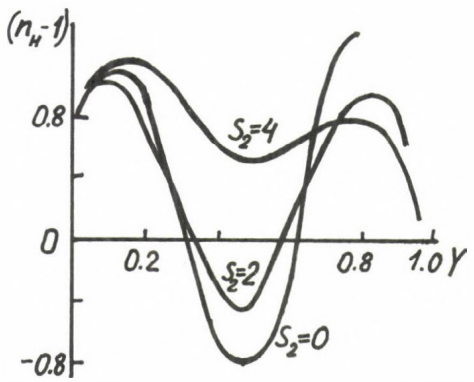

Fig. 4

Substrate-dependent "cooperativity" estimated for aspartate transcarbamoylase in accordance with the proposed model (see Eq. 10).

Self-oscillations in bifunctional enzyme kinetics regulated by phosphorylation/dephosphorylation

Recently a lot of data concerning the evolutional combination of different enzymes into one multi-functional enzyme by the gene fusion have been obtained. Activities of all the enzymes combined become concerted and controlled by conformational dynamics. This concerted behaviour becomes especially effective, in case it is induced by means of specific modificatory enzymes. A very interesting example of such systems has recently been discovered. We mean a bifunctional enzyme 6-phosphofructo-2-kinase/fructose-2,6-bisphospatase (6PF2K-ase/F26P$_2$-

ase), regulated by phosphorylation/dephosphorylation (Hers, 1984). Two reciprocal enzyme activities usually linked to two different enzymes in a substrate ("futile") cycle are here arranged into a single protein, the result being their conformational interrelation. Our analysis shows that the feedback interactions are organized here in such a manner as to produce self-oscillatory regime resulting in time separation of reciprocal flows without futile energy loss. It is interesting that substrates F6P (fructose-6-phosphate) and $F26P_2$ (fructose-2,6-bisphosphate),if arranged in 6PF2K-ase/$F26P_2$-ase, influence the protein kinase modificatory activity. Such feedback control through the modificatory enzyme (so-called "cascade regulation") is really very effective. The system considered is an important regulatory block of metabolic networks. $F26P_2$ has recently been shown to have a strong regulatory effect on glycolysis. Thus, oscillations of this metabolite, predicted in this paper, may supply one more explanation for well known glycolytic oscillations.

The non-linear graph (Goldstein and Shevelev, 1985) for this multi-enzymic system shown in Fig. 5 is pictured according to the mass action law. All of reaction participants (substrates and enzymes) are considered here as time dependent variables. In Fig. 5 they are shown as circles and reactions - as squares.

We designate here F6P as S_1, $F26P_2$ as S_2. E_1 is a dephosphorylated bifunctional enzyme catalyzing the forward reaction $S_1 \rightarrow S_2$, while E_2 is a phosphorylated bifunctional enzyme catalyzing the reaction $S_2 \rightarrow S_1$. Protein kinase E_3 catalyzing the reaction $S_2 \rightarrow S_1$. Protein kinase E_3 catalyzes the phosphorylation $E_1 \rightarrow E_2$. Phosphatase (not shown) catalyzes the dephosphorylation $E_2 \rightarrow E_1$. Substrates S_1 and S_2 are reversibly bound to protein kinase E_3 to form inactive complexes. This fact seems to be very plausible and does not contradict experimental data. Graph of Fig. 5 has been analysed with the help of the graph-theoretic computer programme detailed in (Ivanova and Tarnopolsky, 1979). The applied algorithm is similar to rules of Clarke (1974) and of Goldstein and Shevelev

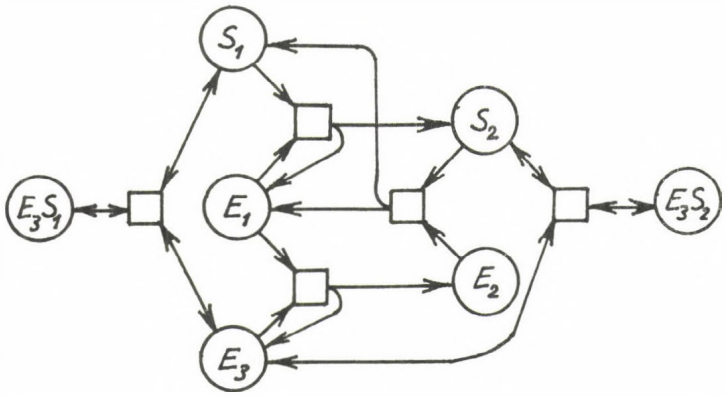

Fig. 5

Graph for bifunctional system 6PF2K-ase/F26P_2-ase controlled by phosphorylation/dephosphorylation with substrate feedback regulation.

(1985). On this basis the conditions for self-oscillations have been obtained and corresponding parameter values have been computed. The oscillatory behaviour for the system discussed is shown in Fig. 6. The computed unstable state is the following: $E_1=10^{-1}$, $S_1=2$, $E_2=10^{-1}$, $S_2=1$, $E_3=10^{-2}$, $S_1E_3=0.2$, $S_2E_3=0.1$. Oscillations arise around this unstable state.

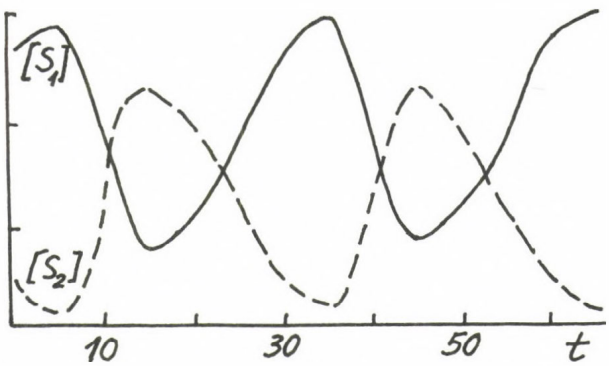

Fig. 6

Self-oscillatory kinetics computed for graph of Fig. 5 (6PF2K-ase/F26P_2-ase system)

Acknowledgements

I am very thankful to Drs. A.N. Ivanova, S.R. Saifullin and E.L. Shevelev for the computer analysis.

References

Cha, S. (1968) A simple method for derivation of rate equations for enzyme-catalyzed reactions under the rapid equilibrium assumption or combined assumptions of equilibrium and steady-state. J. Biol. Chem. 243, 820-825.

Clarke, B.L. (1974) Graph theoretic approach to the stability analysis of steady-states chemical reaction network. J. Chem. Phys. 60, 1481-1492.

Cornish-Bowden, A. (1976) Principles of Enzyme Kinetics. Butterworth, London-Boston.

Goldstein, B.N. (1983) Analysis of cyclic enzyme reaction schemes by the graph-theoretic method. J. theor. Biol. 103, 247-264.

Goldstein, B.N. and Shevelev, E.L. (1985) Stability of multi-enzyme systems with feedback regulation: a graph theoretical approach. J. theor. Biol. 112, 493-503.

Hers, H.G. (1984) The discovery and the biological role of fructose 2,6-bisphosphate. Biochem. Soc. Trans. London, 12, 729-735.

Ivanova, A.N. and Tarnopolsy, B.L. (1979) On an approach to some quantitative features of kinetic system behaviour and its computer simulation (critical phenomena, auto-oscillations). Kinetics and Catalysis, XX, 6, 1541-1548.

King, E.L. and Altman, C. (1956) A schematic method of deriving the rate laws for enzyme-catalyzed reaction. J. Phys. Chem. 60, 1375-1378.

Lazdunski, M. (1974) Half-of-the-sites reactivity and the role of subunit interactions in enzyme catalysis. Progr. Bioorg. Chem. 3, 81-104.

Monod, J., Wyman, J., Changeux, J.-P. (1965) On the nature of allosteric transitions: a plausible model. J. Mol. Biol. 12, 88-118.

Popova, S.V., Goldstein, B.N., Shevelev, E.L. (1983) Steady-state equations for multi-substrate reactions catalyzed by oligomeric enzymes. Studia Biophys. 95, 167-176.

Saifullin, S.R. and Golstein, B.N. (in press) Enzyme model for mixed co-operativity. Molek. Biol.

Severin, S.E., Gomaskova, V.S., Krasovska, O.E., Melnikova, O.F. (1976) Kinetic properties of α-ketoglutarate dehydrogenase. Dokl. Akad. Nauk. 229, 755-757.

Volkenstein, M.V. and Goldstein, B.N. (1966a) A new method for solving the problems of the stationary kinetics of enzymological reactions. Biochim. Biophys. Acta, 115, 471-477.

Volkenstein, M.V. and Goldstein, B.N. (1966b) Allosteric enzyme models and their analysis by the theory of graphs. Biochim. Biophys. Acta, 115, 478-485.

Yagodina, L.O., Shevelev, E.L., Smolyaninova, T.I., Goldstein, B.N., Markovitz, D.S. (in press) The study of kinetic manifestation of slow conformational transitions in lactate dehydrogenase. Molek. Biol.

Goldstein, B.N., Kornilov, V.V., Smetanitz, Y.S. (in press) On the symmetry of polyenzymic complexes. Molek. Biol.

DISCUSSION

BARDSLEY:

Is it possible to incorporate the laws of microscopic reversibility into graph theoretic methods so that the rate equations are properly dimensioned with respect to the correct number of independent rate constants?

GOLDSTEIN:

The laws of microscopic reversibility as well as other physical principles (for example, time-hierarchy and space-symmetry of complicated enzymic systems) should be incorporated, of course, into graph theoretic methods. The application of these principles allows the number of independent kinetic parameters to be reduced. As a consequence we obtain sufficiently simpler rate equations when using graph theoretic methods.

Dynamics of Biochemical Systems
S. Damjanovich, T. Keleti, L. Trón (Eds)

DYNAMICS OF CONFORMATIONAL CHANGES OF ENZYMES AND THE MODULATION OF SUBSTRATE BINDING AND CATALYSIS. EVOLUTIONARY CONSIDERATIONS

JACQUES RICARD and GEORGES NOAT

Centre de Biochimie et de Biologie Moléculaire du C.N.R.S.
BP. 71 - 13402 Marseille Cedex 9 - France

I - INTRODUCTION

Kinetic equations that describe the behaviour of allosteric enzymes, appear to be extremely complex, much more complex than the corresponding substrate-binding isotherms. The substrate-binding isotherm of a four-site enzyme for instance, is a 4:4 equation, that is the ratio of two polynomials of the fourth degree in substrate. For the same type of enzyme, the simplest kinetic scheme would be expressed by a 10:10 rate equation!

By the very nature of their steady state equations one would expect the allosteric enzymes to display a very complex kinetic behaviour [1-3]. Most allosteric enzymes however exhibit a smooth kinetic response when the substrate concentration is varied. In most cases, one observes positive or negative co-operativity as well as substrate inhibition. Although complex rate equations may generate smooth curves [4] , there is little doubt that a large potential of kinetic complexity of allosteric enzymes does not seem to be often encountered in nature. One may therefore wonder whether some constraints between rate constants may not have arisen in the course of Evolution, thus resulting in a partial degenerescence of rate equations and therefore in their simplification. The existence of constraints between rate constants means the existence of some definite structural properties of polymeric enzymes.

Enzyme kineticists have derived the steady state equations of various models of allosteric enzymes.As expected, these equations are exceedingly complex and tell us nothing about the way subunit interactions and conformational constraints modulate the rate of product appearance . On the other hand, the classical models of subunit interactions, namely the Monod et al [5] and the Koshland et al [6] models, have been derived for equilibrium conditions occurring between the protein and a ligand. As it will be seen

later, these models are not applicable to rate data.

The aim of this communication is to precisely study how the dynamics of subunit interactions modulates, under non-equilibrium conditions, the rate of an enzyme reaction and to understand how this process may have been subjected to evolutionary pressure.

II - THE THERMODYNAMIC FORCES THAT CONTROL ENZYME REACTIONS AND THEIR EVOLUTION

The simplest enzyme reaction may be described by the model

$$E \underset{k_{-1}}{\overset{k_1[S]}{\rightleftharpoons}} ES \underset{k_{-c}}{\overset{k_c}{\rightleftharpoons}} EP \underset{k_2[P]}{\overset{k_2}{\rightleftharpoons}} E$$

If one assumes, as done by Albery and Knowles [7], that the improvement of catalytic efficiency is the driving force of evolution, evolutionary pressure must tend to maximize the reaction flux, J, from S to P through the various internal states of the reaction. Improving the catalytic efficiency of the reaction implies that the reciprocal of the flux decreases. The upper limit of functional efficiency, called "catalytic perfection" [8] will be reached when :

- the binding of the substrate and the product are both diffusion-controlled;
- the ratio 1/[S] is small enough to make one of the terms of the flux equation dominant;
- the free energy changes involved when passing through the central transition states are small.

The reaction flux is then solely defined by the diffusion-controlled rate constant and by the overall equilibrium constant.

Another important question is to figure out which kind of molecular device allows this improvement of catalytic efficiency. If $\Delta G^{\neq}$ and $\Delta G^{\neq}{}'$ are the free energies of activation associated with an enzyme reaction process and the corresponding uncatalyzed reaction , one may write for the internal states of the free energy profile

$$\begin{aligned}
\Delta G^{\neq}_{-1} &= \Delta G^{\neq}{}'_{s\bar{s}} + \Delta G^{B}_{s} - X_{s\bar{s}} \\
\Delta G^{\neq}_{c} &= \Delta G^{\neq}{}'_{s\bar{x}} + \Delta G^{B}_{s} - X_{s\bar{x}} \\
\Delta G^{\neq}_{-c} &= \Delta G^{\neq}{}'_{p\bar{x}} + \Delta G^{B}_{p} - X_{p\bar{x}} \\
\Delta G^{\neq}_{2} &= \Delta G^{\neq}{}'_{p\bar{p}} + \Delta G^{B}_{p} - X_{p\bar{p}}
\end{aligned} \qquad (1)$$

In these expressions $\Delta G^{\neq}_{s\bar{s}}$, $\Delta G^{\neq}_{s\bar{x}}$, $\Delta G^{\neq}_{p\bar{x}}$, $\Delta G^{\neq}_{p\bar{p}}$ are the non-enzymatic free energies of activation required to go from a ground to a transition state, namely from S to to $S^{\neq}$, from S to $X^{\neq}$, from P to $X^{\neq}$ and from P to $P^{\neq}$, respectively. $-\Delta G^{B}_{s}$ and $-\Delta G^{B}_{p}$ are the binding free energies of the substrate and of the product. Similarly $X_{s\bar{s}}$, $X_{s\bar{x}}$, $X_{p\bar{x}}$ and $X_{p\bar{p}}$ are the driving forces that allow to pass the free energy barriers, namely which allow to go from S to $S^{\neq}$, from S to $X^{\neq}$, from P to $X^{\neq}$ and from P to $P^{\neq}$. These driving, or thermodynamic, forces exerted in either the forward or the backward direction consist of two contributions : the binding energy of the transition states to the enzyme and the free energy associated with the conformation changes of the enzymes which pass from a strained to a less strained state. These driving forces may be expressed as

$$
\begin{aligned}
X_{s\bar{s}} &= \Delta G^{T}_{s\bar{s}} + \Delta G^{B}_{\bar{s}} \\
X_{s\bar{x}} &= \Delta G^{T}_{s\bar{x}} + \Delta G^{B}_{\bar{x}} \\
X_{p\bar{x}} &= \Delta G^{T}_{p\bar{x}} + \Delta G^{B}_{\bar{x}} \\
X_{p\bar{p}} &= \Delta G^{T}_{p\bar{p}} + \Delta G^{B}_{\bar{p}}
\end{aligned}
\qquad (2)
$$

In these expressions $\Delta G^{B}_{\bar{s}}$, $\Delta G^{B}_{\bar{x}}$, $\Delta G^{B}_{\bar{p}}$ represent the binding free energies of the various transition states. $\Delta G^{T}_{s\bar{s}}$, $\Delta G^{T}_{s\bar{x}}$, $\Delta G^{T}_{p\bar{p}}$ are the free energies released upon the conformation changes of the enzyme in going from a ground to a transition state, namely from ES to $ES^{\neq}$, from ES to $EX^{\neq}$, from EP to $EX^{\neq}$ and from EP to $EP^{\neq}$, respectively.

The evolutionary pressure, which tends to decrease the $\Delta G^{\neq}$ values of the central transition states (equations 1), tends to make ΔG^{B}_{s} and ΔG^{B}_{p} as close to zero as possible and to maximize the driving forces X. When the driving forces are close to their maximum values, the binding and conformational energies ΔG^{B} and ΔG^{T} which appear in equations (2) are independently reaching their own maximum values. A ligand-induced conformation change requires some energy to occur, therefore the binding energies have reached their maximum possible values when all the transition states, $S^{\neq}$, $X^{\neq}$ and $P^{\neq}$ are tightly bound to the free enzyme form without any additional conformation change of this enzyme. Therefore this improvement of catalytic efficiency implies that the enzyme should have the same conformation in all the transition states.

Upon passing a free energy barrier, the enzyme relapses from a strained

to an unstrained conformation. The functional efficiency of the enzyme is maximum when the energy released during this conformation change in maximum, and therefore the same for all the reaction steps. This implies that

$$\Delta G^{T}_{s\bar{s}} = \Delta G^{T}_{s\bar{x}} = \Delta G^{T}_{p\bar{x}} = \Delta G^{T}_{p\bar{p}} = \Delta G^{T} \tag{3}$$

and therefore that

$$X_{s\bar{x}} = X_{p\bar{x}} \tag{4}$$

Moreover, it follows from the above reasoning that substrate and product stabilize the same, or energetically indistinguishable, conformation (S).

Then, the activation free energies associated with the internal states reduce to (equation 1)

$$\begin{aligned} \Delta G^{\neq}_{-1} &\sim \Delta G^{\neq\,\prime}_{s\bar{s}} - X_{s\bar{s}} \\ \Delta G^{\neq}_{c} &\sim \Delta G^{\neq\,\prime}_{s\bar{x}} - X_{s\bar{x}} \\ \Delta G^{\neq}_{-c} &\sim \Delta G^{\neq\,\prime}_{p\bar{x}} - X_{s\bar{x}} \\ \Delta G^{\neq}_{2} &\sim \Delta G^{\neq}_{p\bar{p}} - X_{p\bar{p}} \end{aligned} \tag{5}$$

Therefore if an enzyme has reached its maximum functional efficiency this implies that the two following requirements have been met, namely:
- the enzyme should have the same conformation, along the reaction co-ordinate, in all the transition states;
- the substrate and the product stabilize in the ground states energetically indistinguishable conformations, or even the same conformation [8, 9].

III - THE PRINCIPLES OF STRUCTURAL KINETICS

As outlined previously [9-13] , the aim of the structural kinetic formalism is to express the rate of a chemical process, carried out by a polymeric enzyme, in terms of both the corresponding process carried out by an ideally isolated subunit and the role played in this process by subunit packing and distorsion within the polymer. As a matter of fact, subunit interactions may affect a chemical process in two different ways. Owing to protomer arrangement and association, they can modify the rate of a conformational transition associated with that reaction step . Moreover they may strain the active site and therefore modify the rate of the process. These two types of energy contributions tend to stabilize the polymeric enzyme with respect to the ideally isolated subunit.

Since the conformation of an enzyme has to be relieved at the top of the energy barrier, one may expect the quaternary constraints between subunits to be relieved in the transition states. Obviously there cannot be any experimental proof that quaternary constraints are relieved in the transition states, but this assumption is necessary to explain the occurrence of catalysis.

In its simplest version, the structural kinetic formalism relies on three postulates :

- the postulate that an unstrained subunit occurs under only two conformations, A (unliganded) and B (liganded);
- the postulate of uniqueness of subunit conformation in all the transition states;
- the postulates that quaternary constraints are relieved in the transition states.

These statements are formulated in terms of postulates, but the discussion presented in the above section shows that evolutionary pressure should favour the emergence of these molecular properties.

Let there be any kind of chemical process, involved in a reaction carried out by a polymeric enzyme, the corresponding activation energy may be ideally split up into three energy contributions :

1) The intrinsic energy contribution $\Delta G^{\neq *}$ which corresponds to what the activation energy would be in absence of any subunit interaction. This is the free energy of activation of an ideally isolated protomer.

2) The second energy contribution is termed the protomer arrangement contribution, $\Sigma({}^{\alpha}\Delta G^{int})$. It expresses quantitatively how subunit arrangement and association, apart from any strain of the active sites, may modulate the rate of the conformational transition associated with the chemical process. This energy component corresponds to the free energy of subunit polymerization, on assuming that no conformation change occurs during this process. If there exist l subunits in conformation A and m subunits in conformation B, in a ground or a transition state, this protomer arrangement energy contribution assumes the form

$$(6) \qquad \Sigma({}^{\alpha}\Delta G^{int}) = (\tfrac{l}{2})\,({}^{\alpha}\Delta G_{AA}) + (\tfrac{m}{2})({}^{\alpha}\Delta G_{BB}) + lm({}^{\alpha}\Delta G_{AB})$$

3) The third energy contribution is called the quaternary constraint contribution, $\Sigma({}^{\sigma}\Delta G^{int})$, and expresses how the strain between subunits through quaternary constraints may modify the reaction rate. It may be

expressed by an equation similar to equation (6) above. Since quaternary constraints however must be relieved in the transition states, this contribution applies to ground states only.

Therefore the expression of the free energy of activation for the process carried out by the polymeric enzyme assumes the form

$$\Delta G^{\neq} = \Delta G^{\neq *} + \Sigma({}^{\alpha}\Delta G^{int}) + \Sigma({}^{\sigma}\Delta G^{int}) \tag{7}$$

and the corresponding rate constant is

$$k = k^* \, \Pi\alpha \, \Pi\sigma \tag{8}$$

where

$$k^* = \frac{k_B T}{h} \exp\{-\Delta G^{\neq *}/RT\}$$

$$\alpha = \exp\{-({}^{\alpha}\Delta G)/RT\} \tag{9}$$

$$\sigma = \exp\{-({}^{\sigma}\Delta G)/RT\}$$

k_B, h and T are the Boltzmann constant, the Planck constant and the absolute temperature, respectively. α and σ are dimensionless coefficients analogous to equilibrium constants. They are termed interaction and strain coefficients, respectively. k^* is the so-called intrinsic rate constant [9, 12]. An illustration of the principles of structural kinetics is to be found in references 9 and 12.

IV - STRUCTURAL KINETIC EXPRESSION OF RATE EQUATIONS

The structural formalism allows one to express how subunit interactions and conformational constraints modulate the steady state rate of product appearance. For a dimeric enzyme, if subunits are loosely coupled, the model that describes the rate of product appearance is shown in Figure 1.
In this model, the subunits are assumed to exist in only two unstrained conformations A and B in the ground states, and the corresponding equation is 2:2 in substrate concentration, namely [12]

$$\frac{v}{[E]_o} = \frac{2\bar{k}^* \bar{K}^* [S] + 2 \bar{k}^* \frac{\alpha_{AA}}{\alpha_{AB}} \bar{K}^{*2} [S]^2}{1+2 \frac{\alpha_{AA}}{\alpha_{AB}} \bar{K}^* [S] + \frac{\alpha_{AA}}{\alpha_{BB}} \bar{K}^{*2} [S]^2} \tag{10}$$

In this expression $\bar{k}^*$ and $\bar{K}^*$ are apparent catalytic and affinity constants defined as

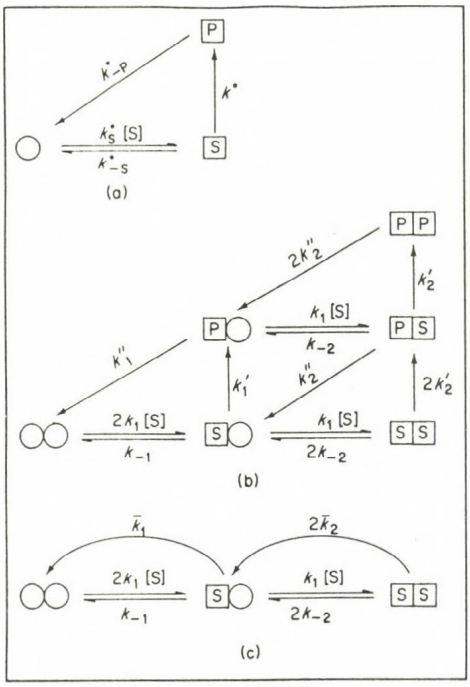

Figure 1 :
Kinetic model for loose coupling in a dimeric enzyme.
(a) The intrinsic process for an ideally isolated subunit.
(b) Kinetic model for a dimeric enzyme.
(c) Kinetic model for a dimeric enzyme after graph reduction.

(11)

$$\bar{k}^* = \frac{k^* \, k^*_{-p}}{k^* + k^*_{-p}}$$

$$\bar{K}^* = \frac{k^*_s (k^* + k^*_{-p})}{k^*_{-p} (k^* + k^*_{-s})}$$

Clearly when no subunit interaction occurs, $\alpha_{AA} = \alpha_{BB} = \alpha_{BB} = 1$ and equation (10) reduces to

(12)

$$\frac{v}{[E]_o} = \frac{2 \, \bar{k}^* \, \bar{K}^* \, [S]}{1 + \bar{K}^* [S]}$$

and the enzyme does not display any co-operativity. Kinetic co-operativity in equation (10) obviously appears as a consequence of subunit interactions which hinder , or facilitate, the rate of the conformational transitions.

If subunits are tightly coupled (Figure 2) , the structural rate equation becomes more complex and one has to take account of the strain of the active sites generated by the inter-subunit conformational constraints. When, as shown in Figure 2 (b), conformational constraints are relieved in

the unliganded and fully liganded states

(13) $$\sigma_{AA} = \sigma_{BB} = 1$$

and

514) $$\sigma_{AB} = \frac{\alpha_{BB}}{\alpha_{AB}} \frac{1}{\sigma_A^*}$$

In this case, the corresponding structural rate equation assumes the form [12]

(15) $$\frac{v}{[E]_o} = \frac{2\,\bar{k}^*\,\bar{K}^*\,[S] + 2\,\bar{k}^*\,\frac{\alpha_{AA}}{\alpha_{AB}}\,\bar{K}^{*2}\,[S]^2}{1 + 2\,\frac{\alpha_{AA}}{\alpha_{BB}}\,\sigma_A^*\,\bar{K}^*\,[S] + \frac{\alpha_{AA}}{\alpha_{BB}}\,\bar{K}^{*2}\,[S]^2}$$

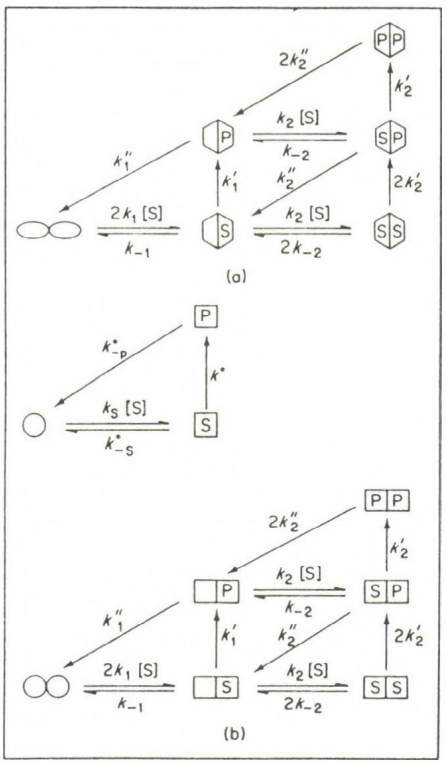

Figure 2:
Kinetic model for tight coupling between subunits in a dimeric enzyme.
(a) Quaternary constraints are not relieved in the non-liganded and fully-liganded states.
(b) Quaternary constraints are relieved in the non-liganded and fully-liganded states. The intrinsic process is shown between (a) and (b).

The same structural formalism allows to derive the expression of the corresponding substrate-binding isotherms under equilibrium conditions. For the model of Figure 1, the corresponding substrate-binding isotherm is

$$(16)\quad \bar{\nu} = 2\,\bar{Y} = \frac{2\,\frac{\alpha_{AA}}{\alpha_{AB}}\,K^*\,[S] + 2\,\frac{\alpha_{AA}}{\alpha_{BB}}\,K^{*2}\,[S]^2}{1 + 2\,\frac{\alpha_{AA}}{\alpha_{AB}}\,K^*\,[S] + \frac{\alpha_{AA}}{\alpha_{BB}}\,K^{*2}\,[S]^2}$$

and for the model of Figure 2 (b) one has

$$(17)\quad \bar{\nu} = 2\,\bar{Y} = \frac{2\,\frac{\alpha_{AA}}{\alpha_{BB}}\,\sigma_A^*\,K^*\,[S] + 2\,\frac{\alpha_{AA}}{\alpha_{BB}}\,K^{*2}\,[S]^2}{1+2\,\frac{\alpha_{AA}}{\alpha_{BB}}\,\sigma_A^*\,K^*\,[S] + \frac{\alpha_{AA}}{\alpha_{BB}}\,K^{*2}\,[S]^2}$$

Clearly, equations (10) and (15) do not reduce to equations (16) and (17). Therefore the important conclusion which may be derived from the use of the structural formalism is that subunit interactions and conformational constraints affect substrate binding and the rate of conversion of substrate into product in a different way. This matter will be discussed later on in this paper.

V - SUBUNIT COUPLING AND KINETIC CO-OPERATIVITY OF POLYMERIC ENZYMES

The maximum or minimum Hill coefficient is a classical measure of co-operativity. For 2:2 substrate binding equations, the extreme (maximum or minimum) Hill coefficient is obtained at half-saturation of the enzyme by the ligand. Under non-equilibrium conditions the extreme Hill coefficient of a 2:2 rate equation

$$(18)\quad \frac{v}{[S]_o} = \frac{\psi_1[S] + \psi_2[S]^2}{\psi_o' + \psi_1'[S] + \psi_2'[S]^2}$$

may be shown to be [13]

$$(19)\quad \tilde{h}_{ext} = \frac{2}{1+\sqrt{\frac{\psi_o' - \psi_2\,\Gamma/2}{\psi_o'}}}$$

where the parameter Γ is defined as

$$(20)\quad \Gamma = \lim_{1/S \to 0} \frac{d^2(E_o/v)}{d(1/S)^2} = 2\,\frac{\psi_2^2\psi_o' - \psi_1(\psi_2\psi_1' - \psi_2'\psi_1)}{\psi_2^3}$$

In expressions (18)-(20) the ψs and ψ's are groupings of rate constants.

For loosely coupled subunits (model of Figure 1), the expression of substrate-binding Hill coefficient at half-saturation of the substrate is

$$\bar{h}_{1/2} = \frac{2\sqrt{\rho}}{1 + \sqrt{\rho}} \tag{21}$$

whereas the extreme kinetic Hill coefficient assumes the form [13]

$$\tilde{h}_{ext} = \frac{2}{1 + \sqrt{2-\rho}} \tag{22}$$

In either equation (21) or (22) the ρ parameter is defined from subunit interaction coefficients αs, namely

$$\rho = \frac{\alpha_{AB}^2}{\alpha_{AB}\,\alpha_{BB}} \tag{23}$$

From the comparison of equations (21) and (22) several interesting conclusions may be drawn [13] .

- For loose coupling between subunits, the concept of kinetic co-operativity is meaningful only if $\rho < 2$.
- A positive substrate-binding co-operativity is "amplified" when expressed under steady state conditions by measuring the conversion of substrate into product.
- A negative substrate-binding co-operativity is "attenuated", under non-equilibrium conditions, by measuring the rate of product appearance.

Therefore loose coupling between subunits does not allow strong negative co-operativity to occur. Moreover for dimeric enzymes, although loose coupling between subunits may generate positive kinetic co-operativity, this co-operativity is not accompanied by any sigmoidicity of the rate curve.

When tight coupling of subunits occurs, as shown in Figure 2 (a), the extreme substrate-binding co-operativity, as expressed by the Hill coefficient is

$$\bar{h}_{1/2} = \frac{2\sqrt{\rho'}}{1 + \sqrt{\rho'}} \tag{24}$$

but ρ' is now defined as

$$\rho' = \frac{\alpha_{AB}^2\,\sigma_{AB}^2}{\alpha_{AA}\,\sigma_{AA}\,\alpha_{BB}\,\sigma_{BB}} \tag{25}$$

and depends on both the interaction (α) and strain (σ) coefficients. The corresponding kinetic Hill coefficient, under non-equilibrium conditions, assumes the form [13]

$$\tilde{h}_{ext} = \frac{2}{1+\sqrt{\frac{\sigma_{AA}}{\sigma_{AB}}\left(2 - \frac{\sigma_{AA}}{\sigma_{AB}}\rho'\right)}} \qquad (26)$$

Here again, comparison of equations (24) and (26) allows some important conclusions [13] :

- The kinetic co-operativity may occur only if $\rho'\sigma_{AA}/\sigma_{AB}<2$.
- The substrate-binding co-operativity is solely defined by the ρ' coefficient, whereas the kinetic co-operativity is expressed by ρ' and the ratio σ_{AA}/σ_{AB}. Moreover ρ' and σ_{AA}/σ_{AB} may take independent values, in such a way that the sign of substrate-binding and kinetic co-operativities may be opposite.
- If the substrate-binding co-operativity is positive ($\rho'>1$), the kinetic co-operativity must be positive as well.
- If the substrate-binding co-operativity is negative ($0<\rho'<1$), the kinetic co-operativity may be negative or positive.
- If $\rho' = 1$, that is if there is no substrate-binding co-operativity, there may exist a positive kinetic co-operativity if $\sigma_{AA}/\sigma_{AB} \neq 1$. Then strain of the active sites, exerted through quaternary constraints, may generate a kinetic co-operativity which is not associated with any real substrate-binding co-operativity. Moreover for a dimeric enzyme, tight coupling between subunits may generate a sigmoidal rate curve.

If now subunits are tightly coupled, but if the strain is relieved in the non-liganded and fully-liganded states (Figure 2b), the substrate-binding Hill coefficient is

$$\bar{h}_{1/2} = \frac{2\sqrt{\rho''}}{1+\sqrt{\rho''}} \qquad (27)$$

but now

$$\rho'' = \frac{\alpha_{BB}}{\alpha_{AA}} \frac{1}{\sigma_A^{*2}} \qquad (28)$$

Thermodynamics imposes that [9,13]

$$\alpha_{BB} \geq \alpha_{AA}\sigma_A^{*2} \qquad (29)$$

which implies that $\rho'' > 1$. Therefore substrate-binding co-operativity can only be positive or nil. The corresponding kinetic Hill coefficient is

$$(30) \qquad \tilde{n}_{ext} = \frac{2}{1+\sqrt{\frac{\alpha_{AB}}{\alpha_{BB}}\sigma_A^* \left(2 - \frac{\alpha_{AB}}{\alpha_{BB}}\sigma_A^* \rho''\right)}}$$

As previously , whereas substrate-binding co-operativity is solely defined by the value of ρ'', kinetic co-operativity is defined by both ρ'' and $\alpha_{AB}\sigma_A^*/\alpha_{BB}$. Comparison of equations (27) and (30) shows that kinetic co-operativity cannot be negative and that a positivie kinetic co-operativity may be generated by a strain of the active sites, even in the absence of substrate-binding co-operativity.

VI - CATALYTIC EFFICIENCY AND FUNCTIONAL SIMPLICITY OF ALLOSTERIC ENZYMES

It has now become possible to answer the basic question raised in the introduction of this paper, namely : is there any mechanistic reason which explains that the potential kinetic complexity offered by allosteric enzymes is only rarely encountered in Nature ? In other words, is there any mechanistic reason for the frequent occurrence of functional simplicity ?

Probably the driving force of neo-darwinian evolution of allosteric enzymes is the improvement of their catalytic efficiency, exactly as for the monomeric enzymes [7, 14, 15]. If one wants to figure out how a polymeric protein may have a catalytic function, one has to postulate that the inter-subunit constraints are, at least in part, relieved in the transition states. Geometric and electrostatic destabilization could not occur otherwise [16-18]. Simple kinetic and thermodynamic considerations have allowed to show that the improvement of catalytic efficiency during evolution involves :

- the complete relief of inter-subunit constraints in the transition states;
- the uniqueness of conformation of the subunits that have bound any of the transition states;
- the uniqueness of conformation of the liganded subunits in the ground states, whatever the nature of the ligand , substrate or product is.

These requirements are precisely those which lead to degenerescence, and therefore to a simplification of the rate equations. For a dimeric enzyme for instance, the simplest kinetic scheme should lead to a 3:3 rate equation. However when the three above conditions apply the rate equation degenerates to a 2:2 one. The mechanistic conditions which lead to

catalytic efficiency, lead to functional simplicity as well. This allows to understand that evolutionary pressure tends to reduce the potential kinetic complexity offered by allosteric enzymes. The existence of this complexity, as expressed by "bumps" and turning points on the rate curves [3] may be viewed as an ancestral character of enzyme function.

VII - CONCLUSIONS

Several interesting conclusions may be drawn from the above theoretical considerations. The classical models of Monod et al [5] or Koshland et al [6] cannot be applied to non-equilibrium conditions which are precisely those of enzyme reactions. A so-called structural formalism, more general than the Koshland formalism, allows to express and to compare how subunit interactions and conformational constraints modulate either substrate binding to the enzymes or the rate of product appearance, under steady state conditions.

Loose coupling between subunits results in an amplification of positive kinetic co-operativity with respect to the corresponding substrate-binding co-operativity. Alternatively, this mode of subunit coupling leads to an attenuation of negative kinetic co-operativity with respect to the corresponding substrate-binding co-operativity.

Tight coupling of subunits may lead to inversion effects. That is negative substrate-binding co-operativity may be associated with positive kinetic co-operativity. Moreover a complete lack of substrate-binding co-operativity may occur together with positive kinetic co-operativity. This surprising effect is due to the strain of the active sites generated by inter-subunit constraints.

The mechanistic conditions which increase the catalytic efficiency of enzymes, increase their functional simplicity as well. Evolution should have favoured the emergence of enzymes that display both catalytic efficiency and functional simplicity.

REFERENCES

1 - Bardsley, W.G. (1977) J. Theor. Biol. 65, 281-316.

2 - Bardsley, W.G., Leff, P., Kavanagh, J.P. and Waight, R.D. (1980) Biochem. J. 187, 739-765.

3 - Teipel, J. and Koshland, D.E. (1969) Biochemistry 8, 4656-5663.

4 - Solano-Munoz, F., Mc Ginglay, P.B., Woolfson, R. and Bardsley, W.G. (1981) Biochem. J. 193, 339-352.

5 - Monod, J., Wyman, J. and Changeux, J.P. (1965) J. Mol. Biol. 12, 88-118.

6 - Koshland, D.E., Nemethy, G. and Filmer, D. (1966) Biochemistry 5, 365-385.

7 - Albery, W.J. and Knowles, J.R. (1976) Biochemistry 15, 5631-5640.

8 - Ricard, J. (1978) Biochem. J. 175, 779-791.

9 - Ricard, J. in Applied Biochemistry and Bioengineering, (1985) G.R. Welch ed., Vol 5, pp. 177-240, Academic Press , New York.

10 - Ricard, J., Mouttet, C. and Nari, J. (1974) Eur. J. Biochem. 41, 479-497.

11 - Ricard, J. and Noat, G. (1982) J. Theor. Biol. 96 , 347-365.

12 - Ricard, J. and Noat, G. (1984) J. Theor. Biol. 111, 737-753.

13 - Ricard, J. and Noat, G. (1985) J. Theor. Biol. in the press.

14 - Cornish-Bowden, A. (1976) J. Mol. Biol. 101, 1-9.

15 - Koshland, D.E. (1976) Fed. Proc. Fed. Am. Soc. Exp. Biol. 35, 2104-2111.

16 - Lumry, R. (1959) in The Enzymes , P.D. Boyer , M. Lardy and K. Myrbäck eds, Vol. 1, pp. 157-231, Academic Press, New YorK.

17 - Jencks, W.P. (1969) Catalysis in Chemistry and Enzymology , Mc Graw Hill New York.

18 - Jencks, W.P. (1975) Adv. Enzymol., 43, 219-410.

DISCUSSION

ATKINSON:

As you said, there is no thermodynamic or kinetic reason why substrate binding curves and velocity response curves must be identical. Whether they are or not depends simply on whether the rapid binding (Michaelis) assumption is valid and whether the intrinsic rate constants are changed by modifiers. But isn't it perhaps significant that in the few cases in which binding curves, and the effects of modifiers on them, have been determined they are nearly identical with the velocity response curves? Do you know of established counter-examples? Evolution may have selected this type of response in many or most cases because of regulatory advantages of such behavior.

RICARD:

The catalytic constants originating from the various enzyme-substrate complexes may, by chance, have similar values but I can hardly believe these values to be identical. The catalytic rate constant values depend on the energy levels of both the corresponding ground and transition states. If my assumption that the intrasubunit strain is relieved in the transition states, were correct, the energy levels of the ground and transition states, along the reaction coordinate, should be different. This indeed, should lead to different catalytic rate constant values. There is little doubt that very different models, for instance the Monod's model and the "simple" Koshland's model may fit pretty closely the same binding data. It is only through best fit estimation procedures that "validity" of the models may be appreciated. The same type of analysis has certainly to be performed when comparing kinetic models, or, when comparing kinetic overbinding models. I do not believe one may safely speak about the "validity" of a given model until the quality of the fit has not been compared with that of possible rival models.

As far as the intrinsic properties of a regulatory enzyme are concerned I can't see any advantage in having kinetic patterns similar to, or different from substrate-binding curves. Our structural formalism may predict the existence of sigmoidal kinetic curves with a degree of co-operativity similar to or higher than that obtained from the substrate binding isotherms.

ATKINSON:

You suggested that subunit interaction might facilitate catalytic action. That is obviously possible, but the opposite effect (a decrease in catalytic activity as a consequence of oligomerization) is also possible and has been observed. The catalytic subunits of aspartate transcarbamylase (which are trimers, but without subunit interactions) catalyse the reaction rapidly with normal ("hyperbolic") kinetics. The intact enzyme catalyzes the reaction considerably more slowly but with sigmoid kinetics, so that sensitivity to substrate concentration is much greater than in the case of the subunits. Similar behaviour is seen in oxygen binding by hemoglobin and by its α-β subunits. It seems that formation of oligomers may involve a sort of negative spring loading that can be overcome by binding interactions, thus producing the steep response that is necessary for regulatory sensitivity. Evolution is selection from among a wide range of thermodynamic and kinetic possibilities. Regulatory sensitivity may well be more biologically important than maximal catalytic effectiveness.

RICARD:

On the whole I agree with these comments. What I simply wanted to outline is that the classical models of co-operativity of necessity implied the binding of a ligand to be decreased if subunit interaction occurred.
The structural formalism we proposed shows that subunit interactions may enhance both catalytic efficiency and

substrate co-operativity, which do not appear as antagonistic anymore.

BARDSLEY:

It is clear that rate equations calculated by graph theoretic or structural techniques must be identical. Do the 3:3 rate equations for your scheme reduce in degree to 2:2?
What interpretation do you propose when the parameter $\rho>2$? Do you just abandon interpretation in the presence of substrate in solution?

RICARD:

The presented rate equations have been derived by conventional techniques (King-Altman method for instance). The structural formalism is not a new way of deriving steady-state rate equations but its aim is to show how enzyme structure modulates reaction rate. The 3:3 rate equations reduce to 2:2 equations because some postulates have been made on the nature of the transition states.
When $\rho>2$, the reaction is inhibited by an excess substrate in the range of investigated substrate concentration. In this range the very concept of the Hill coefficient becomes meaningless.

CORNISH-BOWDEN:

I should like to comment on Dr. Atkinson's first point. He said that in the small number of cases for which experimental evidence existed there was a good correspondence between equilibrium binding behaviour and velocity behaviour. I want to emphasize that the number of such experimental cases is indeed small and to point out that 15-20 years ago similar arguments were advanced to dismiss the possibility of kinetic co-operativity in monomeric enzymes. Although kinetic models were proposed by Ferdinand (Biochem. J. 98, 278-283, 1966), Keleti (Acta Biochim. Biophys. Acad. Sci. Hung. 3, 247-258, 1968) and

others at about the same time as the well known quasi-equilibrium models of Monod et al. and Koshland et al. (Monod, J., Wymann, J. and Changeux, J.-P., J. Molec. Biol. 12, 88-118, 1965; Koshland, D.E.Jr., Némethy, G. and Filmer, D., Biochemistry 5, 365-385, 1966), they were not given serious attention for a long time because all of the known examples of co-operative enzymes were believed to be oligomeric enzymes. We now know from the work of a number of groups, including Dr. Ricard's in particular, that kinetic co-operativity in monomeric enzymes is a real phenomenon in the real world, and we are reminded that we should be cautious about making broad generalizations on the basis of a very small number of experimental examples.

RICARD:

I can only agree with these comments.

Dynamics of Biochemical Systems
S. Damjanovich, T. Keleti, L. Trón (Eds)

DYNAMICS OF DNA STRUCTURE

MAXIM D. FRANK-KAMENETSKII

Institute of Molecular Genetics, USSR Academy of Sciences,
Moscow 123182, USSR

It is an established fact today that, under normal conditions, the structure of DNA is for the most part close to the Watson-Crick right-handed double helix or, as people usually say, the B form. This has been most clearly demonstrated in recent studies of very short DNA rings (comprising a couple of hundreds of bp). Shore and Baldwin (1983a) observed clear oscillations of the ring closure probability as a function of the number of base pairs in DNA with a period of about 10 bp. Horowitz and Wang (1984) concluded that the pitch of DNA in solution is equal to 10.54 bp.

DNA samples used in these studies have only recently become available with the advent of genetic engineering. In general, genetic engineering techniques have revolutionized the whole field of DNA structure and dynamics. It is primarily these techniques that made the recent discoveries possible which have considerably widened our knowledge of the structural range of DNA. The classical B form was shown to be the main but by no means the only possible DNA structure.

What are the alternative (other than the B form) structures and when are they formed? Below, I am going to answer this question.

First of all it should be emphasized that no alternative structures are formed in linear, non-superhelical DNA. A linear DNA molecule is in the B form practically throughout its length, though of course it exhibits small bending and torsional fluctuations (Hagerman, 1981; Shore and Baldwin, 1983a,b; Horowitz

and Wang, 1984; Frank-Kamenetskii, 1985; Frank-Kamenetskii et al. 1985). It is very rarely (after each hundred thousand bp, on the average) interrupted by solitary open, disrupted base pairs. The available data indicate that the lifetime of this open state is as short as 10^{-6} s. A given base pair opens every 10^{-2} s. I restrict myself to these short comments about the dynamics of linear DNA (for a comprehensive discussion of the subject and literature, see my recent paper (Frank-Kamenetskii, 1985)) and will now turn to alternative structures in superhelical DNA.

Negative superhelicity is known to be the universal property of DNA in both prokaryotic and eukaryotic cells. Special enzymes, topoisomerases, maintain the degree of superhelicity in vivo. In the superhelical state the DNA dobule helix is under the stress. As a result, negative superhelicity favours any alternative structure that releases the superhelical stress. In early studies (before 1980) only two candidates, namely the open region and the cruciform structure, were considered. Vologodskii et al. (1979) studied theoretically the competition between these two possibilities and predicted that long palindromic sequences, comprising about 20 bp or more, would from cruciform structures under sufficient superhelical stress. This theoretical prediction has been quantitatively conformed by numerous studies of cruciform formation in palindromic regions of different prokaryotic DNA (Lilley, 1980; Panayotatos and Wells, 1981; Vologodskii and Frank-Kamenetskii, 1982; Singleton and Wells, 1982; Lyamichev et al., 1983; Singleton, 1983).

Probably the most striking feature of cruciformation is its very slow kinetics, especially at a low temperature. This is due to the necessary formation of a large open region as an intermediate state in the course of the cruciformation. This phenomenon has extensively been studied theoretically (Vologodskii and Frank-Kamenetskii, 1983) and experimentally (Mizuuchi et al., 1982; Courey and Wang, 1983; Sinden and Petijohn, 1984; Panyutin et al., 1984). It was also used by Lyamichev et al. (1984) to study the problem of the presence of cruciforms in vivo.

After the left-handed Z form was discovered (Wang et al., 1979) it became clear that this structure should be listed as an additional (and a rather powerful) candidate capable of reducing the superhelical stress. However, as in the case of the cruciforms, the Z form formation requires a specific nucleotide sequence, namely alternating purines and pyrimidines in both DNA strands. There are no such sequences in natural prokaryotic genomes (though they are quite often found in eukaryotic DNA). As a result one could study the B-Z transition in plasmids carrying artificial purine-pyrimidine inserts.

Two-dimensional gel electrophoresis proved to be the most powerful technique for studying the conformational transitions (B-Z, B-cruciform, etc.) under superhelical stress (Wang et al., 1983; Lyamichev et al., 1983; Haniford and Pulleyblank, 1983; Peck and Wang, 1983; Panyutin et al., 1984). This method is based on the fact that when a transition occurs in superhelical DNA which releases the superhelical stress the overall dimensions of the molecule increase and it slows down in the gel. This results in a characteristic discontinuity of the two-dimensional pattern (see Fig. 1).

Such patterns as shown in Fig. 1 made it possible to obtain quantitative information about the energetics and kinetics of cruciformation (Courey and Wang, 1983; Lyamichev et al., 1983; Panyutin et al., 1984) and the energetics of the B-Z transition in $(GC)_n \cdot (GC)_n$ and $(GT)_n \cdot (AC)_n$ sequences (Peck and Wang, 1983; Haniford and Pulleyblank, 1983; Frank-Kamenetskii and Vologodskii, 1984; Vologodskii and Frank-Kamenetskii, 1984). Recently Panyutin et al. (1985) have shown by this method in conjunction with the S1 endonuclease mapping that the $(AT)_n \cdot (AT)_n$ sequences form cruciforms rather than the Z form under superhelical stress.

Treatment with the S1 endonuclease is widely used by biochemists to detect and locate alternative structures in DNA. This method is very efficient in detecting cruciformation as well as the B-Z transition. In the former case the scission is located at the centre of the palindromic region whereas in the latter case it is located at the ends of the purine-pyrimidine tract (Lilley, 1980; Panayotatos and Wells, 1981; Rich et al., 1984).

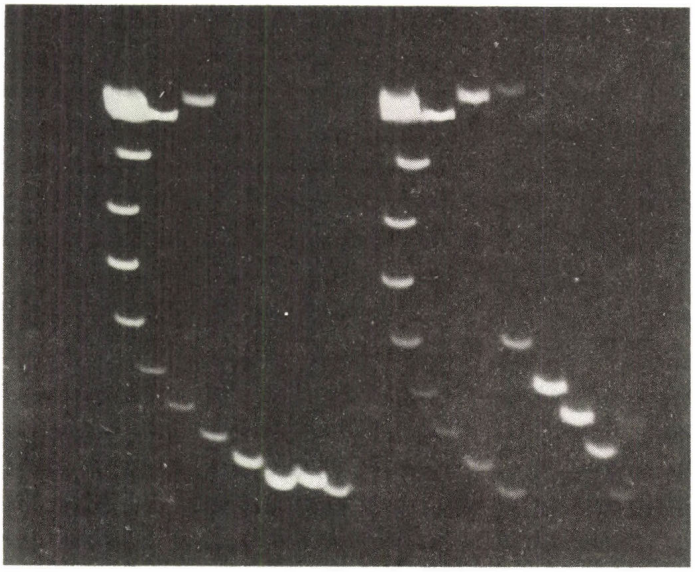

Figure 1

A typical two-dimensional gel electrophoresis pattern for DNA undergoing a superhelical stress-induced conformational transition (the pattern on the right). In the first direction (top to bottom) DNA moved under the tested conditions. In the second direction (left to right) the intercalating dye chloroquine was added. The dye relaxed the negative superhelicity and all alternative structures disappeared. As a result it was possible to calculate the number of each topoisomer. The pattern on the left shows a control experiment for DNA that cannot undergo any structural transition during electrophoresis.

Numerous studies indicate that homopurine-homopyrimidine sequences (such as $(GA)_n \cdot (TC)_n$ are very good substrates for the S1 endonuclease (Hentschel, 1982; Larsen and Weintraub, 1982; Weintraub, 1983; Cantor and Efstradiadis, 1984; Htun et al., 1984). Do these sequences form the cruciform or the Z form or some novel alternative structure? This is the most intriguing question in the field since long homopurine-homopyrimidine tracts are often met in eukaryotic DNA.

Very recently we have studied the problem with the aid of two-dimensional gel electrophoresis (Lyamichev et al., 1985). First of all we constructed a plasmid carrying a 509-bp-long fragment of sea urchin DNA. This fragment included the $(GA)_{16} \cdot (TC)_{16}$ stretch. With the aid of two-dimensional gel

electrophoresis and the S1 endonuclease mapping we have shown that the $(GA)_{16} \cdot (TC)_{16}$ stretch undergoes a sharp structural transition with increasing superhelicity. As in the cases of cruciform and Z form formation, the observed transition partly relaxed the superhelical stress. In contrast with the other two well-documented transitions, the observed transition strongly depended on pH (see Fig. 2).

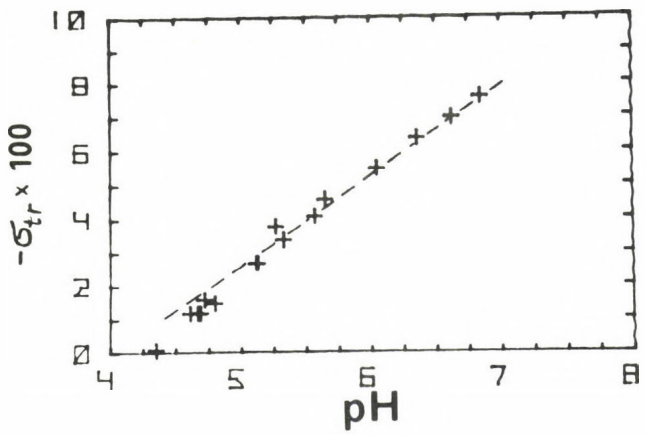

Figure 2

The pH dependence of the $-\sigma_{tr}$ value, the negative superhelical density of DNA corresponding to the transition midpoint.

The data in Fig. 2 clearly indicate that neither cruciform nor the Z form formation can be associated with the observed transition since the equilibrium between these structures and the B form is known to be pH-independent. We arrive at the conclusion that at high negative superhelicity and/or low pH a novel DNA structure is formed in homopurine-homopyrimidine regions. Lyamichev et al. (1985) called this structure the H form. A comprehensive quantitative analysis of the observed transition led Lyamichev et al. (1985) to the conclusion that the H form has the structure shown in Fig. 3.

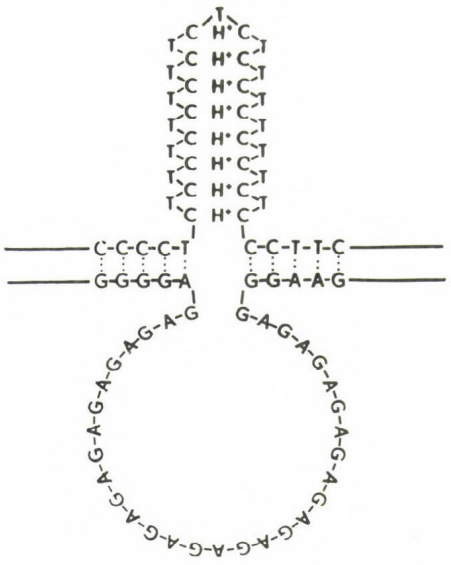

Figure 3

Model of the H form proposed by Lyamichev et al. (1985). The homopyrimidine strand forms stacked singly protonated C·C pairs with thymines looped out of the structure.

Proposing the structure in Fig. 3 Lyamichev et al. (1985) proceeded from the very important works by Gray, Ratliff and their coworkers who studied poly(TC) by CD and other methods. Having studied the yield of photodimers of different types Brown et al. (1985) presented conclusive evidence of the formation at low pH of stacked protonated C·C pairs with thymines looped out of the structure. On the other hand, Gray et al. (1984) demonstrated the formation of C·C+ pairs between antiparallel strands.

The proposed model of the H form makes it possible to explain the asymmetric cleavage by the S1 endonuclease of two DNA strands in the $(GA)_n \cdot (TC)_n$ tracts described by Htun et al. (1984). These authors reported that the homopyrimidine strand was cleaved only in the centre of the tract, whereas the homopurine strand was cleaved virtually throughout the tract. This is exactly what one could expect for the structure in Fig. 3.

Thus, the family of alternative structures which are formed in superhelical DNA has been enlarged by one more member. Now we know three such structures: the curciform formed in palindromic regions, the Z form formed primarily in alternating

purine-pyrimidine tracts and the H form formed in homopurine-homopyrimidine tracts.

Do alternative structures play any role in the functioning of DNA in the cell? At the moment we cannot answer this question. There are a lot of indications that the superhelical stress in vivo is, on the average, lower than in vitro. It is most probably due to this fact that attempts to observe alternative structures in vivo have failed. The available data indicate that alternative structures in vivo have failed. The available data indicate that alternative structures are not stable in vivo without complexing with special proteins. Such proteins shifting the equilibrium towards the formation of alternative structures have been extracted from eukaryotic cells in the case of the Z form (Rich et al., 1984). Among them the Rec1 protein from Ustilago is of the greatest interest since its ability to induce the B-Z transition explains the first stage of homological recognition during genetic recombination. Proteins specifically stabilising the cruciform and/or the H form still await discovery.

One can speculate that negative superhelicity, which dramatically increases the probability of spontaneous formation of alternative structures in DNA, greatly facilitates their recognition by specific proteins.

REFERENCES

Brown, D.M., Gray, D.M., Patrick, M.H. and Ratliff, R.L. (1985) Photochemical demonstration of stacked $C \cdot C^+$ base pairs in a novel DNA secondary structure. Biochemistry, 24, 1676-1683.

Cantor, C.R. and Efstratiadis, A. (1984) Possible structures of homopurine-homopyrimidine S1-hypersensitive sites. Nucl. Acids Res. 12, 8059-8072.

Courey, A.J. and Wang, J.C. (1983) Cruciform formation in a negatively supercoiled DNA may be kinetically forbidden under physiological conditions. Cell, 33, 817-829.

Frank-Kamenetskii, M.D. (1985) Fluctuational motility of DNA. In: Structure and Motion: Membranes, Nucleic Acids and Proteins. (E. Clementi, G. Corongiu, M.H. Sarma and R.H. Sarma, eds.) Adenine Press, pp. 417-432.

Frank-Kamenetskii, M.D. and Vologodskii, A.V. (1984) Thermodynamics of the B-Z transition in superhelical DNA. Nature, 307, 481-482.

Frank-Kamenetskii, M.D., Lukashin, A.V., Anshelevich, V.V. and Vologodskii, A.V. (1985) Torsional and bending rigidity of the double helix from data on small DNA rings. J. Biomol. Struct. Dyn. 2, 1005-1012.

Gray, D.M., Cui, T. and Ratliff, R.L. (1984) Circular dichroism measurements show that C C^+ base pairs can coexist with A T base pairs between antiparallel strands of an oligodeoxynucleotide double-helix. Nucl. Acids. Res. 12, 7565-7580.

Hagerman, P.J. (1981) Investigation of the flexibility of DNA using transient electric birefringence. Biopolymers, 20, 1503-1535.

Haniford, D.B. and Pulleyblank, D.E. (1983) Facile transition of poly(d(TG) d(CA)) into a left-handed helix in physiological conditions. Nature, 302, 632-634.

Hentschel, C.C. (1982) Homocopolymer sequences in the spacer of a sea urchin histon gene repeat are sensitive to S1 nuclease. Nature, 295, 714-716.

Horowitz, D.S. and Wang, J.C. (1984) Torsional rigidity of DNA and length dependence of the free energy of DNA supercoiling. J. Mol. Biol. 173, 75-91.

Htun, H., Lund, E., and Dahlberg, J.E. (1984) Human U1 RNA genes contain an unusually sensitive nuclease S1 cleavage site within the conserved 3' flanking region. Proc. Natl. Acad. Sci. USA, 81, 7288-7292.

Larsen, A. and Weintraub, H. (1983) An altered DNA conformation detected by S1 nuclease occurs at specific regions in active chick globin chromatin. Cell, 29, 609-622.

Lilley, D.M.J. (1980) The inverted repeat as a recognisable structural feature in supercoiled DNA molecules. Proc. Natl. Acad. Sci. USA, 77, 6468-6472.

Lyamichev, V.I., Panyutin, I.G. and Frank-Kamenetskii, M.D. (1983) Evidence of cruciform structures in superhelical DNA provided by two-dimensional gel electrophoresis. FEBS Lett. 153, 298-302.

Lyamichev, V., Panyutin, I. and Mirkin, S. (1984) The absence of cruciform structures from pAO3 plasmid DNA in vivo. J. Biomol. Struct. Dyn. 2, 291-301.

Lyamichev, I.V., Mirkin, S.M. and Frank-Kamenetskii, M.D. (1985) A pH-dependence structural transition in homopurine-homopyrimidine tract in superhelical DNA. J. Biomol. Struct. Dyn. (in press)

Mizuuchi, K., Mizuuchi, M. and Gellert, M. (1982) Cruciform structures in palindromic DNA are favoured by DNA supercoiling. J. Mol. Biol. 156, 229-243.

Panayotatos, N. and Wells, R.D. (1981) Cruciform structures in superhelical DNA. Nature, 289, 466-470.

Panyutin, I., Klishko, V. and Lyamichev, V. (1984) Kinetics of cruciform formation and stability of cruciform structure in superhelical DNA. J. Biomol. Struct. Dyn. 1, 1311-1324.

Panyutin, I., Lyamichev, V. and Mirkin, S. (1985) Structural transition in $d(AT)_n \cdot d(AT)_n$ inserts within superhelical DNA. J. Biomol. Struct. Dyn. 2, 1221-1234.

Peck, L.J. and Wang, J.C. (1983) The energetics of B to Z transition in DNA. Proc. Natl. Acad. Sci. USA, 80, 6206-6210.

Rich, A., Nordheim, A. and Wang, A.H.-J. (1984) The chemistry and biology of left-handed Z-DNA. Ann. Rev. Biochem. 53, 791-846.

Shore, D. and Baldwin, R.L. (1983a) Energetics of DNA twisting. I. Relation between twist and cyclization probability. J. Mol. Biol. 170, 957-981.

Shore, D. and Baldwin, R.L. (1983b). Energetics of DNA twisting. II. Topoisomer analysis. J. Mol. Biol. 170, 983-1007.

Sinden, R.R. and Pettijohn, D.E. (1984) Cruciform transitions in DNA. J. Biol. Chem. 259, 6593-6600.

Singleton, C.K. (1983) Effects of salt, temperature, and stem length on supercoil-induced formation of cruciforms. J. Biol. Chem. 258, 7661-7668.

Singleton, C.K. and Wells, R.D. (1982) Relationship between superhelical density and cruciform formation in plasmid pVH51. J. Biol. Chem. 257, 6292-6295.

Vologodskii, A.V. and Frank-Kamenetskii, M.D. (1982) Theoretical study of cruciform states in superhelical DNAs. FEBS Lett. 143, 257-260.

Vologodskii, A.V. and Frank-Kamenetskii, M.D. (1983) The relaxation time for a cruciform structure in superhelical DNA. FEBS Lett. 160, 173-176.

Vologodskii, A.V. and Frank-Kamenetskii, M.D. (1984) Left-handed Z form in superhelical DNA: a theoretical study. J. Biomol. Struct. Dyn. 1, 1325-1334.

Vologodskii, A.V., Lukashin, A.V., Anshelevich, V.V. and Frank-Kamenetskii, M.D. (1979) Fluctuations in superhelical DNA. Nucl. Acids Res. 6, 967-982.

Wang, A.H.-J., Quigley, G.J., Kolpak, F.J., Crawford, J.L., van Boom, J.H., van der Maler, G. and Rich, A. (1979) Molecular structure of a left-handed double helical DNA fragment at atomic resolution. Nature, 282, 680-686.

Wang, J.C., Peck, L.J. and Becherer, K. (1983) DNA supercoiling and its effects on DNA structure and function. Cold Spring Harbor Symp. Quant. Biol. 47, 85-91.

Weintraub, H. (1983) A dominant role for DNA secondary structure in forming hypersensitive structures in chromatin. Cell, 32, 1191-1203.

Dynamics of Biochemical Systems
S. Damjanovich, T. Keleti, L. Trón (Eds)

CONFORMATIONAL FLUCTUATIONS, THERMAL STABILITY AND HYDRATION OF PROTEINS. STUDIES BY HYDROGEN EXCHANGE KINETICS

ANDREAS ROSENBERG and BÉLA SOMOGYI*

Department of Laboratory Medicine and Pathology, University of Minnesota, Minneapolis, Minnesota 55455, USA

*Permanent address: Department of Biophysics, University Medical School, 4012 Debrecen, Hungary

We are at present aware of three experimentally described types of dynamic behavior characteristic for protein molecules: 1) Reversible thermal unfolding being the best known and most studied of the three. The equilibrium is between the native, globular structure and a far more disroganized state that more or less resembles the time averaged structure of the random coil of a synthetic long chain polypeptide. Efforts have been made to separate the total net energy of stabilization into component parts of which hydrogen bond formation, sidechain solvation and electrostatic interactions are the best understood. 2) Fluctuations of structure. A small system represented by the assembly of atoms constituting a macromolecule is expected to show energy, and density fluctuations which are not negligible (Cooper, 1984). The corresponding time dependent structural changes are less well understood. They can be described within several frames of reference. The deviations from average three dimensional coordinates allow description in terms of amplitudes, "flexibility of chain" (Huber and Bennett, 1983). In dimensionless energy terms the form of the distribution function for energy terms describes the contributions from inter- and intrastate fluctuations. In kinetic terms the same movements are characterized by relaxation times and relaxation time spectra. 3) Most of the properties of a protein molecule are profoundly influenced by its state of hydration. The dehydrated molecule has no biological activity (Rupley et al., 1983). The hydration equilibria are often described in terms of hydrophobic and hydrophilic hydration and expressed as protein/water weight ratio. These equilibria are presumably coupled to most of protein reactions. At the same time the bound water is characterized by abnormal vapor pressure. The object of this paper is to show that methods are available allowing the investigation of the relationships among these three phenomena.

The cooperative thermal unfolding equilibrium per se has not been implicated in the biological function, although it is true that during protein synthesis the nascent chain has to undergo a folding reaction. The overwhelming majority of evidence at hand suggests that the native structure represents a free energy minimum and the chain spontaneously refolds itself from the unfolded state. As a consequence the thermodynamic parameters obtained from the study of unfolding define the forces responsible for maintaining the unique, native three dimensional structures. Careful thermal studies of unfolding have shown (Lumry et al., 1966) that in many cases the transition can be described by a two-state model. This does not mean that unfolding or refolding take place in one step but that the concentration of possible intermediate forms is negligible, compared to the concentration of the end states. This observation, of course, does not hold for all proteins, especially in case of multisubunit, multidomain proteins for which the unfolding sequence can show many separate steps (Privalov, 1982). The free energy associated with stability is the net sum of large and compensatory changes in enthalpy and entropy. The magnitude of the free energy change associated with unfolding, 1-10 kcal, reports that the native structure is marginally stable under biologically significant conditions. Marginal in the sense that we are near enough to the transition region so that the probability of a molecule to be found in the unfolded state, although very small, is not negligible. Although voluminous literature exists describing the probable sources of free energy stabilization in terms of hydrogen bonds, sidechain solvation and electrostatic interactions, our interest here is to develop an argument for linking experimentally the unfolding reaction to the thermodynamic fluctuations around the native state.

Studies of the kinetics and relaxation time spectra of the unfolding reaction have led to the proposal (Tsong, 1982) that every step of the overall reaction representing the unfolding of either the whole molecule or a domain or subunit takes place via two linked consecutive reactions: a rapid initial change representing a more subtle conformational rearrangement followed by the unfolding of the chain on much slower time scale.

The nature of the first step is not so well understood, it represents the adjustment of the native, average state to a new state corresponding to the conditions imposed. It also represents a shift of the free energy minimum towards the transition state. It stands to reason that if the first step is on the path towards the transition state for unfolding it could be compared to the nucleation step in many phase changes. The average of the

native state is shifted and the molecule is sampling more of the states where the number of broken bonds increases until the critical nucleation size, the transition state is reached. The endstates of these thermodynamically predictable fluctuations represent structures of more disordered and solvent accessible nature. It has to be stressed here that this is not a state we usually associate with partial unfolding which is generally considered to involve unfolding of a part of the protein to a state past the transition state and more similar to the unfolded state. We suggest that it is the fluctuations between the transition state analogues that the relaxation measurements of Tsong observe in the fast time range (Tsong, 1982). Regardless of the problems associated with these detailed studies the experimental evidence allows us to describe a tentative model of stability and structural movements. At low temperatures the fluctuations sampled around the native state are predominantly of a non-cooperative nature and of small amplitudes. At higher temperatures larger amplitude and more cooperative fluctuations become more probable. In the transition state region the intrastate fluctuations are complemented by the interstate fluctuation giving rise to large heat capacity changes. Thus the intrastate fluctuations, experimentally observed, are linked to the stability and interstate equilibria.

The model proposed has a quantitative basis in the statistical mechanical treatment of protein unfolding developed mainly by Ikegami (Ikegami, 1981). In this and other similar treatments (Cerf, 1978) the approach is to assume that a homogeneous field of interaction energy exists making all bonds identical, each representing the average interaction energy. Such a mean field simplification of Weiss type allows qualitative predictions about the thermal phase equilibrium but it gives little additional information. The important point emerging from this statistical-mechanical model of denaturation is its possible extension to the case of time dependence. The model predicts that as the temperature increases the native state, a metastable one in our case, relaxes to the stable state at the new temperature (the unfolded one) exhibiting two relaxation times. The first one characterises a very fast process associated with a nucleation type of phenomena followed by a slower process corresponding to the well known unfolding step. The first step, the fast one, is an intrastate rearrangement shifting towards the transition state, the words used to describe it are pretransition, nucleation. We have thus theoretical grounds to believe that the native structure stabilized by the cooperative network of bonds undergoes fluctuations along the reaction coordinate (arrow B in Fig. 1).

These fluctuations are similar to the shift in the energy minimum of the native state at increased temperature, arrow A in Figure 1. A clear relationship is thus established between the thermal unfolding reaction characterizing the thermal stability of the protein and the intrastate fluctuations of the native state at lower temperatures. The role of hydration in these arguments and observations is great. The thermal stability and unfolding enthalpy increase and decrease rapidly when the protein is dehydrated (Fujita and Noda, 1981). The biological activity and conformational fluctuations are as a rule (Rupley et al., 1983) restored at lower levels of hydration than the thermal stability is. This points to preferential interaction of water with the unfolded form. In principle it can be stated that without hydration conformational transitions, both intrastate and interstate are not possible. Solvation reactions are thus linked to the structural transition.

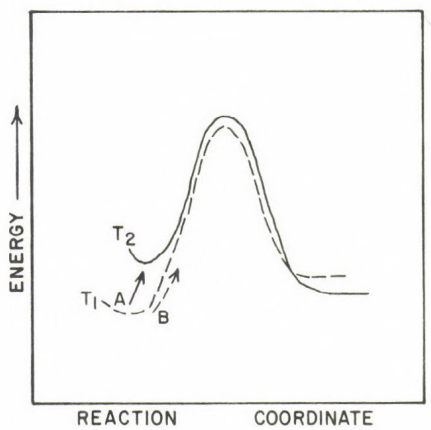

Figure 1.

Schematics of the energy balance for transition state kinetics.

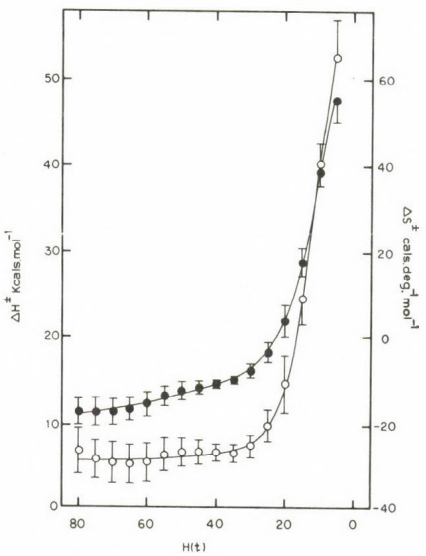

Figure 2.

Average enthalpy (•) and entropy (o) of activation for lysozyme as a function of H(t), hydrogens remaining unchanged at 298 K. From Gregory et al., 1982.

We ask now what evidence do we have to support our model. One of the methods first used to detect fluctuations within the native macrostate was

hydrogen exchange kinetics and most of our investigations have used this method. The exchange reaction CONH + HOH^* ⇄ $CONH^*$ + HOH catalyzed by both hydrogen and hydroxyl ions has an apparent first order rate constant expressed as follows

$$k_{ex} = k_o + k_H (H) + k_{OH} (OH) \quad (1)$$

where k_o stands for water catalysis. The different peptide and sidechain groups on a polypeptide chain exchange in the unfolded state with rates differing somewhat due to the different electrostatic interactions with the nearest neighbors. For most purposes it is sufficient to use an average rate constant $\langle k_{ex} \rangle$. If we investigate an exchanging site found in the globular, native state of the protein we find that the rate is greatly attenuated. We can express the new rate as

$$k_{app} = \beta \langle k_{ex} \rangle \quad (2)$$

The constant β is the structural attenuation factor which contains information about fluctuations and stability. The temperature dependence of the apparent rate constant k_{app} contains both the enthalpy of activation for $\langle k_{ex} \rangle$ a known quantity and temperature dependence of the conformational process. Figure 2 shows the activation energies and entropies for exchange from lysozyme plotted as a function of H_{rem} a quantity representing the point in the complex curve for which the activation energy is calculated. The extraction of average activation energies from a sum of first order reactions is possible because of the extreme spread of the rate constants (8-9 magnitudes). Figure 2 shows as expected an increase in enthalpy because the variable H_{rem} is inversely proportional to the average rate constant at each point. What, however, is more important is that there are indications that the function as depicted is a composite of two functions, one with a moderate slope in the region of low activation energies and a steep function dominating the region of high activation enthalpies, the latter presumably being responsible for the larger more cooperative motion reaching high on the right hand side of the potential well in Figure 1. The most interesting thing, however, is that the unfolded state of the interstate transition, the classical unfolding reaction seems to contribute little to the exchange. For any residue with such a dominating exchange pathway it can easily be shown (Barksdale and Rosenberg, 1982) that.

$$\Delta H^{\ddagger}_{app} = \Delta H^{\ddagger}_{ex} + \Delta H_o \quad (3)$$

The average contribution by $\Delta H^{\ddagger}_{ex}$ is quite well known (Gregory and Rosenberg, 1983) and precise values for ΔH_o are available in literature. Values for the apparent activation energy in Figure 2 never reach values indicative for major contributions by the pathway represented by Eq. (3).

The earlier models for hydrogen exchange (Barksdale and Rosenberg, 1982) associating the high enthalpy exchange with thermal unfolding were based on data not yet of sufficient quality to detect the consistently lower enthalpies. We would like to stress that of course the thermal unfolding does contribute to exchange in the transition region but the competition from intrastate fluctuations of considerable cooperativity and amplitude dominates the exchange. This is in good qualitative agreement with Ikegami's model and our hydrogen exchange data. Tsong argues further that the rapid relaxation should be a structural one in the native state possibly associated with solvent penetration into the protein matrix. Enthalpy and entropy pairs are plotted for a series of H_{rem} values in Figure 3.

The linear portions of the plot, described by $\Delta H^{\ddagger} = a + b\Delta S^{\ddagger}$ are often referred to as the compensation plot. Such an extrathermodynamic relationship is not part of the thermodynamic system of axioms and laws and represents a purely observational phenomenon. The presence of such a plot, however, is an indicator for the existence of certain common properties for the series of reactions differing in the discontinuous variable (Lumry and Rajander, 1970; Eftink et al., 1983; Lumry and Gregory, 1985). The ΔH or ΔS plot, however, might result in a linear relationship with a slope close to the experimental temperature even without the existence of compensation. This is due to the statistical nature of the errors in the two variables and can be avoided by using the Krug plot which is the plot of ΔH agains ΔG. It can be shown that the Krug plot then also results in a straight line with a slope of $b/(b+T)$, where T is the experimental temperature. In our specific case we have to interpret not one linear function but two, each representing about half of the indexed points.

In order to use the parameters a and b provided by the above relationship, we have to establish models for the reaction and show that the reaction schemes representing these models can lead to linear relationships. Hopefully, we should also be able to predict the behavior of our functions when new variables are introduced.

In search for a simple first model we observe that similar values for the slope b (often called T_c) equal to 360^{o} are observed for a series of conformational transitions in proteins (Gregory et al., 1982). The simplest

model for our reaction is the mandatory coupling model of Eftink et al. (1983) used for the study of ligand binding to proteins. We assume thus that the exchange reaction is coupled to a conformational equilibrium according to

$$N \underset{k_2}{\overset{K_{eq}\ k_1}{\rightleftharpoons}} A \xrightarrow{k_3} \text{Exchange} \qquad (4)$$

N represents the nonaccessible and A the accessible state. The scheme is formally identical with the Carlsberg mechanism. For $k_2 >> k_3; k_1$ it can be shown that the measured rate constant is $k_{app} = K_{eq} k_3$. Proceeding now in a similar fashion as Eftink and Ghiron did using the absolute rate theory for any observed, apparent rate constant we write

$$k_{app} = (kT/h) k_3^{\ddagger} K_{eq} \qquad (5)$$

$$R\ln k_{app} = R\ln(kT/h) + R\ln k_3^{\ddagger} + R\ln K_{eq} \qquad (6)$$

Taking the derivative of $R\ln k_{app}$ we arrive at:

$$\Delta H^{\ddagger}_{app} = RT + \Delta H^{\ddagger}_3 + \Delta H_{eq} \qquad (7)$$

We will return to Eq. (6), multiplying both sides with -T and taking a derivative in respect to T

$$\Delta S^{\ddagger}_{app} = R(1 + R\ln T + \ln R/h) + \Delta S^{\ddagger}_3 + \Delta S_{eq} \qquad (8)$$

If we multiply Eq. (8) with -T and combine it with 7 we can rearrange it for constant temperature as

$$\Delta H^{\ddagger}_{app} = \text{Constant} + p\Delta G_o + T\Delta S^{\ddagger}_{app} \qquad (9)$$

Equation 9 is the same form as equations shown by Eftink and Biltonen to yield compensation plots when p is the extrathermodynamic variable. In other words the rates for the points in the range of the linear plot with a slope of 360^{o} are determined by the size of the conformational contribution expressed for the sake of convenience by a multiplier p and an imaginary minimal free energy increment ΔG_o. We have thus two relationships

$$\Delta H^{\ddagger}_{app} = A + \Delta G^{\ddagger}_3 + p\Delta G_o + T\Delta S^{\ddagger}_{app} \qquad (10)$$

$$\Delta H^{\ddagger}_{app} = a + b\Delta S^{\ddagger}_{app} \qquad (11)$$

The subscript app as before refers to the experimentally obtained values.

For the above equations to be valid certain restrictions have to exist. By comparing the corresponding terms we see that if we assume

$$a = A + \Delta G_3^{\ddagger} + p\Delta G_o \qquad (12)$$

the right hand side of the Eq. (12) must remain constant for a limited range. This is true if the $\Delta\Delta$ term (the $\Delta\Delta$ term to be used below refers to change of quantities over the linear range of index points) of $p\Delta G_o$ is small compared to $A + \Delta G_3^{\ddagger}$. A small value for $p\Delta G_o$ is characteristic for a process where the large changes in enthalpy and entropy in Eqs. (7, 8) compensate each other. The $\Delta G_3^{\ddagger}$ for poly-DL-alanine at pH 7 is around 19 kcal (Gregory et al., 1982). The magnitude of $\Delta\Delta p\Delta G_o$ can from our experimental data be estimated as 1.5 kcal at most. The simulations by Eftink and Biltonen show that a 6 % change in the conformational free energy contribution still results in a straight line when data are plotted according to Eq. (11). The precision of our measurements would not allow us to easily see deviations from straight line behavior until $\Delta\Delta p\Delta G_o$ moves into the range of 3 kcal. Having included the varying free energy term into the constant a the constant b will represent the experimental temperature.

We conclude that the apparent compensation plot with a slope corresponding to a compensation temperature of 360^{o} can be explained by the coupling of the exchange process to a conformational equilibrium. As a test for such an assignment we will predict the effect of glycerol addition on the behavior of the compensation plot. Glycerol as a rule stabilizes the native compact conformations of proteins by way of preferential interaction (Gekko and Timasheff, 1984). Such a shift of stability will appear in the $p\Delta G_o$ term, however the $\Delta\Delta p\Delta G_o$ term should show little change. We would thus expect a shift due to the change in absolute value but very little change in slope. As seen in Figure 3 the effect of 5 M glycerol on exchange from lysozyme follows the predicted pattern.

To find a reasonable model for the line representing the fastest hydrogens is somewhat more difficult, the values for the slope, $b,=T_c$ are very high. It is at once evident that mandatory or non-mandatory couplings to some equilibrium involving conformational process are unlikely. The observed values for $\Delta S^{\ddagger}$ and $\Delta H^{\ddagger}$ do not correspond to conformational equilibria. Let us assume that a fast equilibrium, compared to exchange, still exists for the distribution of reactants between the solution and the protein phase, thus Eq. (5) and the transition state approximation still hold only if K_{eq} is now a much smaller number related to the equilibrium of broken

and non broken hydrogen bonds and to the first approximation similar to all the sites in the region represented by the large b. The difference in observed rate lies in k_3 which for our model is dependent both on visosity and orientation factors. For the slower sites the dominating factor was the probability of a structural transition and differences in k_3 we discuss now, although present, did not dominate the observed enthalpy values.

$$k_{3,i} = A_i/\eta d^{-\Delta G^{\ddagger}_3/RT} = A_i/\eta_{oi}\, e^{-\Delta G^{\ddagger}_{\eta_i}/RT}\, e^{-\Delta G^{\ddagger}_3/RT} \qquad (13)$$

The term $G^{\ddagger}_{\eta_i}$ is associated with the surmounting of the barriers for reactant transport within the domain (Beece et al., 1980). A and η_{oi} represent the steric factors and frequency as well as damping. This expression inserted into $k_{app} = K_{eq} k_3$ and derivatives taken in respect to 1/T and T as before lead to the following expressions for the activation enthalpy and entropy observed.

$$\Delta S^{\ddagger}_{app,i} = \Delta S_{eq} + \Delta S^{\ddagger}_3 - R\ln\frac{A_i}{\eta_{oi}} + \Delta S^{\ddagger}_{\eta o} = \Delta S_{eq} + \Delta S^{\ddagger}_3 + \Delta S^{\ddagger}_{\eta i} \qquad (14)$$

$$\Delta H^{\ddagger}_{app,i} = \Delta H_{eq} + \Delta H^{\ddagger}_3 + \Delta H^{\ddagger}_{\eta} \qquad (15)$$

We adopt now the simplest model where packing density provides a change in the n indexed components for enthalpy and entropy according to the following: $\Delta H^{\ddagger}_{\eta} = \Delta H^{\ddagger}_{\eta o} + \alpha_i h$ and $\Delta S^{\ddagger}_{\eta} = \Delta S^{\ddagger}_{\eta o} + \beta_i S$. We insert these expressions into Eqs. (14, 15), combine and rearrange as previously for Eqs. (7, 8 and 9).

$$\Delta H^{\ddagger}_{app,i} = A + \alpha_i h + T\beta_i S + T\Delta S^{\ddagger}_{app,i} \qquad (16)$$

The middle term in Eq. (16) represents the extra quantity varying with index. We know from the data in Figure 3 that in this case the variation term is large enough not to be neglibible compared to A in Eq. (16). Linearity in such conditions can be observed over limited range. Comparing Eq. (16) with the standard compensation plot $\Delta H^{\ddagger} = a + b\Delta S^{\ddagger}$ for the corresponding terms we can write

$$a = A \qquad b = \frac{\alpha_i h + T\beta_i S}{\Delta S^{\ddagger}_{app,i}} + T \qquad (17)$$

At larger values of the two $\Delta\Delta$ terms, $\alpha_i h$ in the range we consider is negative and so is $\Delta S^{\ddagger}_{app,i}$. Consequently the first term in expression for b is positive and b>T. The effect of glycerol is much more difficult to predict. We see from Figure 3 that both the constant term A and the slope change. We know that the presence of glycerol will influence the bond

breaking equilibrium K_{eq}. We cannot predict the direction of all the terms in the presence of glycerol. Data for bond breaking thermodynamics in such solutions are not available. Thus all we can say is that the effect of glycerol does not contradict our second model that accounts for the higher value for b. Also a high value for b has been found for hydration equilibria of proteins, a process directly related to motility of sidechains (Lüscher-Matli and Ruegg, 1982; Schinkel et al., 1985).

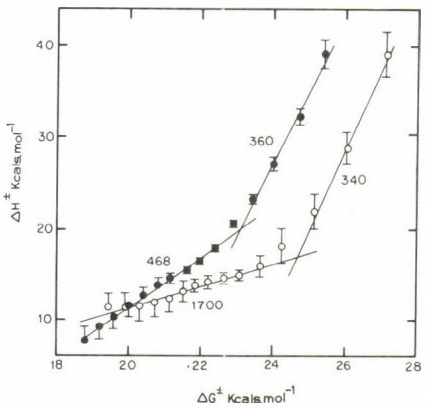

Figure 3.

Enthalpy-Free energy compensation plot $\langle \Delta H^{\ddagger} \rangle$ as a function of $\langle \Delta G^{\ddagger} \rangle$ without glycerol (•) and with 5 M glycerol (o), at 298 K. From Gregory et al., 1985, submitted.

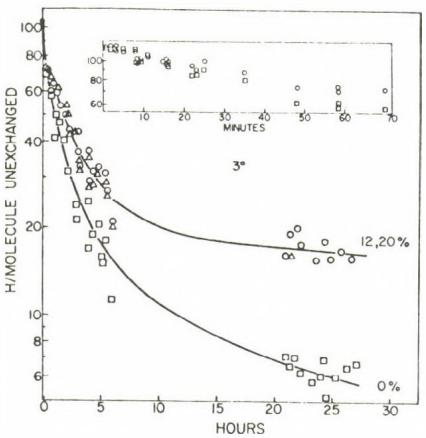

Figure 4.

Out-Exchange kinetics of tritiated trypsin at pH 2 in presence and absence of ethanol. From Woodward et al., 1975.

We have thus reasonable evidence to suggest that the rate of the observed exchange of slower hydrogens is determined by a conformational equilibrium between nonaccessible and more accessible state. The evidence from the enthalpy values here and previously published (Gregory et al., 1982) would indicate that the equilibrium is not identical with the thermal unfolding processes. Whether the difference between accessible and non-accessible state lies in unfolding of a chain segment into solvent or melting and hydration of section in situ represents rather a semantic than physical difference. The important point is that a structural equilibrium is present, an equilibrium where breaking of the hydrogen bond structure represents the

rate determining function in the exchange process.

The rate process for the fastest hydrogens is not dominated by breaking of structures but by a tortuous path type of a transportation process linked to internal and external viscosity.

Experiments on hydrogen exchange in the presence of 10-20 % ethanol (Woodward et al., 1975) give further support for two rate limiting steps. We know that at low temperature ethanol in this concentration range acts similarily to glycerol (Velicelebi and Sturtevant, 1979) but has little viscosity. Our models would predict that the fastest hydrogen would show little effect of ethanol addition whereas the slower ones should be influenced profoundly. This is the actual case as seen in Figure 4.

The data and the models proposed show that hydrogen exchange kinetics combined with study of stability and the effects of viscosity allow some insight into the nature of fluctuations and their relationship to solvent.

(Supported by NSF-PCM 8303027)

REFERENCES

Barksdale, A.D., and Rosenberg, A. (1982) Acquisition and interpretation of hydrogen exchange data from peptides, polymers and proteins. Methods of Biochem. Anal. 28, 1-113.

Beece, D., Eisenstein, L., Frauenfelder, H., Good, D., Mardeu, M.C., Reinisch, L., Reynolds, A.H., Sorensen, L.B., and Yue, K.T. (1980) Solvent viscosity and protein dynamics. Biochemistry, 19, 5147-5157.

Cerf, R. (1978) Molecular field theory of reversible unfolding of biopolymers. Proc. Natl. Acad. Sci. USA, 75, 2755-2758.

Cooper, A. (1984) Protein fluctuations and the thermodynamic uncertainty principle. Prog. Biophys. Molec. Biol. 44, 181-214.

Eftink, M.R., Anusiem, A.C., and Biltonen, R. (1983) Enthalpy-entropy compensation and heat capacity changes for protein ligand interactions: General thermodynamic models and data for the binding of nucleotides to ribonuclease A. Biochemistry, 22, 3884-3896.

Fujita, Y., and Noda, Y. (1981) Effect of hydration on the thermal stability of protein as measured by differential scanning calorimetry. Int. J. Peptide Protein Res. 18, 12-17.

Gekko, K., and Timasheff, S.N. (1981) Thermodynamic and kinetic examination of protein stabilization by glycerol. Biochemistry, 20, 4677-4686.

Gregory, R.B., Knox, D.G., Percy, A.J., and Rosenberg, A. (1982) Thermodynamics of structural fluctuations in lysozyme as revealed by hydrogen exchange kinetics. Biochemistry, 24, 6523-6530.

Huber, R., and Bennett, Jr., W.S. (1983) Functional significance of flexibility in proteins. Biopolymers, 22, 261-279.

Ikegami, A. (1981) Statistical thermodynamics of proteins and protein denaturation. Adv. Chem. Physics, 46, 363-413.

Lumry, R., Biltonen, R., and Brandts, J.F. (1966) Validity of the "two-state" hypothesis for conformational biopolymers. Biopolymers, 4, 917-944.

Lumry, R., and Rajender, S. (1970) Enthalpy-entropy compensation phenomena in water solutions of proteins and small molecules. A ubiquitous property of water. Biopolymers, 9, 1125-1227.

Lumry, R., and Gregory, R. (1986) Free energy management in protein reactions; concepts, complications and compensation. in The Fluctuating Enzyme. Welch, G.R. ed., Wiley-Interscience, New York, in press.

Lüscher-Matte, M., and Ruegg, M. (1982) Thermodynamic functions of biopolymer hydration II. Enthalpy-entropy compensation in hydrophilic hydration processes. Biopolymers, 21, 419-429.

Privalov, P.L. (1982) Stability of proteins. Proteins which do not present a single cooperative system. Adv. Prot. Chem. 35, 1-104.

Rupley, J.A., Gratton, E., and Careri, G. (1983) Water and globular proteins. Trends in Biochem. Sci. 8, 18-28.

Schinkel, J.E., Downer, N.W., and Rupley, J.A. (1985) Hydrogen exchange of lysozyme powers hydration dependence of internal motions. Biochemistry, 24, 352-366.

Tsong, T.Y. (1972) Viscosity-dependent conformational relaxation of ribonuclease A in the thermal unfolding zone. Biochemistry, 21, 1493-1498.

Velicelebi, G., and Sturtevant, Y.M. (1979) Thermodynamics of the denaturation of lysozyme in alcohol-water mixtures. Biochemistry, 18, 1180-1186.

Woodward, C.K., Ellis, L.M., and Rosenberg, A. (1975) The solvent dependence of hydrogen exchange kinetics of folded proteins. J. Biol. Chem. 250, 440-444.

Dynamics of Biochemical Systems
S. Damjanovich, T. Keleti, L. Trón (Eds)

PROTEIN DYNAMICS AS REVEALED BY FLUORESCENCE QUENCHING

BÉLA SOMOGYI* and ANDREAS ROSENBERG

Department of Laboratory Medicine and Pathology, University of Minnesota, Minneapolis, Minnesota 55455, USA

*Permanent address: Department of Biophysics, University Medical School, 4012 Debrecen, Hungary

The dynamic properties of protein molecules, like intramolecular fluctuations of thermodynamic functions, etc., seem to play an important role in the function of proteins (Gurd & Rothgeb, 1979; McCammon & Karplus, 1980; Somogyi et al., 1984a). In the wide spectrum of the different physical methods, fluorescence spectroscopy proved to be a successful one in studying protein dynamics (Lakowicz & Weber, 1973;Eftink & Ghiron, 1975, 1977; Barboy & Feitelson, 1978; Hevessy et al., 1981; Somogyi et al., 1984b; Matko et al., 1984; Jameson et al., 1984).

The subject of the present paper is to show how the quenching of protein fluorescence can be related to and used to obtain information about protein dynamics.

In general case, the excited state of a fluorophore can decay by a few competing and independent pathways:

$$\begin{aligned} &\text{a)}\ A^* \xrightarrow{k_f} A + h\nu \\ &\text{b)}\ A^* \xrightarrow{k_o} A + \text{heat} \\ &\text{c)}\ A^* \xrightarrow{k_+[Q]} A{:}Q \end{aligned} \qquad (1)$$

Here A* and A are the excited and ground state of the fluorophore, k_f is the rate constant of the decay by photon emission, $h\nu$, k_o is the sum of rate constants of processes like local quenching (caused by the neighboring solvent molecules or residues in the case of a protein), and $k_+[Q]$ is the rate constant of decay caused by the collision of the fluorophore in the excited state and a quencher molecule being present in concentration [Q]. (The presence of static quenching, which is due to the complex formation between A and Q, is disregarded here).

On the basis of scheme (a), the average lifetime of the excited state τ can be obtained as:

$$\tau = (k_f + k_o + k_+[Q])^{-1}. \qquad (2)$$

Since the fluorescence intensity measured in steady state circumstances (continuous, relatively low level excitation) is proportional to this lifetime, it is easy to show that the ratio of the fluorescence intensities obtained without and with the presence of quencher Q is described by:

$$\frac{F_o}{F} = 1 + k_+\tau_o[Q], \qquad (3)$$

the Stern-Volmer equation, where F_o and F are the fluorescence intensities in the absence and the presence of quenching, τ_o is the average lifetime when Q=0 and:

$$k_+\tau_o = K_{sv} \qquad (4)$$

is the Stern-Volmer constant. When only $\alpha(<1)$ fraction of the fluorophores are accessible to the quencher, the modified Stern-Volmer or Lehrer equation is useful to analyze the quenching data (Lehrer, 1971):

$$\frac{F_o}{\Delta F} = \frac{F_o}{F_o - F} = \frac{1}{\alpha} + \frac{1}{\alpha K_{sv}} \frac{1}{[Q]}. \qquad (5)$$

During the derivation of the above equations, it is assumed that every collision of the quencher is effective, i.e. we are dealing with "strong" quencher, otherwise K_{sv} contains one additional factor, $0<\gamma<1$, characteristic of how effective the given quencher is. Equation (5) is the usual form applied for the study of protein fluorescence, when part of the emitted light originates from fluorophores (like tryptophan, tyrosine, etc. residues)buried inside the macromolecule. While studying quenching of protein fluorescence, two main problems arise:

1) The proteins usually contain both external (located on or close to the surface) and internal (not exposed to the solvent) fluorophores. In the case of applying ionic quencher, this problem diminishes since these quenchers, just by being strongly charged, can quench only the external fluorophores. In the case of a neutral quencher (like oxygen, acrylamide, etc.) however, the simultaneous quenching of both types of fluorophores occurs

resulting in serious difficulties of how to interpret the "average" quenching constants obtainable. To overcome this problem, it is required to have the separate quenching parameters for the two classes. Such a method will be described here as "double quenching."

2) In contrast to the interpretation of K_{SV} (or k_+ characteristics of the quenching of model compounds like tryptophan, etc., in simple solvent, the detailed molecular description of k_+, and therefore the interpretation of K_{SV}, is not straightforward for proteins. For external fluorophores, there are two possibilities: they are either permanently exposed to the solvent and therefore to the quencher as well, or their transient exposure is controlled by some kind of gating provided by the surface dynamics of the protein, i.e. by the motion of the neighboring groups (McCammon & Northrup, 1981; Szabo et al., 1982). Regarding the internal fluorophores, again there are two different possible mechanisms to account for the quenching. First, like the hydrogen exchange, here the reactants (the excited fluorophore and the quencher) can come into contact (resulting in quenching) either by the transient exposure of the fluorophore to the solvent (partial unfolding) (Englander & Kallenbach, 1984) or by a mechanism in which the quencher penetrates the protein body as it is shown for the case of oxygen (Calhoun et al., 1983; Hagaman & Eftink, 1984). Obviously, depending on which mechanism is involved in the actual quenching, the information contained by K_{SV} will be different.

According to the above, to learn more about protein dynamics, it is necessary to develop appropriate models like the one describing oxygen penetration (Gratton et al., 1984; Jameson et al., 1984). The alternative model, compared to the penetration, has been developed (Somogyi et al., 1985) and will also be described here.

The method of "double quenching"

With one independent variable, the quencher concentration, a linear relationship seen in Eq. (5), yields two parameters α and K_{SV}. If we desire to resolve the mechanism in further detail by characterizing the quenching constants and accessibility for the two main classes of

fluorophores, the external and internal, we have to increase the number of variables. One way to do this is to simultaneously apply two quenchers showing the selectivity in their ability to quench (Somogyi et al., 1985). One of the quenchers should be specific (like I^-, Cs^+, etc.), being able to quench only the external fluorescence, while the other one should be nonspecific (like oxygen or acrylamide). According to the above, let us consider a protein having three classes of fluorophores: a) external, b) internal and quenchable by the nonspecific quencher only, and c) non-quenchable. The fluorescence intensities F_{oe} ($=\alpha F_o$), F_{oi} ($=\beta F_o$) and F_{on} ($=\gamma F_o$) then add up to F_o, the total intensity. Therefore:

$$\alpha + \beta + \gamma = 1. \tag{6}$$

By then using the exact proportionality between the lifetime and fluorescence intensity, and the additivity of fluorescence, one can arrive at:

$$\frac{F_{1,2}}{F_o} = \frac{\alpha}{1+K_{1e}[Q_1]+K_2[Q_2]} + \frac{\beta}{1+K_{1i}[Q_1]} + \gamma, \tag{7}$$

where $F_{1,2}$ is the total fluorescence intensity in the presence of the two quenchers with concentration of $[Q_1]$ for the nonspecific quencher and $[Q_2]$ for the specific one. The K_{1e}, K_{1i} and K_2 are the appropriate Stern-Volmer constants being assigned according to the indexes. It is then obvious, that for the total fluorescence intensities, F_1, measured in the presence of Q_1 and the absence of Q_2, one obtains (by inserting $[Q_2] = 0$ into Eq. (7)):

$$\frac{F_1}{F_o} = \frac{\alpha}{1+K_{1e}[Q_1]} + \frac{\beta}{1+K_{1i}[Q_1]} + \gamma. \tag{8}$$

Combining Eqs. (7) and (8):

$$\frac{F_o}{\Delta F} = \frac{F_o}{F_1-F_{1,2}} = \frac{1+K_{1e}[Q_1]}{\alpha} + \frac{\{1+K_{1e}[Q_1]\}^2}{\alpha K_2}\,\frac{1}{[Q_2]}. \tag{9}$$

Equation (9) shows that by keeping $[Q_1]$ constant and varying $[Q_2]$, the plot of $F_o/\Delta F$ as $1/[Q_2]$ results in a straight line with intercept and slope depending on $[Q_1]$ (see Fig. 1). It should be noted that when $[Q_1]= 0$, Eq. (9) reduces to the modified Stern-Volmer plot for quencher No. 2. Therefore, two parameters out of the six (α and K_2) can be obtained from a titration in the absence of Q_1.

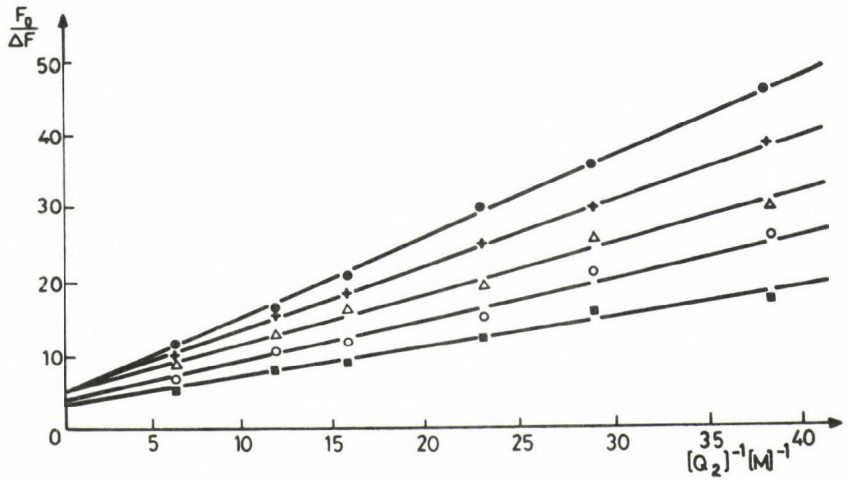

Figure 1. The quenching of lysozyme by iodide (Q_2) in the presence of acrylamide (Q_1) plotted according to Eq. (5). The acrylamide concentrations were: no acrylamide x-x-x, 0.1 M O-O-O, 0.2 M Δ-Δ-Δ, 0.3 M +-+-+, 0.4 M ●-●-●. The concentration of iodide was varied from 0 to 0.18 M. The buffer was on all occasions 50 mM phosphate, pH 7.0, containing 0.1 mM $Na_2S_2O_3$ (to prevent I_3 formation). The excitation wavelength was 297 nm and the emission was monitored at 337 nm. The bandwidth of 5 nm was used in all measurements. The temperature was kept constant at 303 ± 0.1 K. The accessibility and quenching constant characteristic of I^- was calculated from the lowest curve as $\alpha = 0.33$ and $K_2 = 8.13\ M^{-1}$.

To proceed further, a secondary plot should be used by plotting the square roots of slopes, $\xi^{1/2}$, against $[Q_1]$ (see Figure 2):

$$\xi^{1/2} = \frac{1}{(\alpha K_2)^{1/2}} + \frac{K_{1e}}{(\alpha K_2)^{1/2}} [Q_1]. \qquad (10)$$

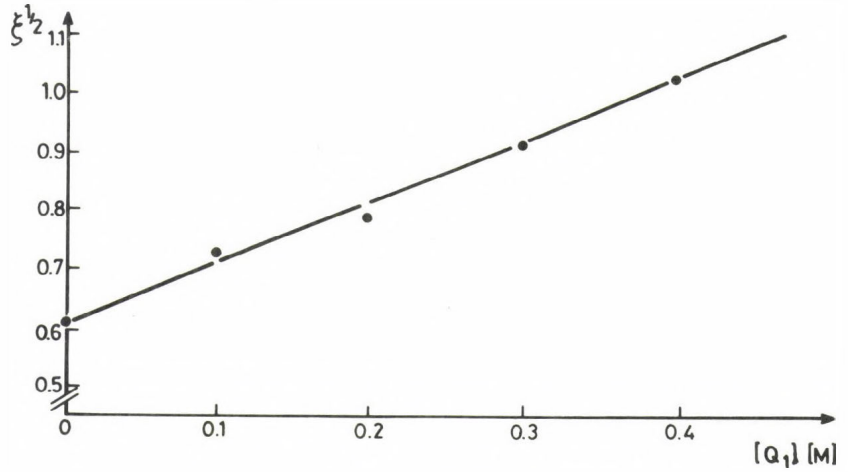

Figure 2. The square root, $\xi^{1/2}$, of the straight lines from Fig. 1 plotted against acrylamide concentration. The value of K_{1e} was calculated as the ratio of the slope and intercept of the straight line shown (K_{1e} = 1.62 M^{-1}).

The value of K_{1e} can be determined either by using the slope and intercept of Eq. (10) or using the already known value of αK_2 and the slope.

The parameters remained then to evaluate are β, γ and K_{1i}. For this, one can define X and calculate its value from the already known parameters as:

$$X = \left[\frac{F_1}{F_o} - \frac{\alpha}{1+K_{1e}[Q_1]} \right] = \frac{\beta}{1+K_{1i}[Q_1]} + \gamma. \qquad (11)$$

Denoting the value of X at $[Q_1] = 0$ by X_o, we write:

$$\frac{1}{X_o - X} = \frac{1}{\beta} + \frac{1}{\beta K_{1i}} \frac{1}{[Q_1]} . \qquad (12)$$

Plotting $1/(X_o-X)$ vs. $1/[Q_1]$ should result in a straight line and the

values of β and K_{1i} can accordingly be calculated from the slope and intercept (see Figure 3). The value of γ then comes from $\gamma=1-\alpha-\beta$.

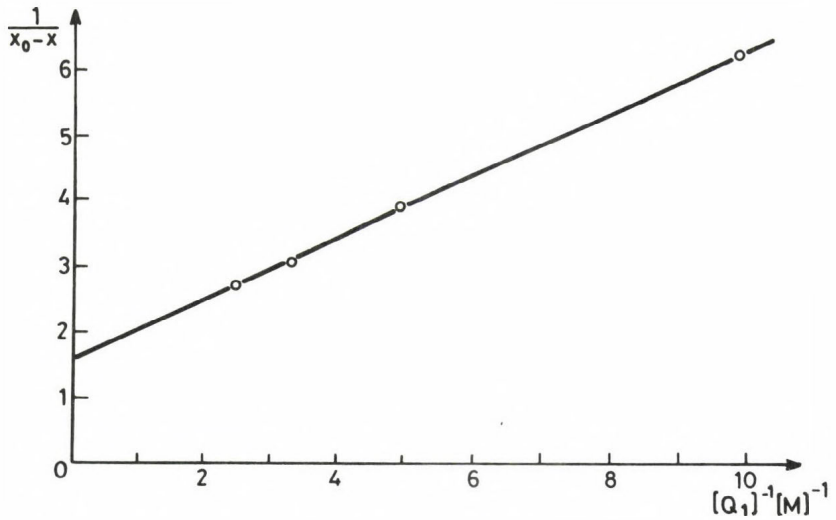

Figure 3. The plot of $(X_o-X)^{-1}$ vs. $[Q_1]^{-1}$. The values of β and K_{1i} were calculated according to Eq. (12) as β = 0.63 and K_{1i} = 3.57 M^{-1}.

Gated quenching of protein fluorescence/phosphorescence

With the exception of permanently exposed fluorophore groups of proteins, there are two main pathways to quench the protein fluorescence/phosphorescence: a) the penetration model assumes the quencher to penetrate the protein matrix; b) the partial unfolding model prescribes that the internal groups of the protein occasionally and transiently become exposed to the solvent.

The latter mechanism is usually discussed in terms of a reaction scheme borrowed from the hydrogen exchange literature (Barksdale & Rosenberg, 1982; Calhoun et al., 1983a,b):

$$A^*_{cl} \underset{k_{cl}}{\overset{k_{op}}{\rightleftarrows}} A^*_{op} + Q \overset{k_+}{\rightarrow} A_{op}{:}Q. \qquad (13)$$

Here, A and A^* stand for the ground and excited states of the fluorophore, subscripts cl and op stand for the nonaccessible (closed) and accessible (open) states, Q is the quencher molecule while k_+ is the bimolecular quenching constant characteristic of the rate of encounter complex formed between the exposed fluorophore and the quencher molecule.

Due to the finite lifetime of the excited state, however, the scheme (13) gives only an approximate description of gated quenching. For example, for the quenching constant K_{sv}, Eq. (13), results in:

$$K_{sv}[Q] = \frac{k_{op}k_+\tau_o[Q]}{k_{cl}+k_+[Q]} \qquad (14)$$

with τ_o being the lifetime of the excited state in the absence of quencher, i.e., it predicts the quenching reaction to be fist order in quencher concentration only in a limited range when $k_+[Q] << k_{cl}$.

To have a more precise description, one has to deal with the extended scheme of:

$$\begin{array}{ccccc} A_{cl} & \leftrightarrow & A_{op} & & \\ \uparrow & & \uparrow & & \\ \downarrow & & \downarrow & k_+[Q] & \\ A^*_{cl} & \leftrightarrow & A^*_{op} & \rightarrow & A_{op}{:}Q \end{array} \qquad (15)$$

In a general case the scheme (15) represents a given fraction, α, of the protein fluorescence. If fraction $1-\alpha$ cannot be quenched by the given quencher, one can apply probabilistic considerations to calculate the probability, W, that the α fraction of the fluorescence will not be quenched by the applied quencher, i.e. the probability that the excited state assigned to α will decay in any other way but quenching:

$$W = \frac{1 + P_{cl}\dfrac{k_+[Q]\tau_o}{1 + \dfrac{\tau_o}{\nu_{cl}} + \dfrac{\tau_o}{\nu_o}}}{1 + \dfrac{\tau_o + \nu_{cl}}{\nu_{cl}}\dfrac{k_+[Q]\tau_o}{1 + \dfrac{\tau_o}{\nu_{cl}} + \dfrac{\tau_o}{\nu_o}}} \qquad (16)$$

Here ν_o and ν_{cl} are the average time of the fluorophore being in the open

and the closed state, τ_o is the lifetime of the excited state in the absence of the quencher and:

$$P_{cl} = (1 - P_o) = \frac{\nu_{cl}}{\nu_{cl} + \nu_o} . \tag{17}$$

By the use of Eq. (16), one can obtain the form of the modified Stern-Volmer equation:

$$\frac{F_o}{F_o - F} = \frac{F_o}{\Delta F} = \frac{1}{\alpha_{obs}} + \frac{1}{\alpha_{obs} K_{sv}} \frac{1}{[Q]} , \tag{18}$$

with the parameters:

$$\alpha_{obs} = \alpha\alpha_g \tag{19}$$

and:

$$K_{sv} = \frac{P_o k_+ \tau_o}{\alpha_g} \tag{20}$$

where:

$$\alpha_g = P_o\left(1 + \frac{P_{cl}}{P_o} \frac{\tau_o}{\tau_o + \tau_{cl}}\right). \tag{21}$$

As it is seen by the inspection of Eqs. (18)-(21), our model describes the quenching to be first order in the quencher concentration. Further, the gating affects the apparent accessibility, α_{obs}, and the Stern-Volmer constant, K_{sv}, depending on the ratio of ν_{cl}/τ_o (see Table 1).

Table 1. The quenching parameters of gated quenching in the limiting cases.

	$\nu_{cl} << \tau_o$	$\nu_{cl} >> \tau_o$
α_{obs}	α	$P_o\alpha$
K_{sv}	$P_o k_+ \tau_o$	$k_+ \tau_o$

The product $\alpha_{obs} K_{sv}$, however, remains $\alpha P_o k_+ \tau_o$ independently of the ratio of ν_{cl}/τ_o. This is characteristic of the model that has diagnostic power. For example, by changing the viscosity, which certainly alters the ratio of ν_{cl}/τ_o but leaves the value of P_o unchanged (altering both ν_{cl} and ν_o in the same way), the above product ($\alpha_{obs} K_{sv}$) would decrease linearly

with the viscosity, while the change of K_{SV} itself would show a different profile depending on the change of ν_{Cl}/τ_o (see Eqs. (20) and (21)).

(Supported by NSF-PCM 8303027)

References

Barboy, N., Feitelson, J. 1978. Fluorescence quenching as an indicator for structural fluctuations in liver alcohol dehydrogenase. Biochemistry 17, 4923-4926.

Barksdale, A.D., Rosenberg, A. 1982. Acquisition and interpretation of hydrogen exchange data. Methods of Biochemical Analysis (Click, D., ed.) Vol. 28, 1-113, Wiley, N.Y.

Calhoun, D.B., Vanderkooi, J.M., Englander, S.W. 1983a. Penetration of small molecules into proteins studied by quenching of phosphorescence and fluorescence. Biochemistry 22, 1533-1539.

Calhoun, D.B., Vanderkooi, J.M., Woodrow III, G.V., Englander, S.W. 1983b. Penetration of dioxygen into proteins studied by quenching of phosphorescence and fluorescence. Biochemistry 22, 1526-1532.

Eftink, M.R., Ghiron, C.A. 1975. Dynamics of a protein matrix revealed by fluorescence quenching. Proc. Natl. Acad. Sci. USA 72, 3290-3294.

Eftink, M.R., Ghiron, C.A. 1977. Exposure of tryptophanyl residues and protein dynamics. Biochemistry 16, 5546-5551.

Englander, S.W., Kallenbach, N.R. 1984. Hydrogen exchange and structural dynamics of proteins and nucleic acids. Quarterly Review of Biophysics 16, 521-655.

Gratton, E., Jameson, D.M., Weber, G., Alpert, B. 1984. A model of dynamic quenching of fluorescence in globular proteins. Biophys. J. 45, 789-794.

Gurd, F.R.N., Rothgeb, T.M. 1979. Motions in Proteins. Adv. Protein Chem. 33, 73-165.

Hagaman, K.A., Eftink, M.R. 1984. Fluorescence quenching of trp-314 of liver alcohol dehydrogenase by oxygen. Biophys. Chem. 20, 201-207.

Hevessy, J., Somogyi, B., Welch, G.R., Papp, S., Matko, J., Damjanovich, S. 1981. A fluorescence parameter reporting on the change of intramolecular fluctuations. Int. J. Luminescence 24/25, 811-814.

Jameson, D.M., Gratton, E., Weber, G., Alpert, B. 1984. Oxygen distribution and migration within $MB^{DES\ Fe}$ and $HB^{DES\ Fe}$. Biophys. J. 45, 795-803.

Lakowicz, J.R., Weber, G. 1973b. Quenching of protein fluorescence by oxygen. Detection of structural fluctuations in proteins on the nanosecond time scale. Biochemistry 12, 4171-4179.

Matko, J., Seres, I., Papp, S., Somogyi, B. 1984. Dynamic interaction between functional groups in the active site of glycogen phosphorylase b. Biochem. Biophys. Res. Comm. 122, 649-655.

McCammon, J.A., Karplus, M. 1980. Simulation of protein dynamics. Ann. Rev. Phys. Chem. 31, 29-45.

McCammon, J.A., Northrup, S.H. 1981. Gated binding of ligands to proteins. Nature 293, 316-317.

Somogyi, B., Welch, G.R., Damjanovich, S. 1984a. The dynamic basis of energy transduction in enzymes. Biochim. Biophys. Acta. 768, 81-112.

Somogyi, B., Matko, J., Papp, S., Hevessy, J., Welch, G.R., Damjanovich, S. 1984b. Förster-type energy transfer as a probe for changes in local fluctuations of protein matrix. Biochemistry 23, 3403-3411.

Somogyi, B., Papp, S., Rosenberg, A., Seres, I., Matko, J., Welch. G.R., Nagy, P. 1985a. A double-quenching method for studying protein dynamics: Separation of solvent exposed and masked fluorophores. Biochemistry, accepted for publication.

Somogyi, B., Norman, J.A., Rosenberg, A. 1985b. Gated quenching of intrinsic fluorescence of globular proteins. Biophys. J. submitted.

Szabo, A., Shoup, D., Northrup, S.H., McCammon, J.A. 1982. Stochastically gated diffusion-influenced reactions. J. Chem. Phys. 77, 4484-4493.

DISCUSSION

CHERRY:

Could you comment on how your rate constant for acrylamide quenching of internal tryptophans in lysozyme compares with the rate constants for oxygen quenching and acrylamide quenching reported for other proteins.

SOMOGYI:

This "double quenching" method gives us the Stern-Volmer constants for the two tryptophan subclasses. Their conversion into bimolecular rate constants is based on the observations by Imoto et al. (Proc. Natl. Acad. Sci. USA, 69, 1151, 1971) saying, that about 90 % of the total fluorescence of lysozyme can be attributed to TRP-108 and Trp-62 residues. According to the Lee-Richards criterion the Trp-62 is a solvent exposed residue while Trp-108 is a deeply buried one. The rate constant for acrylamide quenching of the latter "internal" residue has been estimated using the singlet lifetime measured and assigned to this residue by Formoso and Forster (cf. J. Biol. Chem. 250, 3738, 1975). Regarding the acrylamide quenching data, our value (k_q^{int}: $1.7 \times 10^9 M^{-1} s^{-1}$) is significantly smaller than those assigned to small indole compounds and fully exposed residues in small peptides and proteins ($4\text{-}9 \times 10^9 M^{-1} s^{-1}$). It lies between the values observed for human serum albumin and monellin, which in turn, lie by a factor of $\cong 5$ below obtained for RNAse-T_1, the most often used model for completely buried tryptophanes. Furthermore, our value is smaller than the rate contants for oxygen quenching usually assigned to buried residues, except Trp-314 in LADH, where the rate constant of oxygen quenching is comparable to our value, while the acrylamide quenching constant is extremely small. These relations are not so surprising, since oxygen is expected to diffuse into a protein matrix much more readily than acrylamide (cf. Eftink and Jameson, Biochemistry, 21, 4443, 1982).

DYNAMICS OF MULTIENZYME COMPLEXES AND METABOLIC PATHWAYS

Dynamics of Biochemical Systems
S. Damjanovich, T. Keleti, L. Trón (Eds)

DYNAMIC INTERACTIONS BETWEEN METABOLIC SEQUENCES

DANIEL E. ATKINSON

Department of Chemistry and Biochemistry,
University of California,
Los Angeles, California 90024, USA

A living system is strikingly dynamic. At any moment in a living cell a large number of reactions are occurring, most of them at rates very much greater than they could attain at similar concentrations in the absence of biological catalysts. Living systems differ very strongly from the non-living world in the variety of chemical reactions of which they are composed and in the velocities of those reactions.

But an even more specific difference between living and non-living systems is the intricate pattern of functional correlations and interrelationships that characterize life. Each reaction is a functional part of a metabolic sequence, and each sequence is interrelated functionally with many other sequences. These functional relationships are so obvious that we may sometimes tend to take them for granted and fail to recognize their significance. However, they are so fundamentally important that it may not be an exaggeration to say that, in effect, they constitute life. Thus in discussing dynamic interrelationships between sequences we deal with life at its most fundamental and irreducible level.

The pattern of interrelations is shown at a simplified level in Figure 1, which applies to heterotrophic aerobic cells. The three basic needs of all cells are energy (a suitable ATP/ADP ratio), electrons or reducing power (a suitable $NADPH/NADP^+$ ratio), and starting materials for the biosynthesis of the cell's components. In aerobic heterotrophic metabolism, all three are supplied by oxidation of carbohydrates, fats, and proteins. As the diagram shows, only a few compounds, all

intermediates of glycolysis, the citrate cycle, or the pentose phosphate pathway, serve as starting materials for synthesis of nearly all of the compounds in the cell. Since those compounds are consumed in synthetic sequences, there is a constant flow of carbon atoms through them. In contrast, the flow of energy and electrons from catabolic sequences to biosynthetic and other processes where they are needed is mediated by turnover of essentially constant ATP/ADP and $NADPH/NADP^+$ pools, with little flow of carbon atoms.

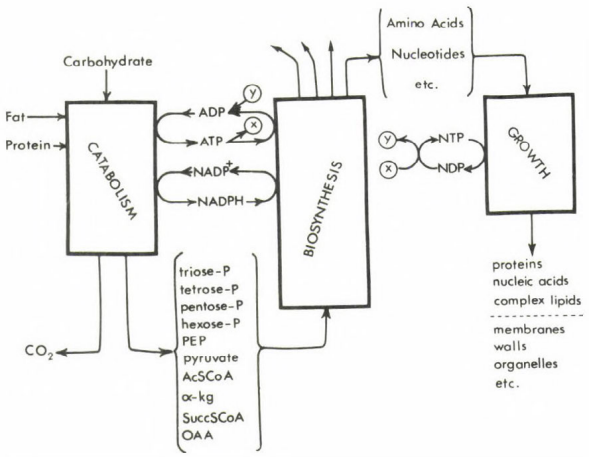

Figure 1.

A functional block diagram of the metabolic organization of a typical heterotrophic aerobic organism.

Chemical energy is potentially available from any system that contains two or more compounds that are related by a feasible chemical reaction, if that reaction is not at equilibrium. Two of the major functions of catabolism are to hold the ratios of ATP to ADP, and of NADPH to $NADP^+$, at essentially constant values that are far from equilibrium for the reactions in which they will serve to transfer energy to other processes in the cell. These two transducing systems, ATP/ADP and $NADPH/NADP^+$, link catabolic and anabolic sequences with definite stoichiometric ratios. It is clear that they must also

be involved in the functional kinetic controls that primarily distinguish living from non-living chemistry.

I suggest that the factors that are involved in dynamic correlations between metabolic sequences can be grouped under four headings:

a) A pattern of relative affinities of enzymes for coupling agents that causes kinase and dehydrogenase reactions to respond to the ATP/ADP or the NADPH/$NADP^+$ ratio rather than to the absolute concentrations of the individual compounds.

b) Organization of metabolism so that nearly every conversion is paired with an oppositely-directed conversion that involves different reactions and a different overall stoichiometry, especially with regard to the coupling agents, ATP/ADP and NADPH/$NADP^+$.

c) High kinetic orders of the reactions that are catalyzed by most regulatory enzymes.

d) Modulation of the activity of regulatory enzymes by modifier or effector metabolites.

a) Response to ratios

In any chemical energy-transducing system, such as an electrical storage cell or the coupling systems of living organisms, the most important operating parameter is the ratio of the components. In order that the ATP/ADP ratio, for example, can be held essentially constant it is necessary that both the regeneration of ATP by phosphorylation of ADP and the conversion of ATP to ADP as metabolic energy is used (for example, in biosynthesis, pumping materials across membranes, or muscular movement) must respond to the ratio of concentrations rather than to absolute concentrations. This type of response has been observed for a number of kinases and dehydrogenases. It is the basis for the pattern of regulatory interactions by which the ATP/ADP ratio, or the adenylate energy charge, is very strongly stabilized in the cell. This is probably the most fundamental manifestation of biological homeostasis, and it depends in a conceptually simple way on the properties of enzymes that catalyze reactions in which ATP and ADP are interconverted. Similar interactions tend to stabilize the reduced-

oxidized ratio of the NADP system. Because the $NADH/NAD^+$ system functions within the block of catabolic sequences rather than between blocks, it does not appear in the metabolic functional block diagram of Fig. 1. It is, however, an important coupling system between substrate oxidation and electron transport phosphorylation, and its ratio is stabilized by the same kinds of interactions that operate in the cases of the ATP/ADP and $NADPH/NADP^+$ couples.

An enzyme will respond to a substrate/product ratio if the $S_{0.5}$ values (the concentrations at which the site is half saturated with the ligand in the absence of competing ligands; sometimes termed the effective Michaelis constant) for both substrate and product are small in comparison with their physiological concentrations. Then the site will always be virtually saturated, and the fraction of the sites at which substrate and product are bound will depend on the ratios of their concentrations to their respective $S_{0.5}$ values. Thus for the nucleotide binding site of a kinase, the ratio of sites binding ATP to those binding ADP will be given by $(ATP/S_{0.5(ATP)})/(ADP/S_{0.5(ADP)})$. If the $S_{0.5}$ values were large in comparison with physiological concentrations, most of the sites would be empty, ATP and ADP would compete only weakly, and the amount of each that was bound would depend mainly on its absolute concentration rather than on the concentration ratio. Energy homeostasis would not then be achievable.

In addition to causing the velocity of the reaction to respond to the ratio of substrate to product, high affinity of an enzyme for S and P also allows the nature of that response to be precisely adjusted to increase its sensitivity and tc meet physiological needs. Figure 2 shows how the fraction of sites that bind A as a function of the mole fraction of A in an A-B pool depends on the relative affinities of the site for A and B. If the $S_{0.5}$ values were equal, the fraction of sites bearing A would merely equal the mole fraction of A, as shown by the central diagonal straight line. If the affinity for A were greater than that for B, one of the upper curves would describe the binding, and if the affinity for product were greater one of the lower curves would apply.

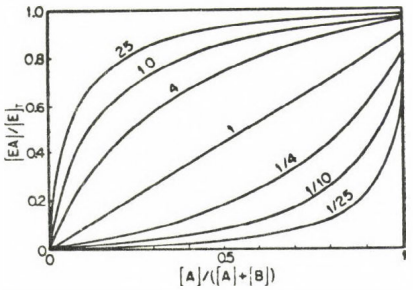

Figure 2.

Fraction of binding sites bearing compound A as a function of the mole fraction of A in an A-B mixture; effects of relative affinities for A and B. The numbers indetifying the curves are the ratios of the dissociation constants K_A/K_B.

Many kinases bind ADP more firmly than ATP, often by a ratio of about 5, giving a response curve that would lie between the 1/4 and 1/10 curves in the figure. This property may at first thought seem undesirable, since it means that ADP will be an effective product inhibitor. The extent of inhibition is shown by the difference between that curve and the uppermost curve, where ADP binds so weakly that competition is negligible. The loss in catalytic activity is much more than compensated for, however, by an increase in regulatory sensitivity. Most of the range of reaction velocity is condensed into a rather narrow range at the high end of the mole fraction scale. The relatively large slope of the curves in that region obviously allows for much greater sensitivity in regulation than would be possible in the absence of ADP inhibition. Similar but reciprocal interactions at catalytic sites of enzymes that contribute to regeneration of ATP lead to curves with complementary slope, as seen in Figure 3. Here R signifies the regeneration, and U the utilization or use of ATP.

The abscissa of Figure 3 is the energy charge, (ATP + 0.5 ADP)/(ATP + ADP + AMP), the effective mole fraction of ATP. It is evident that this pattern of responses will lead to powerful stabilization, since a tendency for energy charge to decrease will be resisted by an increase in the rate at which ATP is regenerated and a decrease in the rate at which it is used. A tendency for the value of energy charge to rise will similarly be resisted by appropriately-directed responses.

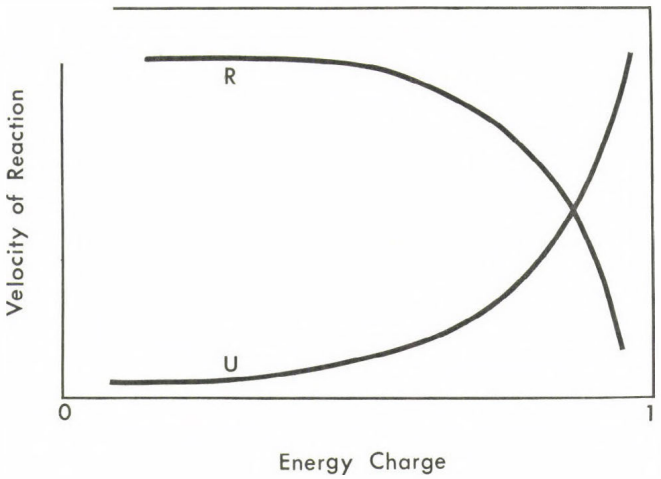

Figure 3.

Generalized responses of regulatory enzymes in ATP-regenerating sequences (R) and in ATP-utilizing sequences (U) to variation in the value of the adenylate energy charge.

b) Oppositely-directed sequences

Enzymes are catalysts, and like all catalysts they affect the rates of reactions but cannot directly determine the direction of reaction. The direction, of course, is determined by thermodynamic considerations: all reactions go in the direction of decreasing ΔG; that is, toward equilibrium. But no matter how finely adjusted were the enzymic responses, a chemical system that hovered sluggishly near equilibrium could not have many of the characteristics that we observe in actual living systems. It is necessary for an organism to be able, for example, to store energy at times and to retrieve the stored energy at others. An organism that operated around equilibrium could store fats only when the concentration of acetyl coenzyme A was high (above the concentration at which it is in equilibrium with palmitoyl coenzyme A), and could retrieve energy from stored fat only if the concentration of acetyl coenzyme A fell below that equilibrium concentration. Thus under

conditions of energy need it would be handicapped by low concentrations of the very intermediates that are required for regeneration of ATP. Such an organism could not respond dynamically and appropriately to changing conditions and metabolic needs, and could not be expected to survive.

We may then seem to have a paradoxical situation or at least a difficult problem of design. If we are to have the dynamic metabolic interactions that are necessary for life, both the direction of conversions and their rates must respond to metabolic signals. Rates depend on the activities of enzymes, and can be modulated (point d below), but the direction of a reaction or reaction sequence, being under thermodynamic control, responds only to the concentrations of the reactants and products. It cannot be reversed by an external signal.

Properly speaking, a problem can exist in advance of its solution only as a consequence of conscious thought or foresight. In the blind world of evolution, where differential reproduction selects from among random mutations, there can be no planning, no foresight, and thus no problems to be solved. Only in retrospect, when we consider evolved mechanisms or structures, can we feel that a problem was solved or a difficulty surmounted. In that retrospective sense, we may say that the arrangement that evolved appears to be the only possible solution to the problem of how to make the directions of metabolic conversions dynamically responsive to metabolic need.

For nearly every metabolic conversion, two separate and distinct pathways exist. The pahtways are composed of different reactions and the overall sequences differ in stoichiometry, especially with respect to the coupling agents ATP/ADP and $NADPH/NAD^+$. Because the ATP/ADP system is maintained very far from equilibrium, a difference in the number of ATP-to-ADP conversions that are stoichiometrically coupled to a metabolic sequence will cause a large difference in the overall equilibrium constant of the conversion. The difference is of the order of 10^7 to 10^8 for each ATP that is converted to ADP. Thus the equilibrium constant for the hydrolytic reaction

fructose-1,6-bis-P + H_2O ⇌ fructose-6-P + Pi

is about 10^4, but for the phosphofructokinase reaction

fructose-6-P +ADP ⇌ fructose-1,6-bis-P + ATP

the equilibrium constant is about 10^{-4}. Thus under any conceivable physiological conditions the phosphofructokinase reaction must go in the direction opposite to that written. In that direction the equilibrium constant is of course about 10^4.

This simple example illustrates the general plan around which metabolism is organized: paired oppositely-directed conversions, containing different reactions or sequences of reactions, with different ATP/ADP stoichiometries. This organization is shown in Fig. 4 for the general case.

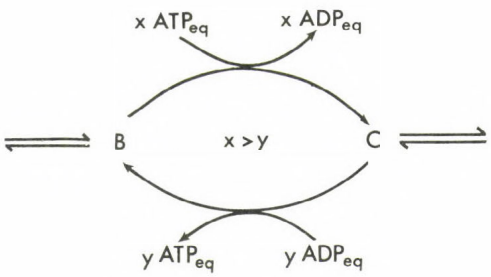

Figure 4.

Two oppositely-directed reaction sequences with different ATP/ADP stoichiometries. The value of x is large enough so that conversion of B to C by the upper pathway is thermodynamically favorable under physiological conditions, and the value of y is small enough (it may be zero or negative) so that conversion of C to B is favorable under the same conditions.

Because of the difference in the equilibrium constants (or in free energy change) of the two conversions, the members of a pair of such sequences are thermodynamically favorable in opposite directions under physiological conditions. Thus the

kinetic controls that determine the fluxes through the two sequences can determine the direction of net conversion. Thermodynamic limitations on regulatory flexibility are thus circumvented, and metabolic signals can control both the directions and the rates of metabolic conversions. Such signals directly affect only rates, but because of the oppositely-directed sequences, coordinated control of rates controls the direction of net conversion. Other examples are glycolysis and gluconeogenesis, storage and mobilization of fats, and, in photoautotrophs, photosynthesis and respiration. These major energy-related conversions illustrate a general feature of metabolic design; such paired sequences, effecting oppositely-directed conversions, are found throughout metabolism. Amino acids, for example, are typically synthesized by one sequence of reactions and oxidized by another with different ATP stoichiometries.

This pairing of sequences may be considered the basic feature of evolved metabolic design. It is the feature that allows metabolic conversions to operate far from equilibrium, where rates can be high and responses rapid, but to be able to reverse direction rapidly in response to metabolic signals. Other aspects of enzymic behavior, including the other features in our list, are part of the mechanism by which the regulatory possibilities of oppositely-directed sequences are effected.

c) High-order reactions

Most enzymes that catalyze first reactions in sequences, or branch-point reactions, bind one or more substrates cooperatively, and the reactions that they catalyze are of kinetic order higher than one with respect to those substrates. The rates of such reactions obviously respond more sensitively to changes in substrate concentrations than do ordinary first-order reactions. This is illustrated in Figure 5, where the cross-sectional area from the bottom of the openings up to the concentration of substrate is proportional to the rate of reaction.

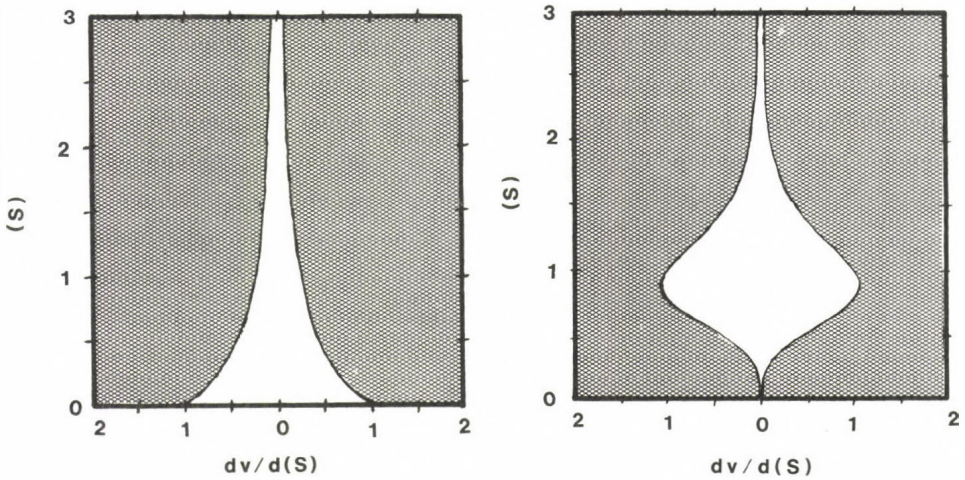

Figure 5.

Schematic representation of the variation of reaction velocity as a function of substrate concentration for a first-order or standard Michaelis enzyme (A) and for a cooperative enzyme that catalyzes a reaction that is fourth order with respect to substrate. Water flow is taken as an analog of reaction velocity. The shaded blocks represent dams or barriers, with openings cut in them to allow flow of water. The level of water behind the dam is analogous to substrate concentration, and for any level the area of the opening through which the water flows is proportional to reaction velocity. For both figures the value of $S_{0.5}$, the concentration at which velocity is half of the maximal velocity, is 1.0. Note that the incremental increase in velocity that results from a small increase in substrate concentration is much greater for the fourth-order enzyme, over a range of concentrations below $S_{0.5}$, than for the first-order enzyme at any substrate concentration.

d) Response to modifiers

The kinetic properties of regulatory enzymes change when specific modifiers, or metabolic signals, bind to modifier sites. The most common effect caused by modifiers is change in the affinity of the enzyme for one or more substrates. The amount of substrate bound to an enzymic site is a function of the ratio $(S/S_{0.5})^n$, where n is the effective kinetic order. Thus a change in $S_{0.5}$ has as large an effect on reaction velocity as does a change in substrate concentration. It is also evident that high kinetic order will render an enzyme more

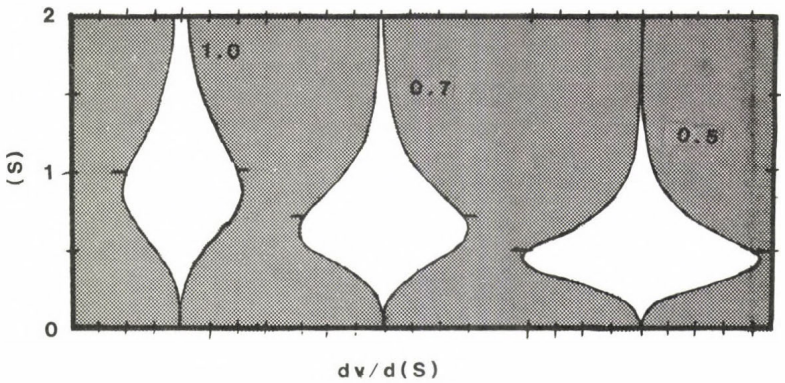

Figure 6.

Schematic representation of variation of reaction velocity as a function of substrate concentration for a fourth-order enzyme; effect of change in $S_{0.5}$. The analogy is the same as in Fig. 5. This figure shows the effect of a modifier that causes the value of $S_{0.5}$ to change. In this analogy, the modifier causes deformation of the shape of the opening, while not affecting its total cross-attentional area (that is, the modifier affects $S_{0.5}$ but not the maximal velocity of the reaction). The ticks on the sides of the openings indicate the value of $S_{0.5}$, and ticks on abscissa are at 0.5-unit intervals.

sensitive to changes in the value of $S_{0.5}$, and hence to changes to changes in the concentration of modifiers that change $S_{0.5}$, than would be possible for a first-order enzyme. The effect of change in $S_{0.5}$ is illustrated in Figs. 6 and 7, where relative values of 1.0, 0.7, and 0.5 are compared. The rate of reaction is changed strongly by a two-fold change in $S_{0.5}$. Much larger changes than this in the value of $S_{0.5}$ are frequently observed in studies on regulatory enzymes.

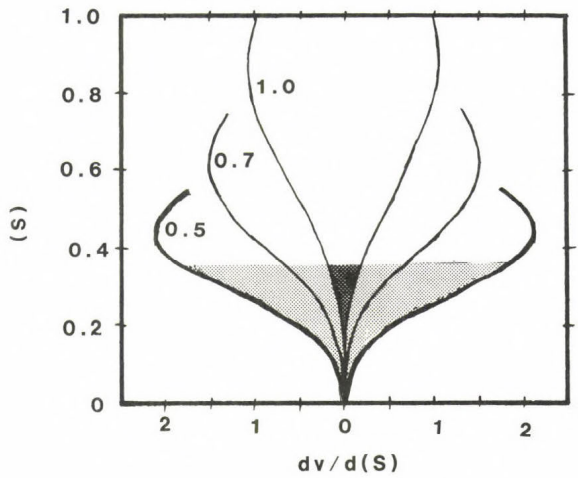

Figure 7.

Schematic representation of variation of reaction velocity as a function of substrate concentration for a fourth-order enzyme; effect of change in $S_{0.5}$. The lower portions of the openings shown in Fig. 6 are superposed for more direct comparison of the effects, at constant substrate concentration, of a change in the value of $S_{0.5}$. The velocity corresponding to the area of dark shading is increased to correspond to the area of the light shading by a two-fold change in $S_{0.5}$.

To summarize, dynamic interactions between sequences are an essential aspect of metabolism, and might be considered to be the basic characteristic of life. The features that are responsible for such interactions may be grouped into four categories. One is a consequence of the organized interactions of many enzymes: metabolic conversions exist typically as paired oppositely-directed sequences, with sufficiently different coupling-agent stoichiometries between members of a pair so that the forward direction is always thermodynamically favorable for one sequence and the reverse direction for the other. This is the fundamental basis of metabolic organization. Without this feature, flexible and dynamic functional responses would not be possible. The other three types of features are behavioral patterns of individual enzymes. The affinities of regulatory enzymes for the coupling agents that link sequences stoichio-

metrically (ATP/ADP and NDPH/$NADP^+$) are typically so great that the binding sites are virtually saturated at all times. This makes the rates of reactions sensitive to ratios such as ATP/ADP and so allows the ratios or mole fractions of such coupling agents to be strongly stabilized. Greater affinity for the product (e.g., ADP in the case of kinases) increases the sensitivity of enzyme response by condensing much of the range of reaction velocity into a narrow range of coupling agent ratio or mole fraction. The affinities of many regulatory enzymes for their substrates are modulated by binding of modifier metabolites. This leads to responses that are appropriate to the metabolic conditions that are signalled by the modifier. Finally, most regulatory enzymes bind their substrates cooperatively, which greatly increases the sensitivity of responses to substrate concentrations and to the effects of modifiers that cause changes in the affinities of enzymes for their substrates. Sensitivity is often further enhanced by cooperative binding of modifiers as well.

All four types of regulatory features appear to be necessary for sensitive functional dynamic interactions between sequences, and it would be difficult or impossible to imagine a metabolic system functioning effectively in the absence of any one of them. By the same token, any mathematical or conceptual model of metabolism must explicitly take all of these four features of metabolic interactions into account if it is to have possible relevance to the chemical activities of actual living cells.

ARAGON:

As you have shown phosphofructokinase exhibits a sigmoidal saturation curve for fructose-6-P, and the extent of this sigmoidicity is dependent on its inhibition by ATP, among other factors. In relation to this matter, when the behavior of this enzyme is studied by using ITP as a phosphate donor instead of ATP, it also exhibits sigmoidicity for fructose-6-P despite of the fact that ITP is not an inhibitor of this enzyme. Could you please make some comment on this subject?

ATKINSON:

Phosphofructokinase is unusual in that ITP, GTP, CTP and UTP can all serve as phosphoryl donors. Only ATP decreases the affinity for F6P, which seems to be related to the special regulatory role of the adenylate nucleotides. I cannot say anything useful about the factors that are responsible for a sigmoid response to F6P concentration.

KRETSCHMER:

Is reversible enzyme phosphorylation a process related to metabolic regulation or rather to signals from outside of the cell?

ATKINSON:

Phosphorylation caused by signals from outside the cell, such as epinephrine or glucagon, often seem to serve to override local regulatory systems. Thus, to take the first case discovered, phosphorylation of liver glycogen phosphorylase converts the adenylate-sensitive form 'b' to the effectively adenylate-independent form 'a'. However, there are also phosphorylations that probably are not responses to external signals.

RICARD:

What is your personal opinion about the "functional advantages" of negative cooperativity which is frequently encountered in nature?

ATKINSON:

I am not convinced that negative cooperativity occurs frequently in nature, although it may do so. Positive cooperativity is useful when, as is generally the case in metabolism, substrate concentrations are to be stabilized by modulation of fluxes. Negative cooperativity would of course facilitate the opposite type of interaction: stabilization of fluxes by modulation of concentrations. It is possible that such a response might sharpen the concentration pulses of regulatory compounds. Thus if phosphodiesterase exhibited negative cooperativity, the cell's response to epinephrine might be enhanced.

OVÁDI:

Can PFK be regulated by changing of the ratio of ATP/ADP which occurs under physiological condition?

ATKINSON:

If the thrust of your question relates to the fact that changes in the ATP/ADP ratio are small, my answer is yes, I think these small changes are regulatory. Indeed the fact that the ATP/ADP ratio (or the ATP mole fraction or the energy charge) remains nearly constant when fluxes vary by several hundred fold seems to me to be conclusive evidence that the metabolic sequences that regenerate ATP and those that use ATP are very effectively and rapidly controlled by the adenine nucleotide system.

Dynamics of Biochemical Systems
S. Damjanovich, T. Keleti, L. Trón (Eds)

APPLICATION OF THE TRANSIENT KINETIC BEHAVIOUR OF COUPLED ENZYME REACTIONS TO THE ANALYSIS OF METABOLIC PATHWAY DYNAMICS

JOHN S. EASTERBY

Department of Biochemistry, University of Liverpool, Liverpool L69 3BX, UK

The regulation of flux through pathways and other sequences of consecutive reactions has received considerable attention. The theoretical basis for the related temporal response of such sequences and their ability to adapt to changing needs within the cell has been less well studied. In any sequence of consecutive enzyme reactions there is a lag in the appearance of end-product following initiation. The lag is due to the accumulation of intermediates within the sequence and is characterised by the transient time. The transient time may be defined as the intercept of the steady-state asymptote to the progress curve in the formation of product with the time axis, taking as the zero time point the time at which the sequence was initiated. The transient time indicates the time scale on which the pathway operates and is a measure of its adaptive capacity or responsiveness to changing flux requirements. Analysis of the transient time falls broadly into three categories:

(a) The analysis and optimisation of coupled enzyme assays.
(b) The analysis of the response and time-scale of metabolic processes.
(c) The analysis of the channelling of intermediates within multifunctional proteins and multienzyme complexes.

The theoretical analysis of transience has largely dealt with freely diffusing systems of enzymes and

substrates. Comparison of theoretically derived transients with experimentally observed values may therefore reveal limitations on diffusion, or compartmentation of components. If τ_t is defined as the theoretically evaluated transient and τ_m that measured, either within the cell or *in vitro*, three situations may arise:

(i) $\tau_t = \tau_m$ enzymes and substrates are freely diffusing.

(ii) $\tau_t > \tau_m$ substrates are channelled between enzymes and diffusion into the bulk medium is restricted.

(iii) $\tau_t < \tau_m$ there is restriction of diffusion and enzymes or substrates may be compartmentalised.

COUPLED ENZYME ASSAYS

The earliest interest in the temporal response of consecutive enzyme systems was directed towards coupled enzyme assay procedures [1,2,3]. To facilitate the analysis and in order to generate linear, homogeneous, differential equations amenable to solution a number of simplifying assumptions were made. The principle assumption was that the sequence would eventually enter a steady-state in which the concentrations of intermediates do not change with time. In order to achieve this it was assumed that the initial enzyme of the sequence would be rate-limiting and additionally, if it were severely rate-limiting, the steady-state concentrations of intermediates would be less than the Km values of the enzymes involved. Under these circumstances first-order rather than Michaelis-Menten kinetics would be observed and the differential equations would be soluble. Also the steady-state rate of product formation would represent the activity of the initial enzyme.

The single auxiliary enzyme system

The analysis of such a system in which a primary,

rate-controlling enzyme is coupled to a single auxiliary enzyme through irreversible reaction gives rise to the following scheme [1,2,3]:

$$S0 \xrightarrow{Vo} S1 \xrightarrow{Vm/Km} P$$

and:

$$d[S1]/dt + Vm/Km.[S1] = Vo \quad \ldots\ldots(1)$$

$$d[P]/dt = Vm/Km.[S1] \quad \ldots\ldots(2)$$

$$[S1] = Vo.\,\tau\,(1 - \exp(-t/\tau)) \quad \ldots\ldots(3)$$

$$[P] = Vo(t + \tau \exp(-t/\tau) - \tau) \quad \ldots\ldots(4)$$

$$\tau = Km/Vm \quad \ldots\ldots(5)$$

with boundary condition [S1] = [P] = 0 at t = 0, where Vo is the required velocity and Vm/Km the pseudo-first-order rate coefficient. In the steady-state ($t \to \infty$) one may also write:

$$[S1]ss = Vo\,\tau \quad \ldots\ldots(6)$$

and:

$$\lim_{t\to\infty} [P] = Vo(t - \tau) \quad \ldots\ldots(7)$$

Equation 7 represents the steady-state asymptote to the progress curve and intersects the time axis at $t=\tau$. Thus the transient time is given by Eq.(5) and is equivalent to the Km/Vm ratio of the auxiliary enzyme and is independent of the primary enzyme whose activity is sought. The intercept on the ordinate axis is -[S1]ss and represents the steady-state concentration of intermediate. In physical terms this means that the concentration of product in the steady-state has been depressed, below that expected if the pathway had entered the steady-state at zero time, by an amount equal to the concentration of intermediate.

The virtue of this simple analysis is that it closely represents the situation in many coupled assay systems and allows prediction of the accuracy of rate measurements. Equation 3 may be written in the alternative form [3]:

$$[S1]/[S1]ss = 1 - \exp(-t/\tau) = v/Vo \quad \ldots\ldots(8)$$

where v represents the rate of product formation at time t.

It is therefore possible to predict the fractional attainment of the required steady-state rate and this can be measured with greater than 1% accuracy ($v/Vo > 0.99$) provided $t > 4.6\,\tau$.

Generalisation to an unlimited number of coupling enzymes

In the example above involving a single auxiliary enzyme, it would have been possible to dispense with the first order approximation and apply Michaelis-Menten kinetics [4]. However, in cases where more than one auxiliary enzyme is involved, Michaelis-Menten behaviour results in simultaneous differential equations with no analytical solution. The problem may still be approached as before and the model extended to include an unlimited number of enzymes resulting in the following scheme [3]:

$$S0 \xrightarrow{Vo} S1 \xrightarrow{V1/K1} S2 \xrightarrow{V2/K2} S3 \;.....\; Si \;.....\; Sn \xrightarrow{Vn/Kn} P$$

with associated equations:

$$d[Si]/dt + [Si]/\tau_i = [Si-1]/\tau_{i-1} \quad i = 2,3,....n \quad ....(9)$$

$$d[P]/dt = [Sn]/\tau_n \quad .....(10)$$

and boundary condition $[Si]=[P]=0$ at $t=0$, where:

$$\tau_i = Ki/Vi \quad .....(11)$$

resulting in:

$$[Si] = Vo\,\tau_i\left(1-\sum_{j=1}^{i} Aj\,\exp(-t/\tau_j)\right) \quad ....(12)$$

where:

$$Aj = \tau_j^{\,i-1} \prod_{k=1,\,k\neq j}^{i} 1/(\tau_j - \tau_k) \quad .....(13)$$

and:

$$[P] = Vo\left(t + \sum_{i=1}^{n} Ci\,\exp(-t/\tau_i) - \sum_{i=1}^{n} \tau_i\right) \quad ..(14)$$

where:

$$Ci = \tau_i^{\,n} \prod_{j=1,\,j\neq i}^{n} 1/(\tau_i - \tau_j) \quad .....(15)$$

Once more in the steady-state ($t \to \infty$):

$$[P] \underset{t\to\infty}{=} Vo\left(t - \sum_{i=1}^{n} \tau_i\right) \quad \ldots\ldots\ldots\ldots\ldots\ldots (16)$$

Thus the transient time for the sequence is simply the sum of the individual enzyme transients $\tau = \sum Ki/Vi$. Similarly the ordinate intercept is given by $-Vo \sum \tau_i$ which is the sum of the steady-state concentrations of the n intermediates . The model is in most respects equivalent to that of the single auxiliary enzyme. However, it differs in one important respect, no generalisation may be made concerning the time required to reach a particular fraction of the steady-state flux. This is dependent on the specific values of the transient times of the enzymes concerned. However, Eqs. (12),(14) & (16) are symmetrical with respect to transient times and the order of auxiliary enzymes within the sequence does not affect the temporal response.

This model, though simple, led to useful generalisations about the behaviour of sequences and pathways. In general the initial enzyme, though rate determining, does not contribute to the transient time. The transient time for the sequence is the simple sum of the individual enzyme transients and the enzymes which dominate the transient response (ie. those having greatest τ values) are not necessarily those of lowest activity. They may have high Km values and possibly low affinity for their substrates. This led to the proposal that 'time-limiting' enzymes might exist which, though of high capacity, would also have high Km's. These enzymes if positioned after a branch point would control the flow of material along the branch and would only respond if the substrate accumulated and was sufficiently long-lived [3]. Such an enzyme was subsequently identified in the arom multifunctional protein complex of Neurospora crassa [5]. Shikimate kinase controlled the anabolic or catabolic fate of aromatic intermediates within the complex. The time-limiting enzyme concept has subsequently gained wider acceptance [6].

The consequences of extending the sequence

When there is more than one auxiliary enzyme it is difficult to generalise about the rate of attainment of a steady-state owing to the presence of multiple transient times. However, it is still of interest to know the effect of extending the sequence. This difficulty can be partially resolved by making the auxiliary enzymes kinetically identical, which in the present context means giving them identical transient times. This can be achieved by adding enzymes in proportion to their Km's, thus keeping the Km/Vm ratio constant. The following scheme describes the situation:

$$S0 \xrightarrow{Vo} S1 \xrightarrow{1/\tau} S2 \xrightarrow{1/\tau} S3 \ldots\ldots\ldots\ldots Sn \xrightarrow{1/\tau} P$$

Each step has the same first-order rate coefficient given by $1/\tau$ (ie. Vm/Km). The analysis of this sequence separates the effects of enzyme kinetic properties from those of pathway length and results in the following solutions [7]:

$$[Si] = Vo\left(\tau - \sum_{j=0}^{i-1} (\tau/j!)\,(t/\tau)^{j} \exp(-t/\tau)\right) \quad \ldots\ldots(17)$$

and:

$$v/Vo = 1 - \sum_{j=0}^{n-1} n^{j}/j!\,(t/\tau_o)^{j} \exp(-nt/\tau_o) \quad \ldots\ldots\ldots(18)$$

$$[P]/[S] = (t/\tau_o) + \sum_{j=0}^{n-1} n^{(j-1)}.(n-j)/j!.(t/\tau_o)^{j}.\exp(-nt/\tau_o) - 1. \quad \ldots(19)$$

where:

$$\tau_o = n\tau \quad \ldots\ldots\ldots\ldots\ldots\ldots(20)$$

v is the velocity of product formation and [S] represents the sum of the steady-state intermediate concentrations.

Thus it is possible to describe the fractional attainment of the steady-state rate in terms of an overall

transient time for the sequence and the number of auxiliary enzymes. The consequences of extending the sequence are shown in Table 1.

TABLE 1

Attainment of the steady-state velocity in a coupled enzyme sequence

The half-time, the time to reach 99% of the steady-state flux and the velocity at the transient time are shown.

No. auxiliary enzymes (n)	t/τ_o		v/Vo
	$v/Vo = 0.5$	$v/Vo = 0.99$	at $t = \tau_o$
1	0.693	4.605	0.632
2	0.839	3.319	0.594
3	0.891	2.802	0.577
4	0.918	2.511	0.567
5	0.934	2.321	0.560
6	0.945	2.185	0.554
7	0.952	2.082	0.550
8	0.959	2.000	0.547
9	0.963	1.934	0.544
10	0.967	1.879	0.542
15	0.978	1.696	0.534
20	0.983	1.592	0.532

This solution has two important consequences. Firstly it is possible to completely describe the generalised time course of a coupled enzyme system providing all enzymes are given the same transient time. Secondly, extending the sequence increases the time required to reach 50% of the steady-state rate but decreases the time required to reach 99% of this rate. Therefore, given two sequences with the same overall transient time, the longer will approach the steady-state first. As the number of enzymes becomes very large the pathway response approaches a step function and no product is seen until the transient time is reached. At

this point product appears and is produced at the steady-state rate [7]. The implication for the design of coupled enzyme assays is clear. The system is best defined if all enzymes have the same transient time and no loss of accuracy of steady-state measurements is incurred by extending the sequence, as the steady-state is approached more rapidly.

GENERALISATION OF THE THEORY OF PATHWAY TRANSIENCE

The previous models rely on detailed kinetic description of the enzyme sequence but have one common property. The transient or lag time in product formation is the result of accumulation of intermediates within the pathway. This suggests a more general approach to the analysis of transience based solely on mass conservation and requiring no detailed kinetic knowledge of the pathway [8,9]. All material input must appear as intermediate, either free or enzyme-bound, or as product [9].

$$\overset{Vo}{S0 \longrightarrow} S1 \longrightarrow S2 \ldots\ldots\ldots\ldots Si \ldots\ldots\ldots\ldots Sn \longrightarrow P$$

$$\int_0^t Vo.dt = \sum [Si] + \sum [ESi] + [P] \qquad \ldots\ldots\ldots\ldots\ldots\ldots (21)$$

where Vo is the rate of input and summation over all intermediates is implied. This yields:

$$[P] = Vo\left(t - 1/Vo. \int_0^{Vo} t.dVo - \sum [Si]/Vo - \sum [ESi]/Vo\right) \ldots (22)$$

in the steady-state one may write:

$$[P] = Vss\left(t - 1/Vss. \int_0^{Vss} t.dVo - \sum [Si]/Vss - \sum [ESi]/Vss\right). (23)$$

this is of the form:

$$[P] = Vss(t - \tau) \qquad \ldots\ldots\ldots\ldots\ldots\ldots (24)$$

where τ is given by:

$$\tau = 1/Vss. \int_0^{Vss} t.dVo + \sum [Si]/Vss + \sum [ESi]/Vss \quad .....(25)$$

The transient time consists of three components, one due to the variation in the rate of input and two due to accumulation of intermediates. If we consider first the case when the rate of input is constant then:

$$\tau = \sum [Si]/Vss + \sum [ESi]/Vss = \sum \tau_i .....(26)$$

Here a dynamic property of the system is described by static parameters, namely the steady-state concentrations and flux. The transient times are generally associated with intermediates and not with individual enzymes and the overall transient is again the sum of the individual transients. The steady-state parameters may be arrived at either by measurement or theoretically from a knowledge of pathway kinetics without need for solution of differential equations. Comparison of theoretical and measured values is therefore possible.

Enzymes obeying Michaelis-Menten kinetics

For a sequence of irreversible reactions obeying Michaelis-Menten kinetics with constant rate of input Vo, the individual transients take the form:

$$\tau = \tau_{free} + \tau_{bound} = Km/(Vm - Vo) + [E]/Vm \quad .....(27)$$

The second term represents the reciprocal of the turnover number of the enzyme involved and is only significant if the enzyme concentration ([E]) is comparable to Km. This is generally not the case and enzyme-bound intermediate does not contribute significantly to the transient. The transient time is then given by τ_{free} and reduces to the pseudo-first-order value when the enzyme capacity is large compared to the rate of input. The ratio of first-order to Michaelis-Menten transients is given by:

$$\tau_{fo} / \tau_{mm} = (1 - Vo/Vm) \quad .....(28)$$

This ratio rapidly converges to unity for Vm/Vo ratios

greater than 2 and the pathway becomes essentially first-order. Similarly, if the time required by a single auxiliary enzyme obeying Michaelis-Menten kinetics to reach 99% of its steady-state rate is compared with that of a first-order enzyme, it is found that the first-order approximation is valid for Vm/Vo ratios greater than 6 [9].

Rate modification by effectors which are intermediates within pathways of the type considered can be accounted for by their effects on Km and Vm values.

Reversible first-order reactions

In this case the individual transients are given by:

$$\tau_i = 1/ki + \sum_{x=i+1}^{n} 1/kx. \prod_{y=i}^{x-1} 1/Ky \quad \ldots\ldots\ldots (29)$$

where k's represent rate coefficients for forward reactions and K's represent equilibrium constants. Thus each individual transient is modified by all subsequent steps up to the next irreversible step (1/Ky=0).

Variation in the rate of input

The term:

$$1/Vss. \int_{0}^{Vss} t.dVo$$

in the description of the transient given in Eq.(25) is due to the variation in the rate of input to the pathway. This may result from substrate depletion, the establishment of a steady-state in the ES complexes of the initiating enzyme or from feedback on the initial boundary or enzyme of the system. In the present context, depletion of substrate or source material for the pathway may be ignored as this would preclude the establishment of a steady-state. Similarly in the absence of feedback it may be shown that this term is

identical to the transient or characteristic time of the initiating enzyme. This is likely to be in the micro- to millisecond range and will generally be negligible compared to the intermediate-associated transient which will be in the millisecond to second range. One may therefore conclude that this term will normally represent the effect of feedback on the initial enzyme of the pathway.

Where feedback is negative the term will also be negative and has the effect of reducing the transient time. This is because material will initially be input at a rate greater than that observed in the steady-state and the intermediate-associated transients will consequently be overestimated. Thus systems involving negative feedback can help to establish the pathway in the steady-state more rapidly. Moreover the effects of feedback may be quantified.

This is amply demonstrated by a study of glycolysis in the perfused rat heart. The temporal response of glycolysis is dominated by the section of the pathway between glucose and fructose 1,6-bisphosphate. Phosphofructokinase is the primary control point but control is also exerted on hexokinase through feedback inhibition by glucose 6-phosphate. This serves to vary the rate of input of glucose to the patnway as the glucose 6-phosphate level changes. The result is a 30-50% reduction of the transient time under most conditions.

Transition between steady-states

The previous equations have referred to pathways entering a steady-state from rest but they may be modified to allow for the more likely occurrence of a transition between steady-states. If a transition occurs from steady-state (a) to (b), Eq.(24) still applies but the transient time is now given by:

$$\tau = \tau_b - Va/Vb.\ \tau_a \quad \ldots\ldots\ldots\ldots\ldots\ldots (30)$$

Here Va and Vb are the appropriate fluxes and τ_a and τ_b are

still given by Eq.(25). Therefore the transition between any two steady-states may be analysed on the basis of the establishment of each state from rest and the transient times are functions of state.

REFERENCES

[1] McClure,W.R. (1969) "A kinetic analysis of coupled enzyme assays" Biochemistry 8, 2782-2786

[2] Hess,B. & Wurster,B. (1970) "Transient time of the pyruvate kinase-lactate dehydrogenase system of rabbit muscle in vitro" FEBS Lett. 9, 73-77

[3] Easterby,J.S. (1973) "Coupled enzyme assays: A general expression for the transient" Biochim.Biophys.Acta 293, 552-558

[4] Storer,A.C. & Cornish-Bowden,A. (1974) "The kinetics of coupled enzyme reactions" Biochem.J. 141, 205-209

[5] Welch,G.R. & Gaertner,F. (1976) "Coordinate activation of a multienzyme complex by the first substrate" Arch.Biochem.Biophys. 172, 476-489.

[6] Heinrich,R. & Rapoport,T.A. (1975) "Mathematical analysis of multienzyme systems: II.Steady state and transient control" BioSystems 7 ,130-136

[7] Easterby,J.S. (1984) "The kinetics of consecutive enzyme reactions. The design of coupled assays and the temporal response of pathways" Biochem.J. 219, 843-847

[8] Bartha,F. & Keleti,T. (1979) "Kinetic analysis of interaction between two enzymes catalyzing consecutive reactions" Oxid.Commun. 1, 75-84.

[9] Easterby,J.S. (1981) "A generalized theory of the transition time for sequential enzyme reactions" Biochem.J. 199, 155-161

DISCUSSION

OVÁDI:

How do you determine the kinetic parameters for the calculation of the theoretical value of τ?

EASTERBY:

In vitro, in homogenates at as near physiological conditions as possible. Intracellular pH and nucleotide concentrations were measured by NMR, together with some of the phosphorylated intermediates of glycolysis. Those not measurable by NMR were measured by conventional enzymic techniques.

CORNISH-BOWDEN:

You made the point that the time required to reach 99 % of the steady-state rate decreases as the number of enzymes in the pathway increases. While this is true, it is a little misleading because it depends on the fact that you are measuring time in units of the transient time. But the transient time itself increases with the number of enzymes, and the time measured in seconds required to reach any fraction of the steady-state rate also increases with the number of enzymes.

EASTERBY:

Yes, what I intended to imply was that of two sequences having the same transient time, the longer will approach the steady-state first.

RICARD:

Do you know whether a linear sequence of enzyme reactions, that independently follow Michaelis-Menten kinetics, may exhibit damped oscillations during the approach of the overall steady-state?

EASTERBY:

It has been claimed to have been observed but I do not believe it is possible.

BARDSLEY:

The characteristic polynomial for topologically linear systems can only have real negative roots. Non real zerus and hence damped oscillators require closed loops in the topological scheme.

DYNNIK:

What kind of tissue was used in your experiments? How is it possible to split glycolytic intermediates in a whole heart, to compare that system with the homogenate?

EASTERBY:

We did not try to reconstitute glycolysis in vitro, we merely determined the kinetic parameters. In the case of the early reactions of the pathway these values were also used for computer simulations.

Dynamics of Biochemical Systems
S. Damjanovich, T. Keleti, L. Trón (Eds)

INTERACTIONS OF SEQUENTIAL METABOLIC ENZYMES OF THE MITOCHONDRIA: A ROLE IN METABOLIC REGULATION

JACK B. ROBINSON, Jr. and PAUL A. SRERE

VA Medical Center (151B) Pre-Clinical Science Unit,
4500 South Lancaster Road, Dallas, TX 75216 USA

Introduction

The isolation of the separate components of sequential biochemical pathways has been extremely useful; historically, this approach has been necessary to the development of our knowledge of metabolism. However, it has always been implicit in the isolation and characterization of biological systems in vitro that these substances had been removed from the natural milieu, and therefore some of the interactions that might occur in vivo were lost. In the case of the enzymes of the Krebs tricarboxylic acid cycle, when mitochondria are disrupted six of the enzymes are released in a soluble form. We present in this work evidence that such solubility need not exist in vivo. These ideas are not novel; indeed they have been presented elsewhere many times (1-4). In order to simplify discussion, we suggest the use of the term "metabolon" to mean a functional complex of enzymes sequential in a metabolic pathway which is bound to a cellular structural element.

Methods

Liver mitochondria from three Sprague-Dawley rats were prepared as described earlier (5). The mitochondrial pellet was resuspended in the isolation medium (220 mM mannitol, 70 mM sucrose, 2 mM HEPES·KOH, pH 7.0) at a protein concentration of 100 to 200 mg/ml. The mitochondrial suspension (5 µl) was assayed for citrate synthase (EC 4.1.3.7) activity with DTNB in 100 mM Tris-Cl, pH 8.1 at 25°C (6) in the absence of any disruptive agent. This value of enzyme activity was always less than 5% of total

activity present. The total activity was measured by assaying citrate synthase activity in the presence of 1% Triton X-100. No effect on enzyme activity was seen over a range of 0.2 to 2% Triton X-100. One ml of the mitochondrial suspension was then placed in a 1.5 ml microfuge tube and subjected to sonic oscillation for 15 s at a power setting of 3 on a Heat Systems 225W sonicator equipped with a tapered microtip. This represents the minimum power setting sufficient to produce cavitation in this system, and heating of sample was negligible at these low power settings. These parameters may vary from preparation to preparation, but each preparation was subjected to sonic oscillation until at least 60% of total citrate synthase was exposed. The sample was then assayed for exposed citrate synthase activity, which refers to that enzyme activity after sonic oscillation measured in the absence of detergent.

Portions of the mitochondrial suspension containing 6 mg protein were pipetted into a volume of 150 mM KCl, 2 mM HEPES·KOH, pH 7.0 sufficient to give a final volume of 0.6 ml. The final pH of the mixture was 6.5. These samples were incubated 20 min on ice to allow whatever structural changes due to changes in ionic strength to occur. Exposed enzyme content was determined (no Triton X-100 added), and then the samples were centrifuged at 32,000 xg for 30 min at 4°. The supernatant solution was then withdrawn and the pellet resuspended in 0.6 ml of 0.1 M HEPES·KOH, pH 7 by gentle scraping with a glass rod followed by expression through a 25 gauge syringe needle three times, and enzyme activities determined. The entrapped water volume of the pellet, determined with [^{14}C]-inulin as described earlier (9), was found to be 2% of the total volume. Multiple determinations of sedimented exposed citrate synthase activity (and total citrate synthase activity determined in the presence of detergent) showed a variation of no more than 10% of the values presented. All data presented in the present work are the average of at least duplicate determinations. A unit of enzyme is that amount catalyzing the formation of 1 µmole/min of product. In all cases, exposed enzyme refers to that enzyme assayed in the absence of detergent. Values of enzyme activity given for the pellet are those found in the sediment produced by 32,000xg for 30 min in the absence of detergents.

Aconitase (EC 4.2.1.3) (8), (NAD^+)isocitrate dehydrogenase (EC 1.1.1.41) (9), fumarase (EC 4.2.1.2) (10), malate dehydrogenase (EC 1.1.1.37) (11), and ß-hydroxybutyrate dehydrogenase (EC 1.1.1) (12) were assayed by the methods previously described. Protein concentration was

determined by the method of Bradford (13). Antiserum to rat heart citrate synthase was prepared as described previously (14), followed by sodium sulfate precipitation and Sephadex G-100 chromatography to obtain purified immunoglobulins.

Results and Discussion

When mitochondria are subjected to gentle sonic oscillation by the method described we find that about 60% of the original total activity measured in the presence of Triton X-100 becomes measurable without added detergent. One half of this exposed citrate synthase can be sedimented at 32,000xg and one half remains in the supernatant solution (Table I). It should be noted that the conditions of isolation were those generally

Table I Citrate synthase activity present in various fractions of gently sonicated mitochondria+

Sample	Citrate Synthase Units
mitochondrial suspension, enzyme assayed with 1% Triton X-100 present (total units present/6 mg protein)	0.36 ± 0.13
mitochondrial suspension after sonic oscillation (units exposed, no detergent present)	0.22 ± 0.06
32,000 xg pellet (1% Triton X-100)	0.27 ± 0.07
32,000 xg pellet (no detergent)	0.12 ± 0.02
32,000 xg supernatant	0.12 ± 0.03

+The values presented are mean ± standard deviation for eight different preparations of mitochondria, from duplicate determinations of bound enzyme per preparation. The amount of enzyme exposed varied from preparation to preparation, leading to higher deviations in the data presented above than is seen on values obtained in single preparations, but no normalization was done.

accepted as representing physiological pH and ionic strength, and that the consistency and reproducibility of this effect was within acceptable limits.

Mitochondria untreated by sonic oscillation show at most 5% of the total citrate synthase activity (and in most preparations no enzyme is measurable without detergent). This demonstrates that the conditions of the standard enzyme assay do not disrupt mitochondrial structure. Sonic oscillation for time periods three to four times longer than described in Methods causes the release of all the citrate synthase as a soluble enzyme into the supernatant solution without diminishing the total amount of enzyme observed (data not shown). Similarly, freezing the mitochondrial sample once, with isopropyl alcohol-dry ice, and thawing caused release of enzyme with all the enzyme activity in the supernatant solution (data not shown).

These results (Table I) could be interpreted as enzyme entrapment in a substrate-permeable but enzyme-impermeable vesicle. This possibility was tested by measuring inhibition of the exposed enzyme by rat heart citrate synthase antibodies. Antibodies (Mr=160,000) would not be expected to penetrate a vesicle that retained citrate synthase (Mr = 100,000). Inhibition of exposed enzyme by antibody was observed (Table II). The presence of citrate synthase in the detergent-disrupted mitochondria in experiment 1

Table 2 Reactivity of citrate synthase exposed by gentle sonication of rat liver mitochondria[+] with anti-rat heart citrate synthase IgG

Experiment 1

Sample	Citrate Synthase Units	
	+ Triton X-100	- Triton X-100
sonicated mitochondria	0.38 ± 0.0	0.16 ± 0.02
sonicated mitochondria + Control IgG	0.36 ± 0.01	0.19 ± 0.01
sonicated mitochondria + anti-RHCS IgG	0.15 ± 0.0	0.0 ± 0.0

Experiment 2

Sample	+ Triton X-100	- Triton X-100
pellet	0.31 ± 0.04	0.18 ± 0.03
pellet + anti RHCS IgG	0.18 ± 0.01	0.025 ± 0.003
pellet + 1% added TX-100 added before anti- RHCS	0.0 ± 0.0	0.0 ± 0.0

[+]In experiment 1, 35 µg IgG were added to samples of sonicated mitochondria (6 mg) in 0.6 ml 150 mM KCl, 2 mM HEPES, pH 7.0, and all samples were incubated on ice for 1 h; and exposed enzyme (-Triton X-100)

and total enzyme (+Triton X-100) were determined. The sonicated mitochondrial sample was then centrifuged and 35% of the exposed citrate synthase was found to be sedimented. In experiment 2, gently sonicated mitochondria were prepared and centrifuged at 32,000 x g for 30 min before addition of antibody, followed by a 1 h incubation on ice before enzyme assay. The two experiments were done on different preparations of mitochondria. Data presented are average $\pm$ ranges for duplicate assays.

after treatment with the antibodies to citrate synthase demonstrated that the antibody cannot penetrate to and inhibit latent enzyme (enzyme within intact mitochondrial structure). The reaction of antibody with citrate synthase requires at least five minutes before the enzyme activity begins to show measurable inhibition. Therefore, those enzyme assays in the presence of Triton X-100 (total reaction time 2 minutes) accurately reflect the amount of latent (unexposed by sonication) enzyme present in these samples even in the presence of antibody. Experiment 2, done on resuspended pellets of sedimented gently disrupted mitochondria shows the same result caused by antibody addition. Therefore, enzyme measured as sedimentable is not latent enzyme exposed by the resuspension procedure before centrifugation. In experiment 1, the enzyme activity measured in Triton X-100 (line 3 column 1 of Table II) represents that citrate synthase within intact mitochondrial structure which cannot be reached by the added antibody. In experiment 2, Triton X-100 is added to make all the enzyme available, and it can be seen in this instance that all the enzyme is inhibited by antibody.

Another possible source of error in estimation of the stability of the complex arises from the purely technical consideration that, in resuspension of pelleted samples of mitochondria even gently treated with disruptive techniques, the application of force necessary to obtain a homogenous suspension might conceivably disrupt intact structures, thus leading to further expression of previously latent enzyme. To a small extent this does happen, as can be seen by examination of Table I. The average recovery of citrate synthase is 110% $\pm$ 22 in the binding assays. To study this effect, we did an experiment where a resuspended pellet was recentrifuged, and resuspended again. The resuspended pellet showed no significant increase in exposed sedimentable citrate synthase, although a small amount

was found in the supernatant of the second centrifugation. This implies that the exposed sedimentable enzyme is not an artifact of the physical stress of resuspensions of pelleted mitochondria.

ß-Hydroxybutyrate dehydrogenase is a well known marker enzyme for the inner membrane of liver mitochondria. The pellet obtained by centrifuging gently-disrupted mitochondria has 93% of the total ß-hydroxybutyrate dehydrogenase activity present in these mitochondria (35% initially exposed by gentle disruption). The total amount of ß-hydroxybutyrate dehydrogenase is measured by sonic oscillation of mitochondria in 15 sec bursts followed by an enzyme assay until a constant amount of enzyme is observed in successive treatments. The remaining 7% is observed in the supernatant solution of the gently disrupted mitochondria.

The effect of pH and ionic strength on the yield of sedimentable exposed citrate synthase was determined (Figure 1). These data were difficult to interpret simply, since mitochondrial structure and stability are influenced by these parameters. Nonetheless, sedimentable exposed enzyme was apparent throughout the range of conditions tested despite any structural changes that may have occurred.

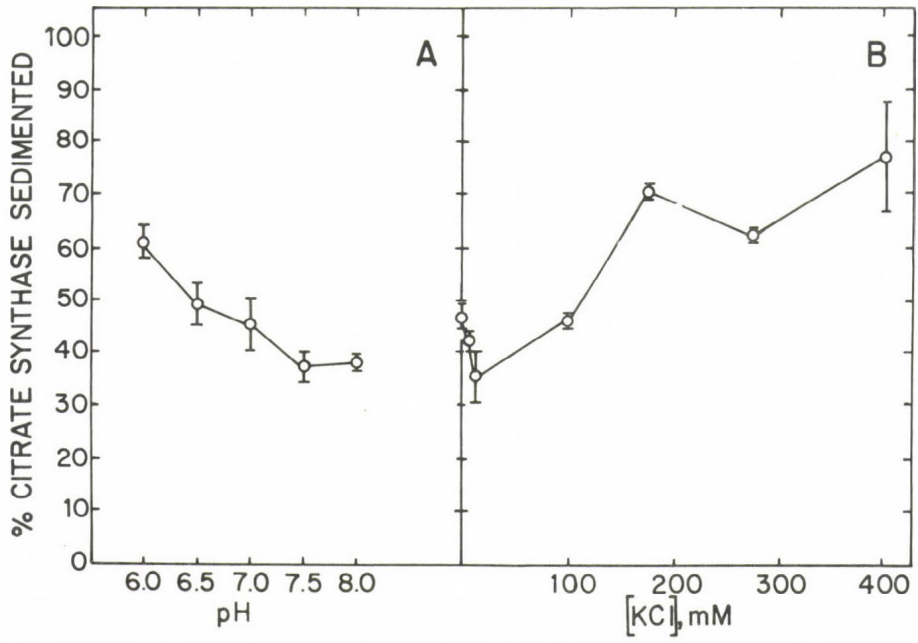

Fig. 1 Effect of pH and ionic strength on formation of a sedimentable exposed citrate synthase in gently disrupted mitochondria. The bars asso-

ciated with each point show the range of duplicates. (A) The effect of pH. Samples were prepared with 20 mM HEPES·KOH at the indicated pH values, also containing 150 mM KCl and 6 mg sonicated mitochondria. The pH values were measured on the supernatant solutions after assay. (B) The effect of ionic strength. Samples were prepared in 2 mM HEPES (pH 7) with KCl concentrations as indicated, and 6 mg gently disrupted mitochondria, and bound exposed citrate synthase measured.

The sedimentable exposed enzyme activity was measured after sonic oscillation followed by incubation at various temperatures. The data (not shown) indicate that the complex is stable at 4°, 25°, and 37° for 30 min.

The effect of including certain metabolites and other compounds in the assays on the amount of exposed sedimentable citrate synthase was also studied. The amount of exposed sedimentable citrate synthase was not affected by 50 μM oxalacetate, 1 mM citrate, 0.1 mM disodium ethylenediaminetetracetic acid 0.1 mM $MgCl_2$ or 0.1 mM $CaCl_2$. However, 0.1 mM or 1 mM potassium phosphate causes the release of all exposed citrate synthase into the supernatant. This is not an effect of ionic strength (See Figure 1) so it must be considered to be a specific effect of phosphate. This observation raises the possibility that the Krebs tricarboxylic acid cycle metabolon may exist on at least two levels of regulation. Additionally, we can prepare sedimentable citrate synthase by hypoosmotic shock (mitochondria diluted to 1 mg/ml to 10 mg/ml in water) treatment with low concentration of detergent (0.005% triton X-100 at 6 mg/ml mitochondria, or hyperosmotic shock at 30% sucrose).

If the enzymes of the Krebs tricarboxylic acid cycle are indeed arranged in a metabolon, it would be predicted that the other enzymes considered to be soluble, i.e., fumarase, malate dehydrogenase, aconitase, and (NAD^+)isocitrate dehydrogenase, would also be present in a sedimentable form. This was tested and found to be the case (Table VI). Succinyl CoA synthase (succinate thiokinase) was not studied here, since the enzyme has previously been shown to be bound to the α-ketoglutarate dehydrogenase complex (15), and its assay in crude systems is difficult. Nonetheless, this previous work and the present results definitely show all the "soluble" matrix enzymes of the Krebs tricarboxylic acid cycle can be present in a bound and potentially organized form.

Table 3 Sedimentation of Krebs Tricarboxylic cycle enzymes from gently disrupted mitochondria[+]

Enzyme	Enzyme Units Exposed	Pellet	Supernatant
Experiment 1			
Citrate Synthase	0.21 ± 0.005	0.12 ± 0.0025	0.14 ± 0.01
Fumarase	0.23 ± 0.0	0.14 ± 0.05	0.07 ± 0.0
(NAD^+) Isocitrate Dehydrogenase	0.05 ± 0.0	0.019 ± 0.0015	0.018 ± 0.001
Experiment 2			
Citrate Synthase	0.31 ± 0.015	0.16 ± 0.0	0.21 ± 0.0
Malate Dehydrogenase	6.3 ± 0.2	2.6 ± 0.1	5.1 ± 0.15
Aconitase	0.09 ± 0.01	0.045 ± 0.003	0.023 ± 0.0

[+]Numbers represent the average enzyme activities of duplicate assays ± ranges, with all enzymes determined in the same samples. Experiments 1 and 2 were different preparations of mitochondria. In experiment 1 the samples were prepared as described in Methods, whereas in experiment 2, 5 mM 2-mercaptoethanol was included in the KCl/HEPES buffer.

The microstructural changes induced by sonic oscillation are shown in Figures 2 and 3.

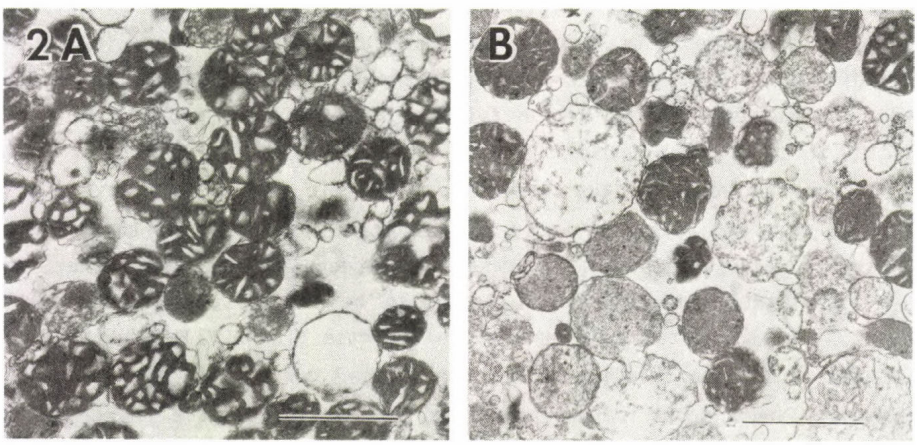

Fig. 2 Transmission Electron Microscopy of thin section of intact and gently disrupted mitochondria. Samples were processed by routine technique and examined on a Phillips 301 electron microscope with an operating voltage of 60 kV. Inset bars present 1 micron. Part A, intact mitochondria. Part B, gently disrupted mitochondria.

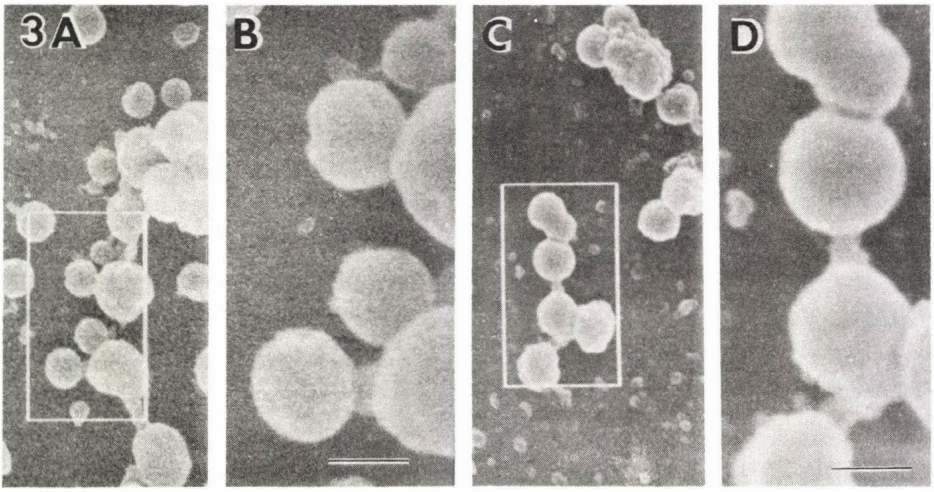

Fig. 3 Scanning Electron Microscopy of intact and gently disrupted mitochondria. Portions of each mitochondrial sample were fixed in glutaraldehyde, transferred to ovalbumin-coated cover slips, osmicated and critical-point dried. The samples were then gold-sputtered and examined in an ISI 40 scanning electron microscope. Insert bars represent 1.5 micron on parts A and C, and 0.5 micron on parts B and D. Parts A and B, intact mitochondria. Parts C and D, gently disrupted mitochondria.

These data demonstrate that there is minimal although significant change in structures by these techniques. It must be considered that the thin-section photographs represent only a portion of each mitochondrion's structure, and with study of the scanning electron micrographs and negatively stained samples (not shown) the most likely conclusion is that the population of mitochondria obtained by gentle sonic oscillation is a homogenous one, with virtually no "intact" structures remaining.

In conclusion, we have investigated an experimental system wherein the enzymes of the Krebs tricarboxylic acid cycle behave in such a manner that a sequential reaction mechanism involving purely soluble activities in the mitochondrial matrix is highly unlikely. The enzymes are available for assay, yet exist in a form sedimentable at moderate centrifugal force. We have preferentially studied the activity of citrate synthase since there is no cytoplasmic isozyme in mammalian systems. This enzyme is easily and accurately assayable in crude systems such as this; it is stable; and specific antibodies were available for it. Citrate synthase shows the properties of accessibility to antibodies, sedimentability under varying conditions of pH, ionic strength, temperature, and presence of substrates which would be expected if in vivo it was present in a metabolon.

Acknowledgments

The authors acknowledge the excellent technical assistance of Mr. Daniel D. Owens and Mr. Reginald Tyiska; the efforts of Dr. Lindsey Inman of the Electron Microscopy Unit of the VA Medical Center at Dallas; and manuscript preparation by Penny Perkins. This work was supported by the Research Service of the Veterans Administration, USPHS, NSF, and the Welch Foundation.

References

1. Robinson, J.B. Jr. and Srere, P.A. (1985) Organization of Krebs Tricarboxylic Acid Cycle Enzymes in Mitochondria. J. Biol. Chem. (in press).
2. Srere, P.A. (1980) The Infrastructure of the Mitochondrial Matrix. Trends Biochem. Sci. 5, 120-121.
3. Srere, P.A. (1982) The Structure of the Mitochondrial Inner Membrane-Matrix Compartment. Trends Biochem. Sci. 7, 375-378.
4. Clegg, J.S. (1984) Properties and Metabolism of the Aqueous Cytoplasm and its Boundaries. Am. J. Physiol. 246, R133-R151.
5. D'Souza, S.F. and Srere, P.A. (1983) Binding of Citrate Synthase to Mitochondrial Inner Membranes. J. Biol. Chem. 258, 4706-4709.
6. Srere, P.A., Brazil, H., and Gonen, L. (1963) The Citrate Condensing Enzyme of Pigeon Breast Muscle and Moth Flight Muscle. Acta Chem. Scand. 17, S129-S134.
7. Moore, G.E., Gadol, S.M., Robinson, J.B. Jr., and Srere, P.A. (1984) Binding of Citrate Synthase and Malate Dehydrogenase to Mitochondrial Inner Membranes-Tissue Distribution and Metabolite Effects. Biochem. Biophys. Res. Commun. 121, 612-618.
8. Fansler, B. and Lowenstein, J.M. (1969) Aconitase from Pig Heart. Meth. Enzymol. 13, 26-30.
9. Plaut, G.W.E. (1969) Isocitrate Dehydrogenase (DPN-Specific) from Bovine Heart. Meth. Enzymol. 13, 34-42.
10. Hall, R.L. and Bradshaw, R.A. (1969) Fumarase. Meth. Enzymol. 13, 91-99.
11. Kitto, G.B. (1969) Intra- and Extramitochondrial Malate Dehydrogenase from Chicken and Tuna Heart. Meth. Enzymol. 13, 106-116.
12. Delafield, F.P. and Doudorff, M. (1969) α-Hydroxybutyrate Dehydrogenase from Pseudonomas lemoignei. Meth. Enzymol. 14, 227-231.
13. Bradford, M.M. (1976) A Rapid and Sensitive Method for the Quantitation of Microgram Quantities of Protein Utilizing the Principle of Protein-Dye Binding. Anal. Biochem. 72, 248-254.
14. Moriyama, T. and Srere, P.A. (1971) Purification of Rat Heart and Rat Liver Citrate Synthases: Physical, Kinetic, and Immunological Studies. J. Biol. Chem. 246, 3217-3223.
15. Porpaczy, Z., Sumegi, B., and Alkonyi, I. (1983) Interaction Between the α-Ketoglutarate Dehydrogenase Complex and Succinate Thiokinase. Biochim. Biophys. Acta 749, 172-179.

SLUSE-COFFART:

Is it possible that, after gentle sonication and centrifugation at 50 000 g, the measurable enzymic activity in the pellet in the absence of detergent is linked to inverted submitochondrial particles?

SRERE:

The electron micrographs show very few submitochondrial particles. We have in addition tried differential centrifugation of the sonicated mitochondria and found no evidence for smaller particles containing exposed enzyme activity.

KACSER:

The close association of enzymes on some matrix could affect the control properties of the pathway of which they form part. For example, if two consecutive enzymes are closely associated, this may result in "channelling" of the substrate/product. The outcome of this is that, from a control point of view, there is only one functional entity and only one control coefficient. This will affect the distribution of control in the system. Has this aspect been considered?

SRERE:

No experiments on the control aspects of the isolated complex has been performed.

AMLER:

Do you think, that the folding of the inner mitochondrial membrane controls matrix enzyme complexes associated with this membrane?

SRERE:

The shape of cristae of mitochondria varies from tissue to tissue, and there are no theories to explain the charge in morphology. We do know that under various metabolic conditions the cristae can change their conformation but there is no evidence that the folding controls the enzymes attached to it.

CHERRY:

Perhaps I could comment on the effect of matrix proteins on mobility of inner mitochondrial membrane proteins. I think it is important to distinguish here between rotational and lateral mobility. We have measured the rotational mobility of cytochrome oxidase and got similar results in intact mitochondria, submitochondrial-particles and in reconstituted vesicles, indicating that there is no significant restriction by matrix proteins. On the other hand, lateral diffusion coefficients for inner membrane proteins determined by other groups are much less than expected for free diffusion in a lipid bilayer so there may well be an effect of the matrix on lateral mobility.

SRERE:

I should have mentioned that Dr. Cherry has shown that some of the electron transport proteins in the inner membrane occur as aggregates.

Dynamics of Biochemical Systems
S. Damjanovich, T. Keleti, L. Trón (Eds)

CHARACTERIZATION OF METABOLITE POOLS BY "ENZYME PROBES"

PETER FRIEDRICH

Institute of Enzymology, Biological Research Center,
Hungarian Academy of Sciences, Budapest, P.O.B.7,
Hungary H-1502

The living cell is a highly organized hierarchy of compartments. According to Kempner /1980/, a metabolic compartment is a subcellular region of biochemical reactions kinetically isolated from the rest of cellular processes. This general definition allows for various physical means in creating a compartment. In the most obvious case a compartment is surrounded by a membrane which determines the traffic of matter in and out of the compartment. Such compartments, e.g. the cytoplasm or the mitochondrial matrix, are usually large relative to an enzyme, let alone substrate, molecule and therefore we refer to them as macrocompartments. Kinetic isolation of a reaction can, however, be achieved by more subtle means. In a multienzyme complex some intermediates may be "channelled" from one enzyme to the other without mixing with the rest of cellular material. Alternatively, both enzymes and metabolites may be attached to binding sites within a macrocompartment, which introduces heterogeneity inasmuch as the enzyme or metabolite pool becomes subdivided into free and bound fractions. Enzyme-enzyme channels and intracellular binding sites are as a rule in the order of the size of a molecule, hence we refer to them as microcompartments /cf.Friedrich, 1984/.

Our attention will be focussed here on microcompartmentation established by binding sites. If an enzyme is attached to some cellular structure, as for example glyceraldehyde-3--phosphate dehydrogenase /GAPD/ is anchored at the erythrocyte membrane /e.g.Kliman and Steck, 1980; Solti et al., 1981/ or

hexokinase at the mitochondrial membrane /e.g.Wilson, 1980/, the given reaction will occur at a certain cellular niche, thus the product metabolite will be abundant in that location. Such anchoring of enzymes may be a physical prerequisite for channelling of metabolite/s/ from one enzyme to the other, i.e.for another type of microcompartmentation. However, the local confinement of catalytic activity may also serve other ends. For example, the specificity of protein kinases, which phosphorylate a number of substrate proteins in vitro, is thought to be largely determined by the subcellular location, i.e. by the juxtaposition of the target protein. Data have been presented suggesting that the binding of protein kinase, and the change of its binding site /translocation/, may be instrumental in the plastic changes of neurons, i.e. in memory mechanisms /Kandel and Schwartz, 1982; Saitoh and Schwartz, 1985/. Cytoskeletal proteins, particularly MAP-2, are thought to harbour protein kinases /Vallee et al., 1984/, which thereby may influence a number of cellular processes, like motility, shape changes, intracellular transport, cell division, etc.

On the other hand, if a metabolite is bound to some macromolecule in a macrocompartment, the consequences are quite different. The immediate result of such a binding is the lowering of the concentration /activity/ of the free metabolite, hence the decrease of metabolic flux using that metabolite. Since binding is reversible, an abundant binding species may serve as a buffer attenuating sharp changes in the production of the metabolite. It must be emphasized, however, that in steady-state a binding species has no effect on flux unless its concentration in the cell can be altered.

It has been recognized for long /e.g.Sols and Marco,1970/ that much of the intracellular metabolite pools is bound to functionally related macromolecules, mainly enzymes. One can even estimate the distribution of a compound between free and bound fractions in the knowledge of the intracellular concentration of the compound, of the binding species and the correspoding dissociation constant/s/. However, such estimates necessarily imply an unstructured reservoir and the validity of the laws of dilute solutions, two assumption hardly applicable to the living cell.

We have earlier devised a simple approach to characterize metabolite pools in respect of free and bound fractions /Solti and Friedrich, 1979/. The rationale of the approach is as follows. The cells /or the tissues/ are disrupted and simultaneously an enzyme is introduced which attacks the metabolite in question. The time course of decay of the metabolite is then followed. In the simplest case, when the total amount of the metabolite is free, one gets a single first order decay curve /provided that the initial metabolite concentration is well below its K_m/ and the rate constant is proportional to the concentration of the degrading enzyme. If in addition to the free fraction there is also a bound fraction of the metabolite, the decay curve will be biphasic,as long as the dissociation rate constant of the metabolite is comparable or smaller than the rate constant of enzymatic degradation. More than one bound fraction, with dissimilar dissociation rate constants, will result in the corresponding number of slow phases.

Since in such an experiment the degrading enzyme is utilized to probe the metabolite pool, we have referred to it as an "enzyme probe" /Solti and Friedrich, 1979/. The scope of the method can be summarized briefly as follows. It is applicable to any compound for which an appropriate degrading enzyme exists, whether endogenous or exogenous. Complexes whose dissociation is considerably faster than the enzymatic decay escape detection. Similarly, different binding species /complexes/ with closely similar dissociation rate constants cannot be distinguished from each other. The activity of the degrading enzyme must not change over the time period of analysis. With the number of bound fractions resolution rapidly deteriorates: more than two bound fractions can be distinguished only under very favourable instances. Obviously, the metabolite must not be generated in the system during analysis.

In the following the application of this "enzyme probe" method for the characterization of metabolite pool heterogeneities will be illustrated through two examples: NAD microcompartmentation in human erythrocytes and cAMP micro-

compartmentation in wild type and memory-mutant Drosophila melanogaster.

In fresh human erythrocytes the NAD + NADH concentration is about 50 μM and the oxidized form of the coenzyme is greatly favoured. We monitored the decay of NAD in packed red cells /haematocrit: 100%/ after cell disruption by sonication /Solti and Friedrich, 1979/. Namely, the enzyme NAD-glycohydrolase /EC 3.2.2.5/, which splits NAD at the nicotinamide-ribose linkage, is located on the outer surface of red cell membrane and gains access to intracellular NAD only after cell disruption. Fig.1 shows the time course of NAD decomposition in the hemolysate and the graphic resolution of overall reaction into three kinetically distinguishable phases. Phase III /$t_{1/2} \approx 1$ min/ corresponds to the reaction of free NAD as evidenced by the closely similar $t_{1/2}$ measured for added NAD in a dilute homogenate. Phase II /$t_{1/2} = 7$ min/ proved to be identical with the reaction of NAD bound to GAPD, whereas in phase I /$t_{1/2} = 4$ hours/ some unidentified NAD-complex decomposes which, however, becomes rapidly destroyed in the presence of 0.01 % Triton X-100. The assignment of pool II as GAPD.NAD complex could be made by measuring NAD decay first at $0^{o}C$ when free NAD is mainly decomposed, and then continuing the reaction at $37^{o}C$, when pool II becomes depleted /Fig.2/. The latter process ran parallel with the "stripping" of NAD from its GAPD-complex, monitored by the decrease of reactivity of the enzyme's essential SH-group against iodoacetate. Namely, bound NAD had been shown to markedly facilitate this alkylation of the enzyme /Cseke and Boross, 1970/. Interestingly, the depletion of pool II led to the arrest of lactate production in the haemolysate /Fig.3/. The results suggest that in the red cell the pool II of NAD is necessary and sufficient to maintain the normal flux of glycolysis.

Recently we have been engaged in the study of cAMP metabolism in memory-mutant Drosophila melanogaster. The dunce mutant strains are defective in a cAMP-specific phosphodiesterase /PDE-II/, have elevated cAMP levels and perform poorly in an electric shock-odour learning paradigm /Dudai et al., 1976; Byers et al., 1981; Dudai, 1985/. We addressed the question

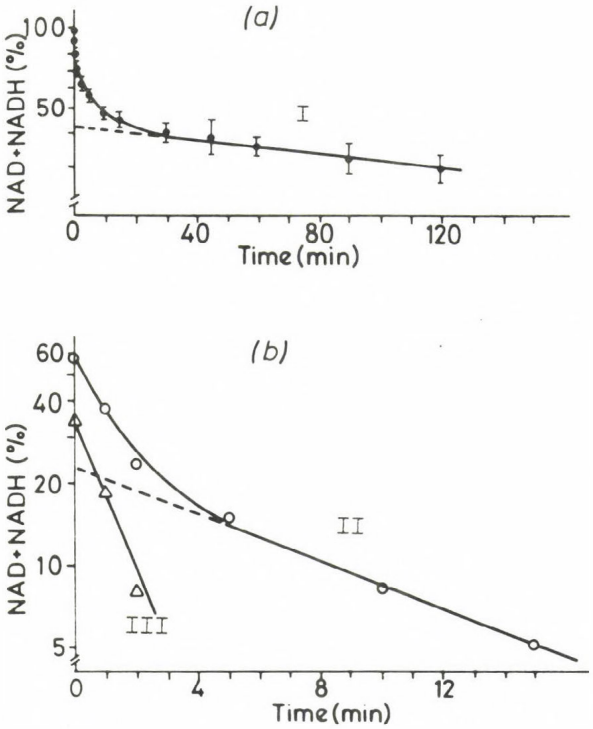

Fig.1. Time course and kinetic resolution of NAD decay in human erythrocyte sonicate at 37°C. 0 time: start of 30 s sonication. At times samples were withdrawn for NAD + NADH determination. (a): Overall decay (•) (b): Curve (o) was derived by subtracting the extrapolated slow phase I /broken line/ from the curve in (a). Curve III (Δ) was obtained from curve (o) in a similar manner. From Solti and Friedrich /1979/.

whether the extra cAMP in the mutant /in wild type Canton-S: 1.6 pmol per mg fly; in <u>dunce</u>^{M11}: 6 to 10 pmol per mg fly/ is free or is sequestered by binding to protein. We applied the "enzyme probe" method, analogously to human erythrocytes: we followed the time course of cAMP decay in fresh homogenate of flies under the effect of endogenous cyclic nucleotide phosphodiesterases /Friedrich et al., 1984/. The decay curve was strongly biphasic

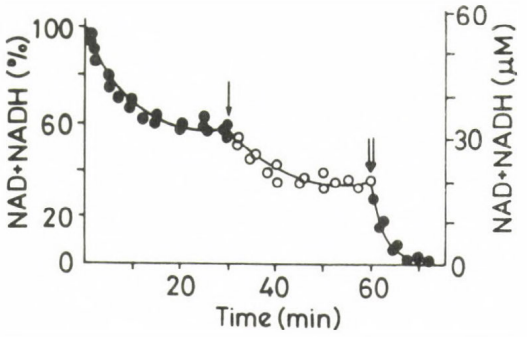

Fig.2. Resolution of NAD pools. The NAD decay was monitored as in Fig.1 but at $0^{o}C$ (●), then at $37^{o}C$ (o), finally after addition of 0.01 % (final concentration) Triton X-100 (▪). From Solti and Friedrich (1979).

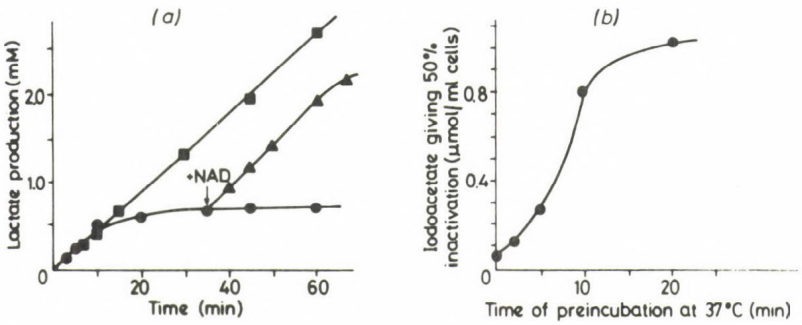

Fig. 3. Lactate production from 5 mM glucose /A/ and development of iodoacetate-resistance /B/ in a 90 % red cell sonicate. a: Lactate production of intact cells /■/, of sonicate /●/, and of sonicate after addition of 100 uM NAD as indicated by the arrow /▲/.
b: Development of iodoacetate resistance of glyceraldehyde-3-phosphate dehydrogenase. Note that the resistance /i.e.stripping of GAPD/ reaches maximum at about the same time /about 15 min/ as lactate production ceases. From Solti and Friedrich /1979/.

with both wild type and mutant flies (Fig.4). A very rapid phase was followed by a slow phase. The apparent first order rate constant of the latter was similar for Canton-S and dunce^{M11} /4.5 /±0.5/x 10^{-2} min^{-1} and 4.2 /±0.6/x 10^{-2} min^{-1}, respectively/. The extrapolated intercepts on the ordinate of the slow phases gave, however, different values for the total amount of slowly-degrading cAMP: in the mutant the slow component was about three times as high as in the normal /1.5 vs. 0.55 pmol cAMP per mg fly/.

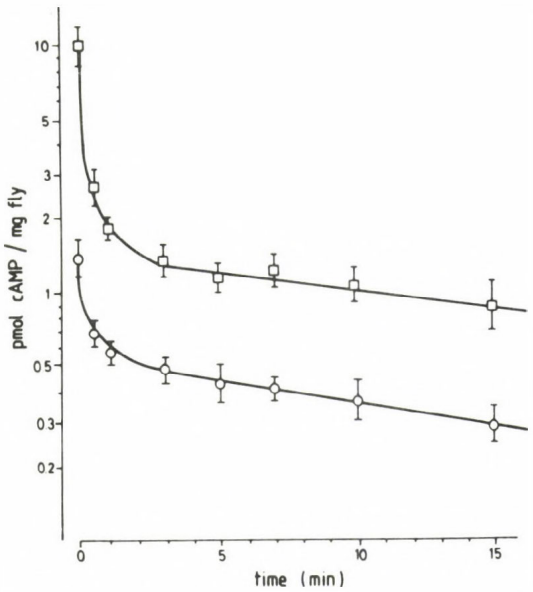

Fig.4. Time course of cAMP decay in Drosophila homogenates /100 mg fly/ml/ at 0°C. cAMP was determined by radioimmunoassay. o, Canton-S flies; □, dunce^{M11} flies. From Friedrich et al. /1984/.

Control experiments indicated that the occurrence of slow phase was not due to inactivation of PDEs in the homogenate. Adenylate cyclase activity was practically nil during the

experiment; with dilute homogenate exogenous cAMP gave a first order decay /cf.Friedrich et al.,1984/. The observed upward shift of the ordinate intercept could also be modelled: if exogenous cAMP was added at the time of homogenization of Canton-S flies, the slow phase moved upward without change of the slope /Fig.5/.

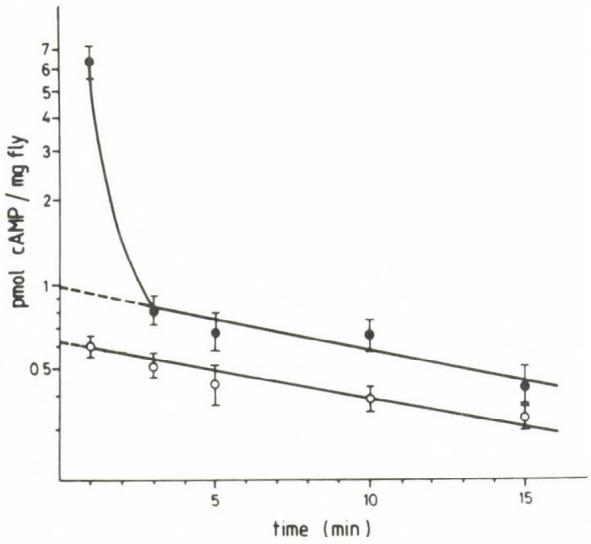

Fig. 5. Effect of exogenous cAMP on the slow phase of cAMP decay in Canton-S homogenate. o, no addition; •, 30 pmole of cAMP/mg fly included in the homogenizing buffer. From Friedrich et al./1984/.

Thus the interpretation of Fig. 4 is that in the mutant part of the extra cAMP is bound to protein, in all probability to the regulatory /R/ subunit of cAMP-dependent protein kinase: in <u>dunce</u>^{M11} the concentration of R.cAMP complex is about threefold the normal. We do not know the exact meaning of this observation. It may indicate that the high cAMP in the mutant keeps the protein kinase holoenzyme in a higher degree of dissociation resulting in some extra protein phosphorylation. Indeed, such phenomena have been demonstrated /Dévay et al.,

1984/. On the other hand, since the catalytic and regulatory subunits of cAMP-dependent protein kinase may be expressed separately, the higher level of R.cAMP may be part of a compensatory mechanism developed by the mutant in order to neutralize the excess of cAMP, which otherwise might be detrimental to physiological processes more vital than associative learning.

In conclusion, the enzyme probe method can be conveniently used to characterize metabolite pools in respect of their reactivity heterogeneity, which generally stems from sequestration by binding. It should be noted that the method is simple and can be widely applied, as endogenous or exogenous degrading enzymes can be found for most naturally occurring compounds. The circumstance that the decay curve is started at the time of homogenization reduces the possibility of post-disruptional rearrangements in binding. The example of cAMP analysis illustrates that physiological metabolizing enzymes can also serve as "enzyme probes", because in the homogenate the degradative processes predominate. Nevertheless, each case should be examined individually to ascertain that the above criteria of analysis are met.

References

Byers, D., Davis, R.L. and Kiger, J.A.,Jr./1981/ Defect in cyclic AMP phosphodiesterase due to the dunce mutation of learning in Drosophila melanogaster. Nature 289, 79-81.

Cseke, E. and Boross, L./1970/ Factors affecting the reactivity of the activated SH-group of D-glyceraldehyde-3-phosphate dehydrogenase. Acta Biochim. Biophys. Acad. Sci. Hung.5, 385-398.

Dévay, P., Solti, M., Kiss,I., Dombrádi, V. and Friedrich,P. /1984/ Differences in protein phosphorylation in vivo and in vitro between wild type and dunce strains of Drosophila melanogaster. Int. J. Biochem.16, 1401-1408.

Dudai, Y./1985/ Genes, enzymes and learning in Drosophila. Trends Neurosci. 8, 18-21.

Dudai, Y., Jan, Y.-N., Byers, D., Quinn, W.G. and Benzer, S.

/1976/ dunce, a mutant of Drosophila deficient in learning. Proc. Natl. Acad. Sci. USA 73, 1684-1688.

Friedrich, P. /1984/ Supramolecular Enzyme Organization. Quaternary Structure and Beyond. Pergamon Press, Oxford, Akadémiai Kiadó, Budapest.

Friedrich, P., Solti, M. and Gyurkovics, H./1984/ Microcompartmentation of cAMP in wild type and memorymutant dunce strains of Drosophila melanogaster. J. Cell. Biochem. 26, 197-203.

Kandel, E.R. and Schwartz, J.H./1982/ Molecular biology of learning: Modulation of transmitter release. Science 218, 433-443.

Kempner, E.S./1980/ Metabolic compartments and their interactions. In Cell Compartmentation and Metabolic Channeling. /Nover, L., Lynen, F. and Mothes, K., eds/, VEB Gustav Fischer Verlag, Jena, Elsevier/North Holland Biomedical Press, Amsterdam-New York-Oxford, pp. 211-224.

Kliman, H. J. and Steck, T.L./1980/ Association of glyceraldehyde-3-phosphate dehydrogenase with the human red cell membrane. J. Biol. Chem. 255, 6314-6321.

Saitoh, T.and Schwartz, J.H./1985/ Phosphorylation-dependent subcellular translocation of a Ca^{2+}/Calmodulin-dependent protein kinase produces an autonomous enzyme in Aplysia neurons. J. Cell Biol. 100, 835-842.

Sols, A. and Marco, R. /1970/ Concentrations of metabolites and binding species. Implications in metabolic regulation. Curr. Top. Cell. Regul. 2, 227-273.

Solti, M. and Friedrich, P./1979/ The "enzyme probe" method for characterizing metabolite pools. The use of NAD-glycohydrolase in human erythrocyte sonicate as a model system. Eur. J. Bichem. 95, 551-559.

Solti, M., Bartha, F., Halász, N., Tóth, G., Sirokmán, F. and Friedrich, P. /1981/ Localization of glyceraldehyde-3-phosphate dehydrogenase in intact human erythrocytes. Evaluation of membrane adherence on autoradiograms at low grain density. J. Biol Chem. 256, 9260-9265.

Vallee, R.B., Bloom, G.S. and Theurkauf, W.E. /1984/ Micro-

tubule-associated proteins: Subunits of the cytomatrix. J. Cell Biol. 99, 38s-44s.

Wilson, J. E. /1980/ Brain hexokinase, the prototype ambiquitous enzyme. Curr. Top. Cell. Regul. 16, 1-44.

DISCUSSION

SLUSE-GOFFART:

My question deals with the first example of kinetically distinguishable compartments. Is it excluded that the three-NAD compartments are due to three different levels of disruption of erythrocytes, namely no disruption, partial disruption and total disruption?

FRIEDRICH:

We have carefully excluded this obvious possibility. We made sure that haemolysis by sonication be complete, which we monitored by the release of haemoglobin. In our standard protocol we applied the minimum time of sonication that produced practically 100 % haemolysis. Further sonication did not change the time course of coenzyme decay shown in Fig. 1.

Dynamics of Biochemical Systems
S. Damjanovich, T. Keleti, L. Trón (Eds)

DYNAMICS OF AEROBIC ENERGY METABOLISM, COENZYME CYCLES, FEEDBACK AND FEEDFORWARD CONTROL AND HOMEOSTASIS

V.V. DYNNIK, R.H. DJAFAROV, I.M. DJAFAROVA

Institute of Biological Physics, Acad. Sci USSR,
Pushchino, SU-142292, USSR

The dynamical properties of energy metabolism (EM) such as stabilization of ATP (or energy charge) (1-3), trigger phenomena (2, 4, 5), self-oscillations (6-8) are due to the presence of a great number of feedback and feedforward loops (both positive and negative) in EM. The regulatory loops of allosteric nature can easily be identified. At the same time, regulatory loops can arise at the stoichiometric level (2, 4, 5, 9-11). The mechanisms of their formation and their functions have hardly been studied. It is not clear, either, why the number of the regulatory loops in EM is as large as it is. Does not this lead to excessive metabolic control?

The aim of the present paper is to attract attention to the peculiarities of the stoichiometric organization of EM and of the system of regulatory loops. The results come from analysis of the available data by mathematical models and from our own experiments.

RESULTS

Structure and regulation of the aerobic EM of animal tissues

The core of aerobic EM is the tricarboxylic acid cycle (TCA-cycle). It is in this system that fragments of the initial substrates in the form of AcCoA are being oxidized to CO_2

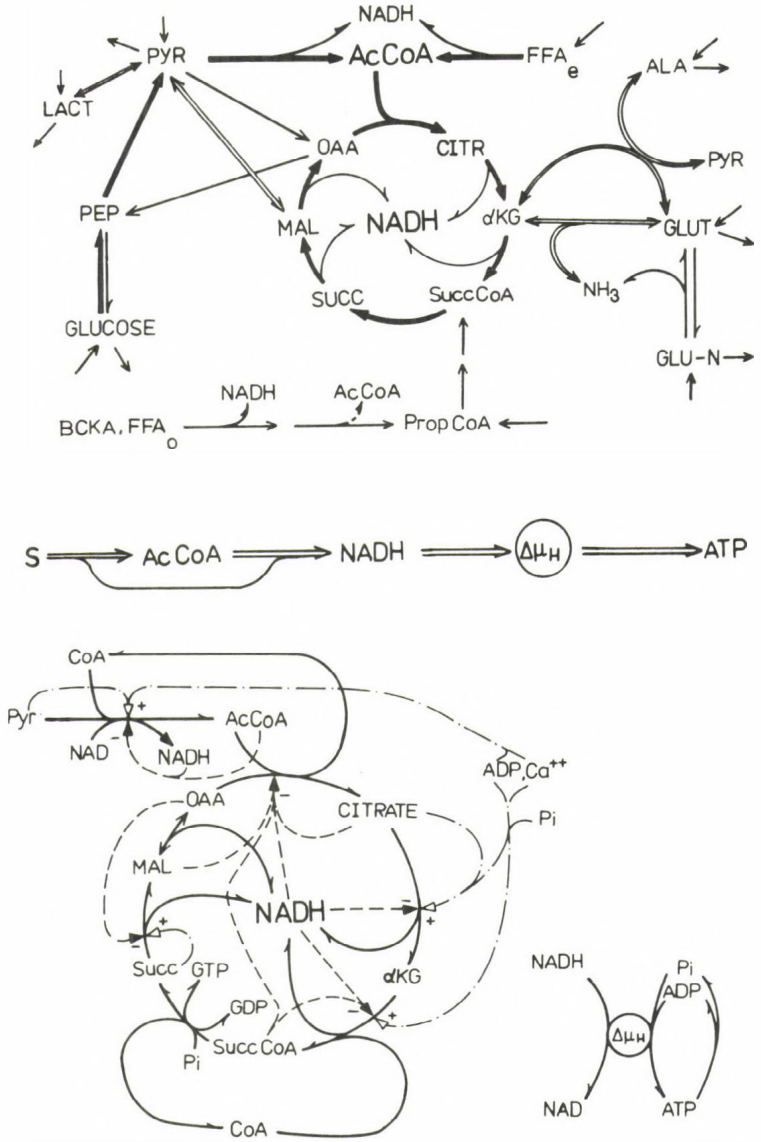

Figure 1

A scheme of the metabolic pathways of the aerobic energy metabolism (top) and various types of regulation of the tricarboxylic acid cycle and pyruvate dehydrogenase (bottom). Activation (+) and inhibition (-) of different reactions are shown by dashed-and-dotted and dotted lines, respectively.

(Fig. 1, top). The cycle cannot be treated as an isolated circular system. The various satellite reactions feeding in and out of the cycle (shown by thin and double lines on the top of Fig. 1) cannot be disregarded. The net fluxes in the reactions do not exceed 10 % of maximal cycle flux in the heart. Owing to these reactions, however, the sum of the cycle intermediates can vary under physiological conditions by one order of magnitude and more (12)

The carbohydrates, even (e) and odd (o) fatty acids (FFA), branched chain ketoacids (BCKA) and propionate enter the cycle as AcCoA and (or) SuccCoA. The bulk of the flux is through AcCoA. The entry through SuccCoA is minor (except for ruminant liver) and its hyperactivation causes severe metabolic disorders (13).

The dashed arrows (Fig. 1, bottom) indicate different types of regulation of the TCA-cycle and of pyruvate dehydrogenase (PDH) reaction. Except for the inhibition of citrate synthase (CS) by malate, all the regulatory mechanisms involve negative feedback loops (NFLs), which may be grouped into local and global ones. All the entries to the cycle undergo a multiple control.

There are also stoichiometric feedback and feedforward loops, which are not as readily evident. Let us consider a few examples of such NFLs. For instance, the CoA - AcCoA pair couples the CS and PDH reactions, owing to a constancy of the sum of CoA-thioesters in the mitochondria. Analogously, all the NADH-producing dehydrogenases are coupled to the reactions of the respiratory chain. The reactions of ATP synthesis are coupled to cellular ATPases. Lipman was the first to notice this property of coenzymes (14).

Coenzyme cycles of EM

Disregarding the complicated structure of EM and focussing attention on the net reactions of coenzyme conversions, we arrive at a scheme (for EM of muscles) containing three coenzyme cycles (Fig. 2).

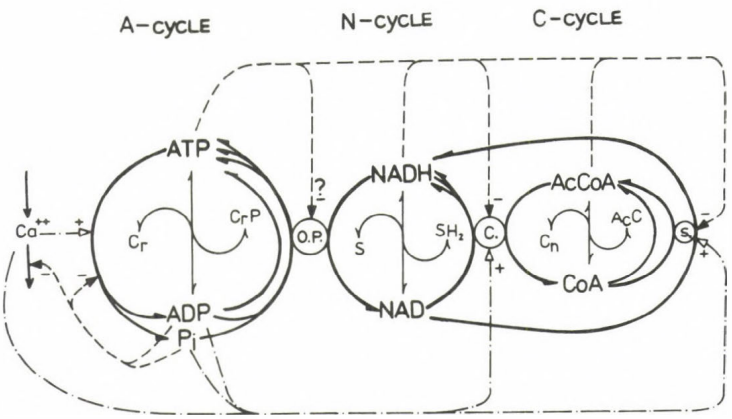

Figure 2

Coenzyme cycles and global negative feedback loops (dashed and dashed-and-dotted lines) in muscle energetics

The C-cycle is formed by the reactions of conversion of the initial substrates (s) to AcCoA and by the CS-reaction of TCA-cycle. The NAD-reducing dehydrogenases and the reactions of respiratory chain constitute the N-cycle, and the reactions of ATP synthesis and hydrolysis - the A-cycle. The coupling between the cycles is due to the systems of the oxidative phosphorylation and TCA-cycle.

Each type of coenzyme has its own buffer. For ATP, NADH and AcCoA, these are CrP, reduced substrates and acetylcarnitine.

This representation of the aerobic EM reveals a hierarchy of global NDLs, which form a family of nested loops (dotted lines in Fig. 2). The NFLs formed by the adenylates and inorganic phosphate, P_i, control fluxes in all cycles. The effect of the pyridine nucleotides is limited by the dehydrogenases of N- and C-cycles. The influence of CoA-thioesters extends to the reactions of C-cycle. Fluxes in the cycles are preset by the ATPase load, i.e. by the net rate of ATP hydrolysis by the ATPases of actomyosin and sarcoplasmic reticulum and by Na^+-K^+ ATPase. Ca^{2+} participates in the control of all coenzyme

cycles. However, it cannot be considered as an external regulator, because its level is regulated by adenylates and P_i.

The system of the coenzyme cycles for liver EM is slightly different due to the synthesis of ketone bodies with the AcCoA to CoA conversion running independently of TCA-cycle. In the liver, the net rate of ATP hydrolysis is determined by Na^+-K^+ ATPase and by "ATPases" of biosynthetic pathways. The CrP-buffer is absent and Ca^{2+} is not involved in the immediate control of EM.

Dynamics of the cycles

It would be now interesting to compare the maximum fluxes and the total content of the coenzymes in the A, N and C-cycles. Their magnitudes for rat heart mitochondria are as follows: 20-23, 7-8, 1.5 μmol/sec/g dry wt and 4-5, 1-1.5, 0.5-1 μmol/g dry wt, respectively. It follows from this comparison that the turnover time in each cycle is less than a second. With these values the jumps in the rates of consumption of ATP, NADH or AcCoA might cause a depletion of the appropriate coenzymes, because of the delays in the metabolic pathways of ATP, NADH and AcCoA synthesis.

However, the depletion never occurs owing to the buffers and to a great number of NFLs, whose immediate effect is the levelling off of the fluxes. The effect is primarily due to adenylates and P_i which activate various pathways of EM and reduce the rates of ATP hydrolysis by ATPases (Fig. 2).

The importance of such a control of ATPases during the transient periods of overload, when the rate of ATP hydrolysis (V_{ADP}) exceeds by far that of its synthesis, is seen from Fig. 3. The system without feedback control of ATPases is critically dependent on workload (right). The increase in its magnitude or duration (periods of workload are marked by black rectangles) will cause ATP depletion and the development of the rigor state. The system with feedback control (left) can stand twice as great a load without ATP depletion (shown by broken lines). In this system the inhibition of ATPases by the

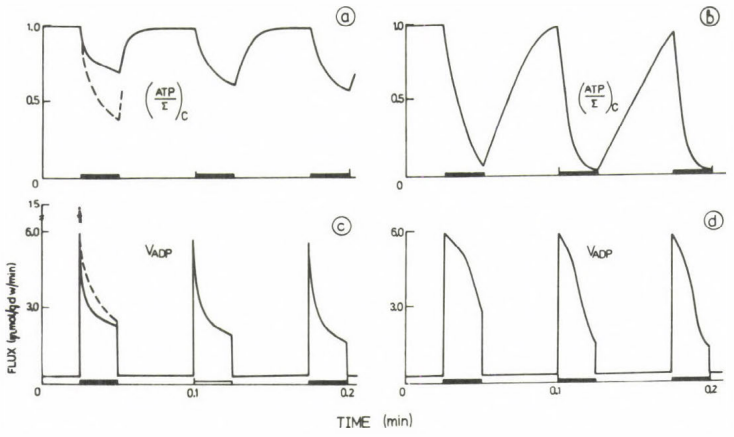

Figure 3

Effect of overload on cytosolic ATP level and the net rate of ATP hydrolysis (V_{ADP}) in a model of muscle energy metabolism. Periods of increased load are marked by black rectangles. Left, a system incorporating the regulation of ATPases by their products; right, a system lacking this feedback regulation.

accumulated ADP will lead to a rapid fall of V_{ADP} and, hence, of the force developed by muscle. It is this spike constituent of the force developed (V_{ADP}) that is important for many voluntary efforts. The above mechanisms of the regulation of ATPases and of Ca^{2+} level in cytosol by adenylates and P_i must be taken into consideration in explaining the autonomous control of EM and in studying the phenomena of muscle fatigue and myocardial failure.

Coupling of fluxes in the coenzyme cycles

In the system considered (Fig. 2) the feedback structure looks like a family of embedded loops, some of them embracing 2 or 3 cycles. The theory of automatic regulation states that the inclusion of NFLs into various technical systems greatly reduces output signal sensitivity to changes in the internal elements. Systems with common NFLs, embracing all unreliable elements, show better suppression of noise than systems with

local loops embracing single elements (15).

In the EM, fluxes are set up by the ATPase load. Hence a low sensitivity of fluxes in the cycles to variations in different parameters can be anticipated.

At the same time, fluxes in the coenzyme cycles are coupled through the reactions of oxidative phosphorylation and TCA-cycle (Fig. 2). Because of the proton conductivity of mitochondrial membrane and the satellite reactions feeding in and draining the TCA-cycle out, the stoichiometry of the production of 12 ATP molecules per 1 AcCoA molecule is not fixed. Due to such slippage in the coupling systems the relationship between fluxes in the C- and A-cycles can be different under different conditions. Consider the EM of the heart as an example. Fig. 4 presents the calculated steady-state characteristics of EM. The upper left figure shows the dependence of flux in the C-cycle (which has the same rate as that of CS-reaction) on the ATPase load, i.e. on the flux in the A-cycle. The dotted, dashed and solid lines correspond to substrate (pyruvate) concentrations of 200 μM, 1 mM and 5 mM. It is easily seen that the flux in the CS-reaction as a function of the ATPase load remains invariant within 1 % with respect to the 25-fold change in pyruvate level. The growing pyruvate concentration will only cause an increase in the operating range of fluxes. This holds to within 2-3 % also for the other reactions of TCA-cycle, except malate dehydrogenase (MDH).

The ATP/ADP ratios, both cytosolic (cyt) and mitochondrial (mit), and the NADH/NAD ratio also show a weak sensitivity to variation of pyruvate in this concentration range (lower left and middle plots of Fig. 4). By contrast, the concentrations of oxaloacetate (OAA) and citrate change by more than one order of magnitude with the same values of ATPase load (upper right and middle plots).

It is important that the rate of the CS-reaction remains constant with the strongly varying level of OAA. The effect of the increased level of the substrate OAA is compensated by the appropriate increase in the level of the inhibitor of CS citrate.

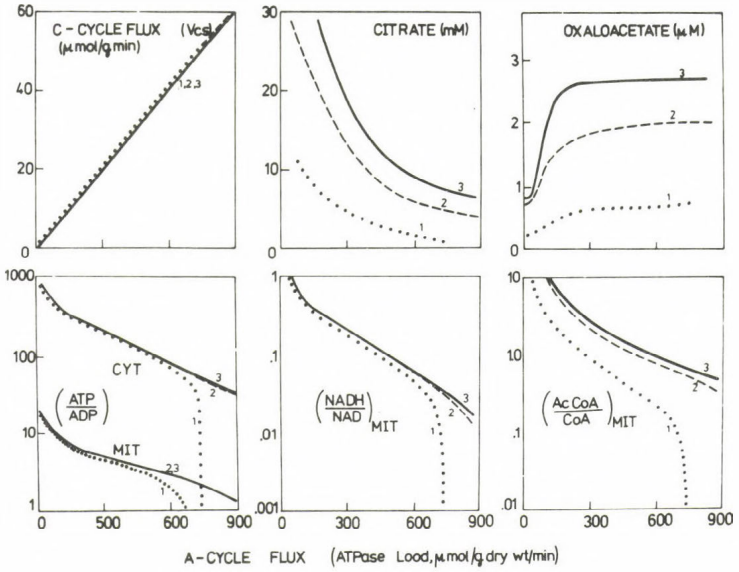

Figure 4

Steady-state characteristics of myocardial energetics, calculated by the model. The dotted, dashed and solid lines correspond to pyruvate concentrations of 200 μM, 1 mM and 5 mM.

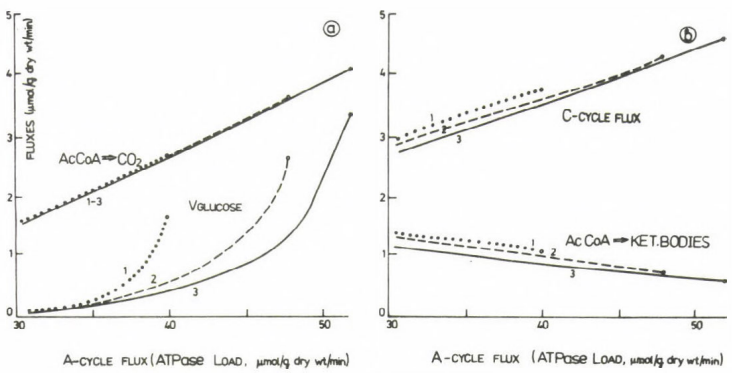

Figure 5

Steady-state characteristics for liver metabolism, calculated by the model for the case of gluconeogenesis from lactate and pyruvate whose concentrations vary in the ranges 100 μM → 4 mM and 10 μM → 0.4 mM, respectively. The dotted, dashed and solid lines correspond to pyruvate carboxylase activities of 5, 10 and 15 μmol/min/g dry wt.

Satellite reactions and regulation of TCA-cycle

The 25-fold increase in pyruvate concentration produces a marked change in the rate of OAA influx to the cycle through the pyruvate carboxylase (PC) reaction (Fig. 1, top). However, the rate of CS-reaction remains unaltered (Fig. 4, left and top) and the excess OAA is utilized by malic-enzyme and phosphoenolpyruvate carboxykinase (see Fig. 1).

The same properties are seen in the αKG-node. The increase in the αKG-influx through glutamate-pyruvate transaminase at excess pyruvate is largely compensated by its outflux through the glutamate dehydrogenase (Fig. 1, top). The effect of increasing αKG concentration in the αKGDH-reaction is compensated by an increase in the level of the inhibitor of αKGDH, SuccCoA.

Thus, in spite of the noticeable variation in the rates of the satellite reactions, the segment of TCA-cycle from CS to succinate dehydrogenase (SDH) behaves as a whole unit. This is achieved due to the great number of global NFLs in the TCA-cycle.

Similar properties of the TCA-cycle have been revealed also in the liver in the case of gluconeogenesis from lactate or alanine. Here the fluxes in the satellite reactions can amount to as much as 30 % of the maximum flux in the TCA-cycle.

The relationships between steady-state fluxes in the C- and A-cycles of liver EM are shown in Fig. 5. The rate of gluconeogenesis is predetermined by lactate, whose concentration changes from 100 μM to 4 mM for each curve in the model. The dotted, dashed and solid lines correspond to PC activity of 5, 10 and 15 μmol/g dry wt/min. Gluconeogenesis is an additional ATPase load for the liver EM. Because of this, the variation of PC activity causes a change in both the maximum rate of gluconeogenesis and the operational range of ATPase loads. However, despite such a strong change in the activity of PC, providing OAA to the cycle, the rate of the CS-reaction as a function of the ATPase load remains unaltered (Fig. 5, left). All the reactions of TCA-cycle, except MDH, also behave as a

single unit (with accuracy of 2-3 %). By contrast, the rate of ketogenesis, not subjected to the global feedback control, changes appreciably (Fig. 5, right). As a result, the net flux in the C-cycle is not stabilized either.

The results obtained show that the satellite reactions affect the concentrations of the intermediates, but not the fluxes and stoichiometry of TCA-cycle. This type of regulation of TCA-cycle and other branches of EM, involving the system of embedded NFLs, makes fluxes in the coenzyme cycles invariant with respect to the changing cellular parameters.

Flexibility of the control and homeostasis

The great number of NFLs in EM is not excessive and it makes the biochemical control flexible. With varying cellular parameters, it permits either synergetic or antagonistic operation and the replacement of one regulatory mechanism by another (16).

In the myocardium, with glucose as a substrate, the main regulators in the TCA-cycle are adenylates, P_i, Ca^{2+} and the concentrations of intermediates in the whole range of workloads (16). The presence of fatty acids causes a large increase in the levels of AcCoA, SuccCoA and NADH in the mitochondria (17) and the regulation of TCA-cycle by these coenzymes becomes pronounced. Owing to the satellite reactions, there is a rise in the concentrations of the intermediates. In these conditions the effect of Ca^{2+} and ADP on the key dehydrogenases is reduced (since they are K-type activators) and is partially replaced by that of NADH (16).

The above examples show that the combinations of the regulatory NFLs are determined by the operational conditions in the EM. Owing to the flexible multiloop control, fluxes in the coenzyme cycles become insensitive to changes in different parameters within a certain range. This means that the fundamental function of the system-balance between energy yields and demands - is well stabilized with ever changing and floating environmental parameters. This is what may be called the biochemical homeostasis.

Destruction of homeostasis and various types of the feedforward inhibition

The reasons for destruction of homeostasis are many. We restrict ourselves to consideration of the mechanisms of the inhibition of fluxes in the coenzyme cycles at the expense of depletion of only one or two coenzyme forms (Fig. 2).

The depletion of NAD and blocking of the flux in the N-cycle occur in the absence of O_2 during anoxia or ischemia. A similar depletion of the coenzymes of C- and Y-cycles can also be observed in certain conditions. For this to occur, it is sufficient to add in excess a substrate which is oxidized as CoA-thioester. With substrates entering the TCA-cycle as AcCoA and SuccCoA, different mehcanisms of flux inhibition in EM are possible (10, 11). We will confine to the case of substrates as AcCoA.

If the TCA-cycle operates as a closed circular system (Fig. 6, left top), then the addition of excess substrate S causes an accumulation of AcCoA coupled with the reduction in the level of free CoA. This reduction is first compensated by the accumulation of αKG so that the flux in the cycle remains unaltered. After the intermediates have largely been converted to αKG, further reduction of CoA level will cause a drop in the rate of the αKGDH-reaction and therefore, in the rate of OAA regeneration in the cycle, which, in turn will result in a reduced rate of the CS-reaction producing free CoA. This leads to a still greater reduction of the level of CoA and to the inhibition of αKGDH. The process, which is an autocatalytic one, stops when αKG becomes a trap for the intermediates and AcCoA for CoA and SuccCoA. In the actual system the inhibition is not complete because of the satellite reactions, which supply OAA, and also because of the deacetylation of AcCoA to CoA. The steady-state rate of the substrate S oxidation slowly decreases with the increasing level of S (Fig. 6, left and bottom). This mechanism is feasible for pyruvate (11).

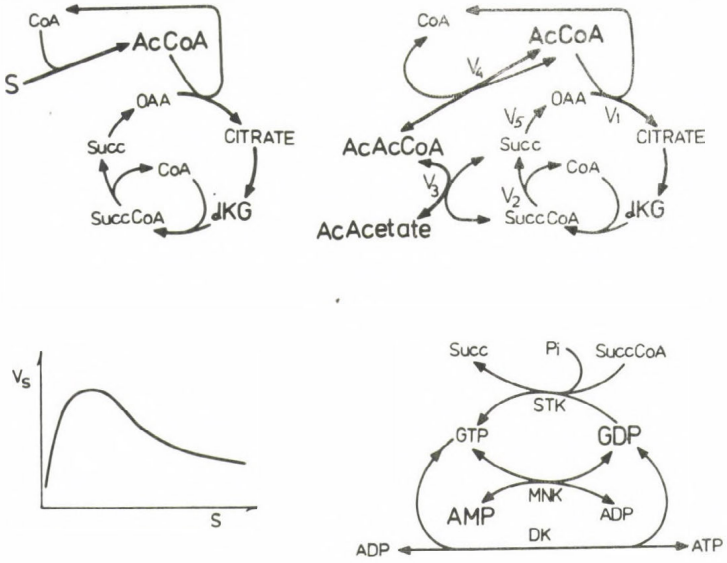

Figure 6

Top, a simplified scheme of the oxidation of different substrates (S, left) and acetoacetate (right) in the tricarboxylic acid cycle of heart tissue. Bottom, steady-state rate of the oxidation of S as a function of its concentration (left) and the reactions of purine metabolism in the mitochondria (right).

Adenylate kinase is known to be absent from the mitochondria of various tissues. Its function is taken by di- and mononucleotide kinases (DK and MNK, Fig. 6, right and bottom). The AMP level in the mitochondria is determined, to a large extent, by the GTP/GDP ratio and by the rate of ATP hydrolysis to AMP.

During the inhibition of flux in the cycle the rate of the GDP-dependent succinate thiokinase (STK) reaction also drops. As a result, the GTP/GDP ratio reduces and AMP is accumulated. This accumulation is particularly prominent with the autocatalytic substrates converted to appropriate acyls at the expense of ATP and GTP hydrolysis. In the inhibited state, the proportion of AMP in the adenylate sum greatly increases, i.e. it becomes a trap for ATP and ADP. This mechanism dominates in the case of TCA-cycle inhibition by excess of

caproic acid (Dynnik, Kosenko, Kaminsky, unpublished).

Both types of trap, the CoA-trap and the ATP, ADP-trap, are realized in different conditions with other substrates, in particular with ketone bodies (KB). In this case (Fig. 6, right top) STK is shunted by 3-oxoacid CoA transferase (OCT), which is equivalent to GTP hydrolysis. That is why the perfusion of isolated heart with excess of KB causes a rapid cessation of contractile activity (18).

Particular attention should be given to the stoichiometry of KB oxidation. In the absence of different sources of AcCoA, this system is a degenerate trigger in which both stable stationary states are inactive.

As seen from the scheme (Fig. 6, top and right), the steady-state regime in the system is possible with equal rates of the STK and OCT reactions ($V_2=V_3$). The rates of the production of AcCoA ($V_4=2V_3$) and OAA ($V_5=V_2+V_3$) will be the same only in this case. However, this state is unstable because it can be realized for any given flux in a system only at a definite concentration of acetoacetate (AcAc). Beyond this concentration, the rate of OAT (V_3) exceeds that of STK (V_2) and AcCoA is formed at a rate higher than that of OAA. As a result of AcCoA accumulation, the above mechanisms become efficient. Below this critical level of AcAc, STK is dominating and the rate of OAA production is higher than that of AcCoA. In this case AcCoA is being depleted in the CS-reaction and OAA becomes a trap for the intermediates of the TCA-cycle.

The oxidation of most substrates and their conversion to AcCoA are regulated by a great number of NFLs. The addition of excess substrates destroys this control in such a way that the excessive production of AcCoA becomes possible. The excess of AcCoA, on the strength of the peculiar stoichiometry of TCA-cycle, leads to the formation of coenzyme traps, which inhibit fluxes in the coenzyme cycles, thus destroying the homeostasis of the whole system.

CONCLUSIONS

1. The aerobic EM includes three conjugated coenzyme cycles regulated by the system of embedded NFLs.

2. The loops formed by adenylates and also by phosphate and Ca^{2+} (muscle, brain and heart tissues) are ranking high in the hierarchy of regulation.

3. The control exerted by the system of NFLs is flexible, depending on the conditions prevailing in the cell.

4. A system so organized appears as a homeostat. It can stabilize its main function (fluxes) under conditions of floating cellular parameters. The effects of Pasteur and Crabtree, the Sparing effect of fatty acids, the phenomena of muscle fatigue and myocardial failure clearly demonstrate this ability.

5. The various stoichiometric negative feedforward loops may lead to destruction of homeostasis.

REFERENCES

1. Atkinson, D.E. (1968) The energy charge of the adenylate pool as a regulatory parameter. Interaction with feedback modifiers. Biochemistry, 7, 4030-4034.
2. Sel'kov, E.E. (1975) Stabilization of energy charge, generation of oscillations and multiple steady states in energy metabolism as a result of purely stoichiometric regulation. Eur. J. Biochem. 59, 151-157.
3. Boiteux, A., Hess, B., Sel'kov, E.E. (1984) Experimental and theoretical studies of the regulatory hierarchy in glycolysis. In: Self-oscillations. Autowaves and Structures far from Equilibrium. (Krinsky, V.I. ed.), Springer-Verlag, Heidelberg, pp. 240-251.
4. Glende, M., Drabsch, H., Reich, J.G., Sel'kov, E.E. (1975) Role of orthophosphate in the energy metabolism of the cells. Studia Biophysica, 52, 141-154.

5. Grinwald, P.W. (1977) Positive feedback in the living process: The role of ATP in ischaemic cell death. Medical Hypotheses, 3, 138-143.
6. Higgins, J. (1967) Theory of oscillating reactions. Ind. Eng. Chem. 59, 18-62.
7. Sel'kov, E.E. (1968) Self-oscillations in glycolysis. A simple kinetic model. Eur. J. Biochem. 4, 79-86.
8. Khibnik, A.I., Dynnik, V.V. (1984) Glycolytic oscillations. Their mechanisms and role. Proc. 16th FEBS Meeting, Moscow, (Abstr.) XXI-030, p. 437.
9. Reich, J.G., Sel'kov, E.E. (1981) Energy metabolism of the cell. A theoretical treatise. Acad. Press, London, p. 345.
10. Dynnik, V.V. (1984) Substrate inhibition in the tricarboxylate cycle. Proc. 16th FEBS Meeting, Moscow, (Abstr.) XXI-011, p. 434.
11. Dynnik, V.V., Kim, Yu.V., Maevsky, E.I., Khasanov, V.A. (1984) Stoichiometric control by CoA-thioesters and inhibition by malate of the tricarboxylate cycle. Studia Biophysica, 102, 197-213.
12. Spydevold, Ø, Davis, E.J., Bremer, J. (1976) Replenishment and depletion of citric acid cycle intermediates in skeletal muscle. Eur. J. Biochem. 74, 155-165.
13. Corkey, B., Martin-Requero, A., Brandt, M., Williamson, J.R. (1980) Regulation of ketoisocaproate and ketoisovalerate metabolism and their interactions with the citric acid cycle in isolated hepatocytes. In: Metabolism and Clinical Implications of Branched Chain Amino and Ketoacids. (Walser, M. et al., eds.) Elsevier, North-Holland Inc. New York, pp. 119-127.
14. Lippman, F. (1981) The ATP-phosphate cycle. Curr. Top. Cell. Regul. 18, 301-311.
15. Truxel, J.G. (1955) Automatic feedback control system synthesis, McGraw-Hill Comp. Inc., New York, p. 615.
16. Dynnik, V.V. (1982) Mechanisms regulating muscle energy metabolism during oxidation of glucose and fatty acids. A mathematical model, Biokhimija (Engl. Transl.) 47, 1072-1081.

17. Kobayashi, K., Neely, J.R. (1979) Control of maximum rates of glycolysis in rat cardiac muscle. Circul. Res. 44, 166-175.
18. Taegtmeyer, H. (1983) On the inability of ketone bodies to serve as the only energy providing substrate for rat heart at physiological work load. Basic Res. Cardiol. 78, 435-450.

DISCUSSION

ATKINSON:

Your simulated system showed a wide range of values of the ratio ATP/ADP, up to 1000 or so. Yet analytical values cluster closely around about 5. (Of course these are determinations of total concentration, and do not take binding into account.) What do you think about this discrepancy?

DYNNIK:

In our models, the ATP to ADP ratio changes 100 times or even more in the whole range of ATPase loads. This may reflect the changes of free nucleotides or their activity ratio.

Up to 90 % of ADP in muscle and about 30-40 % in liver is bound. Biochemists concerned with muscle energetics prefer to estimate it from the CrP/Cr ratio.

There is also a problem with the reliable determination of mitochondrial ATP/ADP ratio. Most of the extraction experiments give a value for it of about 1 or even lower. How is mitochondrial metabolism regulated, if the in vivo ratio is about 0.2? I think all these discrepancies are bound to the applied routine analytical methods.

ATKINSON:

It seems to me that there is a bothersome paradox here, which continues to be puzzling. Most of the ADP in muscle is bound to proteins: much less is bound in yeast or bacteria. We would expect that the constant ratio would be (free ATP)/(free ADP). Yet extraction experiments yield the same ratio of <u>total</u> ATP and ADP concentrations for cells of most if not all types. I do not understand this.

DYNNIK:

If we have equal ratios for total nucleotides in various

tissues, this means that the actual ratios are very different. In any case it would be risky to compare data of excitable tissues of mammals with those of yeast and bacteria. In the mammalian tissues, the free ATP/ADP ratio may change by orders of magnitude; in yeast and bacteria it does not. Which state of muscle metabolism may we compare with that of yeast and bacteria?

Dynamics of Biochemical Systems
S. Damjanovich, T. Keleti, L. Trón (Eds)

DYNAMIC ASSEMBLY OF ENZYMES RELATED TO TRIOSEPHOSPHATES

JUDIT OVÁDI

Insitute of Enzymology, Biological Research Center,
Hungarian Academy of Sciences, Budapest, Hungary
H-1502 Pf 7

INTRODUCTION

Triosephosphates are situated at the branching point of several metabolic pathways. Their physiological concentrations are rather low in the micromolar range /1/. At the same time the concentrations of enzymes catalyzing their conversion in the glycolytic pathway are 10 - 100 μM, which probably means that the enzymes are densely packed /1, 2/. This situation favours the formation of protein-protein complexes and by the same token the functional compartmentation of these metabolites. Therefore, it was important to study whether the rate and direction of triosephosphate conversion could be regulated by enzyme-enzyme interactions.

We have investigated the complex formation between aldolase and three functionally related enzymes, glyceraldehyde-3-phosphate dehydrogenase /GAPD/, triosephosphate isomerase /TPI/ and glycerolphosphate dehydrogenase /GDH/. All of these enzymes are oligomers. The two dehydrogenases dissociate on dilution /Table 1/, moreover, the substrates induce their dissociation. As a result of dissociation in the case of GAPD a more active, in the case of GDH a less active enzyme species is formed /3, 4/. Aldolase and isomerase can be considered as stable oligomers over a wide range of protein concentration.

Table 1. Interactions between enzymes related to triose-phosphates

Homologous interactions	Heterologous interactions	Dissociation constant, μM	Ref.
GAPD T ⟷ 2D		1.0	/5/
D ⟷ 2M		0.8	/5/
	aldolase- D	0.3	/6/
TPI	aldolase- D	1.2	/7/
GDH D ⟷ 2M		4,0	/4/
	aldolase- D	0,2	/8,9/
	aldolase- M	1,0	/8,9/

T, D and M represent the tetrameric, dimeric and monomeric enzyme species, respectively.

Thus the subunit-subunit interactions of dehydrogenases have to be taken into account in the study of heterologous interactions, since preferential binding of enzyme forms of different specific ativities to the other enzymes may ensure in itself a kind of regulation in metabolic flux.

Two approaches have been used: physico-chemical methods, mostly fluorescence polarization measurements, to characterize quantitatively the enzyme complexes, and a kinetic approach based on the analysis of consecutive reactions catalysed by functionally related enzymes.

QUANTITATIVE CHARACTERIZATION OF ENZYME COMPLEXES

A typical experiment of the study of interaction between aldolase and GAPD is shown in Fig.1. The dehydrogenase was covalently labelled with fluorescent dye and the fluorescence polarization was measured in the presence of increasing concentration of unlabelled aldolase. The curve illustrates the change in polarization at the equilibrium state. Inactivation of neither enzymes occured during the experiments. Since there was no free dye in solution to interact with aldolase

and the quantum yield of the dye bound to the dehydrogenase was not affected by addition of aldolase, the increase in anisotropy is suggested to be directly related to the binding of unlabelled aldolase to the labelled dehydrogenase.

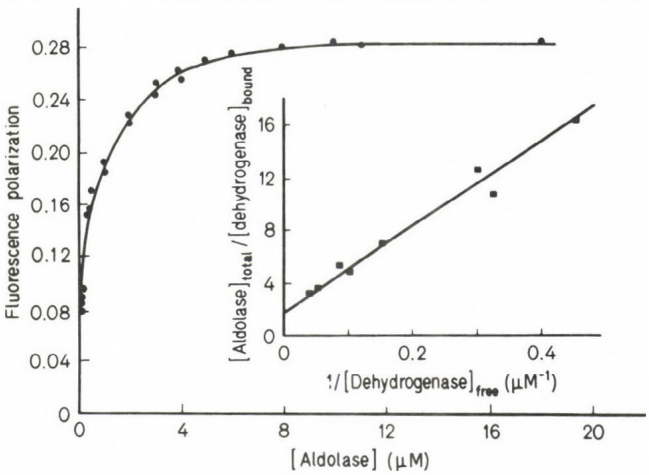

Fig.1. Change in fluorescence polarization of labelled dehydrogenase /0.5 μM/ as a function of aldolase concentration in 50 mM Tris-HCl, 1 mM EDTA, 2 mM NAD, pH 7.5 after 4 h incubation at 20°C. Inset: determination of the dissociation constant and stoichiometry of the labelled aldolase-dehydrogenase complex by Wu-Hammes plot.

From Wu-Hammes plot /Fig.1 inset/ the apparent dissociation constant and apparent stoichiometry were estimated to be 0.3 μM and 2 tetrameric aldolase /tetrameric GAPD, respectively. The latter means that a tetrameric aldolase molecule probably binds a dimeric dehydrogenase /6, 13/.

Similar types of experiments have been carried out with other enzyme complexes /Table 1/. Aldolase interacts with both GAPD and GDH preferentially with their dimeric forms which are catalytically more active species. The dimeric isomerase is also bound to the tetrameric aldolase. The values of dissociation constants of heterologous complexes indicate that the interactions occur at enzyme concentrations considerably lower than those known to exist in cytosol /1/.

Futhermore, since the strengths of interactions are comparable there is a possibility for the interactions to endow the complexes with dynamics that result in dissociation-association phenomena. Therefore, the question arises: have heterologous interactions functional consequences or not?

KINETIC ANALYSIS OF TWO-ENZYME SYSTEM

The complex formation between aldolase and GAPD has been studied in considerable detail in several laboratories /10-12/. We have presented also kinetic evidence for the binding of these enzymes to each other /13/. It was found that the K_M value of GAP for dehydrogenase determined in the coupled reaction was significantly lower than the one determined in the individual reaction /Fig.2/.

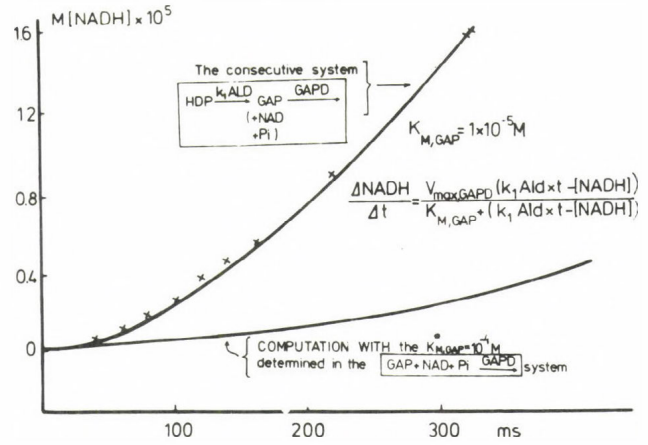

Fig.2. Fitting of the consecutive reaction catalysed by aldolase and GAPD. The concentration of enzymes was 3 μM. The assay contains 3 mM fructose-1,6-P, 2 mM NAD, 6 mM P_i in 50 mM Tris-HCl buffer, pH 7.5, 1 mM EDTA. The solid lines are the theoretical curves calculated according to the Michaelis-Menten equation with the following parameters: V_{max} of GAPD reaction: 9.5×10^{-3} M min^{-1}; V_4 of aldolase reaction: 3×10^{-3} M min^{-1} K_M of GAP: 1.5×10^{-5} M/ measured in separate reaction/ or 1.5×10^{-5} M /measured in coupled reaction/.

Although in aqueous solution glyceraldehyde-3-phosphate /GAP/ exists in equilibrium mixture of the inactive diol and active aldehyde forms, however, the aldehyde-diol conversion is expected to be rapid compared to the transit of the aldehyde form from aldolase to dehydrogenase in a non-interacting enzyme system. Thus the decrease in the K_M value measured in the coupled reaction may indicate that a part of the aldehyde form of intermediate liberated at the active site of aldolase is trapped by dehydrogenase without diffusing into the bulk solution.

In order to get direct evidence for the channelling of the intermediate, GAP, the "isotope dilution" technique has been used.

The scheme of two consecutive reactions catalysed by enzymes E_1 and E_2 in the presence of an external intermediate is the following:

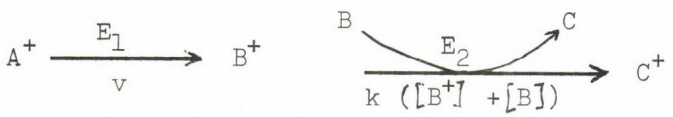

where the asterisk indicates radioactive metabolites.

If $[A^+] \gg K_M$ for E_1 and $([B^+]+[B]) < K_M$ for E_2 then the progress curve of product formation can be described as the sum of the two equations:

$$[C^+] = vt - \frac{v}{k}(1 - e^{-kt})$$

$$[C] = [B_o](1 - e^{-kt})$$

where v is the steady state velocity of the reaction catalysed by a given concentration of E_1 in the absence of added intermediate and k is the pseudo first order rate constant of the conversion of intermediate measured in an independent experiment with the same concentration of E_2 used in the consecutive reaction. $[B_o]$ is the initial concentration of unlabelled B.

To calculate the relative specific radioactivities ($r = [C^+]/([C^+] + [C])$) of the end product which would indicate different interacting mechanisms, kinetic parameters v, τ and k have to be determined from the time courses of coupled and uncoupled reactions at given concentrations of enzymes E_1 and E_2. (v is the seady-state slope of the progress curve of the coupled reaction, τ is the intercept on time axis, k is calculated from the time course of conversion of B in the absence of A^+.) All of the kinetic parameters determined are their weighted sums for reactions catalysed by complexed and uncomplexed enzyme species since the solutions always contain free E_1 and E_2 /14/.

Fig. 3 illustrates the models of different interacting mechanisms and the relevant equations for calculation of relative specific radioactivities. It is to be emphasized that by comparing $r_{measured}$ with r_i (i=1,2,3) values one can identify the mechanism of interaction of functionally related enzymes without knowing the concentration of the heterologous complex in a given enzyme system.

We used this approach to identify the mechanism of interaction in the aldolase-GAPD enzyme system. TPI was added to the system i./ to eliminate the undesirable aldehyde ⟶ diol conversion of GAP; ii./ to have a reconstituted part of glycolytic pathway, hence the consequence of interaction might be examined from the physiological view points. It has to be pointed out that the validity of the equations are not influenced by the presence of TPI if the kinetic parameters are determined in the presence of TPI.

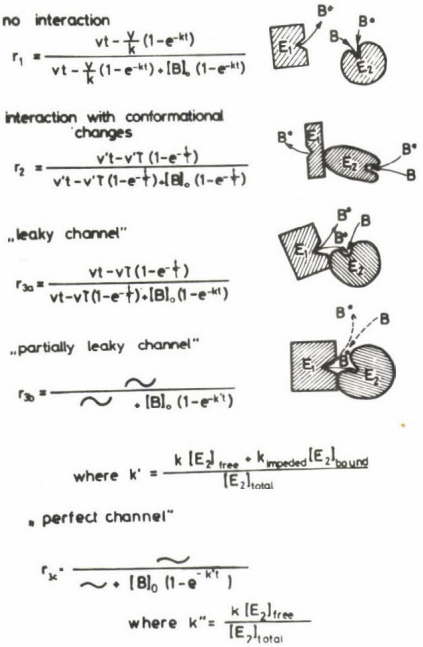

Fig.3. Models of different interacting mechanisms and the relevant equations for calculation of relative specific radioactivities /r/

$\sim$ indicates: $vt - v\tau(1 - e^{-\frac{t}{\tau}})$

The conversion of triosephosphates catalysed by GAPD and TPI can be described by a single pseudo first order reaction /Fig.4, curve 1./ indicating that i./ TPI was in excess to ensure the rapid equilibrium of triosephosphates; ii./ $[GAP] < K_M$ for dehydrogenase as determined in the presence of TPI. Hence the rate constant reflects the activity of GAPD in the given system. In addition, we have found that the time course of GAP conversion is not influenced by the presence of aldolase. The v value was determined from the steady-state part of the curve and the intercept on time axis of the linear part of curve 2 equals τ in the three-enzyme system.

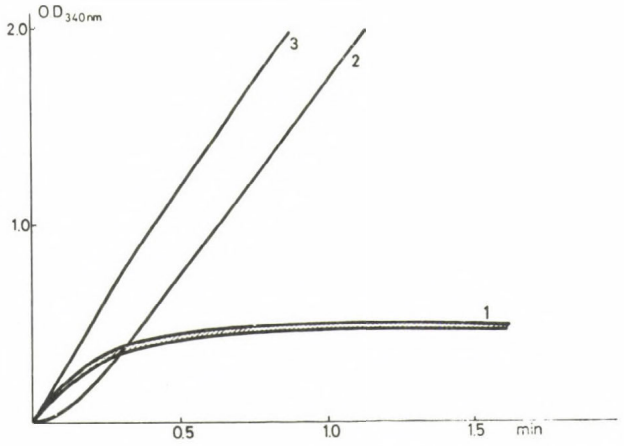

Fig.4. Time courses of enzymatic reactions catalysed by two- or three-enzyme systems GAP oxidation catalysed by GAPD in the presence of aldolase and TPI and in the absence of aldolase; Dashed area represents the deviation from average. /curve 1/ Fructose-1,6-P conversion into phosphoglycerate in the coupled reaction of aldolase, TPI and GAPD /curve 2/; the same as curve 2 with added GAP /curve 3/. Enzyme concentrations are 0.13, 0.53 and 0.60 μM for aldolase, isomerase and dehydrogenase, respectively. Initial concentration of GAP and fructose-1,6-P, if present, 6.4×10^{-2} and 2 mM, respectively.

For isotope incorporation from [^{14}C]- Fructose-1,6-P into phosphoglycerate, the reaction was stopped at time t and the concentrations of labelled and total product were determined by high performance liquid chromatographic analysis followed by scintillation counting /14/ and by NADH production, respectively.

Table 2 illustrates the results of four sets of experiments. The increase in reciprocal τ value as compared to k value does in itself indicate some kind of enzyme-enzyme interaction in the system without revealing the type of interaction.

Table 2. Kinetic parameters measured in the three-enzyme system and the relative specific radioactivities

Exp.	v μMs^{-1}	$1/\tau$ s^{-1}	k s^{-1}	Relative specific radioactivity r_1	r_2	r_3	r_{meas}
1	6.3	0.20	0.043	0.58	0.65	0.75	0.75
2	8.0	0.22	0.054	0.63	0.70	0.76	0.75
3	5.6	0.22	0.054	0.59	0.66	0.72	0.71
4	5.6	0.22	0.054	0.61	0.68	0.74	0.72

The reaction mixtures contained 0.13-0.20 μM aldolase, 0.50-0.60 μM GAPD, 0.50-0.60 μM TPI, 2 mM Fructose-1,6-P, 6 mM NAD, 4 mM arsenate in 40 mM TEA buffer, pH 8.5. GAP: 59-64 μM, t: 23-32 s.

However, by comparing the values of calculated and measured relative specific radioactivities /$r_{measured} = r_{3a}^{calculated}$/ the mechanism of interaction can be identified with the "leaky channel" model. This means that GAP formed endogenously in the coupled reaction reaches GAPD before equilibration with the external GAP and both complexed and uncomplexed dehydrogenase molecules have the same ability to bind and convert exogenous GAP.

KINETIC ANALYSIS OF THREE-ENZYME SYSTEM

In order to get information how TPI takes part in or influences the interaction between aldolase and GAPD the kinetics of three-enzyme system has been analysed and compared with that of the two-enzyme system. The scheme of the consecutive reactions catalysed by aldolase and GAPD in the presence of excess TPI is the following:

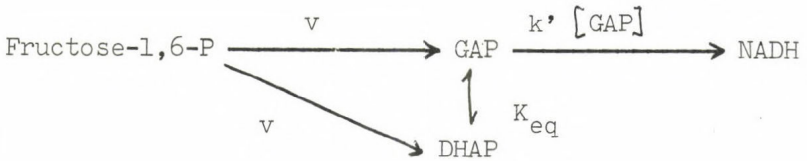

If $[\text{Fructose-1,6-P}] \gg K_M$ for aldolase and $[\text{GAP}] < K_M$ for GAPD, and TPI ensures rapid equilibrium between triosephosphates ($K_{eq} = [\text{DHAP}]/[\text{GAP}]$), NADH concentration can be calculated:

$$[\text{NADH}] = 2vt - \frac{2v}{k'}(1 - e^{-k't})$$

In a non-interacting three-enzyme system the steady-state velocity of NADH formation should be double of the rate measured in the absence of TPI, since the 2:1 stoichiometry of hexosephosphate per GAP conversion does hold. τ value will be comprised in the equilibrium constant /K_{eq}/ of triosephosphates ($\tau = 1/k' = (K_{eq} + 1)k$), where k and k' are the pseudo first order rate constants measured in the absence and presence of TPI. The effect of TPI on the activity of aldolase has been analysed by comparing the steady-state velocities in the two- and three-enzyme systems. For the calculation of the τ value, which is directly related to the activity of dehydrogenase in the three-enzyme system, the pseudo first order rate constant /k'/ of the conversion of GAP catalysed by GAPD was determined in the presence of TPI. It is to be noted that no kinetically significant TPI-GAPD interaction can be detected.

Table 3 summarizes the results of a typical series of experiments measured in the two- and three-enzyme systems. In a system containing aldolase and dehydrogenase the v value represents the steady-state velocity of the consecutive reactions since a two-fold increase in aldolase concentration results in a practically two-fold increase in the v value. This also indicates that the activity of aldolase is not influenced by GAPD. However, the presence of TPI does not produce a two-fold elevation in the value of v as expected for a non-interacting enzyme system. Moreover, by increasing the concentration of TPI, the steady-state rate of the consecutive reactions changes oppositely. However, by increasing the concentration of dehydrogenase a two-fold v value can be measured. Simultaneously, the increase of TPI concentration results in a decrease in the reciprocal τ value indicating an apparent

decrease in the activity of dehydrogenase. The finding that the elevation of TPI concentration causes significant decrease both in the steady-state velocity and in the reciprocal τ values which can be reverted by the increase of GAPD concentration, may indicate the alternative binding of TPI and GAPD to aldolase. This suggestion seems to be supported by our recent fluorescence polarization measurements.

Table 3. Kinetic parameters of the consecutive reactions catalysed by three-enzyme system

aldolase μM	GAPD μM	TPI μM	v_{ss} μM/s	$1/\tau$ s^{-1}	k s^{-1}
-	0.45	-			0.06 diol⟶ ald
0.12	0.45	-	3.5	>1	
0.24	0.45	-	6.9	>1	
-	0.45	0.15			0.043
0.12	0.45	0.15	5.8	0.13	0.043
0.12	0.45	0.49	5.0	0.10	0.043
0.12	0.91	0.15			0.063
0.12	0.91	0.15	6.9	0.14	
0.12	0.91	0.50	5.4	0.11	

The assay contained 6 mM NAD, 4 mM arsenate and 2 mM FDP or 0.05 mM GAP in 50 mM TEA buffer, pH 8.5.

CONCLUSION

The results presented here suggest that in the muscle where the physiological concentrations of proteins are significantly higher than in these experiments, aldolase and GAPD can form heterologous association. Due to the physical interaction between them the apparent activity of dehydrogenase increases since i./ the catalytically more active oligomeric form, GAPD dimer is involved in the complex formation; ii./ the intermediate, GAP, of the coupled reaction is directly transferred from from aldolase to dehydrogenase due to the

juxtaposition of active sites of the enzymes. The active site of dehydrogenase seems not to be buried, at least not completely, by aldolase. Nevertheless, GAP might be functionally compartmentalized at near-physiological conditions by the protein complex even if TPI perturbs the interaction by competing with dehydrogenase for the binding to aldolase. As a consequence of aldolase-TPI interaction the rapid equilibrium between triosephosphates may not be ensured or triosephosphates produced by aldolase-TPI complex probably are not available freely for enzymatic conversion catalysed by aldolase-GAPD complex.

REFERENCES

1. Srere,P.A./1967/ Enzyme concentrations in tissues. Science 158 936-937
2. Ottaway,J.H., Mowbray,J./1977/ The role of compartmentation in the control of glycolysis. Curr.Top.Cell.Reg. 12 107-208
3. Ovádi,J.,Batke,J.,Bartha,F.,Keleti,T./1979/ Effect of association-dissociation on the catalytic properties of glyceraldehyde-3-phosphate dehydrogenase. Arch.Biochem. Biophys. 193 28-33
4. Batke,J.,Asbóth,G.,Lakatos,S.,Schmitt,B.,Cohen,R./1980/ Substrate-induced dissociation of glycerol-3-phosphate dehydrogenase and its complex formation with fructose--bisphosphate aldolase. Eur.J.Biochem. 107 389-394
5. Ovádi,J.,Mohamed Osman,I.R.,Batke,J./1982/ Lokal conformation changes induced by successive NAD binding to dissociable tetrameric glyceraldehyde-3-phosphate dehydrogenase. Quantitative analysis of a two-step dissociation process. Biochemistry 21 6375-6382

6. Ovádi,J., Salerno,C., Keleti,T., Fasella,P. /1978/ Physico-chemical evidence for the interaction between aldolase and glyceraldehyde-3-phosphate dehydrogenase Eur.J.Biochem 90 499-503

7. Salerno,C., Ovádi,J. /1982/ Interaction between D-fructose-1,6-bisphosphate aldolase and triosephosphate isomerase. Mutual protection against perchloric acid denaturation. FEBS Lettr. 138 270-272

8. Ovádi,J., Mohamed Osman,I.R., Batke,J. /1983/ Interaction of dissociable glycerol-3-phosphate dehydrogenase. Quantitative analysis by extrinsic fluorescence probe. Eur.J.Biochem. 133 433-437

9. Ovádi,J., Mátrai,Gy., Bartha,F., Batke,J. /1985/ Kinetic pathways of formation and dissociation of the glycerol-phosphate dehydrogenase and fructose-1,6-bisphosphate aldolase complex. Biochem.J. 229 57-62

10. Patthy,L., Vas,M. /1978/ Aldolase-catalysed inactivation of glyceraldehyde-3-phosphate dehydrogenase. Nature 276 94-95

11. Grazi,E., Trombetta,G./1980/ The aldolase-substrate intermediates and their interaction with glyceraldehyde--3-phosphate dehydrogenase in a reconstituted glycolytic system. Eur.J.Biochem. 107 369-373

12. Masters,C.J., Winzor,D.J. /1981/ Physicochemical evidence against the concept of an interaction between aldolase and glyceraldehyde-3-phosphate dehydrogenase. Arch.Biochem. Biophys. 209 185-190

13. Ovádi,J., Keleti, T. /1978/ Kinetic evidence for interaction between aldolase and D-glyceraldehyde-3-phosphate dehydrogenase. Eur.J.Biochem. 85 157-161

14. Orosz,F., Salerno,C., Ovádi,J. Functional compartmentation of glyceraldehydephosphate in a reconstituted three-enzyme system
In preparation

EASTERBY:

Extrapolation of your data on the "leaky-channel" model to zero concentration of exogenously added intermediate should allow you to calculate the efficiency of transfer of the intermediate between active sites (i.e.: the fraction of intermediate transferred directly). Have you carried out this calculation?

OVÁDI:

The efficiency of transfer of the intermediate between active sites can be calculated if the dissociation constant of the heterologous enzyme complex is known, or E_2 is completely complexed by E_1.

Dynamics of Biochemical Systems
S. Damjanovich, T. Keleti, L. Trón (Eds)

VISCOSITY AND BIOCHEMICAL DYNAMICS IN VIVO

G. RICKEY WELCH

Department of Biological Sciences,
University of New Orleans,
New Orleans, Louisiana 70148, USA

I. INTRODUCTION

Viscosity is an important physical property of a medium, being defined "macroscopically" from the realm of continuum mechanics and "microscopically" from statistical mechanics. Basically, it relates to transfer of momentum (and therefore to particle mobility) in a given medium. The role of viscosity in biochemical processes has been largely ignored, owing primarily to the penchant for extrapolating from dilute aqueous solution in vitro to the (supposedly similar) condition in vivo.

In principle, viscosity plays an intimate role in all aspects of enzyme action, in ligand association/dissociation processes as well as in energization of the protein for catalytic turnover. The basic issue is, whether or not medium viscosity is actually rate-determining in any of these processes. Under in vitro conditions its influence is usually quite insignificant, compared to the chemical events of ligand binding/release and catalysis. A discordant note to this status rerum comes with the increasing realization, that many enzymes of intermediary metabolism operate in vivo in heterogeneous states far different from that of isolated enzymes in vitro.

Here, we shall relate the potential roles of viscosity in enzymatic processes in light of recent information on 1) enzyme organization in the cell, 2) the nature of cellular microenvironments, and 3) the dynamical properties of protein molecules.

II. CELLULAR INFRASTRUCTURE AND THE ORGANIZATION OF METABOLISM

In recent decades electron microscopy has revealed a complex and richly diverse particulate infrastructure in living cells—especially larger eucaryotic cells. This structure encompasses the extensive

membraneous reticulation (e.g., plasmalemma, endoplasmic reticulum, mesosomes [bacteria]), as well as the hyaloplasmic space. The latter region, containing the so-called "ground substance", is laced with a dense array of various cytoskeletal elements (e.g., microtubules, microfilaments, intermediate filaments) and an interlocking microtrabecular lattice (1). With so much surface area, it is not surprising that a significant amount of cellular water is "structured" (i.e., has physical properties unlike that of normal bulk water) (2-5). Estimates vary, as to the exact percentage of the cell water that is so "structured".

What with the ambience of abundant particulate elements and "structured" water, as well as rather high protein concentration, one would intuit that the cytoplasmic viscosity must be large. Thus far, however, measurements indicate values 3-5X that of normal water (for small diffusing molecules the size of most intermediary metabolites) (2-5). Most of the experimental probes, used to determine cytoplasmic viscosity, sample widely different regions of the cellular space during the course of the measurement. Thus, the actual viscosity value so obtained is a statistical averaged quantity. In localized microenvironments, such as those close to the surface elements, the viscosity is surely greater.

Accumulating empirical and theoretical considerations indicate that the majority (if not all) of the enzymes of intermediary metabolism operate in vivo in association with particulate structures. A perusal of the literature reveals evidence for enzyme organization in virtually all major metabolic pathways (for recent reviews see refs. 5-10). The organizational mode, of the multienzyme systems of specific metabolic processes, may entail formation of protein-protein complexes and/or individual adsorption to cytological substructures. Strong evidence has come also from centrifugation studies on whole cells(11-12) and cell fragments (13). Experimental and theoretical calculations (14,15) of protein "concentrations", in association with cytomembranes and organelles, indicate high, crystal-like densities of protein molecules in (on) particulate structures of the cell. There is a remarkable homology, in the surface area-to-volume ratio for all membraneous cytological substructures. Such considerations led Sitte (14) to propose, that all cytomembraneous elements have evolved in a common fashion to function as effective "protein collectors" in the operation of cell metabolism. And, work from Porter's group (16) shows the microtrabecular lattice itself to be "dressed" with a multitude of (as yet unidentified) proteins.

Thus, cell biology presents us with a rather simple, biphasic view of cellular infrastructure: a solid phase, encompassing extensive membraneous surfaces and the fibrous lattice-work; and a soluble phase, containing a considerable amount of "structured" water. We must focus on the solid phase as the primary site of intermediary metabolic processes, with the soluble phase functioning largely in such subservient roles as thermal buffering, distribution of common substrates, regulatory substances, and salt ions, etc. In the remainder of our discussion here, we will consider the specific influence of solvent viscosity on enzymatic processes and its possible relationship to the organizational state of multienzyme systems in vivo.

III. INFLUENCE OF VISCOSITY ON THE BINDING/RELEASE OF SUBSTRATE/PRODUCT ON THE ENZYME

Here (and in subsequent sections), we consider a simple Michaelian enzyme reaction of the form

$$E + S \underset{k_{-s}}{\overset{k_{+s}}{\rightleftarrows}} ES \xrightarrow{k_{cat}} E + P$$

The fundamental role of viscosity in the formulation of the rate constants (k_{+s},k_{-s}) for binding/release of substrate (or product) is well-known in enzymology (17,18). Under diffusion-controlled steady-state conditions, the unitary rate constants reduce in the limit to the Smoluchowski rate coefficient, k_D, given by

$$k_D = \Omega \cdot f_e \cdot D \cdot r_c \qquad (1)$$

where Ω is a factor relating to geometric restrictions on the mode of approach of ligand to the enzyme active site ($0 < \Omega \leq 4\pi$), f_e a factor relating to electrostatic effects, D the diffusion coefficient for the ligand, and r_c a critical reaction radius. Using the Stokes-Einstein inverse relation between diffusion coefficient (D) and viscosity (η), we see that $k_D \propto (1/\eta)$.

The Smoluchowski theory (19) shows how viscosity, in principle, influences the basic binding/release of ligand molecules to the protein. But, realistically, what does it tell us about viscosity and enzyme action? First, its potential is brought to bear only under conditions when the chemical events of ligand binding/release are faster than diffusive processes. Even in this case, it may be difficult to dissect the relative influence of diffusivity from the other parameters in Eq. (1). Obviously, a clear

understanding of the importance of viscosity in the approach of ligands to (and escape from) the enzyme depends on our grasp of the complete mechanistic picture of the given enzyme, as well as a knowledge of the actual transport properties of the ambient medium.

The Smoluchowski rate coefficient has come to play a more general role in enzyme kinetics, serving to delimit the overall dynamics of enzyme activity. Consider the reaction of free substrate with free enzyme to yield product. The apparent second-order rate constant for this reaction is k_{cat}/K_m (20). Rigorous reasoning shows that the upper (evolutionary) limit on k_{cat}/K_m is just k_D (20). That is to say, no matter how effective is the enzyme as a catalyst, from the standpoint of the speed and efficiency of the chemistry of substrate-binding and catalytic-turnover, the overall rate of catalysis can proceed no faster than the rate of diffusion of substrate to the enzyme active site. Recently, Keleti and Welch (21) extended these arguments, to suggest that a more complete evolutionary picture is obtained by conjugating k_{cat}/K_m to the respective enzyme concentration (density) in situ. Accordingly, the "kinetic power", $k_\Gamma = V_{max}/K_m$, emerges as the real measure of the kinetic potential of an enzyme reaction in vivo.

Welch et al. (22) examined an additional role of viscosity in enzyme kinetics, viz., the "cage effect" of the solvent environment on enzyme-ligand recombination. As a nascent ligand (e.g., product) molecule emerges from the enzyme binding site (with a certain impulsive energy), it will feel a translational barrier — whose height is a function of the local solvent viscosity. Theoretical simulation showed that, for the case of an enzyme whose chemistry of recombination is very effective, a marked viscosity ("cage") effect is seen at a viscosity value as low as 3-4X that of water. Coincidentally, that is the range of measured cytoplasmic viscosity (see Section II).

IV. INFLUENCE OF VISCOSITY ON THE TRANSIENT TIME OF METABOLIC PROCESSES

Since enzyme action involves a composite of unitary rate processes, it may be difficult to perceive of the general effect of solvent viscosity on a given enzyme by dissecting it into effects on the individual rate constants. A holistic quantity which is directly related to viscosity is the transient time, τ. As seen for example in the chapter by Dr. Easterby (this volume), τ is an important parameter in the overall dynamics of a multienzyme system. Physically, it is defined by the time required for diffusion and accumulation of intermediate substrate/product species to

levels sufficient to sustain a steady state. Since it depends on mass transfer from one enzyme to another in the sequence, one intuits that τ must be a function of medium viscosity.

Consider the following two-enzyme (irreversible) sequence:

$$S \xrightarrow[E_1]{v_o} I \xrightarrow[E_2]{} P$$

catalyzed by enzymes E_1 and E_2. Let us suppose for simplicity that the overall flux is limited by the first reaction (whose velocity is v_o), such that the second enzyme is subsaturated. Then, the transient time for this system is found to be

$$\tau = K_2 / V_2 \qquad (2)$$

where K_2 and V_2 are the Michaelis constant (K_m) and the maximal velocity (V_{max}), respectively, for the second enzyme. Using explicit expressions for K_m and V_{max}, it was shown (23) that

$$\tau = (\pi \cdot r_I \cdot D_I \cdot [E_2])^{-1} \exp (E_p / k_B T) \qquad (3)$$

where $[E_2]$ is the total number-density of enzyme E_2 molecules, r_I and D_I the molecular radius and diffusion coefficient, respectively, for species I, E_p an activation energy for the conversion $E_2 I \rightarrow E_2 + P$, k_B the Boltzmann constant, and T the absolute temperature.

Equation (3) gives a way of calculating the transient time of an enzyme system as a function of solvent properties — assuming the system to be homogeneously dissolved in a bulk phase. Employing typical values of r_I, [E], and E_p, and taking the solvent viscosity to be 3-5X that of water, we find $\tau \simeq$ 3-5 min (23). (For a multienzyme sequence the individual transient times are additive.) Such numerical values do not correspond to observed metabolic transients. This situation has been used as a general theoretical argument in favor of enzyme organization <u>in vivo</u> (23).

V. VISCOSITY AND THE PROTEIN-DYNAMICAL BASIS OF CATALYTIC TURNOVER

The old notion, that the overall structure of an enzyme serves the singular role of maintaining statically a requisite three-dimensional arrangement of active-site residues, is now outmoded (24-26). Accumulating evidence has revealed a wide variety of internal motions in proteins, span-

ning the gamut of time domains and encompassing various structural levels in the protein matrix. Realization of the dynamic nature of the protein molecule has led to the development of a number of theoretical models of enzyme action (reviewed in refs. 27-29). These models propose that particular classes of fluctuations in the protein provide for high free-energy events at the active site. One finds an emerging view, that the enzyme molecule is an intricate free-energy transducer, serving to link the molecular chaos of the environment and the localized chemical-reaction coordinate. What differentiate the various models are the types of surface phenomena assumed to serve as the source of the free energy ("borrowed" from the medium), and the suggested mode of linkage between the ambient source and the enzyme active site.

Although the mechanistic picture is far from clear, it is apparent that "something" (e.g., collisional processes, binding/relaxation of solvent or ionic species) at the protein-solvent interface, acting through the protein "mediator", is involved in generating the proper phase-space correlation of active-site variables. Viscosity, η, is an appropriate parameter relating to the modality of thermal interaction (at a given temperature) between the protein and solvent medium. At the microscopic level, the mobility of the particles composing the system is proportional to $(1/\eta)$. The thermal "(de)energization" of an enzyme-substrate complex must be determined by that "mobility" — whether it specifies direct diffusional-collisional interaction of the solvent molecules with the protein or binding/relaxation of the solvent/solute particles with the protein. Indeed, numerous theoretical and experimental treatments have demonstrated an explicit role of medium viscosity in enzyme catalysis (reviewed in refs. 26-28).

The rate constant, k_{cat}, characterizing the conversion ES→EP, is our concern here. The overall free-energy change associated with the transition-state passage may be decomposed into two contributions: that from chemical processes (e.g., E-S binding, solvation/desolvation effects) localized specifically at the active site, and that from the protein matrix interacting with the bound chemical subsystem. Considering only the latter contribution, we assume that the rate process can be characterized by a fluctuation enthalpy. Hence, if a catalytic event demands an enthalpy $h^{\ddagger}$ in the protein, the rate will be given by the rate of occurrence of fluctuations, i.e.,

$$k'_{cat} = k_{\nu} \cdot W(h^{\ddagger}, T) \qquad (4)$$

where k_{ν} is a frequency factor and W a probability distribution function describing the fluctuating enthalpy of the protein (ES complex) at temperature T (27,28). (The "prime" on k_{cat} reminds us that we are considering only the protein contribution.)

An explicit dependence of k_{cat} on viscosity enters through k_{ν}. The first mathematical derivation of such dependence was by Damjanovich and Somogyi (30,31), who showed from statistical-mechanical considerations that k_{ν} varies as $(1/\eta)$. This form has been derived from other theoretical approaches in more recent years (reviewed in refs. 27-29). In the context of protein dynamics, there has been much interest recently in the Kramers phase-space diffusion theory of chemical kinetics (32). Early on, Kramers showed how viscosity produces deviations from the transition-state formulation of absolute reaction rates.

A $(1/\eta)$-dependence for k_{cat} agrees fairly well with empirical evidence in moderate viscosity ranges. Deviations at higher solvent viscosities have been attributed to the situation, that the reaction coordinate of the bound chemical subsystem is influenced by two viscosities: that of the solvent and the intrinsic viscosity of the protein matrix (26,28,33).

We are just beginning to unravel the intricacies of the protein-dynamical basis of enzyme action. However, one thing is eminently clear: viscosity plays a distinctly deterministic role in the frequency with which the enzyme body generates high free-energy events at the active site.

VI. VISCOSITY AND ENZYME ACTION IN VIVO

From the empirical and theoretical information accumulated to date, what can we say about viscosity and biochemical dynamics in vivo? First, there is the question of diffusional transit, especially as it applies to larger eukaryotic cells. Experimental measurements thus far indicate that the translational motion of small molecules (e.g., metabolites) is retarded by less than an order of magnitude (compared to water) within the aqueous interstices of the cytomatrix elements. Questions of the physical properties of cell water, of the diffusional impedance of cytological structures, etc., are currently being investigated in a number of laboratories. Generally, one cannot ascertain the specific influence of the rate of material (e.g., substrate) diffusion on an individual enzyme in vivo unless one

knows the mechanistic details of the given enzyme reaction, as well as the nature of the microenvironment *in situ*.

The transient time of a multienzyme sequence provides one indication of the significance of viscosity in the overall dynamics of a metabolizing system. Using known values of cytoplasmic viscosity and average number of enzyme molecules per cell, we find calculated values of transient time which seem too high — if we presume that the enzymes of intermediary metabolism are homogeneously dissolved in the cellular space. This predicament has been invoked as one factor in support of the general notion, that much of the enzymatic machinery is structurally organized *in vivo* (18,23). That there is increasing evidence showing intermediary metabolites and enzymes to be at roughly equimolar concentration *in vivo*, further attests to the validity of this notion.

It is known that the organizational state of many enzyme systems involves association with subcellular surface elements. But, merely binding the enzymes of a metabolic sequence, say to a membrane, does not, in itself, solve the diffusional-transit problem. The local viscosity at the cytosol-surface interface may be higher than that in the bulk (22). This situation would imply, theoretically, that the localized enzymes must be placed in rather close proximity on the surface. Interestingly, studies have shown protein-densities on subcellular membranes to be very high (see Section II).

A problem of perhaps equal importance for these membrane-adsorbed enzymes concerns the effect of the locally high viscosity on the protein-dynamical basis of catalytic turnover. To date, rigorous viscosity studies have been performed on relatively few enzymes *in vitro*. Extrapolating the available data (*viz.*, k_{cat} *vs.* η plots), from *in vitro* conditions to the kinds of viscosity values potentially extant in localized microenvironments *in vivo*, would suggest that many enzymes catalyze reactions at somewhat depressed rates — if activation of the catalytic complex is by purely thermal means. This raises the bizarre possibility that some membrane-associated enzymes may actually be activated by *nonthermal* means, i.e., are designed to "plug into" local nonequilibrium energy sources. One obvious source would be "active protons", which are generated by virtually all energy-transducing biomembranes. This possibility is rendered more palatable, with the realization of the central role of "mobile protons" in the structure, dynamics, function, and evolution of enzymes (34). While highly speculative at present, this idea seems to be physically plausible (35).

Despite the relative paucity of empirical and theoretical information presently accessible to us on viscosity and enzymology, it is imperative that this subject be pursued with exactitude. A knowledge of viscosity effects will provide us a real understanding of the thermal interaction of the enzyme molecule with its surroundings. The road to such an understanding is a convoluted one. Not only must we know more about the enzyme itself, but we must turn increasingly to cell biology to relate to us the physicochemical nature of the local microenvironments. And, we must rely on the rigor of physical chemistry and statistical mechanics, to give us a more exact grasp of the concept of "viscosity" at the microscopic level. This pursuit is sure to yield a fuller appreciation of the unity of the enzyme and its biological habitat in the living cell.

A more detailed discussion of this topic is presented elsewhere (36).

VII. REFERENCES CITED

[1] Porter, K. R. (ed.)(1984). J. Cell Biol. 99, 1s-248s.

[2] Drost-Hansen, W. and Clegg, J. S. (eds.)(1979). Cell-Associated Water. Academic. New York.

[3] Keith, A. D. (ed.)(1979). The Aqueous Cytoplasm. Dekker, New York.

[4] Franks, F. and Mathias, S. (eds.)(1982). Biophysics of Water. Wiley, New York.

[5] Clegg, J. S. (1984). Amer. J. Physiol. 246, R133.

[6] Masters, C. J. (1981). CRC Crit. Rev. Biochem. 11, 105.

[7] Wombacher, H. (1983). Mol. Cell. Biochem. 56, 155.

[8] Friedrich, P. (1984). Supramolecular Enzyme Organization. Akadémiai Kiadó, Budapest and Pergamon, Oxford.

[9] Srere, P. A. (1984). Trends Biochem. Sci. 9, 387.

[10] Welch, G. R. (ed.)(1985). Organized Multienzyme Systems: Catalytic Properties. Academic, New York.

[11] Kempner, E. S. and Miller, J. H. (1968). Exp. Cell Res. 51, 141, 150.

[12] Zalokar, M. (1960). Exp. Cell Res. 19, 14.

[13] Coleman, R. (1973). Biochim. Biophys. Acta 300, 1.

[14] Sitte, P. (1980). In Cell Compartmentation and Metabolic Channeling (Nover, L., Lynen, F., and Mothes, K., eds.), p. 17. Elsevier, New York.

[15] Srere, P. A. (1985). In Organized Multienzyme Systems: Catalytic Properties (Welch, G. R., ed.), p. 1. Academic, New York.

[16] Schliwa, M., van Blerkom, J., and Porter, K. R. (1981). Proc. Natl. Acad. Sci. USA 78, 4329.

[17] Eigen, M. (1974). In Quantum Statistical Mechanics in the Natural Sciences (Kursunoglu, B., Mintz, S. L., and Widmayer, S. M., eds.), p. 37. Plenum, New York.

[18] Welch, G. R. (1977). Prog. Biophys. Mol. Biol. 32, 103.

[19] Rice, S. A. (1985). Diffusion-Limited Reactions (Comprehensive Chemical Kinetics [Bamford, C. H., Tipper, C. F. H., and Compton, R. G., eds.], Vol. 25). Elsevier, New York.

[20] Fersht, A. (1985). Enzyme Structure and Mechanism (2nd ed.). Freeman, San Francisco.

[21] Keleti, T. and Welch, G. R. (1984). Biochem. J. 223, 299.

[22] Welch, G. R., Somogyi, B., Matkó, J., and Papp, S. (1983). J. Theor. Biol. 100, 211.

[23] Welch, G. R. (1977). J. Theor. Biol. 68, 267.

[24] Careri, G., Fasella, P., and Gratton, E. (1979). Ann. Rev. Biophys. Bioeng. 8, 69.

[25] Karplus, M. and McCammon, J. A. (1983). Ann. Rev. Biochem. 53, 263.

[26] De Brunner, P. G. and Frauenfelder, H. (1982). Ann. Rev. Phys. Chem. 33, 283.

[27] Welch, G. R., Somogyi, B., and Damjanovich, S. (1982). Prog. Biophys. Mol. Biol. 39, 109.

[28] Somogyi, B., Welch, G. R., and Damjanovich, S. (1984). Biochim. Biophys. Acta 768, 81.

[29] Welch, G. R. (ed.)(1986). The Fluctuating Enzyme. Wiley, New York.

[30] Damjanovich, S. and Somogyi, B. (1971). In Proc. First Eur. Biophys. Cong. (Broda, E., Locker, A., and Springer-Lederer, H., eds.), Vol. 6, p. 133. Verlag der Wiener Medizinischen Akademie, Vienna.

[31] Somogyi, B. and Damjanovich, S. (1975). J. Theor. Biol. 51, 393.

[32] Kramers, H. A. (1940). Physica 7, 284.

[33] Gavish, B. (1980). Phys. Rev. Lett. 44, 1160.

[34] Welch, G. R. and Berry, M. N. (1983). In Coherent Excitations in Biological Systems (Fröhlich, H. and Kremer, F., eds.), p. 95. Springer-Verlag, New York-Berlin.

[35] Welch, G. R. and Kell, D. B. (1986). In The Fluctuating Enzyme (Welch, G. R., ed.). Wiley, New York.

[36] Somogyi, B., Rosenberg, A., Welch, G. R., and Damjanovich, S. (1986). In Towards A Cellular Enzymology (Klyosov, A., Varfolomeev, S., and Welch, G. R., eds.). Plenum, New York.

DISCUSSION

ATKINSON:

Do you have a feeling for how close together, in terms of substrate molecular dimensions for example, two sites must be in order that there can be effective channeling in the absence of physical constraints on diffusion away from the region?

WELCH:

No, for the moment we do not have an exact idea of the closeness of the active sites. In a pure aqueous medium, preliminary results indicate that the distance cannot be more than about one substrate-molecular diameter (Welch, G.R. et al., J. Theor. Biol. 100, 211. 1983).

CHERRY:

I feel somewhat uneasy about the use of microviscosity in your discussion. I think it is very important when giving a number for microviscosity to know how it was measured and whether the particular number is relevant to the problem. For example, in membranes one might determine a microviscosity from measuring the rotational diffusion of a small lipid probe, but this wouldn't necessarily enable you to predict lateral diffusion coefficients. My question is, therefore, how were the microviscosities in cell cytoplasm which you quoted obtained and are you sure the numbers are the right ones to apply to substrate diffusion and to viscous damping of protein fluctuations?

WELCH:

The actual numerical value of cytoplasmic viscosity (viz., 3-5 X that of water) which I cited in my lecture and used, for example in the calculation of substrate diffusional transit, represents the latest experimentally determined estimate from ESR, NMR, and neutron-scattering techniques applied to intact cells. These techniques

measure the translational mobility of probe molecules (and in some cases water itself) averaged over the entire cell. Of course, various sizes of diffusing probe molecules have been used, in order to get a wide spectrum of viscosity values. The value which I used was for something the size of a glucose molecule. These kinds of experimental results are, at best, crude; but they represent the best assessment of the average viscosity of the bulk cytoplasm presently available. (I would say that the value, 3-5 X that of water, is reasonable, considering the large amount of polyelectrolytic surface and bound water in cells.) The local viscosity on particulate surfaces is certain to be higher. It has not been possible as yet to measure such a "local viscosity" in actual cells. But, a value 10 X that of water would not be unrealistic. In my lecture I wanted just to draw attention to the gross effect of viscosity on substrate/product transit. At short range, the viscosity takes on a discontinuous character - definable theoretically (via statistical mechanics) but rather unapproachable experimentally. This consideration is especially important in trying to understand the effect of viscosity on protein dynamics. To date, there is relatively little reliable data on the actual influence of viscosity on protein motions; only a few proteins have been studied rigorously. Although one can intuit (and show theoretically) that protein dynamics are affected by viscosity, we don't yet have a "local" picture of the phenomenon (see Welch, G.R. et al., Prog. Biophys. Mol. Biol. 39, 109. 1982). Again, in extrapolating to in vivo conditions, I just wanted to draw attention to a gross effect.

BARDSLEY:

Can you clarify whether your theory relies on time-dependent distribution functions or are you really dealing with well-stirred solutions?

Viscosity effects could well be far more complicated if you allowed for the increase in viscosity to set up steeper diffusion gradients. In such a model the empirical effect might be almost entirely a solvent effect on the "on/off" rate constants and the effect on catalysis could be much less important.

WELCH:

No, we did not include explicitly any time dependence. I agree that one should incorporate such consideration, especially at higher viscosity (where local diffusion gradients may be important).

I agree with your assessment of the total effect of viscosity, on the overall kinetics of enzyme action. In my lecture I dissected the viscosity effect (for illustrative purposes) into its influence on substrate/product interaction and on catalytic turnover. In a highly viscous medium it is quite possible that the effect on product release might dominate (see Welch, G.R. et al., J. Theor. Biol. 100, 211. 1983.).

ROSENBERG:

I would like to point to another factor to be considered in case a reaction takes place in a non-ideal solution. Excluded volume is defined as the solution space not available for a molecule by the physical presence of other molecules. The factor is negligible even at quite respectable protein concentrations however, as shown by Ross and Minton it increases very rapidly at protein concentrations around 30-40 %. The models for mitochondrial structure presented at this meeting imply even higher packing densities. The activity coefficients for proteins in such systems are high. The effect on reactions is in opposite direction to the effect predicted for high friction coefficients. The experimentally observed effects on rates are thus sums of at least two functions, microviscosity and excluded volume.

WELCH:

The excluded-volume effect is likely to be very important for *in vivo* microenvironments. It is certainly a factor which we must include in further theoretical analyses.

Dynamics of Biochemical Systems
S. Damjanovich, T. Keleti, L. Trón (Eds)

THE GENERAL PRINCIPLES OF THE CONTROL OF FUNCTIONING ENZYMES AND MULTIENZYME COMPLEXES

B.I. KURGANOV

The All-Union Vitamin Research Institute, Moscow, USSR

In any object of the material world levels of the organization of the matter can be detected. As far as biological objects are concerned the levels of material organization may be represented as follows: enzyme → multienzyme complex → subcellular structure → cell → tissue → organ → functional systems→... When discussing the functioning and the control of biological systems, their structural characteristics should be taken into account. In my opinion the hierarchy of the levels of the control of functioning biological systems is predetermined by the multilevel organization of the matter in living organisms. One can expect that the mechanisms of the control operative on different levels have common features.

The aim of the present paper is to discuss the regulatory mechanisms which are exerted on the levels corresponding to enzymes and to multienzyme complexes. The idea has been suggested that second messengers play the key role in the control of functioning the multienzyme complex as a whole.

ENZYMES AS CONTROLLABLE SYSTEMS

Certain protein molecules exert catalytic functions, the catalytic efficiency of high-molecular biocatalysts being much higher than that of low-molecular analogs. In other words, the assembly of aminoacids in the macromolecule possessing a spatial structure provides the formation of an active site per-

forming the efficient chemical transformation of substrates. However, one should keep in view that the transition to a structurally organized polypeptide system forms simultaneously the pre-conditions for the creaton of sites participating in the control of such a catalytic system. The molecules of enzymes occupying the key positions in the metabolic pathway contain the spatially distinct sites of binding of metabolites exerting regulatory functions. Metabolite regulators differ by their chemical nature from the substrates and the products of the enzymic reaction. In other words, metabolites-regulators are the "external" factors for a given enzymic process. Metabolites exerting their regulatory functions by interactions with spatially distinct binding sites are designated as allosteric effectors.

The following events are involved in the realization of the control mechanism in which the regulatory functions are exerted by metabolites-regulators. The mechanism is initiated by recognition and binding of the metabolite-regulator in a specific site ("allosteric site") of the enzyme molecule. The binding of the metabolite-regulator induces the change in the conformational state of the enzyme molecule (the "classical" allosteric mechanism), the change in the oligomeric state of the enzyme molecule (the dissociative mechanism) or the change in the adsorptive state of the enzyme molecule i.e. the position of the equilibrium between free enzyme and the enzyme adsorbed to subcellular structures (the adsorptive mechanism). Changes in the conformational, oligomeric or adsorptive state cause alterations of the catalytic properties of the active site (the affinity of the enzyme with respect to substrates, the rate of the catalytic breakdown of the complex between the enzyme and substrates, the character of the interactions of the substrate-binding sites in the enzyme oligomer and so on). The final stage of the allosteric and related regulatory mechanisms is the chain of feed-back which is signalled about the achieved result. The change in the rate of the formation of the enzymic reaction products which enters into the metabolic pathway will lead to the alteration of enzyme-functioning producing the metabolite-regulator.

It should be noted that allosteric, dissociative and adsorptive enzyme systems exhibit similar kinetic behaviour (Kurganov, 1982, 1985a,b).

Thus the evolution of low-molecular catalysts has led to the appearance of macromolecules which are characterized not only by the high catalytic efficiency but also by the sensitivity to the control by new material signals. These governing factors are metabolites and they provide the optimum functioning of a given enzyme in the system of a higher order of complexity i.e. in the definite metabolic pathyway.

MULTIENZYME COMPLEXES AS CONTROLLABLE SYSTEMS

The understanding of the fact that each level of material organization gives birth to new control laws which are realized with the participation of new ("external") governing factors allows to analyse the problem of the regulation of cellular metabolism from new positions.

Enzymes participating in the metabolic pathways tend to form ordered multienzyme complexes (Welch, 1977; Keleti, 1984). It is generally accepted that the formation of multienzyme complexes is biologically advantageous from the following points of view. The association of the enzymes of the metabolic pathway leads to the formation of microcompartments where the metabolic process may proceed with higher overall rate in comparison with the rate of the process proceeding in the system with homogenous distribution of enzymes. The reason of this is the diminishing of the time of diffusion of the active sites of corresponding enzymes (Snol', Ermakova and Frank, 1979; Keleti, 1984). It should also be noted that metabolic intermediates are not released into the medium. This circumstance exclude the undesirable involvement of intermediates of other metabolic pathways.

However, the enhancement of the efficiency of proceeding of the metabolic pathway in the microcompartment of the multienzyme complex is not the only advantage of the formation of organized multienzyme structures. The physiological sense of

the formation of multienzyme complexes is that the cell has the possibility to control the metabolic pathway represented by the multienzyme complex as a whole.

The assembly of the complex of glycolytic enzymes

The complex of glycolytic enzymes may serve as an example of the complex of enzymes participating in the common metabolic pathway. In skeletal muscles glycolytic enzymes are localized near the I-band of muscle fibers (Sigel and Pette, 1969; Dölken, Leisner and Pette, 1975). According to the data of biochemical investigations individual glycolytic enzymes are able to bind reversibly to F-actin which is the main structural protein of the I-band (Arnold and Pette, 1968, 1970; Arnold, Henning and Pette, 1971; Westrin and Backman, 1983; Sugrobova et al., 1983). The regulatory proteins of I-band, troponin and tropomyosin, play important role in the adsorption of glycolytic enzymes (Clarke and Morton, 1976: Clarke and Masters, 1976; Stewart, Morton and Clarke, 1980). High affinity to structural proteins of skeletal muscles has been revealed by 6-phosphofructokinase, fructose-bisphosphate aldolase, glyceraldehyde-phosphate dehydrogenase, lactate dehydrogenase and glucosephosphate isomerase (Clarke and Masters, 1975). When analysing the data on the intracellular distribution of glycolytic enzymes, Pette (1975) has drawn the conclusion that high local concentrations of glycolytic enzymes in the adsorption layer should favour the formation of the ordered multienzyme complex.

The ability to bind some glycolytic enzymes is revealed also by the glycoprotein of the erythrocyte membrane, the so called band 3 protein. This glycoprotein is responsible for the transport of anions through the erythrocyte membrane. The binding site formed by band 3 protein may reversibly attach one tetrameric molecule of 6-phosphofructokinase (Higashi, Richards and Uyeda, 1979), two tetrameric molecules of glyceraldehyde-phosphate dehydrogenase (Yu and Steck, 1975) or two tetrameric molecules of fructose-bisphosphate aldolase (Strapazon and Steck, 1977). The formation of the complex of glycolytic enzymes adsorbed to the erythrocyte membrane has been postulated

by Green et al. (1965), Tillmann, Cordua and Schröter (1975) and Higashi, Richards and Uyeda (1979).

Kurganov and colleagues (Kurganov, 1984, 1985a; Kurganov, Sugrobova and Mil'man, 1985) have used the data on adsorption of glycolytic enzymes to the structural proteins of skeletal muscles and erythrocyte membranes, the data on protein-protein interactions among glycolytic enzymes and the data on the regulation of glycolytic enzymes by cellular metabolites for construction of the tentative spatial structure of the complex of glycolytic enzymes. The complex contains one tetrameric molecule of 6-phosphofructokinase and two molecules of each of other glycolytic enzymes (glucosephosphate isomerase, fructose-bisphosphate aldolase, glyceraldehyde-phosphate dehydrogenase, phosphoglycerate kinase, phosphoglyceromutase, enolase, pyruvate kinase, lactate dehydrogenase, triosephosphate isomerase and glycerol-3-phosphate dehydrogenase). 6-phosphofructokinase plays the central role in the formation of the multienzyme complex. The adsorption of 6-phosphofructokinase to the anchor protein of the support is the first step in the assembly process. The tetrameric molecule of 6-phosphofructokinase has three symmetry axes of second order and the enzyme is adsorbed to the support along one of the symmetry axes. Then the attachment of two molecules of fructose-bisphosphate aldolase, two molecules of glyceraldehyde-phosphate dehydrogenase and two molecules of each of other glycolytic enzymes takes place. The fixation of the complex of glycolytic enzymes on the erythrocyte membrane is shown in Fig. 1.

The complex of glycolytic enzymes has a symmetry axis of second order which is perpendicular to the plane of the erythrocyte membrane. There are two microcompartments where glycolysis proceeds without releasing glycolytic intermediates into the medium. The formation of the ordered multienzyme structure ensures the channeling of formed ATP to the ATP-consuming enzyme systems, for example, to myosin ATPase site in muscle fibers.

It should be noted that the complex of glycolytic enzymes has a dynamic structure and a dynamic equilibrium exists between the complex and the free enzymes of the cytosol. The com-

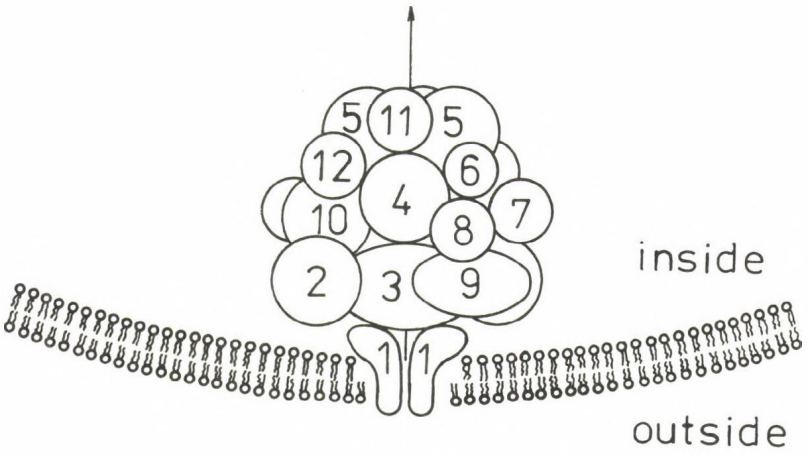

Figure 1

The schematic representation of the attachment of the complex of glycolytic enzymes to the dimers of band 3 protein embedded in the erythrocyte membrane. The used designations are: 1 - band 3 protein; 2 - glucose phosphate isomerase; 3 - 6-phosphofructokinase; 4 - fructose-bisphosphate aldolase; 5 - glyceraldehyde-phosphate dehydrogenase; 6 - phosphoglycerate kinase; 7 - phosphoglyceromutase; 8 - enolase; 9 - pyruvate kinase; 10 - lactate dehydrogenase; - 11 - triosephosphate isomerase and 12 - glycerol-3-phosphate dehydrogenase.

pleteness of the formation of the complex of glycolytic enzymes is sensitive to the variations of the concentrations of cellular metabolites. For example, it is known that fructose-1,6-bisphosphate diminishes the affinity of fructose-bisphosphate aldolase to F-actin (Arnold and Pette, 1970; Clarke and Masters, 1975) and to the erythrocyte membranes (Strapazon and Steck, 1977). Simultaneously fructose-1,6-bisphosphate strengthens the binding of 6-phosphofructokinase to dimers of band 3 protein (Higashi, Richards and Uyeds, 1979). Thus the desorbing effect of fructose-1,6-bisphosphate with respect to fructose-bisphosphate aldolase and the reverse effect of this metabolite with respect to 6-phosphofructokinase favour the formation of the complex of glycolytic enzymes. In addition to the ability to affect the affinity of glycolytic enzymes to the support, fructose-1,6-bisphosphate strengthens the associates between glycolytic enzymes (Clarke and Masters, 1974). Therefore one

can assume that fructose-1,6-bisphosphate acts as a factor which stabilizes the complex of glycolytic enzymes adsorbed to the support.

The control of functioning of multienzyme complexes

The fixation of the multienzyme complex on the biological support results in the formation of a system having a specialized control site. In our opinion, the function of this control site is exerted by the anchor protein of the support. The control site provides the sensitivity of the multienzyme complex to new control factors which are not metabolic intermediates but substances of other chemical nature. We assume that the anchor protein undergoes definite changes with the participation of second messengers (Ca^{2+} ions, cyclic AMP, inositol 1,4,5-triphosphate, diacylglycerol and so on). The appearance of second messengers in the cell is the result of interaction of hormones and neurotransmitters with the corresponding cell receptors (Iyengar et al., 1980; Berridge, 1983, 1984).

The following experimental data may be attracted to support the proposed hypothesis.

It is known that Ca^{2+} ions in concentrations up to 10^{-5} M do not effect the enzymic activities of glycolytic enzymes in solution (Vaughan, Thornton and Newsholme, 1973). However, when bound to the filaments formed by F-actin, troponin and tropomyosin, one of the glycolytic enzymes, fructose-bisphosphate aldolase, becomes sensitive to Ca^{2+} ions. Ca^{2+} ions enhance the affinity of adsorbed enzyme to substrate, fructose-1,6-bisphosphate (Walsh, Clarke and Masters, 1977). Therefore one can assume that the complex of glycolytic enzymes formed within the I-band of myofibrils containing Ca^{2+}-binding protein (troponin C) is regulated by Ca^{2+}-ions. The concentration of Ca^{2+} ions in the resting muscle is about 10^{-7} M. The increase in the content of Ca^{2+}-ions up to 10^{-5} M in response to nervous exitation initiates muscle contraction which is exerted with the use of the energy of ATP hydrolysis. The activation of myosin ATPase by actin becomes possible after the binding of Ca^{2+}-ions by troponin C. It is evident that Ca^{2+}-ions should

stimulate the glycolytic process producing ATP. This stimulation is realized through the anchor protein, troponin C. The complex of glycolytic enzymes adsorbed on the structural proteins of skeletal muscles remains inactive until the binding of Ca^{2+}-ions to troponin C takes place. The binding of Ca^{2+}-ions to troponin C produces conformational changes in the anchor proteins and neighbouring proteins of the complex. This gives the possibility for the substrates to get into the microcompartment and be chemically transformed.

The anchor protein fixing the complex of glycolytic enzymes to the erythrocyte membrane is able to interact with Ca^{2+}-ions like anchor proteins in skeletal muscles. The interaction of Ca^{2+} ions with band 3 protein leads to the inhibition of the transport of anions through the erythrocyte membrane (Passing and Schubert, 1983). One can expect that the functioning of the complex of glycolytic enzymes fixed on the dimers of band 3 protein will be sensitive to Ca^{2+} ions.

CONCLUSION

In summary, I should like to formulate some principles of the regulation of cellular metabolism.

The control of cellular metabolism has multilevel nature. The hierarchy of the levels of the control of cellular metabolism is based on the multilevel material organization of biological objects. The biological system of each level of the complexity has elements which exert working and control functions (for example, active and allosteric sites for the enzymes, the microcompartment and the anchor protein for the multienzyme complexes adsorbed on the biological supports). The regulatory factors which interact with the control site of the system are external ones with respect to the given system. In other words, these factors are not the substrates or the products of the enzymic reaction in the case of single enzymes and are not the metabolic intermediates in the case of multienzyme complexes. The regulatory factors ensure the optimum functioning of the given biological system when included in the system of a higher level of complexity.

As far as the regulation of multienzyme complexes is concerned two levels of control may be identified. The lower level of control is exerted with the participation of metabolites-regulators (allosteric regulation). The higher level of control is exerted with the participation of second messengers affecting the anchor protein of the support which ensures the formation of the multienzyme complex. The control mechanism of the higher level provides the rough regulation of the functioning of the multienzyme complex (switching on - switching off the metabolic pathway), whereas owing to the control mechanisms of the lower level a fine adjustment of the catalytic action of the multienzyme complex is achieved. It should be noted that the control mechanisms which are operative at the higher levels are more rapid.

REFERENCES

Arnold, H. and Pette, D. (1968) Binding of glycolytic enzymes to structure proteins of muscle. Eur. J. Biochem. 6, 163-171.

Arnold, H. and Pette, D. (1970) Binding of aldolase and triose-phosphate dehydrogenase to F-actin and modification of catalytic properties of aldolase. Eur. J. Biochem. 15, 360-366.

Arnold, H., Henning, R. and Pette, D. (1971) Quantitative comparison of the binding of various glycolytic enzymes to F-actin and the interactions of aldolase with F-actin. Eur. J. Biochem. 22, 121-126.

Berridge, M.J. (1983) The role of membrane phospholipids in receptor transducing mechanisms. In: Cell Surface Receptors (P.G. Strange, ed.) Ellis Horwood Ltd., Chichester, pp. 207-226.

Berridge, M.J. (1984) Inositol triphosphate and diacylglycerol as second messengers. Biochem. J. 220, 345-360.

Clarke, F.M. and Masters C.J. (1974) On the association of glycolytic components in skeletal muscle extracts.

Biochim. Biophys. Acta, 358, 103-207.

Clarke, F.M. and Masters, C.J. (1975) On the association of glycolytic enzymes with structural proteins of skeletal muscle. Biochim. Biophys. Acta, 381, 37-46.

Clarke, F.M. and Masters, C.J. (1976) Interactions between muscle proteins and glycolytic enzymes. Int. J. Biochem. 7, 359-365.

Clarke, F.M. and Morton, D.J. (1976) Aldolase binding to actin containing filaments: Formation of paracrystals. Biochem. J. 159, 797-798.

Dölken, G., Leisner, E. and Pette, D. (1975) Immunofluorescent localization of glycogenolytic and glycolytic enzyme proteins and of malate dehydrogenase isozymes in cross-striated skeletal muscle and heart of the rabbit. Histochemistry, 43, 113-121.

Green, D.E., Murer, E., Hultin, H.O., Richardson, S.H., Salmon, B., Brierly, C.P. and Baum, H. (1965) Association of integrated metabolic pathways with membranes. I. Glycolytic enzymes of the red blood corpuscle and yeast. Arch. Biochem. Biophys. 112, 635-647.

Higashi, T., Richards, C.S. and Uyeda, K. (1979) The interaction of phosphofructokinase with erythrocyte membranes. J. Biol. Chem. 254, 9542-9550.

Iyengar, R., Birnbaumer, L., Schulster, D., Houslay, M. and Michell, R.H. (1980) Modes of membrane receptor-signal coupling. In: Cellular Receptors for Hormones and Neurotransmitters (D. Schulster and A. Levitzki, eds.) John Wiley and Sons, Chichester, pp. 55-81.

Keleti, T. (1984) Channelling in enzyme complexes. In: Dynamics of Biochemical Systems (J. Ricard and Cornish-Bowden, eds.) Plenum Publishing Corporation, New York, pp. 103-114.

Kurganov, B.I. (1982) Allosteric Enzymes. Kinetic Behaviour. John Wiley and Sons, Chichester, p. 344.

Kurganov, B.I. (1984) Adsorption of peripheral enzymes to membrane anchor proteins. J. Theor. Biol. 111 707-723.

Kurganov, B.I. (1985a) The physico-chemical mechanisms of regulation of enzyme activity. In: Physical Chemistry. Contemporaneous Problems. (Y.M. Kolotyrkin, ed.) Vol. 5.

(In Russian). Chimija, Moscow, pp. 180-219.

Kurganov, B.I. (1985b) Control of enzyme activity in reversibly-adsorptive enzyme systems. In: Catalytic Facilitation in Organized Multienzyme Systems (G.R. Welch, ed.) Academic Press, New York, pp. 241-270.

Kurganov, B.I., Sugrobova, N.P. and Mil'man, L.S. (1985) The supramolecular organization of glycolytic enzymes. J. Theor. Biol. (in press)

Passing, R. and Schubert, D. (1983) The binding of Ca^{2+} to solubilized band 3 protein of the human erythrocyte membrane. Hoppe-Seyler's Z. Physiol. Chem. 364, 873-878.

Sigel, P. and Pette, D. (1969) Intracellular localization of glycogenolytic and glycolytic enzymes in white and red rabbit skeletal muscle. Histochem. Cytochem. 17, 225-237.

Snol', S.E., Ermakova, E.A. and Frank, G.M. (1979) The diffusional constraints and the evolutional sense of the formation of intracellular structures. In: The Methodological and Theoretical Problems of Biophysics (G.R. Ivanitskii, ed.) Nauka, Moscow, pp. 90-99.

Stewart, M., Morton, D.J. and Clarke, F.M. (1980) Interaction of aldolase with actin containing filaments. Structural studies. Biochem. J. 186, 99-104.

Strapazon, E. and Steck, T.L. (1977) Interaction of the aldolase and the membrane of human erythrocytes. Biochemistry 16, 2966-2971.

Sugrobova, N.P., Eronina, T.B., Chebotareva, N.A., Ostrovskaya, M.V., Livanova, N.B., Kurganov, B.I. and Poglazov, B.F. (1983) Regulation of enzyme activity in adsorptive enzyme systems. III. Interaction of pig muscle lactate dehydrogenase with F-actin. Mol. Biol. (USSR) 17, 430-436.

Tillman, W., Cordua, A. and Schröter, W. (1975) Organization of enzymes of glycolysis and of glutathione metabolism in human red cell membranes. Biochim. Biophys. Acta, 382, 157-171.

Vaughan, H., Thornton, S.D. and Newsholme, E.A. (1973) The effects of calcium ions on the activities of trehalase, hexokinase, phosphofructokinase, fructose diphosphatase and pyruvate kinase from various muscles. Biochem. J. 132, 527-535.

Walsh, T.P., Clarke, F.M. and Masters, C.J. (1977) Modification of the kinetic parameters of aldolase on binding to actin-containing filaments of skeletal muscle. Biochem. J. 165, 165-167.

Welch, G.R. (1977) On the role of organized multienzyme systems in cellular metabolism: a general synthesis. Progr. Biophys. Molec. Biol. 32, 103-191.

Westrin, H. and Backman, L. (1983) Association of rabbit muscle glycolytic enzymes with filamentous actin. A counter-current distribution study at high ionic strength. Eur. J. Biochem. 136, 407-411.

Yu, J. and Steck, T.L. (1975) Associations of band 3, the predominant polypeptide of the human erythrocyte membrane. J. Biol. Chem. 250, 9176-9184.

DISCUSSION

WELCH:

I have a question concerning the regulatory significance of such reversibly adsorptive systems as in the case for the association of phosphofructokinase with erythrocyte membrane. Of particular concern with this enzyme is the fact that its substrate-saturation curve changes from sigmoidal to more hyperbolic when it is bound to the membrane.

KURGANOV:

The changes in the shape of v vs (S) plot which accompany the adsorption of phosphofructokinase to the erythrocyte membrane mean the diminishing of sensitivity of the enzyme reaction rate to the variation of substrate concentration and the weakening of contribution of this enzyme in the regulation of glycolytic processes.

We should realize that the adsorbed phosphofructokinase is a component of the multienzyme complex. The spatial organization of the glycolytic enzymes leads to the formation of the microcompartment where glycolytic process proceeds without the release of the glycolytic intermediates in the medium. The multienzyme complex adsorbed to the dimer of band 3 protein embedded in the erythrocyte membrane has symmetry axis of second order and contains two such compartments. All glycolytic enzymes (with exception of phosphoglycerate kinase) possess oligomeric structure. The definite part of active and effector sites of the glycolytic enzymes face to the microcompartment whereas the other one is located on the surface of the multienzyme complex. The former active and effector sites participate in the glycolytic process which proceeds in the microcompartment. The main product of glycolytic process, ATP, should be channelled to corresponding ATP-consuming enzyme systems (for example, to the active sites of myosin ATPase in myofibrils). The regulatory

links in the microcompartment should be weakened. In particular, effector sites of phosphofructokinase located in the microcompartment should be characterized by less affinity to ATP in order not to prevent the ATP production in the working microcompartment.

On the other hand, active and effector sites located on the surface of the multienzyme complex should retain their sensitivity to metabolites-regulators in order to provide the control of functioning the multienzyme complex by cellular metabolites accumulated in the surrounding (i.e. in the macrocompartment).

Another aspect of functioning phosphofructokinase concerns the appearance of the sensitivity of adsorbed form of the enzyme to new regulatory factors. I assume that phosphofructokinase adsorbed to the support of the biological nature becomes sensitive to second messengers. It is known that anchor proteins revealing the affinity to phosphofructokinase interact with Ca^{2+} ions. One can expect that Ca^{2+} ions will be important regulators of the enzyme activity of adsorbed phosphofructokinase and of the catalytic action of the whole organized glycolytic system.

FRIEDRICH:

The evidence available about the three glycolytic enzymes examined in considerable details, i.e. phosphofructokinase, aldolase and glyceraldehyde-3-phospnate dehydrogenase (GAPD), indicates that these enzymes bind to the red cell membrane mainly under hypotonic conditions, when examined in vitro. This, however, does not exclude that they are bound to the membrane in vivo, in the intact cell. Two papers addressed to the question of localization of GAPD in intact erythrocytes: Kliman and Steck (J. Biol. Chem. 255, 6314-6321, 1980) analysed the kinetics of saponin-induced partial haemolysis and Solti et al. (J. Biol. Chem. 256, 9260-9265, 1981) determined the distribution of ^{3}H-labelled GAPD in fixed erythrocytes by electron-microscopic autoradiography. Both approaches gave the

result that about two-thirds of the total GAPD in red cells is located at the membrane. The model proposed by Dr. Kurganov for a submembrane overall glycolytic complex can only be regarded as a working hypothesis, since only some aspects of it can be supported by experimental evidence.

KURGANOV:

The experimental data which have allowed to suggest the idea about the existence of the ordered complex of the glycolytic enzymes and to dispose the glycolytic enzymes in the complex in the definite manner include the data on the adsorption of the glycolytic enzymes to the erythrocyte membranes and to the structural proteins of the myofibrils, the data on the protein-protein interactions for the glycolytic enzymes and the data on the regulation of the glycolytic enzymes by the glycolytic intermediates. The analysis of these experimental data and the tentative structure of the complex of the glycolytic enzymes will be represented in our paper (Kurganov, B.I., Sugrobova, N.P., Mil'man, L.S., J. theor. Biol. in press).

OVÁDI:

You mentioned that it is known that the mitochondrial AAT dissociates on dilution. Where do those data come from? Do you have any evidence for the occurence of glycolytic multienzyme complex as well as for the location of each enzyme in such a complex?

KURGANOV:

I have discussed the sedimentation of cytoplasmic aspartate aminotransferase from pig heart. The dissociation of the dimeric form of this isozyme into monomers in diluted solution is a well documented fact.

Dynamics of Biochemical Systems
S. Damjanovich, T. Keleti, L. Trón (Eds)

THE DYNAMIC CHARACTER OF THE ENZYME-ENZYME INTERACTIONS IN THE CYTOPLASM OF EVOLUTIONARY DISTANT SPECIES

J. BATKE and P. TOMPA

Institute of Enzymology, Biological Research Center,
Hungarian Academy of Sciences, Budapest, Hungary,
H-1502 Pf. 7

INTRODUCTION, GENERAL PROBLEMS: The continuously increasing number of experimental data of the past ten to twenty years, as well as theoretical considerations, give us more or less the evidence that the macromolecular constituents both of the cytoplasm and the mitochondrial matrix are somehow organized. Let us only briefly refer to the observations concerning the existence of enzyme-enzyme interactions, multienzyme aggregates, protein-membrane interactions, the microcompartmentation of metabolic intermediates etc./cf. 1-4 and references therein/. Beyond these, however, there are examples in which such interactions were not observed /cf. 5-7/. It is also a frequently found discrepancy that interactions clearly demonstrated kinetically could not be detected by ultracentrifugation method /cf. 9,10/. Reasons of this may be the rather high instability of these systems at least in vitro conditions, as well as their sensitivity to even small changes of environmental factors /8/. Influence of such a technical factor as for instance the effect of pressure on the equilibria during ultracentrifugation /cf. 11/ may also be determinative. In short, the choice of the appropriate technique/s/ is one of the most important requirements of the successful detection.

For the analysis of macromolecular interactions in solution nowadays, the use of covalently attached fluorescence probes seems to be the most fruitful technique. This method has several advantages over others, such as the extreme sen-

sitivity, the less time-consumption of the experiment compared to other techniques, the possibility to detect rapid changes /in stopped flow/ and above all its excellent suitability for quantitative analyses. These characteristics determined our choice to apply fluorescence methods, since we wanted to characterize the enzyme-enzyme interactions in quantitative terms.

AIMS: Our present aim is to compare the ability of cytoplasmic enzymes for interactions in phylogenetically distinct species /like a mammal and yeast/. Our attention is focused on fructose-1,6-bisphosphate aldolase /aldolase/ and the enzymes functionally related with it, namely glyceraldehyde-phosphate /GAPD/ and glycerolphosphate /GDH/ dehydrogenase, triosephosphate isomerase /TPI/, phosphofructokinase /PFK/ and fructose--1,6-bisphosphatase /F-1,6-Pase/. These enzymes participate directly in the production and conversion of triosephosphates, glyceraldehyde- and dihydroxyacetone-phosphate, which are common intermediates of at least the glycolysis, the glycerolphosphate-shuttle and the pentose phosphate pathway. At a metabolic crossroad like this, the existence of certain mechanism which would control the proportion of the transforming common intermediates towards various directions are possible. We assume that if such regulation exists, then this is based on the ability of the appropriate enzymes to form complexes in a competitive manner. In such "functional complexes" the intermediate is directly transferred /channelled, cf. 13 and references therein/ to the "next" appropriate enzyme. The competition of the "starting" enzymes of alternative routes to form complex with the enzyme producing the common intermediate will dictate the ratios of the actual metabolic fluxes. Our present experience suggests a dinamically organized assembly of enzyme complexes with a few participants rather, than a large "static"multienzyme aggregate containing all the glycolytic enzymes /glycosome/.

HOMOLOGOUS /SUBUNIT-SUBUNIT/ INTERACTIONS: The susceptibility of the above mentioned enzymes /aldolase, GAPD.../ to form complexes with each other in a buffered system /standard condition: 0.05 M Tris-HCl buffer, pH: 7.5 or 8.5, 20°C/ has

been analysed with purified rabbit muscle and baker's yeast /Saccharomyces cerevisiae/ enzymes. However interpretation of the results was rendered difficult by the fact that some of these enzymes proved to be dissociable oligomers, as this was indicated by the enzyme concentration dependent characteristic change of their fluorescence anisotropy or specific fluorescence intensity of the fluorescence probes attached covalently to the enzymes. According to these observations yeast aldolase /22/ and muscle GDH /12/ exist in rapid dimer-monomer, while muscle GAPD /15/ in a rapid tetramer-dimer-monomer equilibrium in the range of 10-0.01 μM. On the contrary, tetrameric yeast GAPD /20/ and tetrameric muscle aldolase /17/ do not dissociate in the same concentration range in standard conditions.

In such cases if the specific enzymatic activities as well as fluorescence anisotropies were changed /muscle GAPD and yeast aldolase in Fig.1/ we concluded that the different oligomeric forms have distinct specific catalytic activity.

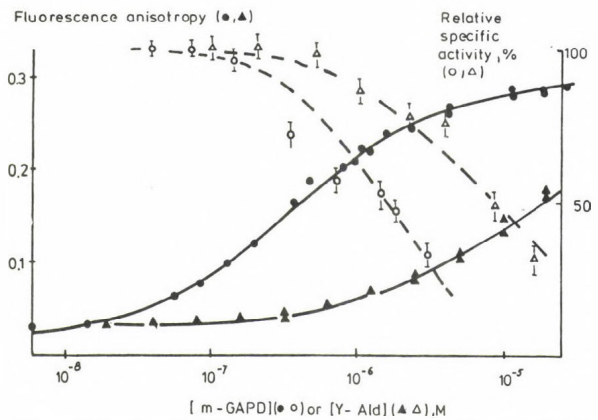

FIG.1 The change of fluorescence anisotropy of muscle GAPD /●/ and yeast aldolase /▲/ both enzymes labeled with ~1 equivalent FITC/, and the change of relative specific enzymatic activities /open symbols/ as the function of their concentrations at our standard condition /see the text, at pH:7.5/. For details see references/15,18,22/. Solid lines indicate computed curves assuming tetramer-dimer-monomer and dimer-monomer equilibria of GAPD/14,15/ and aldolase /22/, respectively, with the dissociation constants given in Table I.

Table I: Summary of the values of the dissociation constants /K/, the association /k_+/ and dissociation /k_-/ rate constants of the homologous /subunit-subunit/ and heterologous interactions of various rabbit muscle/m/ and yeast /y/ cytoplasmic enzymes. Conditions are pH:7.5 or 8.5, 0.05 M Tris-HCl buffer, 20° C.

Interaction	Sources	Enzymes	pH	K /μM/	$k_+ x10^{-6}$ /$M^{-1}min^{-1}$/	k_- /min^{-1}/	Ref.
HOMOLOGOUS	y	Ald/d-m/	7.5 8.5	8-20 4 - 7	- k_-/K:0.03	- 0.1-0.2	22
		GAPD /t/	8.5	< 0.0002	practically non-dissoc.		20,22
		/o-t/ PFK /t-d/		0.5 1.0	-	-	29
	m	Ald /t / /t-d/		practically non-dissociable in 10-0.01 μM 0.1-1			17,22 23 24,25
		GAPD /d-m/	8.5 7.5	0.5-5	-	-	15,19 14
		GDH /d-m/	7.5	3; $(4.6)_{est.}$	$(>1)_{est.}$	$(>4.6)_{est.}$	12,(21)
		PFK/16mer-o- -t-d/		data are not presented			33
HETEROLOGOUS	y	Ald-GAPD	7.5	0.08-0.1	1-2	0.05-0.1	22
			8.5	0.1-0.2	1-2	0.2-0.4	
		Ald-PFK	8.5	0.05-0.1	3	Kk_+:0.2	22
		Ald-TPI	int.can not be detected by fluorim./22/				
	m	Ald-GAPD	7.5	0.2-0.3	0.0025	Kk_+:0.0005	17
			7.5	-	0.05-0.1	-	22
			8.5	-	0.1-0.2	-	22
		Ald-TPI		2	-	-	27
		Ald-GDH	7.5	0.1	-	-	12
				1^{++}	0.02^{++}	0.004^{++}	16,21
				$0.2-0.8^{+}$	$0.5-0.002^{+}$	$0.4-0.002^{+}$	
	liver Ald-fruct.- -1,6-bisphos- phatase		8.5	data are not presented			28
HYBRID H.	m-Ald and y-GAPD		8.5	0.1-0.2	2	Kk_+:0.2-0.4	22
	y-Ald and m-GAPD		8.5	0.05	3.6	Kk_+: 0.2	22

o:octamer, t:tetramer, d:dimer, m:monomer, ++:Ald-GDH_d, +:Ald-GDH_{m1}, and Ald-GDH_{m2} complexes, est.:estimated value.

On the other hand, if anisotropy vs. enzyme concentration was constant /muscle aldolase and yeast GAPD in Fig.2/ and no

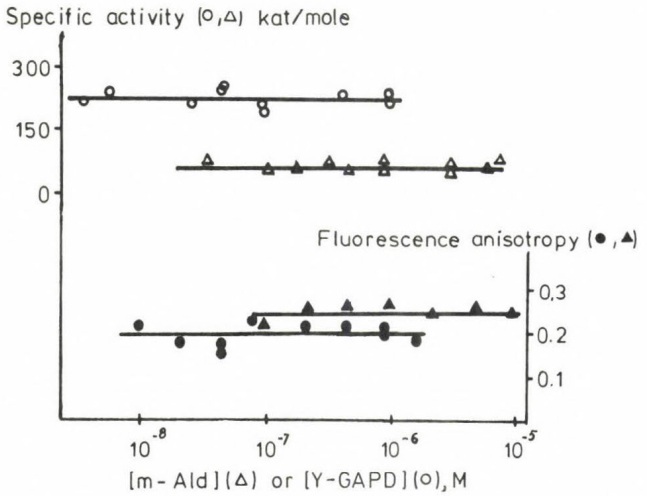

FIG.2 The fluorescence anisotropies /• ,▲/ and the specific enzymatic activities /o ,Δ/ of yeast GAPD /circles/ and muscle aldolase /triangles/ measured at different enzyme concentrations at our standard conditions at pH:7.5 and 8.5 for aldolase and GAPD, respectively. The fluorescence probe, fluorescamine was used since yeast GAPD labeled with FITC was completely inactive. For other details see references 22 and cf. 17,20,26.

change in specific activity was observed, then we concluded that dissociation of the oligomer does not occur. Otherwise these statements have been in good agreement with sedimentation velocity data referring to the non-dissociable character of muscle aldolase /23/ and yeast GAPD /20/, but indicating the dissociation of muscle GAPD /24, 25 and cf. 15/. Dissociation of dimeric GDH was also presented by ultracentrifugation /12/ and a rather good parallelism between the enzyme concentration dependence of the fluorescence anisotropy and specific enzymatic activity was found /Fig. 1. in ref 16/.

INTERACTIONS IN CYTOSOL: Any shift of the oligomeric equilibria of these enzymes may have regulatory consequences. Therefore we examined whether concentration dependences of the specific activities can be observed or not in a mixture of all the cytoplasmic enzymes, i.e. in a mixture which somehow mimics

the macromolecular milieu of the cytoplasm. For this purpose a crude extract was prepared from the disrupted cells by an appropriate centrifugation /100.000 g, 1 h/. The supernatant which contained the cytoplasmic constituents was occasionally filtered on a Sephadex column in order to eliminate small molecular-mass intermediates from the macromolecular components. The activities of the above mentioned enzymes were then determined at different concentrations of this "cytoplasmic--like" macromolecular mixture and the specific activity vs. the dilution of the cytoplasm was calculated. The result was rather surprising since the specific activity even of the non-dissociable muscle aldolase and the yeast GAPD /in muscle and yeast cytosols, respectively/ showed a characteristic concentration dependence /Fig. 3./.

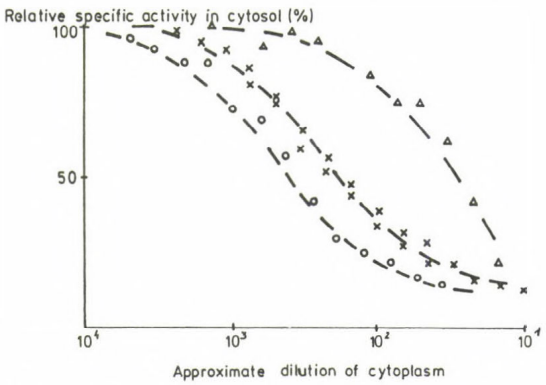

FIG.3 Changes of the relative specific activities of rabbit muscle aldolase/o/ , yeast GAPD /x/ and rabbit liver GAPD /△/ in cytosol as the function of the approximate dilution of the cytoplasm, at our standard conditions /pH:8.5/. For details see reference /22/ and the text.

A possible explanation of such changes is the dissociation of heterologous complexes during the dilution, since in purified form both aldolase and GAPD /muscle and yeast/ constitute complexes with each other and alternatively with other enzymes /cf. Table I and the references therein/ too.

We should like to note here that the characteristic decrease of specific activities- towards the high cytosol concentrations - indirectly suggests the channelling of the intermediate/s/ in the enzyme complex. The added substrate seems to be transformed into product only by the free /non-complexed/ form of the enzyme, while the enzyme which is in the heterologous enzyme complex is not or partially available for the external /added/ substrate. The time-while the initial velocity is determined in the stopped flow measurement /in several 20-40 milliseconds after mixing the substrate with the cytosol/ - is too short for the diffusion of the substrate to the active centre of the appropriate enzyme in the complex. Otherwise other possible reasons of such a decrease of the specific activities at higher enzyme concentrations were carefully analysed /cf. 22/: i./ Activities were measured at substrate saturation and the substrate saturation curves were found to be Michaelis-Menten type even at high cytosol concentration. Moreover the K_m values proved to be independent of the cytosol concentration. ii./ The absorbance changes at 340 nm caused by side reactions after the addition of NAD^+ to the cytosol were negligible compared to the change after mixing NAD^++glyceraldehyde-3-phosphate+arsenate in the GAPD activity test. iii./ Initial velocities /in stopped flow/ were carefully determined from the very linear, initial part of the time curves where not more than 5 % of the added substrate had been transformed.iv./ The possible rate limiting effect of the diol--aldehyde conversion of the glyceraldehyde-3-phosphate /cf.34/ at higher enzyme concentrations was excluded. v./ The rate reducing effect of the increased viscosity even at the highest cytosol concentrations where measurements were carried out was negligible.

In any case the concentration dependence of the specific activities seems to reflect the very complex relations both of the heterologous and homologous enzyme-enzyme interactions in this cytosol fraction. Such a complicated system is not an appropriate subject for a rigorous quantitative analysis, however, conclusions can be drawn from the measurements of interactions between pairs of purified enzymes.

QUANTITATION OF HETEROLOGOUS INTERACTIONS; CONCLUDING REMARKS:

Equilibrium and rate constants of complex formation and dissociation were calculated from the changes of specific fluorescence intensities /relative quantum yields/ and of anisotropy of the fluorescent probe, fluorescein isothiocyanate /FITC/, attached covalently to one of the enzymes analysed. As an illustration, the titration of yeast aldolase /labeled with FITC/ by unlabeled yeast GAPD or yeast PFK is presented in Fig.4. Similarly, the formation or the dissociation of the yeast aldolase-GAPD complex are shown in Fig. 5. Details of

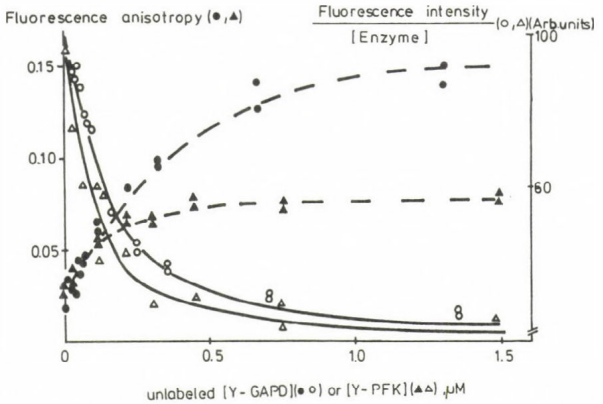

FIG.4 The titration of labeled yeast aldolase /0.05 μM, containing ~1 equivalent FITC/ with unlabeled yeast GAPD /circles/ or with yeast PFK /triangles/ followed by measuring the change of anisotropy /dense symbols/ and the specific fluorescence /open symbols/ at our standard conditions /pH:8.5/. Solid lines are computed curves assuming 1:1 stoichiometry of binding with dissociation constants 0.2 and 0.1 μM for GAPD and aldolase, respectively. For other details see reference /22/.

the calculations are given elsewhere /22/. Data summarized in Table I indicate that heterologous interactions are somewhat stronger /K's are near 0.1 μM/ than homologous ones /K's are near 1 μM/, however essential differences do not exist in yeast and muscle types of interactions. This similarity, but rather the observation that also hybrid interactions between yeast and muscle enzymes can appear in vitro /and the

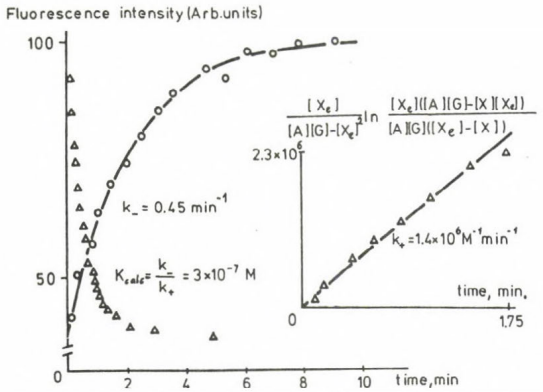

FIG.5 The kinetics of the dissociation /o/ and the formation /Δ/ of the yeast aldolase-GAPD complex followed by the change of fluorescence intensity at our standard condition at pH:8.5. The dissociation kinetics was measured as follows:1.8 and 6 μM aldolase /FITC labeled/ and GAPD, respectively were incubated for 10 minutes, then it was diluted 50 times and the change of fluorescence intensity recorded. Solid line is an exponential / $e^{-k_- t}$ / computed curve with k_-:0.45 min^{-1} .The dissociation kinetics was measured by mixing 0.09 μM aldolase /labeled with FITC/ and 0.65 μM GAPD, and the change of fluorescence intesity was followed. Insert indicates the semilogarithmic plot of the reversible bimolecular complex formation of aldolase/A/+ GAPD/G/ ⇄ complex calculated with the K_d:0.2 μM /from Fig.4/.The slope of this plot is k_+:1.4x10^6 $M^{-1}min^{-1}$. The ratio of k_-/k_+:0.3 μM is in good agreement with the value of 0.2μM determined independently from Fig. 4.

K values are also in 0.1 μM range!/ suggests the possible ancient origin of the organization of these enzymes in the cytoplasm.

The rate constants of the complex formation /k_+: 10^6-10^3 $M^{-1}min^{-1}$/ and that of the the dissociation /k_-:10^0-$10^{-3}$$min^{-1}$/ show larger variability, but as a whole, all cases indicate rapid processes. This high speed of the transformation of enzyme complexes ensures the flexibility of the system in regulatory responses /cf. 21/.

Although the effect of intermediates, pH, temperature and ionic strength on these enzyme-enzyme interactions has not been exhaustively examined in all details, however, a few statements can be made /cf. 22/: i./ Intermediates seem to have an essential effect on homologous interactions, i.e. the presence of substrates or products /or both/ weakens the

associative forces, ii./ increasing ionic strength has the same weakening effect, but iii./ the change of temperature /between 10-25°C/ and the pH /between 6.8-8.5/ have no essential influence on these interactions.

The values of the dissociation constants of the enzyme complexes /determined in the absence of substrates, intermediates/ are near to the 0.1-1 μM range /Table I/, while the physiological "average" concentrations of the glycolytic enzymes are near to the 0.1 mM, so dissociation seems to have no significance in vivo. But the known ability of cell membranes and cellular particules to bind enzymes considering /cf. references in 1/, the differences between K values and the "effective" concentrations of the appropriate enzymes become smaller. Moreover the above mentioned weakening effect of the intermediates as well as the rather high ionic strength in the cell also bring these two factors closer together. In short, dissociation-association dynamics may be important in the physiological effects at in vivo concentrations.

Finally let us consider the possible maximal size of a multienzyme complex in the cytoplasm. Mowbray, Moses and others /30-32/ have demonstrated an enormously large multienzyme aggregate, the glycosome, in E. coli cytosol, which contained all the glycolytic enzymes. Our experience does not provide such a big complex in yeast or in muscle cytosol, since we could never detect any of the glycolytic activities near the exclusion volume of our Biogel A 5M column in the cytosol preparations /corresponding to $M_r \sim 2$ million/, only in the cases if our preparations contained contaminating cell particles or disruption fragments. However, in cytosols, free from these particles, we have never found any glycolytic activities in this extremely high molecular-mass elution region. But even if such a large complex exists, this in itself would not answer the question how the alternative transformations of the intermediate/s/ are regulated. From the standpoint of regulation such a large "static" complex is equivalent to a non-associated, densely packed system. On the other hand, the comparable dissociation constants /cf. Table I/ of the heterologous complexes of aldolase with its functionally

related enzymes suggest the chance of a competition among these enzymes to form distinct complexes with aldolase. The direct transfer /channelling/ of the intermediate/s/ can occur in these complexes into different directions and reorganization of the complexes will determine the changes in the ratios of the fluxes. Unfortunately an experimental demonstration of the competition of GDH and GAPD was not successful, since the two dehydrogenases proved to form complex with each other too /not published/. However recently Ovádi /personal comunication/ succeeded in finding competition between TPI and GAPD /muscle enzymes/ in the alternative formation of complexes with aldolase.

SUMMARIZING A dynamically organized assembly of alternative complexes of aldolase and enzymes functionally related to it is assumed to govern the transformation of triosephosphates in various directions. Regulation of these fluxes would occur by channelling of the intermediates in these complexes. The flexibility of the system, via the chance of fast reorganization of the enzyme complexes, may be the base of an efficient regulation. The interaction of these enzymes can be considered as an ancient characteristic of the cytoplasm, since it is common in phylogenetically distant species like the yeast and a mammal.

Acknowledgements: We are indebted to Prof. F.B. Straub for his inspiration to check the hybrid interactions and to Prof. T. Keleti for his continous interest and helpful discussions.

REFERENCES:

1./ Keleti,T.,Ovádi,J.,Batke,J. /1986/ Kinetic and physico-chemical analysis of enzyme complexes,In: Towards a Cellular Enzymology/eds. Klyosov,A.A., Varfolomeev,S.D., Welch,G.R./ Basic Life Sciences ser., Plenum Press, New York

2./ Friedrich,P. /1984/ Supramolecular Enzyme Organization. Quaternary Structure and Beyond. Pergamon Press, Oxford, Akadémia Kiadó, Budapest

3./ Srivastava,D.K, Bernhard,S.A./1985/ Enzyme-enzyme interactions and the regulation of metabolic reaction pathways. Current Topics Cell.Reg.Vol. 28 in press

4./ Srere,P.A. /1982/ The structure of the mitochondrial inner membrane matrix compartment, TIBS 7 375-378

5./ De Duve,C. /1970/ Is there a glycolytic particle? in: Wennergren Symposium on Structure and Function of Oxidation--Reduction Enzymes, pp. 715-728, Wennergren Center, Stockholm

6./ Anderson,N.G., Green,J.G., /1967/ The globule phase of the cell, in:Enzyme Cytology /ed: Roodyn,D.B./ pp. 475-509 Acad. Press, London, New York

7./ Masters,C.J., Winzor,D.J. /1981/ Physicochemical evidence against the concept of an interaction between aldolase and glyceraldehyde-3-phosphate dehydrogenase, Arch.Biochem.Biophys. 209 185-190

8./ Clarke,F.M., Masters,C.J. /1973/ Multi-enzyme aggregates: New evidence for an association of glycolytic components, Biochim.Biophys. Acta 327 223-226

9./ Horecker,B.L., Melloni,E., Pontremoli,S. /1981/ Aldolase and fructose bisphosphatase: key enzymes in the control of gluconeogenesis and glycolysis, Curr.Top.Cell.Reg. 18 181-197

10./ Fahien,L.A., Smith,S.E./1974/ The enzyme-enzyme complex of transaminase and glutamate dehydrogenase, J.Biol.Chem. 249 2696-2703

11./ Harrington,W.F., Kegeles,G./1973/ Pressure effects in ultracentrifugation of interacting systems, Meth.Enzymology 27 306-330

12./ Batke,J., Asbóth,G., Lakatos,S., Schmitt,B., Cohen,R. /1980/ Substrate-induced dissociation of glycerol-3-phosphate dehydrogenase and its complex formation with fructose bisphoshate aldolase, Eur.J.Biochem. 107 389-394

13./ Keleti,T./1984/ Channelling in Enzyme Complexes, in Dynamics of Biochemical Systems /Eds:Ricard,J.,Cornish-Bowden, A./ Plenum Press, New York pp. 103-114

14./ Batke,J./1982/ Spectrofluorometric Analysis of the Dissociation of Oligomeric Macromolecules: Correction for the Absorption of Exciting and Emitted Light in a Side-Bottom Type Fluorometer, Anal.Biochem. 121 123-128

15./ Ovádi,J., Mohamed Osman,I.R., Batke,J. /1982/ Local conformational changes induced by successive NAD binding to dissociable tetrameric D-glyceraldehyde-3-phosphate dehydrogenase. Quantitative analysis of a two-step dissociation process. Biochemistry 21 6375- 6382

16./ Ovádi,J., Mohamed Osman,I.R., Batke,J./1983/ Interaction of the dissociable glycerol-3-phosphate dehydrogenase and fructose-1,6-bisphosphate aldolase. Quantitative analysis by an extrinsic fluorescence probe. Eur.J.Biochem. 133 433-437

17./ Ovádi,J., Salerno,C., Keleti,T., Fasella,P. /1978/ Physico-chemical evidence for the interaction between aldolase and glyceraldehyde-3-phosphate dehydrogenase. Eur.J.Biochem. 90 499-503

18./Ovádi,J., Batke,J., Bartha,F., Keleti,T. /1979/ Effect of association-dissociation on the catalytic properties of glyceraldehyde-3-phosphate dehydrogenase. Arch.Biochem. Biophys. 193 28-33

19./ Minton,A.P., Wilf,J. /1981/ Effect of macromolecular crowding upon the structure and function of an enzyme: glyceraldehyde-3-phosphate dehydrogenase. Biochemistry 20 4821-4826

20./ Mockrin,S.C., Byers,L.D., Koshland,Jr.D.E. /1975/ Subunit interactions in yeast glyceraldehyde-3-phosphate dehydrogenase. Biochemistry 14 5428-5437

21./ Ovádi,J., Mátrai,Gy., Bartha,F., Batke,J./1985/ Kinetic pathways of formation and dissociation of the glycerolphosphate dehydrogenase and fructose-1,6-biphosphate aldolase complex. Biochem.J. 229 57-62

22./ Tompa,P.,Bär,J., Batke,J. Interactions of some yeast cytoplasmic enzymes. Quantitative analysis by an extrinsic fluorescence probe. In preparation.

23./ Friedrich,P., Arányi,P., Nagy,I. /1972/ Studies on the relationship between quaternary structure and enzymatic activity of rabbit muscle aldolase. Acta.Biochim.Biophys.Acad.Sci.Hung. 7 11-19

24./ Hoagland,V.D., Teller,D.C. /1969/ Influence of substrates on the dissociation of rabbit muscle D-GAPD, Biochemistry 8 594-602

25./ Lakatos,S., Závodszky,P./1976/ The effect of substrates on the dissociation association equilibrium of mammalian D-GAPD. FEBS Lett. 63 145-148

26./ Rutter,W.J., Hunsley,J.R., Groves,W.E., Calder,J., Rajkumar,T.V., Wodfin,B.M./1966/ Fructose bisphosphate aldolase, in: Meth. Enzymol.Vol IX. /ed.by Wood,W.A./ p. 479 Acad.Press New York, London

27./ Salerno,C., Ovádi,J. /1982/ Interaction between D-fructose--1,6-bisphosphate aldolase and triosephosphate isomerase. FEBS Lett. 138 270-272

28./ Pontremoli,S., Melloni,S., Salamino,B., Sparatore,B., Michetti,M., Singh,V.N., Horecker,B.L. /1979/ Evidence for an interaction between fructose-1,6-bisphosphatase and fructose-1,6-bisphosphate aldolase, Arch. Biochem.Biophys. 197 356-363

29./ Kriegel,T., Ovádi,J., Behlke,J., Kopperschläger,G./1985/ Quantitative analysis of substrate-modulated dissociation of yeast phosphofructokinase. Eur.J.Biochem. submitted for publication

30./ Mowbray,J.Moses,V. /1976/ The tentative identification in Escherichia coli of a multienzyme complex with glycolytic activity. Eur.J.Biochem. 66 25-36

31./ Gorringe,D.M., Moses,V./1980/ Organization of the glycolytic enzymes in Escherichia coli. Int.J.Biol.Macromol. 2 161-173

32./ Macnab,R., Moses,V., Mowbray,J./1973/ Evidence for metabolic compartmentation in Escherichia coli. Eur.J.Biochem. 34 15-19

33./ Hesterber,L.K., Lee,J.C./1982/ Self-association of rabbit muscle phosphofructokinase: Effects of ligands. Biochemistry, 21 216-222

34./ Trentham,D.R., McMurray,C.H., Pogson,C.I. /1969/ The active chemical state of D-glyceraldehyde-3-phosphate in its reaction with D-GAPD, aldolase and Triose Phosphate Isomerase. Biochem.J. 114 19-24

KACSER:

I would like to know whether there is a common definition of "channelling". It seems to me that different people use different definitions not simply different methods.

BATKE:

Channelling (perfect, leaky, etc.) means certain kinds of mechanisms having functional importance in order to more or less avoid the diffusion of the intermediate into the bulk medium. Beside indirect evidences there is one direct method for the experimental verification of channelling, the isotope dilution technique.

SRERE:

Channelling of a substrate occurs if that substrate (intermediate) is out of diffusion equilibrium with the bulk medium.

I think in relation to Ovádi's work the separation of leaky vs perfect channelling is not useful for it detracts from the important point that specific protein-protein interaction occurs.

BATKE:

I agree with the definition of channelling.

DYNNIK:

I agree with Professor Kacser. If a whole system might operate as a cluster, its regulation (control) would be inflexible, owing to the low number or independent variables, the disappearance of a number of feedback loops and the drastical changes in the control coefficients. Referring back to the tricarboxylate cycle, we see that such a system with multiloop control behaves as a closed segment (from CS to SDH) as if this segment is spatially separated from the rest of the mitochondria, or is organized in a multienzyme complex.

At the same time, some parts of various metabolic pathways may operate as cluster complexes. It has been shown in the laboratory of Professor B. Hess, that the sum of the total intermediates in the intact yeasts is several times lower than that in the extracts. Such experiments may give further in vivo - in limbo support for the results presented by Dr. Batke, about the organization of these complexes.

BATKE:

Thank you for your comments and suggestion.

MANNERVIK:

It is known that many proteins are composed of more than one domain and it appears that in eukaryotes they may sometimes be encoded in separate exons in the genome. Further, some proteins are multifunctional enzymes with two distinct active sites catalyzing different reactions. It seems conceivable that some enzymes may nave been evolved by gene duplication to form a bifunctional polypeptide chain with two separate catalytically active domains, the coding DNA sequences of which were later separated by introns or otherwise. If so, this evolutionary process might be reflected in the genomic structure so that the genes of some of the enzymes, that interact and express channelling, would be adjacent on the chromosome. In other words, this would explain the association of heterologous protein subunits as a vestige of domain interactions in a common ancestral protein. My question is whether there is any information about the organisation of the genes of the enzymes that we are discussing.

WELCH:

In response to Dr. Mannervik's question, the glycolytic enzymes in bacteria, generally, are not encoded by contiguous genes on the chromosome. There is no direct correlation between gene-contiguity and protein-complex formation, except for the case of "multifunctional proteins"

(which represent single polypeptides with multiple catalytic active sites).

FRIEDRICH:

Pertaining to Dr. Kacser's problem of our definition and detection method of "channelling" of metabolites, I think we all agree that "channelling" is the direct transfer of metabolite from one enzyme to the other without mixing in the bulk medium. It is another question how we can demonstrate such a phenomenon. In fact, there are several ways of doing that, but each approach has certain limitations. A compilation of these can be found in my monograph entitled "Supramolecular Enzyme Organization" Akadémiai Kiadó - Pergamon Press, 1984.

EASTERBY:

Particularly in vitro one may quantify the effects of channelling by comparison of measured transient times with those expected from the known properties of the isolated enzymes.

BATKE:

Thank you for the comment.

ENZYME KINETICS AND REGULATION

Dynamics of Biochemical Systems
S. Damjanovich, T. Keleti, L. Trón (Eds)

MODEL DISCRIMINATION. CONDITIONS WHEN THE CORRECT MODEL CAN BE IDENTIFIED FOR TRANSIENT, STEADY-STATE AND BINDING DATA

W.G. BARDSLEY

Department of Obstetrics and Gynaecology,
University of Manchester, at St. Mary's Hospital,
Whitworth Park, Manchester, M13 OJH, UK

1. INTRODUCTION

A common problem is where experimental measurements, y, are observed with some control variables, x, and it is believed that a functional relationship of the form

$$y_i = f_j(x_i,\theta) + e_i \qquad (1)$$

exists. Here e is the error, θ is a vector of parameters to be estimated and f_j is the correct model from a set of possible models $f = (f_1,f_2,\ldots,f_m)$. When f_j is a linear model and $e = (e_1,e_2,\ldots,e_n)$ is distributed as $N(0,I\sigma^2)$ then exact small sample results are possible (Draper and Smith, 1981) but this is seldom the situation encountered in the biochemical laboratory as the models f_j are usually non-linear. Such non-linearity of f_j has been considered by Beale (1960), Box (1971) and Bates and Watts (1980).

If the correct model is known, then the statistical properties of estimates, the redundancy of parameters and the design of experiments to ensure economical use of data have been summarised by Endrenyi (1981). However, there are many situations when a choice of the appropriate model f_j has to be made either by an examination of residuals or by comparing relative goodness of fit with possible alternative models. This subject has not received so much attention.

With linear models, the variance ratio tests for goodness of fit and relevance of parameters have optimum properties and are widely used. Pettersson and Pettersson (1970) suggested using the F test to fix the empirical rate equation for steady-state enzyme kinetic models but did not consider the effect of non-linearity. When multiple linear regression

models are being investigated, the control variables can often be fixed experimentally in such a way that the relevance of any sub-set of coefficients can be tested. However, with non-linear models, a design matrix cannot be manipulated in this way and the law of diminishing returns operates. As further parameters are added to the model, the ability of any statistical test to detect new coefficients rapidly becomes limited. In this paper I shall attempt to bring these problems into sharper focus.

2. THE DETERMINISTIC MODELS

Often biochemists deal with systems where concentrations of species, X say, are observed as functions of time, t, and rate constants, k, are involved in functional forms such as $F(X, dX/dt, k, t) = 0$. Regression analysis of such stiff systems of non-linear differential equations can be achieved using, for example, Gear's method, but the drawbacks are the need for good starting parameter estimates, expense in computer time and frequently unreliable estimates of k since the equations can be rather overdetermined. Sometimes the system is, or can be, manipulated experimentally to become autonomous and linear with square matrix A as in

$$dX/dt = AX. \tag{2}$$

Thus we have transient kinetics, pharmacokinetics, denaturation of macromolecules or time dependent inhibition of enzymes. Another procedure is to study the zero eigenvalue solution i.e. the pseudo-steady-state, leading to positive rational functions of the form

$$v/E_0 = P(X)/Q(X). \tag{3}$$

An even more extreme example is where $t \to \infty$ or when a rapid equilibrium is assumed, for then all of the saturation behaviour, y, of the system can be obtained from the binding polynomial $N(x)$ as in

$$y = \frac{1}{n} \frac{d \log N(x)}{d \log X} \tag{4}$$

Now statistical tests for model discrimination require that the number of degrees of freedom in the deterministic equation be defined and so we had better be clear what is involved in this. Generally we have a vector of coefficients θ, each component, θ_i, being a function of some directed trees, t, which are functions of rate constants, k. Also there will be constraints such as $F(k) = 0$ due to microscopic reversibility, $G(t) = 0$ caused by degeneracy or $H(\theta) = 0$ resulting from boundary conditions etc.

If $\theta = (\theta_1,\theta_2,\ldots,\theta_n)$, $t = (t_1,t_2,\ldots,t_m)$ and $k = (k_1,k_2,\ldots,k_l)$ but

$$t_i = \alpha_i(k) \quad ; \quad i = 1,2,\ldots,m$$

$$\theta_i = \beta_i(t) \quad ; \quad i = 1,2,\ldots,n$$

$$k_i = \gamma_i(k) \quad ; \quad i = 1,2,\ldots,n$$

and the restrictions F, G and H lead to $\dim(k) = l_o$, $\dim(t) = m_o$ and $\dim(\theta) = n_o$, then the number of degrees of freedom of eq.(1) will be the rank of the Jacobian matrix $J_\gamma = (\partial \gamma_i / \partial k_j)$.

$$\text{Since } J_\gamma = J_\alpha J_\beta$$

$$\text{then rank } J_\gamma \leq \min (\text{rank } J_\alpha, \text{rank } J_\beta)$$

$$\leq \min (l_o, m_o, n_o) \leq \min (l,m,n).$$

3. STATISTICAL TESTS FOR MODEL DISCRIMINATION

Most methods for fitting eq.(1) to experimental data involve optimisation where the objective function is the p-norm of a residual vector r, i.e. $\left\{\sum |r_i|^p\right\}^{1/p}$. Minimising the 1-, 2- or ∞-norms are equivalent to maximising the likelihoods if the error is distributed bi-exponentially, normally or uniformly respectively.

Maximum likelihood parameter estimates have well known asymptotic properties, i.e. $\hat{\theta} \sim N(\theta,(nB_\theta)^{-1})$, where B_θ is the information matrix, and a likelihood ratio test can be constructed (Keeping, 1962; Silvey, 1975). If the test is to discriminate between

H_o : f_j is the correct model (and f_{j+1} is correct since $f_j \subset f_{j+1}$),

H_1 : f_{j+1} is the correct model but f_j is incorrect,

then the likelihood ratio will be

$$\lambda = \frac{\max L(f_{j+1})}{\max L(f_j)}$$

where $L(f_j)$ is the likelihood function restricted to model f_j and $L(f_{j+1})$ the likelihood under model f_{j+1}. The test would be chosen, if possible, to reject H_o when $\hat{\lambda} > c$ where

$$P(\hat{\lambda} > c \mid H_o) = \alpha$$

α being the size of the Type I error. If model f_j has m_j degrees of freedom and gives a sum of squares Q_j with n data points then the test statistic

$$F_j = \frac{(Q_j - Q_{j+1})/(m_{j+1} - m_j)}{Q_{j+1}/(n - m_{j+1})} \qquad (5)$$

is distributed as $F(m_{j+1}-m_j, n-m_{j+1})$ for linear models under H_0 (Lindgren, 1976). With non-linear models the statistic (5) will be approximately F distributed if the non-linearity in f_j and f_{j+1} is not too great. Also a large value for F would be strong evidence for the superiority of model j+1 against model j. So it seems worthwhile then to see how such an uncorrected statistic is distributed with the sort of models and data encountered in biochemistry.

4. THE F TEST. THEORETICAL CONSIDERATIONS

Suppose that we fit models f_j and f_{j+1} with m_j and m_{j+1} degrees of freedom to n data points giving the weighted sumsof squares Q_j and Q_{j+1} where

$$Q_j = \sum_{i=1}^{n} w_i \left\{ y_i - f_j(x_i, \hat{\theta}) \right\}^2 .$$

If $f_j \subset f_{j+1}$ in the sense that restricting parameter values in f_{j+1} yields f_j then, under H_o, F_j of eq.(5) will be approximately F distributed but under H_1, F_j will be inflated. If $f_j \not\subset f_{j+1}$ then it is also possible for F_j to become negative as we shall see later.

With simple H_o and simple H_1 we can define the sizes of a test, α and β, in terms of the probability of a test statistic falling in a critical region under H_o or H_1, and thus leading to Type I or Type II errors. With composite hypotheses there is the power function, $\Pi(\theta)$, defined as the probability of rejecting H_o as θ varies, using a specified test statistic. Clearly the F test could be used in model discrimination even though the size might not be known accurately as long as the power could be shown to be high on H_1, low on H_o and understood as a function of θ, the parameters of the model.

Considering the form of the numerator of eq.(5) it is natural to investigate the distance measure

$$Q = \int_0^{\infty} \left\{ f_j(x,\hat{\theta}) - f_{j+1}(x,\theta) \right\}^2 dx \qquad (6)$$

where θ is the actual parameter set for the correct model f_{j+1} and $\hat{\theta}$ is the estimate obtained for the deficient model f_j. Q as defined by eq.(6)

is a function of θ only since it has been minimised with respect to $\hat{\theta}$. So by varying θ the conditions under which model f_{j+1} can be discriminated from f_j can be explored. Some results from the application of this technique will be presented shortly.

5. THE F TEST. COMPUTER STRATEGY

To extend this type of analysis to higher order cases we have to generate data using known parameter values, add error according to some specified distribution, calculate Q_j and F_j values along with θ estimates and then attempt to analyse the sampling distributions generated.

I have put together a software package to create, then add error repeatedly to an exact data set. Regression analysis is performed in sequence to a hierarchy of models, estimating parameters, covariance matrices and weighted sums of squares. Then F statistics are accumulated, probability integral transforms applied and Kolmogorov-Smirnov and chi squared tests used to test H_o: the transforms are uniform on (0,1). It uses NAG routines C05AZF, E04HBF, E04JAF, E04JBF, F01ABF, F02AAF, G01BAF, G01BBF, G01BCF, G01CBF, G05DDF, G05DYF, G08CAF, M01ANF and S14AAF.

6. THE F TEST WITH EXPONENTIAL FUNCTIONS

Eq.(2) leads to the deterministic equation

$$f_j = \sum_{i=1}^{j} a_i \exp(\lambda_i t) \qquad (7)$$

which is one of three distinct types (Bardsley et al, 1986).

a) Matrix A is diagonal

When a system is uncoupled, as for instance when n distinct, independent first order processes take place, the a_i are constants, independent of the λ_i. In the case of 1 or 2 components, Q of eq.(6) increases monotonically as the rate constants separate as illustrated in figure 1.

b) Matrix A is not diagonal

When several species are interconnected in sequence, the a_i and λ_i of eq.(7) are not independent. They are all functions of the rate constants. For 1 or 2 components, the Q of eq.(6) decreases monotonically as the rate constants separate as illustrated in figure 2.

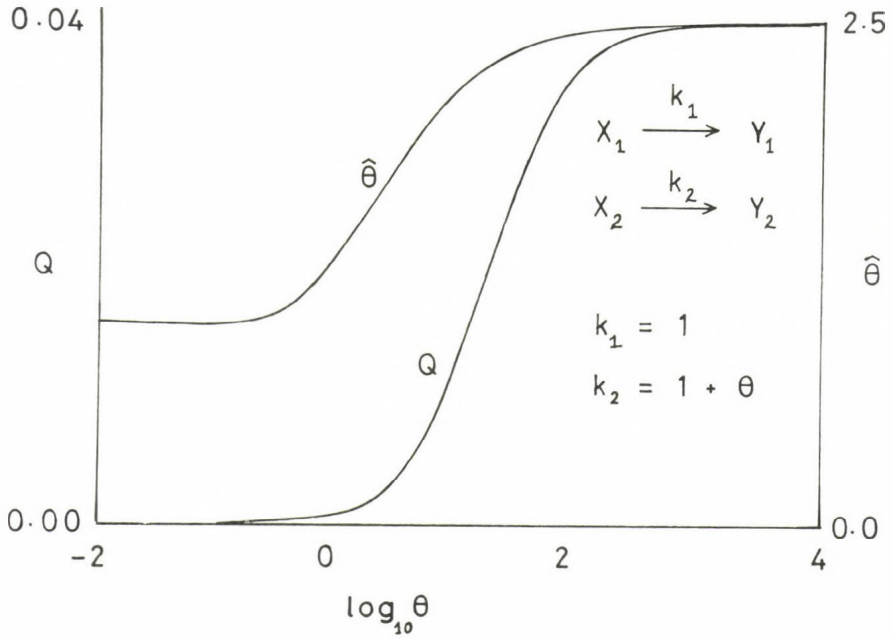

Fig. 1. Q defined by eq.(6) for $f_j = X_1(t)$ and $f_{j+1} = \frac{1}{2}(X_1(t)+X_2(t))$ with a parallel uncoupled scheme. The $Q(\theta)$ and $\hat{\theta}(\theta)$ profiles can be established analytically (Bardsley et al, 1986) but the values shown were calculated using NAG routine G02AEF.

c) The generating scheme is cyclic

When this occurs, the eigenvectors and eigenvalues are again dependent. A new feature is that the characteristic polynomial can have non-real zeros. For a simple cyclic scheme, Q of eq.(6) attained a maximum value when matrix A had non-real eigenvalues and the time profile was a damped oscillation as shown in figure 3. The discriminant of the characteristic polynomial for this cyclic scheme is $\theta(\theta+4)$ and so damped oscillations occur when $-4 < \theta < 0$.

A simulation study was undertaken to see if the principles found to apply with these simple schemes were relevant with higher order models.

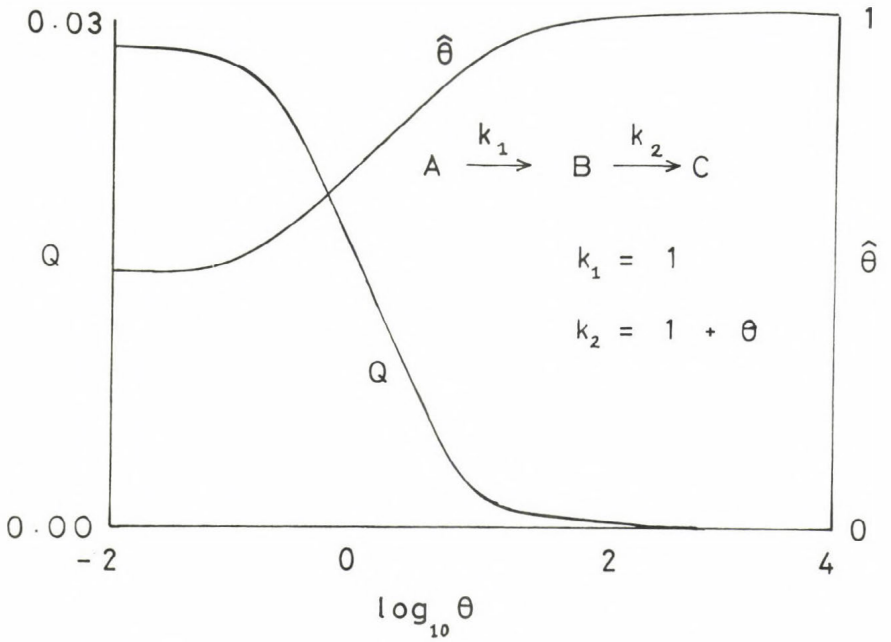

Fig. 2. As for Fig. 1 with $f_{j+1} = C(t)$, $f_j = B(t)$ but $k_2 = 0$.

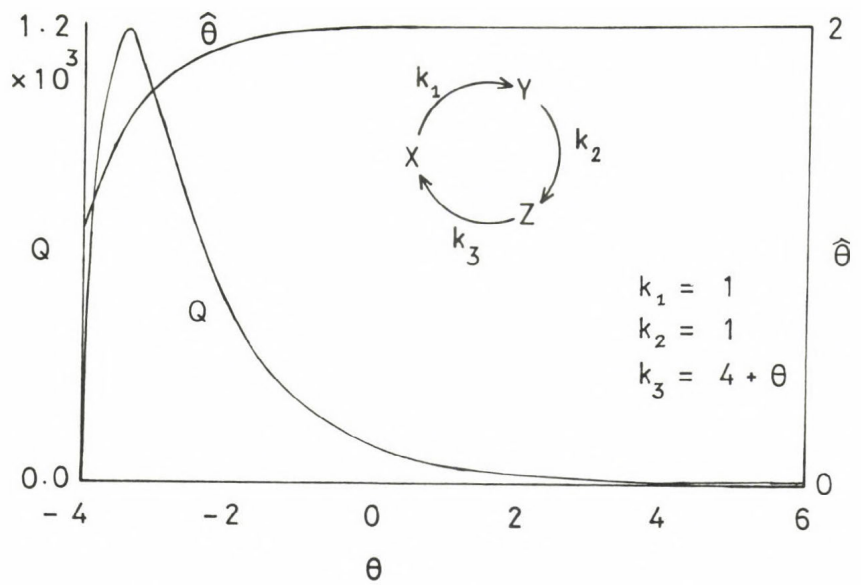

Fig. 3. As for Fig. 1 with $f_{j+1} = X(t)$, $f_j = X(t)$ but Y and Z node compressed

Computation supported these predictions with more complicated schemes (Bardsley et al, 1986). We studied 4 types of data with 15 logarithmically spaced points as follows:

i) 2.5% relative error, range of 5 -95% of f(t) covered,
ii) 5.0% relative error, range of 10-90% of f(t) covered,
iii) 7.5% relative error, range of 15-85% of f(t) covered,
iv) 10.0% relative error, range of 20-80% of f(t) covered.

The k_i values in an example of scheme (a) were varied until the power of the F test was high. As shown in figure 4, the ratio k_{i+1}/k_i had to increase as the order of the model increased to identify correctly the number of relaxing components. The time scale increased steadily as the

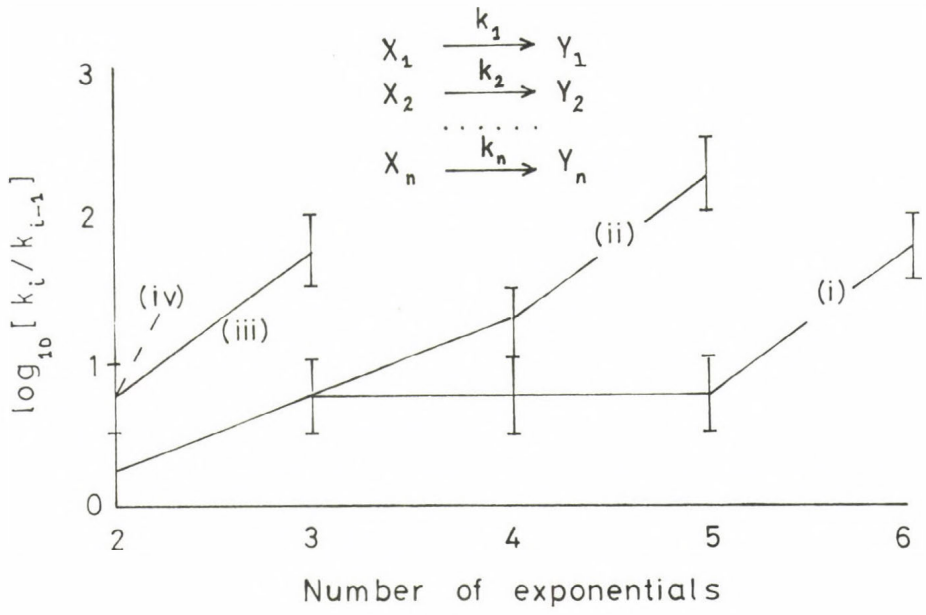

Fig. 4. Vertical bars represent transition regions where the power function of the F test became high using a critical region defined by the 99% F point. The indications (i), (ii), (iii) and (iv) refer to the data structures defined in the text. The deterministic equation was for parallel, uncoupled first order processes as in figure 1. The power was high above the vertical bars, low below them. The F test failed beyond terminated lines.

number of parameters increased. Similarly the k_i values of scheme (b) were varied until the power of the F test was high. As shown in figure 5

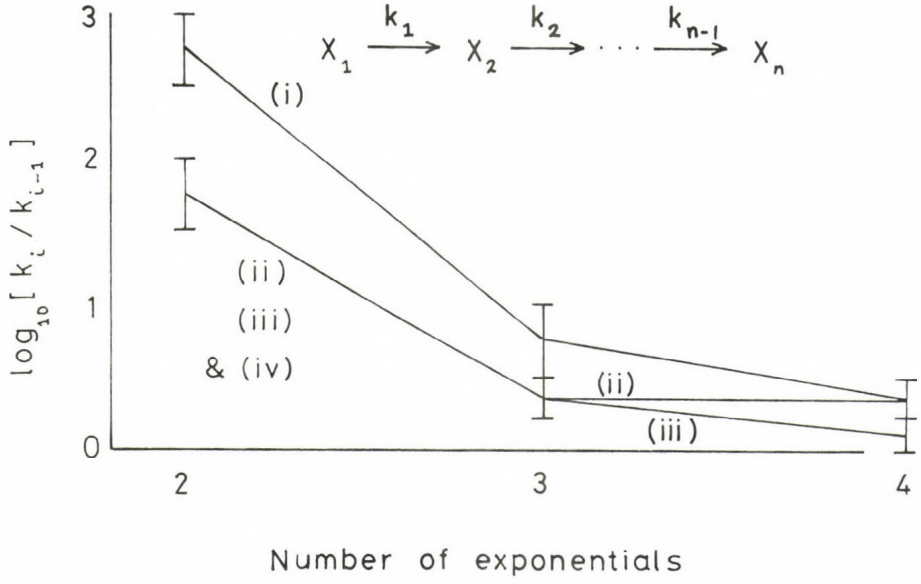

Fig. 5. Details as for Fig. 4, except that the deterministic equation was for a consecutive, coupled series of first order processes as in figure 2. The power was high below the vertical bars, low above them.

the ratio of k_{i+1}/k_i had to decrease as the order of the model increased to identify the number of relaxing components correctly. The time scale altered very little as the number of parameters increased. With the data structures of (i) and (ii) it was possible to detect up to four exponentials but with (iv) only two could be reliably detected. The seeming anomaly, that rate constants had to come close together to be detected, can be easily rationalised by considering what happens if any step in a consecutive scheme becomes rate-limiting.

7. THE F TEST WITH POSITIVE RATIONAL FUNCTIONS

When only one substrate is varied, the steady state solution of eq.(3) can be written as

$$f_j = \sum_{i=1}^{j} \theta_i x^i / (1 + \sum_{i=j+1}^{2j} \theta_i x^{i-j}). \qquad (8)$$

Equation (8) has 2j independent parameters and the equation for the model

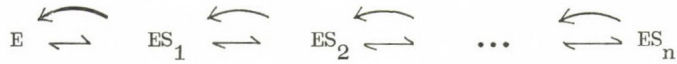

can be expressed with just 2j parameters K_i ; i=1,2,...,j and k_i ; i=1,2,...,j to equal any set of $\theta_i \geqslant 0$. Hence no statistical test could ever indicate a mechanism more complex than this one (Bardsley, 1983). As the degree j in eq.(8) increases, a number of facts can be established by analysis or computation.

i) The number of possible curve shapes, $f_j(x)$, increases rapidly since multiple inflexions and turning points can occur (Bardsley and Wood, 1985).

ii) The maximum complexity in terms of such geometric concepts as sigmoidicity or turning points can be understood by constructing extreme examples (Bardsley and Wright, 1983; Bardsley et al, 1983). Study of these limiting examples as j increases shows that the relative difference between consecutive members decreases rapidly as j exceeds 2.

iii) Although simulation shows that complex profiles are possible (Wardell et al, 1982) nevertheless most examples will look much like second order curves over physiological ranges of substrate concentrations with chemically reasonable rate constant values.

iv) It is easy to detect second order terms by the F test and third order terms can often be identified. However, fourth and higher order terms are extremely difficult to detect (Burguillo et al, 1983).

v) The test statistic for j=1 and 2 is distributed very much like an F variate.

8. THE F TEST WITH SATURATION FUNCTIONS

When the deterministic equation is eq.(4), or a scalar multiple of it as in dose-response curves, analysis is particularly easy. Thus for N, a binding polynomial of order n, we use the form

$$N = 1 + K_1 x + K_2 x^2 + \ldots + K_n x^n$$

for curve fitting but

$$N = 1 + \binom{n}{1} \theta_1 x + \binom{n}{2} \theta_1 \theta_2 x^2 + \ldots + \theta_1 \theta_2 \ldots \theta_n x^n \qquad (9)$$

for theoretical discussion, the connection between θ and K being

$$\theta_j = \frac{j\, K_j}{(n-j+1)\, K_{j-1}} \quad , \quad K_o = 1.$$

The ratios θ_{j+1}/θ_j have been of interest since they define the intrinsic cooperativity of the system as opposed to the apparent cooperativity defined by the Hill slope (Bardsley and Waight, 1978).

At this point it should be emphasised that the saturation functions of order $n > 2$ are disjoint. They do not belong to a hierarchy such as $f_1 \subset f_2 \subset f_3 \ldots \subset f_n$ since by selecting specific θ_i values we cannot pass from f_{j+1} to f_j except for j=1. To do so would require that two polynomials p(x) of degree n and q(x) of degree m satisfied

$$m\, p'(x)\, q(x) = n\, p(x)\, q'(x)$$

for all x. This is only true when p(x) and q(x) are powers of some polynomial r(x) of degree d where (m,n) = d. Hence it is possible for the constrained sum of squares Q_j for the correct model f_j to be less than the unconstrained sum of squares Q_{j+1} even though model f_{j+1} has more degrees of freedom than model f_j. This frequently occurs when fitting saturation data and is not necessarily a deficiency in the optimisation routine.

To apply the method leading to eq.(6), consider data with y(1)=1/2 for all θ_1, θ_2 generated by the true model f(x) defined by

$$f(x) = \frac{\sqrt{\theta_1/\theta_2}\, x + x^2}{1 + 2\sqrt{\theta_1/\theta_2}\, x + x^2} \qquad (10)$$

and let the false model g(x) be fitted where

$$g(x) = \frac{x}{\theta + x} \qquad (11)$$

and θ is chosen to minimise

$$Q = \int_0^\infty \left\{ f(x) - g(x) \right\}^2 dx. \qquad (12)$$

As figure 6 shows, a unique value of θ minimises Q and also $Q=0 \Longleftrightarrow \theta_1=\theta_2$.

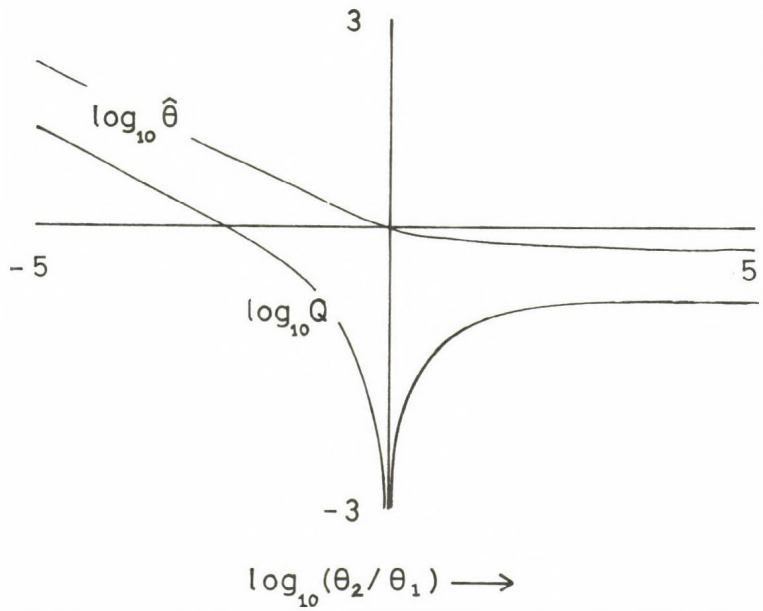

Fig. 6. Q defined by eqs.(6) and (12) with the saturation functions of eqs.(10) and (11). The $Q(\theta)$ and $\hat{\theta}(\theta)$ profiles were calculated using NAG routines C05AZF and D01AMF.

For positive cooperativity Q increases monotonically to an asymptote but Q increases without limit as the intrinsic cooperativity becomes increasingly negative. Hence the cases $\theta_2 > \theta_1$ and $\theta_2 < \theta_1$ are not symmetrical and we could say that it is easier to detect negative than positive cooperativity. This can be rationalised when it is realised that $\theta_2 > \theta_1$ generates a family of curves that rapidly approach a curve of maximum sigmoidicity whereas $\theta_1 < \theta_2$ gives a long slow approach to the asymptote $y(\infty)=1$.

The power of the F test and the distribution of the test statistic have been studied by computation using 15 logarithmically spaced points

for $y(x_1) = 0.05$, $y(x_n) = 0.95$ with 5% constant relative error. Figure 7 shows estimates of the power as a function of θ_2/θ_1 for the cases n=2,3,4 and 5.

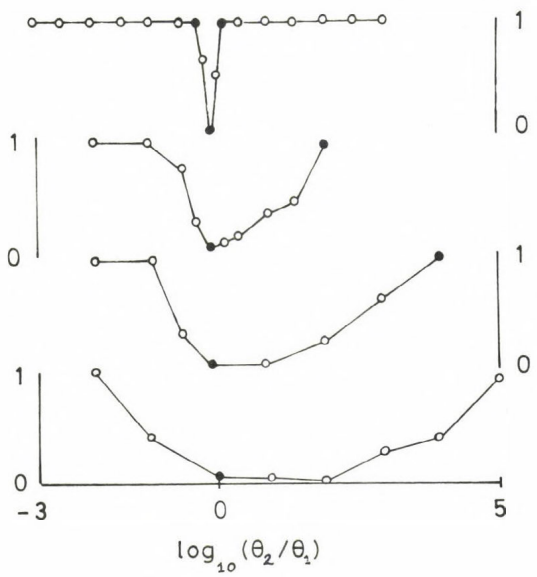

Fig. 7. Power functions for the deterministic eqs.(4) and (9). Sample size was 20 (○) or 100 (●). For the cases $n \geqslant 3$, $\theta_j = \theta_2$ for j=2,...,n. The null hypothesis, H_o: model j is correct, was rejected when the test statistic F_j of eq.(5) exceeded the 95% point of the appropriate F statistic. From the top downwards the true models were n=2, n=3, n=4, then n=5.

These figures show that n=2 is almost an ideal power curve. The cases n=3,4 show how the cusp widens with increasing numbers of parameters and for n=5 the cusp has become very wide and asymmetrical. Hence the second order term can be easily identified, third and fourth order terms are increasingly difficult to identify and fifth order terms can only be detected when the parameter values are very widely separated.

Estimates for the distribution of the test statistic are to be found in table 1 for values of the parameters θ_i on the edges of the cusps in the power functions. When f_j is the correct model it often happens that

TABLE 1. Distribution of F test statistics for saturation functions.

Order of true model	D	P(>D)	C	P(>C)	S(95)	F(95)	S(99)	F(99)
1	.07	.67	13	.16	3.64	4.67	8.82	9.07
2(a)	.12	.09	9	.44	3.93	4.75	9.40	9.33
2(b)	.15	.03	11	.26	4.98	4.75	9.76	9.33
3	.17	.01	21	.01	4.16	4.84	7.83	9.65
4	.51	.00	204	.00	2.33	4.96	8.63	10.00

H_o: probability integral transform is uniform on (0,1)

Sample size = 100

D - Kolmogorov Smirnov statistic
P(>D) - probability of exceeding D
C - Chisquared statistic
P(>C) - probability of exceeding C
S(95), S(99) - average of boundary points for 95% and 99% class intervals
F(95), F(99) - F statistics for the appropriate degrees of freedom

Parameters: 1 , $\theta_1 = 1.0$

2(a), $\theta_1 = 0.5$, $\theta_2 = .28$

2(b), $\theta_1 = 0.5$, $\theta_2 = .89$

3 , $\theta_1 = 0.33$, $\theta_2 = \theta_3 = 3.33$

4 , $\theta_1 = 0.25$, $\theta_2 = \theta_3 = \theta_4 = 2500$

Data: 15 logarithmically spaced points between $y(x_1) = 0.05$, $y(x_n) = 0.95$ with 5% constant relative error.

$Q_{j+1} > Q_j$ so in performing the probability integral transforms F_j was set equal to zero when this occurred. The chi square test and also comparison of the points separating 95% and 99% class intervals of the simulated statistics with the theoretical 95% and 99% F values showed good agreement between the test statistics and the appropriate theoretical F distribution. The Kolmogorov-Smirnov test has higher power and it showed some evidence for skewness to the lower end of the F distribution.

9. CONCLUSIONS

There are no exact small sample tests for model discrimination with non-linear models but in this paper I have argued that the F test can be used with biochemical models even though there are complications and the size is not known accurately. The F test has high power in distinguishing two exponentials from one, a second order rational function from a hyperbola and in detecting two or three binding sites. In these circumstances the test statistics behave very much like F variates.

If dense, accurate data over a wide range can be realised then the power of the F test can be sufficiently high to detect four exponentials,

a fourth order enzyme kinetic model or four binding sites. In order to detect models more complicated than these it is necessary for experimental data to be of a very high quality and for the true parameters to have extreme values, outside of the critical regions described in this paper.

REFERENCES

Bardsley, W.G. (1983) J. theor. Biol. 104, 485-491

Bardsley, W.G. & Waight, R.D. (1978) J. theor. Biol. 72, 321-372

Bardsley, W.G. & Wright, A.J. (1983) J. Mol. Biol. 165, 163-182

Bardsley, W.G. & Wood, R.M.W. (1985) Amer. Math. Monthly 92, 37-48

Bardsley, W.G., Solano-Muñoz, F., Wright, A.J. & McGinlay, P.B. (1983) J. Mol. Biol. 169, 597-617

Bardsley, W.G., McGinlay, P.B. & Wright, A.J. (1986) Biometrika, In press

Bates, D.M. & Watts, D.G. (1980) J.R. Statist. Soc. 42, 1-25

Beale, E.M.L. (1960) J.R. Statist. Soc. 22, 41-88

Box, M.J. (1971) J.R. Statist. Soc. B33, 171-201

Burguillo, F.J., Wright, A.J. & Bardsley, W.G. (1983) Biochem.J. 211, 23-34

Draper, N. & Smith, H. (1981) Applied Regression Analysis, 2nd edn. John Wiley & Sons, New York

Endrenyi, L. (1981) Kinetic Data Analysis. Design and analysis of enzyme and pharmacokinetic experiments. Plenum Press, New York

Keeping, E.S. (1962) Introduction to Statistical Inference. D. Van Nostrand Co. Inc., Princeton, New Jersey

Lindgren, B.W. (1976) Statistical Theory, 3rd edn. Macmillan Publishing Co. Inc., New York

Pettersson, G. & Pettersson, I. (1970) Acta Chem. Scand. 24, 1275-1286

Silvey, S.D. (1975) Statistical Inference. Chapman & Hall, London, New York

Wardell, J.M., Bardsley, W.G., Kavanagh, J.P. & Wood, R.M.W. (1982) J. theor. Biol. 95, 465-487

ACKNOWLEDGEMENTS

I thank A.R. Bowman for statistical advice, T.L. Freeman for help with optimisation and P.B. McGinlay for assisting me with computation.

ENDRÉNYI:

The distance measure Q integrates from 0 to infinity and, therefore, aims at discrimination over the whole sample space. Would the results be different if discrimination were restricted to a region of interest to an investigator, such as the design measure 1 which integrates from x_1 to x_2?

In the scheme of consecutive reactions, the subsequent rate constants increase in magnitude in the demonstrations shown. This means that intermediate products are depleted as soon as they are formed, and that the first reaction dominates the scheme to an extent which increases with larger ratios of consecutive rate constants. Would the results be different if the rate constants of the earlier reactions were higher and the intermediate products had opportunity to accumulate?

BARDSLEY:

You are quite correct to point this out. The range from zero to infinity was used in the integrations for analytical convenience. However, I had in mind a dedicated worker obtaining data over a time interval covering most of the span of total response. So integration over a time range spanning say 5 % to 95 % of the vertical scale of response, would give a very similar result to that obtained for the interval zero to infinity.

Actually all of the schemes that I considered were symmetrical with respect to permutation of the rate constants. I deliberately chose initial conditions and compartments sampled so that the deterministic equation, had this symmetry with respect to the interchange of rate constants. So the rate constants could not be described as either increasing or decreasing in a geometric progression.

CORNISH-BOWDEN:

In considering consecutive reactions you appeared to be assuming that you could only measure the appearance of the final product. In practice, however, spectroscopic methods are often available that allow one to observe intermediates as well. When this is true one has considerably more information available to determine the number and parameters of exponential terms. Also, in this case, monotonically decreasing rate constants will lead to more tractable results than monotonically increasing rate constants. As a separate point, I was disappointed that you dismissed half a century of development of distribution-free methods and about a decade of development of robust regression methods when you said that you need to know the error distribution in order to discriminate between models. Although model-discrimination techniques in the context of robust regression are in their infancy, I cannot agree that model discrimination is impossible without knowledge of error distribution, and I am sure that in the future these methods will improve.

BARDSLEY:

Of course it matters very much which compartments are sampled. A consecutive, reversible, first order, topologically linear scheme, $dX/dt=AX$, has real negative eigenvalues and has a matrix, A, that can usually be diagonalised. So we can then find a real invertible matrix, P, and make the transformation $Y=PX$. Then the scheme becomes $dY/dt=DX$, where D is diagonal and has the same eigenvalues as A. Now the physically observed reciprocal relaxation times are not always rate constants, but they are always the eigenvalues. I have demonstrated that sampling the last compartment in such a scheme leads to higher power in the F test as the eigenvalues come closer together i.e. the condition number of A approaches unity. However $Y=PX$ corresponds to a specific linear combination of the signals measured in all compartments.

With this particular linear combination the system is uncoupled and, by my earlier argument, the power of F test will then be high as the eigenvalues separate.
So I have drawn attention to two extreme possibilities and, in any given experiment, the power of the F test as a function of the eigenvalues will depend upon the precise combination of compartments sampled.
You have misunderstood my attitude as I didn't intend to dismiss robust methods. There are experiments involving expensive reagents, or even human subjects, where only a limited quantity of data of poor quality is available. Here robust methods come into their own. I have in mind a determined experimenter who has gone to a lot of trouble to prepare good reagents and who is prepared to measure sampling variance. If the covariance matrix of data is known with reasonable accuracy, then a likelihood ratio test will have higher power than a robust method. Of course, if the error is not normal, the L_2 norm and F test would not be appropriate and other objective functions and test statistics would be required. I only claim to have identified constraints on parameter values and limitations imposed by data quality in order for the power of the F test to be usefully low on H_o and high on H_1.
Robust tests for model discrimination in a hierarchy of models can, in any case, only be evaluated and compared with likelihood ratio tests when such methods become generally available.

EASTERBY:

I think you have proved what I suggested intuitively yesterday. Namely that when you have a sequence of exponential processes, as in a coupled enzyme system, you can only gain useful information by measuring end-product if you add all enzymes in proportion to their K_m's. Then the coefficient matrix has a single eigenvalue of multiplicity n and the equations can be normalised. Normally the equations are symmetrical with respect to transient

times and the order of enzymes in the sequence has no kinetic consequence for product formation.

BARDSLEY:

If the equations are correct then I don't see why you can only gain useful information in the singular case. Don't forget that in this singular case of coincident eigenvalues the approach to the steady state is determined by a polynomial in time multiplied by a single exponential. As time increases, the polynomial increases thus balancing the decreasing exponential and this is the reason why the relaxation time is greater than that for the single experimental term alone. I see no difference in analysis of data treatment whether the eigenvalues are coincident or not. It is true that for coincident eigenvalues the entire behaviour has only one degree of freedom in that there is only one rate constant. Nevertheless, the scheme is not topologically first order (i.e. 2 compartments) it is still topologically of order n-1 (i.e. n compartments).

SLUSE-GOFFART:

When an equilibrium-binding curve exhibits jumps (the data are supposed to be reliable and jumps reproducible), the number of inflexion points imposes a minimum degree to the Adair's equation. In such a case, a degree higher than 4 could be evidenced. This is the case for the external-oxoglutarate binding to its translocator in rat-heart mitochondria.

BARDSLEY:

The jumps to which you refer may well be highly reproducible. They may therefore contain all sorts of useful information about the mechanism. What is in doubt is whether they can be used to support a high order Adair type of model. I don't think you can use arguments based upon the number of inflexion points to achieve this aim. You may be able to convince yourself this way, but to convince

anybody else you will have to use statistical methods. The advantage of such an approach is partly that everybody will get the same answer, whereas nobody will ever agree to the number of inflexions. Another reason is that a computer fitted curve proves that the mechanism can actually fit the data. Furthermore it yields parameter estimates that can be examined in the light of chemical commonsense.

SLUSE-GOFFART:

If common sense tells us that the jumps are actual structures, we must take them into account. The particular case of the oxoglutarate translocator could be discussed after my lecture.

BARDSLEY:

Perhaps we can discuss this after your talk.

ENDRÉNYI:

Cornish-Bowden and Koshland in a paper published in Biochemistry around 1970, inserted a footnote. This considered a set of binding experiments in which the binding curve showed a masked depression around the binding of the second out of 4 ligands.

The authors noted that if an F-test analyzing the entire binding curve was performed, the models with and without the depression in the binding curve could not be distinguished. Therefore the question was raised whether discrimination should be applied to the whole experiment or only within the experimental region of interest? Intuition would suggest the latter. However, formal procedures are not available for deciding this question.

CORNISH-BOWDEN:

Dr. Endrényi is referring to a paper in which Dan Koshland and I were examining a paper of Anderson and Weber in which they claimed to have observed a highly "kinked" sat-

uration curve in fluorescence measurements for lactate dehydrogenase (Cornish-Bowden, A. and Koshland, D.E.jr., 1970. J. Biol. Chem. 245, 6241-6250; Anderson, S.R. and Weber, G. 1965. Biochemistry, 4, 1948-1957). We applied an F test to the entire curve that appeared to show that the kinked line drawn by Anderson and Weber did not fit significantly better than a smooth curve obeying a 4th degree Adair equation. However, after receiving Weber's comments on a preliminary draft of our paper, we included a footnote conceding that an F test applied to the entire curve might be misleading and that one really ought to examine the significance of the kinked region of the curve in isolation from the rest of the data. For the record, I should add that our actual calculation of the F value was incorrect, though this does not affect the general point in relation to today's discussion.

Dynamics of Biochemical Systems
S. Damjanovich, T. Keleti, L. Trón (Eds)

DESIGN AND ANALYSIS OF ENZYME KINETIC EXPERIMENTS EFFICIENCY AND ROBUSTNESS OF THE PARAMETERS

B. BEZEAU*, M.J. CLEMENTS*, A. CORNISH-BOWDEN#,
L. ENDRENYI* and J. WANG*

*Department of Pharmacology, University of Toronto,
Toronto, Ontario, M5S 1A8, Canada and
#Department of Biochemistry, University of Birmingham,
P.O. Box 363, Birmingham B15 277, England

PARAMETER ESTIMATION BY UNWEIGHTED AND WEIGHTED LEAST SQUARES

Parameters of kinetic models are frequently evaluated by nonlinear regression, a procedure based on the principle of least squares. This aims at selecting those model parameters which minimize the sum of squares (SS), the sum of the squared differences between the observed responses (reaction velocities) and those predicted by the model.

The approach has a variety of theoretical and practical advantages [1-4]. With asymptotically large numbers of observations, the calculated parameters are accurate and precise or, in statistical parlance, unbiased and efficient. This means that the errors of evaluating the parameters average to zero, and therefore that the estimated parameters average to their true but actually unknown value; also, that their variation (expressed by their variance or standard deviation) is as small as possible. Furthermore, asymptotically, the calculated parameters follow the normal distribution.

These favourable properties are preserved to a large extent at moderate sample sizes. However, they imply that the assumptions behind the least-squares approach are fulfilled. These include the belief that the model being considered is in fact correct, that the errors of the observations are additive to the true prediction of the model, that the predictor, independent variables have no error, that the errors are independent, and that all observations have the same distribution and, in particular, the same variability.

If, for instance, the latter assumption for the constancy of variance is not satisfied then the least-squares criterion should be modified. The parameters are chosen to minimize the weighted sum of squares (WSS) in which the squared difference between each observed and model-predicted response is multiplied by a weight. The weight should be proportional to the reciprocal of the variance of the observation. This means, sensibly, that higher weight is assigned to a precise reading (having a small variance), and lower weight is given to an imprecise one.

UNCERTAIN WEIGHTS: THE NEED FOR ROBUST PROCEDURES

The application of weights implies (even when no weights are used in SS) that the variances of the observations are known, at least in comparison with each other. This is true only very infrequently. Usually, such information is either completely absent or is simply quite vague and uncertain. As a result, the weights applied in the calculations, and their relationship, may not be correct.

However, when an inappropriate weighting scheme is used, the estimated parameters can easily lose their favourable properties. They could be biased and their variances can become substantially inflated. Examples of this will be seen later.

Thus, the uncertainties about the behaviour of the variances (the variance model) can have distressing consequences on the calculated parameters. Therefore, it is desirable to consider estimating procedures which are insensitive to the different, possible assumptions about the variances. Two such robust methods will be discussed. The first of these will evaluate the weights from the observations themselves and from the last updated prediction of the model. These calculations will be repeated at each update (or iteration). The second approach will be nonparametric and will not rely on the assumption of a distribution for the errors. In addition to these procedures being robust, they satisfy also a second requirement: they yield parameters quite precisely, i.e. efficiently.

These considerations apply when experiments are designed with the goal of estimating parameters as precisely as possible. The favourable designs also vary sensitively with the assumed behaviour of the variances. Therefore, robust approaches will be considered also for experimental designs. Again, the resulting sampling schemes will yield not only robust parameters but also quite efficient ones, i.e., values with high, close-to-optimal precision.

HILL EQUATION

The robust approaches for the design and analysis of experiments will be illustrated on the example of the Hill equation:

$$v = \frac{Vc^h}{K^h + c^h}$$

Here, v is the response, the reaction velocity in enzymology, measured at various concentrations, c. The purpose of the supposed experimental studies is the evaluation of the 3 model parameters. They are the maximal response (maximal velocity, V), the concentration yielding half of the maximal response (a Michaelis-type constant, K), and the Hill coefficient (h) which determines the steepness of the response curve and can characterize the cooperativity of an enzyme system [5,6].

Essentially, the Hill equation provides an empirical description of the dependence of a response (in our case, the reaction velocity) on concentration. The empirical relationship characterizes a variety of systems, such as the effect of drug doses or concentrations on graded or quantal response [7,9]. The logistic function, favoured by statisticians, is also equivalent to the Hill equation [10,11].

LEAST-SQUARES ESTIMATION OF PARAMETERS

Simple Least Squares

The principles of the method of least squares were described earlier. Now they will be formally presented.

A true, error-free response (y°) depends on the form of the model being considered (f), the value of its controlling, independent variable (x), and the magnitudes of its p parameters (P_1, P_2, ..., P_p):

$$y^\circ = f(x, P_1, P_2, \ldots, P_p) \quad .$$

In the case of the Hill equation, the response is the reaction velocity, the independent variable is concentration, and the 3 parameters to be evaluated are V, K, and h:

$$v^\circ = f(c, V, K, h) \quad ,$$

where f has the form of the equation given above.

The measured responses (y) contain an experimental error (ε) in addition to the true response:

$$y = y^\circ + \varepsilon \quad .$$

Consequently, the error is the difference between the observed and true

responses:

$$\varepsilon = y - y^{\circ} \quad .$$

The true response is not known. It is best estimated from its value predicted by the model (y_{pred}). Consequently, the estimated error (e), is:

$$e = y - y_{pred} \quad .$$

The errors of the observations are generally minimized if the parameters of the model are chosen to yield such predicted responses (y_{pred}) which result in the least sum of the squared errors:

$$SS = Min[\Sigma e^2] = Min[\Sigma(y - y_{pred})^2] \quad .$$

We shall refer to the evaluation of this least sum of squares (SS), or "least squares", by iterative calculations as the simple least-squares (LS) analysis. It assumes that the variances (σ^2) of all errors, ε, are the same.

Weighted Least Squares

If the variances of the various errors, and the corresponding observations, are different, then weights should be used in order to compensate for this divergence. As already noted, the weights (w) should be proportional to the reciprocals of the error variances:

$$w \propto 1/\sigma^2 \quad .$$

The squared errors to be minimized should be multiplied by these weights:

$$WSS = Min[\Sigma we^2] = Min[\Sigma w(y - y_{pred})^2] \quad .$$

The weighted sum of squares (WSS) is computed by the iterative weighted least-squares (WLS) procedure. As a limiting case for the behaviour of errors, the condition of constant relative (or percentage) error:

$$\sigma/y^{\circ} = \text{constant} \quad ,$$

will be considered. Replacing again the true response by its value predicted by the model, the weights applied by WLS are:

$$w = 1/y_{pred}^2$$

(taking unity as the proportionality constant).

We shall now discuss approaches which do not require that the relationship between variance and response, i.e. the error behaviour, be known.

ROBUST ESTIMATION 1: METHOD OF VARIANCE RATIO (SIGMA RATIO)

Variance Model and Its Evaluation

The variance conditions of constant errors or relative errors can be thought of as limiting cases of a more generally prevalent error behaviour:

$$\sigma^2 = \sigma_0^2 + \sigma_2^2 y^{\circ 2} \quad .$$

Of the two components of variance, the first dominates at low levels of the response (such as the constant, background error or white noise observed in many systems of measurement). At high levels of the response, the second component of the variance dominates and constant relative (or percentage) errors are observed.

A procedure will be described which evaluates the two components of variance from the observations. This will enable the direct calculation and application of the appropriate weighting scheme.

If observations are obtained and a preliminary least-squares analysis is performed then the true response is estimated again by its value predicted by the model, and the variance of the error by the square of the estimated error. Consequently, approximately:

$$e^2 = s_0^2 + s_2^2 y_{pred}^2 \quad .$$

(Here s_0^2 and s_2^2 refer to estimated values of σ_0^2 and σ_2^2, respectively.) Therefore, in a plot contrasting e^2 with y_{pred}^2 a straight-line relationship should be obtained with a slope of s_2^2 and intercept of s_0^2. The slope and the intercept can be actually calculated from just two points. The computations can be repeated for all combinations of point-pairs, and a value of s_2^2 and s_0^2 calculated for each. Finally, overall estimates of s_2^2 and s_0^2, such as their medians, can be obtained.

In practice, it is not necessary to evaluate separately s_2^2 and s_0^2. We are essentially interested in the relative contributions of the two components of variance since they unambiguously determine the relative weights of the various observations. Therefore, it is sufficient to estimate σ_0/σ_2 (the "sigma ratio") from pairs of points, and take the median of these values. The following weights can then be used, in the next calculation of the weighted sum of squares, for the observations:

$$w = \frac{(s_0^2/s_2^2) + \bar{y}_{pred}^2}{(s_0^2/s_2^2) + y_{pred}^2} \quad .$$

(Here the numerator is included only to yield a reasonable order of magnitude for w.)

With these weights, the parameters can be modified in order to obtain a reduction of the weighted sum of squares. New predictions by the model are obtained, these yield new error estimates (residuals, e), the sigma ratio is estimated again, and new relative weights are calculated. This process is continued until all of its components, especially WSS, remain unchanged between consecutive updates (iterations).

The method of variance ratio, and its robustness, has been demonstrated for linearizable enzyme kinetic models [12-14] and for exponential functions [15]. It is a procedure which can be applied generally for linear and nonlinear models. We shall illustrate its features on the example of the Hill equation. The method can be combined with protective weighting procedures against the possible presence of unusual, outlying observations. We shall not consider this aspect which has been dealt with elsewhere, in particular in a report in this volume [14].

Illustration of the Robust Method: Hill Equation

1000 computer-simulated experiments were performed by assuming the following conditions. The parameters of V = 1 and K = 1 were chosen arbitrarily but maintaining generality since v and c could be expressed in terms of V and K, respectively. h = 2 was assumed. 6 observations were arranged with concentrations between the limits of c/K = 0.143 and 2.0 (corresponding to the relative velocities of v/V = 0.02 and 0.80) in geometrically increasing progression. The measurement errors were taken to be normally distributed around the true velocities with a mean of zero and a standard deviation which was, at it limits, $\sigma_0 = 0.05$ (with $\sigma_2 = 0$) and $\sigma_2 = 0.10$ (with $\sigma_0 = 0$) for constant and relative errors, respectively. Between these limits, σ_0/σ_2 was varied again in geometric progression in such a way that the variance of an observation at v/V = 0.50 (at half-maximum) would remain the same.

Results of the simulations are shown in Fig. 1 for the precision and accuracy of parameter K. The other two parameters had similar properties. Fig. 1B illustrates a nonparametric measure of the variation among the 1000 K-values calculated by each of three weighting schemes (in addition to a reference scheme). The 1000 values were ordered in each case by magnitude and the difference between the 750th and 250th value was recorded, the so-called inter-quartile interval (IQ or "hinge" [16]). This was related to the IQ obtained by the reference weighting scheme

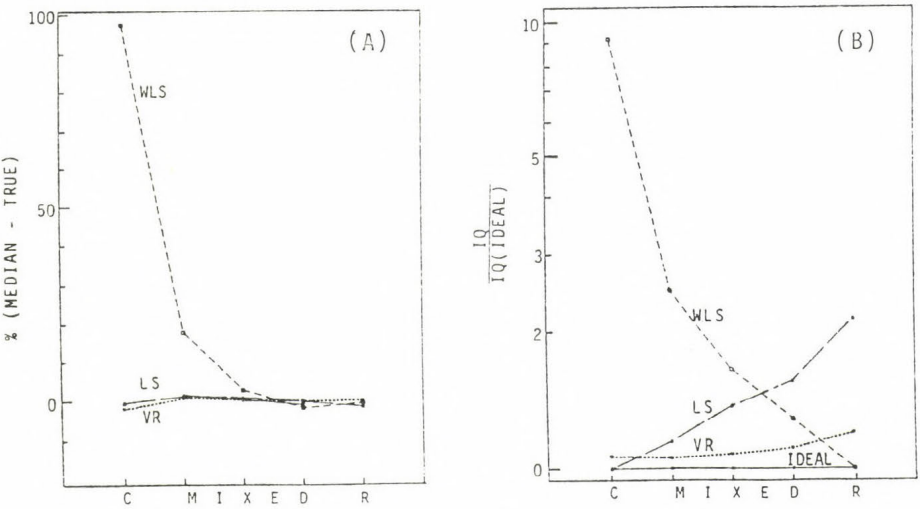

Figure 1. Effect of the error behaviour on the precision and accuracy of parameters estimated by the method of variance ratio.

For comparison, properties of parameters calculated by 3 other methods in 1000 computer-simulated experiments are also shown. (See text for conditions of the simulations.) The illustrations refer to parameter K of the Hill equation.

The error behaviour varies from constant (C) to relative (R) errors with 3 intermediate, mixed conditions in-between. The 4 estimating methods are: LS - unweighted least squares (assuming constant variance), WLS - weighted least squares (with weights assuming constant relative errors), VR - method of variance ratio (error behaviour and weighting scheme evaluated from the observations), IDEAL - ideally-weighted least squares (with weighting schemes corresponding to the true, and supposedly known error behaviour; the condition is useful for simulations but not realistic in practice).

(A) Bias of the estimated parameters. The nonparametric median (m) is calculated, and the percentage bias is evaluated by comparison with the true parameter value (P°): $100(m - P°)/P°$. An accurate parameter has zero bias. (B) Precision of the estimated parameters. The nonparametric measure of the interquartile interval (IQ) of the 1000 estimated parameters is shown in a logarithmic scale. The "Ideal" method is used as a reference and, therefore, its IQ is always 1. For the other methods, a relative IQ close to 1 indicates high estimating precision.

LS is the appropriate method when the variance is constant, WLS is ideal with constant relative errors. When the error properties are removed from these favourable conditions then the variability of the estimated parameters increases and, in some cases, so does their bias. In contrast, parameters calculated by the method of VR show, under all error conditions, high precision and accuracy.

which applied weights corresponding to the true sigma ratio, i.e. implied that the sigma ratio was known. Thus, the IQ ratio for this "Ideal" procedure is always 1.

With constant errors (on the left of the diagram) the unweighted LS is the ideal method of analysis. However, as the sigma ratio shifts towards relative error (on the right), the comparative performance of LS deteriorates and yields a much higher than ideal variability of the estimated parameter. Conversely, WLS with weights corresponding to constant relative error is the ideal method for this error behaviour (on the right). The performance of WLS becomes very much poorer as the error conditions shift towards constant variance.

Throughout the range of error conditions the method of variance ratio yields almost as favourable results as the ideal, but usually unknown, weighting scheme. At the same time, the parameters calculated by the variance ratio procedure are vastly superior to those obtained from least squares using incorrect weights. Thus the VR method is robust against the uncertainty of error behaviour and efficient in comparison with the ideal analysis.

VR performs satisfactorily also when the bias of the parameters is considered (Fig. 1A). In contrast, WLS can yield strongly biased parameters when applied with the incorrect error assumption.

ROBUST ESTIMATION 2: NONPARAMETRIC ANALYSIS

Nonparametric Evaluation of the Hill Parameters

It has been known for over a decade that nonparametric procedures can be usefully applied to the analysis of enzyme kinetic data. The method of the Direct Linear Plot (DLP) was proposed for the evaluation of Michaelis-Menten parameters [17-19]. The estimated parameters of the rectangular hyperbola were demonstrated to be robust against incorrect error assumptions and remarkably efficient with respect to the correctly weighted least-squares analysis [18,20].

The procedure expresses the 2 model parameters by 2 data points and essentially solves 2 equations with 2 unknowns. This is repeated with different pairs of data points and, in each case, the 2 parameters are evaluated. Finally, a single estimate of each parameter is obtained from their numerous values calculated pairwise, for example by taking their medians.

We shall illustrate features of nonparametric estimation on the

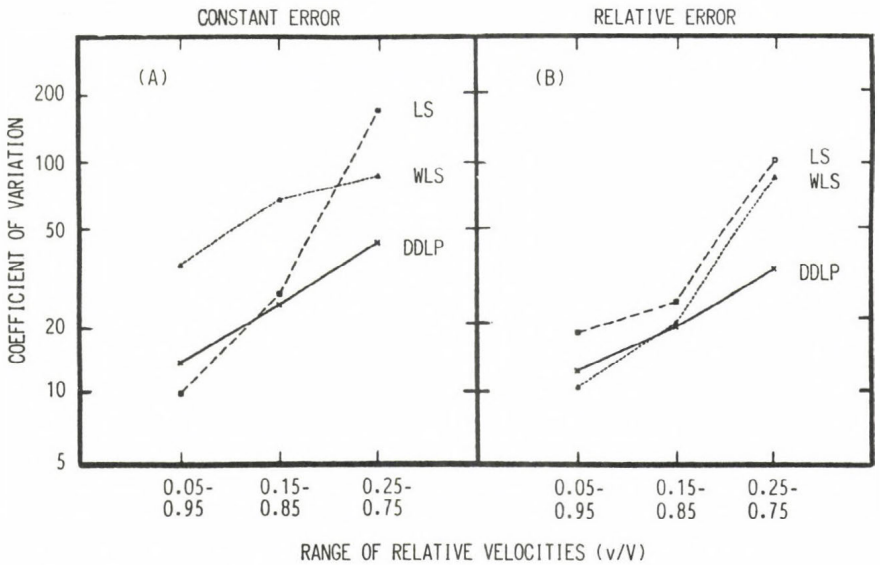

FIGURE 2. Precision of the Hill parameter K evaluated by the nonparametric method of DDLP (Direct Double-Linear Plot).

Coefficients of variation of parameters estimated under various conditions in 100 simulated experiments are shown. The diagrams illustrate the effect of 3 experimental designs (indicated in terms of the range of relative velocities) and 2 limiting error behaviours (Fig. 2A: constant variance, σ = 0.02V, Fig. 2B: constant relative errors, σ = 0.04v). For comparison, the precisions of the parameters calculated by unweighted and weighted least squares are also shown. (These methods are appropriate when the limiting error conditions actually prevail.)

The parameters estimated by DDLP are, under favourable conditions (e.g., with wide range of designs), almost as precise as those yielded by least squares applying the correct weighting scheme. Under unfavourable experimental conditions, the precision of the DDLP parameters in fact exceeds that of the least-squares values even when correct weights are used. The DDLP parameters are always much more precise than the least-squares values based on the inappropriate weighting scheme.

example of the Hill equation. If the ratio of consecutive concentrations is constant (i.e., if the concentrations are spaced logarithmically, or in geometric progression) then the two corresponding, consecutive responses, characterized by the Hill equation, are related according to a rectangular hyperbola [21]. Consequently, from 4 observations (pairs of pairs), the 3 parameters of the Hill equation (V, K, and h) can be evaluated [22]. The calculation can be repeated and the 3 parameters calculated for various selections of 4 readings. Finally, overall estimates of the parameters can be obtained from the medians of their separately calculated values.

Evaluation of the Method of the Direct Double-Linear Plot

Figure 2 illustrates some of the results obtained by the nonparametric procedure. Since it utilizes the principles of the DLP method, and since it doubles-up the required pairs of observations, we shall refer to the approach as that of the Direct Double-Linear Plot (DDLP). In 100 computer-simulated experiments, 6 observations were arranged in geometric progression between concentration limits which yielded the 3 ranges of relative velocities shown in the diagrams. True h = 1 was used in these simulations. The experimental errors were assumed to be normally distributed with means of zero and standard deviations of either $\sigma = 0.02V$ when constant variance was simulated or $\sigma = 0.04v$ for constant relative errors.

Figure 2 shows coefficients of variation (standard deviations expressed as percentages of the true parameter values) of the 100 K-parameters estimated by 3 procedures: unweighted and weighted least squares (LS and WLS assuming constant and relative errors, respectively), and the nonparametric DDLP procedure. Similar results were obtained under various simulated experimental conditions and for the other parameters of the Hill equation. It should be noted that the accuracies of the parameters were similar when calculated by the 3 methods.

The precisions of the parameters calculated by DDLP are not much lower, and in some cases even substantially higher, than those yielded by the ideal weighting scheme for the true error behaviour: LS for constant variances (Fig. 2A) and WLS with constant relative errors (Fig. 2B). The parameters computed by DDLP are consistently and substantially more precise than the corresponding values estimated by the inappropriate weighting procedure (WLS in Fig. 2A and LS in Fig. 2B).

Consequently, the parameters calculated by the method of DDLP are robust with respect to the uncertainty of the error behaviour. They are also quite efficient since their precision is close to the approximately optimal precision when the error features are known. As seen above, the variability of the DDLP parameters is much lower than that yielded by an incorrectly guessed weighting scheme.

Evaluation of the Hill parameters by DDLP is particularly effective and robust under unfavourable experimental conditions. For example, Figure 2 illustrates that with a restricted experimental design the parameters estimated by DDLP show particularly small variation (high precision) in comparison with the least-squares values, regardless of whether these are obtained by applying correct or incorrect weights. The

comparative robustness of the DDLP parameters is also seen when, in the simulations, the observational error is increased.

OPTIMAL AND ROBUST DESIGN OF EXPERIMENTS

Optimal Design of Kinetic Experiments

Before discussing robust approaches to parameter estimation, we considered the method of least squares. It was seen to yield parameters which had favourable properties provided that the assumptions of the method were satisfied. We were especially concerned with the proposition that the scheme of weights applied in the calculation of WLS should correspond to the behaviour of the error variances. Robust procedures were necessitated by the belief that these error features are, in practice, often not known.

In a similar manner, we shall initially consider methods for developing experimental designs which are based on the principle of least squares. They share its favourable properties but also rely on its assumptions. Following this, approaches to experimental design will be discussed which are insensitive to the behaviour of the experimental error. The procedures will be illustrated again on the example of the Hill equation.

Optimally effective experimental designs minimize one of the features of the variance-covariance matrix (V) for the parameters or of a quantity related to this [23-25]. The measures include minimizing the determinant of the matrix (D-optimization) which aims at designs yielding the smallest standard errors (highest precision) of all parameters and their smallest correlations. In the first-order approximation, the design criterion minimizes the (hyper)volume of the joint confidence region of the parameters. When an investigator wishes to reduce only the standard errors of the parameters (but not their correlations), (s)he would minimize only the trace of the matrix V which involves only its diagonal elements (A-optimization). If, on the other hand, protection is sought against the presence of redundant parameters then one might wish to establish designs maximizing the smallest eigenvalue of V (E-optimization). At other times, the smallest errors for predicting the responses would be evaluated (G-optimization).

Thus, the goals of the investigator determine the criterion to be applied for designing efficient experiments. In recent years, the criterion of D-optimization was used in order to explore designs of

biological experiments. These included investigations in enzyme [27-30], tracer [31-33], and pharmacokinetics [30,34-36].

The D-optimal design is often favoured because of an additional useful property: it yields comparatively simple sampling schemes which can be interpreted easily. The number of optimal design points generally equals the number of model parameters, and the points are replicated (nearly) equally. The designs are independent of transformations of the variables or parameters. All these features are not shared by the other design criteria for parameter estimation.

Optimal and Robust Designs for the Hill Equation

In the case of the Hill equation, the optimally efficient designs involve 3 repeating sampling points [37]. One of these is always the highest attainable concentration ($c_1 \to \infty$) yielding the largest possible velocity ($v_1 \to V$). This is necessary for the evaluation of a precise asymptotic velocity, V.

The other two design points depend on the features of the observational errors. If their variance is constant then the parameters are estimated with the highest precision if $(c_2/K)^h = 2.84$ and $(c_3/K)^h = 0.352$ yielding the relative velocities of $v_2/V = 0.740$ and $v_3/V = 0.260$, respectively [37]. If the relative errors are constant (constant percentage error and constant coefficient of variation) then two of the optimal concentrations and velocities should be as small as possible (c_2, c_3, v_2 and $v_3 \to 0$). This is reasonable since the error model assumes that the smallest velocities are observed with the lowest errors.

For intermediate error behaviour the optimally efficient experimental designs can be determined similarly [37]. As the examples given above indicate, these designs depend sensitively on the assumption about the error behaviour. This does not create a problem if the investigator knows the features of the errors. However, if these properties are not known then designs based on a possibly incorrect assumption can yield quite imprecise parameters (with low efficiency) [37].

Various strategies were proposed for dealing with the uncertainty about the error behaviour [37,38]. If the investigator wishes to provide protection against the possibility of a very low estimating efficiency then the minimum efficiency that can be calculated over the range of possible error behaviour should be maximized. However, this approach can result in fairly complicated designs [38].

In contrast, a simple strategy can be applied for the design of

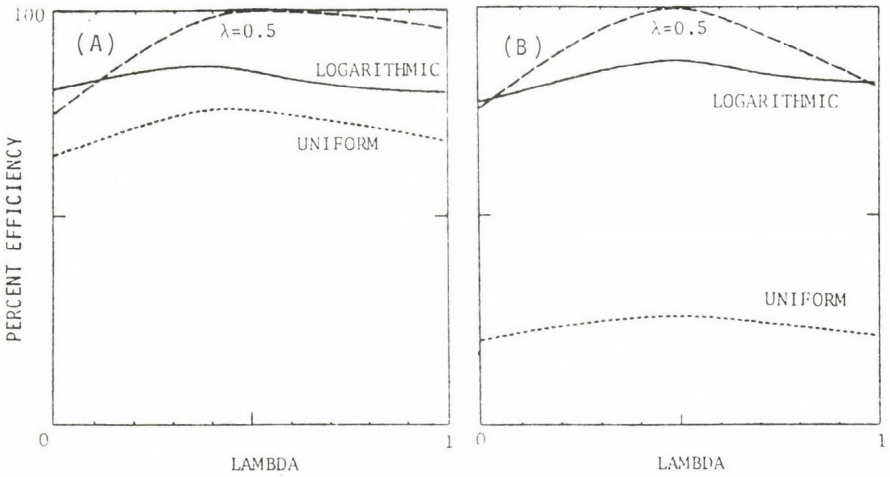

Figure 3. Effect of error behaviour on efficiency when the parameters of the Hill model are estimated from 3 different experimental designs.

The diagrams show the estimating efficiencies obtained at various true error behaviours when 6 concentrations are arranged to yield a range of relative velocities (A) between 0.05 and 0.80, and (B) between 0.05 and 0.99. The effect of 3 sampling schemes is illustrated: the concentrations are arranged within their limits (1) uniformly, (2) in geometrically increasing intervals (logarithmic spacing), and (3) in a replicating design recommended when the behaviour of the experimental error is not known (indicated by $\lambda = 0.5$). Details of this scheme are described below and in the text.

λ (lambda) is a measure of the error behaviour: $\lambda = 0$ indicates constant variance, $\lambda = 1$ corresponds to constant relative errors. The estimating efficiency is reciprocally proportional to the number of observations which are needed to achieve a given magnitude of the parameter errors. (A measure for these errors is now the determinant of the variance-covariance matrix for the parameters.) The efficiencies at each λ are referenced by the optimally attainable measure of parameter errors. For instance, the design optimal at true errors indicated by $\lambda = 0.5$ yields 100% estimating efficiency when the behaviour of the errors actually corresponds to $\lambda = 0.5$. At other actual error behaviours, the efficiency is lower.

The design optimal at $\lambda = 0.5$ is recommended when features of the measurement errors are not known. The design has 3 optimal sampling points which are to be replicated evenly: $c_1 \rightarrow \infty$, $c_2 = 1.38^{1/h}$ K and $c_3 = 0.094^{1/h}$ K. The resulting relative velocities are v/V = 1.0, 0.58, and 0.086.

The recommended design is seen to yield generally higher estimating efficiency than the customarily used schemes. Still, geometrical (logarithmical) spacing of the concentrations usually results in quite precise parameters. In contrast, uniformly distanced concentrations yield imprecise parameters.

experiments when the average estimating efficiency is maximized within the uncertain region of error behaviours. In this case, the most favourable design is very similar to the optimal scheme which is calculated by assuming that the variance (and not the standard deviation) of the observations is proportional to the true response. This parallelism holds for the Hill equation [37] as well as for other models [38].

As a result, the following design is recommended for the Hill equation when the error behaviour is not known: in addition to the highest possible concentration (as before, $c_1 \to \infty$), the other two, repeating sampling points are $(c_2/K)^h = 1.38$ and $(c_3/K)^h = 0.094$, yielding the relative velocities of $v_2/V = 0.581$ and $v_3/V = 0.086$, respectively.

Figure 3 compares the estimating efficiencies obtained by the recommended design with those provided by customarily applied sampling schemes. λ is a measure of the error behaviour; a value of 0 indicates constant errors, a value of 1 corresponds to constant relative errors.

Figure 3 illustrates that the precision of parameters obtained by the recommended design compares favourably with that yielded by the frequently applied sampling schemes containing the same number of observations. The calculated parameters are particularly imprecise when the concentrations are spaced uniformly.

CONCLUSIONS

1. Parameters of kinetic models can be evaluated precisely and efficiently (i.e., with small error and comparatively little effort) by applying the method of least squares, provided that its assumptions are satisfied. For instance, it is essential for the effective design and analysis of kinetic experiments that the behaviour of the observational errors (their relationship to the magnitude of the response) be known.

2. If the error behaviour is not known then it is advisable that robust approaches be followed for the design and evaluation of experiments. These procedures should yield parameters which are not sensitive to the various possible error features and are, at the same time, quite precise, even though not optimally so.

3. 2 procedures are illustrated for the robust estimation of the parameters of the Hill equation. The method of Variance Ratio evaluates, not only the model parameters, but also the error behaviour and the consequent weighting scheme. The method of Direct Double-Linear Plot provides a nonparametric approach for the calculation of Hill parameters.

Computer-simulated experiments demonstrate that both methods

yield robust and efficiently estimated parameters. The precisions of these parameters is close to those yielded by the correctly weighted least-squares calculations. On the other hand, the parameters evaluated by the robust procedures are very substantially more precise than those obtained from least squares when it is incorrectly weighted. The accuracies of the parameters estimated by the various methods are similar.

4. Experiments can be designed for the evaluation of precise parameters again when the error behaviour is known. If this is not the case then the average estimating efficiency can be maximized within the range of plausible error features. The resulting designs compare favourably with frequently applied schemes.

ACKNOWLEDGEMENTS

The support of these investigations by the Medical Research Council of Canada, the Banting Research Foundation, and NATO is gratefully acknowledged.

REFERENCES

1. Jennrich, R.I. (1969) Ann. Math. Statist. 40, 633-643.
2. Malinvaud, E. (1970) Ann. Math. Statist. 41, 956-969.
3. Bard, Y. (1974) *Nonlinear Parameter Estimation*, pp. 40-44, Academic Press, New York.
4. Jennrich, R.I. and Ralston, M.L. (1979) Ann. Rev. Biophys. Bioeng. 8, 195-238.
5. Wyman, J. Jr. (1964) Adv. Protein Chem. 19, 223-286.
6. Whitehead, E.P. (1970) Progr. Biophys. 21, 323-397.
7. Wagner, J.G. (1968) J. Theor. Biol. 20, 173-201.
8. Parker, R.B. and Waud, D.R. (1971) J. Pharmacol. Exp. Ther. 177, 1-12.
9. Holford, N.H.G. and Sheiner, L.B. (1981) CRC Crit. Rev. Bioeng. 5, 273-322.
10. Berkson, J. (1944) J. Amer. Stat. Assoc. 39, 357-365.
11. Ashton, W.D. (1972) *The Logit Transformation*, Griffin, London.
12. Cornish-Bowden, A. and Endrenyi, L. (1981) Biochem. J. 193, 1005-1008.
13. Cornish-Bowden, A. and Endrenyi, L. (1985) Biochem. J., in press.
14. Cornish-Bowden, A. and Endrenyi, L., in this volume.
15. Endrenyi, L. and Wang, J., Amer. J. Physiol., submitted for publication.

16. Tukey, J.W. (1977) *Exploratory Data Analysis*, pp. 32-39, Addison Wesley, Reading, MA.
17. Cornish-Bowden, A. and Eisenthal, R. (1974) Biochem. J. 139, 715-720.
18. Eisenthal, R. and Cornish-Bowden, A. (1974) Biochem. J. 139, 721-730.
19. Cornish-Bowden, A., Porter, W.R. and Trager, W.F. (1978) J. Theor. Biol. 74, 163-175.
20. Atkins, G.L. and Nimmo, I.A. (1975) Biochem. J. 149, 775-777.
21. Endrenyi, L., Fajszi, Cs. and Kwong,F.H.F. (1975) Eur. J. Biochem. 51, 317-328.
22. Clements. M.J. and Endrenyi, L. (1985) Proc. Can. Fed. Biol. Soc. 28, 175.
23. Fedorov, V.V. (1972) *Theory of Optimal Experiments*, Academic Press, New York.
24. Box, G.E.P. and Lucas, H.L. (1959) Biometrika 46, 77-90.
25. St. John, R.C. and Draper, N.R. (1975) Technometrics 17, 15-23.
26. Steinberg, D.M. and Hunter, W.G. (1984) Technometrics 26, 71-97.
27. Kanyár, B. (1978) Acta Biochim. Biophys. Acad. Sci. Hung. 13, 153-160.
28. Duggleby, R.G. (1979) J. Theor. Biol. 81, 671-684.
29. Endrenyi, L. and Chan, F.Y. (1981) J. Theor. Biol. 90, 241-263.
30. Endrenyi, L. (1981) In *Kinetic Data Analysis: Design and Analysis of Enzyme and Pharmacokinetic Experiments* (L. Endrenyi, ed.), pp. 137-167, Plenum Press, New York.
31. DiStefano, J.J. III (1981) Amer. J. Physiol. 240, R259-R265.
32. Landaw, E.M. and DiStefano, J.J. III (1984) Amer. J. Physiol. 246, R665-R677.
33. Nathanson, M.H. and Saidel, G.M. (1985) Amer. J. Physiol. 248, R378-R386.
34. D'Argenio, D.Z. (1981) J. Pharmacokin. Biopharm. 9, 739-755.
35. Endrenyi, L. and Dingle, B.H. (1981) In *Pharmacokinetics During Drug Development: Data Analysis and Evaluation Techniques* (G. Bozler and J.M. van Rossum, eds.), pp. 149-173.
36. Landaw, E.M. (1985) In *Variability in Drug Therapy - Description, Estimation, and Control* (M. Rowland, L.B. Sheiner and J.-L. Steiner, eds.), pp. 187-200, Raven Press, New York.
37. Bezeau, M. and Endrenyi. L., J. Theor. Biol., submitted for publication.
38. Schulz, M. and Endrenyi, L. (1983) Proc. Amer. Stat. Assoc. Comput. Sect. 177-181.

DISCUSSION

MÁTRAI:

You detailed that it is very important to know the exact value of λ, because if it is not correct the evaluated model will be misleading. How can we determine this value in the daily laboratory practice?

ENDRÉNYI:

Dr. Mannervik demonstrated in his lecture that the logarithm of the squared residuals can be plotted against the logarithm of the squared response predicted by the model. The slope evaluated in this plot equals λ.
The same plot can be applied, as Dr. Mannervik showed, if replicate observations are available. (It should be emphasized that true replicates are required for this purpose, those which are separated by all sources of variation of the experiment.) In this case the logarithm of the variance (or the standard deviation or the range) of the replicates can be plotted against the logarithm of their squared averages (or their averages or medians). The slope should again be λ.

BARDSLEY:

What do you think are the differences between using the determinant, trace or condition number etc., of the information matrix as a design criterion? Surely some sort of mean of the relative errors would be better?

I believe you have used the Jacobian exclusively to construct a linear approximation to the covariance matrix. Don't you think the Hessian matrix of the objective function would be better? Surely a second order correction is always an improvement and the Hessian matrix does have such curvature information?

ENDRÉNYI:

The various design criteria place emphasis on different aspects of the estimated variances. If the determinant of the variance-covariance matrix (V) is minimized (D-optimization) then the investigator may aim at the simultaneous optimization of the parameter variances and covariances. The criterion minimizes the (hyper)volume of the joint confidence intervals of the parameters and maximizes their posterior probabilities.

If the trace of V is minimized (A-optimization) then the standard errors of all parameters are to be reduced without any regard of their correlation. Thus, in principle, it is possible to get parameters with small standard errors but high correlations. In such a case, the estimated values of the parameters may be rather meaningless.

The investigator is more concerned with the quality of the model and of the estimated parameters if he intends to obtain a design which maximizes the smallest eigenvalue of V (E-optimization). This would ensure that the estimation would not result in a strange mixture of very good and very poor parameters.

On the other hand, it is possible that the interest of an investigator is focussed on only some, or just one, of the model parameters. In the case of the Hill equation, for example, one often wishes to evaluate the Hill coefficient with little or no interest in the other two parameters. In this case, a subset criterion of D-optimization should be utilized.

In other circumstances, an investigator may wish to minimize the error for predicting the response in a region (G-optimization).

The priorities set by the investigator should determine which one of these criteria would be used for the design of experiments. It is also possible to apply criteria in (linear) combinations. Once the investigator sets a design criterion, and provides the necessary additional information (structural model, variance model, guessed parameters), numerical optimization is generally straight-forward.

Nevertheless, the criterion of D-optimization which is considered in the manuscript, has useful advantages. In practice, perhaps the foremost among these is the observation that the criterion yields simple results. To various degrees, this is not true about the results of the other criteria which can depend on experimental conditions or the approach to the formulation of the problem. The results of D-optimization are also independent of the units of the variables and (monotonic) transformations of the parameters; again not general features of the other criteria.

It is very true that for nonlinear models, first-order statistics represent an approximation. It is also a useful question whether the approximation is satisfactory and useful?
Certainly at the minimum of the (weighted) sum of squares optimization criterion, the linear approximation holds perfectly. The farther away we move from the minimum, in terms of parameter combinations and up on the surface of (weighted) sum of squares, the cruder the approximation will become. The closeness of the approximation depends then on the height of movement on the surface (this is determined by the magnitude of the error variance) and also on the nature of the model.
A practical approach to the design and analysis of experiments involving nonlinear models would evaluate if, with a given variance level and model, tests according to the curvature measures of Bates and Watts would indicate the acceptability of the linear approximation, - or the lack of it. If the first-order approximation is not satisfactory, second-degree statistics involving Hessians should be pursued.
For the design of experiments, Hamilton and Watts will publish in a 1985 issue of Technometrics a paper which will consider the effect of second-order approximation to D-optimization. It is clearly an improvement over the linear treatment. However, it has again the disadvantage of being dependent on the magnitude of the error variance.

Therefore, it could be wise to resort to this higher approximation only when it is sufficiently merited, and apply more generally the linear approximation of D- or other optimizations.

MARKUS:

Instead of using much global design criteria as D- and A-optimality we have had cases where it was useful to minimize just single elements of the covariance matrix.

CORNISH-BOWDEN:

As Dr. Markus says, one may often need to fit a multi-parameter model even though not all of the parameters are of any interest. A familiar example occurs in the preliminary characterization of an unpurified enzyme: we may wish to obtain an estimate of K_m, but we can only get this by estimating V as well, even though the value of V is a function of the unknown enzyme concentration and may be of little interest. In such a case we need a design that maximizes the precision of K_m, not one that maximizes some index of the variance-covariance matrix as a whole.

Dynamics of Biochemical Systems
S. Damjanovich, T. Keleti, L. Trón (Eds)

ESTIMATION OF ENZYME KINETIC PARAMETERS WITHOUT PRIOR INFORMATION ABOUT WEIGHTS OR ERROR DISTRIBUTION

ATHEL CORNISH-BOWDEN* and LASZLO ENDRENYI†

*Department of Biochemistry, University of Birmingham, P. O. Box 363, Birmingham B15 2TT, England and
†Department of Pharmacology. University of Toronto, Toronto, Ontario, Canada M5S 1A8

The method of least squares is the most widely known and used for fitting theoretical equations to experimental data. It depends, however, on numerous assumptions that are often unjustified in practice, and for that reason performs much less well than its idealized properties might lead one to expect. The whole set of assumptions are well set out and discussed by Watts (1981), and here we shall consider only two of the most important reasons why least-squares calculations may be unsatisfactory: (i) the least-squares method gives poor estimates if the errors in the observations are not normally distributed and in particular it is very sensitive to isolated bad observations, or outliers; (ii) if the errors are not all drawn from the same population, i.e. they are heteroscedastic, the proper weighting function must be known and applied.

For fitting the Michaelis-Menten equation or, in principle, any other equation of two parameters, these two problems may be circumvented by avoiding the method of least squares altogether. For example, the median estimates derived from the direct linear plot (Eisenthal and Cornish-Bowden, 1974; Cornish-Bowden and Eisenthal, 1974, 1978) prove to be almost as satisfactory as least-squares estimates when the least-squares assumptions are true, and much better than least-squares estimates when the least-squares assumptions are false. Unfortunately, however, this approach cannot easily be extended to equations of three or four parameters, because the amount of computation required increases very steeply both with the number of parameters and with the number of observations. If one wishes to fit

the equations for two-substrate kinetics or inhibition, etc., one must either proceed in stages, in a computational analogue of using primary and secondary plots, or one must use a robust modification of least squares.

There has been a considerable amount of attention in the statistical literature to the development of robust regression procedures that overcome the problem of outliers. The biweight method of Mosteller and Tukey (1977) is one such procedure that gives excellent protection against outliers in studies with the Michaelis-Menten equation when the correct weighting function is used (Cornish-Bowden, 1981), and it would be optimistic of biochemists to expect to improve appreciably on this. There has, however, been almost no corresponding attention to the second of the problems noted above, possibly because professional statisticians suppose that the correct weighting function is always either known or easily determined. In reality, at least in enzyme kinetics, the correct weighting function is almost never known, and experiments to determine it are rarely carried out. Moreover, when they have been carried out (Storer et al., 1975; Siano et al., 1975; Askelöf et al., 1976; Nimmo and Mabood, 1979), they have indicated that the advice to assume that each measured rate has the same error distribution (Cleland, 1979) is normally incorrect. It appears, therefore, that in the development of methods of robust regression one should pay at least as much attention to the weighting function as to outliers.

Considerations such as these led us to propose a new method of robust regression in which the biweight method of Mosteller and Tukey (1977) is combined with a method of estimating the weighting function from information contained within the data (Cornish-Bowden and Endrenyi, 1981). Tests of this method for fitting the Michaelis-Menten equation were very promising, indicating that in this case it was as effective as the median method, but with the major advantage of being generalizable to equations of more than two parameters. In this chapter we discuss its application to the equations of steady-state enzyme kinetics, most of which can be handled by linear methods. We give particular attention to the equations for two-substrate reactions, but we have elsewhere considered inhibition equations and pH dependences, such as bell-shaped pH profiles (Cornish-Bowden and Endrenyi, 1985). In the following chapter, we consider the more

general problem of non-linear regression of equations that cannot be linearized.

METHODS

Implementation

The method of fitting enzyme kinetic equations described and tested in this chapter has been implemented as a computer program written in Fortran and suitable for use on any computer that accepts standard Fortran. Both the program and a full description of its use have been published (Cornish-Bowden, 1985), and thus only a brief indication of its capabilities is needed here. It can fit any equation of two or three variables and two, three or four parameters that becomes linear when written as an expression for the reciprocal of the dependent variable. This includes all of the equations commonly encountered in studies of steady-state enzyme kinetics except the equation for pure non-competitive inhibition (i.e. mixed inhibition with the constraint that the two inhibition constants are equal), and thirteen of these are built in to the program: these include the Michaelis-Menten equation, the common types of inhibition, two-substrate reactions, bell-shaped pH profiles, etc.; none of these need to be defined by the user, but if additional ones are required they can be defined as data.

As well as implementing the robust method described in this chapter, the program also allows the sigma ratio to be specified in the data and it allows the biweight method to be suppressed. It can, therefore, be used to obtain a conventional least-squares fit if desired, and as an alternative to the kind of intermediate weighting function embodied in Eq. (1) it allows the use of a different approach advocated by Askelöf et al. (1976).

Testing

Computations reported in this chapter were done on a Honeywell Multics computer, using a special version of the program that allows experimental data to be simulated in the computer according to various hypotheses about the error behaviour. Routines from the NAG Library were used for generating random numbers from specified distributions.

THEORY

Error variance

When the true function defining the variance of a measured quantity, such as a rate v, is unknown, it is reasonable to assume that it lies between two limiting hypotheses: (i) "simple errors", where the standard deviation is a constant, and (ii) "relative errors", where the coefficient of variation is a constant. These may be considered as limiting cases of the following equation:

$$\sigma^2(v) = \sigma_0^2 + \sigma_2^2 v_{true}^2 \qquad (1)$$

in which $\sigma^2(v)$ is the variance of v, v_{true} is the true value of v, and σ_0 and σ_2 are constants. In a real experiment all three of the quantities on the right-hand side of Eq. 1 are unknown, but fortunately it is possible to estimate σ_0/σ_2, the "sigma ratio", from the data, and this provides sufficient information to define a weighting function (Cornish-Bowden and Endrenyi, 1981). An initial fit must be obtained with arbitrary or assumed weights, but subsequently one can use this to obtain calculated rates $\hat{v}$. For any rate, one can estimate the error as $\hat{e} = (v - \hat{v})$, and regard $\hat{e}^2$ as a rough estimate of the variance. If one considers all of the observations in pairs (excluding any for which the two $\hat{v}$ values are equal), one can obtain an estimate of the sigma ratio from each pair, defined as shown in Fig. 1. Note particularly that in neither of the situations illustrated in Figs. 1a and 1c can the two points be realistically connected by a straight line, because this would imply negative variances at some positive rates. Instead, therefore, one must take these cases as indicating the most extreme values allowed, 0 (relative errors) for Fig. 1a, or $+\infty$ (simple errors) for Fig. 1c. The best estimate of the sigma ratio is taken as the median of all the individual values, including the zero and infinite values, and is used to calculate new weights w, as follows:

$$w = \frac{(\sigma_0/\sigma_2)^2 + \bar{v}^2}{(\sigma_0/\sigma^2)^2 + \hat{v}^2} \qquad (2)$$

The numerator of this expression is strictly arbitrary, as it can be given any constant value without affecting the final estimates, but if

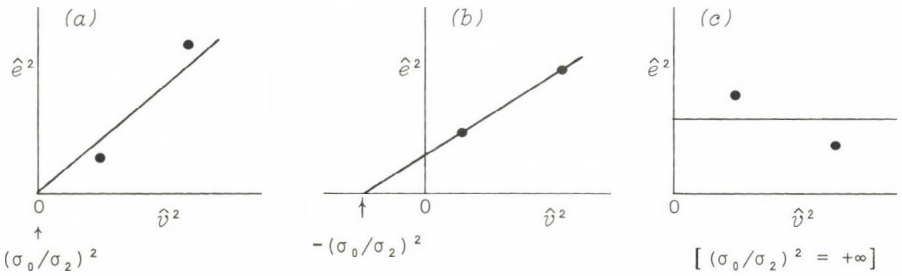

Fig. 1. Estimation of the Sigma Ratio

After a preliminary fit has been obtained, the observations are considered in pairs, with the squared estimated error plotted against the squared calculated rate. When the straight line drawn through the two points gives a negative intercept on the abscissa (Fig. 1b), the square root of the absolute value of this intercept is taken as an estimate of the sigma ratio. When the intercept is positive, the corresponding estimate of the sigma ratio is taken as zero if the slope is positive (Fig. 1a) or infinite if it is negative (Fig. 1c). The best estimate of the sigma ratio is taken as the median of the individual estimates.

$\overline{v}$ is defined as the mean of all the observed rates the resulting weights fall in a numerical convenient range. These weights can then be used to obtain improved parameter values and calculated rates, and the process can be repeated until the results are self-consistent.

Outliers

The traditional approach to handling outliers in least-squares calculations is to try to identify them and then reject them from the regression. However, unless there is independent evidence to justify rejecting a particular observation, rejection must either depend on a subjective assessment of what is a "reasonable" amount of deviation or on some predetermined and ultimately arbitrary criterion. Moreover, if one considers a parameter estimate as a function of the magnitude of one particular error, one will observe that as the error increases its effect on the parameter estimate increases correspondingly but then abrupts vanishes when the error passes the rejection level. This jerky behaviour, reminiscent of the sudden breaking of an elastic band as it is stretched, is hardly very satisfactory.

One can avoid the arbitrariness of choosing a rejection level in advance by allowing the observations themselves to define what is a

"reasonable" amount of deviation, for example by defining an outlier as an observation that deviates from the fitted equation by more than six times the median absolute deviation. This does, however, leave the problem of jerkiness, which can best be handled by smoothing out the rejection: instead of proceeding abruptly from full inclusion to full rejection in one step, one can decrease the weight of deviant observations smoothly from full weight for an observation fitting the model exactly to zero for one deviating by more than six times the median absolute deviation. This approach is implemented in the biweight (a contraction of bi-square weight) method of Mosteller and Tukey (1977). As with the estimation of the sigma ratio, one requires a preliminary fit to the data, which is obtained by giving all observations full weight, i.e. weight of unity if the sigma ratio is not used, but preferably weight w, defined by Eq. (2), using an assumed value of the sigma ratio if no better value exists. One can then define a scaled deviation u, as follows:

$$u = w^{\frac{1}{2}}(v - \hat{v})/6S \tag{3}$$

where S is the median value of $|w^{\frac{1}{2}}(v - \hat{v})|$ and the constant 6 defines the criterion for complete rejection. New weights W are now defined as follows:

$$W = \begin{cases} w(1 - u^2)^2 & \text{if } |u| < 1 \\ 0 & \text{if } |u| > 1 \end{cases} \tag{4}$$

These weights are then used to refine the calculation, which continues until the results are self-consistent. The quantitative effect of Eq. (4) is shown in Table 1.

Combining the two methods

As both the estimation of the sigma ratio and the application of the biweight method are inherently iterative in character, one might suppose that the whole computation would be very lengthy, requiring a complete set of biweight iterations between each pair of sigma-ratio iterations, or vice versa. In practice, however, we have not found

Table 1. Treatment of Outliers

The Table shows the effect of modifying the weight given to the most deviant observations by the biweight method. As discussed in the text, u represents a weighted measure of the deviation of an observation from the fitted equation, scaled such that 50% of observations give values of u less than $\frac{1}{6}$. The final weight W is calculated from Eq. (4) with $w = 1$; thus the values tabulated show the extent to which the weight of a deviant observation is decreased relative to the value calculated from the sigma ratio. Note that almost 50% of observations are assigned more than 95% of full weight.

$\|6u\|$	W
0.0	1.000
0.5	0.986
1.0	0.945
1.5	0.879
2.0	0.790
2.5	0.683
3.0	0.563
3.5	0.435
4.0	0.309
4.5	0.191
5.0	0.093
5.5	0.026
> 6.0	0.000

this to be necessary, as both sets of calculations are done simultaneously: in each iteration the same calculated rates are used both for improving the estimate of the sigma ratio and for modifying the weights according to the biweight method. The only complication that sometimes arises is that if the sigma ratio is allowed to vary between iterations without any restriction it can enter an infinite cycle of oscillation between two values. We overcome this by "damping" the oscillations: in the first iteration there is no restriction on the value, but subsequently it is not allowed to change by more than a preset limit, which is decreased in each iteration.

RESULTS

Estimation of the correct weighting function

We have tested the capacity of the proposed method for estimation of the correct weighting function by reference to the equation for a ternary-complex mechanism:

$$v = Vab/(K_{iA}K_{mB} + K_{mB}a + K_{mA}b + ab) \qquad (5)$$

in which v is the rate measured at concentrations a and b of two substrates A and B respectively, and V, K_{iA}, K_{mB} and K_{mA} are the parameters to be estimated. For purposes of simulation we take the true values of these parameters to be 100, 5, 1 and 1 respectively. Apart

Table 2: Estimation of the Sigma Ratio

Each line of the Table shows the number of times the estimated value of the sigma ratio obtained in 100 simulated experiments fell in the specified ranges, for data obeying Eq. (5) with the true parameter values specified in the text. Each experiment consisted of 25 observations obtained for all combinations of five values (0.5, 1.0, 2.0, 5.0 and 10.0) of a and b. In all cases the errors were normally distributed, but the values of the "constant" standard deviation σ_0 and the "proportional" standard deviation σ_2 were varied as indicated. In the classification of estimated values, "moderate" values of the sigma ratio are between 0.577 and 1.732 times (i.e. between $1/\sqrt{3}$ and $\sqrt{3}$ times) the mean observed rate, "low" values are below this range but non-zero, and "high" values are above this range but finite. The results shown in the first five lines (***A***) were obtained with the full robust method, whereas those in the second five lines (***B***) were obtained with the biweight facility suppressed.

	True values			Estimated values of σ_0/σ_2				
	σ_0	σ_2	σ_0/σ_2	∞	High	Moderate	Low	Zero
A	1.0	0.00	∞	56	26	12	6	0
	0.8	0.01	80	29	37	31	3	0
	0.5	0.02	25	5	12	59	21	3
	0.3	0.03	10	1	3	35	47	14
	0.0	0.05	0	0	0	13	43	44
B	1.0	0.00	∞	62	19	16	3	0
	0.8	0.01	80	34	30	33	2	1
	0.5	0.02	25	4	9	62	22	3
	0.3	0.03	10	0	2	24	59	15
	0.0	0.05	0	0	0	7	34	59

from the arbitrary value of 5 assumed for K_{iA}/K_{mA} there is no loss of generality implied by these values.

Table 2 shows the results obtained in simulated experiments when the true sigma ratio varied from infinity (simple errors) to zero (relative errors). It may be seen that the estimated sigma ratio was in either the correct range or an adjacent range in about 90% of experiments. Thus although one cannot normally hope to estimate the sigma ratio accurately one can certainly obtain an approximate value, and there is no difficulty in distinguishing the extreme cases from one another. The lower part of Table 2 shows that the sigma ratio can be estimated marginally more accurately if the biweight method is not used. However, the improvement is rather slight and one may question whether it is worth the cost of abandoning protection against outliers.

Given that we cannot expect to estimate the sigma ratio exactly from finite data sets, we need to know whether the classification into the approximate range as indicated by the results in Table 2 is ade-

Table 3. Comparison of Methods for Parameter Estimation

The Table refers to the same sets of simulated data as those of Table 2, but it shows a comparison between the values of K_{iA} obtained by fitting the data in various ways, this parameter being chosen because it is the least well-defined for the experimental design considered. The other parameters were, however, examined and showed qualitatively similar behaviour. The values tabulated are root-mean-square deviations from the true value, 5.0. The "full robust" method was as described in the Theory section; in the "variable sigma ratio" method the biweight adjustment was suppressed; in "relative least squares" the coefficient of variation was assumed to be constant; in "simple least squares" the standard deviation was assumed to be constant.

σ_0	σ_2	Full Robust	Variable Sigma Ratio	Relative Least Squares	Simple Least Squares
1.00	0.00	0.669	0.592	1.162	0.596
0.80	0.01	0.581	0.502	1.085	0.488
0.50	0.02	0.476	0.442	0.647	0.511
0.30	0.03	0.512	0.499	0.497	0.727
0.00	0.05	0.746	0.641	0.590	1.016

quate for parameter estimation. This may be judged by considering the results in Table 3, where the estimates of K_{iA} obtained by the robust method are compared with those given by least squares with an assumed weighting function, assuming either simple errors or relative errors. It may be seen that the behaviour with this more complex model is entirely consistent with what we observed previously with the Michaelis-Menten equation (Cornish-Bowden and Endrenyi, 1981): the robust method always gives parameter estimates that are almost as good as those given by the best method, and it is sometimes much better than least squares with assumed weights. When there are no outliers in the data (as here) the inclusion of the biweight method has a deleterious effect on parameter estimation, but this is not serious.

Protection against outliers

To test whether the full robust method gave the expected protection against outliers, we carried out further simulations in which outliers were introduced into the data in various proportions. In these experiments the sigma ratio was not varied but was set at 10, i.e. a low value in relation to the majority of observed rates: this accords with the reasonable view that although for large rates the coefficient

Table 4. Effect of Outliers on Parameter Estimation

Simulated experiments similar to those in Tables 2 and 3 were carried out. However, the sigma ratio was not varied; instead σ_0 and σ_2 were held constant at 0.30 and 0.03 respectively. In addition, outliers were introduced in a proportion varying from 0 to 20%, with standard deviation 5-fold higher than that of the other observations. The top line, for 0% outliers, corresponds to line 4 of Table 3, but the details differ somewhat because of sampling variation. For further explanation, see the caption to Table 3.

Percentage of Outliers	Full Robust	Variable Sigma Ratio	Relative Least Squares	Simple Least Squares
0	0.507	0.473	0.550	0.635
4	0.384	0.421	0.606	0.531
8	0.306	0.483	0.475	0.676
12	0.351	0.466	0.493	0.543
16	0.345	0.481	0.460	0.743
20	0.309	0.399	0.435	0.619

of variation may be virtually a constant one cannot expect to measure a zero rate with perfect accuracy, and so there ought to be a "baseline" effect at small rates. The inclusion of the biweight adjustment in the robust method does indeed provide protection against outliers (Table 4), and there is a marked advantage in using it even with only 4% outliers, i.e. an average of one outlier per experiment.

DISCUSSION

As the robust method discussed in this chapter is intended to fulfil a dual role, not only overcoming the usual need in least-squares calculations for prior knowledge of the weighting function, but also offering protection against outliers in the data, we need to consider these two points separately when examining its performance. In principle, and depending on what prior knowledge one has, the two features can be applied independently of one another, and the computer program based on the method (Cornish-Bowden, 1985) does allow this in practice: if one is confident that there are no outliers in the data one can suppress the biweight adjustment, and if one has independent information about the weighting function one can specify the sigma ratio, or, if preferred, the weighting exponent α favoured by Askelöf et al. (1976).

Considering the results in Table 3, one can see that adjustment of

the sigma ratio without use of the biweight method incurs virtually no cost: in the top line, it gave a slightly better result than correctly weighted least squares (simple least squares in this case), whereas in the bottom line it was only marginally inferior to correctly weighted least squares (now relative). Nonetheless, the biweight method does provide excellent protection against outliers (Table 4), and it incurs relatively little cost in precision when no outliers are in fact present (Table 3). One can conclude, therefore, that the full robust method should be the method of choice in most circumstances.

REFERENCES

Askelöf, P. Korsfeldt, M. and Mannervik, B. (1976) *Eur. J. Biochem.* **69**, 61-67

Cleland, W. W. (1979) *Methods Enzymol.* **63**, 103-138

Cornish-Bowden, A. (1985) in *Protein and Enzyme Biochemistry* (ed. Tipton, K. F.), BS115, pp. 1-22, Elsevier, Limerick

Cornish-Bowden, A. and Eisenthal, R. (1974) *Biochem. J.* **139**, 715-720

Cornish-Bowden, A. and Eisenthal, R. (1978) *Biochim. Biophys. Acta* **523**, 268-272

Cornish-Bowden, A. and Endrenyi, L. (1981) *Biochem. J.* **193**, 1005-1008

Cornish-Bowden, A. and Endrenyi, L. (1985) *Biochem. J.*, in press

Eisenthal, R. and Cornish-Bowden, A. (1974) *Biochem. J.* **139**, 721-730

Mosteller, F. and Tukey, J. W. (1977) *Data Analysis and Regression* pp. 333-379, Addison-Wesley, Reading, Massachusetts

Nimmo, I. A. and Mabood, S. F. (1979) *Anal. Biochem.* **94**, 265-269

Siano, D. B., Zyskind, J. W. and Fromm, H. J. (1975) *Arch. Biochem. Biophys.* **170**, 587-600

Storer, A. C., Darlison, M. G. and Cornish-Bowden, A. (1975) *Biochem. J.* **151**, 361-367

Watts, D. G. (1981) in *Kinetic Data Analysis: Design and Analysis of Enzyme and Pharmacokinetic Experiments* (ed. Endrenyi, L.), pp. 1-24, Plenum, New York

ENDRÉNYI:

Drs. Mannervik and Cornish-Bowden called attention in their presentation at the importance and usefulness of residual plots. These can be applied even when the data are not collected as carefully as in Dr. Mannervik's investigations and, therefore, a single residual plot can be quite scattered and yield little information.
Quite frequently, only a few observations are collected in one experiment, but then other experiments are obtained either repeating the earlier ones or by changing the experimental conditions such as the concentration of an inhibitor or modifier, the pH or temperature. In such cases it can be recommended that the residual plots drawn in all studies be spread out on a table and viewed together. Even when the information from any one of them is slight, collectively they provide a powerful indication about the correctness of the model and about the features of the errors.

MANNERVIK:

I would not like to leave the audience with the impression that we suggest that one should restrict the evaluation of error structure to the use of replicates. As I referred to in my contribution earlier, we have suggested a method to determine the error structure based on analysis of residuals obtained by regression analysis (Mannervik, B., Jakobson, I. and Warholm, M., Biochim. Biophys. Acta, 567, 43. 1979). A precondition is the availability of residuals from a good fit of the data. The rationale for the procedure being that the residuals of a precise and unbiased fit should reflect the experimental variance. Neighbouring residuals are grouped in clusters of at least 5 and the mean of their squared values is used as a measure of the local variance. These estimates are then used to formulate an empirical function expressing the error as a function

of velocity or, more accurately in our case, of substrate and inhibitor concentrations. Thus, the kinetic data set itself, rather than separate replicate measurements, is used to elucidate the error structure.

CORNISH-BOWDEN:

I don't think this requires any addition from me.

KRETSCHMER:

How can one come to the minimum in parameter space; are there reasons for a Monte Carlo (evolution) method to be applied instead of the steepest descent method? This question arises in cases of complicated model equations, perhaps with more than one "best solution".

CORNISH-BOWDEN:

In the particular context of my paper there is no difficulty, because I have been dealing solely with linearizable equations, specifically equations that are linear when written in reciprocal form. The program that I have described also has this restriction, though it is not a necessary one and there is no reason why our approach should not be extended to intrinsically non-linear models. Dr. Endrényi will show shortly that this gives excellent results. As a more complete answer to the question, I have rarely had occasion in recent years to use a general non-linear regression program, but when I have done so I have used a combination of a Nelder-Mead simplex method (Nelder, J.A. and Mead, R., Comput. J. 7, 208-313, 1965) in the early stages with a derivative-based method in the vicinity of the minimum (Wharton, C.W., Cornish-Bowden, A., Brocklehurst, K. and Crook, E.M., Biochem. J. 141, 365-381, 1974). However, I make no special claims for this approach, and I am sure that there have been advances in non-linear regression methodology during the past 15 or so years that I have not been aware of. If there is reason to believe that multiple minima exist then it is certainly

worthwile to use some form of grid search or a Monte Carlo search of the kind you refer to; in many problems this is not necessary, however, and it can greatly increase the amount of computation needed.

Dynamics of Biochemical Systems
S. Damjanovich, T. Keleti, L. Trón (Eds)

EMPIRICAL ERROR FUNCTIONS FOR MODEL DISCRIMINATION AND PARAMETER ESTIMATION IN ENZYME KINETICS

BENGT MANNERVIK and U. HELENA DANIELSON

Department of Biochemistry, Arrhenius Laboratory,
University of Stockholm, S-106 91 Stockholm, Sweden

INTRODUCTION

Rigorous kinetic analysis of enzyme systems should involve statistical methods for optimal design of experiments and proper parameter estimation. Graphical methods, although valuable adjuncts for preliminary evaluation of experimental data, have been largely replaced by regression analysis for more objective discrimination between rival mathematical models as well as for the determination of the constants in the rate equations. The refined techniques for analyzing experimental data make it possible to solve previously intractable problems that are necessary for unravelling the complexities of biochemical phenomena. For example, in steady-state enzyme kinetics it can no longer be considered adequate to restrict the analysis to the Michaelis-Menten equation and to the determination of the values of the kinetic constants V and K_m. The first problem to be addressed is the choice of the "best" model out of a set of alternatives. The second, but not independent, problem is the estimation of accurate and precise parameter values in the model selected. For both these purposes the design of the experiments should be optimized. Since the "best" model and the values of its constants are not known a priori, the optimal experimental conditions can not be defined. Therefore, a sequential procedure involving preliminary assumptions about model as well as constants is normally adopted. The results of the subsequent analysis will then serve as the basis for new and improved acquisition and treatment of data. The experimental and analytical protocol thus becomes an iterative procedure which is expec-- ed to converge towards the optimal solution. Fig. 1 depicts such a

strategy for design and analysis of enzyme kinetic experiments. Detailed accounts of procedures used in our laboratory have previously been published (Mannervik and Bártfai, 1973; Mannervik 1981, 1982). Special emphasis has been put on the fundamental problem of discrimination between alternative models and how the analysis is affected by the location and spacing of the independent variables such as substrate and inhibitor concentrations. For example, a mathematical expression, the discrimination function, has been defined, which can be used for finding the optimal experimental conditions for discrimination between two rival models (Bártfai and Mannervik, 1972). For optimal overall design, the integral or the sum of the values of the discrimination function in all experimental points should be maximized (Markus and Plesser, 1981; Mannervik, 1982).

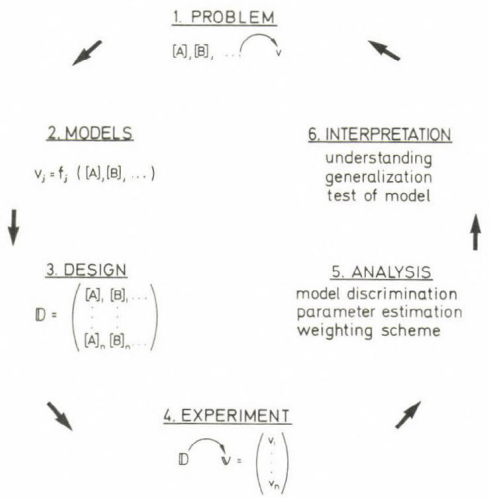

Fig. 1. Sequential strategy of design and analysis in mathematical modelling of enzyme kinetic data. The design matrix for the experiments should be optimized with proper consideration of the error structure of the experimental system as well as the primary goal of the particular experiment (model discrimination or parameter estimation). For each point, the emphasis may shift as the investigation proceeds and the cycle is repeated. (From Mannervik, 1981).

However, neither the design for model discrimination nor the design for parameter estimation, which are normally not the same, can be adequately optimized without considering the error structure of the experimental data (Endrenyi, 1981; Duggleby, 1979, 1981; Mannervik 1981, 1982). The following section will therefore address the experimental variance in some detail.

EXPERIMENTAL ERROR

In enzyme kinetics determinations of reaction rates are used for elucidating the relationships between enzymatic activity and independent variables such as substrate and inhibitor concentrations, pH, and temperature. The determinations are not error-free and it is important to know their nature and how they influence the analysis of experimental data. Traditionally, the experimental error can be divided into systematic error and random error. Most theoretical treatments tacitly assume that systematic errors, in cases where they exist, have been eliminated. In practice, however, it takes great care in the execution and evaluation of kinetic measurements in order to detect and minimize the effect of systematic deviations from the "unbiased" values. Some practical hints have been summarized by Nimmo and Atkins (1981).

The random experimental error is normally referred to as the dependent (measured) variable and is considered due to factors that cannot be controlled by the investigator. For example, fluctuations of temperature in a reaction vessel or random oscillations in the electric current fed into the instrument used to monitor the reaction may contribute to the random error. The following treatment is restricted to what would normally be regarded as random error. However, it will become evident that the error is not necessarily random with respect to the dependent variable, but may be a function of the independent variables (Mannervik 1981, 1982; Mannervik *et al.*, 1986).

In enzyme kinetics, the experimental error has generally been associated with the measured velocity. Two types of errors have been assumed, constant absolute error (*i.e.* independent of velocity) and constant relative error (*i.e.* proportional to velocity). Rigorous experimental

studies have demonstrated that different systems may display different error structures and that neither of these two types may apply. It is therefore mandatory to examine the particular system under investigation for adequate evaluation of its error properties (for references, see Mannervik, 1981, 1982).

In order to study the experimental error, the scatter in a set of measured data should be analyzed. A direct approach is to make replicate measurements ($n \geq 5$) in several experimental points. This procedure will often necessitate a separate experiment exclusively for investigating the error. This may not appear attractive in many cases and an alternative method based on the analysis of the residuals of an adequate fit of data set has been introduced (Mannervik et al., 1979). The rationale behind the latter method is that the residuals of a good fit should be unbiased and reflect only the random error.

In studies of the error structure of enzyme kinetic data, we have demonstrated that in many cases the error is best described as a function of substrate and inhibitor concentrations (Mannervik, 1981, 1982; Mannervik et al., 1986). For some experimental systems, the expression of error as a function of velocity is not only inferior but mathematically inadequate, since a particular velocity value may be generated by several combinations of, e.g., substrate and inhibitor concentrations and the different combinations may be associated with different errors in the measured velocity (Mannervik et al., 1986). In the following, an example illustrating this phenomenon will be given.

EMPIRICAL ERROR FUNCTIONS - AN EXAMPLE INVOLVING GLUTATHIONE TRANSFERASE

It has been proposed that an empirical function should be used to model the error structure (Askelöf et al., 1976). Originally, the treatment involved the variance of the velocity, but in the case that reactant concentrations are used as variables in the modelling, we have found it simpler to use the square root of the variance, i.e., the standard deviation, as the expression of error. Since in the practical applications we are restricted to the use of estimates of the standard deviations, it will be denoted by "s". Thus, the classical models of constant absolute

and constant relative error can be expressed by the following equations, respectively:

$$s = K_1 \tag{1}$$

$$s = K_1 \cdot v \tag{2}$$

where K_1 is an empirical constant, which can be estimated from experimental data, and v is the velocity measured.

In order to account for other error types a more general error function was introduced (Siano et al., 1975; Askelöf et al., 1976):

$$s = K_1 \cdot v^{K_2} \tag{3}$$

where K_2 is an additional empirical constant. (Eq. (3) was actually given in squared form since the variance of v, $Var(v) = s^2$, was considered, but the expressions are equivalent). The previous models, Eqs. (1) and (2), are contained as the special cases where $K_2 = 0$ and $K_2 = 1$, respectively.

In the search for the best error model, it was found that for many experimental systems a function of substrate and inhibitor concentration was superior to Eq. (3) (or its special cases). Originally, power functions similar to Eq. (3), but expressed in reactant concentrations, were tried (Mannervik, 1981). However, more recent studies demonstrated that in many cases an error function similar to the rate equation was a superior alternative (Mannervik et al., 1986). Thus, butyrylcholinesterase data that could be described by the rate equation (Augustinsson et al., 1974):

$$v = \frac{K_1 [A] + K_2 [A]^2}{K_3 + [A] + K_4 [A]^2} \tag{4}$$

where A is the substrate and K_i (i = 1-4) are constants, was found to have an error structure best described by Eq. (5) (Mannervik et al., 1986):

$$s = \frac{K_5[A] + K_6[A]^2}{[A] + K_7[A]^2} \qquad (5)$$

The error function (Eq. 5) lacks the constant term in the denominator, but is otherwise of the same algebraic form as the rate equation, Eq. (4). It was concluded that empirical error functions could mimic the rate equation or its degenerate forms.

A similar, but more extensive study with glutathione transferase 4-4 purified from rat liver (Ålin et al., 1985) is summarized below. Steady-state kinetic experiments involving the concentrations of a substrate (1-chloro-2,4-dinitrobenzene) and an inhibitor (indomethacin) as independent variables have been carried out. Replicate measurements (n = 5) were made for all combinations of 9 inhibitor concentrations (0-100 μM) and 6 substrate concentrations (3-1000 μM). The standard deviation, s, was calculated from the replicates in each experimental point and were analyzed by fitting alternative mathematical models to the data. In addition to Eqs. (1) - (3), several models derived from a general rate equation involving second-degree terms of both substrate and inhibitor concentrations were tested. The simplest model that still accounted for the essential traits of the nonlinear dependence of s on the independent variables was

$$s = \frac{K_1[A] + K_2[I]}{K_3 + [A] + K_4[I]} \qquad (6)$$

where I denotes the inhibitor. Table 1 shows the results of the modelling. The residual sum of squares, obtained upon fitting a model to the estimated errors, shows that Eq. (1) (constant absolute error) is inferior to the alternatives. Eq. (3) is clearly superior, as evidenced by its significantly lower residual sum of squares. It is also noteworthy that the value of K_2 in Eq. (3) is significantly lower than 1.0, which excludes the assumption of constant relative error, i.e. Eq. (2). Equation (6) gives the lowest residual sum of squares and is the best alternative even though the standard deviations of its constant are high. The

Table 1. Alternative empirical models of the error structure of kinetic data obtained with rat glutathione transferase 4-4 using the concentrations of 1-chloro-2,4-dinitrobenzene (substrate) and indomethacin (inhibitor) as independent variables. The initial velocity (v) is the dependent variable, which was measured spectrophotometrically (Ålin et al., 1985). The standard deviation, s, was estimated by replicate measurements (n = 5) at 6 substrate and 9 inhibitor concentrations. Proper units are obtained by considering that concentrations are expressed in μM and velocity in s^{-1}. SD is the asymptotic standard deviation obtained from the regression analysis.

Error model s =	Parameter values ± SD	Residual sum of squares
K_1	K_1 = 0.492 ± 0.091	23.8
$K_1 v K_2$	K_1 = 0.161 ± 0.017 K_2 = 0.484 ± 0.074	3.86
$\frac{K_1[A]+K_2[I]}{K_3+[A]+K_4[I]}$	K_1 = 16.6 ± 21.5 K_2 = 352 ± 509 K_3 = 6060 ± 9010 K_4 = 1730 ± 2340	2.60

reason why an even simpler model was not chosen is that the dependence of s on the substrate and inhibitor concentrations requires terms of each in both numerator and denominator. Lower standard deviations of the constants may be obtained by use of a larger number of experimental data.

The results of modelling the error are also illustrated by plots. Fig. 2 shows standard deviation versus velocity and the corresponding residual plot after fitting Eq. (3) to the data. The left panel appears to show a good fit of the model to the experimentally estimated values, but the right panel reveals the defect that the majority of the residuals are negative and appear in a domain at the lower left corner of the residual plot. Fig. 3. displays standard deviation versus inhibitor

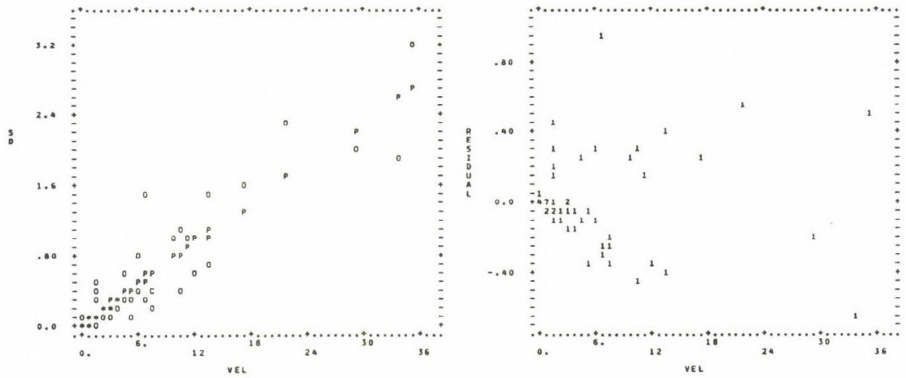

Fig. 2. Error expressed as a function of velocity (dependent experimental variable). The error was estimated by replicate measurements of the velocity of the glutathione transferase 4-4 catalyzed reaction at various combinations of substrate and inhibitor concentrations (cf. Table 1). Equation (3) was fitted to the experimental error values by nonlinear regression. The left panel shows observed (O), predicted (P) and coinciding observed and predicted values (*) plotted versus velocity. The right panel shows the corresponding residual plot; the numerals give the number of coinciding residual values at a given point.

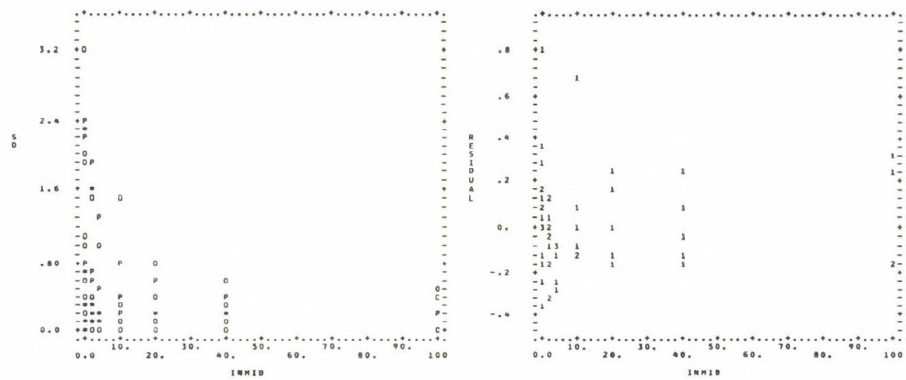

Fig. 3. Error expressed as a function of inhibitor concentration (one of the independent experimental variables). The effect of the inhibitor concentration was tested at several fixed concentrations of substrate. The data are identical to those in Fig. 1 and Table 1, but the error was fitted using Eq. (6), which is a function of substrate and inhibitor concentrations. The cluster of nonrandomly distributed residuals in Fig. 2 was not obtained (in any of a variety of residual plots) upon regression analysis according to Eq. (6).

concentration and the corresponding residual plot after regression according to Eq. (6). The nonlinear dependence on inhibitor concentration is evident (left panel) and the residuals (right panel) are distributed more randomly than for the other models. Even though the advantage of using Eq. (6) rather than Eq. (3) is not dramatic, it is still clear that it represents an improved account of the relationship between error and the experimental variables.

In order to examine the effects of different weighting factors on the estimation of the parameters in the rate equation, the results presented in Table 1 were used. The rate equation that provides the "best" representation of the data was fitted by nonlinear regression according to various weighting schemes. Table 2 shows the equation and the kinetic parameters obtained in three different cases. It is clear that the values of the constants differ significantly when the values computed under the assumption of constant absolute error are compared with the corresponding values computed by use of the alternative error structures. The differences between the values obtained in the last two cases are relatively small, but it may be noted that the ratio between the standard deviations and the parameter values for K_1, K_4 and K_8 are lower when Eq. (6) is used. The values of K_1 and K_4 are of special importance since they contribute heavily to the rate-behavior of the kinetic model. Thus, on the basis of the overall analysis of the results, we conclude that Eq. (6) is the best representation of the experimental error of the alternatives tested.

Since the improvement of using an error model based on substrate and inhibitor concentrations, rather than on velocity, was only moderate for the experimental system presented here, it is worth emphasizing that in the case of acetylcholinesterase, Eq. (3) was clearly inadequate and a model similar to the rate equation was significantly better (Mannervik *et al.*, 1986). The establishing of the best error function may be of importance for the computing of the kinetic constants, and, consequently the prediction of the rate-behavior of the system. This, in turn, will affect the optimal design of experiments both for model discrimination and for parameter estimation.

Table 2. Effect on parameter estimation of using different weighting procedures. Kinetic data for rat glutathione transferase 4-4 were analyzed by weighted nonlinear regression analysis using the rate equation

$$v = \frac{K_1[A]+K_2[A]^2+K_3[A]^2[I]}{K_4+[A]+K_5[A][I]+K_6[A][I]^2+K_7[A]^2[I]+K_8[A]^2[I]^2}$$

where v is initial velocity, A is 1-chloro-2,4-dinitrobenzene (substrate), I is indomethacin (inhibitor), and K_i (i = 1-8) the constants of the equation that should be estimated. The values of the constants are given ± the asymptotic standard deviations obtained from the regression analysis. Initial velocities were determined spectrophotometrically (Ålin et al., 1985). Proper units are obtained by considering that concentrations are expressed in μM and velocity in s^{-1}.

Parameter	Weighting factor ($w_i = s_i^{-2}$)		
	$s = 0.492$	$s = 0.158 \cdot v^{0.849}$	$s = \frac{16.6[A]+352[I]}{6060+[A]+1730[I]}$
K_1	4.306 ± 0.813	5.472 ± 0.813	5.659 ± 0.563
K_2	0.033 ± 0.001	0.031 ± 0.001	0.032 ± 0.002
K_3	0.010 ± 0.003	0.011 ± 0.003	0.017 ± 0.007
K_4	21.30 ± 8.93	34.68 ± 7.57	33.44 ± 3.93
K_5	0.114 ± 0.060	0.129 ± 0.046	0.169 ± 0.069
K_6	0.0020± 0.0018	0.0023± 0.0008	0.0033± 0.0017
K_7	0.0016± 0.0017	0.0016± 0.0002	0.0022± 0.0007
K_8	$(1.3\pm1.5)\cdot10^{-5}$	$(1.3\pm1.2)\cdot10^{-5}$	$(3.1\pm2.6)\cdot10^{-5}$

CONCLUSION

The results showing that experimental error can be adequately represented by an empirical function of substrate and inhibitor concentrations suggest that errors in the independent variables are more important than errors in the determination of the velocity. This conclusion contrasts with the general views on the nature of experimental error in enzyme kinetic experiments. The finding that the rate equation can serve as a model for the error structure raises the question about the origin of the error. In the spectrophotometric assays used in our work, in which the velocities can be determined fairly accurately, it appears as if the error arises primarily in the pipetting of reactant solutions. These errors may be transmitted via the rate equation to be expressed as a composite error in velocity. It should be noted that under general statistical assumptions, the error in velocity, s_v, can be expressed as a linear combination of the errors in substrate, s_A, and inhibitor concentrations, s_I, provided that the covariance between substrate and inhibitor concentrations is zero (which is probable):

$$s_v^2 = \left(\frac{\partial v}{\partial [A]}\right)^2 \cdot s_A^2 + \left(\frac{\partial v}{\partial [I]}\right)^2 \cdot s_I^2 \qquad (7)$$

The partial derivatives of the rate equation with respect to substrate and inhibitor concentrations may be calculated analytically (if the model is known), and it is clear that these values act as multipliers that may magnify a relatively small s_A or s_I. Therefore, as indicated by the present analysis, it is not excluded that the small error that has been estimated for substrate concentration (Askelöf et al., 1976) will contribute significantly to the error measured in velocity. This finding emphasizes even more strongly the necessity of examining the error structure for each experimental system (Mannervik, 1981, 1982).

ACKNOWLEDGEMENTS

A significant part of the analysis of error as a function of the independent variables was initiated and carried out with Drs. I. Jakobson and M. Warholm, whose work is cited in the present paper. This work was supported by the Swedish Natural Science Research Council.

REFERENCES

1. Ålin, P., Jensson, H., Guthenberg, C., Danielson, U.H., Tahir, M.K. and Mannervik, B. (1985) Anal. Biochem. 146, 313-320.
2. Askelöf, P., Korsfeldt, M. and Mannervik, B. (1976) Eur. J. Biochem. 69, 61-67.
3. Augustinsson, K.-B., Bártfai, T. and Mannervik, B. (1974) Biochem. J. 141, 825-834.
4. Bártfai, T. and Mannervik, B. (1972) FEBS Lett. 26, 252-256.
5. Duggleby, R.G. (1979) J. Theor. Biol. 81, 671-684.
6. Duggleby, R.G. (1981) In Kinetic Data Analysis. Design and Analysis of Enzyme and Pharmacokinetic Experiments (Endrenyi, L., ed.), Plenum, New York, pp. 169-179.
7. Endrenyi, L. (1981) In Kinetic Data Analysis. Design and Analysis of Enzyme and Pharmacokinetic Experiments (Endrenyi, L., ed.), Plenum New York, pp. 137-167.
8. Mannervik, B. (1981) In Kinetic Data Analysis. Design and Analysis of Enzyme and Pharmacokinetic Experiments (Endrenyi, L., ed.) Plenum New York, pp. 235-270.
9. Mannervik, B. (1982) Meth. Enzymol. 87, 370-390.
10. Mannervik, B. and Bártfai, T. (1973) Acta Biol. Med. Ger. 31, 203-215.
11. Mannervik, B., Jakobson, I. and Warholm, M. (1979) Biochim. Biophys. Acta 567, 43-48.
12. Mannervik, B., Jakobson, I. and Warholm, M. (1986) Biochem. J., in press.
13. Markus, M. and Plesser, T. (1981) In Kinetic Data Analysis. Design and Analysis of Enzyme and Pharmacokinetic Experiments (Endrenyi, L., ed.) Plenum, New York, pp. 317-339.
14. Nimmo, I.A. and Atkins, G.L. (1981) In Kinetic Data Analysis. Design and Analysis of Enzyme and Pharmacokinetic Experiments (Endrenyi, L., ed.) Plenum, New York, pp. 309-315.
15. Siano, D.B., Zyskind, J.W. and Fromm, H.J. (1975) Arch. Biochem. Biophys. 170, 587-600.

DISCUSSION

MARKUS:

I would like to remark that discrimination design, as you have described it, can be refined to yield more accurate predictions of experiments. In this refined method, which I cannot describe here in detail, the mathematical expectation of the minima of sum of squares fitting with one model and that fitting with the other model are evaluated and compared. This evaluation includes the errors and covariances of the model parameters as well as those of the measurements (V.V. Fedorov and A. Pazman, Fortschr. Physik, 24, 325-355. 1968). Using simulated biochemical experiments, we tested this method, obtaining more accurate results than by just comparing the model predictions (M. Markus and Th. Plesser, in: "Kinetic Data Analysis", 1981, Plenum Press, N.Y., pp. 317-339.). The method can be used for initial rate measurements as well as for progress curves. However, it needs considerably longer computing times than your method.

MANNERVIK:

Thank you for this clarification of how our method can be extended. We have certainly thought about the effect of the experimental error, but we have not incorporated this in our calculations.

ENDRÉNYI:

Dr. Mannervik's excellent and refined experiments are more extensive and more careful than those of most investigators. Therefore, the thoughtful evaluation of the variance relationship may not be available to most. However, it may still be possible to look at the residuals and reach conclusions about the behaviour of the errors. It may also be possible to plot the logarithm of the squared residuals against the logarithm of squares of the velocities predicted by the model. These diagrams would

show rather scattered data points but their trend and qualitative information should be similar to those given more carefully and thoughtfully by Dr. Mannervik.

MANNERVIK:

Let me first remind you that analysis of the residuals of a good fit is indeed a method that we have proposed and used in our studies. However, our attempts to base the analysis on individual residuals, using squared or absolute values, were not successful, since single values were too inaccurate as estimates of the error. Therefore, the error function had to be based on groups of residuals in order to obtain reasonable estimates of the variance. Nevertheless, inspection of plots of individual values, as you suggest, will give a qualitative picture that may be useful.

CORNISH-BOWDEN:

As Dr. Mannervik has shown us, residual plots can be very useful, and now that many experiments are analysed by computer it would hardly be an exaggeration to say that residual plots are the most important kind of plots there are. And the most important thing about them is that they must be plotted! They don't have to be drawn carefully and accurately, as a residual is almost by definition an inaccurate quantity, and they don't have to look beautiful or to be suitable for publication. It is much better to spend a few minutes drawing a residual plot roughly than to spend a week thinking about drawing one carefully and then not doing it. A good computer program should supply residual plots automatically and not rely on the zeal of user.

MANNERVIK:

I agree completely. As stressed in my lecture, examination of residuals is the most informative of the criteria we use for judging goodness-of-fit and for discrimination. The computer program we have adopted provides plots of

residuals versus the dependent and all the independent variables (such as substrate and inhibition concentrations).

MEMBRANE DYNAMICS

Dynamics of Biochemical Systems
S. Damjanovich, T. Keleti, L. Trón (Eds)

THE ROLE OF FcγRECEPTORS IN MEDIATING CONJUGATE FORMATION AND TARGET CELL LYSIS

DAVID M. SEGAL, BORIS KARPOVSKY, DAVID A. STEPHANY, PILAR PEREZ, JULIE A. TITUS and DAVID G. COVELL

Bldg. 10, Rm. 4B17, National Institutes of Health, Bethesda, MD 20205, USA

INTRODUCTION

Antibody-dependent cellular cytotoxicity (ADCC) occurs when target cells coated with IgG anti-target antibodies bind to Fc receptors (FcγR) on effector cells, leading to effector-target conjugates and subsequent target cell lysis (Moller, 1965; Lovchik and Hong, 1977). Because FcγR have been extensively characterized using either solution phase IgG (Dower et al., 1981a) or anti-FcγR monoclonal antibodies (mAb) as ligand (Unkeless et al., 1981), and because target cell lysis occurs shortly after conjugate formation and is easy to measure, ADCC can serve as a convenient prototypic system for examining the process and consequences of cell-cell interactions. In this paper we will discuss the mechanism of conjugate formation between antibody-coated target cells and cells from the $P388D_1$ mouse macrophage line. We will then show that conjugates can be formed artifically using hetero-cross linked antibodies, and examine the requirements for triggering lysis when effector:target conjugates are formed using cross linked antibodies.

RESULTS

Measurement of Conjugates. Figure 1 demonstrates the technique which we have used to measure FcγR-dependent conjugates (Segal and Stephany, 1984a). $P388D_1$ cells and antibody-coated spleen cells were directly labeled with green and red-emitting fluorophores, respectively. They were then mixed and analyzed at various times for red and green fluorescence with a dual laser flow cytometer. After 2 min of incubation (Fig. 1A), most particles were either red (free spleen cells) or green (free $P388D_1$).

Even at this early time, however, a small number of conjugates could be detected (particles that were both red and green), and this number increased progressively with the time of incubation, (Fig. 1B-D). The kinetics of both conjugate formation and the loss of unconjugated spleen or P388D$_1$ cells were followed by measuring the relative percentages of particles within the areas designated in Figure 1D at varying time intervals. Conjugate formation, spleen cell depletion, and P388D$_1$ depletion, follow first order kinetics with similar rate constants for all three processes (Fig. 2).

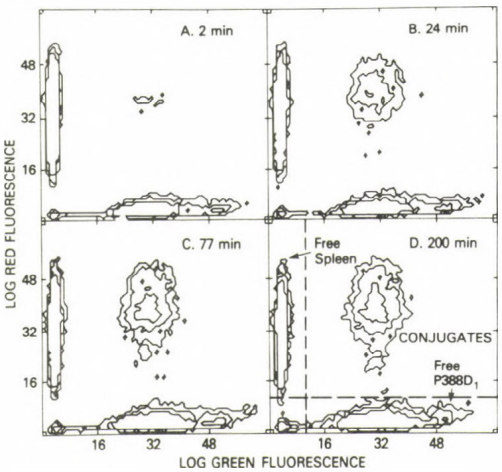

Fig. 1. Formation of conjugates as a function of time. At 0 time, P388D$_1$ cells were mixed with antibody-coated mouse spleen cells. Cells were then incubated at 4°C with slow rotation, and samples were taken for cytometric analysis at varying times. P388D$_1$ cells were labeled with a green fluorophore, fluorescein isothiocyanate, and spleen cells were labeled with a red fluorophore (substituted rhodamine isothiocyanate-XRITC). When analyzed by dual parameter flow cytometry, free spleen cells, free P388D$_1$, and conjugates can be quantitated in a single sample as shown in panel D.

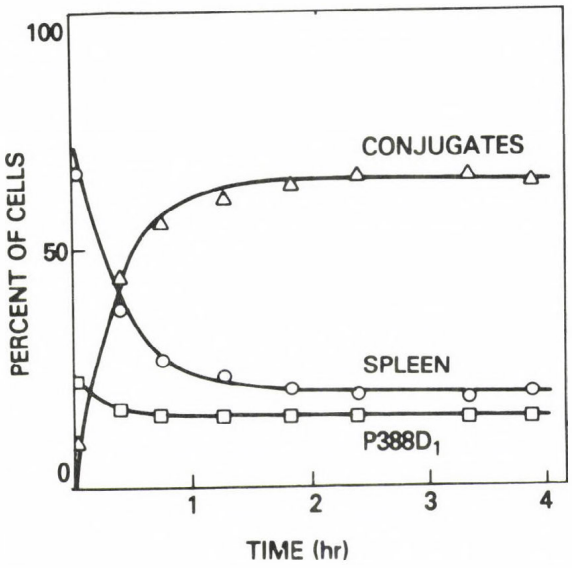

Fig. 2. Kinetics of conjugate formation at 4°C. The percentages of cells in conjugates (△), free spleen cells (○) and free $P388D_1$ cells (□) were determined as indicated in Fig. 1. Data were fit to single exponential functions (curves drawn through data points), yielding first order rate constants of .048, .042, and .062 min^{-1} for conjugate formation, spleen cell depletion, and $P388D_1$ depletion, respectively.

Number of Spleen and $P388D_1$ Cells in Conjugates. In order to examine cellular distributions within conjugates, we mixed varying amounts of antibody-coated spleen cells with a fixed concentration of $P388D_1$ cells and allowed conjugates to form. The cells were diluted and analyzed in the cytometer for free and conjugated cells. The fluorescence of cells within conjugates was then compared with the fluorescence of unconjugated cells. In Figure 3A-C, the green fluorescence of conjugated $P388D_1$ cells (i.e., particles which were both red and green) is plotted as the dashed curve, while the fluorescence of unconjugated $P388D_1$ cells (cells which were red negative) is plotted as the solid curve. Because the fluorescence distributions of free and conjugated $P388D_1$ cells superimpose over a wide range of spleen:$P388D_1$ ratios, the conjugates formed between $P388D_1$ cells and antibody-coated splenocytes contain one $P388D_1$ cell

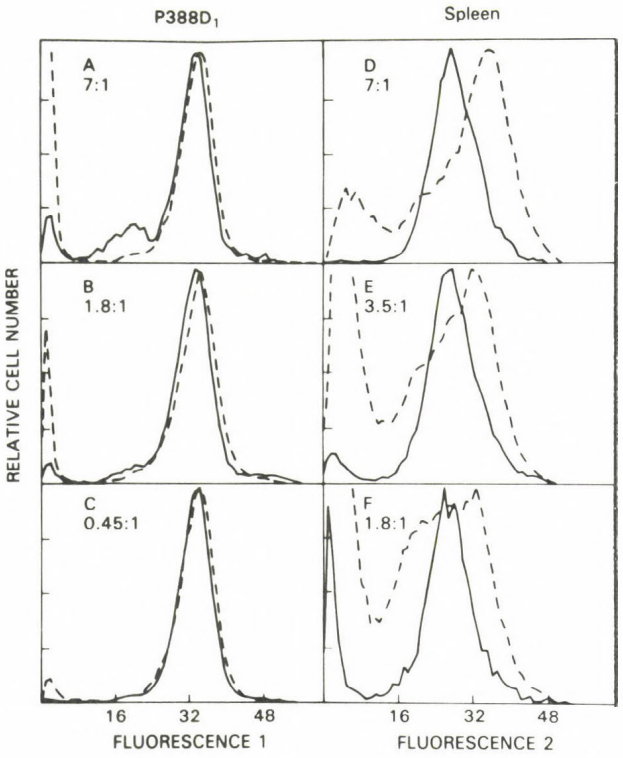

Fig. 3. Comparison of the fluorescence distributions of conjugated and unconjugated cells. In A-C the (green) fluorescence profiles of unconjugated $P388D_1$ cells (solid lines) are superimposed upon those of the conjugated cells (dashed lines). The curves have been scaled so that the fluorescence 1-positive peaks have identical heights. In D-F the (red) fluorescence profiles from spleen cells are plotted for the unconjugated (solid line) and conjugated (dashed line) cells, similar to A-C. Ratios of spleen:$P388D_1$ cells in the original mixtures are indicated in the figure. The density of $P388D_1$ cells was kept constant at $1x10^7$ cells/ml, and the density of spleen cells was varied to give the indicated ratios. Cell mixtures were maintained in suspension for 2-3 h at 4°C prior to analysis.

within experimental error. By contrast, the red fluorescence due to spleen cells in conjugates is greater than the fluorescence of unconjugated spleen cells, and the difference increases as the spleen:$P388D_1$

ratio increases (Fig. 3 D-F). When spleen and P388D_1 cells were mixed at a ratio of about 7:1 (Fig. 3D) most P388D_1 cells within the conjugates were associated with more than one spleen cell. The fluorescence values in Figure 3 are plotted on a logarithmic scale, and a factor of two increase in fluorescence corresponds to about six channels. Using this value we estimate that the conjugate peak in Figure 3D is 2.7 times as bright as that for the unconjugated cells. This suggests that aggregates within this peak contain mainly two and three spleen cells bound to one P388D_1 cell. In addition the conjugates in Figure 3D also exhibited a small shoulder corresponding to one spleen cell bound to one P388D_1. As the ratio of spleen cells:P388D_1 decreases (Fig. 3E) the conjugate peak moves closer to that of the unconjugated cells, corresponding to an average of 1.9 spleen cells per P388D_1 cell. Moreover, the shoulder arising from doublets (i.e., 1 spleen:1 P388D_1) has increased in relative area; and a third shoulder, corresponding to conjugates which exhibit less red fluorescence than a single splenocyte also becomes apparent. At the lowest ratio tested (Fig. 3F), the major peak still corresponds to 1.9 spleen:1 P388D_1, but the two shoulders have become more pronounced. We are not yet certain as to the origin of the population of P388D_1 cells that has bound less red flurophore than is present on an unconjugated spleen cell. Apparently some spleen cells lose some of their bound flurophores after forming conjugates.

Aggregation Rates Plateau at High Cell Densities. Antibody-coated spleen cells were mixed with P388D_1 cells at relative cell densities of 1, 2, 4, 8, and 16. Conjugate formation was followed as a function of time at each cell density, and the kinetics were fit to single first-order equations (Segal and Stephany, 1984b). The kinetic parameters (rate constants and extents of aggregation derived from these analyses) are plotted in Figure 4 vs relative cell density. Figure 4 shows that the rate of aggregation increases hyperbolically with cell density, approaching a plateau at high cell density; by contrast the final extent of aggregation is nearly independent of cell density over the range of densities examined. In the experiment shown in Fig. 4, the cells were constantly mixed in a turbulent suspension. If, instead, the cells were rotated in a non-turbulent suspension so that they were constantly falling at 1 G, then the aggregation rate never became independent of cell density (data not shown). The following experiments were done under conditions where aggregation rate is independent of cell density.

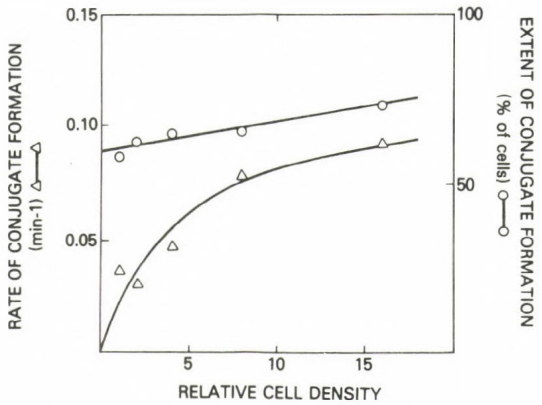

Fig. 4. Formation of conjugates at varying cell densities. Cells were mixed at varying dilutions, and conjugate formation was folowed as a function of time at 4°C. Kinetics of conjugate formation were then analyzed and the rate constants and extents of conjugate formation were plotted vs cell density. A relative cell density of 16 corresponds to $1.1x10^7$ $P388D_1$ cells/ml and $2.1x10^7$ antibody-coated spleen cells/ml. The ratio of spleen to $P388D_1$ cells was kept constant at all dilutions.

Cell Surface Densities of Antibody and FcγR Determine Aggregation Rates. Spleen cells were treated with various concentrations of ^{125}I-labeled antibody, and after washing, the numbers of antibody molecules bound per cell were determined (Segal and Stephany, 1984b). Cells coated with different amounts of antibody were then mixed with $P388D_1$ cells and aggregation was followed in the cytometer. In Figure 5A and B, the extents and rates of conjugate formation are plotted as a function of the antibody density on the spleen cells; these data show that the extent of conjugate formation approaches a plateau for increasing antibody density, in contrast to the rate of aggretation, which continues to increase as the amount of bound antibody increases.

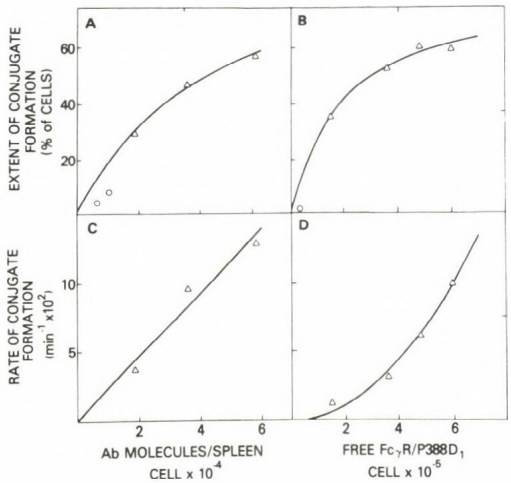

Fig. 5. Kinetics of conjugate formation at varying antibody (A,B) or FcγR (C,D) densities. Spleen cells were treated with varying concentrations of antibody, and P388D$_1$ cells with varying concentrations of anti-FcγR to produce populations of spleen cells with varying cell surface antibody densities and populations of P388D$_1$ cells with varying free FcγR densities. A and B, untreated P388D$_1$ were mixed with the various populations of spleen cells; C and D, a single preparation of antibody-coated spleen cells was mixed with the various P388D$_1$ populations. A and C, extents of conjugate formation, B and D, first-order rate constants.

In a second experiment, P388D$_1$ cells were treated with graded concentrations of the 2.4G2, anti-FcγR monoclonal antibody, and after washing, the numbers of free FcγR were determined by measuring the amount of radiolabeled cross-linked IgG bound at saturation. These cells were then mixed with spleen cells coated with a constant amount of antibody, and the rates and extents of aggregation were measured as a function of time (Fig. 5C and D). Again, the extent of aggregation approaches a plateau while the rate of aggregation continues to rise with increasing free receptor density. In this experiment, the aggregation rate appears to increase exponentially with receptor density, with exponent values of 1.5 to 2.5 giving satisfactory fits to the data. The data of Figure 5 demonstrate that the rate-limiting step of aggregation is critically dependent upon both ligand (antibody) and receptor densities on the cell surfaces.

Reversibility of Conjugate Formation. To test whether aggregation was reversible, antibody-coated spleen cells were mixed with P388D_1 cells at a 6:4 ratio for 2 hr at 4°C (Segal and Stephany, 1984b). At this time 24% of the particles were conjugates with approximately 1.7 spleen cell/P388D_1. Samples of these cells were then diluted 20-fold in either medium alone or in medium containing 10 μg/ml 2.4G2, 45 μg/ml cross-linked IgG, or 100 μg/ml protein A, and were incubated for varying times at room temperature (24°C). Figure 6 shows that conjugates are relatively stable when diluted in medium, decreasing from 23.0 to 19.2% of the particles over a 160-min period. In the presence of reagents that bind to either FcγR (cross-linked IgG and 2.4G2) or the Fc portion of IgG (protein A), however, the conjugates rapidly disaggregate. These experiments demonstrate that conjugates are stable when diluted in medium, but are readily disaggregated by reagents that sequester free ligand or free receptor.

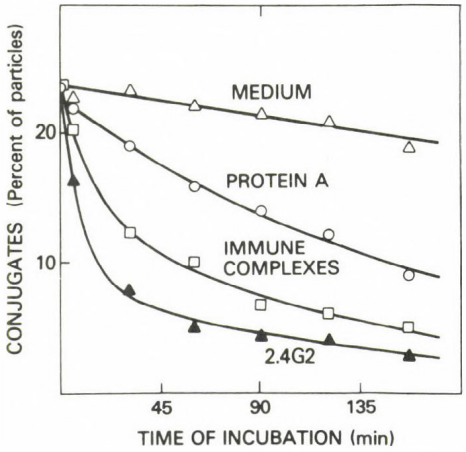

Fig. 6. The disaggregation of conjugates at 24°C. Conjugates between P388D_1 cells and antibody-coated spleen cells were allowed to form for 2 hr at 4°C. Conjugates were then (time zero) diluted 20-fold into medium containing (△) no additives; (○) 100 μg/ml protein A; (□) 45 μg/ml cross-linked IgG; and (▲) 10 μg/ml anti-FcγR antibody. Samples were then slowly rotated at 24°C and samples were taken for analysis at varying times.

Mechanism of Conjugate Formation. Taken together, our data delineate some of the essential features of the mechanism of intercellular aggregation between P388D_1 cells and antibody-coated spleen cells at 4°C. First the observation that the rate of aggregation reaches a plateau with increasing cell density (Fig. 4) suggests that the rate-limiting step in conjugate formation, at high cell densities and with rapid mixing, is not the rate at which cells collide. If it were, then the rate of conjugate formation would increase fourfold for each doubling of cell density, in clear disagreement with the experimental results. Presumably, the collision step is relatively rapid, resulting in unstable intermediates that are not detected because they are disrupted by the flow stream of the cytometer. We can therefore represent aggregation as

$$\text{occurring by the mechanism } P + S \underset{k_{-1}}{\overset{k_1}{<\!\!-\!\!-\!\!>}} PS^* \xrightarrow{k_2} PS, \text{ in which P and S}$$

are free P388D_1 and spleen cells, respectively, PS* is the unstable intermediate, and PS is the stable conjugates. Also, because more than one spleen cell can bind to one P388D_1 cell (Fig. 3), other steps must occur in which one or more spleen cells bind to PS* or PS, giving rise to PS_n. Conceivably, PS* could result from nonspecific weak interactions between cells, or alternatively, from the rapid formation of a few ligand-receptor bonds, insufficient in number to stabilize the conjugate. Our data do not distinguish between these possibilities.

At high cell concentrations, the rate of conjugate formation is strongly dependent upon both antibody and FcγR densities (Fig. 5), suggesting that, on a molecular level, the stabilization of PS* (i.e., the rate-limiting step, k_2) involves the formation of ligand-receptor bonds. In addition, data published elsewhere demonstrate that the formation of ligand-receptor bonds occurs over a small fraction of the P388D_1 and spleen cell surfaces, and utilizes only a small fraction of available antibody molecules or FcγR. Taken together, our results are consistent with a mechanism in which small patches of membrane from the P388D_1 cells rapidly come into contact with patches of spleen cell membrane, followed by a slower formation of bonds between the ligands and receptors present in the areas of intercellular contact. In these areas, we would expect the rate of bond formation to be dependent upon the cell surface densities of ligand and receptor molecules, both of which increase

as the total amounts of bound antibody or free receptors increase. This could explain why the rate of conjugate formation is highly dependent upon bound antibody or free receptors (Fig. 5), even though only a small fraction of the antibodies and receptors are actually used in the formation of conjugates.

Once spleen cells have bound to P388D_1 cells, they remain bound for relatively long periods of time, even in dilute suspension (Fig. 6, upper curve). In previous studies (Dower et al., 1981b), we showed that soluble, multivalent immune complexes also bind stably to P388D_1 cells, but that they rapidly dissociate from the cell surface in the presence of high concentrations of monomeric IgG. Accelerated dissociation of immune complexes occurs because bonds between FcγR and the individual IgG subunits of the complexes are constantly being broken and reformed at the cell surface (Segal et al., 1983). The addition of monomeric IgG accelerates dissociation of the bound complexes by binding to free FcγR, thus preventing the reformation of broken bonds between FcγR and the IgG subunits of the immune complexes. We reasoned that if ligand-receptor bonds were constantly breaking and reforming at the cell:cell interface, similar to the situation with bound immune complexes, then dilution of performed conjugates into media containing reagents that sequested free antibody (protein A) or free receptors (2.4G2 and cross-linked IgG), would markedly accelerate the disaggregation of the conjugates. The data of Figure 6 show that our prediction was correct, and provide strong evidence for a model in which ligand-receptor bonds, although constant in number in the areas of intercellular contact, are continually being broken and reformed.

Conjugate Formation and Lysis Using Antibody Heteroaggregates. In this section, we demonstrate that conjugate formation and lysis can be induced by using covalently cross-linked antibody heteroaggregates that contain both anti-FcγR antibodies and antibodies directed against a target cell determinant. When effector cells bind such heteroaggregates to their FcγR, they will then specifically bind and lyse target cells that have not been opsonized, but which express the appropriate antigen (Karpovsky et al., 1984). Cells which have been coated with hetero-aggregates are termed "franked" effector cells.

The anti-murine FcγR antibody 2.4G2 (Unkeless, 1979), was cross linked with rabbit anti-DNP antibodies using the heterobifunctional reagent, SPDP. P388D_1 cells were incubated with this preparation ("anti-FcγR x anti-DNP"), washed, and tested for lysis against TNP-coated chicken red blood cells (TNP-CRBC). Figure 7 shows that franked P388D_1 cells are potent lytic agents against TNP-CRBC, but do not lyse the target cells in the absence of added antibody. Lysis of antibody-coated target cells (classical ADCC) is shown for comparison. Lysis of TNP-CRBC also occurred when P388D_1 cells were franked with anti-FcγR (Fab) x anti-DNP [F(ab')$_2$], thus demonstrating that the Fc fragments of the antibody heteroaggregates are not involved in promoting lysis by franked effector cells.

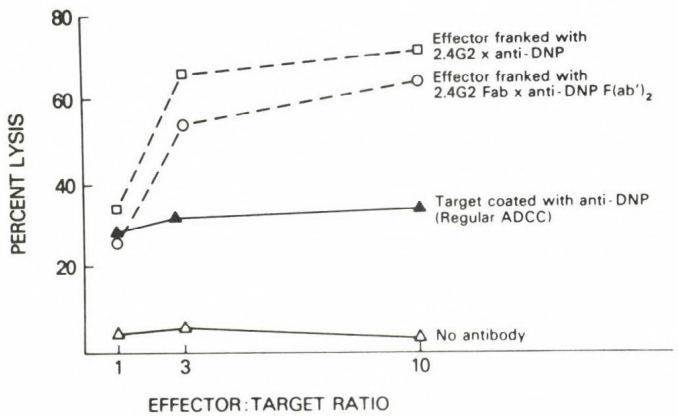

Fig. 7. Lysis of target cells by franked effectors. Lysis of TNP CRBC by P388D_1 cells in a 20-h ^{51}Cr release assay. (□) P388D_1 cells franked with 25 μg/ml anti-FcγR x anti-DNP tested against TNP CRBC. (○) P388D_1 cells franked with 25 μg/ml anti-FcγR Fab x anti-DNP F(ab')$_2$ tested against TNP CRBC. (▲) Untreated P388D_1 cells tested against TNP CRBC coated with anti-DNP antibody. (△) Untreated P388D_1 cells tested against TNP CRBC.

In other experiments (not shown) we demonstrated that lysis of TNP-CRBC by franked effector cells was TNP-specific, and that third party cells were not lysed by franked effector cells.

Inhibition of Lysis and Conjugate Formation by Immune Complexes. Classical ADCC (lysis of antibody-coated target cells) is readily inhibited by immune complexes (MacLenan, 1972). However, because of the extremely high affinity with which 2.4G2 binds to FcγR (Unkeless, 1979), we would expect lysis mediated by franked effectors to be much less sensitive to immune complex inhibition. We therefore tested the ability of immune complexes to inhibit cytolysis and conjugate formation using franked, armed (effected cells incubated with anti-DNP antibody and washed) (Greenberg and Shen, 1973), or untreated effector cells (Karpovsky et al. 1984).

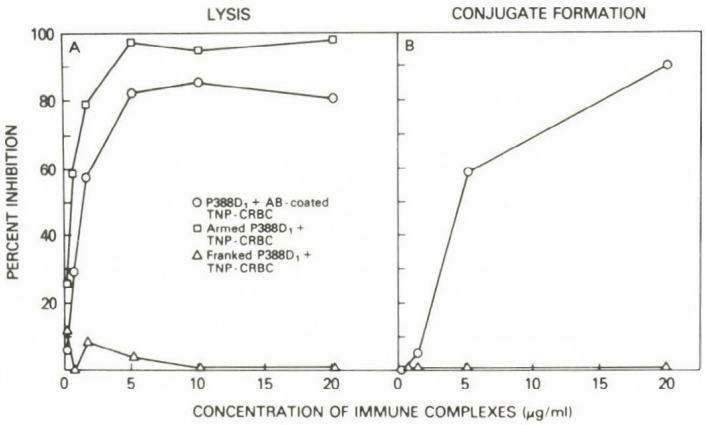

Fig. 8. Inhibition of lysis and conjugate formation by immune complexes. Immune complexes were first added to effector cells, followed by addition of the target cells. In both assays, the immune complexes were present during the entire course of the assay. (A) Inhibition of lysis in a 20-h ^{51}Cr release assay at a 10:1 effector-to-target ratio. (B) Inhibition of conjugate formation as measured by flow cytometry. (O) Untreated $P388D_1$ cells interacting with TNP CRBC coated with anti-DNP antibody. (□) Armed $P388D_1$ cells interacting with TNP CRBC. (Δ) Franked $P388D_1$ cells (anti-FcγR x anti-DNP) interacting with TNP CRBC.

In Fig. 8A, graded concentrations of immune complexes were incubated with effectors and targets in a 20-h ^{51}Cr release assay. This figure shows that both the lysis of antibody-coated target cells by untreated $P388D_1$ cells and the lysis of TNP CRBC by $P388D_1$ cells armed with anti-DNP antibodies are readily blocked by low concentrations of immune complexes.

By contrast, lysis of TNP CRBC by P388D_1 cells franked with anti-FcγR x anti-DNP is totally resistant to inhibition. As expected, the inhibition of conjugate formation followed the same pattern (Fig. 8B); in this experiment, armed effector cells could not be tested for inhibition because too few conjugates formed in the absence of immune complexes.

Linkage of Target Cells to FcγR is Necessary for Lysis. To test whether linkage to FcγR was required for lysis mediated by franked effector cells, we formed conjugates in which the target cells were bound to MHC class I molecules on the effector cells rather than to FcγR. This was done by cross-linking $F(ab')_2$ fragments from 34-1-2, a monoclonal antibody with specificity for K^d and D^d molecules, to $F(ab')_2$ fragments from rabbit anti-DNP antibodies. P388D_1 cells (which are of the H-2^d) haplotype) were then incubated with this material [anti-K^dD^d $F(ab')_2$ x anti-DNP $F(ab')_2$], and their abilities to form conjugates and lyse TNP CRBC were compared with those of P388D_1 cells franked with anti-FcγR x anti-DNP. P388D_1 cells treated with anti-K^dD^d $F(ab')_2$ anti-DNP $F(ab')_2$ were even more effective at forming conjugates than were the P388D_1 cells franked with anti-FcγR x anti-DNP (Fig. 9A). By contrast, only the cells franked with anti-FcγR x anti-DNP mediated a high degree of lysis (Fig. 9B).

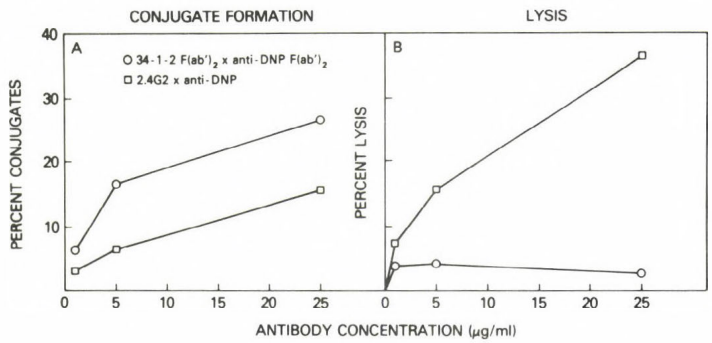

Fig. 9. The requirement of linkage to FcγR for lysis of TNP CRBC by P388D_1 cells. P388D_1 cells were treated with various concentrations of anti-FcγR x anti-DNP (□) or anti-K^dD^d $F(ab')_2$ x anti-DNP $F(ab')_2$ (○) and analyzed for conjugate formation with TNP CRBC (A) or tested for cytotoxicity against TNP CRBC in a 20-h ^{51}Cr release assay (B) at a 10:1 effector-to-target ratio.

TABLE I
Inhibition of Conjugate Formation and Lysis

Inhibitor[a]	$P388D_1$ treated with: Anti-K^dD^d $F(ab')_2$ x anti-DNP $F(ab')_2$	Anti-FcγR x anti-DNP
	Percent conjugates with TNP CRBC	
None	26.8	15.5
Anti-FcγR mAb	23.6	0.6
Anti-K^dD^d mAb	6.2	14.6
	Percent lysis of TNP CRBC[b]	
None	3.1 (1.1)	36.7 (0.9)
Anti-FcγR mAb	0.7 (0.9)	0.5 (0.5)
Anti-K^dD^d mAb	3.8 (0.3)	29.9 (0.6)

[a] $P388D_1$ cells were pretreated with 0.5 mg/ml antibody inhibitor or with medium for 30 min at 0°C. Cross-linked heteroaggregates (25 μg/ml) were then added and the cells were incubated for an additional 30-min period at 0°C and washed.

[b] Means of triplicate samples followed by standard errors in parenthesis. At effector-to-target ratios of 10:1.

The data in Table I show the results of experiments in which $P388D_1$ cells were preincubated with a 20-fold excesses of either anti-FcγR mAb or anti-K^dD^d mAb before treatment with antibody heteroaggregates. As expected, preincubation with free anti-FcγR mAb prevented conjugate formation and lysis mediated by $P388D_1$ cells treated with anti-FcγR x anti-DNP, and preincubation with free anti-K^dD^d mAb inhibited conjugate formation by $P388D_1$ cells treated with anti-K^dD^d $F(ab')_2$ x anti-DNP $F(ab')_2$. When cells franked with anti-FcγR x anti-DNP were pretreated with anti-K^dD^d, only minor effects upon conjugate formation and lysis were observed, which demonstrates that the anti-class I antibody did not suppress lysis. In an attempt to trigger lysis in nonlytic conjugates, $P388D_1$ cells were first treated with anti-FcγR, then with anti-K^dD^d $F(ab')_2$ x anti-DNP $F(ab')_2$, and finally with TNP CRBC. Instead of triggering lysis, pretreatment of the effector cells with anti-FcγR inhibited the small amount of lysis (3.1%) mediated by the anti-K^dD^d $F(ab')_2$ x anti-DNP $F(ab')_2$-treated effectors. This suggests that FcγR were involved

in lysis mediated by even these effectors. Such an involvement could arise, for example, if the anti-K^dD^d $F(ab')_2$ x anti-DNP $F(ab')_2$ preparation contained a small amount of contaminating intact antibody. Further attempts to trigger lysis in nonlytic conjugates by adding immune complexes or Sepharose-linked 2.4G2 to preformed conjugates also failed (data not shown). Therefore, the cross-linking of FcγR in conjugates where the target cells are linked to class I molecules instead of directly to FcγR is not a lytic signal.

Implications for the Mechanism of ADCC. By using antibody heteroaggregates to form effector-target conjugates, several interesting observations have emerged regarding the mechanism of ADCC. First, the data of Fig. 8 show that ADCC can occur when FcγR are linked to the target cells through interactions different from those that normally occur between the ligand and receptor. However, linkage of targets to effectors through at least two other cell surface components, the K^d and D^d molecules, does not result in lysis (Fig. 9). therefore, conjugate formation per se is not sufficient for lysis. Rather, the data suggest that ADCC requires, in addition to conjugate formation, other processes involving FcγR. To test whether the binding of antibody or ligand to FcγR could trigger lysis in nonlytic conjugates, we treated such conjugates with either 2.4G2 (Table I), soluble immune complexes, or 2.4G2 bound to Sepharose beads. In no case did treatment of FcγR in nonlytic conjugates lead to lysis, which suggests that FcγR must be linked directly to the target cell in order for lysis to occur. Since extensive cross-linking of FcγR in nonlytic conjugates (by immune complexes or 2.4G2 Sepharose) did not trigger lysis, we also conclude that either cross-linking of FcγR is not a lytic signal or alternatively, that cross-linking of FcγR does trigger lysis, but that it must occur locally at the region of intercellular contact. The precise nature of the lytic signal remains one of the most intriguing questions concerning the mechanism of ADCC.

ACKNOWLEDGEMENTS

We are grateful to Ms. Judy Kress for excellent secretarial assistance in the preparation of this manuscript.

REFERENCES

1. Dower, S. K., C. DeLisi, J. A. Titus, and D. M. Segal. 1981a. The mechanism of binding of multivalent immune complexes to Fc receptors. I. Equilibrium binding. Biochemistry 20:6326-6332.
2. Dower, S. K., J. A. Titus, C. DeLisi, and D. M. Segal. 1981b. The mechanism of binding of multivalent immune complexes to Fc receptors. II. Kinetics of binding. Biochemistry 20:6335-6341.
3. Greenberg, A. H., and L. Shen. 1973. A class of specific cytotoxic cell demonstrated in vitro by arming with antigen-antibody complexes. Nat. New Biol. 245:282-284.
4. Karpovsky, B., J. A. Titus, D. A. Stephany, and D. M. Segal. 1984. Production of target-specific effector cells using hetero-cross-linked aggregates containing anti-target cell and anti-Fcγ receptor antibodies. J. Exp. Med. 160:1686-1701.
5. Lovchik, J. C., and R. Hong. 1977. Antibody-dependent cell-mediated cytolysis (ADCC): analyses and projections. Prog. Allergy. 22:1-27.
6. MacLenan, I. C. M. 1972. Competition for receptors for immunoglobulin on cytotoxic lymphocytes. Clin. Exp. Immunol. 10:275-283.
7. Moller, E. 1965. Contact-induced cytotoxicity by lymphoid cells containing foreign isoantigens. Science 147:873-875.
8. Segal, D. M., S. K. Dower, and J. A. Titus. 1983. The role of non-immune IgG in controlling IgG-mediated effector functions. Mol. Immunol. 20:1177-1189.
9. Segal, D. M., and D. A. Stephany. 1984a. The measurement of specific cell:cell interactions by dual parameter flow cytometry. The Fc receptor-mediated aggregation of P388D_1 cells with antibody-coated spleen cells. Cytometry 5:169-181.
10. Segal, D. M., and Stephany, D. A. 1984b. The mechanism of intercellular aggregation. I. The kinetics of the Fcγ receptor-mediated aggregation of P388D_1 cells with antibody-coated lymphocytes at 4°C. J. Immunol. 132:1924-1930.
11. Unkeless, J. C. 1979. Characterization of a monoclonal antibody directed against mouse macrophage and lymphocyte Fc receptors. J. Exp. Med. 150:580-588.
12. Unkeless, J. C., H. Fleit, and I. S. Mellman. 1981. Structural aspects and heterogeneity of immunoglobulin Fc receptors. Adv. Immunol. 31:247-270.

DISCUSSION

DAMJANOVICH:

Is there any shearing force in the stream of a flow cytometer separating the weakly bound effector and target cells?
Roughly how many bonds are necessary between the effector and target cells to form strongly bound conjugates.

SEGAL:

There are certainly shearing forces between the effector and target cells. In control experiments, which I didn't mention in my talk, we determined that shear forces had little effect upon the number of conjugates measured. For example the same number of conjugates was detected cytometrically and microscopically, and varying the shear forces by varying the flow rates and nozzle sizes did not affect our results. Vortexing the cells did however reduce the number of conjugates which we detected.
As to the number of bonds required to form conjugates, I can say that it is a low percentage of the total possible number of intercellular bonds, since we have titrated both the free receptor and ligand within conjugates, and have found them to be nearly equivalent to the numbers seen in the unconjugated cells. George Bell has calculated that only a few bonds should be required to form stable conjugates.

TRÓN:

I find it interesting that you have not found higher aggregates in your experiments. I think of aggregates with two or more macrophages linked by spleen cells. You have varied the concentration and the ratio of both kinds of cells, so one would expect, at least in some cases, higher aggregates of this type, too. My question is: do you think it is possible that these do exist, but the primarily formed aggregates are falling apart due to the friction

when speeding up during hydrodynamic focusing.

SEGAL:

This is certainly possible. However, we do not see very many conjugates containing multiple macrophages when we look at cell mixtures in the microscope.

ELSON:

Is there any electron microscopic evidence for localized degranulation of macrophage in the region of contact with target cell, (in analogy with degranulation observed in cytotoxic T-cells)?

SEGAL:

This should certainly be possible to do, especially since the cytometric technique possesses the ability to sort conjugates. However, we have not yet done these experiments.

LUKÁCS:

There should be some Fc receptor cells among the spleen cells which could interact with the other antibody-coated spleen cells. But you showed no conjugate formation among the spleen cells. Did you remove the FcR positive cells from your target cells?

SEGAL:

Thank you for bringing this up. I neglected to mention that the spleen cells had been pretreated with the anti-Fc receptor antibody prior to experimentation.

Dynamics of Biochemical Systems
S. Damjanovich, T. Keleti, L. Trón (Eds)

BIOPHYSICAL APPLICATIONS OF FLUORESCENCE CORRELATION SPECTROSCOPY AND PHOTOBLEACHING RECOVERY

ELLIOT L. ELSON

Department of Biological Chemistry,
Washington University School of Medicine,
St. Louis, Missouri, USA

INTRODUCTION

During the past ten years Fluorescence Photobleaching Recovery (FPR) [also known as "Fluorescence Recovery (or Redistribution) after Photobleaching" or "Fluorescence Microphotolysis"], has been extensively used to characterize the lateral mobility of fluorescence labeled molecules in living cells and in chemically defined systems (Cherry 1979, Peters 1981, Webb et al. 1981, Axelrod 1983, Helmreich and Elson 1984, Elson 1985). A closely related method, Fluorescence Correlation Spectroscopy (FCS), has similar capabilities in principle but has been little used in practice because of technical difficulties in its application to living cells. As will be seen below, however, these difficulties can be circumvented in some applications to cells and need not prevent the application of FCS to appropriate noncellular systems. Both methods can be used to characterize not only lateral mobility but also the kinetics of chemical reaction systems as well, although this latter capability has been

little exploited. Recently FPR has been applied to study cytoplasmic diffusion in living cells (Wojcieszyn et al. 1981, Jacobson and Wojcieszyn 1984) including the diffusion of actin (Wang et al. 1982, Kreis et al. 1982). As discussed below FPR is also being used to study mechanisms of polymerization and interactions of resolved cytoskeletal components. New applications of FCS have also arisen in studies of polymerization and aggregation (Petersen 1984, Petersen 1985). This paper provides an introduction to the basic ideas underlying FCS and FPR and discusses some new directions in the applications of these techniques.

Both methods depend on the same basic experimental process: measurement of the number of molecules of specified types via their fluorescence in a defined open volume of the experimental system as a function of time. In a chemical reaction system these numbers can change due either to their moving into or out of the region (diffusion, flow, or drift) or to their being created or destroyed by the chemical reaction. Hence the standard phenomenological diffusion coefficents and chemical rate constants can be determined from the measured rates of change of the local concentrations of the system components.

In an FPR experiment the system is displaced from equilibrium by using a brief, intense pulse of light to photolyse irreversibly a fraction of the fluorescent molecules in the observation region. Hence there is a macroscopic gradient, $\Delta c(r,t) = c(r,t) - \bar{c}$, between the concentration, $c(r,t)$, at position r and time t in the interior of the region and the equilibrium concentration, $\bar{c}$, in the unperturbed surrounding parts of the system. This is gauged by a corresponding macroscopic displacement of the measured fluorescence, $\Delta F(t) = F(t) - \bar{F}$. The measurement consists of observing the relaxation of $\Delta F(t)$ which results from the dissipation of the concentration gradient (Axelrod et al. 1976).

In an FCS experiment, however, the system rests in equilibrium throughout the measurement. Rather than macroscopic changes of concentration and fluorescence, in an FCS experiment one observes the microscopic changes, $\delta F(t)$, that result from the spontaneous concentration fluctuations, $\delta c(r,t)$, that occur in the system even when in equilibrium. Observation of the dissipation of a macroscopic concentration displacement, as in an FPR experiment or more conventional method for measuring transport or kinetics, allows the determination of the desired phenomenological coefficients from measurements of individual transients. The accuracy of the determination is limited in principle only by the experimental accuracy of the measurement of the fluorescence transient. In contrast many microscopic fluctuations must be measured in an FCS experiment. This is not only because the fluctuations are small and difficult to measure. Even if an individual fluctuation could be measured with high precision, the measurement would not determine the desired phenomenological coefficients with high accuracy. This is because the rates of dissipation of microscopic fluctuations are determined by the phenomenological coefficients only in a statistical sense. Hence for each measurement many fluctuations must be registered and analyzed statistically. This is usually accomplished by computing a fluorescence fluctuation autocorrelation function, $G(\tau)$ (Elson and Magde 1974, Magde et al. 1974, Elson and Webb 1975):

$$G(\tau) = \langle \delta F(0)\delta F(\tau) \rangle = \lim_{\Xi \to \infty} 1/\Xi \int_{0}^{\Xi} \delta F(t)\delta F(t+\tau)\, dt \qquad (1)$$

where $\langle \ldots \rangle$ denotes an ensemble average and the second equation supplies an operational definition. (We have supposed that the system is in equilibrium and therefore is stationary.)

Hence the principal experimental difference between FCS and FPR is in the size and number of the fluorescence transients that must be recorded. Therefore the apparatus, typically based on a fluorescence microscope with a laser light source, is very similar for the two kinds of measurements (Koppel et al. 1976). The requirements differ mainly in that FPR measurements must have specialized electronics, optics and shutters for controlling the photobleaching pulse while FCS measurements demand the capability for computing $G(\tau)$ from the large number of observed fluorescence fluctuations.

RELATION OF MEASUREMENTS TO PHENOMENOLOGICAL COEFFICIENTS

The primary experimental datum is a measurement of the fluorescence emitted from a small open region of the system as a function of time. Then $\delta F(t)$ [or $\Delta F(t)$] must be related to the $\delta c_i(t)$ [or $\Delta c_i(t)$]. The fluorescence emitted by component i from a position r is proportional to the concentration of the component $c_i(r,t)$ weighted by the excitation intensity $I(r)$, and summed (integrated) over all positions:

$$\Delta F(t) = \Sigma_i \, Q_i \int I(r)\Delta c_i(r,t) \, d^2r \qquad (2)$$

where Q_i accounts for the instrumental constants and for the absorption and fluorescence quantum yield of component i and we are assuming for simplicity that the system is confined to a plane. Similarly,

$$G(\tau) = \Sigma_{i,j} Q_i Q_j \int I(r)I(r')\langle \delta c_i(r,0)\delta c_j(r',\tau)\rangle d^2r d^2r' \qquad (3)$$

The dependence of the concentrations on position, time, and the phenomenological coefficients is determined from a system of differential equations which account for diffusion, systematic drift or flow and chemical reaction:

$$\partial\delta c_i(r,t)/\partial t = D_i\nabla^2\delta c_i(r,t) - V_i\delta c_i(r,t) + \Sigma_{i,j} T_{i,j}\delta c_j(r,t) \quad (4)$$

where D_i is the diffusion coefficient and V_i, the uniform drift or flow velocity in the x-direction for component i, and the $T_{i,j}$ characterize the contributions via chemical reactions of component j to the rate of change of the concentration of component i. To use these equations to characterize the macroscopic concentration changes observed in FPR experiments we must assume that the displacements of concentrations from their equilibrium values are small enough so that the kinetic equations describing any nonlinear chemical reactions can be linearized. The systematic translation along the x-direction characterized by the constant velocity V_i could be due to drift in a field (e.g. electorphoresis or sedimentation), to uniform motion of the sample relative to the probe beam, or to a uniform flow process. Nonuniform flow fields, e.g. as in flow through a channel, can be much more difficult to analyze (Magde et al. 1978).

These equations are most simply solved for systems in which the overall dimensions are large compared to the size of the observation area so that $\delta c_i(r,t) = 0$ at $r = (+/-)\infty$. The initial conditions are different for FCS and FPR experiments. For the former one supposes that the system behaves ideally, which is usually justifiable at the low concentrations at which these experiments are carried out. Then, the number of molecules of each component in any volume will be independent of the concentration of any other component and will be governed by a Poisson distribution. Hence the variance of the number of molecules (i.e. the mean square fluctuation) will equal the mean number: $\langle\delta c_i(r,0)\delta c_j(r',0)\rangle = \bar{c}_j\ \delta_{i,j}\ \delta(r-r')$ (Elson and Magde, 1974).

In an FPR experiment the initial concentration gradient, $\Delta c_i(r,0)$, is determined by the duration, T, and the intensity profile, $I'(r)$, of the photobleaching pulse and by the mechanism of the bleaching reactions.

In the simplest FPR experiments the photobleaching intensity profile is an intensified version of the monitoring intensity profile: $I'(r) = BI(r)$ where the constant B is typically in the range 10^3 to 10^4. The simplest mechanistic assumption would hold that each fluorescent component of the system is irreversibly eliminated from the system independently of the others by a single first order process. Then,

$$dc_i(r,t)/dt = -\gamma_i I'(r) c_i(r,t) \qquad (5a)$$

so that

$$\Delta c_i(r,0) = \bar{c}_i\{1 - \exp[-\gamma_i BI(r)T]\} \qquad (5b)$$

where γ_i is the photochemical rate constant. The assumption of an irreversible first order process may be only approximate and should be checked experimentally. Even if the individual bleaching events are irreversible and first order, the assumption that each of the components is eliminated independently of the others is inappropriate for some systems, especially those in which several fluorophores reside on a single kinetic unit as in multiple binding and polymerization systems. Then a more general model is required. If we continue to suppose that all photobleaching processes are first order in fluorophore concentrations, then we can represent the kinetics of a system of coupled reactions as:

$$dc_i(r,t)/dt = I'(r) \Sigma_j P_{i,j} c_j(r, t) \qquad (6)$$

Then a complete evaluation of Equation (2) would in general require the determination of the eigenvalues and eigenvectors of $P_{i,j}$ and the evaluation therefrom of the $\Delta c_i(r,0)$. With these boundary and initial conditions one can conveniently solve the kinetic equations using a Fourier

transform approach (Elson and Magde 1974).

Relatively general expressions for $G(\tau)$ and $\Delta F(t)$ have been published (Icenogle and Elson 1983a, Elson 1985). For our present purpose, however, it is more illustrative to confine our attention to the simplest excitation beam shape and to single component systems. In the simplest and most frequently used "spot" approach a single circularly symmetric region of the system is illuminated by a beam with a Gaussian intensity profile: $I(r) = I_0 \exp(-2r^2/w^2)$ where w is the exp(-2) radius of the intensity distribution and I_0 is the (maximum) intensity at the center of the monitoring beam. Moreover $I'(r) = BI(r)$ as indicated above. Then the characteristic time courses for correlation decay and fluorescence recovery for a single component are as follows:

$$G(\tau) \propto [1 + \tau/\tau_D]^{-1} \qquad (7a)$$

and

$$\Delta F(t) \propto \Sigma_n [(-\kappa)^n/n!][1 + n(1 + 2t/\tau_D)]^{-1} \qquad (7b)$$

for diffusion where $\tau_D = w^2/4D$;

$$G(\tau) \propto \exp[-(\tau/\tau_V)^2] \qquad (7c)$$

and

$$\Delta F(t) \propto \Sigma_n [(-\kappa)^n/(n + 1)!]\exp\{[-2n/(n + 1)](t/\tau_V)^2\} \qquad (7d)$$

for uniform flow or drift where $\tau_V = w/V$;

$$G(\tau) \propto \exp[-(\tau/\tau_V)^2/(1 + \tau/\tau_D)]/[1 + \tau/\tau_D] \qquad (7e)$$

and

$$\Delta F(t) \propto \Sigma_n (-\kappa)^n \exp\{-2(t/\tau_V)^2/[1 + 2t/\tau_D)]\}$$
$$\{n![1 + n(1 + 2t/\tau_D)]\}^{-1} \qquad (7f)$$

for simultaneous drift and flow.

It is sometimes advantageous to bleach patterns more complicated than a circular spot onto the sample (Smith and McConnell 1978, Lanni and Ware 1982, Davoust et al. 1982, Koppel and Sheetz 1983). Using periodic patterns simplifies the data analysis by yielding directly the Fourier components of the detected fluorescence recovery or decay processes (Koppel 1981). Periodic patterns are also useful for detecting anisotropic transport. (Smith et al. 1979).

NEW APPLICATIONS

During the past few years FPR has been used to characterize the mechanism of polymerization of purified actin (Lanni et al. 1981, Tait and Frieden 1982a,b, Lanni and Ware 1984, Mozo-Villarias and Ware 1984) and the interactions of other protein molecules with actin microfilaments (Doi and Frieden 1984, Arakawa and Frieden 1984). When an actin monomer is incorporated into a microfilament, its diffusion coefficient is strongly reduced. Hence measurements of the diffusion coefficients of fluorescence labeled actin could be used as an assay of the extent polymerization. It is possible to gain additional information about polymerization processes using FCS. This is due to the fact that FCS and FPR report different moments of the distribution of aggregate or polymer sizes. This is readily illustrated by considering the initial values $G(0)$ and $\Delta F(0)$ for a distribution of aggregates or polymers, $\{A_i\}$. We shall suppose that the number of fluorophores on an A_i molecule is equal or proportional to i. Assuming a circular Gaussian intensity profile as above, $G(0) = (P^2/\pi w^2)$ $\Sigma_i \; Q_i^2 \bar{c}_i$. We shall also make the reasonable assumptions that the fluorescence quantum yield is independent of i while the absorption probability is proportional to i. Then, $Q_i = iQ_1$. Hence $G(0) =$

$(P^2Q_1{}^2/\pi w^2)$ Σ_i $i^2\bar{c}_i$. To facilitate comparison with this FCS result we shall suppose that the correpsonding FPR measurements are performed in the limit of low extents of bleaching. Then from Eq. (6) $\Delta c_i(r,0) = I'(r)T \Sigma_j P_{i,j}\bar{c}_j$ where T is the duration of the photobleaching pulse and we have assumed that the system components were present at their equilibrium values prior to photobleaching. Let $L_i = \Sigma_j P_{i,j}\bar{c}_j$. Then the initial concentration distributions can be represented as $\Delta c_i(r,0) = I'(r)TL_i$. Hence $\Delta F(0) = (p^2BT/\pi w^2) \Sigma_i Q_iL_i$. In this limit the mechanism which seems most plausible would account for the first order disappearance of c_i due to bleaching itself and the first order appearance of c_i due to bleaching c_{i+1}: $dc_i/dt = I'(r)[-\gamma_i c_i + \gamma_{i+1}c_{i+1}]$. The probability of a photobleaching event should be proportional to the number of fluorophores, $\gamma_i = i\gamma_1$. Hence $L_i = -\gamma_i\bar{c}_i + \gamma_{i+1}\bar{c}_{i+1} = \gamma_1[-i\bar{c}_i + (i+1)\bar{c}_{1+1}]$. This yields $\Delta f(0) = (-P^2Q_1\gamma_1BT/\pi w^2) \Sigma_i i\bar{c}_i$. Hence the amplitude G(0) is proportional to the second and the amplitude $\Delta F(0)$ to the first moment of the distribution of aggregate concentrations.

This instance provides a simple example of how the result of an FPR experiment can depend on the mechanism of the photobleaching process. If, all the fluorophores were to be eliminated simultaneously in a single photochemical event rather than one at a time as proposed above, then it can be shown that $\Delta F(0)$ would also be proportional to the second moment of the distribution of aggregate sizes and therefore would be proportional to G(0). This sort of highly coupled bleaching process seems unlikely in the absence of an extraordinary extent of electronic coupling among the fluorophores. The dependence of FPR measurements on the mechanism of bleaching has been discussed in greater detail elsewhere (Icenogle and

Elson 1983a,b, Elson 1985).

The dependence of $G(\tau)$ on the second moment of the fluorophore aggregate distribution renders it potentially useful for characterizing multiple binding and polymerization equilibria. This potential is enhanced by methods for circumventing some of the technical difficulties that restrict the application of FCS experiments. One of these difficulties stems from the need for observing many fluctuations to obtain a sufficiently accurate $G(\tau)$ and the consequent need for long periods of data acquisition. The period of data acquisition depends on the average duration of the fluctuations. If the principle mode of fluctuation relaxation is via diffusion, then the integration time for the experiment, Ξ [the time required to measure enough fluctuations to yield a sufficiently accurate $G(\tau)$, cf Eq. (1)], will be proportional to $\tau_D = w^2/4D$. Hence Ξ may be diminished by reducing w. The extent to which this may be done is, however, limited by the resolution limit set by the excitation wavelength. Another approach was used in one of the first fluorescence fluctuation experiments, a measurement of the molecular weight of DNA labeled with ethidium bromide (Weissman et al. 1976). The DNA-ethidium sample in a cylindrical cell was rotated through a laser beam which served as an excitation source. Hence, rather than measuring fluctuations in fluorophore concentration over time in a single region of the solution, this approach measures concentration fluctuations over space. In a homogeneous system in a steady state the two approaches should give equivalent results. The rate of rotation was sufficiently fast that each sampled region of the solution was traversed by the laser beam several times before there was substantial diffusional redistribution of the DNA molecules in the region. This provided a two-fold advantage. First, the

time scale of the measured fluctuation was set by the rotation rate rather than the rate of diffusion of the DNA molecules. Hence $G(\tau)$ could be acquired in a much shorter period of time. Second, the repetitive sampling of the regions gave rise to a periodic component to $G(\tau)$ which could then be more readily separated from other fluorescence noise sources which were aperiodic (Weissman et al. 1976). Rotating the sample is not so readily accomplished with microscopic samples such as cells. Nevertheless the same concept can be applied either by scanning the laser beam over the cell (Koppel 1979) or by uniformly translating the cell through the laser beam (Petersen 1985). Suppose that the cell is translated at a constant velocity, V, which is sufficiently fast that no significant redistribution of fluorescent components in each sampled region occurs during the time required for the beam to traverse the region. Then $G(\tau) = G(0)\exp[(-\tau/\tau_V)^2]$ [cf Eq. (7c)] and $G(0) = (P^2/\pi w^2)\ \Sigma_i\ Q_i^2\bar{c}_i$ as shown above. Hence a very useful aspect of this approach is that the measured $G(\tau)$ should have a predictable time behavior, determined by V, which can be set as desired. This approach, called scanning FCS (s-FCS), has been developed by Petersen and applied to measure the extent of aggregation of fluorophores on the surfaces of cells (Petersen 1984, 1985). The fact that the scanning rate can be set as desired is useful both to increase the rate of acquisition of $G(\tau)$ and to permit fitting the measured $G(\tau)$ to a known functional form. Furthermore as shown above the FCS signal increases as the square of the number of fluorophores per aggregate and so becomes more readily measurable in systems of large aggregates such as polymers. Hence s-FCS circumvents some of the difficulties that impede the application of FCS to cells, and appears to be potentially quite useful for characterizing aggregate distributions both on the surface and in the cytoplasm of cells and in cell-free systems.

Another recent development is the coupling of spot photobleaching with digital analysis of video images acquired using very low excitation intensities from fluorescence labeled cells. This approach has been used in an investigation of anisotropic diffusion of a lipid probe in lecithin bilayers above and below the lipid phase transiton (Kapitza et al. 1985). This work also demonstrated the applicability of the method to observing the growth of ligand-receptor clusters on cell surfaces. The approach has also been used to investigate the motions of actin microfilaments in the extending and retracting lamellipodia of migrating fibroblasts (Felder 1984). In this work rhodamine-labeled actin was microinjected into fibroblasts in culture and allowed to integrate into the microfilament system (Kreis et al. 1982). Then, in an active cell a spot was bleached into the labeled actin a few microns behind the edge of an active lamellipodium. The labelled actin in microfilaments does not diffuse significantly on the time scale of the experiment. Hence, the bleached spot can be observed over a period of time. The motion of the spot was compared to that of the edge of the extending and retracting lamellipodium. It was observed that the spot did not experience detectable translation as the edge was advancing. In contrast, when the edge retracted the spot also retracted although at a slower velocity. This led to the conclusion that extension of the lamellipodium does not result from protrusion of formed microfilaments driven by forces generated within the cell body. Rather it appears that the extension results from polymerization of actin at the cell edge.

CONCLUSIONS

Although FCS and FPR are closely related methods which can be used for measuring reaction kinetics and lateral mobility, they have different domains of applicability. FPR is more suitable for studies on living cells and has been used extensively to characterize lateral diffusion on the surfaces and in the cytoplasm of living cells. Due to its dependence on the acquisition of an extended data record, FCS is less useful for studying dynamic processes on living cells but does seem likely to find applications in characterizing aggregation and multiple binding equilibria both in cells in cell-free systems.

ACKNOWLEDGEMENTS

I am grateful to my coworkers in the development of various phases of FCS and FPR: Watt Webb, Douglas Magde, Daniel Axelrod, Dennis Koppel, Joseph Schlessinger, and Ron Icenogle. Our recent work on FCS and FPR has been supported by NIH grant GM 30299.

REFERENCES

1. Arakawa, T., Frieden, C. 1984. "Interaction of Microtubule-associated Proteins with Actin Filaments." J. Biol. Chem. 259:11730-11734.

2. Axelrod, D. 1983. "Lateral Motion of Membrane Proteins and Biological Function." J. Membrane Biol. 75:1-10.

3. Axelrod, D., Koppel, D. E. , Schlessinger, J., Elson, E., Webb, W. W. 1976. "Mobility Measurements by Analysis of Fluorescence Photobleaching Recovery Kinetics." Biophys. J. 16:1055-1069.

4. Cherry, R. J. 1979. "Rotational and Lateral Diffusion of Membrane Proteins." Biochim. Biophys. Acta, 559:289-327.

5. Davoust, J., Devaux, P. F., Leger, L. 1982. "Fringe Pattern Photobleaching. a New Method for the Measurement of Transport Coefficients of Biological Macromolecules." EMBO J. 1:1233-1238.

6. Doi, Y. Frieden, C. 1984. "Actin Polymerization." J. Biol. Chem. 259:11868-11875.

7. Elson, E. L. 1985. "Fluorescence Correlation Spectroscopy and Photobleaching Recovery," Ann. Rev. Phys. Chem. 36:379-406.

8. Elson, E. L., Magde, D. 1974. "Fluorescence Correlation Spectroscopy. I. Conceptual Basis and Theory." Biopolymers, 13:1-27.

9. Elson, E. L., Webb, W. W. 1975. "Concentration Correlation Spectroscopy: A New Biophysical Probe Based on Occupation Number Fluctuations." Ann. Rev. Biophys. Bioeng. 4:311-334.

10. Felder, S. 1984. Mechanics and Molecular Dynamics of Fibroblast Locomotion PhD thesis. Washington University, St. Louis, MO.

11. Helmreich, E. J. M., Elson, E. L. 1984. "Mobility of Proteins and Lipids in Membranes." Adv. Cyclic Nucleotide Protein Phosphoryl. Res. 18:1-62.

12. Icenogle, R. D., Elson, E. L. 1983. "Fluorescence Correlation Spectroscopy and Photobleaching Recovery of Multiple Binding Reactions. I. Theory and FCS Measurements." Biopolymers, 22:1919-1948.

13. Icenogle, R. D., Elson, E. L. 1983. "Fluorescence Correlation Spectroscopy and Photobleaching Recovery of Multiple Binding Reactions. II. FPR and FCS Measurements at Low and High DNA Concentrations." Biopolymers, 22:1949-1966.

14. Jacobson, K., Wojcieszyn, J. 1984. "The Translational Mobility of Substances within the Cytoplasmic Matrix." Proc. Natl. Acad. Sci. USA. 81:6747-6741.

15. Kapitza, H. G., McGregor, G., Jacobson, K. A. 1985. "Direct Measurement of Lateral Transport in Membranes Using Time-Resolved Spatial Photometry (TRSP)." Proc. Natl. Acad. Sci. USA. 82:4122-4126.

16. Koppel, D. E. 1981. "Association Dynamics and Lateral Transport in Biological Membranes." J. Supramol. Struct. and Cellular Biochem. 17:61-67.

17. Koppel, D. E., Axelrod,D., Schlessinger, J., Elson, E. L., Webb, W. W. 1976. "Dynamics of Fluorescence Marker Concentration as a Probe of Mobility." Biophys. J. 16:1315-1329.

18. Koppel, D. E., Sheetz, M. P. 1983. "A Localized Pattern Photobleaching Method for the Concurrent Analysis of Rapid and Slow Diffusion Processes." Biophys. J. 43:175-181.

19. Kreis, T., Geiger, B., Schlessinger, J. 1982. "Mobility of Microinjected Rhodamine Actin within Living Chicken Gizzard Cells Determined by Fluorescence Photobleaching Recovery." Cell, 29:835-845.

20. Lanni, F., Ware, B. R. 1982. "Modulation Detection of Fluorescence Photobleaching Recovery." Rev. Sci. Instrum. 53:905-908.

21. Lanni, F., Ware, B. R. 1984. "Detection and Characterization of Actin Monomers, Oligomers, and Filaments in Solution by Measurement of Fluorescence Photobleaching Recovery." Biophys. J. 46:97-110.

22. Lanni, F., Taylor, D. L., Ware, B. R. 1981. "Fluorescence Photobleaching Recovery in Solutions of Labeled Actin." Biophys. J. 35:351-364.

23. Magde, D., Elson, E. L., Webb, W. W. 1974. "Fluorescence Correlation Spectroscopy. II. An Experimental Realization." Biopolymers, 13:29-61.

24. Magde, D., Webb, W. W., Elson, E. L. 1978. "Fluorescence Correlation Spectroscopy. III. Uniform Translation and Laminar Flow." Biopolymers, 17:361-376.

25. Mozo-Villarias, A., Ware, B. R. 1984. "Distinctions Between Mechanisms of Cytochalasin D Activity for Mg2+- and K+-induced Actin Assembly." J. Biol. Chem. 259:5549-5554.

26. Peters, R. 1981. "Translational Diffusion in the Plasma Membrane of Single Cells as Studied by Fluorescence Microphotolysis." Cell Biol. Int. Rep., 5:733-760.

27. Petersen, N. O. 1984. "Diffusion and Aggregation in Biological Membranes." Can J. Biochem. Cell Biol. 62:1158-1166.

28. Petersen, N. O. 1985. "Scanning Fluorescence Correlation Spectroscopy: Theory and Simulation of Aggregation Measurements." Biophys. J. in press.

29. Smith, B. A., McConnell, H. M. 1978. "Determination of Molecular Motion in Membranes Using Periodic Pattern Photobleaching." Proc. Natl. Acad. Sci. USA. 75:2759-2763.

30. Smith, B. A., Clark, W. R., McConnell, H. M. 1979. "Anisotropic Molecular Motion on Cell Surfaces." Proc. Natl. Acad. Sci. USA. 76:5641-5644.

31. Tait, J., Frieden, C. 1982. "Polymerization-Induced Changes in the Fluorescence of Actin Labeled with Iodoacetamidotetramethylrhodamine." Arch. Biochem. Biophys. 216:133-141.

32. Tait, J., Frieden, C. 1982. "Polymerization and Gelation of Actin Studied by Fluorescence Photobleaching Recovery." Biochemistry, 21:3666-3674.

33. Wang, Y.-L., Lanni, F., McNeil, P. L., Ware, B. R., Taylor, D. L. 1982. "Mobility of Cytoplasmic and Membrane-associated Actin in Living Cells." Proc. Natl. Acad. Sci. USA. 79:4660-4664.

34. Webb, W. W., Barak, L. S., Tank, D. W., Wu, E.-S. 1981. "Molecular Mobility on the Cell Surface," Biochem. Soc. Symp. 46:191-205.

35. Weissman, M., Schindler, H., Feher, G. 1976. "Determination of Molecular Weights by Fluctuation Spectroscopy: Application to DNA." Proc. Natl. Acad. Sci. USA. 73:2776-2780.

36. Wojcieszyn, J., Schlegel, R., Wu, E.-S., Jacobson, K. 1981. "Diffusion of Injected Macromolecules within the Cytoplasm of Living Cells." Proc. Natl. Acad. Sci. USA. 78:4407-4410.

DISCUSSION

ZIDOVETZKI:

The diffusion process you described seems to be three-dimensional. Why, then, you treated it as a two-dimensional diffusion?

ELSON:

There is no need to take diffusion parallel to the optic axis of the microscope into account in the application of FPR to measure the lateral mobility of actin in lamellar regions of fibroblasts. This is because the thickness of the lamellar regions are comparable to or less than the depth of focus of the objective which was used. Hence motion parallel to the optic axis does not produce a change in fluorescence intensity and therefore does not contribute to the fluorescence recovery.

TRÓN:

Thinking only about the application of FRAP and FCS to determine protein lateral diffusion coefficients, the sensitivity of the former is definitely superior to that of the FCS. However, using data averaging the signal/noise ratio can be increased remarkably in the case of FCS. I wonder whether the significant difference in the frequency of application of FRAP and FCS is entirely due to these different sensitivities or are there any other reasons?

ELSON:

The principal reason that FCS has found few applications is that it can be applied only to very stable systems and requires long periods of data acquisition to yield sufficiently accurate correlation functions. FRAP is much less restricted by either of these considerations, since it requires the measurement only of a single fluorescence recovery transient. Signal averaging can be applied to FRAP measurements to improve precision in favourable

instances in which 100 % fluorescence recovery is obtained (e.g. R.D. Icenagle and E.L. Elson, Biopolymers, 22, 1949-1966, 1983.). This however, is merely a matter of improving the signal to noise ratio. In contrast, in FCS statistical analysis of many microscopic fluctuation transients is required in principle to obtain accurate estimations of phenomenological parameters. (c.f. D.E. Koppel, Phys. Rev. A. 10, 1938-1944, 1974.).

CHERRY:

Did I understand correctly that the theory of coupled photobleaching permits an experimental distinction to be made between monomeric and oligomeric proteins in membranes?

ELSON:

In principle, FCS can be used to measure the degree of aggregation of proteins in membranes and in solution. This results from the fact that FCS reports the second moment of the distribution of aggregate sizes. (c.f. D. Magde, W.W. Webb, E.L. Elson, Biopolymers, 17, 361-376, 1978.) This approach is now being developed by N.O. Petersen (Can. J. Biochem. Cell. Biol. 62, 1158-1166, 1984). The theory of coupled photobleaching explains why FPR, in contrast, reports the first moment of the size distribution (under typical conditions of low levels of photobleaching) and is, therefore, not as useful for characterizing aggregate sizes.

GOLLOP:

What is the evidence that the laser beam doesn't cause changes in the cell other than photobleaching?

ELSON:

A variety of studies have shown that although the laser beam may cause adventitious photochemical reactions in the cell, those do not have a detectable effect on the diffusion coefficient measurements. (c.f.: K. Jacobson,

Y. Hou, I. Wojcieszyn, Exp. Cell. Res., 116, 179-189, 1978; D.E. Wolf, M. Edidin, P.R. Dragsten, Proc. Natl. Acad. Sci. USA, 77, 2043-2045, 1980; C.-L. Wey, R. Cone, M. Edidin, Biophys. J. 33, 225-232, 1981; D.E. Koppel, M.P. Sheetz, Nature, 293, 159-161. 1981.)

Dynamics of Biochemical Systems
S. Damjanovich, T. Keleti, L. Trón (Eds)

THE DYNAMICS OF ENDOCYTIC PROCESSING

CHARLES DELISI and MARIANNE GEX-FABRY

Laboratory of Mathematical Biology, Building 10, Room 4B-56
National Institutes of Health, Bethesda, Maryland 20205, USA

INTRODUCTION

The means by which cells swallow substances in their environment can be classified into two general categories. One includes a set of non specific processes such as fluid phase endocytosis in which villous surface structures bend back on themselves, trap fluid as they fuse with the membrane, and then pinch off as vesicles at the cytoplasmic surface. The other process avoids ingestion of large quantities of fluid and is mediated by ligand specific receptors. This review will focus on the latter, ligand specific mechanism.

Endocytosed receptors and ligand are often degraded, suggesting that at least one role for ligand specific endocytosis is the regulation of blood levels of signaling molecules. Another role is the regulation of intracellular concentrations of various substances such as low density lipoproteins which are needed for membrane synthesis. A considerable amount of dynamic and steady state data has appeared in recent years, describing various aspects of endocytosis such as binding, internalization, degradation and recycling in various receptor ligand systems. Mathematical models of some of these processes have been developed. In this paper we outline and briefly review the implications of a mathematical model which integrates the various features of endocytic processing including the relation between sorting pathways, and the modification of pathways when more than one ligand is present.

THE MODEL

The cell surface is considered to be a two dimensional fluid in which receptors are more or less free to move, typically with diffusion coefficients of order 10^{-10} cm^2/sec(Schlesinger et al, 1978). Most receptors that are unbound by ligand move freely in and out of coated pits, specialized surface structures that under normal conditions continually close on themselves to form vesicles at the cytoplasmic side of the membrane, and subsequently return to the surface. There are some exceptions to free mobility—the receptor for low density lipoprotein being a prominent example—in which the receptors appear to be a permanent part of the pit. The description of the dynamics of such exceptions will clearly be a special case of the more general description in which receptors are mobile.

Metabolically active cells at physiological temperatures are continuously endocytosing coated pits along with whatever receptors happen to be associated with them at the time of ingestion. When ligand is present, receptor ingestion is enhanced. The fate of the internalized ligand and receptor is variable and depends on the particular system (Gex Fabry and DeLisi, 1985). Thus, in the LDL and α macroglobulin systems, the receptor is recycled and the ligand degraded, while in the epidermal growth factor (EGF) system both receptor and ligand are degraded, with perhaps some recycling of the ligand. The insulin system behaves symmetrically to the EGF system: the molecule is degraded while its receptor appears to undergo degradation with some recycling. For the transferrin system both ligand and receptor are recycled.

These observations can be thought of in terms of a general system in which the ligand and receptor to varying degrees sort separately; the degree depending on local environment, which in turn could be a function of cell type or could to some extent be controlled by signals provided by the particular receptor-ligand system. The mechanistic basis for these differences is not essential to the model presented below, which incorporates sorting phenomenologically and can therefore be applied to any of the systems. That is to say, we are not attempting to explain why some

receptors recycle and others are degraded, but we are instead presenting a model that accounts for the dynamics of these processes in any given system. To the extent that changes in parameter values of such a model allow us to interpret the dynamics of a number of different systems, we will at least have a simple quantitative characterization of these differences. In the present paper our goal is more modest. We will review the model and assess the extent to which it is able to simulate and predict the dynamics of just one system—epidermal growth factor and its receptor—and discuss some of the biological implications of the analysis.

The mathematical model, its justification, and its relation to models of endocytosis presented by others have been reviewed previously(Gex Fabry and DeLisi, 1984a and ref cited therein; See also Wofsy and Goldstein, 1984). The basic idea is simple and not new: when a ligand binds a receptor, the receptor undergoes a conformational change which enables it to interact with a (hypothesized) coated pit molecule, perhaps a glycoprotein. The specificity for ligand is in the receptor only, with all receptor ligand complexes interacting with the same, or at most relatively few, coated pit proteins. Such two step binding with specificity in the first step only, is one mechanism by which ligand specific receptor internalization is increased over background and, as outlined below, it accounts quantitatively for a wide range of dynamic data on binding, endocytosis, recycling and degradation. The minimal mathematical expression of this idea requires seven variables: free ligand, free surface receptors, receptor-ligand complexes on the surface, free molecules in coated pits to which the ligand-receptor complex binds; receptor-ligand-coated pit protein complexes, free internalized ligand and free internalized receptor. Receptor-ligand complexes inside surface coated pits are assumed to be in equilibrium with receptor-ligand complexes outside coated pits (Fig 1). Depending on the data being analyzed, the model also readily incorporates intracellular ligand–receptor complexes which exist prior to independent sorting of the ligand and receptor.

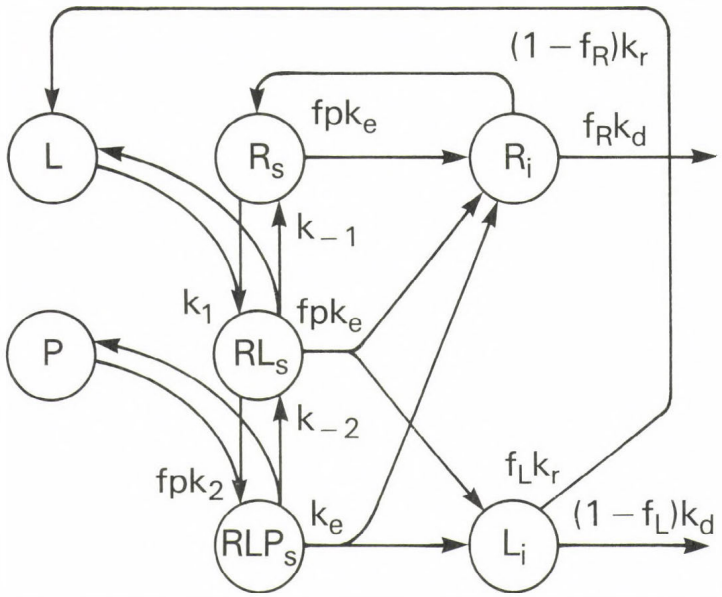

Fig 1. Receptor ligand complexes formed on the cell surface are internalized with coated pits and may then sort independently along one of several paths, some directed toward lysosomal degradation with rate proportional to k_d and others toward the surface with rate porportional to k_r. L is free ligand; R_s is free surface receptor; RL_s is the ligand receptor complex; P is the coated pit protein concentration; RLP_s is the ligand-receptor coated pit protein complex; L_i and R_i are the internalized ligand and receptor.

RESULTS AND DISCUSSION

We will be focusing almost entirely on the kinetic implications of the model, the steady state characteristics having been reviewed in detail elsewhere (Gex Fabry and DeLisi, 1984a,b). Briefly, however, we note that the steady state has a number of features with widespread implications including the following. (a) Variations in the number of coated pit proteins from one cell system to another can lead to substantial variations in the slope and intercept of linear Scatchard plots even when the number of ligand specific receptors is invariant. This variability may therefore contribute to the large variability seen in the affinities of EGF for its receptor, as well as to variations in receptor number determined for a variety of systems by Scatchard analysis. (b) As the number of coated pit

proteins decreases, the Scatchard plot can change from linear to non linear, even though only a single class of receptors is present. (c) Preincubation of cells with phorbol esters can change a non-linear plot to a linear plot. The first two effects are consequences of the two step binding mechanism (ligand to its receptor followed by interaction of the ligand-receptor complex to the coated pit protein); the last from a postulated competition between the EGF-receptor complex and the phorbol ester-receptor complex for the same coated pit protein. We now outline some dynamic consequences of the model.

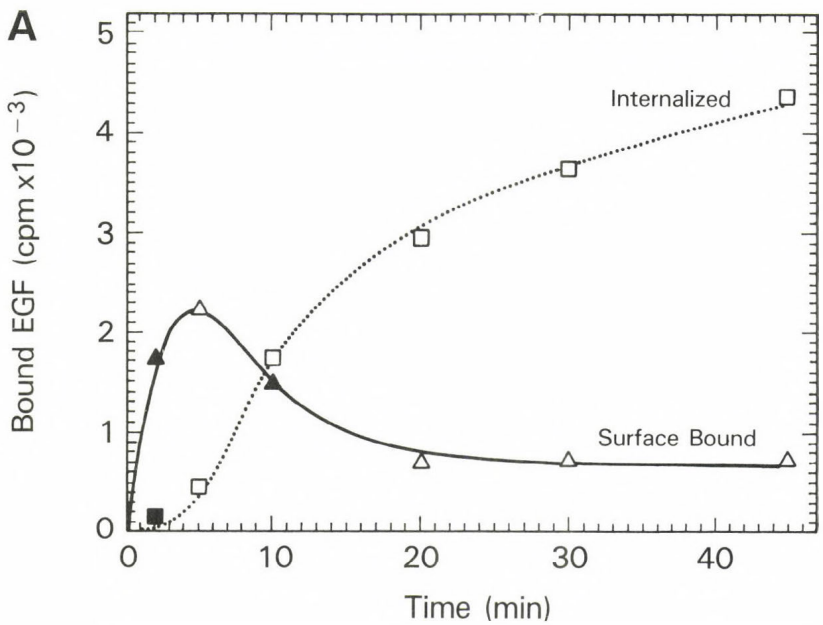

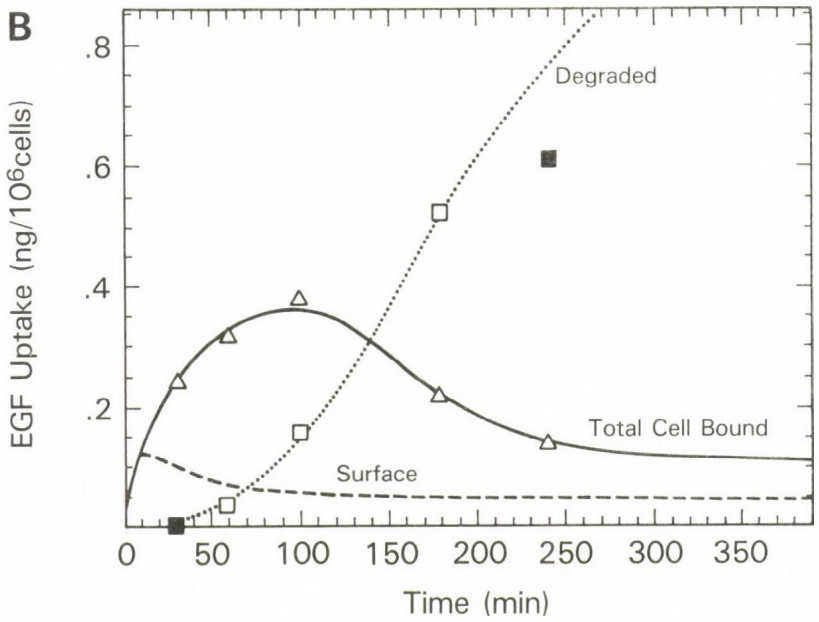

Fig 2. The amount of EGF on the surface of 3T3 cells peaks within the first 5 minutes and then falls due to internalization(A). On a longer time scale, internalization (and thus the total cell associated EGF) continues to increase, peaking at about 100 minutes, when the effects of degradation become prominent (B). Although data sets A and B were taken in different laboratories under slightly different conditions, the model fits both (lines through data points) with approximately the same set of parameter values. Data from Haigler et al (A) and Brown et al (B).

1. The kinetics of cell association, internalization and degradation of EGF

Simultaneous determinations of the kinetics of EGF bound to the surface of 3T3 cells and internalized by those cells display, over the first hour, a classic precursor-product relation. The surface bound concentration increases for about 5 minutes and then starts decreasing as the concentration of internalized EGF builds (Fig 2A) (Haigler et al, 1980). Longer time measurements performed by Brown et al (1979) (Fig 2B), also on the EGF-3T3 cell system, show degradation beginning at about 40 minutes, with the total cell associated EGF starting to drop shortly afterwards. We call attention to two aspects of the analysis. First, the model accounts quantitatively for these data sets with pretty nearly the same set of parameters, the small variations of generally less than a factor of two

arising in part because the experiments were performed in different laboratories under slightly different conditions including different temperatures. The parameter values, obtained by fitting the model to the data, have been presented elsewhere (Gex Fabry and DeLisi, 1984b). Briefly, the forward and reverse rate constants for EGF interacting with its receptor on 3T3 cells are about 10^8 $(M\text{-}min)^{-1}$ and $.59min^{-1}$ respectively. The average internalization time is somewhat over a minute; the average degradation time is about 50 minutes, and the average recycling time is about 20 minutes.

A second feature of the analysis is the distinction between two possible mechanisms for ligand induced receptor internalization. One possibility is that receptor internalization is enhanced solely as a consequence of an increased concentration of receptors in coated pits due to the affinity of ligand-receptor complexes for coated pit proteins. Another possibility, which is not exclusive of the first, is that the coated pit internalization rate depends on the presence of ligand. In fact the analysis indicates an eight-fold increase in the endocytic rate during the first 10 minutes subsequent to exposing the cells to ligand. It is the increased rate, and not coated pit clustering of ligand receptor complexes in itself, that makes the major quantitative contribution to the loss of receptors from the surface. This finding suggests that clustering is tightly linked to some relatively early biochemical event (e.g. activation of a nodal enzyme), leading to an increased rate of coated pit endocytosis. Since coated pits carry with them any receptors which happen to be present, the enhanced rate of endocytosis is not receptor specific, an observation that provides a basis for explaining both homologous and heterologous down regulation; i.e. the decreased ability of cells to bind some ligand shortly after preincubation with the same or a different ligand.

2. Regulatory Effects of Interacting Populations

Although *in vitro* experiments are easily performed under conditions in which cells are exposed to only a single well defined ligand, numerous populations, often highly interactive, are present *in vivo*, and it is important to begin to consider how they might effect one another. A system

which has been extensively studied is the mutual modulation of EGF and phorbol esters, the latter being potent tumor promoters which activate a Ca and phospholipid dependent protein kinase. The effect of incubating embryonal carcinoma cells with 12-O-tetradecanoyl phorbol-13-acetate (TPA) at 37^{o} for 30 minutes prior to adding EGF, is to reduce the binding of EGF at 4^{o} (not shown) and 37^{o} (Fig. 3).

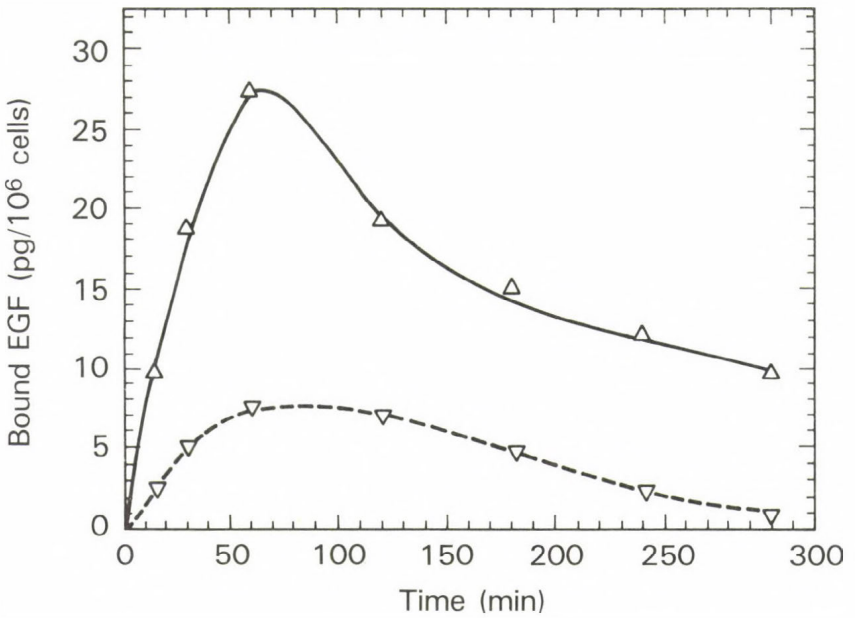

Fig 3. Embryonal Carcinoma (EC) Cells were preincubated in the presence (∇) and absence (Δ) of TPA for 30 minutes at 37^{o}. Cells were then incubated with 1 ng/ml EGF at 37^{o}. The curves were obtained by a best least squares fit of the data from Salomon (1981)

Such heterologous down regulation is in keeping with the observation made in the preceding paragraph on ligand enhanced endocytosis of coated pits, and hence of any receptors they might contain. Of note is that heterologous down regulation of unoccupied transferrin receptors by phorbol esters has recently been observed by Klausner (1984) and May (1984). It is worth emphasizing here that specificity in the first step, and its absence

in the second, suggests that receptor sequences consist of a portion or portions which vary from receptor to receptor and which therefore serve to recognize a particular ligand, and another portion which is evolutionarily conserved and acts as the link to the coated pit protein. Since a certain degree of conservation must be dictated by the apolar environment of the membrane, the cost of maintaining a relatively invariant portion of a receptor sequence would be minimized if the segment were membrane embedded.

The effects of the sequential or simultaneous presence of multiple ligands on cells is more complex than heterologous down regulation. Cells preincubated for three hours with EGF bind less phorbol 12,13 dibutyrate(PDB) than cells which had not been preincubated with EGF, but at later times, the former cell population shows enhanced binding (Fig 4).

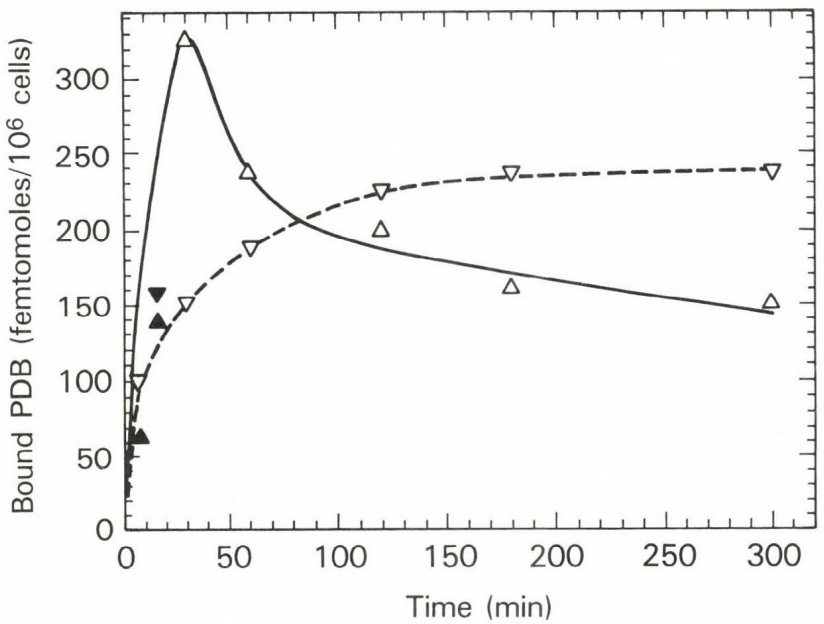

Fig 4. EC cells were preincubated for 3 hrs at 37° in absence (Δ) or presence (α) of 1μg/ml EGF. They were then incubated with 30nM PDB at 37°. The curves are best least square fits of the data, which were taken from Salomon (1981).

The early time decrease can be again explained by heterologous down regulation. Some insight into the subsequent increase might be provided by the fact that the simplest parameter adjustment required to fit the data is a delay in the delivery of the second ligand to lysosomes. Such a delay could lead to accumulation of ligand receptor complexes in prelysosomal organelles, shifting the equilibrium for their separation, and therefore, possibly the amount of material that sorts to a given pathway. The net result is the retardation and possible partial sparing of ligand degradation by the lysosomal machinery.

As a final illustration of the concerted action of several ligands on cell activity, possibly resulting in shifts in sorting pathways, we note that the ratio of surface to total cell associated EGF is somehwat larger in the presence of TPA than in its absence (Salomon, 1981). Analysis of the data (Gex Fabry and DeLisi, 1985) indicates that the difference is most likely the result of increased release of intact ligand from the intracellular volume when TPA is present. The effect might be relevant to the observations of Lee and Weinstein (1980) who found that the addition of phorbol esters at various times after mixing with EGF was associated with decreases in cell bound EGF and increases in the amount of intact EGF in the medium. Although the result can be simply explained by assuming that TPA induces dissociation of EGF from the surface, our results suggest that TPA affects intracellular sorting of EGF, producing a bias toward release of intact ligand rather than degradation.

REFERENCES

Brown, K.D., Y.C. Yeh and R.W. Holley (1979) J. Cell Physiol. 100: 227-238.

Gex-Fabry, M. and C. DeLisi (1984a) Math. Biosci. 72: 245-261.

Gex-Fabry, M. and C. DeLisi (1984b) Am. J. Physiol. 247: R768-R779.

Gex-Fabry, M, and C. DeLisi (1985) Regulation of Interacting Populations During Endocytic Processing: Models of Growth Factor Tumor Promoter Dynamics, in press.

Haigler, H.T., F.R. Maxfield, M.C. Willingham and I. Pastan (1980) J. Biol. Chem. 255: 1239-1241.

Klausner, R.D., J. Harford and J. VanRenswoude (1984) Proc. Natl. Acad. Sci. USA 81: 3005-3009.

Lee, L.S. and I. B. Weinstein (1980) Carcinogenesis 1: 669-679.

May, W.S., S. Jacobs and P. Cuatrecasas (1984) Proc. Natl. Acad. Sci. USA 81: 2016-2020.

Salomon, D.S. (1981) J. Biol. Chem. 256: 7958-7966.

Schlessinger,J., Y. Schechter, P. Cuatrecasas et al (1978) Proc. Natl. Acad. Sci. USA 75: 5353-5357.

Wofsy, C. and B. Goldstein: Coated Pits and Low Density Lipoprotein Receptor Recycling in Cell Surface: Concepts and Models (A. Perelson, C. DeLisi and F.W. Wiegel, eds) Dekker, New York, 1984, pp. 405-456.

Dymamics of Biochemical Systems
S. Damjanovich, T. Keleti, L. Trón (Eds)

INTERACTIONS BETWEEN MAJOR HISTOCOMPATIBILITY COMPLEX GLYCOPROTEINS AND PEPTIDE HORMONE RECEPTORS

MICHAEL EDIDIN

Department of Biology, The Johns Hopkins University,
Charles and 34th Streets, Baltimore, MD21218, USA

A major histocompatibility complex (MHC), a group of linked genes whose products play important roles in immune recognition and function, has been defined in all mammals examined and such complexes exist in birds, and likely in all vertebrates (Goetze, 1977). The similarities of function of linked MHC genes in mice and humans, the two species whose MHC has been carefully studied, is striking and suggests that the complex is a functional unit whose genes remain associated due to pressure of natural selection. The wide distribution of MHCs and the evidence that the component genes have been linked for over 30 million years (that is from before the time that rodent and primate stocks separated from the main mammalian stem) are striking. They suggest that the complex has evolved, probably by gene duplication, from a primitive MHC with other functions than the regulation of immune responses and the interactions of immunocytes with other cells.

The most commonly held view is that the products of the MHC evolved from primitive general systems for recognition at the cell surface (see, for example, Burnet, 1971, Bodmer, 1972, Ohno, 1977, Dausset and Contu, 1980 and Scofield et. al., 1982). Indeed, present structural evidence suggests that MHC antigens, imunoglobulins and some other surface glycoproteins are all derived from a small, ancestral, membrane protein (Hood et.al., 1985). We might expect then to detect ancestral functions of the MHC even in the existing MHC's and their products. Indeed, though the immune functions of the MHC have always been foremost, there has always been a background of ideas and experiments about other, non-immune functions of the complex (reviewed by Ivanyi, 1978). While some

associations of MHC and non-immune function are due to products of genes linked to the traditional MHC genes, most of the data on MHC/functional associations cannot be associated with unknown genes, and, rather must be explained in terms of unknown functions of known MHC gene products.

The products of the MHC have been classified as class I, class II and class III. Class III products are complement components and enzymes which are not readily related to the primary immune functions of the MHC. We will not discuss them further. Class II products are polymorphic surface glycoproteins, principally involved in recognition of antigen by helper T cells. They are limited in their distribution to a few cell types, principally macrophages, endothelial cells and B cells. These antigens will receive only passing mention in our discussion. Finally, there are class I antigens, plasma membrane glycoproteins consisting of a 44,000 heavy chain, non-covalently associated with a 11-12,000 light chain. These antigens are the most polymorphic molecules known, with literally hundred of alleles of each of two class I loci. The antigens are present on almost every cell of the body (muscle and brain may be exceptions), including: liver, kidney and intestinal epithelia, lymphocytes, fibroblasts and even erythrocytes. They are present in moderate to high numbers, ranging from around 10^3/cell in mouse erythrocytes to around 10^5/cell on lymphocytes. (Kimball and Coligan, 1983)

The class I antigens function immunologically as contexts for recognition of foreign, especially viral, antigens by effector T cells. That is, they are receptors for effector T cells, and they are highly specific receptors. T cells active against a viral antigen presented with a particular MHC class I allele will not lyse cells bearing the viral antigen together with a different allele of the same MHC antigen. (Zinkernagel and Doherty, 1979).

If these antigens retain some of their primitve recognition/ receptor function, then we expect them to influence the binding of non-immunologic ligands to cell surfaces. For a number of years my laboratory has explored this possiblity, studying peptide hormone binding to specific receptors as a system, outside of the immune system, in which MHC class I antigens might be expected to influence recognition.

We have worked on both the, H-2K and H-2D class I antigens of mouse and on the HLA-A,B,C antigens of humans. At this point we have considerable, though indirect, evidence that class I antigens do affect the binding of peptide hormones by their receptors. The time is rapidly approaching when physical techniques, such as resonance energy transfer, and measurement of rotational and lateral diffusion in membranes, may be used to detect and characterise interactions between MHC antigens and other cell surface receptors.

The general approach to testing MHC dependence of cell recognition phenomena has been through systems in which some aspects of recognition can be quantitated. The assumption is made, correctly, that while MHC antigens may modify or modulate recognition, they cannot act to abolish a recognition system and also cannot, by their presence create a new, qualitatively distinct recognition system. Thus all of the work in the area of "non-immune recognition" has been on the quantitation of specific recognition events such as cell-to-cell adhesion or the binding of hormones to specific receptors and subsequent cellular responses.

We began our work with a study of the resultant of peptide hormone action in liver, the steady-state level of adenosine 3':5'-cyclic monophosphate (cyclic AMP), cAMP. Our strategy was to measure and compare cAMP levels in livers of animals of congenic stains, differing only for the MHC. The strategy was successful, for we could show that the $H\text{-}2^b$ haplotype was consistently associated with levels of cAMP about 50% higher than those in animals of $H\text{-}2^k$ haplotype, irrespective of the strains carrying the H-2 chromosomes (Meruelo and Edidin, 1974) [Figure 1] The difference in levels segregated in F2 and backcross individuals derived from $H\text{-}2^b$ x $H\text{-}2^k$ congenic mice, and were later shown to segregate with H-2 in fully segregating crosses. Mapping studies with mice bearing recombitant MHC's indicated that the gene(s) affecting cAMP levels mapped telomerically in the complex, in or to the right of H-2D (Lafuse and Edidin, 1978)

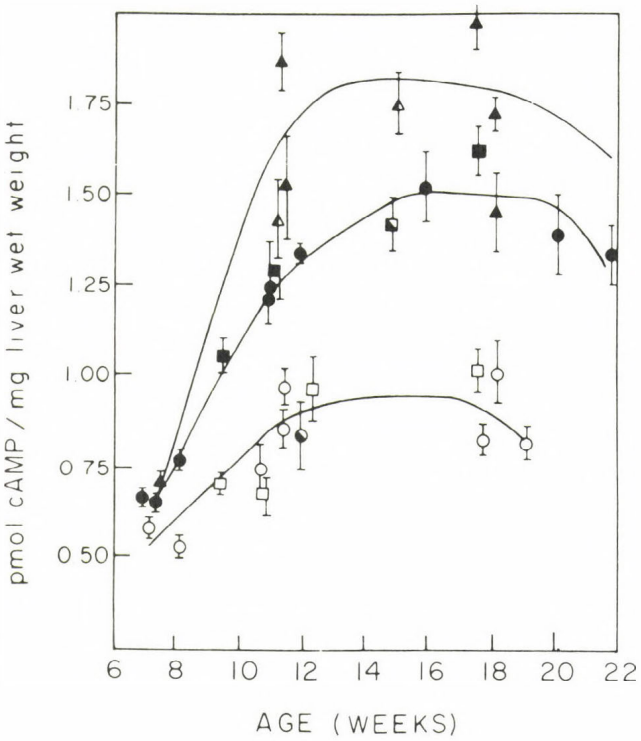

Figure 1. Effects of age and H-2 haplotype on levels of cAMP in liver. The top line, Δ's, gives levels for $H\text{-}2^a$ animals of various strains. The middle line, ●, ■'s, gives levels for $H\text{-}2^b$ animals, and the lower line, O, □'s, gives levels for $H2^k$ animals. From Meruelo and Edidin, 1974.

Steady-state levels of cAMP are a function of hormone binding, coupling of receptor to adenylate cyclase via the GTP-binding protein, activity of the cyclase itself, and activity of degredative enzymes, cyclic nucleotide phosphodiesterases. Careful comparisons of all of these systems between congenics led to the clear conclusion that H-2 affected the glucagon-stimulated adenylate cyclase, but none of the other components of the system. This led to further studies in which we showed that glucagon, which is the major hormone elevating liver cAMP, binds to receptors of different affinity in $H\text{-}2^b$ animals than in $H\text{-}2^k$ animals. Scatchard analysis of the data even indicated that glucagon receptors of $H\text{-}2^k$ animals interacted in a different way than receptors in animals of other haplotypes [Figure 2] (Lafuse and Edidin, 1980)

There are a number of other experiments, by us and others which similarly indicate that MHC haplotype influences the binding of insulin, prostaglandin and cholera toxin to cells. However, none of the experiments discriminates between the effects of products of MHC-linked genes and the effects of known MHC antigens. At this point we ought to consider the ways in which the MHC might affect peptide hormone receptors:

1. MHC antigens are peptide hormone receptors (Svejgaard and Ryder, 1976).

2. Genes for hormone receptors are linked to the MHC.

3. MHC antigens are obligate parts of functional hormone receptors (Simonsen et. al., 1984).

4. MHC antigens interact (weakly) with peptide hormone receptors, modifying their affinity and their interactions with one-another (Meruelo and Edidin, 1974: Chvatchko et. al, 1983).

5. The products of the MHC or of linked genes enzymatically modify hormone receptors.

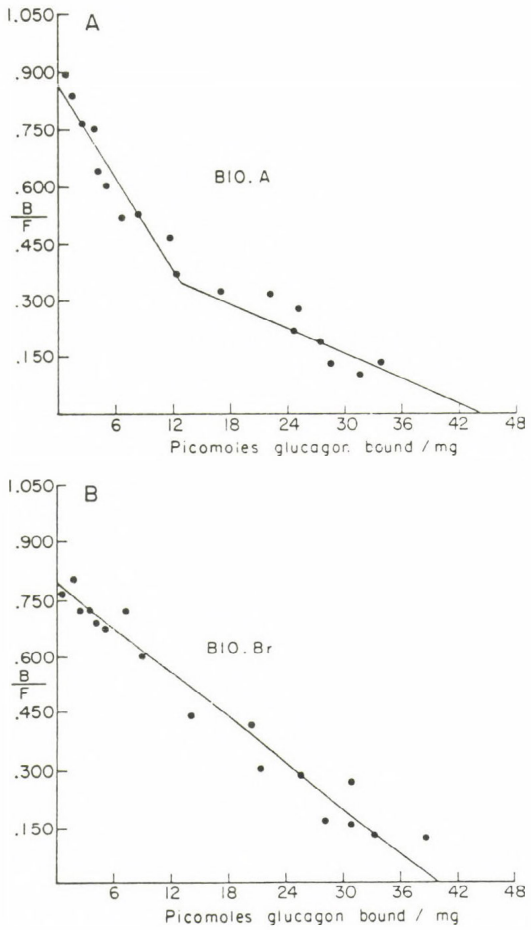

Figure 2. Scatchard plots of glucagon binding to liver plasma membranes A, from B10.A (H-2^a) and B, from B10.Br(H-2^k) animals.

The first two possibilities are the least likely. The structure of authentic peptide hormone receptors is quite unlike that of MHC antigens. Hence, the antigens are not themselves the receptors. MHC effects have been shown for three characterised receptors, for insulin, for glucagon and for epidermal growth factor (Czech et al, 1983). Genes for two of these receptors, EGF and insulin have been mapped to chromosomes other than the MHC chromosome of humans. Given the very great similarity in organisation of mouse and human MHC's and linked genes it is likely that the receptor genes will not map to the MHC in mice.

The idea that MHC antigens are obligate parts of peptide hormone receptors was developed by Simonsen and co-workers (1984), from their finding that Daudi cells which do not express MHC antigens also fail to bind insulin, and from experiments on the reciprocal effects of peptide hormones and of anti-HLA antibodies on each other's binding to HL-60 cells. In contrast, we found that Daudi cells (from the American Type Culture Collection) bear insulin receptors detected both by insulin binding and with anti-receptor antibodies. The Daudi insulin receptor has a K_D in the nanomolar range and there are a few thousand high affinity receptors per cell (K. Hosoi and M. Edidin, unpublished). This discordance may relate to clonal variation in Daudi cells, but it seems to tell against an obligate role for class I antigens in insulin receptor function.

Though we have not been able to use anti-H-2 or anti-HLA antibodies to specifically inhibit insulin binding to IM-9 or to liver cell membranes (Hosoi, unpublished), we have shown that anti-HLA antibodies and EGF reciprocally one another's binding to receptors in A431 cells (Schreiber et. al., 1984). Binding of either ligand sets in train a complicated series of internalizations and changes in cell metabolism and hence the results are not readily interpreted in terms of simple physical models of receptor-antigen association.

The possibility that MHC antigens interact weakly with peptide hormone receptors was proposed to explain several sets of results, including our own on associations of cAMP levels with MHC haplotype. This interaction is also in line with mainstream immunology's ideas about

the function of MHC antigens in the recognition of other surface antigens. Direct chemical evidence for such association was obtained by Chvatchko and co-workers(1983). They photoaffinity labelled insulin receptors in mouse liver membranes and showed that antibodies to class 1 antigens, but not normal serum or irrelevant anti-I-A antibodies, precipitated about 5% of the labelled insulin receptor together with the expected MHC heavy chain. The experiments suggest a weak association bewteen insulin recpetor and MHC antigens.

The last possibility on my list, enzymatic modification of receptors by MHC antigens, is the most speculative. No enzymatic activities have been associated with known MHC antigens, though some years ago Parish and co-workers (1981) speculated that the antigens might be glycosyltransferases, the enzymes which transfer sugars from sugar-nucleotides to specific macro-molecular acceptors. Roth (1985) has recently speculated that MHC antigens and glycosyltransferases are related by descent and has published some preliminary evidence that a galactosyltransferase co-purifies with a class II MHC antigen (Furukawa et. al., 1985). If other MHC antigens also have transferase properties, then one can readily see how some MHC haplotype might modify receptor glycoproteins.

We have now discussed all of my list of the possibilities for MHC effects on peptide hormone binding. Though the first two can likely be ruled out, we have not resolved the last three of these possibilities. While experiments of several sorts suggest themselves, it would be of particular interest to make physical measurements of MHC antigen-peptide hormone receptor proximity in intact cells.

Acknowledgements

Original work reported in this paper was supported by NIH grants AI-14584 and AI-19814. This is contribution number 1286 from the Department of Biology.

References

Bodmer, W.F. 1972. Evolutionary significance of the HL-A system. Nature 237: 139.

Burnet, F.M. 1971. "Self-recognition" in colonial and marine forms and flowering plants in relation to the evolution of immunity. Nature 232: 230.

Chvatchko, Y., van Obberghen, E., Kiger, N., and Fehlman, M. 1983. Immunoprecipitation of insulin receptors by antibodies against class 1 antigens of the murine H-2 major histocompatibility complex. FEBS Letters 163: 207.

Czech, M., Oppenheimer, C., and Massague, J. 1983. Interrelationships among receptor structures for insulin and peptide growth factors. Fed. Proc. 42: 2598.

Dausset, J. and Contu, L. 1980. Is the MHC a general self-recognition system playing a major unifying role in an organism? Human Immunology. 1: 5.

Furukawa, K., Higgins, T., and Roth, S. 1985. An affinity-purified major histocompatibility complex (MHC) antigen with high N-acetylgalactos-aminyltransferase activity. J. Cell Biol. in the press.

Goetze, D. (ed). 1977. The major histocompatibility system in man and animals. Springer-Verlag, Berlin.

Hood, L., Kronenberg, M., and Hunkapiller, T. 1985. T cell antigen receptors and the immunoglobulin supergene family. Cell 40: 225.

Ivanyi, P. 1978. Some aspects of the H-2 system, the major histocompatibility system in the mouse. Proc. Roy Soc. Lond. B 202: 117.

Kimball, E.S. and Coligan, J. E. 1983. Structure of class I major histocompatibility antigens. Contemp. Topics Molec. Immunol. 9: 1-64.

Lafuse, W. and Edidin, M. 1978. The genetic control of liver cAMP levels in mice. Immunogenetics 9: 57.

Lafuse, W. and Edidin, M. 1980. Influence of the mouse major histocompatibility complex, H-2, on liver adenylate cyclase activity and on glucagon binding to liver cell membranes. Biochemistry 19: 49.

Meruelo, D. and Edidin, M. 1975. Association of mouse liver adenosine 3':5'-cyclic monophosphate (cyclic AMP) levels with Histocompatibility-2 genotype. Proc. Nat. Acad. Sci. USA 72: 2644.

Ohno, S. 1977. The original function of MHC antigens as the general plasma membrane anchorage site of organogenesis-directing proteins. Immunol. Rev. 33: 59.

Parish, C.R., O'Neill, H.C. and Higgins, T. J. 1981. Glycosyltransferases and T-cell recognition. Immunology Today 2: 98.

Roth, S. 1985. Are glycosyltransferases the evolutionary antecedents of the immunoglobulins? Quart. Rev. Biol. 60 in the press.

Schreiber, A.B., Schlessinger, J., and Edidin, M. 1984. Interaction between major histocompatibility complex antigens and epidermal growth factor receptors on human cells. J. Cell Biol. 98: 725.

Scofield, V.L., Schlumpberger, J.M., West, L.A., and Weissman, I. 1982. Protochordate allorecognition is controlled by a MHC-like gene system. Nature 295: 499.

Simonsen, M., Skjodt, K., Crone, M., Sanderson, A., Fujita-Yamaguchi, Y., Due, C., Ronne, E., Linnet, K., and Olsson, L. 1984. Compound receptors in the cell membrane. Ruminations from the borderland of immunology and physiology. Prog. Allergy 36: 151.

Svejgaard, A. and Ryder, L.P. 1976. Interaction of HLA molecules with non-immunological ligands as an explanation of HLA and disease associations. Lancet ii: 547, 1976.

Zinkernagel, R.M. and Doherty, P.C. 1979. MHC-restricted cytotoxic T cells: Studies on the biological role of polymorphic major transplantation antigens determining T-cell restriction specificity, function and responsiveness. Adv. Immunol. 27: 51-177.

PECHT:

Is there any evidence for specificity in the interactions between MHC components and hormone/growth factor-receptors?
Have any experiments been done in order to detect such interactions (e.g. covalent crosslinking)?

EDIDIN:

Chvatchko and co-workers (FEBS Letters, 163:201) have co-precipitated a small fraction of affinity-labelled insulin receptor with MHC antigens, using anti-MHC antibodies. I do not know of any other chemical evidence for such associations.

SRERE:

Does the quantity of immobile protein change in the mutant cells or in the "tailless" construct? Does the distribution of diffusion coefficients change in these cases?

EDIDIN:

The quantity of immobile label appears higher in cells expressing mutant antigens, than in cells expressing wild-type antigens. However, the level of mutant antigens is lower than that of wild type and part of the immobile fraction is probably in fact background, autofluorescence or scattered light. We have to re-determine the mobile fraction of mutant antigens using a more sensitive photomultiplier tube.

CHERRY:

The diffusion coefficient you measured for the antigens is close to 10^{-9} cm^2s^{-1} and hence not as low as often observed for plasma membrane proteins. Bearing in mind that diffusion is known to decrease with measuring protein concentration, it seems to be just possible that you do have free diffusion in this case, which would explain

the similarity in diffusion coefficients of the mutant antigens.

EDIDIN:

This may be possible. However, I should note that diffusion of the mutant antigens is completely inhibited (0 % mobility) in many cells from dense cultures. This effect of culture density on antigen mobility is the same as seen for wild-type antigens. That is, diffusion of mutant antigens can be reduced to immeasurably low rates despite the antigens' lack of cytoplasmic tails.

FÉSÜS:

Have you quantitated the number of mutant proteins on the surface in your transfection experiment? If yes, wasn't the difference among these numbers too high (because of the unpredictability of the transfection experiment) to permit comparative experiments regarding the diffusion of hormone receptors?

EDIDIN:

We have not measured diffusion of hormone receptors, only their affinity. The number of H-2 antigens expressed after transfection does vary, but this does not appear to affect their lateral diffusion.

ELSON:

Is haplotype correlated with susceptibility to diabetes?

Is the efficiency of B-cell activation by antigen or by crosslinking surface immunoglobulin (SIg) correlated with haplotype? If so, does H-2 antigen cocap with surface immunoglobulin?

EDIDIN:

Yes. The main correlation is with a Dr antigen, apparently associated with juvenile-onset diabetes (probably involving the immune response to a viral infection). However, there

are also claims of HLA-A and B alleles associated with diabetes.

There was one abstract some years ago that claimed haplotype-associated differences in lectin activation of mouse lymphocytes. I don't know of any other.

DAMJANOVICH:

There is a contraversy concerning the role of the cytoskeletal elements in controlling the lateral diffusion of integral membrane proteins. Would you mind commenting this problem?

Do you know any quantitative data on the number of insulin receptors per cell surface area when you measure lower K_d for insulin binding?

EDIDIN:

Four sets of experiments suggest that cytoskeletal elements affect lateral diffusion of integral membrane proteins. 1.) Cytochalasin B, which interacts with actin filaments, inhibits lateral diffusion. 2.) Lateral diffusion of membrane proteins is increased ten-fold in membranes that have ballooned away from their underlying cytoplasm. 3.) Purified membrane proteins in synthetic membranes diffuse at least an order of magnitude faster than the same proteins in native membranes. 4.) In fibroblasts with highly organized cytoskeletons, lateral diffusion is anisotropic, being about 50-fold faster parallel to the orientation of the cytoplasmic filaments than perpendicular to the filaments.

The number of insulin receptors per cell is highly variable in these lines.

TRÓN:

I think the detailed mechanism of slowing down lateral diffusion of proteins in biological membranes is pretty

far from being wholly understood. There are several possibilities to do this. You have presented here nice evidence which rules out the decisive role of friction between the intracellular part of the MHC antigens and the cytosole.

Data are presented in the literature on very slow protein diffusion in erythrocyte ghosts. However, getting rid of the spectrin when preparing ghosts, the rate of diffusion is increased practically to the level found with artificial bilayers. There have been an increasing amount of publications during the last years reporting about spectrin-like proteins in cells other than erythrocytes. I wonder if the network of spectrin or spectrin-like proteins on the surface of the cytoplasmic membranes can be a general feature of a broad range of cells. Furthermore, I think, instead of the model with steadily decreased diffusional rate or that describing specific interactions between membrane proteins and the cytoskeleton one can set up another one explaining the slowing down phenomenon in the following way. There is a non-inhibited fast diffusion of intramembraneous proteins within each individual region of the spectrin-like network and the slow diffusion rate in the μm range is simply the consequence of the dynamics of eventual opening and closing of gates (pores) acrosss the network of the spectrin-like proteins, in the case of a great variety of cells. Would you comment that, please?

EDIDIN:

There are data indicating that extraction of the erythrocyte membrane cytoskeleton increases lateral diffusion of band 3 proteins (Golan and Veatch, Proc. Natl. Acad. Sci. USA, 77, 2537, 1980). The lateral diffusion of band 3 is also increased in erythrocytes which, genetically, lack spectrin (Koppel et al., Proc. Natl. Acad. Sci. USA, 78, 3576, 1981) and the model that you suggest, of a spectrin network limiting lateral diffusion without directly interacting with trans-membrane proteins, has been proposed

by the authors of the latter paper. It remains to be seen if similar, spectrin-dependent, constraints exist in nucleated cells.

Dynamics of Biochemical Systems
S. Damjanovich, T. Keleti, L. Trón (Eds)

TWO-BINDING-SITE MODEL OF Fc RECEPTORS ON HUMAN K CELLS

JÁNOS GERGELY and GABRIELLA SÁRMAY

Department of Immunology, Eötvös L. University,
H-2131 Göd, Hungary

Fc receptors (FcR) which interact with the C-terminal domains of immunoglobulins of various isotypes are expressed on a wide range of cells, most of them belonging to the immune system. The signals and functions mediated by these receptors are manifold and represent partly effector functions (such as release of mediators, opsonized phagocytosis, antibody dependent cellular cytotoxicity (ADCC)), and partly regulatory mechanisms (e.g. regulation of B cell proliferation, isotype regulation). Different isotypes of FcR-s are expressed on the same T-cells and the prevalent expression of one of the isotypes on the account of the others can be induced by a given isotype of immunoglobulin.

To understand this functional diversity and flexibility in expression one has to consider the structural basis of FcR heterogeneity. Similarly to their natural ligands, the immunoglobulin binding receptors on various cells are very heterogenous. This fascinating heterogeneity of FcR-s might mean first of all differences in the primary structure, and one might suppose that immunoglobulins and FcR-s diverge parallelly during phylogenesis (1). Besides this obvious form, another type of FcR heterogeneity was suggested by us. Studying the structural and functional characteristics of IgG-binding FcR-s on human peripheral lymphocytes a phenomenon, called "receptor conversion" was described by us, showing that the binding specificity (consequently the function) of different conformational forms of the same FcR molecule might be different (2-7).

In the present paper we summarize our data showing that

- depending on the prevailing stimuli and/or actual level of differentiation IgG FcR-s are expressed either in monomeric or polymeric (crosslinked) form;
- the monomeric receptor possesses one active binding site interacting with the CH3 domain of IgG;
- the crosslinking of the monomeric receptor units results in the expression of a second, CH2 domain specific binding site (receptor conversion);
- the functions of the two-binding-sites are different.

Monomeric and polymeric forms of IgG FcR-s. The finding that human peripheral lymphocytes shed their IgG FcR-s after 4-37°C temperature shift while another population does not shed the FcR-s under identical experimental conditions allowed us to distinguish between two forms of IgG binding structures. The shed receptors were found to be monomeric, monovalent, 60.000 m.w. molecules possessing only one active binding site interacting with the CH3 domain of IgGFc, while two active binding sites, one of them CH3, the other CH2 domain specific, were found to be expressed on the polymeric (crosslinked, anchored) form. In in vitro experiments (6, 7) the crosslinking of the isolated monomeric FcR-s either on actomyosin or by transglutaminase resulted in "receptor conversion", i.e. in the expression of the second binding site for the CH2 domain, besides the preexisting CH3 specific one. "Receptor conversion" in both directions was observed on the cell membrane as well (8, 9). Thus ligand binding Concanavalin A (Con A) or α-IF stimulation resulted in the expression of the polymeric, "two binding site" form, while anti-β_2-microglobulin antibodies induced shedding and depolymerization of the crosslinked receptors. Moreover, since IgG FcR-s were found to be expressed only in polymeric form on K and NK cells (10), one may suppose that receptor conversion might not only be the consequence of prevailing stimuli but also reflects the actual level of cell differentiation.

The "two-binding-site-model" of IgG FcR-mediated killing in ADCC. It is generally accepted that K-cells in ADCC need functionally intact IgG FcR-s (11, 12). On the other hand, data dealing with the localization of submolecular sites on IgGFc reacting with the FcR-s on K-cells are conflicting, and the preferential role either of the CH2 or CH3 domains is still an unsettled question. The finding that FcR-s are expressed in polymeric form on K cells gave us a good opportunity to study

- the two-binding-site character of the FcR-s;
- to localize the groups within the CH2 and CH3 domains interacting with the FcR binding sites;
- to identify the function of the individual binding sites.

Supposing that the prerequisite of killing in ADCC is the simultaneous binding of both IgG Fc domains to both receptor binding sites, we studied whether the killing could be abolished when the bindings of domains to the corresponding sites were inhibited separately. To achieve the individual blocking of CH2 and CH3 specific binding sites, Clq (interacting with CH2) and soluble monomeric FcR (binding to CH3), synthetic polypeptides comprising sequences of human γ-1 chains, as well as monoclonal antibodies recognizing epitopes expressed within CH2 or CH3 domains of IgG1, were used. The results can be summarized as follows:

a. Both Clq and soluble monomeric IgG FcR inhibited ADCC dose dependently (10);

b. Three synthetic polypeptides representing CH2 domain sequences and a slightly modified CH3 domain sequence showed dose dependent inhibitory activity in ADCC (10). A stable specific interaction between these synthetic peptides and K-cells was found, showing that a portion of the synthetic peptides adopted the biologically active conformation allowing the high affinity binding to the FcR binding sites.

c. Some monoclonal antibodies having specificity for CH2 or CH3 domain epitopes inhibited ADCC dose dependently and significantly, whilst others gave no inhibition. Similar inhibition was obtained with antibodies specific for IgG1 sub-

class, while an other monoclonal antibody having specificity for a CH1 domain epitope exerted no inhibitory effect (13).

These data proved that

- IgG FcR possessing two-binding-sites characterize the effector lymphocytes of ADCC;
- the simultaneous interaction of the Fc-domains of the target-sensitizing antibody with both binding sites is the prerequisite of killing;
- the groups reacting with one of the binding sites are situated within the CH2 domain in the region of 274/Lys/-301/Arg/, while the groups interacting with the other binding site involve the residues of 408/Ser/-416/Arg/ of the CH3 domain.

Different functions of the two FcR binding sites. The observation showing that only simultaneous ligand binding to both binding sites is able to induce killing activities does not necessarily mean that both sites equally transfer killing signals. An experimental system described by us allowed to study the individual role of each binding site of FcR in ADCC.

We described earlier that Con A stimulated T-cells express C3b-acceptor (C3b-A) sites interacting with the metastable binding site of nascent C3b molecules. Cell surface proteases on Con A activated T cells split C3 which binds to the newly expressed C3b-A-s and the cells, armed by the C3b-A-bound C3b are ready to form bridges to C3b-receptor (CR) bearing target cells. Using C3b-armed Con A-blasts as effectors and CR1-bearing human red blood cells sensitized with anti-D IgG as targets, an enhanced ADCC was measured (14). Testing the influence of CH2 and CH3 domain specific monoclonal antibodies on the killing capacity in this system enlighted us on the possible function of the CH2 and CH3 specific FcR binding sites (13).

Comparing the effect of F(ab) fragments of the CH2 (A55) and CH3 domain specific (x3A8) monoclonal antibodies on EA rosette formation as well as on ADCC it was found that the CH2 domain specific antibody did not significantly affect the EA rosette formation in contrast to the CH3 domain specific

antibody. On the other hand, the former markedly inhibited ADCC activity both of non-stimulated effector cells and Con A stimulated cells in the presence of C3. The inhibitory effect of the CH3 specific x3A8 monoclonal antibody was considerably smaller and the enhancing effect of C3 on the killing capacity of Con A stimulated effectors was not influenced by this antibody.

These results speak for the role of CH3 domain specific binding sites in the target-effector binding and emphasize the importance of the CH2 specific site in the transfer of killing signal.

References

1. Haeffner-Cavallion, N., Klein, M., Dorrington, K.J. (1975) Studies on the Fcγ receptor of the murine macrophage-like cell line P388D1. I. The binding of homologous and heterologous immunoglobulin G. J. Immunol. 123, 1905-1913.
2. Sármay, G., István, L., Gergely, J. (1978) Shedding and reappearance of Fc, C3 and SRBC receptors on peripheral lymphocytes from normal donors and chronic lymphatic leukemia patients. Immunology, 34, 315-321.
3. Sándor, M., Füst, G., Medgyesi, G.A., Erdei, A., Gergely, J. (1979) Heterogeneity of Fc receptors on human peripheral mononuclear blood cells. Immunology, 38, 553-560.
4. Sándor, M., Füst, G., Medgyesi, G.A., Gergely, J. (1978) Isolation and characterization of Fc receptors shed from human peripheral mononuclear cells. Immunology, 35, 559-566.
5. Gergely, J., Erdei, A., Sándor, M., Sármay, G., Uher, F. (1982) The Fc receptor model of membrane cytoplasmic signalling. Molec. Immunol. 19, 1223-1228.
6. Uher, F., Jancsó, A., Sándor, M., Pintér, K., Bíró, E., Gergely, J. (1981) Interaction between actomyosin complexes and Fc receptors on human peripheral mononuclear blood cells. Immun. Letter, 2, 213-217.
7. Fésüs, L., Erdei, A., Sándor, M., Gergely, J. (1982) The influence of tissue transglutaminase on the function of Fc receptors. Molec. Immunol. 19, 39-43.

8. Gergely, J., Sándor, M., Sármay, G., Uher, F. (1984) Fc receptors on lymphocytes and K cells. Biochem. Soc. Transactions, 12, 739-743.
9. Sármay, G., Gergely, J. (1983) Activation of lymphocytes alters Fc receptor-β_2-microblobulin interrelationship on the lymphocyte surface. Cell. Immunol. 78, 73-82.
10. Sármay, G., Benczur, M., Petrányi, Gy., Klein, É., Kahn, M., Stanworth, D.R., Gergely, J. (1984) Ligand inhibition studies on the role of Fc receptors in antigen-dependent cell-mediated cytotoxicity. Molec. Immunol. 21, 43-51.
11. Spiegelberg, H.L., Perlmann, H., Perlmann, P. (1976) Interaction of K lymphocytes with myeloma proteins of different IgG subclasses. J. Immunol. 117, 1464-1471.
12. Klein, M., Neauport-Sautes, C., Ellerson, J.R., Fridman, W.H. (1977) Binding site of human IgG subclasses and their domains for Fc receptors of activated murine T cells. J. Immunol. 119, 1077-1088.
13. Sármay, G., Jefferis, R., Klein, E., Benczur, M., Gergely, J. (1985) Mapping the functional topography of Fcγ with monoclonal antibodies: localization of epitopes interacting with the binding sites of Fc receptor on human K cells. Eur. J. Immunol. 15, 1037-1042.
14. Erdei, A., Benczur, M., Fábry, Zs., Dietrich, M.P., Gergely, J. (1984) C3 cleaved by membrane proteases binds to C3b-acceptors expressed on Con A-stimulated human lymphocytes and enhances antibody dependent cellular cytotoxicity. Scand. J. Immunol. 20, 125-131.

DISCUSSION

SEGAL:

Is there a relationship between the Leu-II antigen and the type II Fcγ receptor?

How do you envision that polymerization of the type I receptor gives rise to the CH2 binding site on the type II receptor?

GERGELY:

It was not investigated.

The consequences of in vitro receptor polymerization were studied in rosette inhibition tests. The monomeric receptor inhibits only the EA rosette formation of FcR^+ cells in contrast to the polymerized soluble FcRI, which inhibits the FcRII bearing cells as well.

PECHT:

Did I understand it correctly that those binding sites of FcγR interacting with CH2 do not interact with the CH3 domains and possibly vice versa? This would be in line with the report by Baird and Holowka concerning the mode of binding of IgE to $Fc_\varepsilon R$.

GERGELY:

The binding sites of Fc-γ-receptors on K cells are domain specific, i.e., one of them interacts only with the CH2 the other with the CH3 domain of IgG. This has been proved in inhibition experiments using domain specific monoclonal antibodies, synthetic polypeptides represe-ting linear sequences of CH2 or CH3 domains, moreover, recently by separate inhibition of the binding sites with CH2 or CH3 domain-deleted myeloma proteins.

EDIDIN:

Does the anti-β-2-microglobulin react directly with the Fcγ receptor, to depolymerize it, or is the effect of the antibody indirect?

GERGELY:

The binding of anti-β-2-microglobulin antibodies to lymphocyte membrane results in reordering of the membrane including the co-shedding of β-2-microglobulin-antibody complexes and Fc receptors. The Fc receptors are present in the supernatants of the cells in monomeric form (see ref. 9).

Dynamics of Biochemical Systems
S. Damjanovich, T. Keleti, L. Trón (Eds)

ON THE ROLE OF CELL SURFACE DYNAMICS AND TRANSMEMBRANE INFORMATION TRANSFER: CYCLOSPORIN A CHANGES PHYSICAL PROPERTIES OF CELL MEMBRANES

L. TRÓN*, S. DAMJANOVICH*+, A. ASZALOS+, J. SZÖLLŐSI*, SALLY A. MULHERN+ and M.J.FULWYLER++

*Department of Biophysics, Medical University School of Debrecen, H-4012 Hungary,
+Food and Drug Administration, USA, Washington DC, 20204
++Laboratory for Cell Analysis, Department of Laboratory Medicine, UCSF, San Francisco, CA 94143

INTRODUCTION

Protein and lipid elements of the outer cytoplasmic membrane do not form a rigid, static entity despite the role of the membrane as border between cell interior and the extracellular space. Every major element of the cell membrane has mobility with different degree of freedom in the plane of the membrane as well as perpendicular to it (1, 2). Biophysical approach to study these complicated two and three dimensional movements of the cell surface elements has been hindered by the lack of suitable methodology. The advent of new techniques like Fluorescence Recovery After Photobleaching (FRAP), Flow Cytometric Energy Transfer (FCET), measurement of transmembrane potential of living cells, determination of rotational parameters of lipid and protein elements of the cell membrane, and many other methods brought about new possibilities to study dynamic properties of the membrane (1-6, 24, 30, 31, 36).

The general mechanism of transmembrane signalling is not independent of the dynamic properties of the cell surface lipids and proteins. An accepted scheme of cell activation generally starts with an increase of intracellular Ca^{2+}, generating Ca^{2+}-ATP activating calmodulin and phosphokinase systems, ultimately leading to the regulation of DNA replication (36). The most elementary step in the long line of events is the increased permeability of membrane to different ions, among them Ca^{2+}. Since any ion transport changes across the membrane are connected to opening and closing the ion channels

is question, the proximity of membrane proteins, their mobility (translational or rotational) in the plane of and perpendicular to the membrane, as well as the altered membrane potential as a consequence of the altered ion transport are of paramount importance from the view point of information transfer through the membrane.

Herewith we present some of our data dealing with the altered properties of lymphocyte membranes when cyclosporin A (CsA) a well-known drug, with largely unknown mode of action is applied to these cells.

CsA, a cyclic endecapeptide antibiotic, has become essentially indispensable in solid organ transplantation (7-8) for suppressing allograft rejection without compromising humoral immunity (8). The cellular and molecular mechanism of this selective effect of CsA on cytotoxic T lymphocytes has not yet been explained despite many thorough investigations resulting in data on quite a few biochemical interactions of the drug with cellular metabolism. The dose-response relationship of CsA is generally studied by observing the suppression of cell mediated cytotoxicity in mixed lymphocyte cultures. Thus, in mixed human, mouse or guinea pig lymphocyte cultures suppression of proliferation and generation of cytotoxic T lymphocytes was observed in association with inhibition of interleukin-2 (IL-2) production (9-11). Subsequently it was shown that IL-2 production was inhibited by CsA at the level of mRNA synthesis (12, 13). CsA inhibited IL-2 synthesis, but the IL-2 receptor expression remained intact and the receptors were responsive to IL-2 in mouse lymphocyte cultures of Balb/c and C57BL/6J mouse spleen cells (14). An inhibition of mitochondrial and lysosomal functions was observed after CsA treatment of cultured mouse spleen lymphocytes (15). Studies with radio-labeled CsA and thymoma cells of mice indicated an association of the drug with a specific intracellular protein fraction (16), and recently it has been found that CsA may inhibit the function of calmodulin through binding to the protein (17). Efforts were made to investigate the preferential uptake of dansyl-labeled CsA by different subsets of human peripheral blood lymphocytes. These investigations found a "dim" and a "bright" population of cells, classified on the

basis of their dansyl-CsA content (18, 19). Due to this wide variety of effects of CsA at the cellular and molecular levels it was suggested by us that an earlier effect of CsA on lymphocytes may be the common denominator for the above mentioned and far from complete list of different activities of the drug (20, 21). In order to approach this complex question, efforts were made to find the earliest possible effect(s) of the CsA. Since the very first theater of any drug-cell encounter is per se the cell membrane, characteristic functional and morphological changes were sought to monitor the drug-membrane interaction. As we reported earlier, CsA and CsG decreased the cytoplasmic membrane potential of splenic and thymus cells of A/J mice without differentiating between T and B cells (20, 21).

In our present study on human peripheral blood mononuclear cells and mouse spleen and thymus lymphocytes, selected techniques were applied to study the properties of the cytoplasmic membrane immediately after CsA treatment; namely (i) flow cytometric membrane potential measurements; (ii) combined effects of specific ionophores and CsA in a flow cytometric as well as in a spectrofluorimetric system; (iii) flow cytometric measurements of fluorescence resonance energy transfer on a cell by cell basis; (iv) ion flux measurements on CsA treated lymphocytes, (v) ESR measurements of lymphocyte membrane in the absence and presence of CsA.

The data obtained from the above experiments support the view that the addition of the cyclosporin immediately influences the properties of the cytoplasmic membrane in such a fashion that these effects could subsequently be responsible for the later biochemical changes in cell metabolism and ultimately for the biological response of lymphocytes to the CsA treatment.

MATERIALS AND METHODS

Cells. Peripheral blood (40-100 ml) from normal human volunteers was drawn into EDTA containing tubes. The blood was diluted three times with 1.5 mM potassium containing phosphate buffered saline (PBS), pH 7.2, and fractionated on Ficoll-Hypaque gradients according to the method of Boyum (22) and

counted in a Coulter counter. HUT-102 cells were a present from Dr. Thomas Waldman (NIH). Mouse spleen cells were prepared from spleen of A/J mice in the same PBS and were also fractionated on Ficoll-Hypaque. Thymus cells of A/J mice were used without Ficoll gradient purification. The cell suspensions were kept on ice, until they were rewarmed to room temperature for use in experiments. The experiments were carried out within 1-3 hours. Viability of cells, determined by the fluorescein diacetate test in a cell sorter, was higher than 95 % (23)

Determination of the membrane potential in a flow cytometer. For membrane potential measurements the cells were labeled with the translocating dye, dihexyloxacarbocyanine iodide ($DiOC_6(3)$, Molecular Probes Inc., Junction City, OR) (24). A stock solution of the dye was prepared in DMSO (spectroscopic grade, Zellerbach Inc.) and diluted to 50 µM concentration. This dye solution was added to 1 ml of cell suspension containing $1\text{-}2\text{x}10^6$ cells so that the final concentration was 125-250 nM. This dye concentration was non-toxic during the measurement. Fluorescence intensity of labeled cells was measured in a Coulter Epics V flow cytometer (25). The laser was tuned to 488 nm and the output was usually kept at 400 mW. The forward angle light scatter and right angle green fluorescence intensities were collected correlatedly for each cell. The fluorescence signal was gated with the light scatter so that the measured cells were lymphocytes. Since peripheral blood lymphocytes and mouse lymphocytes are purported to have no or only very few mitochondria, no mitochondrial poison was required to avoid the interference of mitochondria potential with the cytoplasmic one. Changing the extracellular potassium concentration from 1.5 to 160 mM was rapidly followed by changes in the fluorescence intensity indicating that the measured values signaled cytoplasmic potentials. The scaling with potassium made possible to arrange such an instrumental setting that the zero potential (non-responding fluorescence) was positioned at the furthest left of the histograms. Depolarization with gramicidin and hyperpolarization with valinomycin also signaled a change in cytoplasmic potential and helped to determine the upper and lower limits. Histograms taken in the flow

cytometer were evaluated by calculating the peak, mean, CV and integral values. Flow cytometers "see" only the cell, including the intracellular and the membrane compartments of the three compartments (membrane, extra- and intracellular space) into which the $DiOC_6(3)$ is distributed after staining the cells. Thus, the usual equation describing the distribution over the compartments will have only two terms on the right side:

$$r = \sum_i r_i \qquad \text{with}$$

$$r_i = \sum_j a_{ij}\,(t)\, e^{b_I t}$$

where r_i is any quantitative signal measuring the volume of the i^{th} compartment, t is time, a_{ij} and b_I are coefficients and e is the base of natural logarithm. However, due to the higher solubility of the dye in lipid, the numerical calculation of the membrane potential has great difficulties, thus relative scaling of the measurable changes in cytoplasmic membrane potential values was achieved as described above. At low extracellular potassium concentration the potential and the fluorescence signal were maximal, at high potassium concentration the potential was low.

Determination of esterase activity. The activity of non-specific esterases of the cell membrane was determined essentially as described by Rotman and Papermaster (23). Briefly, the amount of the strongly fluorescent fluorescein trapped inside the cells was taken as a measure of the enzyme activity. Since the fluorescence was measured in a flow cytometer, possibilities for sensitivities of different subpopulations upon different CsA treatment could be investigated. The fluorescein diacetate test was performed after incubating the cells for 5 minutes at $37^{o}C$ with CsA or DMSO, the solvent for CsA.

Spin labeling of the cell membranes. The spin label, 5-doxyl-stearic acid, was dissolved in ethanol and the appropriate volume was vacuum dried in glass test tubes. The usual amount of spin label was $8x10^{-8}$ mole for $2x10^{7}$ spleen lymphocytes. The cell suspension was added in about 30 µl PBS to the test tubes containing the spin label. To evaluate the effect of

CsA on lymphocyte membrane $2x10^7$ spleen cells were spin-labeled as described above and an ERS spectrum was obtained. The cells were recovered from the capillary tube and treated immediately with 100 µg CsA dissolved in 1 µl DMSO, after which another ESR spectrum was obtained. A similar procedure was followed for assessing the effect of 1 µl DMSO on identical spleen cell suspensions. The amount of CsA used for the ESR measurements was 10 times the highest amount used in the membrane potential experiments. ESR spectra were recorded at x-band with a Varian E-9 Century series spectrometer. The temperature of the probe was set to $20^{\circ}C \pm 0.5^{\circ}C$ by a Varian variable temperature accessory, using N_2 gas flow. The ESR spectra were evaluated using the equation for these calculations of Hubbell and McConnell (26) as used in experiments similar to ours by Butterfield et al. (27).

Measurement of cellular K^+ concentration. Cells were prepared either from blood of healthy human volunteers or from the spleen of A/J mice by Ficoll gradient as described above. The cell number was adjusted to $5x10^6$ cells/ml. Samples were incubated in a CO_2 incubator with ^{42}KCl, 2 µCi/ml (spec. act. 0.19 µCi/mg) in RPMI 1640 medium for 16 hours at $37^{\circ}C$. After washing the cells with low potassium PBS, aliquots were taken and treated with CsA, ionophores, hormones or combinations thereof. At the end of the treatment, cells were layered over a 0.5 ml gradient of butylphthalate and oil (10:3 v/v) in Eppendorf microcentrifuge tubes. The tubes were centrifuged at 8000 g for 90 s, frozen in liquid nitrogen and the tip of the tube containing the cell pellet was amputated into a counting vial and the radioactivity was determined. The method was essentially the same as that described by Segal and Lichtman (28).

Measurement of fluorescence energy transfer on a cell-by-cell basis. Flow Cytometric Energy Transfer Measurement (FCET) were carried out in a FACS 440 flow cytometer as described earlier (29-31). Briefly, the HUT-102 cells were harvested and labeled by dansyl-CsA (a present of Dr.Alan Hess, Johns Hopkins Univ.) and FITC-conjugated anti-Tac. The anti-Tac monoclonal antibody in ascites fluid was a gift from Dr.Thomas Waldman (NIH). The antibody was further purified and labeled with FITC as described earlier

(29). The labeled cells were analysed using a broad band UV excitation of the dansyl. Emission of the dansyl and fluorescein dyes was detected correlatedly for each cell, and the energy transfer was calculated (30).

Measurement of intracellular calcium content. The intracellular calcium content was measured either with the quin-2 method (32), or with the indo-1AM dye introduced recently (33). Briefly, the changes in the fluorescence intensity of the quin-2, were recorded as described earlier (32). The indo dye changes its spectral characteristics upon binding the calcium thus in this case the changes in fluorescence were observed simultaneously at two wavelengths 405 and 480 μm as described earlier (33).

RESULTS

Flow cytometric membrane potential measurements. Human peripheral blood lymphocytes were treated with CsA prior to the addition of the membrane potential probe $DiOC_6(3)$. CsA slowed down the uptake kinetics of dye molecules across (or rather into) the membrane. The preincubation usually lasted for 5 minutes with various concentrations of CsA. The upper histograms in Figure 1 show the effect of 10 μg/ml of CsA on the uptake of 125 nM $DiOC_6(3)$. The lower part of the Figure 1 shows the effect of CsA when added to cells which were incubated with 125 nM $DiOC_6(3)$ first, until equilibrium was reached as indicated by two subsequently taken identical histograms. As shown in Figure 1, the CsA treatment decreased the amount of the dye bound to the cells. Calibration of the histograms according to the method of Shapiro (24), demonstrated that the CsA sensitive movement of the dye belonged to the membrane potential responsive fraction. Similar depolarizations were observed with 0.5-10 μg/ml of CsA as well as CsG concentrations. The corrected emission and excitation spectra of the dye alone or with cells did not show any observable difference (shown in Fig. 2).

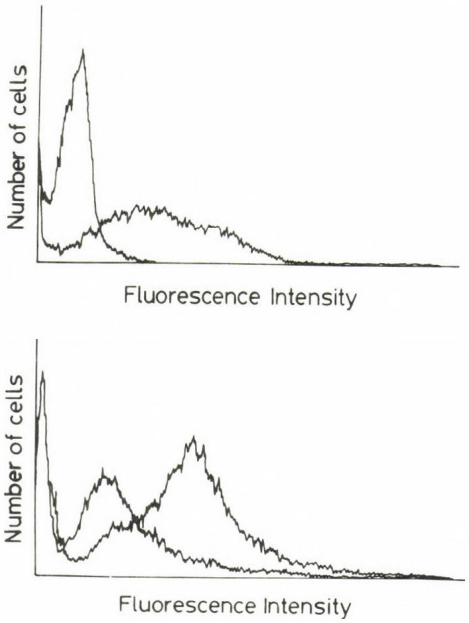

Figure 1.

Upper curves: Human lymphocytes pretreated with 10 µg/ml CsA for 5 minutes were stained with 125 nM $DiOC_6(3)$, (left side histogram). The right side histogram serves as control with pretreatment of 10 µl DMSO. Histograms were taken after 10 minutes incubation with the membrane potential probe. Lower curves: Human lymphocytes were incubated with 125 nM $DiOC_6(3)$ until equilibrium was reached. The left side histogram shows the effect of 10 µg/ml CsA within 2 minutes, the right side one is the DMSO treated control.

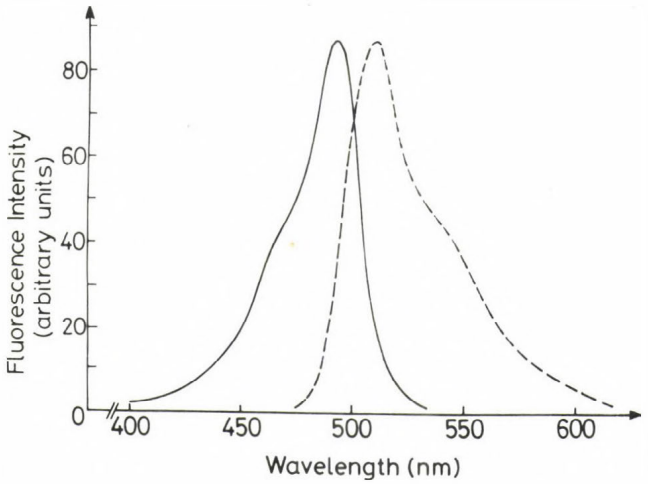

Figure 2.

Corrected fluorescence excitation (solid line) and emission (dashed line) spectra of 100 nM $DiOC_6(3)$ with 10^6 mouse thymus cells/ml PBS. The spectra were taken at 25°C. Fluorescence was monitored at 508 nm for the excitation spectra and the emission spectra were measured with 485 nm excitation. Similar spectra taken without cells gave essentially identical curves.

A similar shift of the histograms was followed also with thymus and the spleen lymphocytes from A/J mice, showing somewhat higher sensitivity to CsA than human peripheral blood cells. Insulin pretreatment prevented the depolarizing effect of the lower doses of CsA (0.5-1.0 g/ml CsA after 2 units/ml/ $/10^6$ cells) on spleen cells (Fig. 3). Insulin was ineffective when human cells were tested, since resting human lymphocytes practically have no insulin receptors (28).

Effect of CsA on ^{42}K loaded lymphocytes. As shown in Table I mouse spleen and human peripheral lymphocytes released potassium upon treatment with CsA. The ^{42}K loaded cells were incubated with 0.2-40 µg/ml CsA for about 5 minutes and the intracellular potassium content was determined in control and CsA treated samples. The insulin pretreatment provided a protection for the spleen cells against the ^{42}K releasing effects

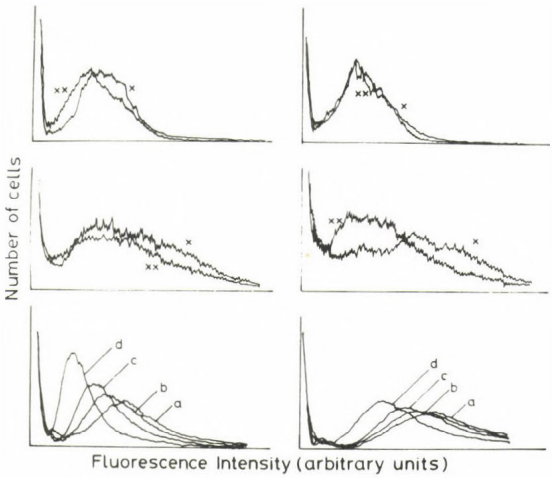

Figure 3.

Effect of hormone pretreatment on the effectiveness of membrane depolarization by CsA. The upper histograms show that pretreatment of human lymphocytes with 10^3 units/ml of human recombinant gamma-interferon abolished the effect of 10 µg/ml CsA. The middle histograms show that recombinant IL-2 (10-100 units/ml) enhanced the effect of 10 µg/ml CsA. The lower curves show the dose dependent depolarization of mouse lymphocytes with two units/ml of insulin. The left side figures are treated only with CsA, while the right side ones show the effects of hormones. The x means the histogram before, the xx the histogram taken after CsA treatment (with a: none; b: 0.5; c: 1.0 and d: 10 µg/ml CsA). Cell number was uniformly 10^6/ml.

of CsA. The ionophores valinomycin, ionomycin and A-23187 also released ^{42}K to different extents, as it also shown in Table I (10).

Interaction of hormones and CsA. The hormones IL-2, and gamma-interferon which are known to influence the maturation of lymphocytes (35), were tested for their effects on the cytoplasmic membrane potential. Gamma-interferon had almost no effect on the fluorescence of $DiOC_6(3)$, thus indicating no effect on the membrane potential. However, high doses of gamma-interferon protected human lymphocytes against the depolarization caused by CsA. Interleukin-2 itself decreased the membrane

Table I.

K^+ concentration in lymphocytes before and after CsA treatment

Treatment	K + concentration
None	129 ± 8.6
2 µg/ml CsA	110 ± 7.5
4 µg/ml CsA	98 ± 10.0
20 µg/ml valinomycin	79 ± 18.0
2 units/ml insulin	125 ± 5
2 units/ml insulin ± 2 µg/ml CsA	123 ± 3.6
20 µg/ml gramicidin	20 ± 1.8
2.5 µg/ml ionomycin	80 ± 7.2
1.0 µg/ml A23187	76 ± 9.3

The data represent the mean ±SD of 5 experiments in mmol/l cell water (23). The insulin treatment was carried out with mouse spleen cells, all other data were obtained with human peripheral blood lymphocytes.

potential of human as well as that of mouse lymphocytes. Depolarization due to IL-2 pretreatment was not only additive with the depolarization caused by the CsA, but slightly enhanced the effect of the latter (Fig. 3).

Combined effect of ionophores and CsA. Combined effects of ionophores and CsA were also tested in order to specify the nature of the changes in the ion-fluxes upon CsA treatment. Since the cytoplasmic membrane potential of resting lymphocytes is for all practical purpose a Donnan-potential, generated by the uneven distribution of extra- and intracellular potassium, the potassium specific ionophore valinomycin was first tested. The valinomycin itself can cause hyperpolarization at very low concentrations by its potassium specific carrier function. The larger concentrations of valinomycin result in a severe loss of potassium and a consequent decrease in the cytoplasmic membrane potential (35). Doses of valinomycin which caused a slight hyperpolarization of the membrane prevented the depolar-

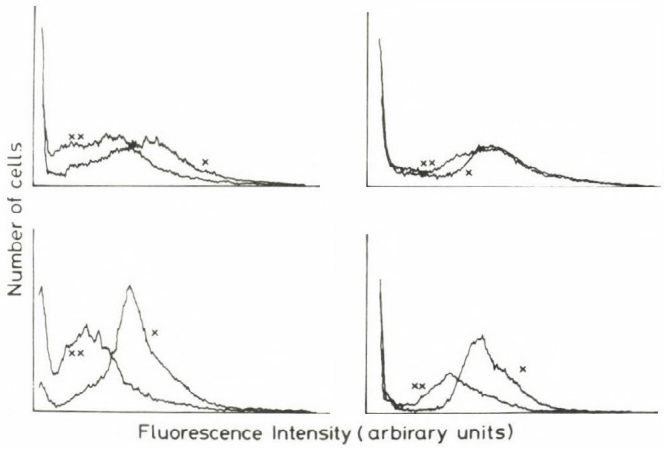

Figure 4.

Effect of valinomycin pretreatment on the depolarizing effect of CsA. The two upper figures show the changes of histograms upon addition of 10 μg/ml CsA before or after (right side picture) adding 5 μg/ml valinomycin. The samples were treated with valinomycin and CsA after the membrane potential probe reached equilibrium with the cells. The two lower pictures show the effect of valinomycin preincubation (5 minutes) on the effect of CsA upon the $DiOC_6(3)$ uptake ($DiOC_6(3)$ was added 5 minutes after CsA addition). The concentration of valinomycin and CsA were as above, 125 nM $DiOC_6(3)$ was applied in all cases. The left side figures were taken with samples treated only with CsA and the right side ones show the effect of valinomycin pretreatment. x: histograms taken before CsA treatment; xx: histograms taken after CsA treatment.

izing effect of CsA (Fig. 4). Higher doses of CsA could partially overcome of this type of protection (data not shown). The antagonistic effects of valinomycin and CsA were also observed when the kinetics of the uptake of the $DiOC_6(3)$ was the indicator of the effects. The nonspecific channel forming ionophore gramicidin always depolarized the membranes regardless of the presence or absence of CsA. Similarly, increased extracellular potassium concentration depolarized the membrane independently of the effects of CsA. Ionomycin, a calcium specific mobile ionophore, caused a small depolarization of the

cytoplasmic membrane potential (see Table I). When the effect of CsA was tested either on the release of the dye from cell at equilibrium or on the uptake kinetics, a pretreatment with ionomycin showed additivity or enhancement of the effects in the case of human lymphocytes. On the contrary after ionomycin pretreatment of mouse spleen lymphocytes, a slight but well detectable decrease in the effect of CsA was observed (data not shown).

The calcium and also magnesium specific ionophore A-23187 decreased the membrane potential at higher concentration. When the addition of A-23178 was combined with CsA, the effects were additive, regardless of the sequence of the addition. On the other hand, variations in the amount of the extracellular free calcium ions obtained by using calcium free buffer or adding EDTA to the cell suspension did not influence the membrane depolarizing effects of CsA.

Miscellaneous experiments with CsA. Although the uptake of the Ca^{2+} was not a prerequisite for the effect of CsA, the release of calcium by the drug could not be excluded without experimentation. Flow cytometric measurement with quin-2 did not show any calcium release. In another experiment human cells were loaded with indo-1 AM dye and the changes in the 405 and 480 nm fluorescence were followed in a spectrofluorimeter as well as in a flow cytometer (33). CsA increased the ratio of the 405/480 fluorescence in a dose dependent fashion indicating an increase in the intracellular calcium 0.5 µg/ml CsA could increase the 405/480 nm fluorescence ratio by a factor of two.

Monoclonal antibodies available against lymphocyte subclass specific antigens were incubated with human as well as with mouse cells prior to treatment with CsA. Most of the available antibodies, characteristically binding different subsets of T and B lymphocytes did not influence the overall effect of CsA. Preincubation of human cells with 10 µg/ml of OKT4 or OKT8 antibodies before addition of $DiOC_6$(3) and 5-10 µg/ml of CsA provided a slight protection against the depolarizing effect of CsA. When cells were incubated with CsA, and fluorescein conjugated antibodies were added to the cells, the binding of the antibodies was not influenced by the CsA pre-

treatment.

Fluorescein diacetate, a non-fluorescent compound, is a substrate of membrane bound esterases. The hydrolysis of FDA into fluorescein and acetate results in an accumulation of fluorescein inside the cells (23). This reaction is also used as a viability test because any leakage of the membrane can be easily monitored. As is shown in Figure 5, the fluorescence was decreased in the presence of CsA.

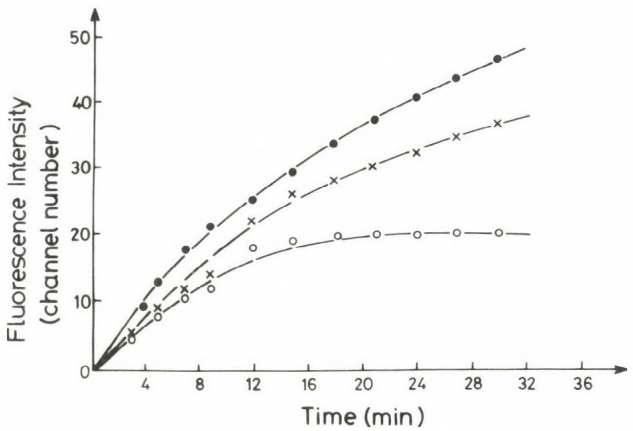

Figure 5.

Effect of CsA on the fluorescein diacetate hydrolysis test. The curves starting from above show the kinetics of the development of fluorescein fluorescence after pretreating mouse spleen lymphocytes with 0 (o), 2 µg/ml (x) and 10 µg/ml (o) CsA for 5 minutes. Data were obtained in a flow cytometer.

Experiments were carried out with HUT-102 cells which have an abudance of IL-2 receptors at their surface and were labeled with fluoresceinated anti-Tac antibody and dansylated CsA. The binding of antibody was not influenced by the presence of the CsA. If the respective binding sites were close enough i.e., within 2.0-10 nm, an effective energy transfer should

occur (29). We could not find energy transfer, thus a close proximity of the IL-2 receptors and CsA localization was not indicated. The very low energy transfer that was occasionally observed could come from energy tunneling between dansyl-CsA dissolved in the lipid-phase and the receptor bound FITC conjugated monoclonal antibody.

As Table II and Figure 6 demonstrate, the spin probe, 5-doxyl stearic acid indicated an immediate uptake of the CsA into the lipid phase of human peripheral (and also mouse spleen) lymphocytes. The increased order parameter also shows a limited motional freedom of the spin probe in the presence of CsA.

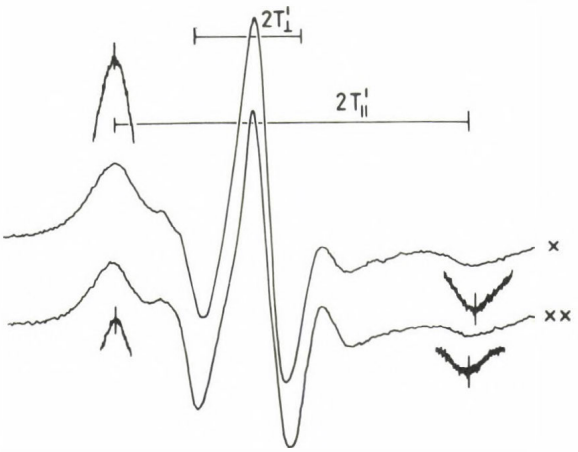

Figure 6.

ESR curves of 5-doxyl stearic acid probe in human lymphocyte membranes before (x) and after (xx) CsA treatment. Further experimental details are shown in Table II.

Table II.

Characteristic ESR parameters of lymphocytes before and after CsA treatment

Cell treatment	$T_{\parallel}'$	$T_{\perp}'$	$T'=T_{\parallel}'-T_{\perp}'$	a_N'	S	n
Human lymphocytes, $2x10^7$ (control)	23.90	8.45	15.45	13.60	0.635	6
Human lymphocytes, $2x10^7$ + DMSO (1 µl)	24.05	8.60	15.45	13.65	0.639	2
Human lymphocytes, $2x10^7$ + 100 µg of CsA in 1 µl DMSO	24.62	8.30	16.32	13.72	0.667	3

Standard deviation for $T_{\parallel}'$ = ±0.29.
Standard deviation for S = ±0.011.

DISCUSSION

A prerequisite to understanding how the CsA acts on particular T cell subsets is to find the earliest possible functional parameter, indicating this particular drug-cell encounter. Biochemical changes in the transmembrane signaling mechanisms undoubtedly occur in the presence of CsA as it was shown in a number of studies (7-16). However, these studies, by their nature, in most cases follow the changes several hours or days after drug treatment. Studies on the possible changes in membrane potential and especially flow cytometric membrane potential measurements offerred the great advantage of obtaining data on a cell by cell basis and gaining information over the total or preselected cell population within minutes after addition of CsA (19-21).

The most important observation of the present paper is the dramatic decrease in the membrane potential of both human and mouse lymphocytes immediately upon addition of CsA regardless of their T or B origin. This membrane depolarizing effect of CsA on mouse lymphocytes was prevented or significantly decreased in the presence of insulin. On the contrary the human lymphocytes responded to the CsA also in the presence of the

same amount of insulin that protected the mouse lymphocytes, a finding in accordance with earlier reports that human lymphocytes do not bind insulin (34).

Depolarization of cytoplasmic membrane as indicated by translocating dyes like $DiOC_6(3)$ can occur by many different mechanisms involving several cations and anions. In unstimulated lymphocytes, usually having a low amount of mitochondria and a cytoplasmic membrane potential that is more than 80 % due to the potassium concentration gradient between the extra and intracellular spaces as described by the Nernst equation, the likeliest ion to be involved in the depolarization is the potassium (36). A decrease in the membrane potential upon addition of CsA when the cells are already equilibrated with $DiOC_6(3)$ can easily be explained by a potassium release. The release of potassium by CsA was directly demonstrated with ^{42}K loaded cells. The CsA may change the transport of potassium either directly, by binding proteins belonging to or located nearby the potassium channels, or indirectly through influencing the structure and function of potassium channel forming proteins from the lipid domain of the membrane. Since quinine did not influence the effect of CsA (unpublished observation), it was unlikely that the voltage gated K^+ channels were involved (37). The sensitive indo-1 dye revealed an increase of intracellular Ca upon addition of CsA. We suggest that this is closely connected with the potassium release, and not an independent phenomenon. The observed decrease in the rate of the uptake of the potential probe in the presence of CsA suggests that the structure of the lipid domains have been changed, since their permeability to the $DiOC_6(3)$ significantly decreased in the presence of CsA. Again, direct evidence was obtained by the ESR measurements wherein the immediate decrease of the motional freedom of spin probes incorporated into the cytoplasmic membrane was observed upon addition of CsA. The corrected emission and excitation spectra of the $DiOC_6(3)$ were very similar or rather identical in the presence and absence of cells. This indicates the lack of a strong interaction of the dye and the cellular lipids. This, and the substantial changes upon changing the extracellular potassium concentration, again provided

additional evidence that the decisive factor determining the distribution of the dye is the electrochemical potential gradient, and among the conditions applied, the interactions of the dye and the lipids play a lesser role. The experiments in which combinations of CsA and ionophores, specific for potassium, calcium or calcium and magnesium, were applied showed strong interactions with CsA. The valinomycin, ionomycin and A-23187 belong to the group of the so-called mobile carriers which have hydrophobic characteristics and shuttle their ions between the outside and inside borders of the membrane; thus these ionophores, influenced by the CsA while dissolved in the lipid domains of the membrane, supported the notion that the CsA was principally merged into the lipid phase of membrane and its effects on ion movements, i.e., the observed depolarization of the cytoplasmic membrane, could be an indirect effect upon the potassium channels. It is interesting that the calcium and calcium and magnesium specific ionophores can also release potassium, most likely by an indirect mechanism. Gramicidin, an ionophore, which forms a hydrophilic channel for ions to cross the membrane, was not influenced by the presence of CsA. Similarly, an increase in the extracellular potassium concentration decreased the membrane potential independent of CsA. Since the CsA has a cyclic peptide structure like many of the mobile ionophores an ionophore-like effect of CsA cannot be excluded. Of course, to test such a specific role demands further investigations. The CsA inhibits the synthesis of gamma-interferon (38). We investigated the possible direct interaction between the membrane-receptor binding hormone, the gamma-interferon, and CsA. Human recombinant gamma-interferon showed a strong interaction with CsA at the membrane level, by preventing the depolarizing effect of CsA on human peripheral blood mononuclear cells. Alternative possibilities of direct and indirect interactions are feasible.

None of the observed effects of CsA at this level could be linked to any of the well characterized subpopulations of mouse spleen or human peripheral blood leukocytes. A comparison of the effects on cells from mouse thymus and spleen respectively did not show a difference. A number of the available

monoclonal antibodies was incubated with human lymphocytes prior to addition of CsA. The membrane potential was not significantly changed upon incubation with the antibodies which did not modify the depolarizing effect of CsA. The only exception in which consistent, although a small protection was observed in the experiments did occur when cells were preincubated with OKT-4 and OKT-8 antibodies. Since these types of monoclonal antibodies are directed against the helper and cytotoxic T cell subpopulation and bind 65 % of the peripheral T lymphocytes, a strong interaction should have produced a readily observable signal. Nonetheless, the helper and cytotoxic lymphocytes are those, supposed to be among the targets of the immunosuppressive agent CsA (8). Another question concerning the interaction of monoclonal antibodies and CsA, was whether the binding of the former was influenced by the latter. The labeling of human lymphocytes with FITC conjugated OKT-3, 4 and 8 binding 90, 65 and 35 % of peripheral human lymphocytes, respectively, was not influenced even at high CsA concentrations. Interestingly enough, the binding of recombinant IL-2 to human peripheral blood lymphocytes, (the existence of the receptors was verified also with FITC-anti-IL-2 receptor antibodies in parallel samples) enhanced the effect of the CsA on the cytoplasmic membrane potential. IL-2 alone did decrease somewhat the cytoplasmic membrane potential.

The observed depolarization of the cytoplasmic membrane in the presence of CsA is apparently the earliest observable effect of the drug on cells. Its indiscriminate action on the membrane potential of both T and B lymphocytes is not surprising since the CsA also influences the B cell activation in a dose dependent fashion (39). The changes in ion fluxes are known to initiate or abolish cell activation. Blockade of the sodium-hydrogen antiport abolished growth factor induced DNA synthesis in fibroblasts (40). Likewise a mutation abolishing this antiport activity in hamster fibroblasts precluded growth at neutral and acidic pH (41). The role of the increase in the intracellular calcium in the activation of leukocytes by A-23187 is well-known, it is noteworthy, however, that CsA prevents activation of leukocytes by A-23187 but this blockade can occur

at different sites as well as at the membrane (42). The possibility that all of the known effects of the CsA on human and mouse cells depend upon, or are initiated by, the early depolarization has to be considered. An explanation for the high degree of selectivity, of CsA for the cell-mediated cytotoxicity is now crucial. The key to this explanation may be found in the highly selective response of the different types of cells. As in the case of the known major intercellular messengers, the hormones, which can also have nonspecific binding to other cells as well as their primary targets, CsA may act nonspecifically and indiscriminately, yet the answer of certain types of cells can be specific and coming only from selected, specifically sensitive populations.

Evidence provided here support the view that closer investigation of cell membrane dynamics, even by indirect means like membrane potential measurements, can significantly contribute to the understanding of cell-drug and cell-hormone interactions.

REFERENCES

1. Damjanovich, S., Trón, L., Szöllősi, J., Mátyus, L., Szabó, G.jr. (1984) Dinamic properties of the murine histocompatibility H-2K^{k} antigen in cytoplasmic membrane. Mol. Immunol. 21, 1151-1155.
2. Axelrod, D. (1983) Lateral motion of membrane proteins and biological function. J. Membr. Biol. 75, 1-10.
3. Shapiro, H.M., Natule, P.J., Kamenetsky, L.A. (1979) Estimation of membrane potentials of individual lymphocytes by flow cytometry. Proc. Natl. Acad. Sci. USA, 76, 5728-5730.
4. Chan, S.S., Arndt-Jovin, D.J., Jovin, T.M. (1979) Proximity of lectin receptors on the cell surface measured by fluorescence energy transfer in a flow system. J. Histochem. Cytochem. 27, 56-64.

5. Austin,R.H., Chan, S.S., Jovin, T.M. (1979) Rotational diffusion of cell surface components by time-resolved phosphorescence anisotropy. Proc. Natl. Acad. Sci. USA, 76, 5650-5654.
6. Waggoner, A.S. (1979) Dye indicators of membrane potential. Ann. Rev. Biophys. Bioeng. 8, 47-68.
7. Borel, J.F., Feuer, C., Gubler, U., Stahelin, H. (1976) Biological effects of cyclosporin A: a new antilymphocytic agent. Agent and Action, 6, 468-475.
8. Cohen, D.J., Loertscher, R., Rubin, M.F., Tilney, N.L., Carpenter, C.B., Storm, T.B. (1984) Cyclosporine: a new immunosuppressive agent for organ transplantation. Ann. Intern. Med. 101, 667-682.
9. Hess, A.D., Tutschka, P.J., Pu, Z., Santos, G.W. (1982) Effect of cyclosporin A on human lymphocyte responses in vitro. IV. Production of T cell stimulatory growth factors and development of responsiveness to these growth factors in CsA-treated primary MLR cultures. J. Immunol. 128, 360-367.
10. Larson, E.L. (1980) Cyclosporin A and dexamethasone suppress T cell responses by selectively acting at distinct sites of the triggering process. J. Immunol. 124, 2828-2833.
11. Bunjes, D., Hardt, M., Rollinghof, M., Worgnes, H. (1981) Cyclosporin A mediates immunosuppression of primary cytotoxic T cell responses by impairing the release of interleukin 1 and interleukin 2. Eur. J. Immunol. 11, 657-661.
12. Krönke, M., Leonard, W.J., Depper, J.M., Arya, S.K., Wong-Staal, F., Gallo, R.C., Waldmann,T.A., Greene, W.C. (1984) Cyclosporin A inhibits T-cell growth factor gene expression at the level of mRNA transcription. Proc. Natl. Acad. Sci. USA, 81,5214-5218.
13. Elliott, J.F., Lin, Y., Mizel, S.B., Bleackley, C.R., Harnis, G.D., Paetkau, V. (1984) Induction of interleukin 2 messenger RNA inhibited by cyclosporin A. Science, 226, 1439-1441.

14. Kaufmann, Y., Chang, A.E., Robb, R.J., Rosenberg, S.A. (1984) Mechanism of action of cyclosporin A: inhibition of lymphokine secretion studied with antigen-stimulated T cell hybridomas. J. Immunol. 133, 3107-3111.
15. Koponen, M., Grieder, A., Loor, F. (1984) Interference of cyclosporin with lymphocyte activation: blockage of the mitogen-induced increases of lysosomal and mitochondrial activities. Immunology, 53, 55-62.
16. Merker, M.M., Handschumacher, R.E. (1984) Uptake and nature of the intracellular binding of cyclosporin A in a murine thymoma cell line, BW5147. J. Immunol. 132, 3064-3070.
17. Colombani, P.M., Robb, A., Hess, A.D. (1985) Cyclosporin A binding to calmodulin: a possible site of action on T lymphocytes. Science, 228, 337-339.
18. Hess, A.D., Colombani, P.M., Donenberg, A.D., Fischer, A., Ryffel, B. (1985) Binding of dansylated cyclosporine discriminates functional lymphocyte-T subsets. Transplantation Proc. 17, 1419-1426.
19. Aszalós, A., Damjanovich, S., Colombani, P.M., Mulhern, S. A., Hess, A.D. (1985) Lymphocyte subpopulations with different sensitivity to CsA have different plasma membrane potential. J. Cell Biol. (submitted)
20. Damjanovich, S., Aszalós, A., Mulhern, S.A., Marti, G., Balázs, M., Mátyus, L. (1985) Coupled transport: intracellular ion regulation. Biophys. J. 47, 271a.
21. Damjanovich, S., Aszalós, A., Mulhern, S.A., Balázs, M., Mátyus, L. (1985) Cytoplasmic membrane potential of mouse lymphocytes is decreased by cyclosporin. Molec. Immunol. (in press)
22. Böyum, A. (1968) Isolation of mononuclear cells and granulocytes from human blood. Isolation of mononuclear cells by one centrifugation, and of granulocytes by combining centrifugation and sedimentation at 1 g. Scand. J. Clin. Lab. Invest. 21, Suppl. 97. 77-90.
23. Rotman, B., Papermaster, B.W. (1966) Membrane properties of living mammalian cells as studied by enzymatic hydrolysis of fluorogenic esters. Proc. Natl. Acad. Sci. USA, 55, 134-141.

24. Shapiro, H.M. (1981) Flow cytometric probes of early events in cell activation. Cytometry, 1, 301-312.
25. Sims, P.J. Waggoner, A.S., Wang, C.H., Hoffman, J.F. (1974) Studies on the mechanism by which cyanine dyes measure membrane potential in red blood cells and phosphatidylcholine vesicles. Biochemistry, 13, 3315-3330.
26. Hubbell, W.L., McConnell, H.M. (1971) Molecular motion in spin-labeled phospholipids and membranes. J. Am. Chem. Soc. 93, 314-316.
27. Butterfield, D.A., Roses, A.D., Cooper, M.L., Appel, S.H., Chesnut, D.B. (1979) A comparative electron spin resonance study of the erythrocyte membrane in myotonic muscular dystropy. Biochemistry, 13, 5078-5082.
28. Segel, G.B., Lichtman, M.A. (1978) The effect of method on the measurement of K^+ concentration in PHA-treated human blood lymphocytes. Exp. Cell. Res. 112, 95-102.
29. Damjanovich, S., Trón, L., Szöllősi, J., Zidovetzki, R., Vaz, W.L.C., Regateiro, F., Arndt-Jovin, D.J., Jovin, T.M. (1983) Distribution and mobility of murine histocompatibility $H\text{-}2K^k$ antigen in the cytoplasmic membrane. Proc. Natl. Acad. Sci. USA, 80, 5985-5989.
30. Trón, L., Szöllősi, J., Damjanovich, S., Helliwell, S.H., Arndt-Jovin, D.J., Jovin, T.M. (1984) Flow cytometric measurement of fluorescence resonance energy transfer on cell surfaces. Biophys. J. 45, 939-946.
31. Szöllősi, J., Trón, L., Damjanovich, S., Helliwell, S.H., Arndt-Jovin, D.J., Jovin, T.M. (1984) Fluorescence energy transfer measurements on cell surfaces. A critical comparison of steady-state fluorimetric and flow cytometric methods. Cytometry, 5, 210-216.
32. Tsien, R.Y., Pozzan, T., Rink, T.J. (1982) Calcium homeostasis in intact lymphocytes cytoplasmic free calcium monitored with a new, intracellularly trapped fluorescent indicator. J. Cell. Biol. 94, 325-334.
33. Grynkiewicz, G., Poenie, M., Rink, T.J. (1982) A new generation of Ca^{2+} indicators with greatly inproved fluorescence properties. J. Biol. Chem. 260, 3440-3450.

34. Schwartz, R.H., Bianco, A.R., Handwerger, B.S., Kahn, C.R. (1975) Demonstration that monocytes rather than lymphocytes are the insulin-binding cells in preparations of human peripheral blood mononuclear leukocytes: implications for studies of insulin-resistant states in man. Proc. Natl. Acad. Sci. USA, 72, 474-478.
35. Waggoner, A.S. (1979) The use of cyanine dyes for the determination of membrane potentials in cell, organelles and vesicles. Methods in Enzimology, 55, 689-697.
36. Alberts, D., Bray, D., Lewis, J., Raff, M., Roberts, K., Watson, J.D. (1983) Molecular Biology of the Cell. Garland Publ. Inc., New York, London
37. DeCoursey, T.E., Chandy, K.G., Gupta, S., Cahalan, M.D. (1984) Voltage-gated K^+ channels in human T lymphocytes: a role in mitogenesis? Nature, 307, 465-468.
38. Room, G.H., Cook, L.A., Vilcek, J. (1983) Gamma interferon synthesis by human thymocytes and T lymphocytes inhibited by cyclosporin A. Science, 221, 63-65.
39. Muraguchi, A., Butler, J.L., Kehnl, K.H., Falkoff, R.J., Fauchi, A.S. (1983) Selective suppression of an early step in human B cell activation by cyclosporin A. J. Exp. Med. 158, 690-702.
40. Pardee, A.B., Dubrow, R., Hamlin, J.L., Kletzien, R.F. (1978) Animal cell cycle. Ann. Rev. Biochem. 47, 715-750.
41. L'Allemain, G., Frachi, A., Cragoe, E.Jr., Pouyssegur, J. (1984) Blockade of the Na^+/H^+ antipart abolishes growth factor-induced DNA synthesis in fibroblasts. Structure-activity relationships in the amiloride series. J. Biol. Chem. 259, 4313-4319.
42. Kay, J.E., Benzine, C.R., Borhetti, A.F. (1983) Effects of cyclosporin A on the metabolism of unstimulated and mitogen-activated lymphocytes. Immunology, 50, 441-446.

DISCUSSION

ZIDOVETZKI:

Did you check, if there is a direct interaction between valinomycin and cyclosporin A?

DAMJANOVICH:

Yes, we did. There is no interaction.

PECHT:

Have the ionophoric properties of cyclosporin B been examined? How much of its biological activity could be explained by such an ionophoric behavior?

DAMJANOVICH:

Several preliminary experiments have been done to get an answer to that question. On the basis of these we cannot rule out that cyclosporin B may have some ionophoric activity. Experiments are in progress in order to clear that point.

ZS.-NAGY:

Do you have any data about the effect of CsA on the lateral diffusion constant of membrane proteins?

DAMJANOVICH:

No, I haven't. It is an excellent idea to look for that question.

Dynamics of Biochemical Systems
S. Damjanovich, T. Keleti, L. Trón (Eds)

DEPOLYMERIZATION OF MICROTUBULES INCREASES MOTIONAL FREEDOM OF LIPID AND PROTEIN PROBES IN THE CELLULAR MEMBRANE AND ALTERS PLASMA MEMBRANE POTENTIAL

ADORJAN ASZALOS , MICHAEL M. GOTTESMAN[+] , SÁNDOR DAMJANOVICH[++]

Division of Drug Biology, Food and Drug Administration, Washington, D.C., USA
[+]National Cancer Institute, NIH, Bethesda, MD. USA
[++]Department of Biophysics, University Medical School of Debrecen, Hungary

Three lines of evidence were obtained indicating that microtubule depolymerization affects the function and the physical state of the plasma membrane in Chinese hamster ovary (CHO) cells. One line of evidence was obtained with a membrane potential sensing dye and flow cytometry. Mictrotubule depolymerization with vincristine, colcemid and colchicine resulted in membrane depolarization. These effects were due to drug interaction with microtubules because 1.) effects were time dependent, 2.) required the entry of the drugs into the cell as indicated by the lack of membrane depolarization in a multidrug resistant mutant, 3.) a colcemid-resistant tubulin mutant did not show membrane potential changes and 4.) taxol, the microtubule stabilizing drug, prevented the action of the depolymerizing drugs. Similar conclusions could be drawn from ESR studies using maleimid spin probes attached to proteins in the membrane. The third line of evidence comes from ESR probing of the lipid domain of plasma membranes. These studies indicate that the motional freedom of the probes, as expressed by the order parameter S, is higher in microtubule depolymerized cell membrane than in membrane of untreated cells.

Previous studies indicate that microtubules modulate the functions of plasma membranes by changing membrane potential (1), hormone responsiveness (2, 3), receptor capping (4, 5) and exocytosis (6). Connections between microtubules or tubulins with cell membrane components have been observed before (7, 8, 9, 10) but the mechanism by which microtubules modulate different membrane functions is not fully understood yet. How-

ever some studies have demonstrated that the microtubule system can directly influence plasma membrane dynamics (11, 12).

In our studies we have shown that depolymerization of microtubules results in increased motional freedom of fatty acid probes inserted into the plasma membrane and of probes attached to sulfhydryl groups of proteins embedded in the lipid domain of membranes of CHO cells. In addition to this, the plasma membrane potential is changed if microtubules are depolymerized. Our results support models based on the anchorage theory in which microtubules interact directly or indirectly with the cell membrane and influence various membrane functions. Some of these studies have been previously reported in the J. Cell Biology (12).

MATERIALS AND METHODS

Growth of cells for electron spin resonance (ESR) Measurements: CHO cells were grown in α-modified minimal essential medium (α-MEM) containing 10 % fetal bovine serum (M.A. Bioproducts, Walkersville, MD), and the antibiotics penicillin (50 U/ml), and streptomycin (50 μg/ml) (Flow Laboratories, Inc., McLean, VA) in monolayer culture as previously described (13, 14). The β-tubulin mutant cell line Cmd-4 was selected for growth in colcemid (15) and the multiple drug-resistant cell line C5 (gift of V. Ling) was selected for growth in colchicine, but has been shown to be resistant to different drugs including adriamycin, puromycin and actinomycin-D (16). 20 h before spin labeling, cells were treated with 0.25 % trypsin, 2 mM EDTA in Tris-dextrose buffer and suspended at a density of $2\text{-}4\times10^6$ cells/ml in 20 ml complete α-MEM medium in 120-ml glass bottles. The bottles were sealed after gassing, and incubated at 37°C in a gyrorotatory shaker bath (New Brunswick Scientific Co., Edison, NJ) at 160 rpm. When spin labels were added, cells were at a density of 8×10^5/ml and were 90 % viable as measured by trypan blue exclusion.

For most studies, cells were grown in suspension in individual bottles. Prior to spin labeling, they were combined and divided into equal portions. Drugs were added as described

and incubation was continued for an additional 45 min. When two drugs were used, as in the case of taxol and colcemid, the second drug was added 10 min after the first one. Cells were then collected by centrifugation and resuspended in phosphate-buffered saline (PBS) to a concentration of 10^6 cells/0.06 ml of PBS. With the mutant cells, direct comparison between mutant and wild-type cell lines was not possible since we were able to show that cells grown to different densities have membranes with different fluidities. 10^6 cells were sufficient to obtain good quality ESR spectra.

Spin labeling: To study the membranes of CHO cells, we used two spin labels: 5-doxyl stearic acid (SA) and 16-doxyl methylstearate (MS), both purchased from Syva Co., Palo Alto, CA. and stored in ethanol for several months at $-20^{\circ}C$. Appropriate volumes of spin label were put into glass centrifuge tubes and diluted with 1-2 volumes of ether, prior to evaporation of the solvents under vacuum. $8x10^{-8}$ mol of spin label was used to label 10^6 cells. The cell suspension in 0.05-0.07 ml of PBS was added to the spin label-containing test tubes. To get essentially all the spin label into the cellular membrane required approximately 30s for the 5-doxyl SA label and 90-120s for the 16-doxyl MS, at room temperature. The majority of the spin probes are probably located in the plasma membrane as suggested by Bales et al. (17). After preincubation with spin labels, the cell suspension was sucked into a 50 µl micropet capillary (Clay Adams Div., Parisippany, NJ) and sealed at the bottom with Critoseal (Syva Co.). Direct contact of the cell suspension with Critoseal was avoided to present leakage of Mn^{2+} ions from the seal into the cell suspension.

Labeling of the membrane proteins: Spin labeling of the membrane proteins was done basically as described by Grof and Belágyi (18). 20 ml of a solution of maleimide nitroxide (1 mg/ml) in ethanol was dried in a conical centrifuge tube. The spin label was then dissolved in 0.1 ml PBS, and 50 µl of a cell suspension of $2-4x10^7$ cell/ml was added. After 15 minutes at room temperature, the suspension was pelleted for 30 seconds and then washed 3 times by repeated cycles of centrifugation-resuspension in the 0.2 ml PBS. The ESR signals of

the final pellets were measured in 50 µl micropet capillary tubes (Clay Adams Co., Parisippany, NJ) sealed with Critoseal (Syva Co., Palo Alto, CA).

Evaluation of the ESR spectra: Evaluation for the fatty acid type probes was as described earlier by Aszalós et al. (19) and is based on the equation used by Hubbel and McConnell (20) and Butterfield et al. (21). Evaluation of the ESR spectra obtained with maleimid type spin probe attached to proteins was done as described by Gróf and Belágyi (18).

Membrane potential measurements: For membrane potential measurements untreated and drug treated aliquots of a CHO cell suspension of $3x10^6$ cells/ml were stained with dihexyloxacarbocyanine iodide ($DiOC_6(3)$), (Molecular Probes Inc., Junction City, OR) dissolved in DMSO, in growth medium. The dye concentration was 0.5 µM, a concentration which was non-toxic to cells as determined by a steady fluorescence intensity for the duration of the measurements (up to 1 h). The fluorescence intensity changes as the cells die and is a very sensitive indicator of cell viability (22). The fluorescence intensity being indicative of the membrane potential was shown by the addition of agents known to change membrane potential according to Waggoner (23). Elevated concentration of extracellular K^+ (up to 160 mM), 2 µg/ml gramicidin-S and 10 µg/ml cyclosporin A decreased while 2 µg/ml valinomycin increased the fluorescence intensity as expected for viable cells.

A Coulter EPICS V flow cytometer and its software were used for data acquisition and analysis. The laser was tuned to 488 nm and the output was kept at 400 mW. The flow rate of the cells was kept low (10^3 cells/sec.) to provide good resolution. The forward angle light scatter and right angle green fluorescence signals were collected. To reduce artifacts, the fluorescence was usually gated on the scatter signal. For each histogram, the coefficient of variation and the means were calculated, and $3x10^4$ cells were analyzed.

Immunofluorescence localization of microtubules: Cells were grown in 35-mm dishes, were fixed and stained with mouse monoclonal antibody to chick α-tubulin (Miles Laboratories Elkart, IN) as previously described (12). Microtubules were

visualized with a Zeiss fluorescence microscope and the degree of microtubule depolymerization was estimated by counting the fraction of cells with well-formed microtubule systems.

RESULTS

Microtubule-depolymerizing drugs affect motional freedom of ESR probes in the membranes: CHO cells treated with various anti-microtubule agents were analyzed using spin labels to determine the effect of microtubule depolymerization and stabilization on the motional freedom of the spin probes in the plasma membrane. The parameters which we evaluated from the ESR spectra were, $2T_{\parallel}$ and $2T_{\perp}$. These are components of the motionally averaged nitrogen hyperfine tensor from which the nitrogen isotropic coupling constant, a_N', and the order parameter, S, can be calculated. In a crystal lattice, where there is no motional freedom of the probe, the S value would be one, whereas S values less than one indicate increasing motion of the spin label probe which has been interpreted to imply increased membrane fluidity.

When the 5-doxyl SA was inserted into membrane of CHO cells treated with taxol, which stabilizes microtubules, no effect on ESR spectra was seen, but cells treated with microtubule depolymerizing agents showed significant differences. The calculated parameters for untreated cells and CHO cells treated with 0.5 μg/ml colcemid (1.3 μM), 2.5 μg/ml colchicine (6.3 μM), 5 μg/ml podophyllotoxin (12 μM), 2.5 μg/ml vincristine 3 μM), and 125 μg/ml griseofulvin (350 μM) are shown in Table 1. These drug treatments were sufficient to cause complete depolymerization of microtubules in CHO cells as measured by indirect immunofluorescence using anti-tubulin antibodies (data not shown).

If the difference between the two values of $T_{\parallel}$ was less than 0.1 gauss, only two measurements were made since the standard deviations of S for untreated and colcemid-treated cells were found to be 0.004 and 0.005, respectively. Hence, the difference between the S values of untreated CHO cells, 0.680, and of colcemid-treated CHO cells, 0.664, is significant.

Table I.

ESR parameters of 5-doxyl SA inserted into CHO cells[x]

Treatment, µg/ml	$T_{\parallel}'$	$T_{\perp}'$	$T'=T_{\parallel}'-T_{\perp}'$	a_N'	S	N
no treatment	27.58 (0.15)	9.06 (0.2)	18.41	15.20	0.680[+]	9
colcemid, 0.5	27.11 (0.2)	9.20 (0.01)	17.91	15.17	0.665[+]	5
colchicine, 2.5	27.10 (0.1)	9.10 (0.1)	18.00	15.16	0.662	2
podophyllotoxin, 5.0	27.15 (0.1)	9.15 (0.1)	18.00	15.16	0.665	2
vincristine, 2.5	26.75 (0.1)	9.40 (0.1)	17.35	15.20	0.638	2
griseofulvin, 125	26.75 (0.1)	9.35 (0.05)	17.40	15.10	0.641	2
taxol, 10	27.66 (0.3)	9.07 (0.2)	18.58	15.20	0.684	4
taxol, 10, followed by colcemid 0.5	27.45 (0.1)	9.02 (0.1)	18.42	15.10	0.687	2
beta lumicolchicine, 2.5	27.35 (0.1)	9.00 (0.1)	18.30	15.12	0.676	2

[x]Experiments performed as described in Materials and Methods, 22°C.

N is the number of data points, S values are calculated as described in Materials and Methods. $T_{\parallel}'$, $T_{\perp}'$, and a_N' are in gauss.

[+]Standard deviations 1: 0.004, 2: 0.005.

Table II.

Dose-dependent effect of colcemid on $T_{\parallel}'$ of 5-doxyl SA-treated CHO cells correlates with microtubule depolymerization

µg/ml colcemid	$T_{\parallel}'$	Microtubule depolymerization[x]
0	27.70	none
0.1	27.45	few short microtubule segments seen
0.2	27.15	complete
0.5	27.10	complete

[x]Assayed by immunofluorescence.

Significant differences were also found between untreated cells and cells treated with the other microtubule depolymerizing agents. We also determined a dose response of CHO cells to colcemid. As seen in Table II, the effect of colcemid on T_{II} ' was observed only with amounts of colcemid that detectably depolymerize microtubules. Treatments with taxol and with taxol followed by colcemid, which block microtubule depolymerization, blocked the observed changes in the motional freedom of the probe (Table I). A colchicine analog with no biological activity, β-lumicolchicine, resulted in no significant changes in membrane fluidity as expressed by the S values (Table I).

Changes in the motional freedom of membrane probes do not occur in a colcemid-resistant β-tubulin mutant: The CHO cell mutant, Cmd-4, which was selected for resistance to colcemid and expresses an altered β-tubulin (15), was compared to the parent cell line for membrane fluidity changes when both cell lines were exposed to colcemid. As shown in Table III, the parent cell line responded to 0.1 μg/ml colcemid treatment with a change in S value from S=0.675 to S=0.659. On the other hand, the treated and untreated mutant cell lines showed no significant difference in the order parameter, i.e., S=0.661 and 0.659, respectively. The lower S value found for the mutant may be due to a somewhat lower density of mutant cells in this experiment (see Table III).

Motional freedom of membrane proteins of CHO cells: The motional freedom of membrane proteins was determined using ESR parameters of a maleimid spin probe which reacts with sulfhydryl groups of proteins. Two types of sulfhydryl groups bind this spin label: easily accessible, mobile sulfhydryl groups, and slow moving sulfhydryl groups seeded deeper in the hydrophobic region of the membrane (19). ESR spectra indicate the motional freedom of both types of proteins, from which the slow moving proteins can be characterized by the outer hyperfine couplings, $2T_{II}$. The two experimental spectra of the two types of proteins made it impossible to calculate order parameters, however, in this case a larger $2T_{II}$ could be interpreted as either less motional freedom or less polar vicinity of the ESR probe (25). Figure 1 shows a typical spectrum obtained

Table III.

ESR parameters of 5-doxyl SA in colcemid resistant (β-tubulin mutant) and wild-type CHO cells[x]

Cells/treatment	$T_{\parallel}'$	$T_{\perp}'$	$T'=T_{\parallel}'-T_{\perp}'$	a_N'	S
resistant mutant no treatment	27.25	9.25	18.00	15.25	0.659
resistant mutant 0.1 µg/ml colcemid	27.20	9.20	18.00	15.20	0.661
wild-type no treatment	27.45	9.10	18.30	15.20	0.675
wild-type 0.1 µg/ml colcemid	27.00	9.15	17.85	15.10	0.659

[x] Experiments performed as described in Materials and Methods, 22°C.

S values are calculated as described in Materials and Methods.

$T_{\parallel}'$, $T_{\perp}'$ and a_N' in gauss.

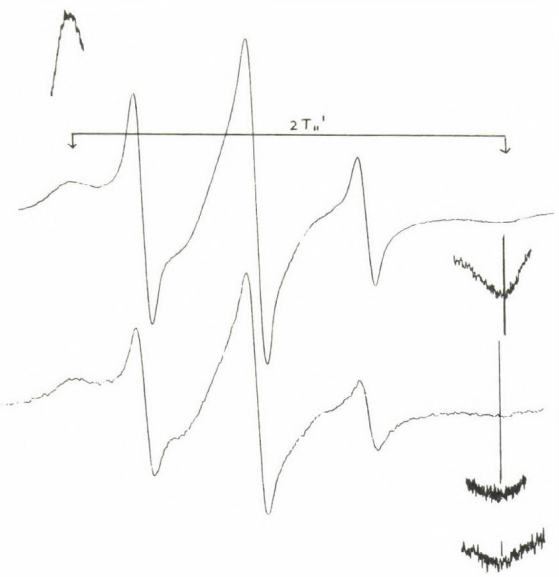

Figure 1

ESR spectra of maleimid type spin probe attached to untreated (upper curve) and 2.5 µg/ml vincristine treated (lower curve) wild-type CHO cells. Labeling and spectroscopic details are described in Materials and Methods.

with the maleimid probe reacted with sulfhydryl groups of proteins of CHO cells. Results obtained with several different microtubule depolymerizing agents and taxol, the depolymerization hindering agent, are shown in Table IV.

Table IV.

ESR parameter of maleimide spin probe in CHO cells[x]

Treatment (μg/ml)	$2T_{\parallel}'$, S.D.
no treatment	58.4 ± 0.2 (n=8)
colchichine (2.5)	57.2 ± 0.3 (n=8)
vincristine (2.5)	57.4 ± 0.2 (n=8)
colcemid (0.2)	57.3 ± 0.1 (n=4)
taxol (10)	58.1 ± 0.2 (n=4)
taxol (10) followed by colcemid (0.2)	58.3 ± 0.2 (n=4)

[x]Cells were labeled with the maleimid spin probe as described in Materials and Methods. SD = standard deviation.

Each applied depolymerizing drug (colchichine, vinblastine and colcemid) decreased the value of $2T_{\parallel}$. Taxol, 10 μg/ml had no effect alone. Also, no significant change in the $2T_{\parallel}$ value could be seen when cells were pretreated with taxol (10 μg/ml) prior to colcemid (0.2 μg/ml) treatment. Changes in the $2T_{\parallel}$ values caused by the microtubule depolymerizing drugs are statistically significant.

Microtubule depolymerization changes membrane potential: The plasma membrane potential of wild-type and mutant CHO cells untreated and treated with microtubule depolymerizing agents was measured with the fluorescent translocating dye method as described in Materials and Methods. Use of a flow cytometric technique allowed us to obtain information on a cell by cell basis. The fluorescence of $3x10^4$ cells was measured to obtain one histogram. The fluorescence intensity was a measurement of the membrane potential since appropriate fluorescence intensity shifts were seen upon addition of known membrane potential

changing agents as detailed in Materials and Methods. Light scatter histograms of treated and untreated CHO cells were superimposable, indicating that treated and untreated cells had similar shapes. Membrane potential shifts of wild-type CHO cells after treatment with 2.5 µg/ml vincristine or 2.5 µg/ml colchicine are shown in Fig. 2. Fluorescence intensity measurement of cells within 3 min after addition of 2.5 µg/ml vincristine indicated very little fluorescence intensity change as compared to that seen after 45 min. This time dependence rules out an ionophoric effect of the microtubule depolymerizing agents. The dose dependence of the membrane potential shift after addition of 0.05, 0.070 and 0.1 µg/ml colcemid was the same as the dose dependence of microtubule depolymerization indicating a good correlation between these two phenomena (data not shown).

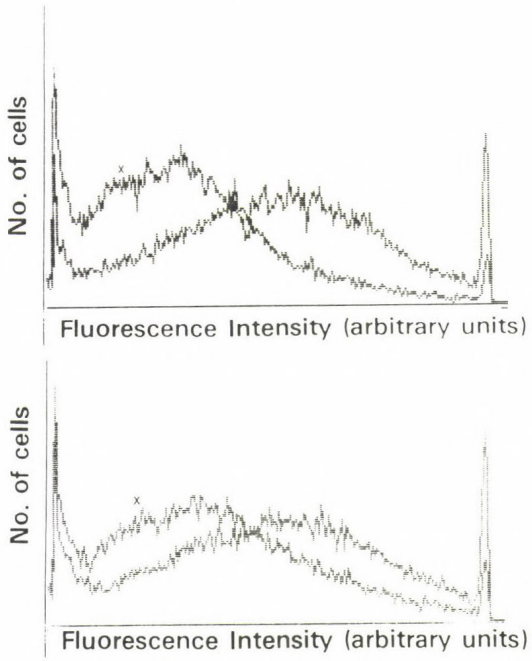

Figure 2

Histograms of 2.5 µg/ml vincristine (top histogram) and 2.5 µg/ml colchicine treated and untreated CHO cells. In both cases treated cells yielded the left histograms. Histograms were obtained as described in Materials and Methods and were suerimposed electronically.

Histograms with fluorescence intensities after addition of 2.5 µg/ml colcemid, 10 µg/ml taxol and 10 µg/ml taxol followed by 2.5 g/ml colcemid to wild-type CHO cells are shown in Figure 3. Colcemid alone caused depolarization while taxol

hyperpolarized CHO cells. Addition of colcemid after taxol treatment, however resulted in no significant change in the fluorescence intensity as would be expected since taxol blocks colcemid-induced microtubule depolymerization.

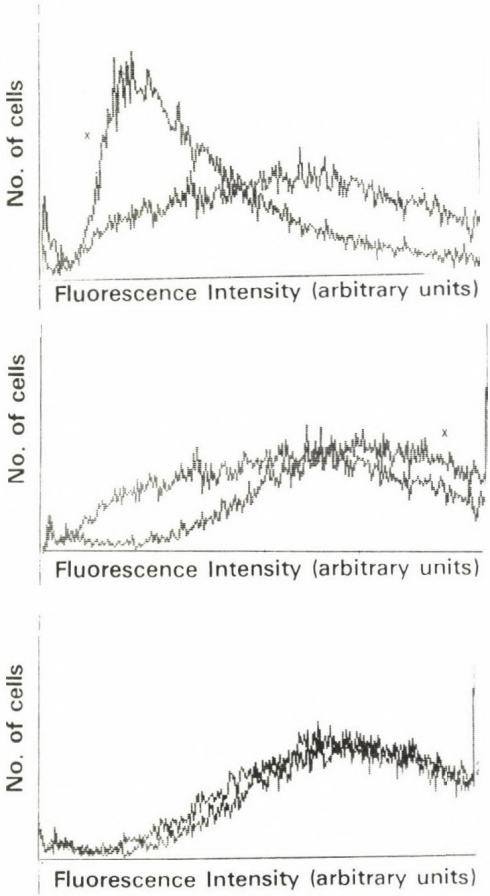

Figure 3

Histograms of 2.5 µg/ml colcemid (top), 10 µg/ml taxol (middle) and 10 µg/ml taxol followed by 2.5 µg/ml colcemid treated CHO cells (bottom). Histograms of treated cells are marked X in each case. Histograms were obtained as described in Materials and Methods and were superimposed electronically.

Two mutant cell lines, a tubulin mutant (Cmd-4) and a multidrug resistant mutant which does not accumulate many drugs (C5), were tested for membrane potential change after addition of 0.1 or 0.075 µg/ml colcemid. The wild-type CHO cells responded to these treatments, but no fluorescence intensity changes were observed with either mutant cells (data not shown). These results imply that the colcemid must enter cells and must also interact with microtubules to have effects on membrane potential.

DISCUSSION

The motion of spin probes in the lipid domain of plasma membranes or attached to transmembrane proteins is a sensitive and reliable indicator of the physical state of the lipid domain of membrane of CHO cells (26) and of membrane bound proteins (19).

This work demonstrates significant increases in the motional freedom of two ligand probes and one sulfhydryl protein probe as a result of depolymerization of microtubules. These changes are not the result of a direct effect of the drugs on the cell membranes since they are not seem immediately after addition of the drugs and are not seen with β-lumicolchicine, a nonfunctional analog of colchicine.

Uptake of the drug by the cells is a prerequisite for the observed effects on membrane potential and motional freedom of the proteins since the colchicine-resistant drug permeability mutant, C5, fails to respond with changes in the motional freedom of ESR membrane probes and in the membrane potential (data not shown).

We have obtained three kinds of evidence that the anti-microtubule agents must interact with microtubules to alter the motional freedom of the spin label in the membrane or to alter plasma membrane potential: (a) the dose response of the effect of colcemid is similar to the dose response for depolymerization of microtubules for this drug: (b) taxol, a drug known to stabilize microtubules in cultured cells (27), blocks the effect of colcemid on membranes; and (c) a CHO mutant resistant to colcemid because of an alteration in β-tubulin (15) shows no effect of colcemid on the motional freedom in the membrane or on the plasma membrane potential.

Lai and coworkers, using the same spin label probes to study CHO membranes, found that there are differences in the motional freedom of the spin probe in the membrane throughout the cell cycle with an increase during mitosis and decreases in G1 and S (24). We speculate that this increase in the motional freedom of the probes during mitosis could be the result of a reorganization of microtubules as spindles are

formed. The results of Lai et al. (24) are consistent with our evidence that depolymerization of microtubules increases motional freedom of spin labels in unsynchronized cell populations. Both studies agree with previous structural observations of Porter, who found cell cycle-specific changes in the appearance of the cell surface in CHO cells (28). Taken together, these results suggest a possible role for microtubules in the mediation of some of these morphologic phenomena.

Spin label studies of the motionally restricted protein sulfhydryl groups are entirely consistent with results obtained with ESR probes of the lipid domain (Table IV). The motional freedom of the protein bound spin probes increases if the microtubule system is depolymerized and these changes are also hindered by taxol (Table IV). More freely moving protein functions seem to parallel the increased motional freedom of the lipid domain in cell membranes with depolymerized microtubule systems. It is interesting to speculate that some of the labeled sulfhydryl groups may belong to ion channels or ion pumps. By this argument, ion flux changes across the plasma membrane may manifest changes in membrane potential after microtubule depolimerization.

The dye $DiOC_6(3)$ which we used for the membrane potential measurements can also measure mitochondrial membrane potential changes (29). In our studies, we believe that only plasma membrane potential changes were recorded for the following reasons: taxol pretreated cells did not respond to colcemid treatment and the tubulin mutant cells Cmd-4 did not respond to colcemid treatment either. The observed fluorescence intensity changes being indicative of membrane potential changes was ascertained as described in Materials and Methods

Another way to relate changes in motional freedom of lipid and protein probes to altered membrane potential comes from the work of Vassilev et al. (1). They have suggested that polymerized microtubules increase ionic conductance through the microtubule lumen. However, both arguments require i.e., microtubule lumen vs ion pumps that microtubules directly or indirectly are connected to the plasma membrane as has been proposed by others based on independent evidence (7).

REFERENCES

1. Vassilev, P., Kanzirska, M. and Ti Tien, H. 1985. Intramembrane linkage mediated by tubulin. Biochem. Biophys. Res. Comm. 126, 559-565.
2. Hagmann, J. and Fishman, P.H. 1980. Modulation of adenylate cyclase in intact macrophages by microtubules. Opposing actions of colchicine and chemotactic factor. J. Biol. Chem. 255, 2659-2662.
3. Insel, P.A. and Kennedy, M.S. 1978. Colchicine potentiates β-adrenoreceptor-stimulated cyclic AMP in lymphoma cells by an action distal to the receptor. Nature (Lond.) 273, 471-472.
4. Albertini, D.F. and Clark, J.I. 1975. Membrane-microtubule interactions: concanavalin A capping induced redistribution of cytoplasmic microtubules and colchicine binding proteins. Proc. Natl. Acad. Sci. USA, 72, 4976-4980.
5. Malawista, D.E., Oliver, J.M. and Rudolph, S.A. 1978. Microtubules and cyclic AMP in human leukocytes on the order of things. J. Cell Biol. 77, 881-886.
6. Wehland, J., Willingham, M.C., Gallo, M.G. and Pastan, I. 1982. The morphologic pathway of exocytosis of the vesicular stomatitis virus G protein in cultured fibroblasts. Cell, 28, 831-841.
7. Bernier-Valentin, F., Aunis, D. and Rousset, B. 1983. Evidence for tubulin-binding sites on cellular membrane: plasma membranes, mitochondrial membranes, and secretory granule membranes. J. Cell. Biol. 97, 209-216.
8. Bhattacharya, E. and Wolff, J. 1975. Membrane-bound tubulin in brain and thyroid tissue. J. Biol. Chem. 250, 7639-7646.
9. Collot, M., Louvard, D. and Singer, S.J. 1984. Lysosomes are associated with microtubules and not with intermediate filaments in cultured fibroblasts. Proc. Natl. Acad. Sci. USA, 81, 788-792.
10. Pfeffer, A.R., Drubin, D.G. and Kelly, R.B. 1983. Identification of three coated vesicle components as α- and β-tubulin linked to a phosphorylated 50.000 dalton polypep-

tide. J. Cell Biol. 97, 40-47.
11. Berlin, R.D. and Fera, J.P. 1977. Changes in membrane microviscosity associated with phagocytosis: Effect of colchicine. Proc. Natl. Acad. Sci. USA, 74, 1072-1076.
12. Aszalós, A., Yang, G.C. and Gottesman, M.M. 1985. Depolymerization of microtubules increases the motional freedom of molecular probes in cellular plasma membranes. J. Cell Biol. 100, 1357-1362.
13. Gottesman, M.M. 1985. Growth properties of Chinese hamster ovary cells. In: Molecular Cell Genetics, M.M. Gottesman, editor. Wiley-Interscience, New York, pp. 139-154.
14. Gottesman, M.M., LeCam, A., Bukowski, M. and Pastan, I. 1980. Isolation of multiple classes of mutants of CHO cells resistant to cyclic AMP. Somatic Cell Genet. 6, 45-61.
15. Cabral, F.M., Sobel, E. and Gottesman, M.M. 1980. CHO mutants resistant to colchicine, colcemid or griseofulvin have an altered β-tubulin. Cell, 20, 20-36.
16. Ling, V. and Thompson, L.H. 1973. Multidry resistant mutants. In: Molecular Cell Genetics: the Chinese hamster cell. M.M. Gottesman, editor, John Wiley, N.Y. pp. 773-787.
17. Bales, B.L., Lesin, E.S. and Oppenhelmer, S.B. 1977. On cell membrane lipid fluidity and plant lectin agglutinability. A spin label study of mouse ascites tumor cells. Biochim. Biophys. Acta, 465, 400-407.
18. Gróf, P. and Belágyi, J. 1983. The effect of anaesthetics on protein conformation in membranes as studied by the spin-labeling technique. Biochem. Biophys. Acta, 734, 319-328.
19. Aszalós, A., Bradlaw, J.A., Reynoldo, E.F., Yang, G.C. and El-Hage, A.N. 1984. Studies on the action of nystatin on cultured rat myocardial cells and cell membranes, isolated red heart and intact rats. Biochem. Pharmacol. 33, 3779-3786.
20. Hubbell, W.L., McConnell, H.M. 1971. Molecular motion in spin-labeled phospholipids and membrane. J. Am. Chem. Soc. 93, 314-326.

21. Butterfield, D.A., Chesnut, D.B., Roses, A.D. and Appel, S.H. 1974. Electron spin resonance studies of erythrocytes from patients with myotonic muscular dystrophy. Proc. Natl. Acad. Sci. USA, 71, 909-913.
22. Shapiro, H.M. 1981. Flow cytometric probes of early events in cell activation. Cytometry, 1, 301-312.
23. Waggoner, A.S. 1979. Dye indicator of membrane potential. Ann. Rev. Biophys. Bioeng. 8, 47-68.
24. Lai, C.S., Hopwood, L.E. and Swartz, H.M. 1980. Electron spin resonance studies of changes in membrane fluidity of Chinese hamster ovary cells during the cell cycle. Biochim. Biophys. Acta, 602, 117-126.
25. Freed, J.H. 1972. Electron spin resonance. Ann. Rev. Phys. Chem. 11, 265-310.
26. Lai, C.S., Hopwood, L.E. and Swartz, H.M. 1980. ESR studies on membrane fluidity of Chinese hamster ovary cells grown on microcarriers and in suspension. Exp. Cell. Res. 130, 437-442.
27. Manfredi, J.J., Parness, J. and Horwitz, S.B. 1982. Taxol binds to cellular microtubules. J. Cell Biol. 94, 688-696.
28. Porter, K., Prescott, D. and Frye, J. 1973. Changes in surface morphology of Chinese hamster ovary cells during the cell cycle. J. Cell Biol. 57, 815-836.
29. Rottenberg, H. 1979. The measurements of membrane potential and pH in cells, organelles and vesicles. In: Methods in Enzymology, Vol. LV, part B (S.T. Leischcher and L. Pacher, eds.) Academic Press, New York, pp. 547-569.

DISCUSSION

ZS.-NAGY:

The order parameter you measured is strongly dependent on the cell number/volume. How can you assure absolutely identical numbers in your test system?

Would you predict how e.g. the passive permeability for K^+ will change, if the lateral mobility of proteins changes in the membrane?

ASZALÓS:

After culturing the cells at well defined conditions and measuring the same order parameter, S, many times, you can be sure that you have always the same membrane "fluidity" of your cells. Also before drug treatment, cells were pooled and divided into treated and untreated parts.

I have no data to answer your question. I have not seen a good discussion on this topic yet either.

CHERRY:

Is it possible that the small changes in order parameters are caused by changes in membrane potential, rather than vice versa. I ask this because membrane potentials of tens of millivolts correspond to high electric field strengths across the lipid bilayer which could in turn cause compression of the lipid chains.

ASZALÓS:

It is entirely possible what you propose is true. I do think that protein conformational change must be first followed by membrane potential change. Change in the motional freedom of lipid molecules may follow these events.

Dynamics of Biochemical Systems
S. Damjanovich, T. Keleti, L. Trón (Eds)

DYNAMIC STRUCTURE OF BIOLOGICAL MEMBRANES

AKIRA IKEGAMI and KAZUHIKO KINOSITA, Jr.

The Institute of Physical and Chemical Research,
Hirosawa 2-1, Wako-shi, Saitama 351-01, Japan

I. INTRODUCTION

From the liquid crystal two-dimensional nature of membrane architecture, molecular motions of membrane constituents are restricted by the anisotropic structural factor in addition to the isotropic frictional factor. Translational motion of proteins or lipids in membranes is structurally restricted in the plane of membrane. Rotational motion of membrane proteins across the plane of membrane is practically restricted by the amphipathic nature of these molecules. Thus, the major rotational diffusion of membrane proteins must be anisotropic rotation around a molecular axis perpendicular to the plane of membrane[1,2].

Rotational motion of deuterated lipids and spin labeled lipids in membranes has been studied by nuclear magnetic resonance (NMR)[3] or electron spin resonance (ESR)[4]. The results are usually analyzed by the assumption that the rotational motion of lipid chains around the chain axis is much faster than the characteristic time scale of the magnetic resonances. Then the spectra give only the "order parameter s" which indicates the angular distribution of chain axis around the membrane normal.

Abbreviations: DPH, 1,6-diphenyl-1,3,5-hexatriene; DMPC, dimyristoyl-phosphatidylcholine; DPPC, dipalmitoyl-phosphatidylcholine; DOPC, dioleoyl-phosphatidylcholine; PAPC, 1-palmitoyl-2-arachidonoyl-phosphatidylcholine; PLPC, 1-palmitoyl-2-linoleoyl-phosphatidylcholine; POPC, 1-palmitoyl-2-oleyl-phosphatidylcholine.

The steady state fluorescence anisotropy of fluorescent dyes embedded in membranes have been used as the measure of membrane fluidity. Its value is in most cases interpreted in terms of "microviscosity"[5] on the assumption of isotropic rotation of probes. Rotational diffusion of a small but unspherical molecule embedded in lipid bilayer, however, should reveal the anisotropic rotation of lipid hydrocarbon chains in the membrane.

In 1977, we studied[6] the molecular motion of a rod like fluorescent probe, 1,6-diphenyl-1,3,5-hexatriene (DPH), in lipid bilayers with the time-resolved fluorescence depolarization technique, and proposed the wobbling in cone model[7]. By this model, we emphasized that the rate and range of the rotational motion were important factors to describe the dynamic structure of membrane. In this paper we briefly summarize our own fluorescence depolarization studies[8,9] on various model and biological membranes.

II. TIME RESOLVED FLUORESCENCE DEPOLARIZATION AND WOBBLING IN CONE MODEL

1) Fluorescence depolarization

Molecular rotation of fluorescent probes can be followed directly by the fluorescence depolarization measurement. Excitation of probes with a vertically polarized light pulse produces an ensemble of excited probes of whose transition moments are preferentially aligned along the vertical direction. Then, the excited probes undergo rotational diffusion and their orientations become randomized with time. If one observesthe vertical (I_v) and horizontal (I_h) components of the fluorescence intensity,their time courses depend on both the lifetime and the rotational correlation time. To separate these dependences, the observed intensities are usually analyzed using the fluorescence anisotropy r(t) defined by

$$r(t) = (I_v(t) - I_h(t))/I_T \quad (1)$$

where $I_T(t) = I_v(t) + 2I_h(t)$ is the total fluorescence intensity. The fundamental anisotropy r_o, the value of r in the absence of rotation, is expressed by

$$r_o = 0.4(3\cos^2\lambda - 1)/2 \quad (2)$$

where λ is the angle between the absorption and emission transition moments. The factor 0.4 is given when the initial distribution of the chromophore is isotropic. The anisotropy decay r(t) of a spherical probe in isotropic media is expressed by

$$r(t) = r_o \exp(-t/\varphi) \quad (3)$$

where φ is the rotational correlation time. For a non-spherical probe, a single exponential term in equation (3) should be replaced by the sum of several exponential terms. The steady state fluorescence anisotropy r^s is given by

$$r^s = \int_0^\infty I_T(t)r(t)dt \; / \; \int_0^\infty I_T(t)r(t)dt \quad (4)$$

2) Fluorescence anisotropy decays in membrane

Typical results of the fluorescence probe, DPH, embedded in model and biological membranes are shown in Fig. 1. The anisotropy decay of DPH observed for all membranes so far studied in our laboratory is biphasic consisting of an initial rapid decrease and a following stationary phase. The process can be expressed by the approximate form:

$$r(t) = (r_o - r_\infty)\exp(-t/\varphi) + r_\infty \quad (5)$$

The first term indicating the decay from r_o to r_∞ should be replaced by the sum of exponential terms for the strict expression. The second stational value r_∞ indicates the presence of structural restriction on the range of rotational motion of probes.

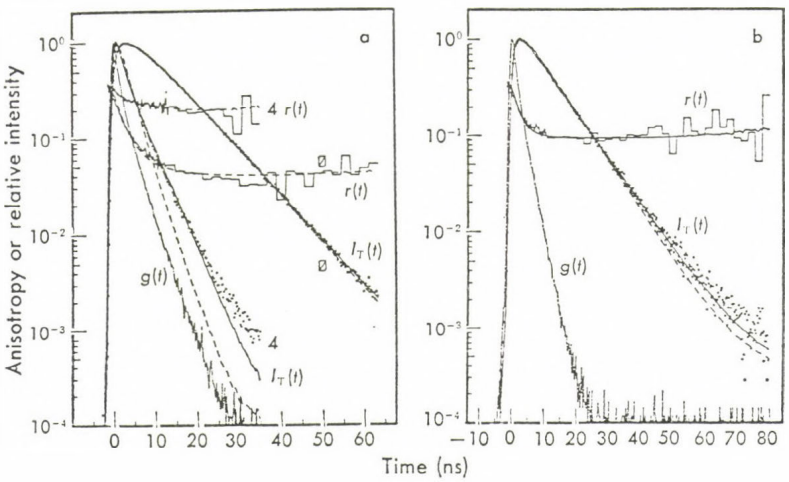

Fig.1 Typical fluorescence decays of DPH in model and biological membranes. a) In pure DMPC vesicles (curves 0) and in vesicles of the oxidase-DMPC molar ratio of 4/100 (curves 4). b) Mitochondrial membranes. $g(t)$, the instrumental response function; $I_T(t)$, the total fluorescence intensity (dots, experimental data; dashed and solid lines, calculated best-fit curves for single- and double-exponential approximations); $r(t)$, fluorescence anisotropy (zigzag lines, experimental; smooth lines, calculated best-fit curves for the exponential-plus-constant approximation).

3) Wobbling in cone model

Wobbling in cone model was proposed to interpret the biphasic decay of equation (5), in terms of two essential factors, the rate and range of restricted rotational diffusion. In the model, the long axis of the fluorescent probe wobbles freely in a cone of semi-angle θ_C with a wobbling diffusion constant D_W. Although the exact form of anisotropy decay r(t) calculated from this model is given by a sum of infinite number of exponentials, it can be closely approximated by a simpler form[7]:

$$r(t) = (r_o - r\infty)\exp(-D_W t/\sigma_S) + r\infty \qquad (6)$$

where σ_S is a constant that depends solely on θ_C, or equivalently on $r\infty/r_o$ (see Table I). Then, if an experimental anisotropy decay r(t) is approximated by the equation (5), the wobbling diffusion constant D_W can

be determined by

$$\varphi = \sigma_S / D_W \qquad (7)$$

Futhermore, the residual anisotropy r_∞ is related to the cone angle θ_C

$$r_\infty / r_0 = (\cos\theta_C (1+\cos\theta_C)/2)^2 = s^2 \qquad (8)$$

where s is the "order parameter", which is usually used as a measure of the chain orientation in NMR or ESR studies.

In the wobbling in cone model, we assume a box type orientational distribution, though the real distribution will be a smooth one. To examine the effect of this simplification on the analysis, we calculated[8] the model of gaussian distribution and compared it with the original cone model (Table I). The result indicates that, when only two parameters are extracted from an experiment, the shape of distribution function is not crucial as long as the model contains the two essential factors describing the rate and angular rangesof probe rotation

TABLE I
COMPARISON BETWEEN STRICT CONE AND GAUSSIAN MODELS

r_∞/r_0	Strict cone model		Gaussian model		σ_G/σ_s
	θ_c	σ_s	θ_e	σ_G	
1.000	0.0	0.0	0.0	0.0	
0.989	5.0	0.0022	5.0		
0.955	10.0	0.0088	10.0		
0.901	15.0	0.0196	15.0		
0.831	20.0	0.0342	20.1		
0.746	25.0	0.0522	25.2		
0.653	30.0	0.0731	30.3		
0.555	35.0	0.0962	35.7		
0.458	40.0	0.121	41.6	0.101	0.83
0.364	45.0	0.146	48.1	0.119	0.82
0.279	50.0	0.170	55.1	0.132	0.78
0.204	55.0	0.193	61.9	0.143	0.74
0.141	60.0	0.214	67.7	0.152	0.71
0.0904	65.0	0.231	72.3	0.158	0.68
0.0527	70.0	0.245	75.7	0.162	0.66
0.0265	75.0	0.253	78.1	0.165	0.65
0.0104	80.0	0.257	79.9	0.166	0.65
0.0022	85.0	0.255	81.2	0.167	0.65
0.0	90.0	0.250	82.2	0.167	0.67

III. DYNAMICS OF LIPID HYDROCARBON CHAINS

1) Phase transition

The temperature dependence of the steady state fluorescence anisotropy r^S of DPH embedded in the lipid bilayers of DMPC DPPC is shown in Fig. 2. Sharp changes in r^S observed at about 23 °C (DMPC) and 44°C (DPPC) indicate the order-disorder phase transition. The corresponding changes in wobbling parameters, θ_C and D_W, were determined[9] (Fig. 3). The orientational distribution of DPH in hydrocarbon regions is highly anisotropic in the ordered state.

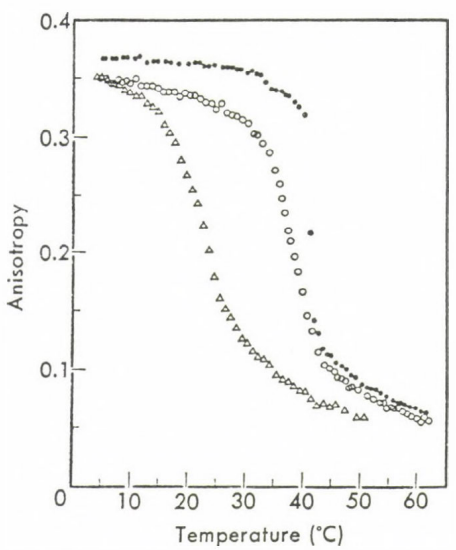

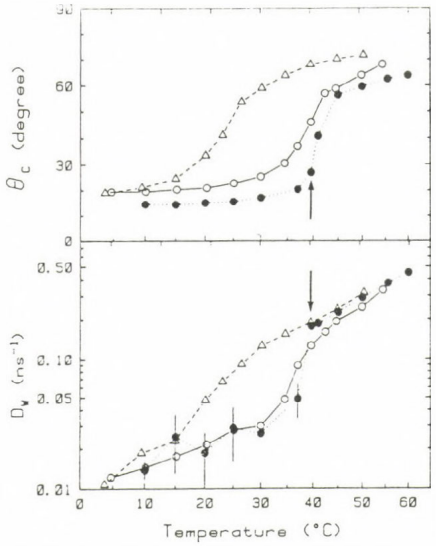

Fig. 2 (left) and Fig. 3 (right). Temperature dependences of the steady-state fluorescence anisotropy (r^S) of DPH (left) and of the wobbling diffusion constant, D_W, and the cone angle, θ_C (left), in lecithin membranes. ● DPPC multibilayer liposomes; ○ DPPC sonicated vesicles; △ DMPC sonicated vesicles.

2) Viscosity in the cone

In the disordered state at higher temperature than T_t, the estimated values of θ_C are about 70° . These values indicate that the fairly large space must be attributed to the cone for the wobbling diffusion. It is

unnatural to keep such a large void space around DPH molecules. A major part of the cone should be occupied by hydrocarbon chains and the probe wobbles around due to collision with these chains. The wobbling diffusion constant D_w indicates the diffusion rate of probe in such a hydrocarbon chain region. The "viscosity in the cone" η_c can be estimated by

$$D_w = kT/(6\eta_c V_e f) \qquad (9)$$

where V_e and f denote the effective volume and the shape factor of the probe. The value of $V_e f$ of DPH in hydrocarbon chains of lipids can be obtained from the observed $r(t)$ of DPH in liquid paraffin because of the similar molecular properties of both solvents. The viscosity in the cone represents purely the friction against the wobbling motion, and should be distinguished from the "microviscosity". The microviscosity is calculated from the value of steady state anisotropy on the assumption of isotropic rotation of a probe. Then, the structural restriction on the rotation is implicitly imposed on the microviscosity. Thus, the estimated values of η_c are an order of magnitude smaller than the "microviscosity" values.

3) Effect of double bonds

The effect of double bonds on the dynamic structure of lipid bilayers is clearly demonstrated by the changes in θ_c and D_w shown in Fig. 4[10]. The large increases in the rate and angular ranges are produced by the first double bonds introduced into the saturated lecithin molecules (DPPC). The values of θ_c and D_w of unsaturated lecithins definitely indicate the disordered state at a temperature lower than T_t of DPPC. The effect of the second and subsequent double bonds is relatively small.

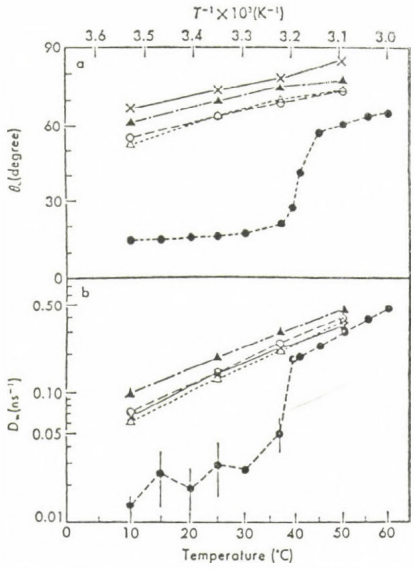

Fig. 4. Temperature dependence of the wobbling diffusion constant, D_W, and the cone angle, θ_C, for DPH in multilamellar phospholipid liposomes. ● DPPC; △ POPC, ○ PLPC, x DOPC, ▲ PAPC.

4) Effect of cholesterol

Since cholesterol is a major lipid component of many biological membranes, its effect on the dynamic structure of lipid bilayers was investigated[9,11] through the molecular motion of DPH in DMPC-cholesterol vesicles. In the disordered state at 35°C, incorporation of cholesterol decreases θ_C sharply, while D_W remained almost the same value. In the ordered state at 10°C, on the other hand, cholesterol increases D_W without changing θ_C. Similar different effects on the ordered and disordered states of lipid bilayers were observed in the reconstituted DMPC-protein systems described in the next section.

IV. PROTEIN-LIPID INTERACTION AND DYNAMIC STRUCTURE OF BIOLOGICAL MEMBRANES

1) Effect of proteins on lipid dynamics

The effect of protein-lipid interaction on the dynamic structure of

lipid bilayers was investigated in systems composed of purified cytochrome oxidase and synthetic lipids[12]. The difference between the effects of cytochrome oxidase on the ordered and on the disordered states of DMPC is shown in Fig. 5.

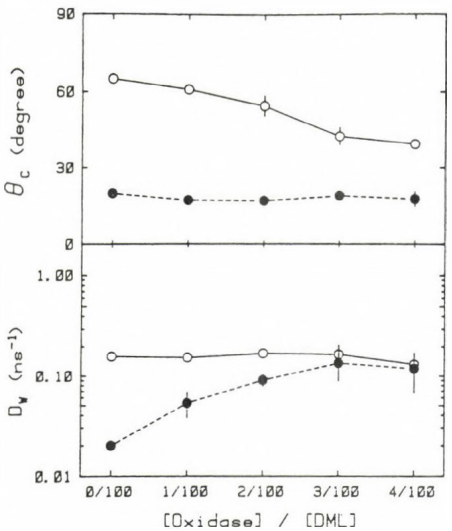

Fig. 5. The wobbling diffusion constant, D_w, and the cone angle, θ_c, for the wobbling motion of DPH in oxidase-DMPC vesicles. ○ , at 35℃ ; ● , at 10℃ .

At the disordered state above T_t, incorporation of the protein progressively reduces the range of wobbling motion θ_c, while it is not affected below T_t. On the other hand, the rate of wobbling motion, D_w, is little affected by the protein at the disordered state though it is increased at the ordered state. At the highest oxidase/lipid ratio of 4/100, virtually all DPH molecules are at the protein surface and reflect the dynamics of hydrocarbon chains in the vicinity of the protein. Here it should be noted that the angular range θ_c estimated from the fluorescence anisotropy decay referes to the motion in the nanosecond time range.

Reduction of the range of motion by the protein was also reported by

electron spin resonance (ESR) study[13] using spin-labeled fatty acid or phospholipid. ESR spectra show that the exchange between these lipids at boundary of protein surface and at bilayer lipids takes at least 50 ns. Deuterium nuclear magnetic resonance studies for membranes containing cytochrome oxidase indicate that exchange rate between the boundary and bilayer lipids exceeds 10^3 sec^{-1}[14]. These results of fluorescence, ESR and NMR studies can be accounted for in a unified manner[12], as shown in Fig. 6.

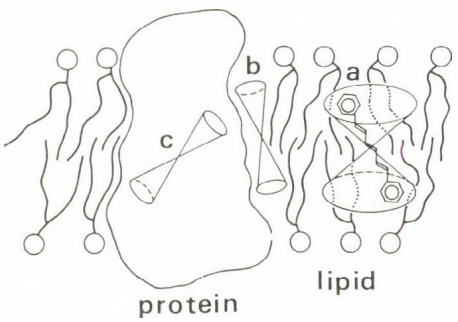

Fig. 6. Diagramatic representation of the wobbling motion of DPH in membrane. Cone A shows the approximate range of the nanosecond wobbling motion of DPH in bilayer part, which, in this figure, is assumed to be in the disordered state. A DPH molecule is depicted in this cone. Cones B and C show the motion on the surface of the protein.

In the nanosecond time range, lipid hydrocarbon chains in the disordered bilayer region exhibit the fast wobbling motion in the cone of large θ_C (see cone A in Fig. 7). Lipid chains at the protein surface are wobbling in the cones with reduced θ_C by the restriction of the irregular protein surface while their rate is not affected (cones B or C in Fig. 7). In the microsecond range, the lipid chains can move around freely among these cones and the apparent range of wobbling motion increases.

2) Dynamic structure of biological membranes.

Nanosecond fluorescence depolarization measurements were

performed[15] at two temperatures 10 and 35°C for typical biological membranes. Anisotropy decay r(t) for all these cases was biphasic, and was interpreted in terms of the wobbling in cone model. The results are shown in Fig. 7.

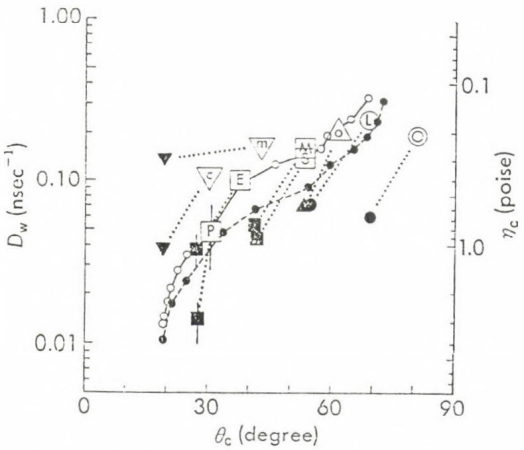

Fig. 7. Wobbling parameters of DPH in model and biological membranes (ref. 15). In two large symbols connected with a dotted line, the open symbol with a letter in it denotes D_w and θ_c at 35 or 37°C, and the closed symbol at 10°C. P, purple membrane; E, erythrocyte membrane; M, mitochondrial membrane; S, sarcoplasmic reticulum membrane; L, PLPC; O, DOPC; m, DMPC + cytochrome oxidase; o, DOPC + cytochrome oxidase; c, DMPC + cholesterol. The right-hand scale for η_c is an approximate one.

The temperature dependence of D_w and θ_c of biological and model membranes are quite similar in spite of the large differences in compositions of the membranes. Activation energies of 7-8 kcal/mole are attributed for the temperature dependence of D_w of all membranes and unsaturated lecithin vesicles (see Fig. 4). Thus, the dynamics of lipid hydrocarbon chains in membranes is basically that of the disordered state of unsaturated lipids.

There is a strong correlation between θ_c and the composition of the membranes. The correlation may be explained by the effects of protein and cholesterol discussed in previous sections. Reduction of θ_c in

sarcoplasmic and mitochondrial membranes compared to θ_c in pure unsaturated lecithin vesicles is explained by the presence of proteins, for cholesterol content of these membranes is very low. Relatively small θ_c values of erythrocyte membrane can be attributed to its high cholesterol content in addition to protein. In the purple membrane, the rigid crystalline structure of bacteriorhodopsin molecules (75wt%) apprently reduces θ_c and D_w.

In summary of our fluorescence studies[16,17], the dynamic structure of biological membranes in the lipid hydrocarbon chain region may be understood by the relative composition of unsaturated phospholipids, proteins and cholesterol, and by their interactions.

References

1) R. J. Cherry, *Biochim. Biophys. Acta.*, **559**, 289 (1979).
2) M. Edidin, *New Compr. Biochem.*, 1, 37 (1981).
3) J. Seelig and A. Seelig, *Q. Rev. Biophys.*, **13**, 19 (1980).
4) S. Ohnishi, *Adv. Biophys.*, 8, 35 (1975).
5) M. Shinitzky and Y. Barenholz, *Biochim. Biophys. Acta*, **515**, 367 (1978).
6) S. Kawato, K. Kinosita, Jr., and A. Ikegami, *Biochemistry*, **16**, 2319 (1977).
7) K. Kinosita, Jr., S. Kawato, and A. Ikegami, *Biophys. J.*, **20**, 289 (1977).
8) K. Kinosita, Jr., A. Ikegami, and S. Kawato, *Biophys. J.*, **37**, 461 (1982).
9) K. Kinosita, Jr. and A. Ikegami, *Biochim. Biophys. Acta*, **769**, 523 (1984).
10) C. D. Stubbs, T. Kouyama, K. Kinosita, Jr., and A. Ikegami, *Biochemistry*, **20**, 4257 (1981).
11) S. Kawato, K. Kinosita, Jr., and A. Ikegami, *Biochemistry*, **17**, 5026 (1978).
12) K. Kinosita, Jr., S. Kawato, A. Ikegami, S. Yoshida, and Y. Orii, *Biochim. Biophys. Acta*, **647**, 7 (1981).
13) P. C. Jost, O. H. Griffith, R. A. Capaldi, and G. Vanderkooi, *Proc. Natl. Acad. Sci. U. S.*, 70, 480 (1973).
14) A. Seelig and J. Jeelig, *Hoppe-Seyler's Z. Physiol. Chem.*, **359**, 1747 (1978).
15) K. Kinosita, Jr., R. Kataoka, Y. Kimura, O. Gotoh, and A. Ikegami, *Biochemistry*, **20**, 4270 (1981).
16) A. Ikegami, K. Kinosita, Jr., T. Kouyama, and S. Kawato, Structure, Dynamics, and Bioenergetics of Biomembranes, ed. by R. Sato and S. Ohnishi, Japan Scientific Societies Press, Tokyo, p.1 (1982).
17) K. Kinosita, Jr., S. Kawato, and A. Ikegami, *Adv. Biophys.*, **17**, 147 (1984).

Dynamics of Biochemical Systems
S. Damjanovich, T. Keleti, L. Trón (Eds)

CALCIUM CHANNELS LINKING ANTIGEN STIMULATION WITH SECRETION FROM MAST CELLS AND BASOPHILS

I. PECHT, B. RIVNAY and A. CORCIA

Departments of Chemical Immunology and Membrane Research,
The Weizmann Institute of Science, Rehovot 76100, Israel

The role of cytosolic free Ca^{+2} ions as a messenger coupling extracellular stimuli to an eventual cellular activity is well established (1). In mast cells and basophils, aggregation of the high affinity Fc receptors specific for IgE by antigen initiates a chain of biochemical events which culminates in the secretion process (2). Identification of these events and their temporal sequence are major research challenges. One of the earliest events, identified in mast cells and basophils, as following the $Fc_\varepsilon R$ aggregation is the increase in free cytosolic calcium ion concentration (3). This has been ascribed predominantly to an increase in the plasma membrane permeability allowing Ca^{+2} influx down its steep concentration gradient. Several characteristics of the Ca^{+2} influx were interpreted as reflecting the opening of ion channels in the plasma membrane (4).

An important tool in our effort to resolve the membranal elements involved in forming the Ca^{+2} channels has been the anti-allergic drug cromolyn (1,3-bis(-2-carboxychromon-5-yloxy)-2-hydroxy propane. This drug can inhibit Ca^{+2} influx into rat peritoneal mast cells or rat basophilic leukemia cells (RBL-2H3 line) and suppress their degranulation process (5,6). Employing this drug, a membrane protein has been isolated from the RBL-2H3 cells by affinity based procedures (7,8). This cromolyn binding protein (CBP) was shown to play an essential role in coupling Fc_ε aggregation with Ca^{+2} influx into the RBL-2H3 cells (9). Later on,conductance studies on model membranes yielded evidence for the ion-channel forming properties of the CBP (10). A comparison of conductance behavior of lipid bilayers reconstituted either with unfractionated plasma membranes of the RBL cells or with CBP alone or together with $Fc_\varepsilon R$,led to the following conclusions: 1) Cation fluxes display channel characteristics. 2) This activity is most probably

contained within the CBP since aggregation with monoclonal anti-CBP antibodies induced channel activity in membranes reconstituted with CBP alone. 3) All the components required for linking IgE mediated aggregation with channel opening are found in the unfractionated RBL plasma membrane and can be incorporated functionally into planar lipid bilayers. 4) Channel opening is specific, as it is induced only by ligands that aggregate the Fc_ε receptor or directly the CBP (10,11).

These results set the stage for a more quantitative examination of the channel activity in terms of its amplitude and open time properties. Furthermore, a comparison of these parameters as affected by the channel activation mode (i.e. antigen or anti-CBP) is essential for identifying the active elements and their mechanism of operation. Therefore, we have quantitatively examined in model membranes co-reconstituted with the two isolated membrane elements, CBP and the IgE-$Fc_\varepsilon R$ complex, the conductance induced upon their aggregation.

RESULTS AND DISCUSSION

Electric currents across bilayers formed at a tip of a micropipette were measured. These bilayers were attached to the tip from the lipid monolayer at air interface of vesicles resuspended in buffer (Fig. 1). The vesicles were prepared from lipids reconstituted (12,13) with either CBP or the IgE-$Fc_\varepsilon R$ complex or with both. Conductance activity was induced either by aggregating the $Fc_\varepsilon R$ or the CBP by specific agents. Several precautions were taken to ensure that the observed conductance is a specific process and not reflecting artifactual behavior (e.g. due to breakdown induced by the electrical potential itself). Moreover, it was imperative to examine whether the $Fc_\varepsilon R$ by itself does have ion channel properties. This possibility was raised, for example, by the reports of J.D-E. Young, J. Unkeless and Z. Cohn and their associates who observed that the $Fc_{\gamma 2b}$ receptor isolated from macrophages has intrinsic Na^+ channel forming properties (14). Thus, experiments in which the pipette-supported membrane contained only the IgE-$Fc_\varepsilon R$ complex, were carried out. No channel activity ($\gtrsim$ 1pS) could be detected in membranes containing only IgE-$Fc_\varepsilon R$ complexes upon aggregation, irrespective of whether specific antigen or anti-IgE antibodies were used. In each of the eight separate experiments of this kind carried out, records were monitored for a minimum of twenty minutes and up to 45 after adding the aggregating agent,yet no conductance was detected.

As mentioned above, CBP containing bilayers were shown to allow channel activity upon specific aggregation by monoclonal anti CBP antibodies (10). In order to quantitatively compare the properties of channels activated via $Fc_{\varepsilon}R$ by antigen to those activated directly by monoclonal anti-CBP antibodies, we started of with measurements on membranes containing both proteins. Experiments where anti CBP was the triggering agent resulted in channel activity very similar to that induced by specific antigens. Figure 2a shows several traces from such experiments. Trace 1 (Fig. 2a) contains two short lived channels (open times of several ms), the first one with a conductance of 4.5 pS and the second 1.5 pS. The channels in this trace appear distorted due to the effect of the filtering on such short-lived channels. Trace 2 shows a channel of 3.5 pS with longer open time (60msec). Like the antigen induced channels (see below), these low conductance and short-lived channels induced by anti-CBP appear scattered, with intervals up to several hundred milliseconds.

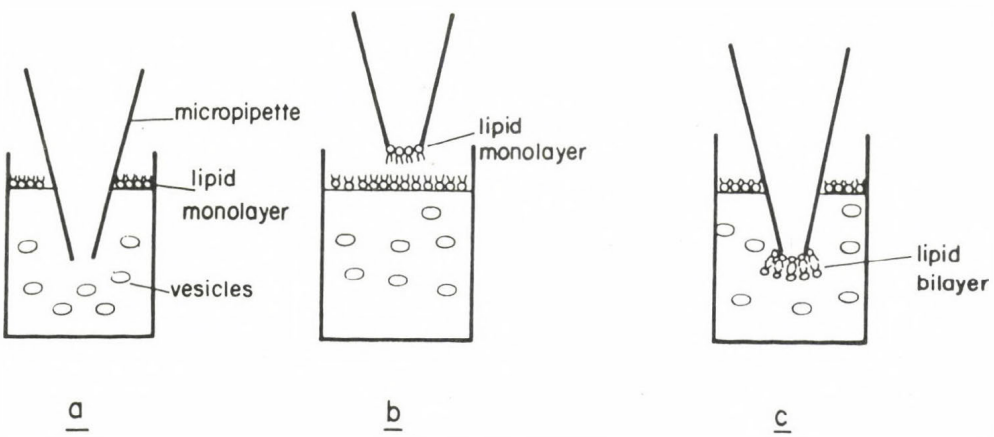

Fig. 1. A schematic illustration of the process of lipid bilayer formation at the micropipette tip. In step a the lipid monolayer is formed from the vesicles. The pipette is already in the buffer vesicle suspension. Step b - removing the pipette, which was kept under positive presence, leads to the formation of a monolayer at the tip. Reimmersion in step c leads to the apposition of lipid chains of the monolayer to that at the water-air interface and a bilayer is formed.

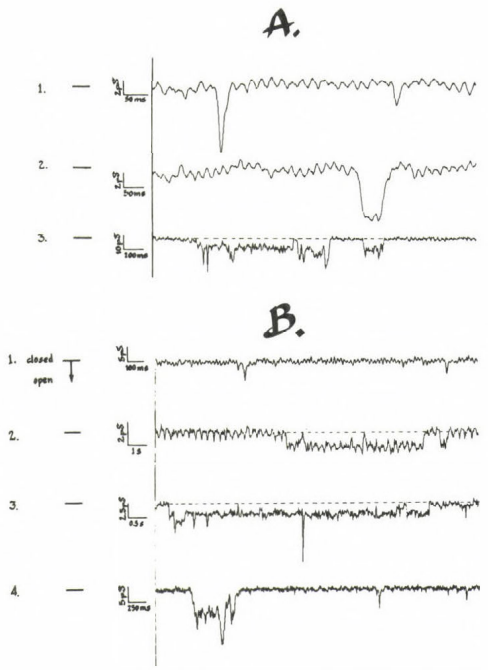

Fig. 2. Channel conductances induced in pipette-supported lipid membranes containing both the CBP and IgE-$Fc_\varepsilon R$. The downward deflection in the current trace signifies channel opening. The line at the left of each trace indicates the closed state level. A: Channels induced by anti-CBP antibodies. Clamp potential was 100 mV in traces 1 and 3 and 40 mV in trace 2. Data were low-pass filtered at 100 Hz in traces 1,2 and 3 and digitized at 3 KHz. B: Channel activity induced by specific antigen (DNP_{16}-BSA). The transmembrane potential was clamped at 40 mV (pipette interior negative) in traces 1,2 and 4 and at 60 mV in trace 3. Data were low-pass filtered at 100 Hz in traces 1 and 4 and 50 Hz in traces 2 and 3 and digitized at a sampling frequency of 3 KHz.

Trace 3 presents an example of a small channel with a long open time. Several closing and reopening as well as superimposed higher conductance levels are also resolved.

In bilayers containing both isolated CBP and $Fc_\varepsilon R$ receptors, channel

activity was now examined when specific IgE aggregating agents were employed. Characteristic conductance is induced by specific antigen ($DNP_{16}BSA$, 5 nM) added to a membrane containing both the IgE-$Fc_\varepsilon R$ complex and the CBP. Several types of events could be resolved: The most frequently observed channels are of low conductance and they remain open for time periods in the range of 10-20 msec. Trace 1 of Fig. 2B shows a 2 seconds recording containing three such channels, detected by our screening program. Due to the filtering required to detect these small channels, the precise conductance values are difficult to determine, yet the most frequently observed channels have a conductance between 1-2 pS. In a few cases, these small channels remain open for significantly longer periods, in the range of seconds (Fig. 2B, trace 2). Higher conductance levels, as high as 10 pS, sometimes appear superimposed on the basic low conductance of the long lived channels (Fig. 2B, trace 3). The last type, comprising a small fraction (10%) of all the channels observed after addition of specific antigen, are characterized by high values of conductance, ranging between 10-30 pS. The higher conductance levels appear either isolated or as bursts of activity with several different conductance levels as illustrated in Fig. 2B, trace 4.

All the above results clearly suggest that IgE aggregation leads, via the $Fc_\varepsilon R$, to channel opening most probably by co-aggregating the CBP. We did a quantitative statistical analysis of the properties of channels induced by either of the two different modes of activation. This required the accumulation and processing of a large number of events. We have analyzed the characteristics of 568 separate single channel events, 397 of which were detected in experiments using antigen and the rest with anti-CBP monoclonal antibodies.

Histograms of channel conductances were drawn from data obtained either by $Fc_\varepsilon R$ mediated aggregation (Fig. 3A), or by anti-CBP mediated aggregation (Fig. 3B). The elementary conductance values were similar in all the experiments, although each of the experiments was carried out at a given potential in the 40-100 mV range. In this analysis only conductance values assignable to the elementary-single channel events are included. Burst behavior containing different higher conductance levels as illustrated above in Fig. 2 were not included. As figure 3A shows, the majority of the detected channels (67%) have conductances in the range 1-2 pS. The number of events with larger conductance decreases rapidly with rather few events having conductances of 7 pS or more.

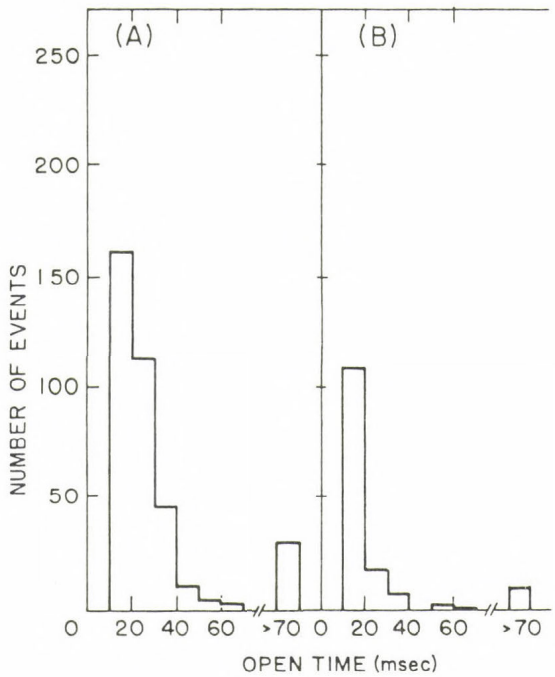

Fig. 3. Conductance histograms constructed from single channel events. A) induced by antigen (DNP_{16}-BSA), B) induced by anti-CBP. Total number of events analysed is 397 in A and 171 in B.

The majority of channels observed with anti-CBP as agonist also fall in the two bins of lower conductance (Fig. 3B) but the fraction of channels in the 1-2 pS range is not as large as in panel A. Although this difference in the histograms may be due to having less data in panel B than in panel A, other possibilities (see below) cannot be excluded.

The second parameter examined for both sets of conductance experiments was the characteristic time the channel remains open. Histograms were also constructed from the observed open-time in the channel records. Figure 4A illustrates events triggered by antigen and Figure 4B those induced by anti-CBP. Events shorter than 10 milliseconds though detectable, were not included in the histograms since the distortion induced by filtration, particularly in channels of very short open times, made them less reliable. (This limitation imposed by the necessity to filter the data in order to resolve channels with small amplitudes, introduces an uncertainty in the calculated values of the average open time discussed elsewhere.)

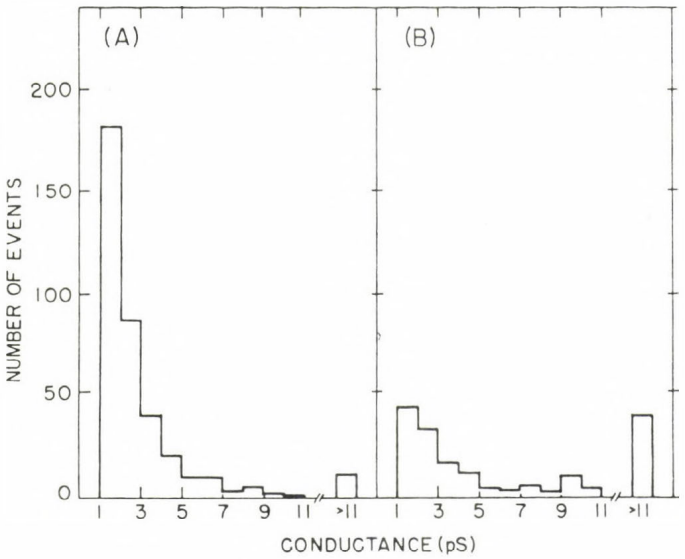

Fig. 4. Open time histograms constructed from single channel events. A) induced by antigen, B) induced by anti-CBP. Number of events in each histogram is the same as in Fig. 3.

Bearing this reservation in mind, the marked similarity of the open time histograms shown in the different panels of Fig. 4, regardless of the channel triggering mode, is still evident. In both cases the majority of channels open for short periods, of the order of 10-30 msec and only a small fraction of the events have open times of 70 msec or more.

The best fitting of the experimental data to a single exponential function is shown in Figure 5. In order to examine the fit of the experimental data to a function of the form $y = A.e^{(-t/\tau)}$, where y is the number of events with an open time t, we calculated the best linear regression fitting the logarithmic function: $\ln y = \ln A + (-t/\tau)$. The slope of this regression line is $-1/\tau$, (i.e. the reciprocal value of the average open time of the distribution). Fig. 5 shows the linear correlations for each set of data. The three groups present good linear correlations with

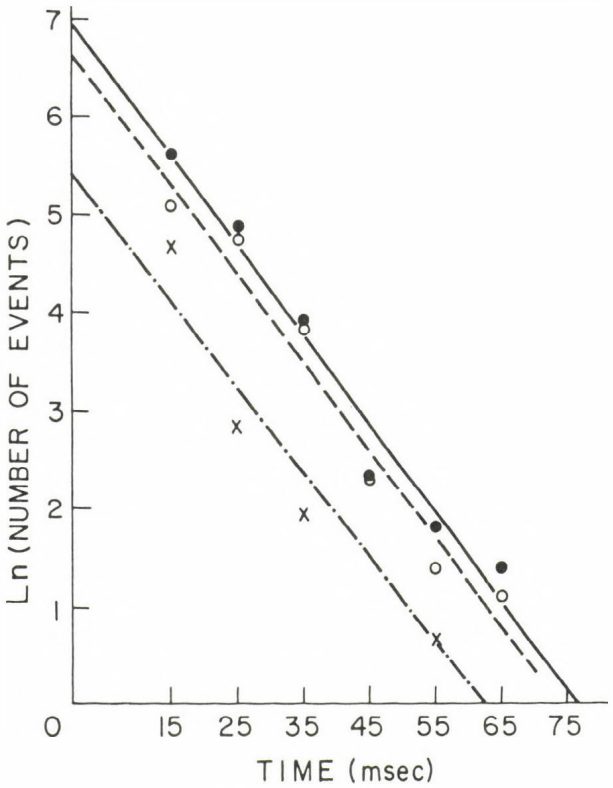

Fig. 5. Linear regression analysis of the open time distributions observed for single channel events. Each open time distribution was fitted to the equation: ln(number of events) = A - t/τ (see text). Mean open times (τ) derived from the slopes of the straight lines were: 11.1 ms for antigen-induced channels (o--o), 11.6 ms for anti-CBP induced channels (x--x) and 11.0 ms for the combined data set (•--•).

coefficients of 0.982, 0.972 and 0.982, respectively, justifying the fitting to a single exponential function. More significantly, the three regression lines are practically parallel, yielding average open times of 11.1, 11.6 and 11.9 milliseconds, respectively. This is a good indication that the channels analysed, irrespective of whether triggered by antigen or by anti-CBP, have the same open-time characteristic. Recalling the limitations involved in this analysis (see above), the value of 11 ms for the average open time of these channels must be considered as an upper limit for this

parameter.

The conductance measurements described here yield a new insight into the initial phase of antigen stimulated secretion from mast cells and basophils. They provide evidence for the direct activation, by the IgE-$Fc_\varepsilon R$ membrane complex of another plasma membrane protein component, the CBP, to form an open Ca^{+2} channel. These observations imply mutual interactions between the CBP and $Fc_\varepsilon R$ and raise a number of further interesting questions, first with respect to the structure and operation mechanism of these membrane components, their stoichiometry and control. Another essential aspect is how other cellular events couple with this Ca^{+2} influx.

Experiments now in progress will hopefully extend the quantitative characterization of the ion channel in physico-chemical terms. The marked similarity observed for the elementary conductance and open-time values observed irrespective of whether triggering is attained via the $Fc_\varepsilon R$ or by anti-CBP antibodies has to be further substantiated. Still, it clearly suggests the common element which forms the ion channel - the cromolyn binding protein.

Acknowledgment: The research work done in the lab of I.P. is supported by a grant in aid by the Hermann and Lilly Schilling Foundation for Medical Research which is gratefully acknowledged.

REFERENCES

1. Gomperts, B.D. (1976) "Calcium and Cell Activation" in Receptors and Recognition 2, 45-102. Cuatrecasas, P. and Greaves, M.F. eds.
2. Ishizaka, T. and Ishizaka, K. (1984) Prog. Allergy 34, 188-235.
3. Beaven, M.A., Rogers, I., Moore, I.P., Hesketh, T.B., Smith G.A. and Metcalf, J.C. (1984) J. Biol. Chem. 259, 7129-7136.
4. Foreman, J., Mongar, J.L. and Gomperts, B.D. (1973) Nature 245, 249-251.
5. Spataro, A.C. and Bosman, H.B. (1976) Biochem. Pharmacol. 25, 505-510.
6. Pecht, I. and Sagi-Eisenberg, R. (1985) in Calcium, Neural Function and Transmitter Release (Katz, B. and Rahamimoff, R. eds.) Martinus-Nijhoff, Boston.
7. Mazurek, N. (1983) Ph.D. Thesis, The Feinberg Graduate School, The Weizmann Institute of Science, Israel
8. Hemmerich, S., Ortega, E. and Pecht, I., in preparation.

9. Mazurek, N., Bashkin, P., Loyter, A. and Pecht, I. (1983) Proc. Natl. Acad. Sci. USA 80, 6014-6018.
10. Mazurek, N., Schindler, H., Schurholz, Th. and Pecht, I. (1984) Proc. Natl. Acad. Sci. USA 81, 6841-6845.
11. Pecht, I., Dulic, V., Rivnay, B. and Corcia, A. (1985) in Heterogeneity of Mast Cells. Millcroft-Inn Symposium. Bienenstock, J., Denburg, J. and Befus, A.D. eds.) in press.
12. Suarez-Isla, B.A., Kee Wan, Lindstrom, J. and Montal, M. (1983) Biochemistry 22, 2319-2323.
13. Coronado, R. and Lattore, R. (1983) Biophys. J. 43, 231-236.
14. Young, D-E.J., Unkeless, J.C., Young, T.M., Mauro, M. and Cohn, Z.A. (1983) Nature 306, 186-189.

DISCUSSION

EDIDIN:

I'm surprised at the long time (more than 1 minute) between adding agonist to reconstituted membrane preparations and observing increased conductance. Have you any explanation for this?

PECHT:

The kinetics of initiating the conductance may involve several factors including the binding and aggregation of the membrane-residing IgE antigen. In the absence of stirring, this might be the cause for the long delay. Still, a detailed examination has to be done in order to provide a proper answer.

ELSON:

Have you examined the dependence of the rate of initiation of conductance in reconstituted bilayers as a function of the concentration of protein in the bilayer?

PECHT:

No, not yet. We naturally did look at single channel behavior at lower protein concentrations but not at the initiation rates.

SEGAL:

In the reconstituted membranes containing both IgE receptor and CBP, do you find desensitization after cross linking the receptor?

PECHT:

I presume you refer to decay of the conductance, rather than to desensitization. (Desensitization is the cell's decay in response to addition of Ca^{2+} ions after antigen triggering in its absence and is observed in most cells and usually not in the RBL-2H3 cells.) In the lipid bi-

layers there is a decay of conductance after long periods (15-20 min) but we have not pursued that in detail.

ZS.-NAGY:

One of your slides showed the highest conductivity value for the artificial membrane when Na^+ was present. I wonder whether this fact is connected to the observations of a group in Chicago (M. Villereal) showing that mitogenic Ca^{2+}-effects are realized through the alteration of the monovalent (Na^+) permeability of the cell membrane.

PECHT:

Indeed, in the absence of Ca^{2+}, conductance of Na^+ ions seems to take place and with a higher value per single channel as shown in the slide you referred to. The relevance of this to mitogenic effects of Ca^{2+} on Na^+ permeability is unclear as we deal with different cells (Lymphocytes vs. RBL cells). We do observe interesting effects of cytosolic Na^+ on secretion from RBL. Yet this is a topic of its own.

ASZALÓS:

Could the increase of internal (Ca^{2+}) come from bound Ca^{2+} of your binding protein instead of from Ca^{2+} influx?

PECHT:

No, the transient rise in cytosolic free Ca^{2+} is a result of a net influx from outside the cell. That has been first shown by Foreman and his associates using $^{45}Ca^{2+}$ (for mast cells) and more recently by M. Beavan and Rivnay for RBL-2H3 cells using the Quin-2 and $^{45}Ca^{2+}$, respectively.

FÉSÜS:

Is CBP unique to basophils and mast cells? Have you looked for it in other types of cells with your monoclonal antibody?

PECHT:

We have looked at cromolyn binding to a limited number of different cell types and found that only mast cells and basophils bound it. The best tool to check this is indeed the monoclonal antibodies but we did not do this yet.

ELSON:

Can you relate changes in calcium transport via the CBP to action of protein kinase C?

PECHT:

We have indeed looked the potential modulation of the cytosolic Ca^{2+} levels by kinase C as effected by phorbol esters (cf. R. Sagi-Eisenberg and I. Pecht, Immunol. Lett. 1984; R. Sagi-Eisenberg, H. Lieman and I. Pecht, Nature, 1985). Rather interesting synergism (at low concentrations 1-7 nM) and inhibitory (at concentration greater than 10 nM) effects on secretion have been components of the RBL-2H3 cells by kinase C is being investigated.

ASZALÓS:

Do you know that other cells, also activated by Ca^{2+} influx would have the same type Ca^{2+} influx mechanism?

PECHT:

Ligand activated Ca^{2+} channels are suggested to operate in several other cell types. An interesting possible analog to the mast cell case could be the T-cell. There are several recent reports suggesting that one of the T-3 membrane complex in T-lymphocytes is acting as a Ca^{2+} channel.

GOLLOP:

Did you try to check the inhibitory effect of cromolyn on the trans-side of the bilayer (the side which has not been reconstituted with the different proteins).

PECHT:

Yes, we did and as you would have expected the drug does not have any effect when added to the trans compartment. Neither can you activate it when the agonist is added to the wrong side.

SEGAL:

Have you any direct evidence that CBP binds to cross linked IgE-receptor, for example by co-precipitation or covalent X-linking?

PECHT:

Not yet. We are planning such studies in the very near future. There is, however, indication for such interactions from co-patching experiments which naturally do not provide direct evidence.

MANNERVIK:

Is it possible that, apart from the effects on the cell membrane, the clinical usefulness of cromolyn may be due to inhibition of leukotriene biosynthesis? Leukotrienes are believed to be orders of magnitude more potent as mediators of the effects of asthma.

PECHT:

As I stressed, the detailed mode of cromolyn's pharmacological action is not settled. Still, as far as I can recall it does not interfere with the biosynthesis of leukotrienes. Hence it is not affecting this aspect of allergic disorders.

Dynamics of Biochemical Systems
S. Damjanovich, T. Keleti, L. Trón (Eds)

EFFECT OF MELITTIN AND MEMBRANE POTENTIAL ON THE MOBILITY OF BAND 3 PROTEINS IN HUMAN ERYTHROCYTE MEMBRANES

RICHARD J. CHERRY

Department of Chemistry, University of Essex,
Colchester CO4 3SQ, UK

INTRODUCTION

In recent years there has been considerable interest in measuring rotational and lateral diffusion of membrane proteins. Rotational motion has been extensively studied by observing transient dichroism of either intrinsic chromophores or triplet probes (Cherry, 1978). In the case of triplet probes, increased sensitivity has been obtained by methods based on the detection of phosphorescence (Austin et al. 1979) or fluorescence depletion (Johnson and Garland, 1981).

Some of the most detailed investigations to date have been performed with band 3 proteins, both in erythrocyte membranes (Nigg and Cherry, 1979a, 1980; Austin et al., 1979) and in reconstituted vesicles (Mühlebach and Cherry, 1985). In the erythrocyte membrane, slightly more than half of the total band 3 appears to rotate freely, while the remainder is restricted by interactions with cytoskeletal proteins (Nigg and Cherry, 1980). Long range lateral motion of all of band 3 is strongly restricted, probably because even 'free' band 3 is entrapped in the interstices of the cytoskeletal network (Koppel et al., 1981).

A particular feature of rotational diffusion measurements is that relaxation times are very sensitive to associations between membrane proteins. This has been exploited to study, for example, the existence of dimers of band 3 in erythrocyte membranes (Nigg and Cherry, 1979b) and complex formation between components of electron transport chains in mitochondrial and microsomal membranes (Kawato et al. 1981, Gut et al. 1983). The present paper describes further recent applications of this approach to erythrocyte membranes. Transient dichroism studies of eosin-labeled band 3 demonstrate that the basic polypeptide, melittin, promotes the self-aggregation of band 3. Moreover this property appears to correlate with its haemolytic activity. In further experiments it is shown that a membrane potential can also cause band 3 to aggregate and this effect may well be mediated by a potential-dependent conformational change of the protein.

METHODS

The transient dichroism technique used to measure rotational

diffusion of membrane proteins is described in detail elsewhere (Cherry, 1978). Essentially the sample is excited by a brief linearly polarized light pulse from a Nd-YAG laser. Transient absorbance changes are recorded for light polarized parallel ($A_{\parallel}(t)$) and perpendicular ($A_{\perp}(t)$) with respect to the exciting pulse and the absorption anisotropy r(t), at time t after the pulse, calculated from the expression

$$r(t) = \frac{A_{\parallel}(t)-A_{\perp}(t)}{A_{\parallel}(t)+2A_{\perp}(t)} \qquad (1)$$

The time dependence of the anisotropy depends on rotational diffusion. For proteins in membranes, the anisotropy normally decays to a constant value r_3. If an immobile fraction is present, r_3 is increased. The parameter $r_3\%$ is a convenient measure of the immobile fraction, where $r_3\% = 100r_3/r_0$ and r_0 is the anisotropy at t = 0.

Band 3 was labeled in intact human erythrocytes with the triplet probe eosin-5-maleimide (Molecular Probes Inc) as described by Nigg and Cherry (1979a). All measurements of rotational diffusion were performed in ghosts prepared by osmotic lysis. In the case of experiments involving melittin, the ghosts were suspended in 5 mM sodium phosphate buffer, pH 7.4 and not resealed. For studies of the effect of membrane potential, right side out resealed ghosts were prepared as described previously (Richards and Eisner, 1982). The ghosts were resealed in a phosphate buffer containing 150 mM KCl to give a high internal K^+ concentration. The resealed ghosts were resuspended in media containing varying concentrations of KCl with isotonicity maintained by addition of the appropriate amount of NaCl. A membrane potential was created by adding the ionophore valinomycin in the presence of a K^+ gradient. The existence of a membrane potential was checked using the fluorescent probe 3-3' dipropyl thiodicarbocyanine (diS-C_3-(5) as described by Waggoner (1979).

Native melittin was purified in the laboratory of Dr. R.C. Hider from whole Apis mellifera venom. The product contained no detectable phospholipase A_2 activity. Succinyl and acetyl melittin derivatives, in which the free amino groups are modified, were prepared by methods based on those of Habermann and Kowallek (1970). Bacteriorhodopsin was obtained from Halobacterium halobium and reconstituted into dimyristoyl-phosphatidylcholine vesicles as previously described (Cherry et al. 1978).

EFFECTS OF MELITTIN ON BAND 3 MOBILITY

Melittin is the major constituent of Honey Bee (Apis mellifera) venom and is largely responsible for the inflammation and tissue damage that follows a sting from this insect. It is a powerful lytic agent and haemolysis of erythrocytes is often used to monitor and study its activity. Melittin is a polypeptide of relatively simple structure and for this reason has attracted much interest as to its mode of action. The sequence of 26 amino acids is notable for a cluster of 4 basic residues close to the blocked C-terminus and a stretch of mostly apolar residues towards the N-terminus (Habermann, 1972).

In spite of extensive studies of the secondary, tertiary and quaternary structures of melittin in a variety of environments, its mechanism of action remains elusive. Previous work has tended to concentrate on mechanisms involving the lipid component of membranes (Dawson et al., 1978; Brown and Wüthrich, 1981; Dasseux et al., 1984, while the possible role of membrane proteins has been largely neglected. The aim of the experiments described here was to test whether melittin had any effect on band 3 proteins in erythrocytes which could be detected as an altered rotational mobility. If so, a further aim would be to discover whether these effects were likely to be important for understanding the lytic activity of melittin.

Initial experiments quickly revealed that melittin does indeed have a dramatic effect on the rotational mobility of band 3 (Dufton et al., 1984). Typical results are shown in Fig. 1 where it can be seen that increasing melittin concentrations cause increasing retardations in the rate of decay of anisotropy. This indicates that melittin causes a loss of rotational mobility of band 3. When melittin is present at a concentration of 1.1 x 10^{-7} moles/mg of membrane protein, band 3 is almost totally immobilised over the time scale of the measurements.

Analysis of the anisotropy decay curves indicates that the immobilising effect is 50% complete at a melittin concentration of 4-5 x 10^{-8} moles/mg of membrane protein. By comparison about 2-3 x 10^{-8} moles melittin/mg of membrane protein are required to produce 50% hemolysis of intact erythrocytes. The fact that melittin immobilises band 3 at a concentration similar to that required for haemolysis provides the first indication that membrane proteins may be involved in the lytic mechanism.

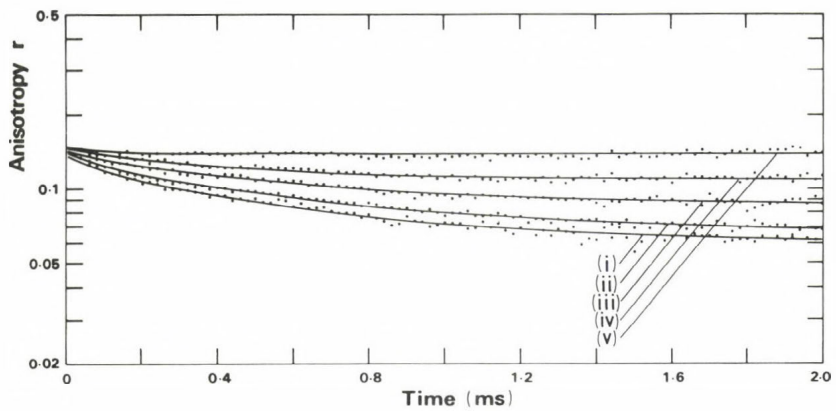

Fig. 1 Anisotropy decay curves for erythrocyte membranes at different concentrations of native melittin. r(t) was measured at 37°C with membranes suspended in 5 mM sodium phosphate buffer, pH 7.4. Concentrations of melittin are expressed as moles per milligram of ghost protein. (i) Without melittin. (ii) 1.8 x 10^{-8} mol/mg. (iii) 3.5 x 10^{-8} mol/mg. (iv) 4.9 x 10^{-8} mol/mg. (v) 1.1 x 10^{-7} mol/mg. Ghost protein concentration was 0.6 mg/ml.

Native melittin contains 6 positive charges (2 Arg, 3 Lys and the N-terminus). The free amino groups can be acetylated to leave a net charge of 2+ or succinylated when the net charge becomes 2-. Acetylation reduces the haemolytic activity of melittin whilst succinylation abolishes it altogether. We have investigated the effects of acetyl- and succinyl melittin on band 3 mobility. We find that in the case of acetyl-melittin the concentration required to produce 50% immobilisation is about 6 x 10^{-8} moles/mg of membrane protein whilst succinyl melittin produces no effect on band 3 mobility. This good correlation between the effects of derivatisation on haemolytic activity and immobilising activity strengthens the proposal that membrane proteins are involved in the lytic action of melittin.

What is the mechanism whereby melittin immobilises band 3? The simplest explanation is that melittin promotes self-association of band 3 into relatively immobile aggregates. The formation of aggregates has previously been invoked to explain the effects of varying cholesterol content on band 3 mobility (Mühlebach and Cherry, 1982). Very recently we have collaborated with Dr. S.W. Hui (Roswell Park Memorial Institute, Buffalo), who has obtained freeze-fracture electron micrographs of erythrocyte membranes treated with melittin or its derivatives. These show that native melittin causes aggregation of intramembranous particles, acetyl melittin produces the same effect but at higher concentrations and succinyl melittin is without effect. The concentration of melittin required to aggregate intramembranous particles (which principally comprise band 3) is similar to that required to immobilise band 3. These results thus provide excellent confirmation that immobilisation by melittin is indeed due to band 3 aggregation in the membrane.

There are a number of ways by which melittin could promote aggregation of band 3. Direct interaction between melittin and band 3 is the most obvious possibility but indirect mechanisms mediated by other membrane proteins can also be envisaged. In addition it is conceivable that aggregation results from a change in the physical state of the lipids induced by melittin.

Experiments are in progress to attempt to distinguish between the above possibilities. In addition we have turned to a simpler model system to further elucidate the nature of melittin-membrane protein interactions. The rotational diffusion of bacteriorhodopsin reconstituted into dimyristoylphosphatidylcholine vesicles has been previously studied in considerable detail (Cherry and Godfrey, 1982). The effects of melittin and its derivatives on bacteriorhodopsin mobility in these lipid vesicles have recently been investigated and found to be essentially similar to those already observed with band 3 (Hu et al. 1985). An important advantage of the model system is that it is possible to vary the lipid:protein mole ratio (L/P) and hence test whether melittin-lipid or melittin-protein interactions are principally responsible for the observed effects. Table 1 summarises the results of a series of experiments in which the change in r_3% is used as a measure of the fraction of bacteriorhodopsin immobilised by melittin.

Table 1 Immobilization of Bacteriorhodopsin by Native Melittin at different Lipid/Protein Ratios

(a) Experiments at constant melittin/protein ratio. (b) Experiments at constant melittin/lipid ratio. Note: L/P, Melittin/L and Melittin/P are mole ratios. $\Delta r_3\%$ is the change in $r_3\%$ from the control value. L, lipid; P, protein

	L/P	Melittin/L	Melittin/P	$\Delta r_3\%$
(a)	50	0.063	3.2	23.5
	99	0.032	3.2	22.7
	161	0.020	3.2	21.4
(b)	50	0.021	1.0	8.6
	99	0.021	2.0	19.0
	161	0.021	3.3	24.2

The results in Table 1 show that the degree of immobilisation is determined by the melittin/protein mole ratio and not by the melittin/lipid ratio. This argues strongly for a direct interaction between melittin and bacteriorhodopsin and suggest that there may be a similar direct interaction with band 3.

A plausible molecular basis for the direct interaction between melittin and band 3 or bacteriorhodopsin can be deduced by consideration of known structural features. Both band 3 and bacteriorhodopsin possess hydrophobic segments which span the lipid bilayer and hydrophilic moieties bearing negative charges which reside in the aqueous phase. Melittin also possesses hydrophobic and hydrophilic segments but the latter is positively charged. Melittin could thus be embedded in the lipid bilayer via its hydrophobic segment while its cationic C-terminal segment crosslinks the membrane proteins by electrostatic binding to anionic residues. Some degree of hydrophobic interaction could also be involved in the interaction. The role of electrostatic binding is supported by the loss of activity resulting from modification of melittin's free amino groups.

The significance of the aggregation effects for the mode of action of melittin is twofold. Firstly the results presented above for erythrocyte membranes indicate that the mechanism of lysis is likely to depend on melittin-intrinsic protein interactions as well as melittin-lipid interactions. Secondly, they provide a possible basis for understanding the high degree of synergism that exists between melittin and phospholipase A_2, the second major component of bee venom, in cell lysis (Yunes et al., 1977). In cells, uniformly distributed intrinsic membrane protein may restrict the access of phospholipase A_2 to the lipids, especially as many of these proteins have large extracellular carbohydrate moieties attached. Aggregation of proteins by melittin would clear regions of lipid bilayer which would subsequently be more readily susceptible to enzymatic attack.

EFFECTS OF MEMBRANE POTENTIAL ON BAND 3 MOBILITY

The effects of membrane potential on the mobility of membrane proteins has been very little investigated. Edidin and Wei (1977) reported that depolarization of cells resulted in an increase in the rate of intermixing of surface antigens following fusion of two different cell types. It was proposed that the effect is due to increased entry of Ca^{2+} into cells, with a consequent effect on restraints to lateral mobility by cytoskeletal elements. Apart from this interesting observation, there is virtually no information on whether protein mobility is responsive to changes in membrane potential. Whilst it is by no means clear that effects are to be expected, the topic appears well worth investigating in view of the ubiquity of potentials across cell membranes.

Here, preliminary results are presented on the effect of membrane potential on band 3 rotational mobility in erythrocyte membranes. These experiments were performed on right side out resealed ghosts prepared as described under Methods. The membrane potential was detected by the fluorescent probe diS-C_3-(5). A decrease in the fluorescent intensity of the probe was observed upon addition of valinomycin for resealed ghosts with the external K^+ concentration $[K]_o$ = 0 mM (nominally) corresponding to hyperpolarization. An increase in fluorescent intensity was observed for $[K]_o$ = 150 mM, whilst a null point was found at $[K]_o$ = 100 mM.

The effect of membrane potential on band 3 mobility is illustrated by the results shown in Figure 2. The anisotropy decay curve was first determined for resealed ghosts with $[K_o]$ = 0 mM. Then valinomycin was added and the anisotropy decay remeasured within 2-3 minutes. It is clear that hyperpolarization of the membrane has a dramatic effect. The decay in anisotropy is abolished corresponding to immobilization of band 3 on the millisecond time scale.

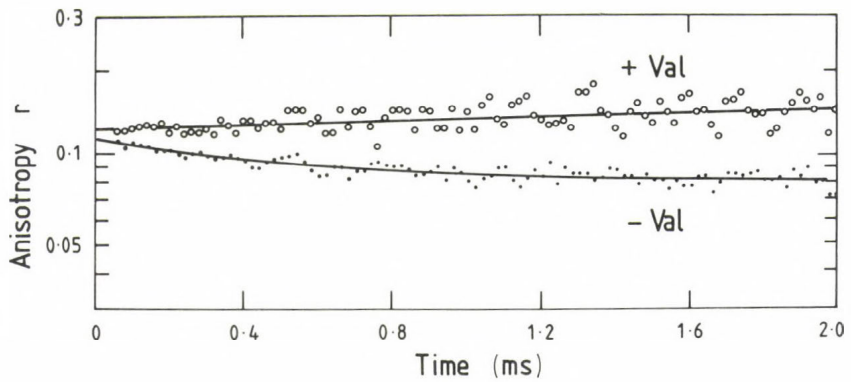

Fig. 2 Anisotropy decay curves for resealed erythrocyte ghosts in the presence and absence of valinomycin. r(t) was measured at 37°C with ghosts suspended in 0 mM KCl, 150 mM NaCl, 4 mM Hepes buffer, pH 7.5.

When similar measurements were performed with $[K_o]$ = 100 mM, no change in the anisotropy decay was detected upon addition of valinomycin. Moreover, valinomycin had no effect on band 3 mobility when added to leaky ghosts. Finally, different K^+ concentrations in the range 0-150 mM had no effect in the absence of valinomycin on either resealed or leaky ghosts. These control experiments clearly show that the immobilization of band 3 occurs only under conditions where a membrane potential is produced across the erythrocyte membrane.

The change in band 3 mobility is accompanied by a further entirely unexpected result. In the deoxygenated samples used for rotation measurements, the triplet state lifetime of the eosin probe is about 2 ms. Under the same conditions which produce an immobilization of band 3, a large drop in triplet lifetime to about 0.5 ms was observed. Again no effect was detected unless a membrane potential was produced.

Further experiments were performed in which the membrane was depolarized by addition of valinomycin to resealed ghosts with $[K_o]$ = 150 mM. Somewhat surprisingly, the effects were rather similar to those obtained with $[K_o]$ = 0 mM, namely immobilization of band 3 and decrease in the eosin triplet lifetime.

We have not attempted to quantify the membrane potentials produced in these experiments, since there is considerable uncertainty in the leakiness of resealed ghosts. Probably the potentials are not too far from the K^+ Nernst potential which implies values in the order of tens of millivolts. In considering possible explanations of the effects on band 3 mobility, it should be noted that potentials of this magnitude applied across a lipid bilayer of thickness 5 nm correspond to an electric field in the order of 10^7 V/m. Conceivably, this high electric field could affect band 3 either directly by inducing a change in conformation or indirectly via compression of the lipids. The large change in triplet lifetime of the eosin probe is a strong indication that a conformational change in band 3 occurs. It is known that tryptophan is a quencher of the eosin triplet state (Kraljić and Lindqvist, 1974) and hence a conformational change which brought the probe closer to such a residue could conceivably explain the lifetime change. The conformational change could in turn lead to aggregation of band 3, which would account for the loss of mobility.

The experiments described here demonstrate that structural changes in the erythrocyte membrane result from changes in membrane potential. It is interesting to conjecture whether similar effects might occur with membrane proteins present in excitable systems. At present we have very little understanding at the molecular level of how, for example, an electrical signal causes release of neurotransmitters from presynaptic terminals or how depolarization of muscle leads to release of Ca^{2+} stored in sarcoplasmic reticulum. A recent electron microscopic observation that acetylcholine release from synaptosomes may be accompanied by aggregation of intramembranous particles (Israel et al. 1981) is a hint that aggregation of membrane proteins may be an important phenomenon. The experiments described here represent an approach by which such phenomena might be further investigated.

ACKNOWLEDGEMENTS

I am indebted to my co-workers, Dr. Mark Dufton, Hu Kun-Sheng, Ian Morrison and Ibrahim Abd. Rahman for their contributions to the work described here. I also wish to thank the MRC and the SERC for financial support.

REFERENCES

Austin, R.H., Chan, S.S. and Jovin, T.M. (1979) Rotational diffusion of cell surface components by time-resolved phosphorescence anisotropy. Proc. Natl. Acad. Sci. USA 76, 5650-5654.

Brown, L.R. and Wüthrich, K. (1981) Melittin bound to dodecylphosphate micelles: Proton NMR assignments and global conformational features. Biochim. Biophys. Acta 647, 95-111.

Cherry, R.J. (1978) Measurement of protein rotational diffusion in membranes by flash photolysis. Methods Enzymol. 54, 47-61.

Cherry, R.J. and Godfrey, R.E. (1981) Anisotropic rotation of bacteriorhodopsin in lipid membranes. Biophys. J. 36, 257-276.

Cherry, R.J., Müller, U., Henderson, R. and Heyn, M.P. (1978) Temperature-dependent aggregation of bacteriorhodopsin in dipalmitoyl and dimyristoylphosphatidylcholine vesicles. J. Mol. Biol. 121, 283-298.

Dasseux, J-L., Faucon, J.F., Lafleur, M., Pezolet, M. and Dufourcq, J. (1984) A restatement of melittin-induced effects on the thermotropism of zwitterionic phospholipids. Biochim. Biophys. Acta 775, 37-50.

Dawson, C.R., Drake, A.F., Helliwell, J. and Hider, R.C. (1978) The interaction of bee melittin with lipid bilayer membranes. Biochim. Biophys. Acta 510, 75-86.

Dufton, M.J., Hider, R.C. and Cherry, R.J. (1984) The influence of melittin on the rotation of band 3 protein in the human erythrocyte membrane. Eur. Biophys. J. 11, 17-24.

Edidin, M. and Wei, T. (1977) Diffusion rates of cell surface antigens of mouse-human heterokaryons. II Effect of membrane potential on lateral diffusion. J. Cell. Biol. 75, 483-489.

Gut, J., Richter, C., Cherry, R.J., Winterhalter, K.H. and Kawato, S. (1983) Rotation of cytochrome P-450: Complex formation of cytochrome P-450 with NADPH-cytochrome P-450 reductase in liposomes demonstrated by combining protein rotation with antibody-induced crosslinking. J. Biol. Chem. 258, 8588-8594.

Habermann, E. (1972) Bee and wasp venoms. Science 177, 314-322.

Habermann, E. and Kowallek, H. (1970) Modification of the amino groups and the tryptophan residue of melittin as an aid to studies on the relationship between structure and mode of action. Hoppe-Seyler's Z.

Physiol. Chem. 351, 884-890.

Hu, K.S., Dufton, M.J., Morrison, I.E.G. and Cherry, R.J. (1985) Protein rotational diffusion measurements on the interaction of bee venom melittin with bacteriorhodopsin in lipid vesicles. Biochim. Biophys. Acta 816, 358-364.

Israël, M., Manaranche, R., Morel, N., Dedieu, J.C., Gulik-Krzywicki, T. and Lesbats, B. (1981) Redistribution of intramembrane particles related to acetylcholine release by cholinergic synaptosomes. J. Ultrastruct. Res. 75, 162-178.

Johnson, P. and Garland, P.B. (1981) Depolarization of fluorescence depletion: A microscopic method for measuring rotational diffusion of membrane proteins on the surface of a single cell. FEBS. Lett. 132, 252-256.

Kawato, S., Sigel, E., Carafoli, E. and Cherry, R.J. (1981) Rotation of cytochrome oxidase in phospholipid vesicles: Investigations of interactions between cytochrome oxidases and between cytochrome oxidase and cytochrome bc_1 complex. J. Biol. Chem. 256, 7518-7527.

Koppel, D.E., Sheetz, M.P. and Schindler, M. (1981) Matrix control of protein diffusion in biological membranes, Proc. Natl. Acad. Sci. USA 78, 3576-3580.

Kraljić and Lindqvist, L. (1974) Laser photolysis study of triplet eosin and thionine reactions in photosensitized oxidations. Photochem. Photobiol. 10, 351-355.

Mühlebach, T. and Cherry, R.J. (1982) Influence of cholesterol on the rotation and self-association of band 3 in the human erythrocyte membrane. Biochemistry 21, 4225-4228.

Mühlebach, T. and Cherry, R.J. (1985) Rotational diffusion and self-association of band 3 in reconstituted lipid vesicles. Biochemistry 24, 975-983.

Nigg, E.A. and Cherry, R.J. (1979a) Influence of temperature and cholesterol on the rotational diffusion of band 3 in the human erythrocyte membrane. Biochemistry 18, 3457-3465.

Nigg, E.A. and Cherry, R.J. (1979b). Dimeric association of band 3 in the erythrocyte membrane demonstrated by protein diffusion measurements. Nature 277,493-494.

Nigg, E.A. and Cherry, R.J. (1980) Anchorage of a band 3 population at the erythrocyte cytoplasmic membrane surface: protein rotational diffusion measurements. Proc. Natl. Acad. Sci. USA 77, 4702-4706.

Richards, D.E. and Eisner, D.A. (1982) Preparation and use of resealed red cell ghosts: in Red cell membranes - a methodological approach, eds. Ellory, J.C. and Young, J.D., Academic Press, London/New York, pp. 165-177.

Waggoner, A.S. (1979) Dye indicators of membrane potential. Ann. Rev. Biophys. Bioeng. 8, 47-68.

Yunes, R., Goldhammer, A.R., Garner, W.K. and Cordes, E.H. (1977) Phospholipases: Melittin facilitation of bee venom phospholipase A_2 catalysed hydrolysis of unsonicated lecithin liposomes. Arch. Biochem. Biophys. 183, 105-112.

DISCUSSION

DAMJANOVICH:

We observed a phenomenon, namely when we reached equilibrium after addition of valinomycin at high K^+ concentration, the fluorescence was further decreased upon addition of gramicidin. It was assumed that in the latter case the membrane itself was also equilibrated. It would be interesting to check this phenomenon in your system.

CHERRY:

Yes, we should try other ways of influencing the membrane potential and it would certainly be worthwhile to perform further experiments with gramicidin A.

ZIDOVETZKY:

What was the behavior of the rotational correlation times during the band 3 aggregation?

It looked, as though your freeze-fracture results indicate the non-randomization rather than aggregation of band 3.

CHERRY:

Because there are probably different sized aggregates present it is not possible to extract meaningful correlation times. All one can say is that with increasing melittin there is an increasing contribution from more slowly rotating species.

I agree. It is hard to tell from freeze-fracture whether you have true aggregation.

ZIDOVETZKI:

So, the best evidence for aggregation is coming from the rotational diffusion measurements rather than from freeze-fracture.

CHERRY:

Yes, but it is more convincing when the two techniques agree.

PECHT:

Could the effect of melittin still be accounted for by the interaction with the lipid rather than with band 3 or rhodopsin? It seems difficult to reconcile a direct effect of the peptide on two such different proteins. Hence interaction with the lipid indirectly modifying the respective lipid-protein behavior seems to me a still viable possibility.

CHERRY:

I think the data I presented for bacteriorhodopsin clearly indicate a direct melittin-protein interaction. We do not know yet if this conclusion can be applied to band 3. However, they both possess anionic residues in their hydrophilic regions which could participate in melittin binding.

SRERE:

Since your proposal and data indicate an ionic interaction between melittin and band 3 is there evidence for an effect of ionic strength on the interaction.

CHERRY:

This is a tricky question to answer because high ionic strength (e.g. 1 M NaCl) dissociates ankyrin leading to an enhancement of band 3 mobility and break up of ghosts into smaller vesicles which themselves have significant tumbling. The experiments we have performed at high ionic strength are therefore difficult to interpret but they are consistent with reversibility of the melittin-induced band 3 aggregation.

KELETI:

What is the effect of the proteins which are known to be bound to band 3 protein?

CHERRY:

These are experiments we still have to perform. For example, it would be interesting to know if removal of cytoskeletal proteins influenced the effect of melittin on band 3.

Dynamics of Biochemical Systems
S. Damjanovich, T. Keleti, L. Trón (Eds)

NUCLEAR MAGNETIC RESONANCE STUDY OF THE INTERACTION OF PHOSPHOLIPID BILAYERS WITH POLYPEPTIDE ANTIBIOTICS

RAPHAEL ZIDOVETZKI*, UTPAL BANERJEE**, ROBERT R. BIRGE***
and SUNNEY I. CHAN*

*Dept. of Biology, University of California, Riverside, USA,
**Dept. of Chemistry, California Institute of Technology, Pasadena, CA, USA,
***Dept. of Chemistry, Carnegie-Mellan University, Pittsburg, PA, USA

ABSTRACT

In this work we examine the interaction of three cell membrane-active polypeptide antibiotics: polymyxin B, gramicidin S, and valinomycin with artificial phospholipid bilayers using a combination of ^{2}H- and ^{31}P-nuclear magnetic resonance (NMR) spectroscopy. This combination of NMR measurements allowed to distinguish a character of interaction of the antibiotics with either single phospholipid bilayers or with bilayers with composition similar to the outer cell membrane of gamma-negative bacteria. The results showed that only weak surface interaction takes place between the antibiotics and the neutral phospholipid membranes. However, each of the antibiotics studied interacts strongly with negatively charged phospholipids, penetrating into the interior of the membranes.

INTRODUCTION

In recent years, there has been considerable interest in the mechanism of action of polypeptide antibiotics. Polymyxin B sulfate is a cyclic polypeptide which carries five positively charged diamino-butyric acid residues (Storm et al., 1977). Lipid-polymyxin B interactions were studied using a variety of biophysical methods, including fluorescence polarization, electron microscopy (Hartman et al., 1978), electron paramagnetic resonance spectroscopy (Galla and Trudell, 1982), calorimetry (Sixl and Galla, 1982), and Raman spectroscopy (Mushaya-

karara and Levin, 1984). Some data suggest that polymyxin B does not bind to zwitterionic lipids (Teuber and Miller, 1977; Hartmann et al., 1978), while in the other works the presence of interactions of polymyxin B with such lipids was reported (Mushayakarara and Levin, 1984).

Gramicidin S is a cyclodecapeptide antibiotic, isolated by Gaux and Brazhnikova (1944). It is effective against the gram-negative bacteria, and it was suggested that the action of gramicidin S on both artificial and natural membranes is mainly due to interactions with negatively charged lipids (Ishida and Mizushima, 1969; Shezhkova et al., 1975). It was suggested in other works, that after initial absorption on the membrane surface via ionic interactions, the hydrophobic residues of gramicidin S interact with the lipids' acyl side-chains (Yonezawa et al., 1982).

Valinomycin is a cyclododecadepsipeptide antibiotic produced by Streptomyces fulvissimus. Valinomycin alters the ionic permeability of natural (Moore and Pressman, 1964) and artificial (Lev and Buzhinsky, 1967) lipid membranes. Previous works using ^{1}H-NMR (Hsu and Chan, 1973) and Raman spectroscopy (Susi et al., 1979) suggested that valinomycin penetrates into the bilayers of dimyristoyl lecithin (DML), but does not increase the ordering of the lipid chains.

Using a combination of ^{31}P- and ^{2}H-NMR, we compared the interactions of these three antibiotics with lipid bilayers composed of a single lipid, DML and composed of a mixture of phospholipids similar to the lipid composition of outer cell membrane of gram-negative bacteria. The obtained results clarified the character of interactions of the antibiotics with the phospholipid bilayers and the possible cause of the toxicity of these antibiotics.

MATERIALS AND METHODS

Dimyristoyl phosphatidylcholine (DML) was obtained from Sigma Chemicals and was checked for purity by thin layer chromatography. All other phospholipids listed below, and all ^{2}H-labelled lipids were purchased from Avanti Polar Lipids,

Birmingham, Alabama. The lipids were pure by thin layer chromatography. Unlabelled synthetic lipids: dipalmitoylphosphatidylethanolamine (DPPE), and dipalmitoylphosphatidylglycerol (DPPG). Unlabelled lipid extracts from E. coli cell membrane: phosphadidylethanolamine (PE) and diphosphatidylglycerol (DPG, cardiolipin).

^{2}H-labelled synthetic lipids: diperdeuteromyristoylphosphatidyl-choline (DML-d_{54}); diperdeuteropalmitoylphosphatidylethanolamine (DPPE-d_{62}) and diperdeuteropalmitoylphosphatidylglycerol (DPPG-d_{62}).

Gramicidin S dihydrochloride (Sigma) was dissolved in H_2O-dioxane (5:2 v/v), filtered and lyophilized prior to use. Polymyxin B sulfate was purchased from Sigma. Valinomycin was purchased from Calbiochem.

Multilamellar dispersions used in this study were made as follows: first, the lipids, or the lipid-antibiotic mixture, were dissolved in methanol or $CDCl_3$ in an NMR tube. The solvent was then evaporated off with dry nitrogen and the tube was kept under vacuum for at least eight hours. The thin film thus formed was hydrated with a 25 mM Tris buffer solution (pD 7.4) in D_2O by repeated vortexing on a mixer and gentle warming with a heat gun. The vortexing was continued for about five minutes until a uniform white suspension was obtained. The samples were always fully hydrated and was typically 1:10 w/v in lipid to water. When polymyxin B was used, it was added to the dry lipids as a solution in the Tris buffer. The multilayers with composition similar to the E. coli membranes (model E. Coli membranes) had the following lipids: 59 % PE; 19 % DPPE; 19 % DPPG; 3 % DPG. In ^{2}H-NMR experiments either DPPE or DPPG was substituted with DPPE-d_{62} or DPPG-d_{62}, respectively.

^{31}P- and ^{2}H-NMR-spectra were acquired at 11.74T (500.13 MHz ^{1}H frequency) on a Bruker WM500 spectrometer as previously described Banerjee et al., 1985).

RESULTS AND DISCUSSION

The typical ^{31}P spectra of DML multilayers with and without added antibiotics are given in Fig. 1. Fully hydrated DML multilayers were used, at temperature above the temperature of gel-liquid crystalline phase transition (T_c). The ^{31}P spectrum of control DML sample is characteristic to the bilayer conformation of the lipids molecules (Seelig, 1978). The rapid intramolecular isomerization of the head group and the rotational diffusion of the lipid molecules about the axis, perpendicular to the plain of the bilayer (director) cause the axial averaging and only two components of chemical shift tensor (σ) can be obtained, which correspond to the orientations parallel (σ), or perpendicular (σ) to the director. The chemical shift anisotropy, arising from the dependence of the ^{31}P chemical shift of a lipid molecule on its orientation relative to the magnetic field, is defined in such a case as $\Delta\sigma=\sigma -\sigma$. From the spectra in Figure 1 $\Delta\sigma$ can be determined from the splitting between the edges of the spectrum of the half height of the low-frequency "foot". The chemical shift anisotropy $\Delta\sigma$ depends on molecular motions and orientation of the phospholipid headgroups. As the motional state of the lipids depends on temperature, and undergoes a sharp change of the phase transition temperature, $\Delta\sigma$ is a sensitive measure of the gel-liquid crystalline phase transition temperature. We used the measurements of $\Delta\sigma$ to compare the motional state of DML in the absence and presence of the antibiotics, and the effect of an antibiotic on the phase transition temperature. The lineshapes of all four spectra in Fig. 1 are characteristic of the phospholipids in multi-lamellar phase. That implies that at the molar ratio of DML to antibiotic of 5.7:1 the bilayer phase is still maintained for all three antibiotics studied. Further increase of antibiotic concentration led to disruption of bilayer structure only in case of gramicidin S (see below). The comparison of spectra with and without antibiotics shows that the effects of the presence of antibiotics on $\Delta\sigma$ are different in each case. Figures 2-4 summarize the temperature dependence of $\Delta\sigma$ for DML in the presence and absence of different concentrations of antibiotics.

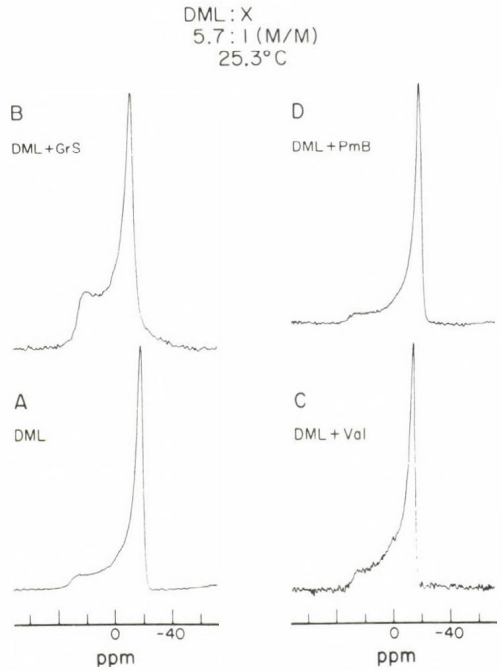

Figure 1.

^{31}P-NMR spectra of lipid headgroups in fully hydrated DML-antibiotic mixtures. The spectra were recorded at 202.49 MHz frequency at 25.3°C. The samples with antibiotics had 5.7:1 DML:antibiotic mole ratio. (A) DML; (B) DML plus gramicidin S; (C) DML plus valinomycin; (D) DML plus polymyxin B.

The temperature dependence of $\Delta\sigma$ in the presence and absence of different concentrations of polymyxin B is given in Fig. 2. The results show that the $\Delta\sigma$ is largely unaffected by the presence of polymyxin B up to a molar ratio of polymyxin B: Lipid of 1:5.7. Only at even higher concentration (1:3) there is a small (4^{O}) change in the phase transition temperature of DML, but even at that high concentration, the presence of polymyxin B does not change the values of $\Delta\sigma$ either above or below the phase transition temperature. These results are consistent with the studies showing that polymyxin B does not interact with neutral lipids (Teuber and Miller, 1972). The effect of valinomycin on $\Delta\sigma$ in shown in Fig. 3. The results show that $\Delta\sigma$ is <u>decreased</u> above T_c in the presence of valinomycin.

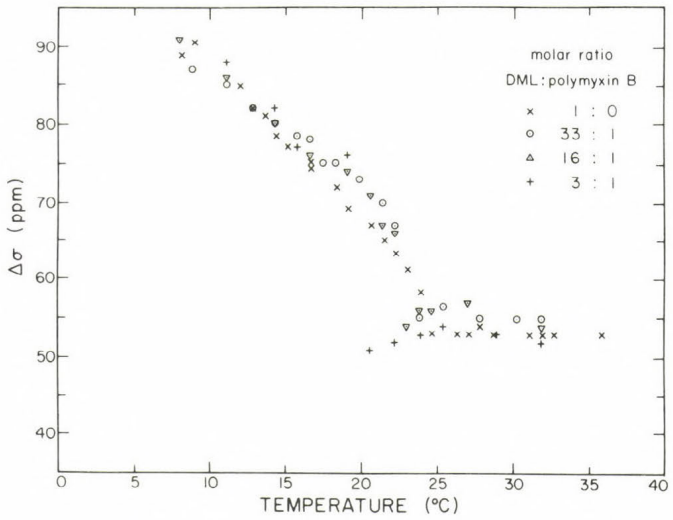

Figure 2.

Plot of Δσ versus temperature for polymyxin B containing DML multilayers (x-x) no polymyxin B mole ratio; (▽-▽) 16:1 DML:polymyxin B mole ratio (+-+) 3:1 DML:polymyxin B mole ratio.

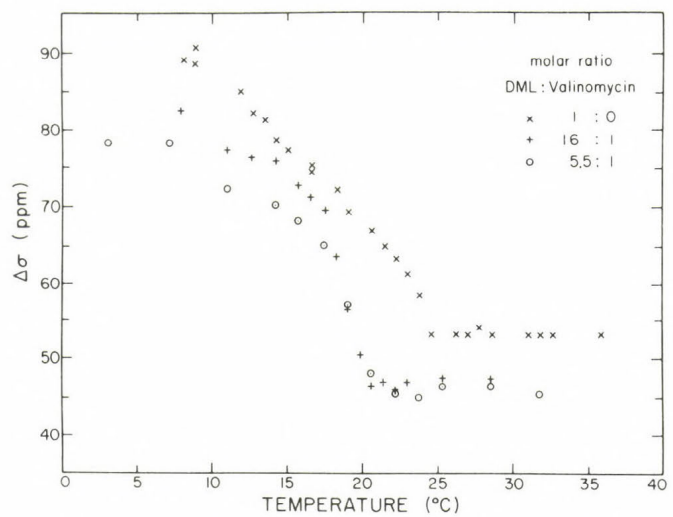

Figure 3.

Plot of Δσ versus temperature for valinomycin containing DML multilayers. (x-x) no valinomycin, (+-+) 16:1 DML:valinomycin mole ratio; (o-o) 5.5:1 DML:valinomycin mole ratio.

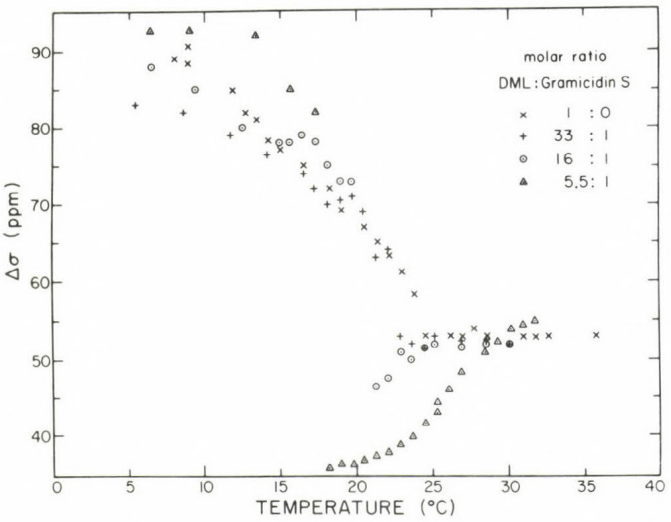

Figure 4.

Plot of $\Delta\sigma$ versus temperature for gramicidin S containing DML multilayers. (x-x) no gramicidin S added; (+-+) 33:1 DML:gramicidin S mole ratio; (o-o) 16:1 DML:gramicidin S mole ratio; (∇-∇) 5.5:1 DML:gramicidin S mole ratio.

The phase transition temperature is decreased by 5^{o}. These results indicate that valinomycin, unlike polymyxin B does react with phospholipid bilayers. The effect of gramicidin S on $\Delta\sigma$ is quite different from those of the other antibiotics studied (Figure 4). The strongest effect of molar concentrations of up to 17 % is observed in the vicinity of the phase transition temperature. Little effect is observed of gramicidin S concentration of 3 mol % (Fig. 1). Increase of gramicidin S concentration to 6 mol % changes T_c by 3^{o}, but does not change significantly at the temperatures higher than 4^{o} above the T_c, or immediately below T_c. However, $\Delta\sigma$ starts to decrease monotonously at $T_c + 3^{o}$, then increases to the values of the control DML immediately below T_c, forming sharp singularity in $\Delta\sigma$ curve at T_c (Fig. 4). This behavior is even more pronounced at gramicidin S molar concentration of 12 %, when decrease in $\Delta\sigma$ starts at $T_c + 10^{o}$, and $\Delta\sigma$ reaches the lowest value observed by us: 36 ppm (Fig. 4). Even at that concentration of gramicidin S, $\Delta\sigma$ is less affected by the presence of the antibiotic

below T_c. Interesting effect is observed in the ^{31}P spectra lineshape at 17 mole % of gramicidin S in the vicinity of T_c. The spectra obtained are consistent with both gel and liquid crystalline phases present simultaneously (Figure 5, right).

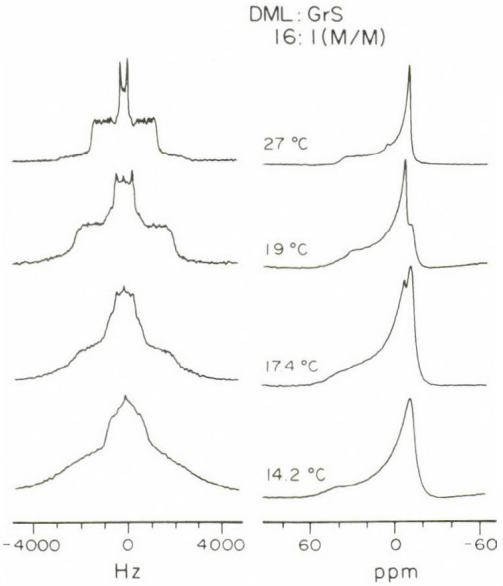

Figure 5.

^{31}P- (right) and ^{2}H-NMR (left) spectra of DML with added gramicidin S at different temperatures. The mole ratio DML:gramicidin S was 16:1.

Such a behavior was not observed by us for the other antibiotics studied in the present or previous (Banerjee et al., 1985) work. Further increase in gramicidin S concentration to 37 mol % led to the change in ^{31}P-NMR lineshape to produce a single peak at a position characteristic of isotropic motions of the phospholipid molecules. Even in that case, however, decrease in temperature resulted in the formation of a bilayer lineshape and finally most of the ^{31}P intensity was in the bilayer lineshape (data not shown). In our previous work on in-

teraction of another polypeptide antibiotic, alamethicin, with DML, we performed extensive simulations of the ^{31}P-NMR spectra lineshape in order to determine what parameters can account for the observed change of $\Delta\sigma$ (Banerjee et al., 1985). Applying the results of these simulations to the present case, we can attribute a decrease of $\Delta\sigma$ in both valinomycin, and gramicidin S case, to the change of the tilt angles θ and Φ of the phospholipid headgroups relative to the director. In case of valinomycin, this change in tilt angles is temperature independent above T_c, as illustrated by horizontal line for $\Delta\sigma$ (Fig. 3). In case of gramicidin S, however, the changes in tilt angles are temperature dependent above T_c, with maximal deviation immediately above the phase transition temperature. The ^{31}P-NMR results show that valinomycin and gramicidin S interact with phospholipid bilayers at temperatures above T_c. The previous simulations showed that the spectral shape, though not $\Delta\sigma$, is affected by change in T_2. Especially affected is the low field "foot" of a spectrum (Banerjee et al., 1985). We observed such a change in the present case upon addition of gramicidin S, indicating that gramicidin S decreases T_2 of the phospholipid headgroups.

Further information on interaction of the antibiotics with DML was attained ^{2}H-NMR of chain perdeuterated DML in the presence and absence of antibiotics. The ^{2}H-NMR spectra of DML-d_{54} at a temperature slightly above the phase transition are shown in Figure 6. Each of these spectra represents the superposition of axially averaged power patterns arising from the different deuterons for each CD_2 segment along the chains. The CD bond order parameter for the i^{th} segment, S_{CD} can be derived from the quadrupolar splitting observed at the perpendicular orientation, where

$$\Delta\nu_D^i = \left(\frac{3}{4}\right) (e^2qQ/h)\ S_{CD}^i$$

and $\frac{e^2qQ}{h}$ is the CD deuteron quadrupolar coupling constant. It has been shown by specific deuteration of lipids that the order parameter profile along the chains of a phospholipid molecule in a multilayer shows a plateau for the methylene seg-

ments near the glycerol backbone (Seelig, 1977). The corresponding quadrupolar patterns due to these segments are nearly coincident with one another and the signals at the perpendicular orientations overlap near the edge of the spectrum. Since the lower parts of the chains are more disordered, the quadrupolar patterns from these methylene segments show well-resolved peaks at the perpendicular orientation. The quadrupol splittings are also sensitive to temperature, even above T_c. The resolution allows to distinguish up to thirteen splittings above T_c (Banerjee et al., 1985). We performed the ^{2}H-NMR measurements with each antibiotic as a function of temperature and antibiotic concentration parallel with the ^{31}P-NMR measurements. The ^{2}H-NMR spectra of DML-d_{54} in the presence and absence of each of the antibiotics studied are given in Fig. 6. A comparison of the spectra in the presence and absence of polymyxin B (Figure 6 A,D) shows that this antibiotic has no effect on the hydrocarbon chains of the bilayer. The ^{31}P spectra (Figures 1, 2) showed that polymyxin B does not change either orientation of the phospholipid headgroups or the phase transition temperature of DML. We therefore conclude that polymyxin B does not interact with DML. Different picture emerges when one considers valinomycin. The ^{2}H-spectra of DML-d_{54} in the presence of valinomycin shows that the effect of this antibiotic on the hydrocarbon chains is minimal. Small change is observed for the outermost peak which arises from the methylene segments near the glycerol backbone, with all other peaks remaining unchanged. The spectrum with valinomycin also does not show broadening observed upon incorporation of proteins into bilayers (Seelig and Seelig, 1978; Rice et al., 1979). The effect of valinomycin on ^{31}P- and ^{2}H-NMR spectra of DML is consistent with the antibiotic molecule interacting with the surface of the bilayers.

The ^{2}H-NMR spectrum of DML-d_{54} in the presence of gramicidin S is given in Figure 6C. The presence of gramicidin S led both to the broadening of the spectrum and to the change of the spectral shape. These results, together with the ^{31}P-NMR measurements indicate that gramicidin S does penetrate into the bilayer above the phase transition temperature. In the

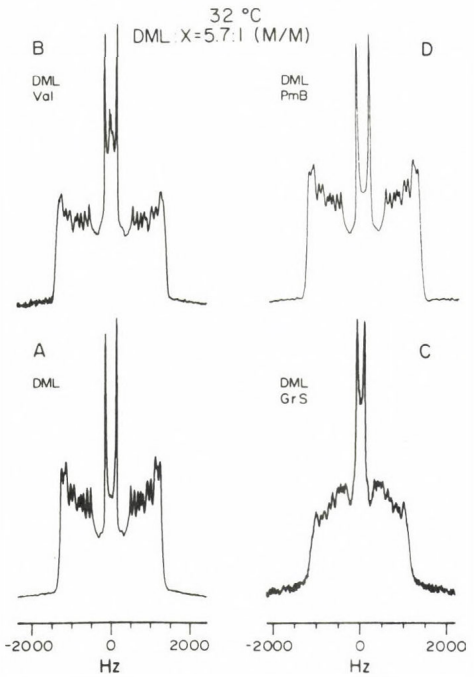

Figure 6.

^{2}H-NMR spectra of DML-d_{54} multilayers with added antibiotics at 32°C. The samples had 5.7:1 DML-d_{54}-antibiotic molar ratio: (A) no antibiotic added; (B) with valinomycin; (C) with gramicidin S; (D) with polymyxin B.

vicinity of the phase transition temperature the combination of ^{31}P- and ^{2}H-NMR shows the presence of the bilayers at two phases, corresponding to liquid crystalline and gel phases. Further increase in gramicidin S concentration causes complete disruption of the bilayer. However, even in this case, cooling of the sample leads to the formation of bilayers.

We used a mixture of E. coli lipid extracts and synthetic lipids (see Methods) to construct bilayers with a composition similar to the composition of the outer cell membrane of E.coli. We then proceeded to study the interaction of such bilayers with the antibiotics using ^{31}P- and ^{2}H-NMR. The ^{31}P spectra of the multilayers in the presence and absence of the antibiotics

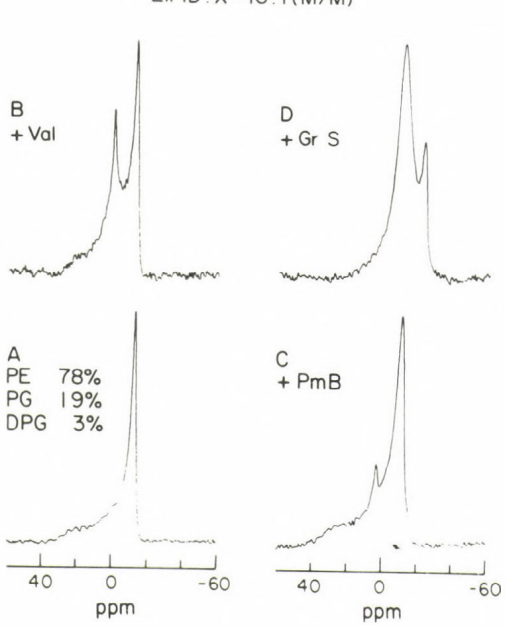

Figure 7.

^{31}P-NMR spectra of lipid headgroups of model E. coli membranes (see text) with added antibiotics at 25.3°C. The samples with antibiotic had 16:1 lipid:antibiotic mole ratio: (A) no antibiotics added; (B) with valinomycin; (C) with polymyxin B; (D) with gramicidin S.

are given in Figure 7. The ^{31}P spectrum of the fully hydrated lipids indicates that the lipids are in bilayer conformation (Figure 1A).

The ^{31}P-spectra of the lipids with each of the antibiotics studied show a peak at 0 ppm, corresponding to a fully averaged by fast isotropic motion NMR spectrum of phospholipids. That indicates that the presence of antibiotics induces, in various degrees, the formation of lipid micelles already at a concentration of 6 mol %. This effect is the smallest one in the case of polymyxin B, with only a minor portion of the intensity of the signal being in the isotropic peak (Figure 7C). The iso-

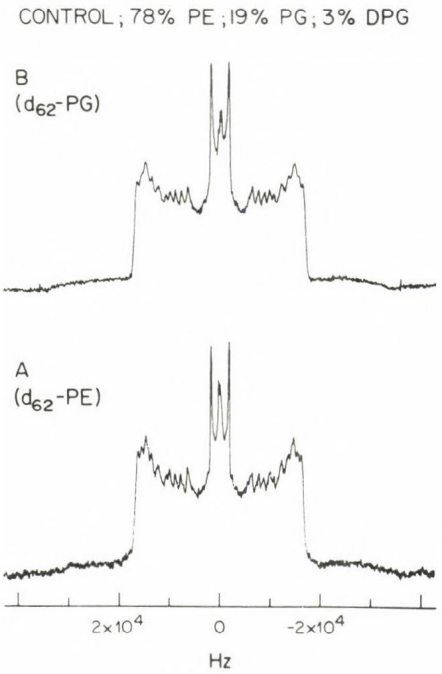

Figure 8.

^{2}H-NMR spectra of model E. coli membranes with added ^{2}H-labelled lipids. (A) with DPPE-d_{62}; (B) with DPPG-d_{62}.

tropic peak becomes more prominent in the case of added valinomycin (Figure 7B), and becomes dominant in the presence of gramicidin S (Figure 7D). In order to further characterize the interaction of the antibiotics with model E. coli membranes, we substituted part of the lipids with the synthetic lipids with perdeuterated side chains. In one type of samples we substituted DPPG with DPPG-d_{62}, and in another we substituted 25 % of E. coli PE extract with synthetic-DPPE-d_{62}. Figure 8A is identical to the spectrum of DPPG-d_{62} (Figure 8B) in chemically identical model E. coli membrane. This means that the distribution of order parameters along the side chain is the same for both PE and PG and indicates the uniform distribution of these lipids in the bilayers. The ^{2}H-spectra of both PE and PG are significantly altered upon the addition of 6 mol % ofpolymyxin B (Figure 9). The shapes of both spectra are still characteris-

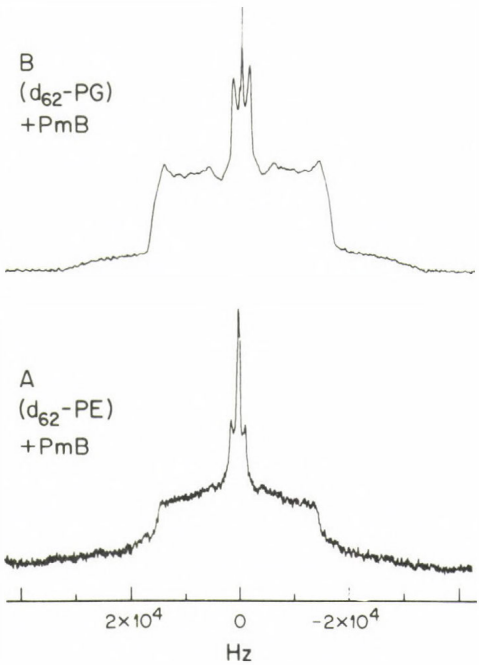

Figure 9.

^{2}H-spectra of model E. coli membrane with added polymycin B of 32°C. Mole ratio lipid:polymyxin B was 5.7:1 (A) with ^{2}H-labelled PE; (B) with ^{2}H-labelled PG.

tic of the bilayer conformation, with only small portion of intensity being in the isotropic peak in the center, which is consistent with the ^{31}P-spectrum of the lipids with polymyxin B (Figure 7C). The spectra, however, exhibit line broadening, making the fine structure observed for pure lipids (Figure 8) unresolvable. Both the broadening effect and the intensity of the isotropic peak are somewhat more pronounced in the spectrum of DPPE-d_{62} (Figure 9B), probably indicating that polymyxin B, while perturbing the structures of both PE and PG, interacts stronger with the former. The preferential interaction of an antibiotic with the PE component of the membrane is more pronounced in the case of gramicidin S (Figure 10). The ^{2}H-spectrum of DPPG-d_{62} in the presence of 6 mol % of gramicidin S

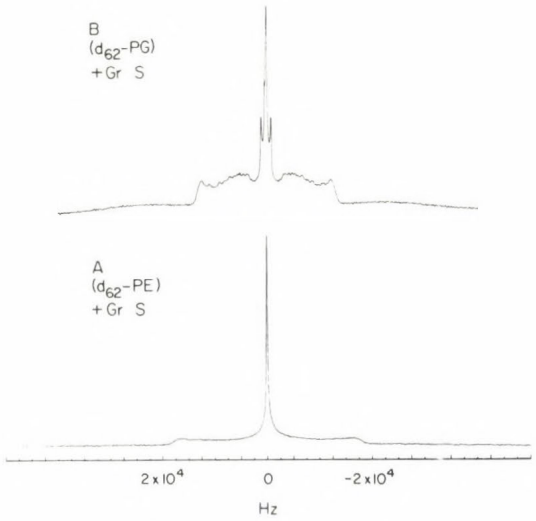

Figure 10.
^{2}H-spectra of model E. coli membranes with added gramicidin S at 32°C.

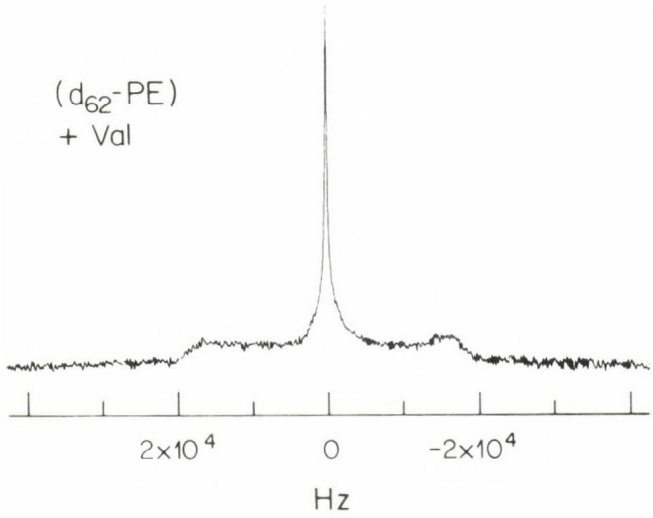

Figure 11.
^{2}H-NMR spectrum of model E. coli membranes with added valinomycin at 32°C. Mole ratio lipid-valinomycin was 5.7:1. In this experiment the ^{2}H-labelled lipid was PE.

still has most of the intensity in the bilayer shape (Figure 10B). It does exhibit line broadening similar to the one observed in the case of polymyxin B. The bilayer structure is maintained, however, only by a small percentage of the PE component, most of this lipid giving the isotropic ^{2}H-NMR peak (Figure 10A). The PE composes 78 % of model bilayers, and the PG only 19 %. Thus, the isotropic peak of the ^{31}P-spectrum of the lipids with gramicidin S can be probably attributed to PE, while the bilayer part of the spectrum to both the PG and the part of the PE. The ^{2}H-spectrum of DPPE-d_{62} in the model *E. coli* membrane in the presence of valinomycin is given in Figure 11. As in the case of gramicidin S, valinomycin also disrupts the bilayer structure significantly.

CONCLUSIONS

The combined use of ^{31}P-NMR of the lipid headgroups and ^{2}H-NMR of the acyl side chains showed the extent of the interaction of each of the antibiotics studied with the lipid membranes.

No perturbation of the lipid bilayer structure is observed by ^{31}P- or ^{2}H-NMR of DML in the presence of polymyxin B, and only small change in T_c when concentration of polymyxin B is raised to 37 mol %. We thus conclude that polymyxin B does not interact with DML.

Relatively small perturbation of DML bilayer structure was observed upon addition of up to 6 mol % of either valinomycin or gramicidin S. The perturbation was reflected mostly in the change of $\Delta\sigma$ in the ^{31}P spectrum, and minor change in the outer peaks of ^{2}H-spectrum. This is consistent with valinomycin interacting with the surface of the bilayers only.

Unlike the other two antibiotics, gramicidin S perturbs the structure of both phospholipid headgroups and the acyl side chains, which indicates that this antibiotic does penetrate into the DML bilayer. The interaction takes place, however, only above the phase transition temperature of the lipids. Only a very high concentration of gramicidin S (37 mol %) was sufficient to disrupt the bilayer structure.

The effect of the antibiotics on model E. coli membranes was very different from that on DML. A completely different picture emerged from the data where the model E. coli bilayers were used. Polymyxin B molecule is probably inserted into the membrane, which stays largely in the bilayer comformation. Both valinomycin and gramicidin S have a strong destructive effect on the model E. coli membranes. Gramicidin S primarily perturbs the structure of the PE component of the model membranes.

The interaction of valinomycin with the PE is also very strong. The interaction of each of these antibiotics with PE is probably one of the sources of their toxicity, as PE is one of the major components of the mammalian cell membranes.

REFERENCES

Banerjee, U., Zidovetzki, R., Birge, R.R. and Chan, S.I. (1985) Biochemistry (in press)

Galla, H.J. and Trudell, J.R. (1980) Biochim. Biophys. Acta, 602, 522-530.

Gaux, G.F. and Brazhnikova, M.G. (1944) Nature, 154, 703.

Hartman, W., Galla, H.J. and Sackmann, E. (1978) Biochim. Biophys. Acta, 510, 129-139.

Hsu, M.C. and Chan, S.I. (1973) Biochemistry, 12, 3872-3876.

Ishida, M. and Mizushima, J.S. (1969) J. Biochem. 66, 33-43.

Lev, A.A. and Buzhinsky, E.P. (1967) Tsitologiya, 9, 102-106.

Moore, C. and Pressman, B.C. (1964) Biochem. Biophys. Res. Commun. 15, 562-567.

Mushayakarara, E. and Levin, I.W. (1984) Biochim. Biophys. Acta, 769, 585-595.

Shezhkova, C.G. et al. (1975) Bioorg. Khim. (Russian) 1, 347.

Sixl, F. and Galla, H.J. (1982) Biochim. Biophys. Acta, 633, 466-478.

Susi, H., Sampugna, J., Hampson, J.W. and Ard, J.S. (1979) Biochemistry, 18, 297-301.

Teuber, M. and Miller, I.R. (1977) Biochim. Biophys. Acta, 467, 280-289.

Yonezawa, H., Okamoto, K., Kaneda, M., Tominaga, N. and Izumiya, N. (1982) 20th Symp. on Peptide Chemistry, Tojonako, Japan pp. 283-288.

PECHT:

Could you elaborate on the correlation between the structure of the different antibiotics and their interactions with the lipid bilayers?

ZIDOVETZKI:

Each antibiotic studied is an amphipathic molecule, and has surfaces which can interact with both polar and hydrophobic regions of a bilayer. There is a lot of information in literature on conformational structures of those molecules, and their state of aggregation, which is critical for establishing the mode of interaction with the membranes. For example, polymyxin B has positively charged tail, which probably binds to negatively charged phospholipid head groups, and hydrophobic ring, which penetrates into the bilayer.

ELSON:

Do you have any information about the influence of a potential difference across the membrane on the interactions between alamethicin and membrane lipids?

ZIDOVETZKI:

It is technically very difficult to introduce an electric potential difference in a sample inside the bore of 11.7 Tesla magnet. Besides that we need milligram amount of lipids in experiments, orders of magnitude more than is used in channel recording experiments. So, I don't think it will be done by NMR in the near future.

DAMJANOVICH:

I was looking for some biphasic effect of valinomycin, depending on concentration, as it is known that valinomycin can either hyper- or hypopolarize membranes. Would you mind commenting on this question?

ZIDOVETZKI:

It is too early to say now, but, interestingly, we did observe that the effect of valinomycin on ^{31}P-NMR spectrum of DML at some point does decrease with the increased concentration of the antibiotic.

ASZALÓS:

Have you thought about trying amphotericin B in your system, since the intercalation of this antibiotic into lipid domains is known.

ZIDOVETZKI:

Indeed, that probably would be interesting.

CHERRY:

Were the ^{2}H-NMR experiments with valinomycin performed in the presence or absence of K^{+}?

ZIDOVETZKI:

Yes, we already started it, at one concentration of K^{+}. We were surprised not to see any difference. We plan to increase the concentration of K^{+}.

CHERRY:

Can you put an upper limit on the proportion of valinomycin which is in the interior of the bilayer.

ZIDOVETZKI:

In the measurements I referred to, probably not more than 10 %.

KRETSCHMER:

Did you look for changes in the spectra of antibiotics (^{13}C, ^{1}H, ^{15}N) interacting with bilayers?

ZIDOVETZKI:

A spectrum of an antibiotic bound to a membrane becomes too broad to be observed under normal conditions. We used ^{1}H-NMR to make sure that all of the antibiotic in a sample is bound to membranes, which is indicated by the absence of a well-resolved spectrum.

Dynamics of Biochemical Systems
S. Damjanovich, T. Keleti, L. Trón (Eds)

KINETICS AS A TOOL FOR THE STUDY OF TRANSMEMBRANE EXCHANGES EXEMPLIFIED BY THE STUDY OF THE OXOGLUTARATE TRANSLOCATOR

CLAUDINE M. SLUSE-GOFFART and F.E. SLUSE

Faculté des Sciences, Département de Chimie Générale et de Chimie Physique, et Faculté de Médecine, Laboratoire de Biochimie et de Physiologie Générales, Institut de Chimie (B-6), Sart-Tilman, B-4000 Liège, Belgium

INTRODUCTION

In heart, the malate/aspartate shuttle is the main transferring device of reducing equivalents (NADH formed during glycolysis) from the cytosol to the mitochondrial respiratory chain. In this shuttle, cytosolic malate enters into the mitochondria while matricial oxoglutarate goes out. These two fluxes of anions through the inner mitochondrial membrane are coupled by the oxoglutarate translocator, which performs a one-to-one exchange.

To know the way of action of the oxoglutarate translocator, the first thing to do is to determine its kinetic mechanism *in situ*. Fortunately, isolated rat-heart mitochondria can be treated to contain only one kind of exchangeable anion, the concentration of which can be varied to some extent. Moreover, by working at 2 °C, we have achieved good conditions to measure initial rates. When possible, initial-rate analysis is in fact the best method to determine a kinetic mechanism because no assumption has to be made *a priori*.

THE KINETIC MECHANISM [1]

The double reciprocal plots of the exchange between external labelled malonate and internal malonate catalysed by the oxoglutarate translocator, exhibit straight lines with a common point situated on the abscissa. This kinetic behaviour has been observed for twelve exchanges, homologous or heterologous, with malate, oxoglutarate, malonate or succinate as substrates. The position of the common point is characteristic of the substrate for which the concentration is varied, it does not depend on the nature of the partner anion. These observations indicate a rapid-equilibrium random mechanism with independent binding of the two substrates. The oxoglutarate translocator spans the membrane and has two independent sites : one site acces-

sible to the external substrate and one site accessible to the internal substrate.

DETAILED STUDY OF THE CYTOSOLIC FACE OF THE TRANSLOCATOR [2,3]

Of course, we have initially explored rather limited ranges of substrate concentrations and we have found that all the substrates apparently behaved according to Michaelian kinetics. But, if the range of external oxoglutarate concentration is widely extended, things become much more complicated : the kinetic and binding saturation curves of external oxoglutarate (from 0.05 to 300 µM) are not hyperbolic but have four jumps (Fig.1) which are more pronounced in the binding curve. The well-defined intermediary plateau in Fig.1B corresponds to half saturation.

The fact that similar structures have been observed in both curves sug-

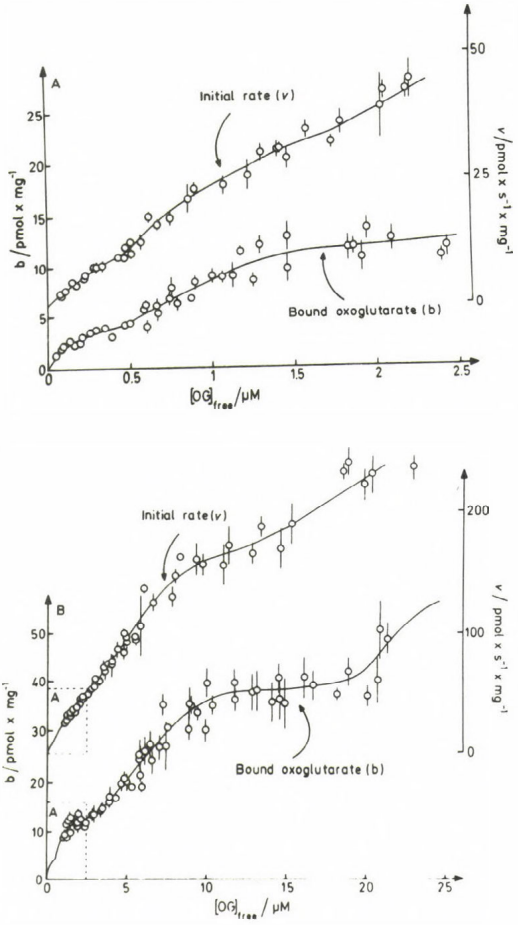

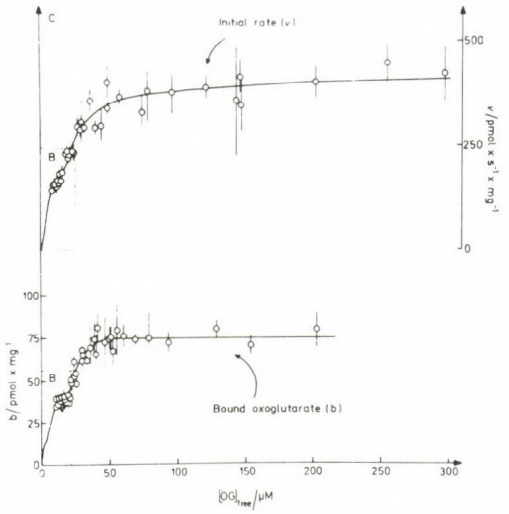

Fig. 1. *Saturation curves by external oxoglutarate.* Lower curve : equilibrium binding. Upper curve : initial uptake rate against 4 mM-internal malate.[4]

gests that these structures are not accidental and must have some significance. They are indeed reproducible [4]. However, reproducible artefacts could be introduced by the method used to obtain the data. In that case we would expect the same type of artefacts for other substrates. This is not the case : the double reciprocal plot of malate uptake is linear over a wide concentration range (from 0.05 to 840 μM).

If malate and oxoglutarate have the same binding sites, their very different behaviour could simply be due to the fact that the oxoglutarate translocator is an oligomer made of identical subunits in which malate binding does not induce any conformational change while oxoglutarate binding does. In order to be sure that malate has the same binding sites as oxoglutarate we have studied the effect of external malate on the initial rate of oxoglutarate uptake : the rate of oxoglutarate uptake in the presence of malate is equal to the rate in the absence of malate on condition that oxoglutarate concentration is divided by one plus the ratio between the external malate concentration and its Michaelis constant. This equality implies that malate and oxoglutarate are competitive and that malate does not modify the affinity of the unloaded sites for external oxoglutarate (and reciprocally). This strongly suggests that malate binding does not induce a conformational change while the conformational change induced by oxoglutarate is localized to the

oxoglutarate loaded subunit without modification of the neighbouring subunits. It must be emphasized that the conformational change induced by the external oxoglutarate is localized on the external face of the translocator. It cannot be perceived by the internal substrate because we know that internal and external binding are independent.

We can now consider the possible meanings of the four jumps in the external-oxoglutarate binding curve. The first point is that these jumps and their intermediary plateaus can be described as changeovers of negative and positive cooperativities. The mean affinity of an unloaded site for external oxoglutarate (Fig.2), first decreases, indicating negative cooperativity. It is followed by an increase of affinity, thus, positive cooperativity. This changeover repeats three times because the binding curve has three intermediary plateaux. This macroscopic behaviour may either reflect actual changeovers of cooperativities at the microscopic level or not. We will successively consider these two possibilities.

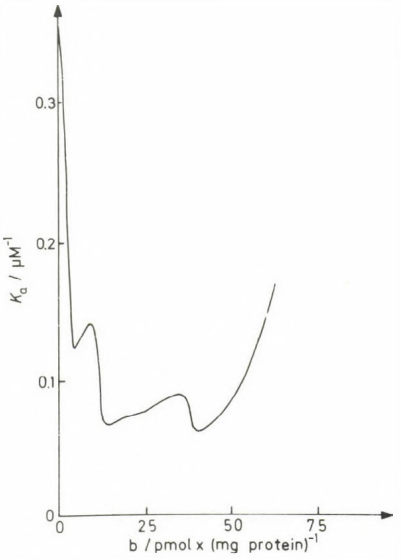

Fig.2. *Mean affinity (K_a) of an unloaded site for external oxoglutarate as a function of bound oxoglutarate (b).* The curve has been obtained by smoothing of the experimental points. K_a = b/((B-b)[OG]) where [OG] is the free external-oxoglutarate concentration and B is the maximal binding.

We will first assume that we deal with a single type of oligomer. In that case, the oxoglutarate binding must obey to an Adair's equation whose

degree, n, is equal to the number of subunits. Of course, we would like to know how many subunits are necessary to observe four jumps. This will be done through the number of necessary inflexion points : six in this case. The abscissae of the inflexion points are the roots of a polynomial that is obtained when we do the second derivative of the Adair's function. The degree of this polynomial is 3n-3, so that it cannot have more than 3n-3 positive roots. This leads to a minimum of 3 subunits. However, it is impossible to obtain four jumps with an Adair's equation of degree three and even four : only two jumps are possible. It can be demonstrated that the polynomial of degree 3n-3 cannot have more than n-1 positive roots (to be published). In our case this means that at least seven subunits are associated to form an oxoglutarate translocator if it is assumed that a single type of oligomer is responsible for the four jumps. Actually, the number of binding subunits would probably be higher than seven according to the following estimation : if the first jump of the binding curve is taken as the saturation of one site per translocator, three sites are loaded after the second jump, nine after the third and eighteen after the last jump.

Let us see the other possible interpretation : could the four jumps of the binding curve be due to four independent contributions ? It is possible if these contributions are not Michaelian. Indeed the sum of hyperbola cannot give a curve with inflexion points. The different contributions, except perhaps that of the first jump,have to be sigmoidal. We will thus suppose now that four oligomeric species of isozymic translocators, exhibiting positive cooperativity, coexist in our mitochondrial preparation. To make this hypothesis compatible with the fact that malate uptake is Michaelian we have to assume that the isotranslocators are made with the same subunits which may be associated in various ways to form various types of oligomers or that it is the membranous environment which may differ. Contrary to oxoglutarate, malate which binds without conformational change of the translocator, will not perceive such differences which concern only the interactions of the subunits between themselves or with the environment. However, this interpretation is not so simple as it seems at first sight. The reason is the internal/external independence observed in the kinetics. The general form of the initial-rate equation for an exchange between A and B is the product of the maximal rate which depends of the studied exchange, a function f of the concentration of the external substrate A, function which is specific to this substrate, and a function g specific to the internal subs-

trate B :

$$v_{A/B} = V_{A/B} \times f_A([A]) \times g_B([B]) \ .$$

If the measured rate is the sum of different contributions which have different f functions for the external substrate, they must have the same g function for the internal substrate so that the f functions can be gathered in one factor :

$$v_{A/B} = V_{A/B} \times \left(\frac{V_1}{V_{A/B}} f_1 + \frac{V_2}{V_{A/B}} f_2 + \ldots\right) \times g_B([B]) \ .$$

Since the resulting f function cannot depend on B, the ratios of the individual maximal rates to the total one must have fixed values whatever B : the influence that B has on the individual maximal rates is the same for each contribution. These two constraints indicate that the oxoglutarate isotranslocators must be equivalent for the internal substrate. They would differ only on their cytosolic face. It is difficult to say if such a situation is more plausible than our first hypothesis of a single oligomer with a great number of interacting subunits.

THE CATALYTIC STEP [3]

Is the catalytic step (the rate limiting step) accompanied by a conformational change ?

When alone in the external medium, malate has a Michaelian kinetics. It is clear that, during the catalytic step, a conformational change of a subunit to reach the activated state cannot be detected because the resulting changes in the subunit interactions are independent on the degree of saturation of the translocator by external malate. But, external oxoglutarate, by modifying the conformation of the subunit to which it binds, will influence the catalytic rate constant of malate uptake.

If, on the contrary, the conformation of the subunit which translocates malate does not change, the catalytic rate constant of a malate-loaded subunit will be the same whatever conformation of the neighbouring subunits show. In that case, the only effect of oxoglutarate will be to competitively inhibit the binding of malate. It is easy to deduce that the initial rate of malate uptake inhibited by oxoglutarate, v', will be equal to its value in absence of oxoglutarate, v, multiplied by the proportion of sites unoccupied by oxoglutarate. This relation can easily be tested by plotting the ratio v'/v as a function of the bound oxoglutarate : it varies linearly between 1 in the absence of oxoglutarate and zero when oxoglutarate is saturating. A non-linear variation between these two points indicates that the activation

is accompanied by a conformational change (Fig.3). Most of the experimental

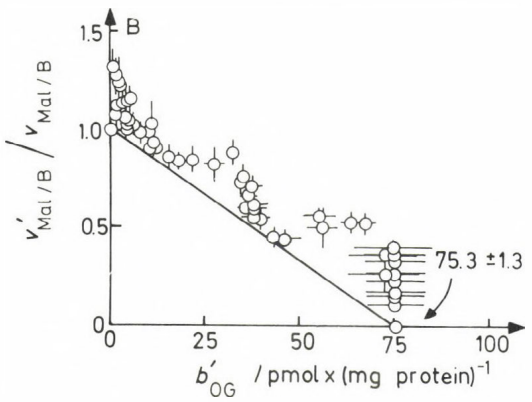

Fig.3. *Effect of external oxoglutarate on malate uptake.* $v'_{Mal/B}$ is the initial rate of malate uptake in the presence of bound oxoglutarate (b'_{OG}). $v_{Mal/B}$ is the initial rate of malate uptake in the absence of external oxoglutarate. Redrawn from [3]

points are above the straight line indicating that oxoglutarate can activate the uptake of bound malate. Oxoglutarate thus has a mixed effect : it inhibits malate binding competitively but can activate the catalytic step of malate uptake. The net effect, when the translocator is poorly saturated with external oxoglutarate, is an increase of the initial rate of malate uptake. At higher saturations by oxoglutarate the net effect is an inhibition of the malate uptake. An important conclusion of this experiment is that the catalytic step of malate uptake is accompanied by a conformational change. We have proposed the following interpretation :

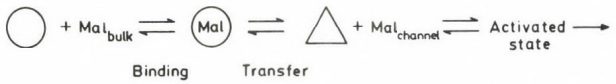

A conformational change of the external surface part of the translocator is likely to occur when malate leaves its surface site to penetrate deeper in the translocator. Malate is probably transferred into a channel in which it can migrate to the other side in exchange with the internal substrate. It is also likely that in this new conformation, the surface site is no longer accessible to the bulk solution so that only one malate can bind to one subunit and penetrate into the channel. The transfer step of malate has a very

small equilibrium constant : if it was not the case, Δ species would not be in negligible concentration and malate uptake would not be Michaelian. Because of its small equilibrium constant, the transfer step is seen as the first step of the catalytic event and not as part of binding.

Let us imagine now that external malate is exchanged with internal oxoglutarate. Oxoglutarate will arrive in front of the triangular conformation and will be transferred to the surface site with a conformational change of the external part of the translocator. It means that the conformation reached by the external part of the translocator after the transfer step of an external substrate is the same whatever the substrate is. The surface site cannot remember the substrate which has passed through it.

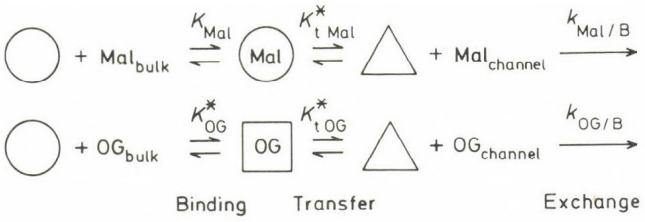

When a step is accompanied by a conformational change, the kinetic parameters, in this case equilibrium constants, will depend on the changes in the interactions of the subunit with the neighbouring subunits and with the membrane. In brief, it will depend on the environment of the subunit. The asterisk indicates the value that this equilibrium constant would have if its interactions with the environment were kept constant. These values with an asterisk, are the intrinsic values of the equilibrium constants. As we suspect that all the subunits are identical,we will suppose that they all have the same set of intrinsic values.

Considering the case where malate and oxoglutarate are both present in the external medium, the ratio of their uptake rates in exchange with the internal substrate B is :

$$\frac{v'_{Mal/B}}{v'_{OG/B}} = \frac{\sum_i [O]_i [Mal]\, K_{Mal}\, K^*_{t\,Mal}\, \frac{(K_{int\,\Delta})_i}{(K_{int\,O})_i}\, k_{Mal/B}}{\sum_i [O]_i [OG]\, K^*_{OG} \frac{(K_{int\,\square})_i}{(K_{int\,O})_i}\, K^*_{t\,OG} \frac{(K_{int\,\Delta})_i}{(K_{int\,\square})_i}\, k_{OG/B}}$$

To obtain the initial rate of malate uptake (numerator) we have done the sum for every possible environment i of the subunit, following the scheme above from the left to the right. For the first step, we have to multiply the concentration of unloaded subunit by the concentration of malate and by the affinity of the subunit for malate in order to obtain the bound-malate concentration. Among these three factors, only the first one depends on the environment. For the transfer step, the intrinsic equilibrium constant has to be multiplied by a factor which accounts for the change of interactions with the environment due to the conformational change. Finally, we have the rate constant of the exchange step. In the denominator, the same process has been followed with oxoglutarate instead of malate. We have a simplification here, because the square conformation which has been formed during the oxoglutarate binding disappears during the transfer step. We can now take out those factors that do not depend on the environment and we see then that the sum over i is the same in the numerator and in the denominator. We thus obtain a simple law (for a more rigorous presentation see [3]), which tells us that when two substrates are present together in a compartment, the ratio of their initial rates of exchange with a substrate of the other compartment, is proportional to the ratio of their concentrations :

$$\frac{v'_{Mal/B}}{v'_{OG/B}} = \frac{k_{Mal/B}\, K_{Mal}\, K^{\ddagger}_{t\ Mal}}{k_{OG/B}\, K^{\ddagger}_{OG}\, K^{\ddagger}_{t\ OG}} \times \frac{[Mal]}{[OG]}$$

This linear relationship verified experimentally is important because it strongly supports the view that all the subunits are identical even if we have a mixture of isotranslocators. In these experiments the internal substrate is malate so that the slope of the line indicates that each subunit is about 9 times more efficient in exchanging oxoglutarate with malate than in exchanging malate with malate.

We still have to provide an experimental evidence for the existence of a conformational change during the oxoglutarate transfer step. This can be done by showing that the catalytic rate constant of oxoglutarate uptake varies with the degree of saturation of the translocator by oxoglutarate. The mean catalytic rate constant of an external site loaded with oxoglutarate is simply the ratio between the initial rate and the binding. It fluctuates with the binding value (Fig.4). The catalytic cooperativity is initially positive in contrast to the binding cooperativity which was first negative. There are three changeovers from positive to negative cooperati-

vity. The cooperative effects on the catalytic rate constant show that a conformational change takes place during the catalytic step of oxoglutarate exchange.

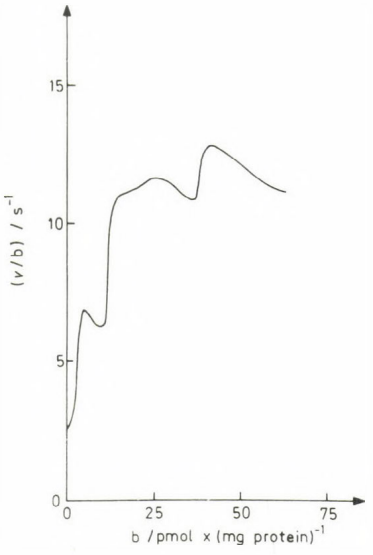

Fig.4. *Mean apparent catalytic rate constant of an oxoglutarate-loaded external site as a function of bound oxoglutarate.* The internal substrate is 4 mM malate. The curve has been obtained by smoothing the experimental points.

THE POSSIBLE REGULATORY ROLE OF THE OXOGLUTARATE TRANSLOCATOR [4,5]

Despite the fact that the complex effects induced by external oxoglutarate are not yet fully understood, it is clear that the translocator is oligomeric and undergoes conformational changes leading to cooperative phenomena. The oxoglutarate translocator is thus comparable to oligomeric enzymes known to play a regulatory role *in vivo* by controlling metabolite fluxes. However, it could be objected that the comparison is not valid because our observations have been made at 2 °C and not at physiological temperature. The observed complexity could result from an aggregation of a monomeric translocator during the lowering of temperature and leading, at 2 °C, to a mixture of monomers, dimers, trimers and so on. To this, it can be answered that it is not sure that the inner membrane of heart mitochondria is fluid enough to allow such aggregation. The protein content is high and some works suggest the existence of a rigid protein network. Further-

more we have a strong argument to exclude the possibility of a mixture of oligomers of various sizes. Indeed, in such a mixture, the proportions of the various oligomers will differ if the total concentration of subunit in the membrane is modified. For example, if the concentration of monomer at physiological temperature is increased the ratio of dimer to monomer at 2 °C will normally increase. Consequently, the shape of the external oxoglutarate binding curve will change. Of course, we are not able to vary the translocator concentration in the membrane but fortunately, nature has done it for us. We have observed an increase in the oxoglutarate binding by a factor 1.6 not depending on the oxoglutarate concentration and thus without modification of the shape of the binding curve. This binding increase can only be due to an increase in the translocator concentration and shows that all the translocators have the same number of subunits, even if several isozymes are present. An aggregation process during the lowering of temperature appears improbable and it is likely that the behaviour of the translocator at physiological temperature is similar to that at 2 °C. We maintain our suggestion that the oxoglutarate translocator could play a regulatory role *in vivo*.

Very interesting is the fact that the increase in concentration of the translocator that we have fortuitously observed seems to be a response of the organism to a mutation which has decreased the efficiency of the translocator. This may be considered as further indication that it plays a regulatory role. In accordance with this view, the oxoglutarate translocator has natural effectors. We have observed an inhibition by external free ADP and an activation by internal aspartate.

CONCLUSIONS

The kinetic and binding studies of the oxoglutarate translocator *in situ* have been fruitful despite their great complexity. The kinetic mechanism has been determined, and we now have a more precise idea of the structure of the translocator and of the conformational changes it undergoes during its activity cycle.

In summary (Fig.5) a functional subunit of the translocator seems to have three domains which could be either specialized subunits or parts of a single polypeptide . Two binding parts are situated near the two membrane surfaces, and are separated by a central catalytic part that we have called channel. Here is represented the exchange between an external oxoglutarate anion and an internal malate anion. Binding of external oxoglutarate to the external binding part induces a conformational change of this part. We have

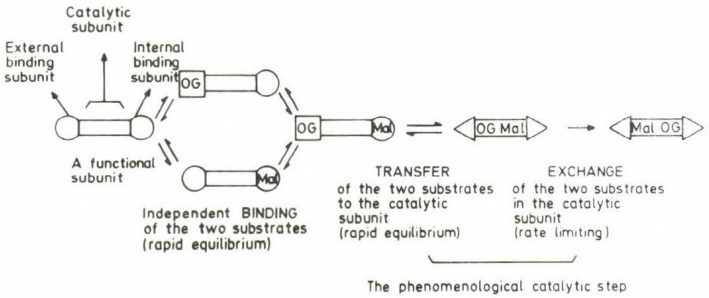

Fig.5. *Schematic representation of a functional subunit of the oxoglutarate translocator exchanging external oxoglutarate with internal malate.* Steps involved in the initial rate. Redrawn from [4]

supposed that internal malate behaves in the same way as external malate and does not induce a conformational change during its binding. The central catalytic part is not modified by the substrate binding so that in any case the two substrates bind independently. The binding steps leading to the ternary complex, are in rapid equilibrium. The phenomenological catalytic step begins with a near-equilibrium transfer of the two substrates into the channel accompanied by a conformational change of the two surface parts. It is likely that, in this new conformation, the binding sites are no longer accessible to substrates in the aqueous solution. The next step, the exchange of the two substrates within the channel, is rate limiting. We have represented the steps that are implied in the initial-rate equation. Of course, complete reaction involves the transfer of the products to the surface parts and their release into the aqueous solutions. The translocator could be made by association of several such functional subunits. It is also possible that the two ends of a single channel are surrounded by several binding subunits.

Thorough kinetic studies of the other anion translocators of mitochondria are still lacking. It is regrettable that the so widely accepted single site carrier model (ping-pong mechanism) be not yet supported by clear kinetic evidence . On the contrary it is excluded for the oxoglutarate translocator and is made questionable for the adenine-nucleotide translocator [6] and for the glutamate-asparate translocator [7].

REFERENCES

1. Sluse, F.E. & Liébecq, C. (1973) Kinetics and mechanism of the exchange reactions catalysed by the oxoglutarate translocator of rat-heart mito-

chondria, Biochimie, 55, 747-754.

2. Sluse, F.E., Duyckaerts, C., Liébecq, C. & Sluse-Goffart, C.M. (1979) Kinetic and binding properties of the oxoglutarate translocator of rat-heart mitochondria, Eur. J. Biochem. 100, 3-17.

3. Sluse-Goffart,C.M., Sluse, F.E., Duyckaerts, C., Richard, M., Hengesch, P. & Liébecq, C. (1983) Conformational changes and possible structure of the oxoglutarate translocator of rat-heart mitochondria revealed by the kinetic study of malate and oxoglutarate uptake, Eur. J. Biochem. 134, 397-406.

4. Duyckaerts, C., Sluse-Goffart, C.M., Sluse, F.E., Gosselin-Rey, C. & Liébecq, C. (1984) Spontaneous modification of the oxoglutarate translocator *in vivo*, Eur. J. Biochem. 142, 203-208.

5. Sluse, F.E., Duyckaerts, C., Sluse-Goffart, C.M., Fux, J.P. & Liébecq, C. (1980) Oxoglutarate translocator of rat-heart mitochondria : regulation by aspartate, FEBS Lett. 120, 94-98.

6. Duyckaerts, C., Sluse-Goffart, C.M., Fux, J.P., Sluse, F.E. & Liébecq, C. (1980) Kinetic mechanism of the exchanges catalysed by the adenine-nucleotide carrier, Eur. J. Biochem. 106, 1-6.

7. Murphy, E., Coll, K.E., Viale, R.O., Tischler, M.E. & Williamson, J.R. (1979) Kinetics and regulation of the glutamate-aspartate translocator in rat liver mitochondria, J. Biol. Chem. 254, 8369-8376.

RICARD:

I quite agree with the idea that a conformation change has to occur during catalysis, but I believe, that during the conversion of a ground state to a transition state, the energy required to reach the top of a barrier has to come from the protein. Therefore, the protein has to be strained in the ground state and unstrained in the corresponding transition state.

SLUSE-GOFFART

I don't disagree with that. Actually, our catalytic step is not a single step. The conformational change occurs during the first sub-step, not during the activation: the state reached after the transfer step is a ground state.

KELETI:

I wonder whether you have any independent physico-chemical evidence of the steric change of the translocator or is the theory based only on kinetic data?

SLUSE-GOFFART:

The theory is based only on kinetic data.

BARDSLEY:

Did you try statistical tests on the data or have you relied upon counting inflexions? The maximum number of critical points is an invariant for a given order but these are more subtle invariant features, such as the curvature as a function of the distance along the curve.

If statistical tests require a fairly low order Adair equation but for close fit to your data as judged by your hand-drawn curves you need a very high order Adair equation, it suggests that the Adair model is the wrong one.

SLUSE-GOFFART:

No statistical tests have been tried. Our conviction regarding the number of inflexion points is supported by the reproducibility, by the fact that they are present in both the binding curve and the kinetic curve (the two methods are somewhat different) and by the fact that an analogous substrate (which has been proved to have the same binding sites) does not exhibit any deviation from a Michaelis-Menten behavior (and this excludes the occurrence of systematic error).

The equilibrium binding curve must obey either to an Adair's equation or to a sum of Adair's equations. In any case the whole order must be high to account for the structures in the curve. Rejection (or support) of this by means of statistical tests would require the use of well adapted tests taking local structures and not only the whole curve into account.

Dynamics of Biochemical Systems
S. Damjanovich, T. Keleti, L. Trón (Eds)

ACCESS CHANNELS IN CARRIER SYSTEMS: EVIDENCE DERIVED FROM INHIBITION STUDIES OF THE CHOLINE AND GLUCOSE TRANSPORT SYSTEMS OF ERYTHROCYTES

R.M. KRUPKA and R. DEVES

Research Centre, Agriculture Canada, University Sub Post Office, London, Ontario, Canada N6A 5B7 and Department of Physiology and Biophysics, University of Chile, Santiago, Chile

According to the conventional carrier model, transport depends on a substrate site that is alternately exposed on opposite sides of the membrane. When the idea was first proposed, a sort of ferryboat was envisaged, which forms a reversible complex with the substrate and diffuses across the membrane (1). This has turned out to be true of certain small ion translocators, or ionophores, such as valinomycin and nonactin (2). However, a mechanism of this kind is extremely unlikely in the case of the transporters that normally function in the cell membrane, which in all systems investigated have been shown to be protein molecules that span the membrane and are relatively fixed in position. Nevertheless, in terms of the kinetics of transport, these systems have often been shown to behave like a ferryboat, with a substrate binding site first exposed on one side of the membrane and then on the other. The explanation may well be that the substrate site is located in a closed channel, which is first open at one end, connecting the site with the solution on that side of the membrane, and then closed here and opened at the other end, thus connecting the site with the solution on the opposite side (3). Hence, transport would depend on the occurrence of conformational changes, the opening and closing of channels connecting the substrate site with either side of the membrane giving rise alternately to two different carrier forms: an inward-facing form in which the substrate site is accessible via an open channel to the cell interior, and an outward-facing form,

in which it is accessible to the medium outside (Fig. 1).

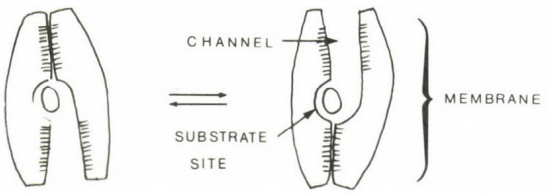

Figure 1. Diagrammatic representation of a transport protein (carrier) with a gated channel mechanism. The carrier spans the membrane, and alternates between outward-facing and inward-facing conformations, in which the substrate site is accessible, via a channel that opens and closes, to the outer or inner solution, respectively. The hatched areas lining the channels represent complementary protein structures that alternately adhere closely, blocking the channel, or separate, opening it.

The existence of highly specific substrate binding sites in carriers was established long ago, and evidence has accumulated in several different transport systems for the involvement of carrier conformational changes in transport, and for the existence of distinct inward-facing and outward-facing carrier forms. The channels that would open and close in concert on opposite sides of the membrane remain hypothetical, however, and it is the purpose of this paper to consider evidence that could bear on their involvement in transport. The approach is indirect, and depends on the investigation of sites that affect the rate of transport but are partly or wholly outside the substrate site: the question posed will be whether the sites are accessible on only one side of the membrane, and further, whether they become accessible on the same side of the membrane as the exposed substrate site. It may be inferred that such sites, if exposed or masked in unison with the appearance and disappearance of the substrate site, are likely to be located within the hypothetical channels.

To investigate this problem, evidence will be reviewed on

the action of inhibitors on two facilitated transport systems in erythrocyte membranes, those for choline and glucose. The object is to determine the sidedness of the action of an inhibitor with reference to both (a) the orientation of the substrate site in the carrier (inward-facing or outward-facing), and (b) the inner and outer surfaces of the membrane.

OBSERVATIONS

A. Glucose transport

This system equilibrates glucose across the red cell membrane. The carrier has been isolated, and is an integral membrane protein with an apparent molecular weight of 46,000 (4). Controversy continues about the details of the mechanism, despite a long history of experimental investigation, but at present the conventional carrier model appears to provide the most satisfactory explanation of the results (4-6). The experiments to be reviewed have to do with the inhibition of the system by three different substances: two reversible inhibitors, cytochalasin B and phloretin, and an irreversible inhibitor, sodium tetrathionate.

1) Cytochalasin B

The first questions to be answered are whether the inhibition is asymmetric, and if so, to which carrier form, inward--facing or outward-facing, the inhibitor is bound. As cytochalasin B, when added to a suspension of red cells, rapidly crosses the membrane by simple diffusion, it could conceivably add to the carrier on both sides and inhibit symmetrically. In fact, it inhibits asymmetrically, the inhibition of exit being competitive, and the inhibition of entry noncompetitive (7,8). The carrier model predicts exactly this behavior when a competitive inhibitor is restricted to the cell interior (9). The reason is as follows: in an exit experiment, the substrate and inhibitor are present in the same compartment and can compete with one another, but in an entry experiment, they are in different compartments and therefore cannot compete (though the inhibitor, by tying up the carrier on the inside, would still reduce the rate of transport). We may con-

clude that cytochalasin B adds exclusively to the inward-facing form of the carrier, and hence, that a cytochalasin B binding site is present in the inward-facing but not the outward facing form.

The second question is whether cytochalsin B attacks the carrier at the same surface of the membrane as the exposed substrate site, that is, the inner surface. Since carriers span the membrane and are simultaneously exposed on both sides, it is possible, in theory, for the substrate site to be exposed on one surface of the membrane while an inhibitor site is exposed on the other surface.

The location of the cytochalasin B site with respect to the inner and outer surfaces of the membrane was established by showing that the site is susceptible to digestion by proteolytic enzymes introduced into the cell interior, but resistant to attack by enzymes in the suspending medium (10). Further, the site was shown to be near the N-terminal end of the glucose transporter protein (11,12), which is exposed on the cytoplasmic surface of the cell membrane.

The third question is whether the cytochalasin binding site is separate from the substrate site. It has been suggested that this inhibitor may form an attachment within the substrate site (13,14), but the following evidence indicates that its main attachment is elsewhere. (1) Cytochalasin B gives strong protection, probably steric in nature, against the irreversible inhibitor 2,4-fluorodinitrobenzene (15,16), while equilibrated substrates increase the rate of reaction of fluorodinitrobenzene with the system (17). (2) Substrates and substrate analogs give protection, again probably steric, against the irreversible inhibitor butanedione, while cytochalasin B accelerates the reaction of the inhibitor (16,18). (3) Cytochalasin B is a much larger molecule than glucose and is non-polar, in contrast to the highly polar glucose; nevertheless, it is bound about 100,000 times more strongly than the substrate (15,19). It is still possible that the cytochalasin site partly overlaps the substrate site, which would explain its competitive mechanism.

In answer, then, to the above questions, it may be said that cytochalasin B binds to the inward-facing carrier, that it adds on the inner surface of the membrane, and that its site of attachment is largely outside the substrate site.

2. Phloretin

The action of phloretin is also asymmetric, but the pattern of inhibition is opposite to that seen with cytochalasin B: the inhibition of entry is competitive, and the inhibition of exit non-competitive. It follows that phloretin is bound to the outward-facing form of the carrier but not to the inward-facing form, even though it readily enters the cell (20,21).

The following evidence suggests that phloretin binds to the carrier on the same surface of the membrane as the exposed substrate site, that is, on the outer surface. Phlorizin, the glucoside of phloretin, also inhibits glucose entry competitively and glucose exit noncompetitively, showing that it too adds to the outward-facing carrier form (6). Since phlorizin fails to penetrate the cell membrane (22), its binding site must lie on the outer surface, and it would be reasonable to assume that phloretin also exerts its effect from the outside, by binding at the same site. It could, however, be argued that owing to its glucose residue, phlorizin binds at a site to which phloretin does not bind, but for the following reasons this does not seem likely: first, the glucose residue has been shown to play no role in phlorizin binding (23); second, the affinity of phlorizin is 100 times greater than that of glucose (19,20); and third, the binding site appears to be in a hydrophobic region of the carrier (23). The evidence suggests that phloretin and phlorizin could well bind at the same site, on the outer surface of the membrane.

Though the binding of phloretin and glucose is mutually exclusive, as if both added at the substrate site, the following evidence argues for separate binding sites. First, the structure of phloretin, and its nonpolar character, contrasts with the structure of the highly polar glucose molecule; on this account, phloretin should bind less strongly than glucose

at the substrate site, but in fact it binds to the carrier 10,000 times more strongly than glucose (19,20). Second, transported substrates, as well as maltose, a non-transported glucose analog, protect the carrier against reaction with butanedione, but phloretin fails to do so, indicating that the chemical reacts in the substrate site, in a region outside the phloretin site (16,18). Phloretin's competitive mechanism could be explained by assuming that the inhibitor site partly overlaps the substrate site; but it is possible that wholly separate allosteric sites are involved.

3. Sodium tetrathionate

Tetrathionate reacts with thiol groups in proteins, and on reaction with the glucose carrier it produces a partial inhibition of transport, which persists after removal of the unreacted inhibitor (24). The inhibition develops gradually, as expected where a covalent bond is formed. The rate of the reaction, i.e. the rate at which the transport system is inactivated, is not significantly altered by equilibrated glucose (24), showing that the reaction takes place outside the substrate site. Reversible competitive inhibitors bound exclusively to the outward-facing carrier (maltose and phloretin) sharply increase the rate of inactivation; whereas reversible competitive inhibitors bound exclusively to the inward-facing carrier (cytochalasin B and androstenedione) almost completely protect the system against tetrathionate (6). It follows that tetrathionate reacts with the outward-facing but not the inward-facing carrier, as the following line of reasoning shows. In the absence of substrates or inhibitors, the carrier should be an equilibrium mixture of the inner and outer conformations, with only the outer form reacting with tetrathionate; and in the presence of equilibrated glucose, the equilibrium of inner and outer forms is not greatly disturbed, i.e. the proportion of the outer form is much the same as in the absence of glucose, and the rate of inactivation is therefore about the same. In the presence of an inhibitor bound exclusively to the outer conformation, all the carriers are drawn into the form of the outward-facing complex, and the

rate of inactivation therefore increases greatly. In the presence of an inhibitor bound exclusively to the inner conformation, on the other hand, all the carriers are drawn into the form of the inward-facing complex, which is unreactive with tetrathionate, and the inactivation rate is therefore reduced to near zero.

The question remains whether tetrathionate reacts with the carrier on the outer surface of the membrane, the inner surface, or both. Tetrathionate, being a large anion, would not be able to penetrate the cell membrane by passive diffusion. However, it does slowly enter the red cell, as a substrate of the anion-exchange carrier (25). When this system was inhibited, blocking the entry of tetrathionate, the rate of inactivation of glucose transport was unchanged (6). It may therefore be concluded that tetrathionate reacts only on the external surface of the red cell membrane.

B Choline transport

This carrier allows choline to equilibrate across the red cell membrane. It has a high degree of steric specificity for the substrate, and forms an exceptionally strong electrostatic bond with it. Distinct inward-facing and outward-facing carrier conformations function in transport, and the conventional carrier model has been found to provide a simple, unified explanation of diverse observations on the system.

1. N-Ethylmaleimide (NEM)

NEM, a small, lipid-soluble molecule that rapidly enters the cell by passive diffusion across the cell membrane, progressively inhibits transport by reacting with a thiol group in the carrier (26). The reaction must be outside the substrate site, as equilibrated choline gives the carrier no protection. The effects of substrate analogs located on either side of the membrane show that the thiol group with which NEM reacts is exposed in the inner carrier form and masked in the outer (26,27). The evidence may be summarized as follows. Non-transported substrate analogs bound exclusively or almost exclusively to the inward-facing carrier form (dipropylamino-

ethanol and dibutylaminoethanol) sharply increase the rate of inactivation. By contrast, non-transported analogs bound exclusively to the outward-facing carrier, such as N,N,N-dimethyl-n-pentyl (2-hydroxyethyl) ammonium ion, give almost complete protection. This evidence is similar to that for the case of tetrathionate inhibition of glucose transport, though in the reverse sense. Further evidence was obtained with a series of choline analogs transported at intermediate rates (27): the effect of an analog present in the external solution was found to be quantitatively related to its ability to alter the carrier partition between its inward-facing and outward-facing forms in the steady state. A well transported analog, the carrier complex of which moves much faster than the free carrier, shifts the partition inward and accelerates the inactivation. Analogs in the series with progressively lower transport rates are progressively less able to alter the partition and to increase the rate of inactivation. Thus, an analog whose complex moves at the same rate as the free carrier would disturb neither the carrier partition nor the inactivation rate. A slowly transported analog, whose complex is less mobile than the free carrier, shifts the partition outward and, to a corresponding degree, reduces the rate of inactivation.

The question of whether NEM reacts with the carrier on the inner or outer surface of the membrane may be approached as follows: since inactivation increases sharply as the pH is raised, the sidedness of the reaction may be determined by comparing the effects of internal and external pH. In the red cell, pH equilibration depends on the operation of the anion exchanger, and when this system is blocked by a specific inhibitor, the pH inside and outside the cell may be controlled independently. The reaction with NEM is found to be independent of the external pH, but sensitive to the internal pH (R. Deves and R. M. Krupka, to be published), and it may be concluded that the reactive thiol group is only exposed on the cytoplasmic surface of the cell membrane.

HYPOTHESIS

In each of the cases discussed, we find that an inhibitory site is located partly or wholly outside the substrate site. The inhibitory site is accessible on only one side of the membrane, though not continuously so: rather, it is exposed when the substrate site is exposed on that side of the membrane, and masked when the substrate site moves to the other side. A further point is that inhibitory sites -- different inhibitory sites -- are associated with both surfaces of the membrane.

An essential difference is apparent between the behavior of the substrate site and that of an inhibitory site, which could possibly provide a clue as to the function of the latter: the substrate site, in effect, moves right across the membrane, allowing a bound substrate molecule to do the same, while the region of the carrier containing an inhibitory site could at best move part way across the membrane. On the other hand, the coincident exposure and closure of the two sites suggest that their functions could be interrelated. This coincidence, as well as the confinement of an inhibitory site to one side of the membrane, may be explained by assuming that the site lies within a channel on one side of the membrane, through which the substrate gains access to the substrate site; and more particularly, that it lies within the region of the channel postulated to open and close alternately, whose function, central to the operation of a transport protein, is to expose the substrate site on one side of the membrane in one carrier conformation, and then to seal it off in the other conformation (see Fig. 1).

It would follow that the investigation of these inhibitory sites might provide evidence on the nature of the complementary protein surfaces that may reasonably be postulated to form the channel walls: these structures would appear to adhere closely to one another in one state, so as to prevent the diffusion of even small molecules or ions into the closed channel, and yet to separate from one another rather freely, coming into contact with the aqueous solution in the other

state. The rates of separation and apposition must be relatively high, since the rate of carrier reorientation, which limits the rate of transport, is dependent on this process. Possibly, therefore, the forces of association between the complementary surfaces would not be too strong, and would be balanced by the energy released when they are surrounded by water. It may be proposed that the two surfaces are formed by different domains in the carrier polypeptide chain.

If such surfaces form the sites of attachment for phloretin and cytochalasin B, then they are likely to be partly nonpolar, corresponding to the nonpolar character of the inhibitors. They may also contain the relatively nonpolar thiol group, which is involved in both the choline and glucose carrier. Other evidence (Deves, R. and Krupka, R.M., to be published) suggests that in the choline carrier an ionizing group of pKa 6.8 may be present in the same area. Possibly these regions of the polypeptide chain comprise a mosaic of polar and nonpolar amino acid side chains, allowing them either to associate closely with one another, or to separate and interact with the aqueous solution.

ACKNOWLEDGEMENTS

This work was supported in part by Grant B1540-8545 from the University of Chile.

REFERENCES

1. LeFevre, P.G. 1975. The present state of the carrier hypothesis. Top. Membr. Transp. 7:109-215.
2. Pressman, B.C. 1976. Biological applications of ionophores. Annu. Rev. Biochem. 45:501-530.
3. Singer, S.J. 1974. Lipid-protein interactions in membranes. in Comparative Biochemistry and Physiology of Transport (Bolis, L., Block, K., Luria, S.E. and Lynen, F., eds.) North Holland Publishing Co., Amsterdam. pp. 65-101,.
4. Wheeler, T.J., Hinkle, P.C. 1985. The glucose transporter of mammalian cells. Ann. Rev. Physiol. 47:503-517.
5. Krupka, R.M., Deves, R. 1981. An experimental test for cy-

clic versus linear transport models. J. Biol. Chem. 256:5410-5416.

6. Krupka, R.M. 1985. Reaction of the glucose carrier of erythrocytes with sodium tetrathionate: Evidence for inward-facing and outward-facing carrier conformations. J. Membrane Biol. 84:35-43.
7. Basketter, D.A., Widdas, W.F. 1978. Asymmetry of the hexose transfer system in human erythrocytes. Comparison of the effects of cytochalasin B, phloretin and maltose as competitive inhibitors. J. Physiol. (Lond.) 278:389-401.
8. Deves, R., Krupka, R.M. 1978. Cytochalasin B and the kinetics of inhibition of biological transport. A case of asymmetrical binding to the glucose carrier. Biochim. Biophys. Acta 510:339-348.
9. Krupka, R.M., Deves, R. 1983. Kinetics of inhibition of transport systems. Intern. Rev. Cytol. 84:303-352.
10. Baldwin, J.M., Lienhard, G.E., Baldwin, S.A. 1980. The monosaccharide transport system of the human erythrocyte. Orientation upon reconstitution. Biochim. Biophys. Acta 599:699-714.
11. Cairns, M.T., Elliot, D.A., Scudder, P.R., Baldwin, S.A. 1984. Proteolytic and chemical dissection of the human erythrocyte glucose transporter. Biochem. J. 221:179-188.
12. Shanahan, M.F., D'Artels-Ellis, J. 1984. Orientation of the glucose transporter in the human erythrocyte membrane. Investigation by in situ proteolytic dissection. J. Biol. Chem. 259:13878-13884.
13. Taylor, N.F., Gagneja, G.L. 1975. A model for the mode of action of cytochalasin B inhibition of D-glucose transport in the human erythrocyte. Can. J. Biochem. 53:1078-1084.
14. Griffin, J.F., Rampal, A.L., Jung, C.Y. 1982. Inhibition of glucose transport in human erythrocytes by cytochalasins: a model based on diffraction studies. Proc. Natl. Acad. Sci. USA 79:3759-3763.
15. Bloch, R. 1973. Inhibition of glucose transport in the human erythrocyte by cytochalasin B. Biochemistry 12:4799-4801.
16. Krupka, R.M., Deves, R. 1980. Evidence for allosteric in-

hibition sites in the glucose carrier of erythrocytes. Biochim. Biophys. Acta 598:127-133.

17. Bowyer, F., Widdas, W.F. 1958. The action of inhibitors on the facilitated hexose transfer system in erythrocytes. J. Physiol. (Lond.) 141:219-232.
18. Masiak, S.J., D'Angelo, G., Sternberg, D.M. 1977. Inhibition of human erythrocyte glucose transport by dione compounds. Evidence for an arginyl residue at the glucose binding site. Fed. Proc. 36:563.
19. Miller, D.M. 1971. The kinetics of selective biological transport. V. Further data on the erythrocyte-monosaccharide transport system. Biophys. J. 11:915-923.
20. Krupka, R.M., Deves, R. 1980. Asymmetric binding of steroids to internal and external sites in the glucose carrier of erythrocytes. Biochim. Biophys. Acta 598:134-144.
21. Krupka, R.M. 1985. Asymmetrical binding of phloretin to the glucose transport system of human erythrocytes. J. Membrane Biol. 83:71-80.
22. Lepke, S., Passow, H. 1973. Asymmetric inhibition by phlorizin of sulfate movements across the red cell membrane. Biochim. Biophys. Acta 298:529-533.
23. Stein, W.D. 1967. The movement of molecules across cell membranes. Academic Press, New York. pp. 281-289.
24. Bloch, R. 1974. Human erythrocyte sugar transport. Identification of the essential residues of the sugar carrier by specific modification. J. Biol. Chem. 249:1814-1822.
25. Haest, C.W.M., Deuticke, B. 1976. Possible relationship between membrane proteins and phospholipid asymmetry in the human erythrocyte membrane. Biochim. Biophys. Acta 436:353-365.
26. Martin, K. 1977. Choline transport in red cells. in Membrane Transport in Red Cells (Ellory, J.C., Lew, V.L. eds.) Academic Press, London. pp. 101-113.
27. Deves, R., Krupka, R.M. 1981. Evidence for a two-state mobile carrier mechanism in erythrocyte choline transport: effects of substrate analogs on inactivation of the carrier by N-ethylmaleimide. J. Membrane Biol. 61:21-30.

DISCUSSION

RICARD:

I have two questions:
Is there any evidence for a role played by electrostatic attraction effects in choline transport? Is the transport process altered by a change of ionic strength?

Are there any inhibitors bound to the two sides of the gate? If so, they should behave as non-competitive for the entry and exit processes. Is that so?

KRUPKA:

We have not studied the effect of ionic strength on choline binding, partly because at low salt concentrations the cells tend to become unstable; there is also the problem that with whole cells, which are used in our experiments, changes in the chloride concentration in the external solution produce large changes in membrane potential, and one would have to sort out the two effects. We do know, however, that the positive charge in the substrate choline makes an unusually large contribution to the strength of binding, which is several orders of magnitude larger than in the case of acetylcholinesterase: a very strong electrostatic bond between the substrate and the carrier site must therefore be formed.

In answer to the second question, there are indeed inhibitors bound on both sides, for example certain steroids in the case of the glucose carrier. Here the inhibition of both entry and exit should be noncompetitive. However, such inhibitors do not have the properties we are looking for, and for this reason we have not considered them here.

CORNISH-BOWDEN:

You seem to be assuming in your models that your substrate and inhibitor are always competitive in the mechanistic sense, i.e. that one or other may be bound but

not both simultaneously. However, given that the two are quite different in structure, it seems likely that the inhibitor might bind after the substrate but might prevent the translocation (catalytic) step. It is not clear to me that any of your data exclude this possibility.
Second, you discussed whether phloretin and phlorizin might act in different ways at different sites. Although I agree with you that plausibility arguments make this unlikely, I suspect that experiments with both inhibitors present simultaneously would resolve this unambiguously.

KRUPKA:

Generally speaking, if the inhibitor is noncompetitive in the mechanistic sense, then the inhibition kinetics would be noncompetitive in all experiments, including entry and exit. The observed competitive inhibitors are therefore evidence for a competitive mechanism. The kinetic analysis of inhibition shows that equilibrium exchange provides the best test, and experiments in the literature, by Widdas and others, have also shown that the inhibition by phloretin and cytochalasin B is competitive in mechanism.
In answer to the second question, I am afraid that even this test would not absolutely prove that both inhibitors bind at the same site, since one could postulate, rather implausibly it is true, that they bind at separate but interacting sites. Nevertheless, the demonstration of competition between the inhibitors would add to the likelihood that they bind at a single site, and this would probably be an experiment worth doing.

ASZALÓS:

Do you have any experience with quinine the voltage gated K^+ channel inhibitor?

KRUPKA:

No, we do not, though I think it would be interesting to examine the effect of quinine on the choline transporter.

LIST OF PARTICIPANTS

AMLER, E. Czechoslovakian Academy of Sciences, Institute of Physiology, Prague, Czechoslovakia

ÁDÁM, G. Institute of Enzymology, Biological Research Center, Hungarian Academy of Sciences, Budapest, Hungary

ARAGON, J.J. Departamento de Enzimologia del Instituto de Investigaciones Biomédicas del CSIC y Departamento de la Facultad de Medicina de la Unive-sidad Autonoma, Madrid, Spain

ATKINSON, D.E. Department of Chemistry and Biochemistry, University of California, Los Angeles, CA, USA

ASZALOS, A. Food and Drug Administration, Washington, DC, USA

BALÁZS, M. Department of Biophysics, University Medical School of Debrecen, Debrecen, Hungary

BARDSLEY, W.G. Department of Obstetrics and Gynaecology, University of Manchester, Manchester, United Kingdom

BATKE, J. Institute of Enzymology, Biological Research Center, Hungarian Academy of Sciences, Budapest, Hungary

BELEZNAY, Zs. Institute of Enzymology, Biological Research Center, Hungarian Academy of Sciences, Budapest, Hungary

CHERRY, R.J. Department of Chemistry, University of Essex, Colchester, United Kingdom

CORNISH-BOWDEN, A. Department of Biochemistry, University of Birmingham, Birmingham, United Kingdom

DAMJANOVICH, S. Department of Biophysics, University Medical School of Debrecen, Debrecen, Hungary

DELISI, Ch. Laboratory of Mathematical Biology, National Institute of Health, Bethesda, MD, USA

DYNNIK, V.V. Institute of Biological Physics, Acad. Sci. USSR, Pushchino, USSR

EASTERBY, J.S. Department of Biochemistry, University of Liverpool, Liverpool, United Kingdom

EDIDIN, M. Department of Biology, The Johns Hopkins University, Baltimore, MD, USA

ELSON, E.L. Department of Biological Chemistry, Washington University School of Medicine, St. Louis, MO, USA

ENDRENYI, L. Department of Pharmacology, University of Toronto, Toronto, Canada

ERNSTER, L. Department of Biochemistry, Arrhenius Laboratory, University of Stockholm, Stockholm, Sweden

FÉSÜS, L. Department of Biophysics, University Medical School of Debrecen, Debrecen, Hungary

FRANK-KAMENETSKII, M.D. Institute of Molecular Genetics, USSR Academy of Sciences, Moscow, USSR

FRIEDRICH, P. Institute of Enzymology, Biological Research Center, Hungarian Academy of Sciences, Budapest, Hungary

GÁSPÁR, R. Department of Biophysics, University Medical School of Debrecen, Debrecen, Hungary

GERGELY, J. Department of Immunology, Eötvös L. University, Göd, Hungary

GOLDSTEIN, B.N. Institute of Biological Physics, USSR Academy of Sciences, Pushchino, USSR

GOLLOP, N. Ben Gurion University of the Negev, Department of Biology, Beer Sheva, Israel

HONG, P.T. Central Institute for Biological Research, Department of Biophysics, Hanoi, Vietnam

IKEGAMI, A. Institute of Physicsl and Chemical Research, Wako, Japan

JEZEK, P. Czechoslovakian Academy of Sciences, Institute of Physiology, Prague, Czechoslovakia

KACSER, H. University of Edinburgh, Department of Genetics, Edinburgh, United Kingdom

KELETI, T. Institute of Enzymology, Biological Research Center, Hungarian Academy of Sciences, Budapest, Hungary

KILÁR, P. Department of Neurology and Psychiatry, University Medical School of Pécs, Pécs, Hungary

KISPÁL, Gy. Department of Biochemistry, University Medical School of Pécs, Pécs, Hungary

KRETSCHMER, M. Institute of Physiological Chemistry, Karl-Marx University, Leipzig, GDR

KRUPKA, R.M. Research Centre, Agriculture Canada, London, Canada

KURGANOV, B.I. The All-Union Vitamin Research Institute, Moscow, USSR

LUKÁCS, K. 3rd Department of Internal Medicine, University Medical School of Debrecen, Debrecen, Hungary

MANNERVIK, B. Department of Biochemistry, Arrhenius Laboratory, University of Stockholm, Stockholm, Sweden

MATKÓ, J. Department of Biophysics, University Medical School of Debrecen, Debrecen, Hungary

MARKUS, M. Max-Planck Institut für Ernährungsphysiologie, Dortmund, FRG

MÁTRAI, Gy. Institute of Enzymology, Biological Research Center, Hungarian Academy of Sciences, Budapest, Hungary

MÁTYUS, L. Department of Biophysics, University Medical School of Debrecen, Debrecen, Hungary

MOLNÁR, E. Department of Biochemistry, University Medical School of Szeged, Szeged, Hungary

OVÁDI, J. Institute of Enzymology, Biological Research Center, Hungarian Academy of Sciences, Budapest, Hungary

PECHT, I. Department of Chemical Immunology, The Weizmann Institute of Science, Rehovot, Israel

PERSSON, L.-O. Department of Biochemistry, Chemical Center, Lund, Sweden

PINTÉR, M. Institute of Enzymology, Biological Research Center, Hungarian Academy of Sciences, Budapest, Hungary

RICARD, J. Centre de Biochimie et de Biologie Moléculaire du C.N.R.S., Marseille, France

ROSENBERG, A. Department of Laboratory Medicine and Pathology, University of Minnesota, Minneapolis, MN, USA

ROSSI, G.L. Istituto di Biologica Moleculare, Universitá degli Studi, Parma, Italy

SEGAL, D.M. Department of Health and Human Services, National Institute of Health, Bethesda, MD, USA

SERES, I. Department of Biophysics, University Medical School of Debrecen, Debrecen, Hungary

SIMON, I. Institute of Enzymology, Biological Research Center, Hungarian Academy of Sciences, Budapest, Hungary

SLUSE, F. Université de Liege, Laboratoire de Biochimie et de Physiologie Générales, Liége, Belgique

SLUSE-GOFFART, C.M. Département de Chimie, Université de Liége au Sart-Tilman, Liege, Belgique

SOMOGYI, B. Department of Biophysics, University Medical School of Debrecen, Debrecen, Hungary

SOULIÉ, J.-M. Attaché de Recherche, C.N.R.S. - C.B.M., Marseille, France

SRERE, P.A. Veterans Administration Medical Center, Pre-Clinical Science Unit, Dallas, TX, USA

STRAUB, F.B. Institute of Enzymology, Biological Research Center, Hungarian Academy of Sciences, Budapest, Hungary

SZÖLLŐSI, J. Department of Biophysics, University Medical School of Debrecen, Debrecen, Hungary

TOMPA, P. Institute of Enzymology, Biological Research Center, Hungarian Academy of Sciences, Budapest, Hungary

TRÓN, L. Department of Biophysics, University Medical School of Debrecen, Debrecen, Hungary

VASS, M. Institute of Enzymology, Biological Research Center, Hungarian Academy of Sciences, Budapest, Hungary

VÉRTESI, B. Institute of Enzymology, Biological Research Center, Hungarian Academy of Sciences, Budapest, Hungary

WELCH, G.R. Department of Biological Sciences, University of New Orleans, New Orleans, LA, USA

ZIDOVETZKI, R. Department of Biology, University of California, Riverside, CA, USA

Zs.-NAGY, I. F. Verzár International Laboratory for Experimental Gerontology, Hungarian Section, University Medical School of Debrecen, Debrecen, Hungary

INDEX

A 23187 417
Adenylate cyclase 393
Aldolase 203
Allosteric enzymes 59
Allosteric regulation 41, 231
Alternative enzyme-enzyme complexes 247
Alternative structures of DNA 91
Anisotropy decay 487
Anisotropic diffusion 359
Antibody dependent cellular cytotoxicity 341, 409
Antibody heteroaggregates 341
Antigen stimulated secretion 473
Asymmetric inhibition 537

Bacteriorhodopsin 487
Band 3 487
- protein of erythrocyte membrane, the participation in the formation of the complex of glycolytic enzymes 231
- self-aggregation of melithin 487
Basophils 443
β-2-microglobulin 393
Bifunctional enzyme 59
Bilayers 501
Bimodality 11
Binding isotherms 73
Binding polynomials 267
Biological membrane 461
Biorhythm 11
Biorhythmicity 11

Carbocyanine dyes 417
Carrier model 537
Cascade mechanism 59
Cell: cell interactions 341
Cellular cytotoxicity (ADDC) 341
Cellular microenvironment 217
Channel 537
-conductance 473

- open time 473
Channelling 203, 247
Chaos 11
Chemical shift anisotropy 501
Chinese Hamster Ovarium (CHO) cells 443
Cholesterol 461
Choline carrier 537
Cholinesterase 289
Citratesynthase, antibody structure 159
Citric and cycle 159
Coated pits 381
Coenzyme cycles 185
Colcemid 443
Colchicine 443
Collisional quenching 113
Compartmentation 173
Compensation plot for hydrogen exchange kinetics 101
Concanavalin A 409
Conformational changes 521, 537
Conformational fluctuation of proteins 101
Control coefficient 3
Control theory 3
Cooperativity changeovers 521
Coupled enzyme assays 145
Crisis 11
Cromolyn 473
Cromolyn binding proteins 473
Cruciform 91
Cyclic AMP 173, 393
Cyclosporin A 417
Cytochalasin 537

Degrees of freedom 267
Design of experiments 289, 323
Dimyristoylphosphatidylcholine vesicles 487
1,6-diphenyl-1,3,5,-hexatriene (DPH) 461
3-3-dipropyl thiocarbocyanine 487
DNA
B form of - 91
H form of - 91
superhelical - 91
Z form of - 91
Double direct linear plot 289
Drosophila 173
Dunce mutant 173
Dynamic structure of membranes 461
Dynamics
- of DNA 91
- of enzyme-enzyme interaction 147
- of metabolic pathways 145

Effector cells 341
Efflux of Ca^{2+} from mitochondria 27
Efflux of Mg^{2+} from mitochondria 27
Elasticity coefficient 3
Electron spin resonance 417 443, 461

Endocytosis
non specific - 381
receptor mediated - 381
Energy metabolism 185
Entrainment 11
Enzyme
- action in vivo 217
- enzyme interactions 231, 247
- evolution 3, 247
- kinetics 267, 289, 309, 323
Krebs cycle - 159
- probe 173
- regulation 41, 159, 231
Equilibrium binding 521
Erythrocyte membrane 461, 537
Erythrocytes 537
Ethanol, effects on hydrogen exchange 101
N-ethyl-maleimid 537
Evolution of enzyme-enzyme interactions 247
Experimental error 323
Exponential functions 267

Fc receptor 341, 409
Feedback and feedforward control 185
Flow cytometry 341, 417
Flow cytometric energy transfer 417
Fluorescence
- anisotropy 247, 461
- correlation spectroscopy 359
double quenching of - 113
time resolved - 461
tryptophane - 113
quantum yield of - 247
- pattern bleaching 359
- photobleaching recovery 359
- polarization 203
Fluorescent probes 247
Fourier transform 323
Franked effector cells 341
Fructose-1,6-bisphosphate 231
F test 267
Functional efficiency 73
Functional simplicity 73

Gated quenching model 113
Glucagon 393
Glucose carrier 537
Glutathione transferase 323
Glyceraldehyde-3-phosphate dehydrogenase 203
Glycerol, effect on protein stability 101
Glycolysis 11, 41, 173, 217
Glycolytic enzymes 231
Glycosome 247
Glycosyl transferase 393
Gramicidin S 501

Hill coefficient 73
Hill equation 289
HLA 393
Homeostasis 185
Homologous and heterologous interaction 247

Human erythrocyte ghosts 487
Human γ interferon 417
Human peripheral lymphocytes 409, 417
Hybrid heterologous interaction 247
Hydrogen exchange kinetics of proteins 101
Hyperpolarization 487
Hysteresis 11

IgE 473
IgG
- CH2 domain 409
- CH3 domain 409
- F(ab) fragments 409
Ion channels (Ca^{2+}) 473
Ionophore 417, 487, 501
In situ assay 41
Insulin 393, 417
Interleukin-2 (IL-2) 417
Intracellular Ca^{2+} 417, 473
Intra-subunit strain 73

Kinetic power 3
Kinetics of exchange reactions 521

Lateral diffusion 359, 393
Liapunov exponent 11
Ligand binding 267
Likelihood ratio tests 267
Long-lived transients
β-lumicolchicine 443
Lysozyme 113

Macromolecular environment 41
Major histocompatibility complex 393
Mast cells 473
Membrane fluidity 393, 443, 461, 487
Membrane potential 393, 443, 473
Metabolic control 541
Metabolic regulation 129
Metabolites 231
Metabolon 159
Microtubules 443
Mitochondria
- exposed enzyme activity 159
heart - 521
sonicated - 159
uptake of Ca^{2+} by - 27
uptake of Mg^{2+} by - 27
Mitochondrial 159
- matrix 159
- membrane 461
- transport 27
Model discrimination 267
Modelling 59, 267, 323
Models of error 323
Motional freedom of lipid probes 443
Motional freedom of protein probes 443
Multienzyme complex 203, 231, 247
Multiple oscillatoring states 11

NAD 173
-glycohydrolase 173
Non-linear phenomena 11
Non-linear regression 267
Nuclear magnetic resonance 461, 501

Order parameter 461
Oscillation 11
Oxoglutarate translocator 521

Parameter estimation 289 309, 323
Phase transition 461
Phloretin 537
Phosphodiesterase 173
Phosphofructokinase 41, 231
Polymyxin B 501
Polypeptide antibiotics 417, 487, 501
Pool heterogeneity 173
Power functions 267
Propagation of error 323
Protein
- aggregation 359
- dynamics 101, 113
- kinase 173
- lipid interaction 461
- protein interaction 41
unfolding of -s 101
Purple membrane 461
Pyruvate kinase 41

Quadrupol splitting 501
Quasiperiodicity 11
Quaternary constraints 73

Rational functions 267
Receptor
- aggregation 473
- conversion 409
- crosslinking 409
- down regulation 381
- shedding 409
Recycling
- of ligands 381
- of receptors 381
Regression analysis 323
Regulation
enzyme - and multienzyme complexes 231
- of energy metabolism 185
- of metabolic fluxes 247
- of Ca^{2+} uptake by mitochondria 27
- of Mg^{2+} uptake by mitochondria 27
Residual 323
Robust
- estimation 289
- design 289
- methods 309
Rotational
- correlation time 461, 487
- diffusion 461, 487
- relaxation of lipids 393

Sarcoplasmic membrane 461
Saturation functions 267
Second messengers 231
Self-oscillations 59
σ ratio method 289
Skeletal muscles 185
Standard deviation 323

Statistical methods 309
Statistical tests 267
Steady-state 267
Stochasticity 11
Strange attractors 11
Structural kinetics 73
Structural poroteins of
skeletal muscles 231
Structural rate equations
73
Substrate site 537
Subunit
loose - coupling 73
- subunit interaction 203
tight - coupling 73
Superhelical DNA 91
Supramolecular organization
203, 231, 247

Target cells 341
Taxol 443
Theory of graphs 59
Tetrathionate 537
Thermal unfolding of
proteins 101
Transient dichroism 473
Transient in enzyme
kinetics 267
Transient time 145
Transition states 73
Transport dynamics 521
Tricarboxylate cycle 185
Triosephosphate dehydrogenase
203
Triosephosphates 247
Triplet probe 487
Tryptophane-phosphorescence
113

Unfolding 101

Valinomycin 417, 487, 501
Variance ratio method 289
Vincristine 443
Viscosity
effects of - on hydrogen ex-
change kinetics 101
- and enzyme organization
217
- and metabolic processes
217
- and protein dynamics 217

Weighted regression 289
Weighting 309
Weighting factors 323
Wobbling in cone model 461

Yeast 11

mation of enzyme systems — two binding sites model of IgG R_c receptor — interaction of MHC antigens and receptors for peptide hormones — membrane dynamics and information transfer — mobility of membrane proteins.

The reader may expect to obtain a broad update on current issues in dynamic features of molecular and cellular systems.

Field of interest: this volume will be of great value and interest to enzymologists, biochemists, transport physiologists, biophysicists, immunologists, cell biologists, and others studying dynamic properties of biochemical systems and wishing to keep abreast of advances in this rapidly expanding field.

AKADÉMIAI KIADÓ
BUDAPEST

Distributors:
KULTURA
Hungarian Foreign Trading Co.
P. O. B. 149
H-1389 Budapest
Hungary

ISBN 963 05 4356 7